

Projecting boreal bird responses to climate change considering uncertainty, refugia, vegetation
lags, and post-glaciation history

by

Diana Stralberg

A thesis submitted in partial fulfillment of the requirements for the degree of

Doctor of Philosophy

in Ecology

Department of Biological Sciences
University of Alberta

© Diana Stralberg, 2016

ABSTRACT

Often referred to as North America's bird nursery, the boreal forest biome provides a productive environment for breeding birds, supporting high species diversity and bird numbers. These birds are likely to shift their distributions northward in response to rapid climate change over the next century, resulting in population- and community-level changes. To anticipate the pattern and extent of such changes, and to inform climate-change adaptation and conservation planning, species distribution models (SDMs) are often used to describe and map species' climatic niches through time. SDMs provide invaluable insights into climatic suitability patterns and potential distributional responses, but they are most useful when assumptions are acknowledged and the resulting limitations are addressed. Each chapter of my thesis focuses on understanding and addressing one of four major limitations of SDMs: (1) model uncertainty in current and future projections, (2) time lags in ecosystem responses to climate change, (3) the static nature of correlative models, and (4) the influence of historical biogeography in determining current distributions.

In my first chapter, using a continental-scale avian dataset compiled by the Boreal Avian Modelling project, I developed models to project climate-induced changes in the distribution and relative abundance of 80 boreal-breeding passerine species. For such projections to be useful, however, the magnitude of change must be understood relative to the magnitude of uncertainty in model predictions. I found that the mean signal-to-noise ratio across species increased over time to 2.87 by the end of the 21st century, with the signal greater than the noise for 88% of species. I also found that, among sources of uncertainty evaluated, the choice of climate model was most important for 66% of species, sampling error for 29% of species, and variable selection for 5% of species. The range of uncertainty exhibited across species and geographic regions suggests a

basis for differential quantitative weightings in assessments of species vulnerability and spatial conservation priorities under climate change.

Many species and ecosystems will likely be unable to keep pace with rapid climate change projected for the 21st century, however. In my second chapter, I evaluated an underexplored dimension of the mismatch between climate and biota: limitations to forest growth and succession affecting habitat suitability. I found dramatic reductions in suitable habitat for many species over the next century when vegetation lags were considered. I used these results to identify conservative and efficient boreal conservation priorities anchored around climatic macrorefugia that are robust to century-long climate change and complement the current protected areas network.

Vegetation change may also be delayed in the absence of disturbance catalysts. In the western boreal region, a combined increase in wildfires and human activities may aid these transitions, also resulting in a younger forest. In my third chapter, I developed a hybrid modelling approach based on topo-edaphically constrained projections of climate-driven vegetation change potential, coupled with weather- and fuel-based simulations of future wildfires, and projections of large-scale industrial development activities, to better understand factors influencing decadal-scale upland vegetation change. I simulated scenarios of change in forest composition and structure over the next century, conservatively concluding that at least one-third of Alberta's upland mixedwood and conifer forest is likely to be replaced by deciduous woodland and grassland by 2090. During this timeframe, the rate of increase in fire probability diminished, suggesting a negative feedback process by which a warmer climate and more extensive near-term fires leads to an increase in deciduous forest that in turn, due to its relatively low flammability, leads to a long-term reduction in area burned.

Finally, boreal species' projected range shifts could be impeded by the northwestern cordillera, which spans from boreal Alaska to the rest of the North American boreal region, and may have inhibited the expansion of many species into climatically suitable habitat after the last glacial maximum (LGM). Using paleoclimate simulations for the past 20,000 years, I analyzed the relative importance of migratory and life-history characteristics vs. current and historical climatic suitability on the distributions of North American boreal-breeding species. The high relative importance of climatic suitability within the northwestern cordilleran region suggests a capacity for several species to disperse into Alaska once climatic connectivity is achieved in the future, which is supported by recently recorded signs of breeding activity.

PREFACE

Some of the research for this thesis was conducted as part of the Boreal Avian Modelling (BAM) project, an international research collaboration led by a steering committee consisting of Fiona K.A. Schmiegelow and Erin M. Bayne at the University of Alberta, Samantha J. Song at Environment Canada, and Steven G. Cumming at Université Laval. All chapters consist of my own original work, supported by co-authors as indicated below. I conducted all of the data analyses personally, with the exception of density offsets (P. Sólymos, Chapter 1), bird-forest age summaries (P. Sólymos, Chapter 2), and some of the fire simulations and data input preparations (X. Wang and F.-N. Robinne, Chapter 3). I wrote all of the original text, which was modified by edits from co-authors.

Chapters 1 and 2 of this thesis have been published in scholarly journals:

Stralberg, D., S. M. Matsuoka, A. Hamann, E. M. Bayne, P. Sólymos, F. K. A. Schmiegelow, X. Wang, S. G. Cumming, and S. J. Song. 2015. Projecting boreal bird responses to climate change: the signal exceeds the noise. *Ecological Applications* 25:52–69.

Stralberg, D., E. M. Bayne, S. G. Cumming, P. Sólymos, S. J. Song, and F. K. A. Schmiegelow. 2015. Conservation of future boreal forest bird communities considering lags in vegetation response to climate change: a modified refugia approach. *Diversity and Distributions* 21:1112-1128.

Chapters 3 and 4 are being prepared for journal submission, with proposed author lists as follows:

Stralberg, D., X. Wang, M.-A. Parisien, F.-N. Robinne, C. L. Mahon, P. Sólymos, and E. M. Bayne. In prep. Scenarios of future climate- and disturbance-driven changes for the boreal forest region of Alberta.

Stralberg, D., S. M. Matsuoka, C. M. Handel, E. M. Bayne, F. K. A. Schmiegelow, and A. Hamann. In prep. Biogeography of boreal passerine range dynamics: past, present, and future.

In addition, as part of my PhD research and affiliation with the BAM project, I have contributed to the following co-authored thesis-related papers:

- Sólymos, P., S. M. Matsuoka, E. M. Bayne, S. R. Lele, P. Fontaine, S. G. Cumming, D. Stralberg, F. K. A. Schmiegelow, and S. J. Song. 2013. Calibrating indices of avian density from non-standardized survey data: making the most of a messy situation. *Methods in Ecology and Evolution* 4:1047-1058.
- Cumming, S. G., D. Stralberg, K. L. Lefevre, P. Sólymos, E. M. Bayne, S. Fang, T. Fontaine, D. Mazerolle, F. K. A. Schmiegelow, and S. J. Song. 2014. Climate and vegetation hierarchically structure patterns of songbird distribution in the Canadian boreal region. *Ecography* 37:137-151.
- Barker, N. K. S., P. C. Fontaine, S. G. Cumming, D. Stralberg, A. Westwood, E. M. Bayne, P. Sólymos, F. K. A. Schmiegelow, S. J. Song, and D. J. Rugg. 2015. Ecological monitoring through harmonizing existing data: Lessons from the Boreal Avian Modelling Project. *Wildlife Society Bulletin* 39:480-487.

I performed post-hoc model analyses and led the writing of Cumming et al. (2013), for which I was designated an equal-contribution lead author. I contributed to the writing of Barker et al. (2015), and assisted with data analysis and editing for Sólymos et al. (2014).

ACKNOWLEDGEMENTS

Chapters 1, 2, and 4 were made possible by the Boreal Avian Modelling (BAM) Project, an international research collaboration on the ecology, management and conservation of boreal birds. I am extremely grateful to the BAM Project's members, data partners, and funding agencies (including Environment Canada and the U.S. Fish & Wildlife Service), listed in full at <http://www.borealbirds.ca/index.php/acknowledgements>. Chapter 3 was enabled by data from the Alberta Biodiversity Monitoring Institute (ABMI), Environment Canada, Natural Resources Canada, and Alberta Environment and Parks (Ecosite Information System).

Funding for my research was provided by the Natural Sciences and Engineering Research Council (Vanier Canada Graduate Scholarship), Alberta Innovates (Alberta Ingenuity Fund Scholarship), the University of Alberta (Killam Graduate Scholarship, Doctoral Prize of Distinction), the Department of Biological Sciences (McAfee Estate Scholarship in Zoology), the Climate Change and Emissions Management Corporation, Environment Canada, the U.S. Fish and Wildlife Service (Neotropical Migratory Bird Conservation Act and Arctic Landscape Conservation Cooperative grants), the Alberta Biodiversity Monitoring Institute, and the Alberta Conservation Association.

I am especially grateful for guidance from my co-supervisors, Erin M. Bayne and Fiona K.A. Schmiegelow, as well as committee members Andreas Hamann and David S. Hik, and external examiners Mark S. Poesch, Evelyn Merrill, and Falk Huettmann. This work was also greatly improved by collaborations with additional co-authors Samantha J. Song, Steven G. Cumming, Péter Sólymos, Steven M. Matsuoka, Xianli Wang, Colleen M. Handel, Marc-André Parisien, Francois-Nicolas Robinne, and C. Lisa Mahon. Other colleagues also provided various forms of assistance (in alphabetical order): Harry Archibald, Craig Aumann, Nicole Barker, Matt Carlson, Easwaramurthyvasi Chidambaravasi, Steven Crawford, Jacqueline Dennett, QiongYan Fang, Dan Farr, Trish Fontaine, Tom Habib, Samuel Haché, Melynda Johnson, Meg Krawchuk, Hedwig Lankau, Jeff Lane, Suzanne Lavoie, Scott Nielsen, Amy Nixon, Daiyuan Pan, Rick Pelletier, Wayne Pettapiece, Terry Rich, Jim Schieck, Rick Schneider, Brian Simpson, Jessica Stolar, Alberto Suarez Esteban, Cassidy van Rensen, and Mike Willoughby. Additional thanks are extended to members of the BAM Team, the Alberta Biodiversity Management and Climate Change Adaptation Project, the Canadian BEACONS project, the Bayne-Boutin lab, the Schmiegelow lab, and the Nielsen lab, for encouragement, support, and intellectual challenge.

Finally, I would like to thank my masters advisor, Terry L. Root, for her inspiration to tackle the difficult issue of climate change and broad-scale ecological questions, as well as my former colleagues and mentors at PRBO Conservation Science in California—especially Ellie M.Cohen, John A. Wiens, Nils Warnock, and Nadav Nur—for motivating and encouraging my research.

TABLE OF CONTENTS

List of Tables	xiv
List of Figures	xv
Introduction.....	1
CHAPTER 1. Projecting boreal bird responses to climate change: the signal exceeds the noise ..	5
1.0 Summary	5
1.1 Introduction	5
1.2 Methods.....	9
1.2.1 Study area and avian survey data.....	9
1.2.2 Climate data	10
1.2.3 Land-use and topography data	11
1.2.4 Density models.....	11
1.2.5 Abundance projections.....	13
1.2.6 Quantifying prediction uncertainty.....	13
1.3 Results	14
1.3.1 Model evaluation	14
1.3.2 Projected changes in potential abundance	15
1.3.3 Prediction uncertainty relative to change.....	16
1.3.4 Spatial and temporal uncertainty	16
1.4 Discussion	17
1.4.1 Signal versus noise in projections of abundance	17
1.4.2 Uncertainty due to GCM projections.....	18
1.4.3 Uncertainty due to sampling error	18
1.4.4 Uncertainty due to predictor variables.....	19
1.4.5 Other potential sources of uncertainty	20
1.4.6 Conservation and management implications	21
1.5 Appendices.....	24

1.6	Tables	25
1.7	Figures	28
CHAPTER 2. Conservation of future boreal forest bird communities considering lags in		
	vegetation response to climate change: a modified refugia approach.....	33
2.0	Summary	33
2.1	Introduction	33
2.2	Methods.....	36
2.2.1	Avian Density Models and Future Projections	37
2.2.2	Seral-stage associations and time lags	39
2.2.3	Modified future distributional trajectories	39
2.2.4	Conservation priorities.....	40
2.2.5	Evaluation of protected areas and conservation priorities	40
2.3	Results	41
2.3.1	Habitat age associations and projected distributional shifts	41
2.3.2	Conservation priorities.....	43
2.4	Discussion	44
2.4.1	Successional lags affect climate-change projections	44
2.4.2	Seral-stage-modified macrorefugia approach yields robust land rankings.....	44
2.4.3	Conservation priorities must complement the current protected areas network.....	46
2.4.4	Conservation priorities minimally sensitive to habitat suitability assumptions.....	46
2.4.5	Model limitations	47
2.4.6	Conclusion	48
2.5	Appendices	49
2.6	Tables	49
2.7	Figures	51
CHAPTER 3. Scenarios of future climate- and disturbance-driven changes for the boreal forest		
	region of Alberta	62
3.0	Summary	62

3.1	Introduction	62
3.2	Methods	66
3.2.1	Study Area	66
3.2.2	Model and Simulation Overview	67
3.2.3	Ecosite and Vegetation Data	68
3.2.4	Climate and Terrain Data	69
3.2.5	Fire and Weather Data	70
3.2.6	Anthropogenic Disturbance Data	70
3.2.7	Ecosite and Vegetation Models	71
3.2.8	Fire and Vegetation Change Simulation	73
3.2.9	Fire and Forest Change Analysis	76
3.3	Results	77
3.3.1	Ecosite Models	77
3.3.2	Vegetation Models	77
3.3.3	Predicted Ecosites and Vegetation	77
3.3.4	Fire Simulation	78
3.3.5	Forest Composition	78
3.3.6	Forest Age	79
3.4	Discussion	79
3.4.1	Caveats and limitations	82
3.4.2	Conclusion	83
3.5	Appendices	84
3.6	Tables	85
3.7	Figures	92
CHAPTER 4. Biogeography of boreal passerine range dynamics in western North America: past, present, and future		105
4.0	Summary	105
4.1	Introduction	105
4.1.1	Glaciation history shapes boreal bird distributions	105

4.1.2	Migratory habits reinforce geographic segregation	107
4.1.3	Will climate-projected range shifts be impeded by the northwestern cordillera?	109
4.2	Methods	110
4.2.1	Study area and species	110
4.2.2	Paleo-hindcasting	111
4.2.3	Climate suitability variables	111
4.2.4	Life-history variables	112
4.2.5	Phylogenetic logistic regression analysis	113
4.2.6	Evaluating future habitat potential	113
4.3	Results	114
4.3.1	Model fit and variable importance	114
4.3.2	Model predictions for current and future climate	115
4.4	Discussion	116
4.4.1	Past and present climatic suitability account for barrier effect	116
4.4.2	Migratory strategy also influences Alaskan boreal occupancy	117
4.4.3	Perceived cordilleran barrier may easily be weakened	118
4.4.4	Range expansions may lead to community reshuffling	119
4.4.5	Conclusion	120
4.5	Appendices	120
4.6	Tables	121
4.7	Figures	132
	Conclusion	137
	References	142
	Appendices	181
	Appendix 1-A. Global climate model summary and downscaling methods	182
	Appendix 1-B. Covariate correlations	187
	Appendix 1-C. Individual species model evaluation	189
	Appendix 1-D. Individual species climate-change projections	197
	Appendix 1-E. R Code for boosted regression tree models	279

Appendix 2-A. Projected proportional change in core habitat area for 53 boreal forest species under alternative vegetation-lag scenarios by 2071-2100.	284
Appendix 2-B. Methods for identification of species' minimum forest age thresholds.....	287
Appendix 2-C. Alternative distributional assumptions for 53 boreal species.	288
Appendix 2-D. R code to calculate core areas, strict refugia, and modified refugia.....	342
Appendix 2-E. Zonation settings and inputs.....	349
Appendix 3-A. Confusion matrix for random forest vegetation predictions.....	353
Appendix 3-B. Vegetation type projections (km ²) by GCM for scenarios A, B1, and B2.....	357
Appendix 4-A. Projected current and paleo-historical core area distributions based on the CCM1 global climate model.....	361
Appendix 4-B. Projected current and paleo-historical core area distributions based on the GFDL global climate model.	389
Appendix 4-C. Values of climate suitability variables for each species.	417
Appendix 4-D. Values of calculated competition indices.	421
Appendix 4-E. Predicted probability of occurrence within Alaska Boreal Interior ecoregion.	423

LIST OF TABLES

Table 1-1. Frequency of projected percentage change in abundance across 80 species.....	25
Table 1-2. Projected changes in indices of spatial distribution across 80 species.	25
Table 1-3. Variance components for four sources of variability (+ interactions).....	26
Table 1-4. Sources of prediction uncertainty (coefficient of variation) over time.....	27
Table 2-1. Proportional change in core habitat area.....	49
Table 2-2. Sensitivity of Zonation land rankings.....	50
Table 3-1. Ecosite and vegetation types considered.	85
Table 3-2. Climate, terrain, geology, and wetland variables included in random forest models for ecosite and vegetation.	87
Table 3-3. Confusion matrix for ecosite classification model.	88
Table 3-4. Confusion matrix for vegetation classification model, grouped by fuel type.....	89
Table 3-5. Variance partitioning of projected burn probability.	90
Table 3-6. Variance partitioning of projected upland vegetation cover type.....	91
Table 3-7. Simulated changes in median upland forest stand age within study area.	91
Table 4-1. Range characteristics of 80 boreal study species.....	121
Table 4-2. Mean bioclimatic variable values by time period, boreal ecoregion, and GCM.	124
Table 4-3. Climate and life-history variables included in phylogenetic logistic regression analysis.....	125
Table 4-4. AICc scores for candidate phylogenetic logistic regression models.	127
Table 4-5. Mean logistic regression model coefficients and model diagnostics.....	128
Table 4-6. Numbers of species projected to breed regularly in the Alaska Boreal Interior currently and during future 30-year periods,	129
Table 4-7. Species most likely to move into the Alaska Boreal Interior currently and during future 30-year periods.	130

LIST OF FIGURES

Figure 1-1. Boreal and southern arctic study area.	28
Figure 1-2. Projected change in species richness and density over time.	29
Figure 1-3. Change in the distribution of signal-to-noise ratios (Cohen’s <i>d</i>) over time.	30
Figure 1-4. Magnitude of projected proportional change plotted against magnitude of uncertainty.....	31
Figure 1-5. Uncertainty due to three sources of variation over time.	32
Figure 2-1. Boreal and southern arctic study area.	51
Figure 2-2. Conceptual diagram of assumptions for seral-stage modified refugia approach.	52
Figure 2-3. Distributions of minimum age thresholds for 53 boreal forest species.	53
Figure 2-4. Alternative distribution scenarios for an example species.	55
Figure 2-5. Zonation results (land ranking maps).	57
Figure 2-6. Combined Zonation results (land ranking maps) for three future time periods.	58
Figure 2-7. Sensitivity of Zonation land rankings to habitat age thresholds.	59
Figure 2-8. Proportion of diversity and minimum species distribution conserved.	61
Figure 3-1. Study area and data locations with data source / project funding information.	92
Figure 3-2. Workflow diagram for modelling process.	94
Figure 3-3. Disturbance footprints, study area, and Burn-P3 buffer area.	95
Figure 3-4. Predicted ecosite type (relative soil moisture/nutrient combination).	96
Figure 3-5. Predicted current vegetation type as a function of ecosite, terrain, and climate.	97
Figure 3-6. Mean burn probability for each time period and scenario under the HadCM3 model.	98
Figure 3-7. Projected change in mean annual burn probability by scenario within study area. ..	99
Figure 3-8. Projected climate-driven vegetation potential for current and future time periods.	100
Figure 3-9. Projected change in upland vegetation cover type over time by GCM and scenario.	101
Figure 3-10. Predicted proportional change in conifer, mixedwood, deciduous, and grassland vegetation types for current and three future time periods.	103
Figure 3-11. Projected change in age class distribution for upland forest fuel types.	104
Figure 4-1. North American ecoregions.	132

Figure 4-2. Climatically suitable core habitat for an example species in current and future time periods..... 133

Figure 4-3. Northwestern cordillera mountain ranges that present potential barriers between non-mountain boreal ecoregions in Canada and Alaska. 134

Figure 4-4. Sample phylogeny for the 80 boreal-breeding species analyzed. 135

Figure 4-5. Climatically suitable core habitat in current, mid-Holocene, and LGM periods for two example species. 136

INTRODUCTION

With the rapid rate of warming recently experienced at northern latitudes and the large magnitude of future change projections (IPCC 2013), there is increasing need to understand and anticipate ecological impacts of climate change on northern ecosystems (Price et al. 2013, Gauthier et al. 2015). The boreal forest biome, by virtue of its large size and relative intactness, is thought to provide a large proportion of North America's avian breeding habitat (Blancher 2003), with the large majority of breeding species migrating from Neotropical and subtropical wintering grounds (Erskine 1977). Many boreal bird species have breeding ranges that extend south of the boreal region, and their strong positive temperature associations suggest range expansions in response to climate change are possible (Cumming et al. 2014). Indeed, recent northward breeding bird range expansions have been documented and attributed to climate change in parts of North America (Hitch and Leberg 2007, Zuckerberg et al. 2009), as well as in Great Britain (Thomas and Lennon 1999). However, species that are restricted to boreal and arctic regions may experience range reductions if their ecological niches are pushed northward. Although trailing-edge range contractions are not widely documented—and are likely confounded with land-use change—some cases of avian latitudinal (McClure et al. 2012) and altitudinal (Tingley et al. 2009) range contractions have been attributed to climate change.

Given the paucity of broad-scale, long-term species trend data, species distribution models (SDMs, aka bioclimatic or niche models) are widely used to project future responses to climate change for a variety of taxa (e.g., Iverson and Prasad 1998, Araújo et al. 2004, Thuiller et al. 2005, Lawler et al. 2013), including birds (Peterson et al. 2002, Huntley et al. 2008, Stralberg et al. 2009, Matthews et al. 2011). SDMs are based on the premise that the environmental niche of a species (*vis-à-vis* Grinnell 1917) may be quantified and used to develop spatial predictions of species' distributions under given environmental conditions, including future climates (Guisan and Zimmermann 2000, Peterson 2001). In a climate context, such correlative models depend on several inter-related assumptions (Pearson and Dawson 2004, Araújo and Pearson 2005, Wiens et al. 2009): that species' distributions are controlled by climatic factors (directly or indirectly), that niches are conserved over time (Wiens and Graham 2005), and that species' distributions are at equilibrium with climate.

In general, the notion that climate governs broad-scale avian distribution patterns is well-established (Thomas 2010, Araújo and Peterson 2012). Current climate variables have been found to be strong predictors of avian distributions (Root 1988, Araújo et al. 2009, Jiménez-Valverde et al. 2011, Cumming et al. 2014) and diversity patterns (Rahbek and Graves 2001, Hawkins and Porter 2003). Niche conservatism remains difficult to evaluate (Wiens et al. 2010), but evidence suggests that it is fairly strong for birds (Lovette and Hochachka 2006, Barnagaud et al. 2014). Climatic equilibrium is probably the most tenuous of SDM assumptions, leading many to call for greater mechanistic representation of fundamental physiological relationships (Kearney and Porter 2009), biotic interactions (Gilman et al. 2010), and/or demographic processes (Keith et al. 2008). However, because information on such mechanisms is often lacking or subject to temporal and spatial scale mismatches (Soberón and Nakamura 2009), SDMs remain the most viable option for multi-species projection of climate-change response (Pearson and Dawson 2003, Wiens et al. 2009). Insomuch as all models are a simplification of reality, SDMs provide invaluable insights into climatic suitability patterns, niche shifts, and potential distributional responses. They provide working hypotheses about the future that can be evaluated with further empirical study.

In a climate-change adaptation context, however, SDMs are most useful when assumptions are acknowledged and the resulting limitations are addressed. Thus, each chapter of my thesis focuses on understanding and addressing one of four major limitations of SDMs:

1. Model **uncertainty** in current and future projections
2. **Time lags** in ecosystem responses to climate change
3. The **static** nature of correlative models
4. The influence of **historical biogeography** in determining current distributions

I employed a climate-based SDM approach to model the distribution and abundance of boreal-breeding passerine birds and to project the influence of climate change. Taking advantage of an extensive, high-quality avian dataset compiled by the Boreal Avian Modelling project (borealbirds.ca, Cumming et al. 2010, Barker et al. 2015), and a new data standardization approach for point-count data (Sólymos et al. 2013), I developed bioclimatic models for 80 boreal-breeding passerine species, downscaled global climate model projections for North America, and developed future avian distributional projections for three 30-year periods from 2011-2100. Chapters 1, 2, and 4 are derived directly from these models, while Chapter 3

evaluates decadal-scale change potential in a more mechanistic fashion, focusing on projected vegetation responses to the combined effects of climate, wildfire, and land-use.

In Chapter 1, I described and evaluated SDMs and projections, and then assessed the **uncertainty** surrounding future projections. The objectives were to:

1. Evaluate the signal-to-noise ratio for projected changes in boreal bird abundance over the next century;
2. Compare different sources of uncertainty related to factors extrinsic (global climate model uncertainty) and intrinsic (sampling and variable uncertainty) to SDMs; and
3. Evaluate spatial, temporal, and species-specific variation in each source of prediction uncertainty.

In Chapter 2, I used SDMs for a subset of 53 strictly forest-associated species to identify spatial conservation priorities in consideration of differential anticipated **time lags**. The objectives were to:

1. Classify species by seral-stage affinity, and identify the most likely future distributional trajectory for each species;
2. Generate seral-stage-modified projections of changes in species' core habitat distributions using species distribution models and quantify differences compared to unconstrained projections;
3. Identify multi-species boreal conservation priority areas over the 21st century, and evaluate the sensitivity of land rankings to seral-stage affinity and species' weightings; and
4. Assess the conservation potential of the existing protected areas network relative to the best, equal-area solutions identified for each of three future periods.

In Chapter 3, to overcome the limitations of correlative models based on **static** relationships, I developed a hybrid simulation modelling approach to evaluate the role of natural and anthropogenic disturbance and resulting forest age structures—in concert with local topographic conditions—in determining local vegetation in Alberta. My objectives were to:

1. Assess the combined impacts of wildfire, anthropogenic disturbance, and climate change on upland vegetation composition and age structure over the next century;
2. Project changes in area burned over time and compare disturbance-mediated fuel scenarios with climate-driven and static fuel scenarios; and

3. Compare disturbance-mediated and climate-driven scenarios of change in upland forest vegetation composition and age and quantify the variability that can be attributed to global climate model differences.

Finally, in Chapter 4 I evaluated the role of **historical biogeography**, using paleo-ecological hind-casting to assess the nature of the northwestern cordillera as a barrier to range expansion, and the likelihood that it will break down in the future. My objectives were to:

1. Use logistic phylogenetic regression analysis to analyze the relative importance of life-history characteristics versus post-glaciation climatic factors on the distributions of North American boreal-breeding species west of the northwestern cordillera in the Alaskan boreal region; and
2. Use this information to predict which species are most likely to shift their distributions from Canada into boreal Alaska in the future.

CHAPTER 1. PROJECTING BOREAL BIRD RESPONSES TO CLIMATE CHANGE: THE SIGNAL EXCEEDS THE NOISE

1.0 Summary

For climate-change projections to be useful, the magnitude of change must be understood relative to the magnitude of uncertainty in model predictions. We quantified the signal-to-noise ratio in projected distributional responses of boreal birds to climate change, and compared sources of uncertainty. Boosted regression tree models of abundance were generated for 80 boreal-breeding bird species using a comprehensive dataset of standardized avian point counts (349,629 surveys at 122,202 unique locations) and 4-km climate, land-use and topographic data. For projected changes in abundance, we calculated signal-to-noise ratios, and examined variance components related to choice of global climate model (GCM) and two sources of species distribution model (SDM) uncertainty: sampling error and variable selection. We also evaluated spatial, temporal, and inter-specific variation in these sources of uncertainty. The mean signal-to-noise ratio across species increased over time to 2.87 by the end of the 21st century, with the signal greater than the noise for 88% of species. Across species, climate change represented the largest component (0.44) of variance in projected abundance change. Among sources of uncertainty evaluated, choice of GCM (mean variance component = 0.17) was most important for 66% of species, sampling error (mean = 0.12) for 29% of species, and variable selection (mean = 0.05) for 5% of species. Increasing the number of GCMs from four to 19 had minor effects on these results. The range of projected changes and uncertainty characteristics across species differed markedly, reinforcing the individuality of species' responses to climate change and the challenges of one-size-fits-all approaches to climate change adaptation. We discuss the usefulness of different conservation approaches depending on the strength of the climate change signal relative to the noise, as well as the dominant source of prediction uncertainty.

1.1 Introduction

Based on recent warming trends and global climate model (GCM) projections for the next century, the North American boreal forest is likely to experience particularly large changes in temperature and moisture availability (Balling et al. 1998, IPCC 2001). Climate change within the boreal region has already led to increased drought- and insect-induced tree mortality (Allen et al. 2010, Michaelian et al. 2010, Peng et al. 2011b), wetland drying (Klein et al. 2005), and

wildfire activity (Podur et al. 2002, Gillett et al. 2004, Soja et al. 2007). By virtue of its large size and relative intactness, the boreal forest is thought to provide a large proportion of North America's breeding bird habitat (Wells and Blancher 2011). Therefore, species presently restricted to boreal regions may experience range reductions if those biomes shift northward and decrease in area, as projected for North America (Rehfeldt et al. 2012). However, positive temperature affinities and broad climatic tolerances suggest that many other species could expand their breeding distributions within the boreal region (Cumming et al. 2014). Recent northward range expansions of breeding birds have already been documented and attributed to climate change in temperate North America (Hitch and Leberg 2007), as well as in Europe (Thomas and Lennon 1999, Devictor et al. 2008).

As evidence has mounted for anthropogenic climate change and its widespread effects on species' distributions, it has increasingly been incorporated in systematic conservation planning efforts (e.g., Hannah et al. 2007, Carroll et al. 2010, Shaw et al. 2012). Accordingly, there is growing interest in forecasting the potential ecological impacts of climate change with an understanding of the associated uncertainties. Species distribution models (SDMs) have been widely used to project geographic changes in species' climatic habitat suitability (e.g., Peterson et al. 2002, Thuiller et al. 2005, Huntley et al. 2008). This correlative approach is based on the premise that the environmental niche of a species (*sensu* Grinnell 1917) may be quantified and used to develop spatial predictions of species' distributions under given environmental conditions, including future climates (Guisan and Zimmermann 2000, Peterson 2001). Paleo-ecological analysis of fossil pollen data suggests that, in the absence of climate conditions with no current analog, substitution of space for time is generally valid (Prentice et al. 1991, Huntley et al. 1993, Roberts and Hamann 2012), although differences in short-term predictability across taxa and ecological traits do exist (Kharouba et al. 2009, Dobrowski et al. 2011, Eskildsen et al. 2013). Passerine birds are not well-represented in the fossil record, but molecular analyses are consistent with avian tracking of changes in climate and vegetation throughout Pleistocene glaciation cycles (Mengel 1964, Weir and Schluter 2004, Lovette 2005). Current climate has been found to be an important predictor of continental-scale avian distributions (Araújo et al. 2009, Jiménez-Valverde et al. 2011, Cumming et al. 2014), although not without skepticism (Bahn et al. 2006, Beale et al. 2008). Species' realized niches are also limited by biotic interactions (Hutchinson 1957), but empirical (Lovette and Hochachka 2006, Rubidge et al.

2011) and theoretical (Soberón 2007, Siegel et al. 2014) evidence suggests that interactions that cannot be defined climatically are mostly local-scale processes that have minimal influence on broad-scale distribution patterns (Rehfeldt et al. 2012).

Assuming that climatic niches of species are conserved over time (Wiens et al. 2010) and equilibrium with climate is maintained (Araújo and Pearson 2005), projecting species' long-term distributional responses to climate change will be problematic when uncertainty overpowers the prediction signal. Uncertainty surrounding future climate change trajectories (Murphy et al. 2004) combined with high variability among the SDMs themselves (Elith et al. 2006), has raised concerns about the utility and reliability of future projections. This has led to the development of ensemble forecasting approaches that use multiple models (Araújo and New 2007, Dormann et al. 2008b) as well as efforts to quantify and compare different aspects of prediction uncertainty. Although several studies have partitioned the variance in SDM-based future projections (Dormann et al. 2008a, Buisson et al. 2009, Diniz-Filho et al. 2009, Mbogga et al. 2010, Garcia et al. 2012), few have evaluated uncertainty with respect to the magnitude of predicted change (but see Thuiller 2004). High prediction error may be outweighed by large directional changes in distribution and abundance. Thus, species-specific estimates of uncertainty (“noise”) vs. change magnitude (the “signal”) are needed over space and time.

A primary source of noise in future projections is the extrinsic variation among GCMs (hereafter “GCM uncertainty”). Although different GCMs are mostly based on the same physical principles (Jun et al. 2008, Masson and Knutti 2011, Pennell and Reichler 2011), the projections they produce can be quite variable (Murphy et al. 2004, Kingston et al. 2009). Some GCMs are clearly better than others (Wang et al. 2007, Scherrer 2011), but metrics for model evaluation are not straightforward, and prediction patterns among GCMs can vary spatially as well as temporally (Tebaldi et al. 2005, Kang and Cressie 2013). Thus, the influence of GCM variability on SDM predictions depends not only on which model is considered, but also the variables, seasons, and geographic areas that are important for a given species.

Given the large variation among GCM projections, it is notable that intrinsic variation among SDM algorithms has often been found to be even larger (Dormann et al. 2008a, Buisson et al. 2009, Diniz-Filho et al. 2009, Garcia et al. 2012; but see Mbogga et al. 2010). However, high SDM variability may be driven by many factors, including the use of lower-performance algorithms (Elith et al. 2006, Hijmans and Graham 2006), sparse or inconsistent data (Araújo et

al. 2005, Dormann et al. 2008a), poor or inconsistent model-building strategies (Meynard et al. 2013), extrapolation outside the range of data (Elith and Graham 2009), and improper handling of spatial dependence. Some of these sources of error can be manipulated or controlled to reduce prediction uncertainty. In particular, by reducing model variability due to spatial dependence, inappropriate extrapolation, and model specification, one can focus on evaluating two fundamental sources of SDM-based (intrinsic) uncertainty: predictor variable selection and sampling error.

Predictor variable or model selection (hereafter “variable uncertainty”) may have a large influence on SDM predictions (Mbogga et al. 2010, Synes and Osborne 2011, Braunisch et al. 2013), especially when important correlated variables decouple in the future. For example, many species’ distributions are limited by the extent of agricultural land use (e.g., Siriwardena et al. 2000) or by the distribution of wetlands (e.g., Calmé and Desrochers 2000) more than climate. Agriculture is constrained by current climate, particularly in northern environments, and the effects of climate and land use on bird distributions can be hard to disentangle (Clavero et al. 2011). However, land use will not necessarily track climate in the future, such that present confounding of climate and land use could lead to errors in future projections. Northern wetland distribution is also correlated with climate at continental extents, due to the propensity for excess moisture to persist in colder environments. Despite reports of rapid boreal wetland drying attributed to recent climate change (e.g., Klein et al. 2005), loss of wetlands may take longer depending on size and local hydrology, providing another mechanism by which presently-correlated variables could become decoupled.

Sampling error (hereafter “sampling uncertainty”) results from various elements of epistemic uncertainty (“uncertainty associated with knowledge of the state of a system”; Regan et al. 2005), including measurement error, sampling bias, and inherent variability in the abundance of organisms across space and time (Elith et al. 2002). This type of uncertainty is often reflected in the differences among SDM algorithms that produce a wide range of individual model specifications. Multi-model predictions based on a diverse assortment of SDM techniques can therefore produce more robust predictions than single models (Thuiller et al. 2009). However, ensemble methods based on a single type of model (e.g., boosted regression trees) have similar strengths (Lawler et al. 2006), and bootstrapping methods may be used to estimate sampling error.

Here, we used an extensive boreal bird dataset for North America (Cumming et al. 2010) to evaluate the signal-to-noise ratio for projected changes in boreal bird abundance over the next century. We also compared different sources of uncertainty related to factors extrinsic (GCM uncertainty) and intrinsic (sampling and variable uncertainty) to SDMs. We evaluated spatial, temporal, and species-specific variation in each source of prediction uncertainty.

1.2 Methods

1.2.1 Study area and avian survey data

We developed climate-change projections for boreal and southern arctic level II ecological regions as delineated by the Commission for Environmental Cooperation (CEC 1997). This included all subunits within the Taiga, Hudson Plain, and Northern Forests ecological regions, as well as the southern subunits of the Tundra ecological region (Alaska Tundra, Brooks Range Tundra, Southern Arctic), and boreal portion of the Northwestern Forested Mountains ecological region (Boreal Cordillera) (Figure 1-1). We used data from avian point-count surveys (Ralph et al. 1995) that were conducted from 1992–2010 within the Nearctic boreal region (Brandt 2009), as compiled by the Boreal Avian Modelling (BAM) project (Cumming et al. 2010). This included primarily off-road data from numerous inventory, monitoring, research, and impact assessment projects, including Provincial Breeding Bird Atlases and the Alaska Landbird Monitoring Survey, but also roadside point-count surveys conducted as part of the North American Breeding Bird Survey (BBS; Sauer et al. 2011). To account for anticipated shifts of southern climate conditions into currently boreal regions, we included point-count data from the same period collected in ecoregions within the continental U.S. and southern Canada that are south of the current boreal region, with climate conditions that are projected to shift northwards into the study area within the next 100 years (Rehfeldt et al. 2012). This primarily consisted of BBS data, but also included off-road data from the western Great Lakes region (Hanowski and Niemi 1995).

Our initial compilation included data from 128 distinct projects with a total of 356,018 surveys at 125,547 unique locations (Figure 1-1). To reduce the confounding influence of anthropogenic disturbance on modelled climate relationships, we removed surveys that had been conducted at agricultural, urban, or barren sites, according to the CEC's North American Land Change Monitoring System (NALCMS) landcover dataset. We also removed surveys known to be conducted after recent timber harvest or other anthropogenic disturbance activities (not

including fire), as mapped by Global Forest Watch Canada, the Alberta Biodiversity Monitoring Institute, and the United States LANDFIRE program. 349,629 surveys at 122,202 unique locations remained.

1.2.2 *Climate data*

Interpolated climate data were generated based on the parameter-elevation regressions on independent slopes model (PRISM) for the 1961-1990 normal period (Daly et al. 2008) and bioclimatic variables were derived according to Wang *et al.* (2012) and Hamann *et al.* (2013). Climate variables were chosen based on several criteria including relevance to vegetation distributions (Hogg and Bernier 2005), avoidance of extreme collinearity (Dormann et al. 2013), and a preference for seasonal over annual variables when they showed high correlations. The final set of variables included extreme minimum temperature (EMT), chilling degree days (DD01), growing degree days (DD51), seasonal temperature difference (TD), mean summer precipitation (MSP), climate moisture index (CMI), and summer climate moisture index (CMIJJA). See [Appendix 1-A](#), Table A1 for complete variable definitions.

To represent potential future climates for three consecutive 30-year periods (2011–2040, 2041–2070, and 2071–2100), we used projections from the CMIP3 multi-model dataset, corresponding to the fourth IPCC assessment report (Meehl et al. 2007). To limit computation time, we selected a subset of four complementary GCMs that spanned a range of projected growing season temperatures and precipitation levels within our study area: the German MPI ECHAM5, the Canadian CCCMA CGCM3.1, the United States GFDL CM2.1, and the United Kingdom Met Office HadGEM1 ([Appendix 1-A](#), Table A2 and Figure A1). Model projections were added as anomalies to the 4-km resolution 1961-1990 baseline data using the delta method and bi-linear interpolation according to Wang *et al.* (2012). The data used in this study is part of a more comprehensive dataset for North America, described in [Appendix 1-A](#) and available as [Supplement 1](#). For this analysis, we adopted a scenario of high and monotonically increasing emissions (SRES A2, IPCC 2001), reflecting actual emissions during the decade elapsed since the scenario was defined (Raupach et al. 2007). Nineteen GCMs had runs available under the A2 emissions scenario.

The most highly correlated climate variables within our model-building dataset (averaged across bootstrap samples, as described in the next section) were EMT and DD01 ($r = -0.88$), followed by MSP and CMIJJA ($r = -0.80$) ([Appendix 1-B](#), Table B1). Within the boreal and

subarctic study area, the most highly correlated variables were CMI and CMIJJA ($r = 0.91$) and CMI and MSP ($r = 0.87$). Averaging across all 19 GCMs available for scenario A2, we found limited future decoupling (decrease in correlation over time) within the set of climate variables used, although there were differences between the model-building dataset and prediction datasets ([Appendix 1-B](#), Figure B1). EMT, DD01, and TD were the variables among which study area-wide correlations changed the most over time and were the most different from correlations within the model-building dataset.

1.2.3 Land-use and topography data

For a second set of models, we included a set of key land-use/landcover variables that may influence bird abundance. We used the 250-m NALCMS landcover dataset to calculate the current proportions of agriculture (AGRICULT), urban development (URBAN), open water (WATER), and wetlands (WETLAND) within each 4-km grid cell. We also derived a compound topographic index (CTI; Gessler et al. 1995)—or wetness index—from a 4-km digital elevation model and used it as a surrogate for wetland areas. The CTI was intended to differentiate lowland vs. upland vegetation types, in order to constrain future projections accordingly. These variables were not highly correlated with the seven climate indices or with each other ([Appendix 1-B](#), Table B1), and only minor future decoupling was observed.

We did not include proportions of natural upland landcover types, given the strong climatic basis for vegetation distribution at this resolution (Hamann and Wang 2006, McKenney et al. 2007a). Limitation of data quality and coverage prevented adequate modelling and prediction of these remotely-sensed landcover types relative to climate at such a broad scale.

1.2.4 Density models

We made use of the abundance information contained in point-count data by using survey- and species-specific correction factors, as described in Sólymos et al. (2013), to standardize density estimates across diverse protocols and environmental conditions. We examined 80 boreal-breeding passerine species with mapped breeding ranges (Ridgely et al. 2005) covering at least 10% of the boreal region (P. Blancher, unpublished data), as defined by Partners in Flight bird conservation regions 4, 6, 7, and 8 (Rich et al. 2004), which coincide with the boreal portion of our study area ([Figure 1-1](#)). Each species also had surveys conducted with multiple time and/or distance intervals—general requirements for fitting the distance sampling

(Buckland et al. 2001) and removal models (Sólymos et al. 2013) used to generate the correction factors.

We used boosted regression trees (BRT; De'ath 2007, Elith et al. 2008) to model avian densities at the level of the individual point-count station. We used the ‘dismo’ (Hijmans et al. 2011), ‘gbm’ (Ridgeway 2012) and ‘raster’ (Hijmans and van Etten 2012) packages for R (R Core Team 2012) to build BRT models for each species and then generate spatial predictions. We used the raw survey count at a point-count location as the response variable and included the log-transformed correction factors derived by Sólymos et al. (2013) as offsets to model avian density (males per ha). For these count data we specified a Poisson generalized boosted model (GBM) in the BRT estimation. The Poisson GBM uses an exponential function of the linear predictor within a gradient boosting algorithm (Friedman 2001, Ridgeway 2012).

We defined sampling units as the combination of the site (route, plot, or other local grouping of point counts) and 4-km grid cell ($n = 39,186$ total sampling units) and, from each sampling unit with > 10 surveys, we randomly selected a single point-count survey in each bootstrap iteration. This was to minimize spatial autocorrelation in surveys among points at the same site and temporal autocorrelation among surveys at the same point. We accounted for additional spatial autocorrelation among nearby sampling units by weighting the selection probabilities of each sampling unit by the inverse of the total number of surveys within the 20-km x 20-km area surrounding the sampling unit. We minimized the influence of single data points by randomly selecting only $1/3$ of the sampling units with ≤ 10 surveys in each bootstrap replicate. This procedure resulted in a total of 18,299 sampling units for each bootstrap replicate.

For each BRT model, we used a stepwise procedure and 10-fold cross-validation to identify the optimal number of trees needed to maximize the mean deviance explained. In each model run, we used a tree complexity of 3, learning rate of 0.001, and a bag fraction of 0.5. To ensure that the optimal number of trees could be found (Elith et al. 2008), we increased the learning rate to 0.005 if the limit of 10,000 trees was achieved, and reduced it to 0.0001 if fewer than 1,000 trees were obtained. Using the optimal number of trees, we calculated 10-fold cross-validation statistics (proportion of deviance explained and Pearson’s correlation coefficient) to assess prediction accuracy. For each species, we compared these statistics between the two variable sets (climate-only and climate + land use + topography) using paired t-tests ($n = 11$ bootstrap replicates). Significance values were adjusted for multiple comparisons using a Holm

(1979) correction. The importance of each model covariate was assessed by averaging the proportion of total deviance explained by a particular variable over all 11 bootstrap replicates.

1.2.5 Abundance projections

For each of the 80 species we applied the fitted BRT models to current and future climate conditions to predict avian density in each 4-km grid cell in the boreal / southern arctic study area. We multiplied the predicted density estimates for each grid cell (males/ha as an estimate of breeding pair density) by the grid-cell area (1600 ha), and summed these values across grid cells to estimate total potential abundance.

We evaluated two sets of covariates: climate-only and climate + land use + topography. We generated models for 11 bootstrap samples, which were identical across species and covariate sets. We evaluated fitted BRTs under projected climates of alternate GCMs for three future time periods (2011–2040, 2041–2070, 2071–2100).

For each species we produced a total of 22 models from 11 bootstrap replicates and two variable sets for the 1961–1990 baseline period. We then produced a balanced set of future projections (264 total) for each species. This included predictions for all combinations of 11 bootstrap replicates, two variable sets, four GCMs, and three future time periods, for a total of 286 predictions for each species. To better assess the full range of variability across GCMs, we also generated an additional set of projections across the remaining 15 GCMs using just one bootstrap replicate, two variable sets and three future time periods. This resulted in an additional 90 predictions, for a grand total of 376, including projections for the 1961-1990 baseline period.

1.2.6 Quantifying prediction uncertainty

To evaluate the overall signal-to-noise ratio for the projected change in overall abundance, we calculated Cohen's d —defined as the difference between means divided by the pooled standard deviation (Cohen 1992)—for each species and each future time period compared to the baseline period, with variances pooled across the two time periods of interest for each calculation. For each time period, d was calculated for the full-factorial combination of 11 bootstrap replicates, two variable sets, and four GCMs ($n = 88$).

Next, to compare the climate-change effect size to the variance components attributable to each source of uncertainty, we conducted two analyses of variance (ANOVA) for each species. Using projected change in overall abundance as the dependent variable, we first conducted four-factor ANOVAs with balanced data using just the four complementary GCMs (n

= 264; 11 bootstrap replicates x 2 variable sets x 4 GCMs x 3 future time periods). We partitioned the sums of squares among the effects of time period (climate-change effect), sampling uncertainty, variable uncertainty, and GCM uncertainty, as well as the interactions between GCM and time, and variable and time. Variance components for each of these factors were calculated as the partial sum-of-squares divided by the total sum-of-squares (aka η^2). To evaluate the additional uncertainty introduced by considering the full suite of available GCMs (an additional 15 models), we also conducted an unbalanced ANOVAs using type II sums of squares (Langsrud 2003) ($n = 354$; 264 original + 90 additional) with the ‘car’ (Fox and Weisberg 2011) package for R. For comparison across species, proportional abundance change was plotted against total uncertainty (sum of variance components for all uncertainty sources, including residuals).

Finally, to evaluate the relative magnitudes of each uncertainty source with respect to abundance projections, we calculated several versions of the coefficient of variation (CV)—i.e., the standard deviation divided by the mean. For each species and time period we calculated the CV in overall abundance for each source of uncertainty: sampling, variable, and GCM (future time periods only). Calculations were based on the full factorial set of predictions (four complementary GCMs), and CV values for each uncertainty source were calculated with predictions for the other sources of uncertainty held constant at their average values. To evaluate spatial patterns of uncertainty for each species, using the same method, we also calculated the CV in density (males/ha) at the 4-km grid-cell-level for each source of uncertainty in each time period.

1.3 Results

1.3.1 Model evaluation

All confidence ranges represent 5th and 95th percentiles except when otherwise noted. Across 80 species, prediction success of climate-only BRT models, assessed via cross-validation, averaged 0.222 (0.069, 0.462) in the deviance explained, and 0.225 (0.071, 0.474) in the Pearson correlation coefficient ([Appendix 1-C](#), Table C1). On average across species, the addition of land-use and topographic variables to the climate-only models did not markedly improve cross-validation correlation (difference = 0.003 ± 0.014 SD) or deviance explained (difference = 0.002 ± 0.011 SD). However, for 18 of 80 species the climate-only models were significantly improved by adding the land-use and topography variables, in terms of one or both diagnostics after

multiple comparison correction. The climate-only model was significantly better for only one species.

Across species, temperature variables explained on average 0.145 (0.038, 0.330) of total deviance and moisture variables explained 0.074 (0.017, 0.156) in climate-only models ([Appendix 1-C](#), Table C2). With models that also included land use and topographic variables, 0.040 (0.002, 0.114) of the deviance explained was accounted for by these additional variables, primarily agricultural land-use proportion and compound topographic index ([Appendix 1-C](#), Table C3). Based on visual inspection of variable response curves from all 11 bootstrap runs, a total of 32 species exhibited clear monotonic decreases in abundance in response to agricultural land use proportion across bootstrap iterations; 7 species had a clear negative response to urban land use proportion.

1.3.2 Projected changes in potential abundance

Of the 80 species modelled, 30 were projected to decline in potential abundance across the boreal and southern arctic regions by 2040; 34 species by 2070; and 37 species by 2100 ([Appendix 1-D](#), Table D1). Considering all sources of prediction uncertainty, projected declines were unequivocal (i.e., confidence intervals around projected change values did not contain zero) for 15 species by 2040, 18 by 2070, and 30 by 2100. Projected increases were unequivocal for 35 out of 50 species by 2040, 37 out of 46 by 2070, and 35 out of 43 by 2100. The distribution of projected species' responses shifted negatively and became increasingly dispersed over time, reflecting larger magnitudes of increase and decrease in abundance ([Table 1-1](#)).

Most species exhibited a northward and upslope (towards higher elevations) distributional shift in response to climate change ([Appendix 1-D](#), Figure D1). Species' range centroids shifted an average of 18 m upward in elevation, 3 degrees north in latitude, and 3 degrees west in longitude by the end of the century ([Table 1-2](#)). Although areas of high boreal-species richness were projected to shift northward in distribution, total potential abundance across all species was projected to decline within the study area. Decreases in boreal species richness and density over time were most apparent in the interior west ([Figure 1-2](#)). Projected current and future density layers (mean and CV across all sources of uncertainty) are available to view and download at <http://borealbirds.databasin.org/>.

1.3.3 Prediction uncertainty relative to change

On average across 80 species, the signal-to-noise ratio, as measured by Cohen's d , was greater than 1 (i.e., signal > noise) for all three future time periods (Figure 1-3). For the 2011-2040 time period, mean d was 1.42 (0.11, 3.49), and greater than 1 for 46 species (Appendix 1-D, Table D2). For the 2041-2070 time period, mean d increased to 2.38 (0.31, 5.32), and was greater than 1 for 59 species. By 2071-2100, mean d was 2.87 (0.73, 5.33), and was greater than 1 for 70 species.

Results from the balanced ANOVA indicated that the greatest source of variability in abundance predictions across species was attributed to the effect of climate change over time, with mean variance component = 0.442 (0.134, 0.760) (Table 1-3). When 19 GCMs were considered in an unbalanced ANOVA, the mean variance component of climate change decreased slightly to 0.397 (0.098, 0.725) (Table 1-3). For 21 species, sampling error represented the largest source of uncertainty (mean variance component = 0.118 across all 80 species) (Table 1-3; Appendix 1-D, Table D2). For 13 of these species, sampling uncertainty was greater than the climate-change effect. For 53 species, GCM represented the largest source of uncertainty (mean variance component = 0.174). However, it was only greater than the climate-change effect for 10 species. When all 19 GCMs were considered, the mean variance component of GCM uncertainty increased to 0.228, compensating for a decrease in time- and sampling-related components. Variable selection resulted in a large variance component (up to 0.745) for a few species, but it was the greatest source of uncertainty for only four species (mean variance component = 0.047).

By definition, prediction uncertainty—calculated as the sum of all variance components except climate change from the balanced ANOVA—was negatively related to the magnitude of projected change in total abundance (Figure 1-4), but a wide range of response magnitudes was seen along the range of prediction uncertainty. Prediction uncertainty was generally low relative to the projected magnitude of change for species with large projected increases. Species with the highest overall prediction uncertainty were evenly split between those with high sampling uncertainty and those with high GCM uncertainty.

1.3.4 Spatial and temporal uncertainty

The magnitude and relative importance of the three components of prediction uncertainty changed over time (Table 1-4). Averaging across all 80 species, sampling error was the greatest

source of uncertainty in current predictions of potential population size (as measured by CV) but uncertainty decreased over time, from an average of 0.129 (0.036, 0.390) in the current period to 0.099 (0.032, 0.228) by the end of the century. Variable-related uncertainty exhibited the opposite trend, increasing in importance over time from 0.058 (0.009, 0.163) to 0.115 (0.007, 0.347), as did uncertainty across the four GCMs, which more than doubled in magnitude from 0.092 (0.028, 0.161) in the 2011-2040 period to 0.216 (0.054, 0.505) in the 2071-2100 period (Table 1-4). When 19 GCMs were considered, the CV attributed to this component further increased to 0.266 (0.086, 0.630) by the end of the century.

Spatial patterns of uncertainty in the density predictions varied widely across species (Appendix 1-D, Figure D2), but for the current period it was concentrated in northern portions of the study area, where data are sparser (Figure 1-5). Over time, areas of high sampling uncertainty were greatly reduced, as northern areas were projected to warm and thus more closely resemble the current climates of well-sampled boreal regions (Figure 1-5a). By the end of the century, the small remaining areas of high variable uncertainty were concentrated in the western interior boreal region (Figure 1-5b). Uncertainty based on four complementary GCMs increased over time, eventually overshadowing the other two sources of uncertainty in most of the study area (Figure 1-5c), with pockets of high GCM uncertainty concentrated in the northwest.

1.4 Discussion

1.4.1 *Signal versus noise in projections of abundance*

For projections of species' responses to future climate change to be useful, the magnitude of a species' projected response needs to be understood relative to the magnitude of uncertainty (Thuiller 2004). We found that for 58% of 80 boreal songbird species over the next 30 years—increasing to 88% of species by the end of the century—the climate-change “signal” in projections of abundance was greater than the “noise” generated by uncertainty due a combination of sampling error, variable selection, and choice of global climate model (GCM). Despite the future increase in GCM uncertainty over time, this variability was swamped by the increasing magnitude of the projected directional change—positive or negative—in species abundance. This suggests that the predicted trajectories of avian responses to future climates are relatively robust for informing conservation planning and resource management decisions under climate change. Although the strength of a projected warming signal compared to GCM “noise” has been demonstrated (Kang and Cressie 2013), we found that the additional uncertainties

introduced by the species modelling process—specifically, sampling error and variable selection—generally did not overwhelm the climate change signal. This result appears consistent with Thuiller (2004), who found a majority (56%) consensus among different combinations of GCMs and SDMs for mid-century species turnover projections in European plant communities.

1.4.2 Uncertainty due to GCM projections

By the end of the century, the largest source of prediction uncertainty across species was the choice of GCM, indicating that multiple complementary GCMs should be used to capture the range of alternative futures. Direct comparison with other variance partitioning studies (Dormann et al. 2008a, Buisson et al. 2009, Diniz-Filho et al. 2009, Mbogga et al. 2010, Garcia et al. 2012) is complicated by differences in taxa, geographic regions, data resolution, and specific GCMs and time periods. However, our high-end estimate of 23% of variation due to GCM was comparable to the other study in this group (Garcia et al. 2012) that considered a full suite of available GCMs (17 vs. 19 in our study). The relatively small (6%) increase in variance from 4 to 19 GCMs reflects the high redundancy among these models (Masson and Knutti 2011) and suggests that a well-selected subset can appropriately reflect climate model uncertainty. Furthermore, GCMs are not of equal accuracy (Scherrer 2011), so the use of poorly-performing GCMs may be counterproductive (Räisänen 2007). Despite the large amount of uncertainty contributed by choice of GCM, we identified just 10 species for which the GCM-related uncertainty was consistently greater than the overall climate-change effect (up to 21 when all 19 GCMs were considered). For these primarily deciduous-forest-associated species, e.g., Mourning Warbler (*Geothlypis Philadelphia*) and Canada Warbler (*Cardellina canadensis*), future abundance trajectories were often non-linear, and diverged substantially over time, with larger projected decreases associated with the drier GCMs ([Appendix 1-D](#), Figure D3). Areas of high GCM uncertainty were primarily located in the western interior boreal region, where available moisture is generally low, and small fluctuations in moisture may lead to major vegetation differences such as grassland vs. forest, or conifer vs. deciduous tree species (Hogg 1994, Schneider et al. 2009, Mbogga et al. 2010).

1.4.3 Uncertainty due to sampling error

Sampling error in the data used to build the model explained approximately 10% of the variance on average, but much more for approximately a dozen species. The species with highest sampling error were generally less well-represented in our dataset, mostly due to their high-

latitude affinities but also likely due to low densities—e.g., Rusty Blackbird (*Euphagus carolinus*) and American Pipit (*Anthus rubescens*). This reflects the obvious fact that SDM accuracy may be reduced when limited occurrence data are available (Stockwell 2002), especially when using more complex methods such as boosted regression trees (Wisz et al. 2008). For this small subset of species with sparse data, current models could likely be improved by targeted surveys, especially in climatically under-represented northern regions. However, despite large error bounds, most of these species were projected to decrease in abundance over time, with high signal-to-noise ratios. As such, their models are still informative, especially from the standpoint of identifying species most vulnerable to climate change. For almost all species examined, the sampling uncertainty decreased over time, as poorly sampled climates to the north were replaced by better-sampled climates to the south, i.e., eastern deciduous forest and interior grassland biomes. The relative lack of projected novel climate emergence (Williams et al. 2007) within our large study area (Rehfeldt et al. 2012) makes sampling uncertainty a much smaller problem than might otherwise be the case (e.g., Stralberg et al. 2009, Zurell et al. 2012). However, the regions with highest future sampling-related prediction uncertainty (mostly in Alaska) did tend to correspond with projected non-analog climates according to Rehfeldt et al. (2012), suggesting that signal-to-noise ratios may be much lower in regions that experience major novel climate development. These high-uncertainty regions may also be related to the partial decoupling of minimum annual temperature from temperature seasonality and growing season heat sums ([Appendix 1-B](#)).

1.4.4 Uncertainty due to predictor variables

Variable uncertainty was a minor component of the variability in future projections for all but a handful of the species we evaluated. This likely reflected the low overall correlation between climate and land-use variables in our dataset, as well as the relatively strong predictive power of climate, compared to land use and topography, at a 4-km resolution. However, this source of uncertainty was important for a few species, primarily those with strong agricultural land-use relationships such as Clay-colored Sparrow (*Spizella pallida*, positive) and Blue-headed Vireo (*Vireo solitaries*, negative). This suggests that, when variable relationships are strong, minimal broad-scale decoupling is sufficient for local variations in projections to arise. When climate and land use are confounded, the effects of climate on species' distributions may be overestimated, thereby misleading both the climate-change projections (Clavero et al. 2011) and

the conservation decisions based upon them. Consequently, there is a need for observational datasets that span a range of land-use and climate conditions. This requirement is not always satisfied by roadside data from the North American Breeding Bird Survey (McKenney et al. 2001, BBS; Sauer et al. 2011), which comprise the primary distributional data available for climate-change projection purposes in North America (e.g., Matthews et al. 2011, Distler et al. 2015). In the boreal region in particular, roads and therefore BBS routes are simultaneously biased toward southern climates and agriculturally-dominated landscapes (NABCI Canada 2012). Our extensive dataset, which included data from more remote parts of the boreal region, markedly reduced this bias.

Although the inclusion of land-use and topography variables did not strongly influence range-wide predictions for most species, it was sometimes quite important locally. By the end of the century, variable uncertainty was concentrated in the southern portions of the boreal region, where the potential to support agricultural land uses in the future is greatest due to projected transition to prairie ecosystems (Frelich and Reich 2009). Unfortunately, boreal-wide spatially-explicit projections of agricultural expansion generally do not exist, except for coarse (0.5° grid cell resolution) global projections that do not indicate any noticeable projected land-use conversion for the region (Jetz et al. 2007, Hof et al. 2011, Meehl et al. 2014). Other modelling efforts have focused on climatic suitability and plant hardiness zones (McKenney et al. 2001), which can be considered equivalent to our climate-only model and used to infer change (i.e., agricultural land uses shift with climate). However, projections that include socio-economic and other policy drivers (e.g., Bierwagen et al. 2010, Radeloff et al. 2011) would be necessary to adequately project local responses to the combined effects of climate and land-use change.

1.4.5 Other potential sources of uncertainty

It is rarely possible to evaluate and quantify all potential sources of uncertainty, some of which stem from vagueness of terms (Regan et al. 2005). For example, our models were intended to predict potential breeding-bird abundance based on climatic suitability. Actual bird numbers will depend on multiple demographic factors—e.g., over-winter survival and dispersal—that are not easily incorporated into a distribution modelling approach (but see Keith et al. 2008, Zurell et al. 2009, Fordham et al. 2013). Even within the more tangible sources of ‘epistemic’ (known) uncertainty (Regan et al. 2005), we could not evaluate every potential contributor. Given the strong climatic basis for vegetation distribution at this resolution (Hamann and Wang 2006,

McKenney et al. 2007a), we assumed that avian responses to climate change would be driven by climate's direct effects on vegetation, and we did not attempt to disentangle these effects. Thus the accuracy of short-term projections may be compromised when vegetation is in disequilibrium with climate (Svenning and Sandel 2013). However, because our intent was to evaluate trajectories of potential change rather than projected conditions for specific time periods, the specific years were less important than the climate conditions they represent.

Furthermore, our evaluation of variable uncertainty was limited to a subset of climate and land-use variables among which future decoupling was limited and localized. There may be other correlated but unmeasured climate variables—e.g., inter-annual variability (Cumming et al. 2014)—that also decouple in the future, leading to additional prediction uncertainty. However, we were limited to existing GCM projections that do not yet adequately model changes to inter-annual climate variability (Mehta et al. 2010). More dramatically, inadequate representation of major positive feedbacks such as changes in albedo due to snow/ice (Screen and Simmonds 2010) and cloud cover (Fasullo and Trenberth 2012) may also mean a substantial underestimation of climate sensitivity among current GCMs (Hansen et al. 2013). Consideration of more extreme scenarios could overwhelm the signal with noise, but we have focused here on generally accepted projections based on the so-called “fast feedbacks” (Rohling et al. 2012) for which short-term responses are better understood. Our results must be interpreted within these boundaries.

1.4.6 Conservation and management implications

A striking aspect of our results is the wide range of projected changes and uncertainty characteristics exhibited across species. Without quantitative analysis, we found some consistent and anticipated patterns among the species modelled. Species with the most northerly distributions often had high sampling uncertainty, due to sparse data, but also had large projected declines, leading to high signal-to-noise ratios that increased over time. Southern grassland-associated species were all projected to increase, but a combination of high variable uncertainty (due to positive associations with agriculture) and high GCM uncertainty led to low signal-to-noise ratios among this group. Deciduous forest-associated species tended to have high GCM uncertainty given the potential for rapid broad-scale conversion of deciduous and mixed forest to grassland, depending on “tipping points” in available moisture (Price et al. 2013). Although less common species generally had high sampling uncertainty, the signal-to-noise ratio for these

species could easily be much higher than for common, high abundance species with little projected response to climate change. Variability among species responses to climate change may be attributed to a variety of traits, the importance of which are not well-understood (Kharouba et al. 2013). For birds, larger ranges are generally associated with lower model accuracy (Stockwell 2002, McPherson et al. 2004, Segurado and Araújo 2004, McPherson and Jetz 2007). Other factors such as migratory behavior, trophic level / feeding guild, habitat specialization, and habitat association (especially wetland affinity) have been found important, but not consistently across regions and taxonomic subsets (Brotons et al. 2004, Huntley et al. 2004, Hernandez et al. 2006, McPherson and Jetz 2007). Further analysis is needed to better explain inter-specific variation in climate-change response, uncertainty, and signal-to-noise ratio.

However, this reinforces the individuality of species' responses to climate change (Williams and Jackson 2007, Stralberg et al. 2009), and highlights the challenges of adopting one-size-fits-all approaches to climate change adaptation. Where feasible, land-based approaches that maintain natural disturbance dynamics (Noss 2001, Leroux et al. 2007) and facilitate broad-scale distributional shifts, e.g. along gradients (Halpin 1997, Noss 2001, Hodgson et al. 2009), may prove most effective in maintaining species diversity without requiring certainty about long-term outcomes. Such approaches are particularly viable in northern regions that are still relatively intact, such as the North American boreal forest.

However, individual species management is warranted for species of high conservation concern. Several studies have demonstrated the long-term inadequacy of relying solely on current environmental conditions to conserve and manage future species populations (Araújo et al. 2004, Veloz et al. 2013). Nevertheless, different conservation approaches may be justified depending on the strength of the climate change signal relative to the noise. When prediction uncertainty is high, there is greater risk associated with focusing on areas of predicted future climatic suitability (Fuller et al. 2008, Carroll et al. 2010, Carvalho et al. 2011). In these cases, a greater emphasis on areas of predicted overlap between current and future climatic distributions, i.e., macrorefugia (Keppel et al. 2012) may be appropriate. Conversely, justification is greater for an emphasis on future climate space when prediction uncertainty is low compared to the magnitude of change (Oliver et al. 2012, Hamann and Aitken 2013). The range of uncertainty exhibited across species also suggests a need for differential and quantitative weighting in assessments of climate-change vulnerability (e.g., Gardali et al. 2012).

The dominant source of prediction uncertainty is also an important consideration in evaluating conservation and research strategies. For some species, especially those that are sensitive to changes in moisture balance, different GCMs result in distinctly different future trajectories. These species may be most effectively managed in an adaptive framework that considers the likelihood of alternative climate futures, updated as new information becomes available about GCM accuracy and reliability. Long-term monitoring at stationary locations will be a critical component of adaptive management efforts (Nielsen et al. 2009). For species with high sampling or variable uncertainty, the choice of GCM is less important within the already large range of future trajectories. In such cases, short-term efforts may be well spent by improving models through additional targeted sampling, e.g., in our case, in under-represented northern regions, and in agricultural landscapes within marginal climates, respectively. It will also be important to study potential climate-change effects on agricultural land uses (David and Marshall 2008), so that they may be factored into conservation decisions.

Finally, of immediate conservation concern within the boreal region is the rapid rate of industrial development, including forestry, energy, and other resource extraction, which could dramatically alter forest habitat over coming decades (Schneider et al. 2003, Hauer et al. 2010). Landscape-level effects of anthropogenic disturbance on avian communities (Schmiegelow et al. 1997, Drapeau et al. 2000, Hobson and Bayne 2000), and avian vegetation type/age-class relationships (Hobson and Schieck 1999, Schieck and Song 2006) have been identified regionally, and could be quantified across larger spatial extents with the development of comprehensive, standardized vegetation (e.g., Beaudoin et al. 2014, Cumming et al. 2015) and anthropogenic disturbance (e.g., Pasher et al. 2013) datasets. With a better understanding of future development and vegetation trajectories, more temporally and spatially refined avian projections can also be generated. In the meantime, we suggest that bioclimatic models, when constructed carefully with accompanying uncertainty estimates, can provide useful projections for a majority of passerine species and should be interpreted in the context of associated uncertainties to inform conservation and management decisions.

1.5 Appendices

[On-line at *Ecological Applications*](#):

[Supplement 1](#). Current and projected climate data for North America.

[Appendix 1-A](#). Global climate model summary and downscaling methods

[Appendix 1-B](#). Covariate correlations

[Appendix 1-C](#). Individual species model evaluation

[Appendix 1-D](#). Individual species climate-change projections

[Appendix 1-E](#). R code for boosted regression tree models and predictions

1.6 Tables

Table 1-1. Frequency of projected percentage change in abundance across 80 species.

Mean change values for each species are based on 11 bootstrap iterations, two variable sets, and four GCMs. See [Appendix 1-D](#), Table D1 for individual species projections.

	>50% decrease	25-50% decrease	25% decrease to 25% increase	25-50% increase	50-100% increase	>100% increase
2011-2040	0	7	50	18	4	1
2041-2070	2	10	33	7	16	10
2071-2100	10	16	17	6	10	21

Table 1-2. Projected changes in indices of spatial distribution across 80 species.

Values represent means (5th and 95th percentiles). Species-level values are based on 11 bootstrap iterations, two variable sets, and four GCMs.

	Mean latitude (deg N)	Mean longitude (deg W)	Mean elevation (m)
Current	56.2 (49.9, 63.3)	-98.7 (-115.7, -86.4)	473.2 (371.6, 686.8)
2011-2040	57.2 (50.3, 63.2)	-99.9 (-116.0, -88.0)	477.7 (375.1, 698.1)
2041-2070	58.0 (50.9, 64.1)	-100.8 (-116.3, -88.4)	481.4 (378.8, 674.5)
2071-2100	59.2 (52.4, 64.9)	-101.7 (-114.2, -89.3)	490.9 (387.5, 642.5)

Table 1-3. Variance components for four sources of variability (+ interactions).

Variance in projected abundance change summarized across 80 boreal- and arctic-breeding species, based on an analysis of variance with 3 future time periods (climate change effect), 2 variable sets, 11 bootstrap sampling iterations, (a) four complementary GCMs and (b) all 19 GCMs available for the A2 emissions scenario (IPCC AR4). # Largest = number of species for which that source of uncertainty was greatest; # >Time = number of species for which that source of uncertainty was greater than the time effect. See [Appendix 1-D](#), Table D2 for species-specific results.

#					GCM	Variable		
GCMs	Statistic	Time	Sampling	Variable	GCM	x Time	x Time	Remaining
a. 4	Mean	0.442	0.118	0.047	0.174	0.107	0.017	0.095
	2 SD	0.404	0.298	0.190	0.224	0.154	0.050	0.172
	5%	0.134	0.005	0.028	0.000	0.018	0.000	0.014
	95%	0.760	0.424	0.388	0.146	0.260	0.066	0.246
	# Largest	N/A	21	4	53	1	0	1
	# > Time	N/A	13	3	10	6	0	9
b. 19	Mean	0.397	0.090	0.045	0.228	0.134	0.016	0.090
	2 SD	0.417	0.261	0.187	0.250	0.172	0.047	0.188
	5%	0.098	0.004	0.076	0.000	0.039	0.000	0.011
	95%	0.725	0.327	0.457	0.146	0.327	0.061	0.216
	# Largest	N/A	10	4	58	8	0	0
	# > Time	N/A	13	3	21	14	0	11

Table 1-4. Sources of prediction uncertainty (coefficient of variation) over time.

Coefficient of variation averaged across 80 boreal- and arctic-breeding species. Confidence intervals represent 5th and 95th percentiles. Sampling uncertainty is due to variation across 11 bootstrap samples; model uncertainty is due to variation between climate-only and climate + land use + topography models; GCM uncertainty is due to variation across (a) 4 complementary GCMs and (b) all 19 GCMs available for the A2 emissions scenario (IPCC AR4).

Time period	Sampling	Variable	GCM-4	GCM-19
1961-1990	0.129 (0.036, 0.390)	0.058 (0.009, 0.163)	N/A	N/A
2011-2040	0.110 (0.028, 0.305)	0.051 (0.010, 0.136)	0.092 (0.028, 0.161)	0.131 (0.034, 0.276)
2041-2070	0.097 (0.027, 0.247)	0.072 (0.002, 0.230)	0.146 (0.041, 0.344)	0.184 (0.065, 0.385)
2071-2100	0.099 (0.032, 0.228)	0.115 (0.007, 0.347)	0.216 (0.054, 0.505)	0.266 (0.086, 0.630)

1.7 Figures

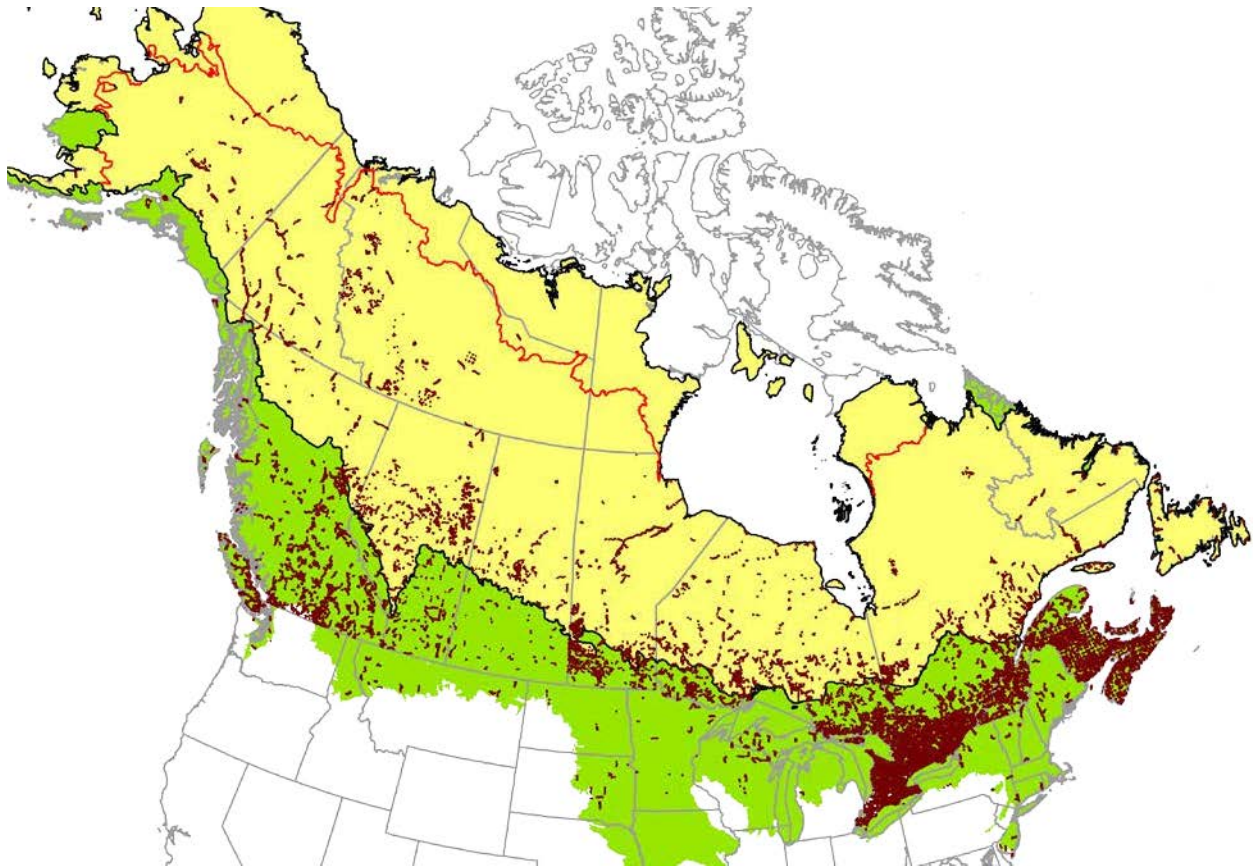


Figure 1-1. Boreal and southern arctic study area.

Study area is shown in yellow with boreal/arctic boundary in red. Additional ecoregions projected to move into the study area by 2100 are depicted in light green. Point-count locations sampled for modelling are shown in dark red.

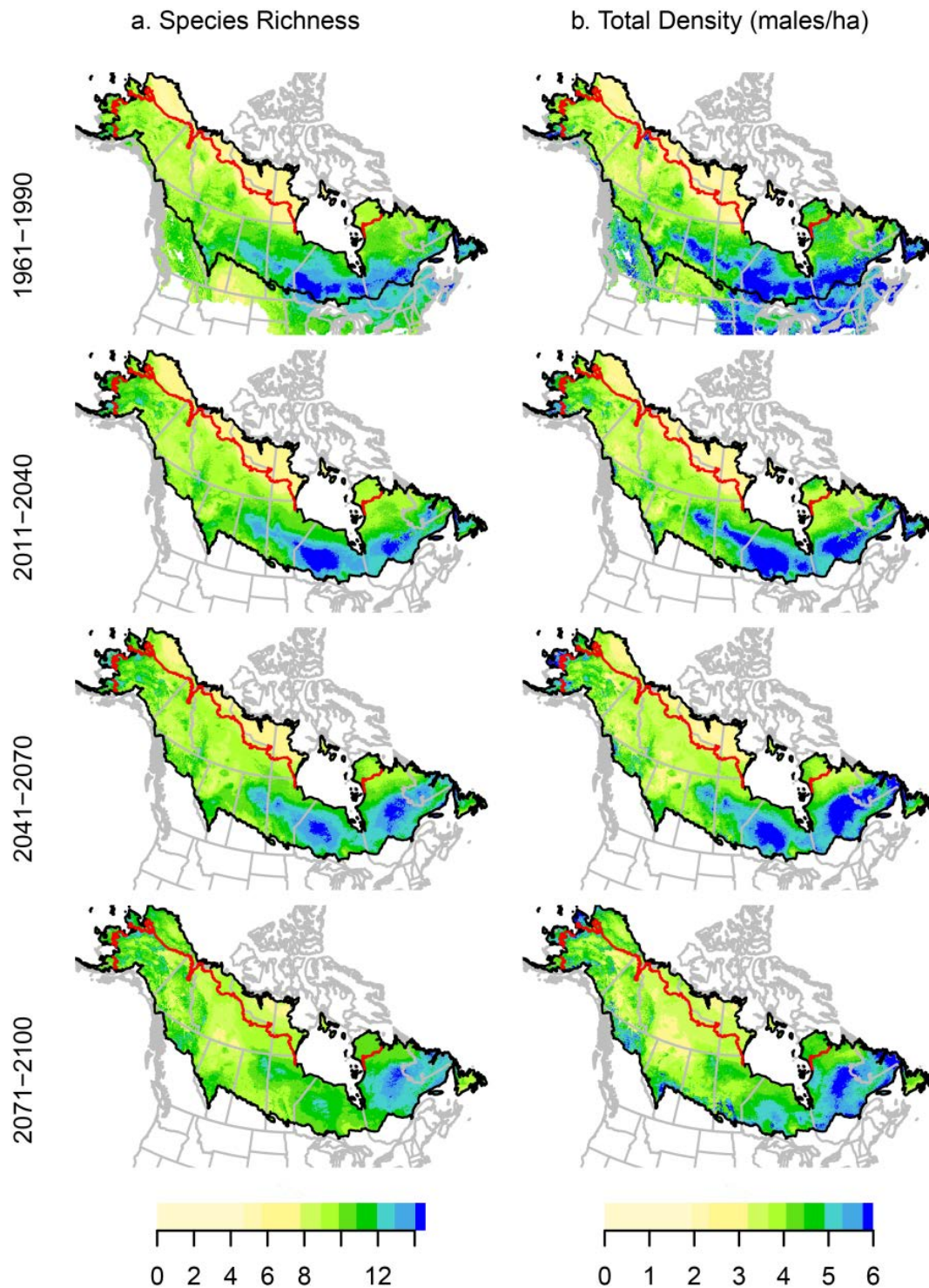


Figure 1-2. Projected change in species richness and density over time.

(a) Boreal breeding bird species richness and (b) Total density (males/ha). Species richness within each 4-km grid cell was calculated by converting density to probability of occurrence and summing probabilities across 80 species. Boreal/arctic boundary shown in red.

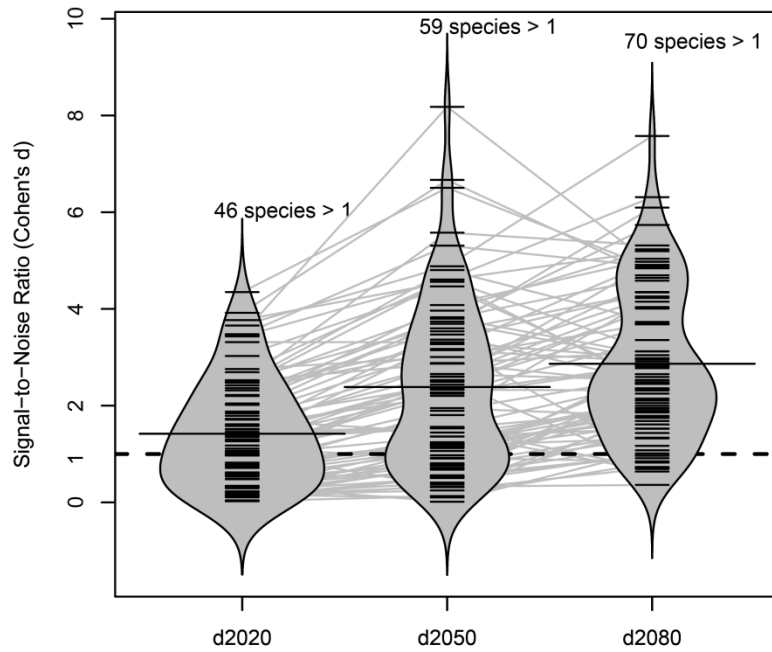


Figure 1-3. Change in the distribution of signal-to-noise ratios (Cohen's d) over time. The violin plots show the shapes of the distribution for each time period, with wider regions representing more common d values. Gray lines link each of 80 species through the different time periods. The dashed line represents $d=1$; above this line, the climate-change signal is greater than the noise due to the sources of uncertainty examined. Solid lines represent mean d values for each time period.

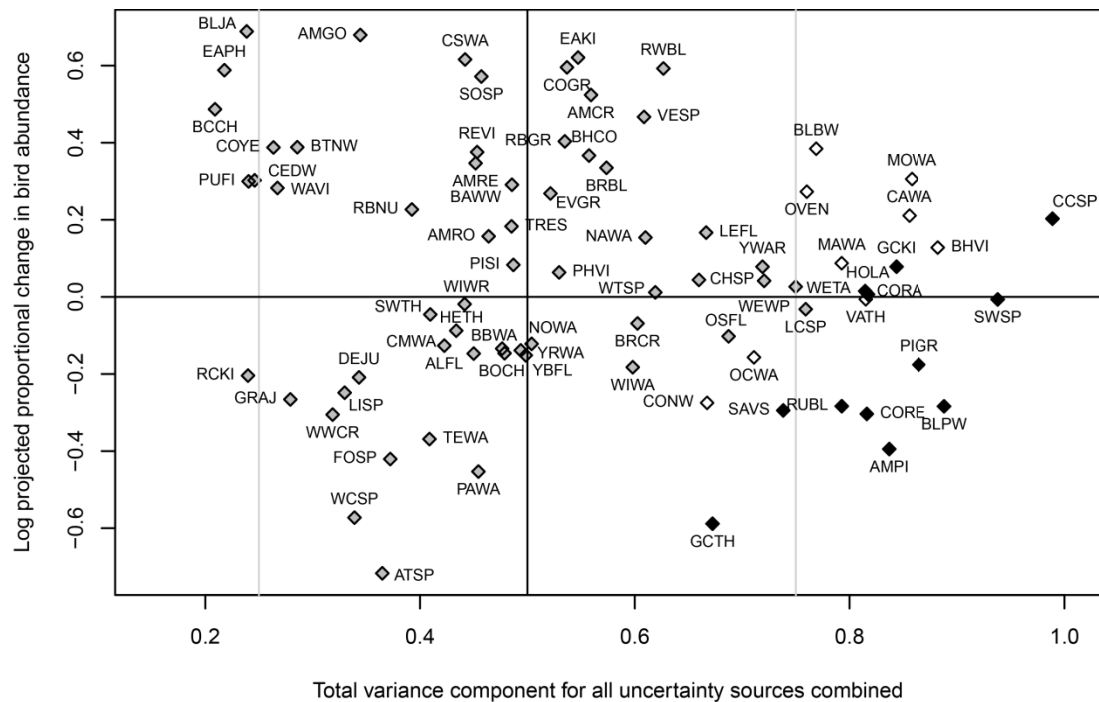


Figure 1-4. Magnitude of projected proportional change plotted against magnitude of uncertainty.

Relationships by the end of the century (2071-2100) for 80 boreal species based on four complementary GCMs. See [Appendix 1-C](#), Table C1 for species code definitions. Gray = climate change effect is greatest source of variability; white = GCM is greatest source of variability; black = sampling or variable selection (CCSP only) is greatest source of variability. The x-axis represents the sum of all variance components except the climate-change effect. The y-axis represents the log-transformed projected proportional change + 1 ($y = 0$ indicates no change).

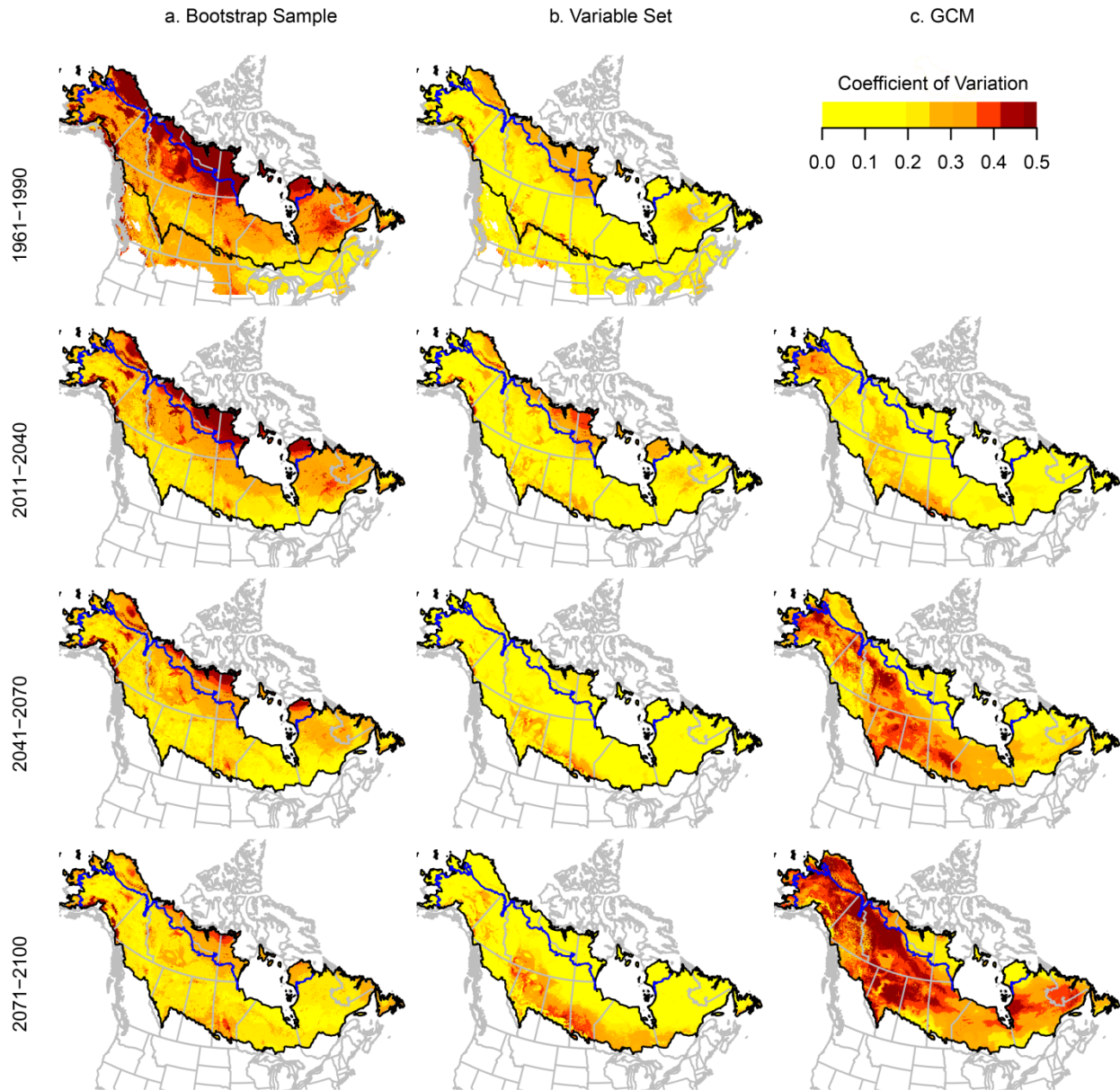


Figure 1-5. Uncertainty due to three sources of variation over time.

Spatial and temporal representations of the coefficient of variation in projected abundance at the 4-km grid-cell level across multiple sources of uncertainty, averaged over 80 boreal breeding bird species. (a) sampling uncertainty due to variation across 11 bootstrap samples; (b) variable uncertainty due to variation between climate-only and climate + land use + topography models; (c) and GCM uncertainty due to variation across four complementary GCMs.

CHAPTER 2. CONSERVATION OF FUTURE BOREAL FOREST BIRD COMMUNITIES CONSIDERING LAGS IN VEGETATION RESPONSE TO CLIMATE CHANGE: A MODIFIED REFUGIA APPROACH

2.0 Summary

Species and ecosystems may be unable to keep pace with rapid climate change projected for the 21st century. We evaluated an underexplored dimension of the mismatch between climate and biota: limitations to forest growth and succession affecting habitat suitability. Our objective was to inform continental-scale conservation for boreal songbirds under disequilibria between climate, vegetation, and fauna. We used forest inventory and avian survey data to classify 53 species by seral-stage affinity, and applied these to generate alternative projections of changes in species' core habitat distributions based on different vegetation lag-time assumptions. We used our seral-stage-modified refugia approach and the Zonation algorithm to identify multi-species boreal conservation priorities over the 21st century. We evaluated the sensitivity of land rankings to seral-stage affinity and species' weights, and assessed the conservation value of the existing protected areas network compared to Zonation results.

End-of-century projected changes in songbird distribution were reduced by up to 169% when vegetation lags were considered. Zonation land rankings based on unconstrained climate projections were concentrated at high latitudes, whereas those based on strict and modified refugia scenarios were concentrated in coastal and high elevation areas, as well as biome transition zones, which were fairly consistent over time and species weights. The existing protected areas network covering 14% of the study area was estimated to conserve 12-14% of baseline avian biodiversity across time periods and scenarios, compared to 16-25% for top-ranked Zonation areas.

2.1 Introduction

The global climate is expected to undergo profound changes during the 21st century (IPCC 2013). Over long periods, ecological communities should generally track these changes, as occurred throughout most of the Holocene (Prentice et al. 1991, Huntley et al. 1993). However, in the short term, disequilibria between climate and biota will arise because of lags in biological response (Svenning and Sandel 2013, Wu et al. 2015). Dispersal limitation, for example, may prevent organisms from relocating to suitable habitat in pace with climate change,

and much effort has been invested to quantify and incorporate species-specific dispersal rates into distributional change projections (e.g., Iverson et al. 2004, Barbet-Massin et al. 2012, Schloss et al. 2012). However, for mobile organisms like migratory songbirds, lags in vegetation responses to climate change are likely more limiting than dispersal rates, given that many songbirds exhibit strong associations with certain forest types and seral stages (Hobson and Schieck 1999, Schieck and Song 2006), somewhat independent of climatic conditions.

In boreal systems, variation in forest type along climatic gradients is typically characterized more by differences in the physical structure and composition of plant communities than by latitudinal or elevational range limits of the constituent species. For example, the boreal forest region of North America is dominated by a few broadly-distributed tree species within the genera *Picea*, *Abies*, *Pinus*, *Populus*, *Betula*, and *Larix* (Lenihan 1993, McKenney et al. 2007b). Given the widespread distributions of these species, the potential for boreal forest vegetation to keep pace with climate change in the short term is likely to be more limited by local plant growth and regeneration processes than by dispersal (Price et al. 2013). In general, warmer temperatures should result in increased drought-induced tree mortality where moisture becomes limiting (Allen et al. 2010, Zhang et al. 2015), an increase in primary productivity where it does not (Burton and Cumming 1995, Friend et al. 2014), and a disturbance-mediated competitive shift from shade-tolerant species such as white spruce, *Picea glauca*, and balsam fir, *Abies balsamifera*, to early-successional, more drought-tolerant species such as trembling aspen, *Populus tremuloides*. Understanding the future of avian distributions in the boreal biome therefore requires consideration of what changes in forest structure are likely to occur, and at what rate.

Within the next century, soil moisture deficits are projected along the southern forest–prairie ecotone in western Canada (Price et al. 2011, Price et al. 2013), where increased tree mortality may cause relatively rapid conversion of forest to grassland or open woodland (Hogg and Hurdle 1995, Schneider et al. 2009). Drought-induced increases in fire and insect outbreaks may hasten these transitions (Hogg and Bernier 2005). Along the northern forest–tundra ecotone, forests are projected to expand into areas currently dominated by shrub and herbaceous tundra vegetation (Rehfeldt et al. 2012), and such expansion has already been documented (Scott et al. 1987, Danby and Hik 2007). Less predictable are future vegetation trajectories within the core of the boreal region (Chapin et al. 2004, Scheffer et al. 2012). There, warmer temperatures and

increased disturbance frequencies could result in a shift from conifer-dominated to deciduous-dominated stands (Soja et al. 2007, Johnstone et al. 2010), although local topo-edaphic conditions may limit these tendencies. Nevertheless, one point appears fairly certain: the mean age of boreal forest stands should decrease as natural disturbance events such as fire increase in frequency (Flannigan et al. 2005, Boulanger et al. 2014), and timber harvest and other industrial development activities continue (Lee et al. 2006, Cyr et al. 2009, Hauer et al. 2010).

Generalist and early-seral bird species may keep pace with climatically-driven changes in forest vegetation, assuming a continued high rate of natural disturbance, as is characteristic of the Canadian boreal region (Parisien et al. 2011a). In contrast, bird species that are associated closely with late seral-stage forest may be at increased risk from climate change, as they are unlikely to take advantage of newly-suitable climates beyond their current range before suitable forest habitat there reaches an appropriate age. Late-seral species are particularly dependent on *in situ* climate refugia: areas of relatively greater projected habitat stability in spite of climate change (Ashcroft 2010, Keppel et al. 2012). At a broad continental scale, this also includes younger forest within so-called ‘macrorefugia’, aka ‘classical refugia’, which can provide future suitable habitat over large areas and which are identified on an individual species basis from relatively coarse-resolution climate projections (Ashcroft 2010). Addressing species-specific time lags in habitat suitability provides a temporal complement to the concept of climate velocity (Loarie et al. 2009, Hamann et al. 2014), which determines the distance that an organism must move to keep pace with climate change (Sandel et al. 2011).

Conservation planning in the face of climate change must therefore consider both protection of the most climatically stable baseline habitats for species that cannot shift quickly, and the availability of newly suitable habitats for those that can. The relative importance of old and new habitats will change as baseline habitats become increasingly unsuitable climatically and forest dynamics create new habitat in climatically-suitable areas. This balance should also be informed (i.e., weighted) by differences among species in climate-change vulnerability and uncertainty of responses (Stralberg et al. 2015b). Significant biological turnover is projected within Canadian protected areas by the end of the century, with approximately half of current national parks expected to occupy the climate space of a different biome (Scott et al. 2002). Thus, the existing protected areas network, which is generally considered inadequate to protect current boreal biodiversity (Andrew et al. 2014), will need to be amended in a manner that

efficiently and strategically maximizes biodiversity protection in a changing climate (Badiou et al. 2013).

Recent advances in systematic conservation planning (Margules and Pressey 2000) have incorporated projected future climate conditions into land prioritization frameworks, with various approaches proposed to address the dynamic nature of climate change and its uncertainty (e.g., Kujala et al. 2013, Loyola et al. 2013, Watson et al. 2013). Other studies have considered dispersal limitations to impose realistic constraints on future distributions (e.g., Carroll et al. 2010, Carvalho et al. 2011, Summers et al. 2012). We build on these advances to address an underexplored dimension of the potential future mismatch between climate and biota: limitations to forest growth and succession affecting habitat suitability. Our objective was to inform continental-scale conservation for boreal songbirds under anticipated disequilibria between climate, vegetation, and fauna, expanding on the macrorefugia concept (Ashcroft 2010). We focused on identifying boreal-wide conservation priorities for songbird species that account for differences in seral-stage preferences and likely trajectories of distributional change over the next century. Such priorities can be incorporated into planning for protected areas large enough to be self-sustaining under local disturbance regimes (Leroux et al. 2007, Schmiegelow et al. 2014). This modified refugia approach thus has the potential to integrate the dynamics of climate change, natural disturbance and vegetation succession in large-scale conservation planning.

We used forest inventory and avian survey data to classify species by seral-stage affinity, and identified the most likely future distributional trajectory for each species. We then generated seral-stage-modified projections of changes in species' core habitat distributions using species distribution models and quantified the differences compared to unconstrained projections. We applied the Zonation hierarchical prioritization algorithm and conservation planning software (Moilanen 2007) to identify multi-species boreal conservation priority areas over the 21st century, and evaluated the sensitivity of land rankings to seral-stage affinity and species' weightings. Finally, we assessed the conservation potential of the existing protected areas network relative to the best, equal-area solutions identified for each of three future periods.

2.2 Methods

Our 7.45 million km² study area (Figure 2-1) consisted of the boreal and southern arctic level II ecological regions mapped by the Commission for Environmental Cooperation (CEC 1997). The area is characterized by a strongly continental climate, but with maritime influences

toward the coasts. Geologically, the region includes the boreal shield, a flat to undulating expanse of granite and gneiss spanning the Canadian portion of the study area; the boreal plain, an area of deep marine sediments south of the shield in western Canada; and the mountainous boreal cordillera, ranging from western Canada into Alaska (United States). Soil moisture deficits are common in the western boreal region, where fire is the predominant natural disturbance. The region east of $\sim 95^\circ$ W longitude, in comparison, is characterised by greater annual precipitation, little or no soil-moisture deficit, and a much greater importance of insect defoliators as a natural disturbance. Both regions exhibit distinct vegetation gradients, with the ratio of coniferous to deciduous trees generally increasing northward and upward in elevation. In the west, aspen parkland is ecotonal between mid-continental grasslands and closed-canopy forests, which then grade into open lichen woodlands and, finally, tundra. Upland forests are composed primarily of *Populus tremuloides* and *Picea glauca* in various mixtures, with the former dominating on warm, exposed, and disturbed sites, and the latter dominating on cold, sheltered, and late-successional sites; extensive forested wetlands are also found, where sparse black spruce (*P. mariana*) and/or larch (*Larix laricina*) dominate on cold, poor wetland soils. Forests on the western boreal shield are composed mostly of black spruce and pine (*Pinus banksiana* in the east and *P. contorta* in the west). On the eastern shield, southern temperate hardwood forests grade into assemblages of fir (*Abies balsamea*) and birch (*Betula* spp.), followed by black spruce forest, open lichen woodlands, and tundra.

2.2.1 Avian Density Models and Future Projections

We used data from avian point-count surveys (Ralph et al. 1995) conducted within the study area and adjacent hemiboreal ecoregions (Figure 2-1) between 1992 and 2010, as compiled by the Boreal Avian Modelling project (BAM; Cumming et al. 2010). After removing surveys known to be affected by anthropogenic disturbance, 349,629 surveys at 122,202 unique locations remained for analysis (Stralberg et al. 2015b)

Species density models were developed using baseline climate data derived from monthly climate normals of temperature and precipitation averaged over the 1961–1990 period (Wang et al. 2012). The data were based on a 1-km digital elevation model, but sub-sampled at 4-km vertical and horizontal intervals. This preserves the full range of climate values, and captures elevational gradients, temperature inversions, and rain shadows in mountainous landscapes. Climate variables used were extreme minimum temperature, chilling degree days, growing

degree days, seasonal temperature difference, mean summer precipitation, climate moisture index, and summer climate moisture index. Future climate projections were downscaled from the Coupled Model Intercomparison Project Phase 3 multi-model dataset (Meehl et al. 2007), and are available as a data supplement to Stralberg *et al.* (2015b). Current land-use/landcover variables (assumed static over time) consisted of current proportions of agriculture, urban development, open water, and wetlands within each 4-km grid cell, according to the CEC's North American Land Change Monitoring System 2005 landcover dataset. To better represent large wetland areas, we also included a 4-km compound topographic index (CTI; Gessler et al. 1995).

Using these variables, we developed models for 53 forest-associated passerine species with breeding ranges (Ridgely et al. 2005) covering at least 10% of the boreal region ([Appendix 2-A](#)). We standardized relative abundance data to estimates of absolute density using location-, survey- and species-specific correction factors (Sólymos et al. 2013). We used boosted regression trees (De'ath 2007) to model avian densities at the point-count level. To reduce spatial autocorrelation, one point was randomly selected from each of 18,299 sampling units (4-km grid cell intersected with survey transect/site) for each bootstrap sample. For each species, we produced a total of 22 density models from a combination of 11 bootstrap samples and two variable sets (climate-only and climate + topography and land use) for the 1961–1990 baseline period. Modelling methods are detailed in Stralberg et al. (2015b).

From these, we produced a set of 264 future projections for each species (88 per time period) based on the A2 emissions scenario (IPCC 2001), four global climate models (GCM; German MPI ECHAM5, Canadian CCCMA CGCM3.1, United States GFDL CM2.1, and United Kingdom Met Office HadGEM1), and three future time periods: 2011–2040, 2041–2070, and 2071–2100. GCMs were selected to represent a complementary range of future climate scenarios. See Stralberg et al. (2015b) for details.

Finally, core habitat for a given species, time period, and model was defined as the grid cells where the model-predicted density exceeded the mean baseline (1961-1990) predicted density for that species within the model-building area (see [Figure 2-1](#)). For each species and time period, we mapped the proportion of the 88 (22 x 4) combinations of species density models and GCMs for which grid cells were classified as core habitat, reflecting sampling and variable-selection variability.

2.2.2 Seral-stage associations and time lags

Most boreal bird species are not unique to a particular seral stage, although density (Schieck and Song 2006, Mahon et al. 2014), and presumably, fitness (Hannah et al. 2008, Haché et al. 2013) differ markedly with age. We used standardized forest inventory data (Figure 2-1) intersected with bird data to estimate a minimum suitable forest age for each species (methods described in Appendix 2-B). To avoid overstating the habitat potential of young forest for old-forest specialists, especially given attribute errors inherent in large composite datasets (McInerney and Purves 2011), we did not calculate absolute forest-age thresholds. Rather, we identified a forest age value (y) for each species corresponding to a common percentile value (x), for which $100 - x\%$ of overall abundance was predicted to occur in forests of age y and older. For x in our core analysis we used the 15th percentile, bracketed by the 5th and 25th percentiles as a sensitivity analysis.

2.2.3 Modified future distributional trajectories

We evaluated future species' distributions under three alternative scenarios:

- A. Unconstrained: bird species' distributions track climate with no time lags for forest habitat development;
- B. Strict refugia: species cannot shift distributions within the 90-year time frame evaluated;
- C. Modified refugia: species track climate with lags of 0, 30, 60, or 90 years, depending on the minimum forest age (y) corresponding to the 15th percentile of their predicted density distribution.

Unconstrained projections (scenario A) were based directly on density model projections for future periods, calculated as the proportion of core habitat across 88 model projections. Strict refugia (scenario B) for each future time period were calculated as the overlap between baseline and future core areas, calculated separately for each model and then combined as a proportion across models. The modified refugia projections (scenario C) were calculated similarly to the strict refugia, except that baseline core areas were replaced with appropriate future core areas in the presence of corresponding time lags, as determined by the minimum forest age threshold for that species (Figure 2-2). For example, for 2041-2070, a species with a 30-year lag would be assumed to occupy the intersection of its projected 2011-2040 and 2041-2070 core areas. For 2071-2100, the same species would be assumed to occupy the intersection of its projected 2041-2070 and 2071-2100 core areas. A species with a 60-year lag would occupy the intersection of its

projected 2011-2040 and 2071-2100 core areas, while a species with a 90-year lag would occupy only the strict refugia (overlap between baseline and 2071-2100 core areas). For comparison purposes, as an expansion of scenario C, we generated distributional projections for all combinations of species and lag periods (30/60/90 years), not just those determined by the minimum forest age threshold.

2.2.4 Conservation priorities

We used Zonation (Moilanen 2007) to rank 4-km grid cells within the study area according to their bird conservation value in the baseline period and the three future 30-year time periods. We used Zonation’s core-area option to maximize the joint representation of all 53 species in the top-ranked cells. For each time period, we obtained solutions for each of the three scenarios. We compared results based on the 15th percentile minimum forest age threshold with those based on 5th and 25th percentile thresholds.

For the 15th percentile threshold, we also compared Zonation solutions obtained for all species weighted equally with those based on an *a priori* weighting factor reflecting risk, defined as the mean ($n = 88$) of 1 – proportional change in species abundance, truncated at 0 and 2. Values close to 2 indicated a species with very high proportional decline on average, while values close to 0 indicated species with large increases. For scenario A, weights were based on mean climate-projected changes in core habitat. For scenario B, weights were based on mean climate-projected changes in refugia, therefore always greater than 1. For scenario C, weights were based on mean climate-projected changes in core habitat, adjusted for seral-stage preferences, so they were intermediate between scenarios A and B.

2.2.5 Evaluation of protected areas and conservation priorities

To assess the adequacy of current protected areas (CEC 2010) vs. Zonation-identified priority areas for all 53 species under climate change, we used two metrics:

1. Zonation’s weighted range-size corrected richness index (WRSCR), a measure of species richness adjusted for baseline distribution size:

$$\text{WRSCR} = \sum_{i,j} w_j q_{ij}$$

where w_j is the weight of species j and q_{ij} is the fraction of the distribution of the species in grid cell i (Moilanen et al. 2012)

2. The minimum proportion of a species predicted/projected range contained within a given area, i.e., “the situation of the worst-off species” (Moilanen et al. 2012):

$$MP = \min_j \sum_i q_{ij}$$

We calculated and compared the sum of WRSCR and MP for the protected areas and for equivalent areas of Zonation solutions in each time period and under each equal-species-weighting scenario (i.e., $w_i = 1$). At 4-km resolution, 14% of the study area is currently protected. Therefore, we used Zonation’s top-ranked 14% of the study area for comparison purposes. Evaluation of other priority thresholds did not yield sufficient additional information to merit inclusion; i.e., species accumulation was close to linear for equal-weighting scenarios.

2.3 Results

2.3.1 *Habitat age associations and projected distributional shifts*

Of the 53 boreal forest species evaluated, 79% (42 species) demonstrated time lags greater than 15 years in their use of forests after disturbance; the remaining 11 species were categorized as early-seral-associated ([Appendix 2-A](#)). Twenty-three species had minimum forest age thresholds ranging from 16-45 years (30-year lag); seventeen species had minimum age thresholds from 46-75 years (60-year lag); and two species were almost entirely found in forest 75 years and older (90-year lag) ([Appendix 2-A](#)). These classifications were found to be largely consistent with findings of Schieck and Song (2006).

Lag-time classifications shifted substantially with changes in minimum age thresholds ([Figure 2-3](#)). With a lower threshold (5th percentile), 75% of species (40/53) were considered early-seral, and only one species was assigned a 60-year lag time. With a higher threshold (25th percentile), only 9% of species (5/53) were considered early-seral, 21% of species (11/53) were assigned a 30-year time lag, and 62% (33/53) were assigned a 60-year lag. These alternate classifications were less consistent with Schieck and Song (2006) than those based on the 15th percentile threshold.

Projected changes in core areas over the century averaged +40% for scenario A (unconstrained), -61% for scenario B (strict refugia), and -22% for scenario C (modified refugia) based on the 15th percentile threshold ([Table 2-1](#)). For scenario C, projected changes ranged from +131% to -92% ([Appendix 2-A](#)). The majority of species (37/53) were projected to experience

decreases in core habitat area under scenario C, compared with 24 decreasing species under scenario A, and 53 decreasing species under scenario B ([Appendix 2-A](#)).

Species associated with older forest were most sensitive to the differences among the three scenarios ([Appendix 2-A](#), [Appendix 2-C](#)). For example, Bay-breasted Warbler (*Setophaga castanea*), exhibited a 79% decrease in its projected end-of-century distribution when the lag of 60 years was taken into account (

Figure 2-4). By end-of-century, divergences among scenarios ranged from 0% for several species to 169% for Blackburnian Warbler (*Setophaga fusca*), which went from a projected 156% increase to a projected 13% decrease ([Appendix 2-A](#)). The largest differences were generally found in species that were projected to increase based solely on climate, but had projected decreases when vegetation time lags were considered.

2.3.2 Conservation priorities

Results of a Zonation core-area prioritization analysis with all 53 species weighted equally indicated rapid change in the top-ranked grid cells (i.e., conservation priorities) over time under scenario A, where no time lag was considered ([Figure 2-5a](#)). End-of-century priorities were heavily focused on high latitudes. Priority regions based on strict (Scenario B, [Figure 2-5b](#)) or modified (Scenario C, [Figure 2-5c](#)) refugia were less variable through time and included fewer areas in the far north. For both lag-adjusted scenarios, end-of-century priority areas appeared less compactly configured than those for the baseline period, and were distributed throughout the boreal region, with an emphasis on coastal and high elevation areas, as well as the boreal-taiga and taiga-tundra transition zones. For scenario C (modified refugia), conservation priorities across multiple time periods had substantial overlap ([Figure 2-6](#)). The top 10% of boreal bird habitat in the baseline plus three future time periods could be conserved with 27.9% of the land area; the top 20% would require 47.8%, and the top 30% would cover 63.8% of the study area. These combined solutions were slightly more efficient (by 2-3-5% respectively) than solutions based on unconstrained projections, and less efficient (by 3-4-4% respectively) than those based on strict refugia assumptions.

Decreasing the minimum forest age threshold from the 15th to the 5th percentile strongly affected Zonation land rankings, with rankings from the latter closely resembling those for the unconstrained scenario ([Figure 2-7a-b](#), [Table 2-2](#)). Increasing the minimum forest age threshold from the 15th to the 25th percentile had only minor effects on Zonation land rankings ([Figure 2-7c](#), [Table 2-2](#)), although the strict refugia scenario resulted in relatively large differences, with a much greater emphasis on current centres of diversity in southern regions ([Figure 2-7d](#), [Table 2-2](#)).

When species were weighted according to magnitude of projected distributional change, end-of-century conservation priorities changed somewhat for the unconstrained scenario ([Table](#)

2-2). However, future conservation priorities under strict and modified refugia scenarios were not noticeably affected by species weights.

For all scenarios and time periods, the top-ranked 14% of areas according to Zonation conserved 16-25% of avian biodiversity, based on WRSCR calculations. By the same measure, 12% of current avian biodiversity was estimated to be conserved by the existing protected areas network covering 14% of the study area (Figure 2-8a). In the absence of time lags, the total avian biodiversity value contained in current protected areas was estimated to increase over time, eventually exceeding 14%. Increases in diversity within protected areas over time were much less pronounced for the lag-adjusted scenarios. Patterns were similar for minimum percent species protection, except that strict refugia had relatively lower levels of proportional distribution coverage than diversity coverage (Figure 2-7Figure 2-8b).

2.4 Discussion

2.4.1 Successional lags affect climate-change projections

Time lags in biological responses to climate change may have major consequences for natural communities in a climate-altered world. We have evaluated an important yet underexplored dimension of this mismatch between climate and biota: limitations to forest growth and succession affecting habitat suitability. For boreal songbirds associated with mature forest habitat, these limitations may result in dramatic reductions in suitable habitat over the next century. Considering vegetation time lags based on seral-stage habitat associations could reduce the projected change in core area of a species within this century by up to 169% compared to projections that do not account for time lags. The effect was especially pronounced for a suite of mixed coniferous-deciduous forest species that were otherwise projected to experience sizeable increases in suitable climates, including Canada Warbler (*Cardellina canadensis*), an at-risk species in Canada (Threatened, *Species at Risk Act*, Schedule 1). Accounting for lag effects exacerbated projected decreases in the amount of habitat for several coniferous-forest species, including the already declining (Sauer et al. 2011) Blackpoll Warbler (*Setophaga striata*) and Cape May Warbler (*S. tigrina*).

2.4.2 Seral-stage-modified macrorefugia approach yields robust land rankings

To account for inter-specific differences in habitat suitability related to lags in vegetation response, we developed a seral-stage-modified refugia approach to identify priority areas for bird

conservation. Our approach identifies conservative and efficient conservation solutions anchored around climatic macrorefugia for the boreal forest region. Although local microrefugia may also be found on north-facing slopes and in cold-air drainages (Ashcroft 2010, Dobrowski 2010), they will typically not be big enough to sustain dynamic disturbance regimes, and local populations occupying these areas will be more vulnerable to demographic fluctuations and consequent extirpation. At a continental scale, it is important to identify macrorefugia within which climate-vulnerable forest species may be conserved through climate transitions. Our approach uses climatic projections for a suite of boreal bird species with a wide range of distributional characteristics to identify common multi-species refugia over time. This approach may be more biologically meaningful than refugia identified from climate-type classifications that may or may not be biologically unique. The seral-stage modification acknowledges the widespread rapid changes in climate that are projected to occur, rather than focusing priorities solely on the regions of highest climatic stability.

Comparison of species weighting schemes suggested that identified refugia are robust to different permutations of forest-associated bird species. By extension, these areas may represent boreal forest refugia for multiple taxa via the concept of environmental surrogacy (Arponen et al. 2008). Generally speaking, these refugia can be characterized in at least one of two ways: (1) as areas of relatively moderate climates—e.g., marine and lacustrine coastal areas, and mountain areas; or (2) as latitudinal and elevational ecotones that currently constitute leading edges for multiple species' populations (e.g., the boreal-taiga transition zone). In a rapidly-warming climate, these areas are projected to remain cooler and/or wetter, with a lower probability of reaching a critical threshold for available moisture that results in the loss of trees. Although there may be some overlap between topographically-based refugia and geophysically diverse enduring features (Anderson and Ferree 2010, Lawler et al. 2015), ecotonal refugia are not explicitly captured by geophysically-based conservation approaches.

Although mature-forest-associated species may remain primarily in refugia over coming decades, early-seral and generalist species may shift distributions more rapidly, especially given concomitant land-use change (Warren et al. 2001). Furthermore, variations in responses based on a range of life-history characteristics such as lifespan, fecundity, and migration strategy, are likely to produce additional shuffling of future bird communities (La Sorte et al. 2009). As a result, transient novel communities are likely to emerge (Blois et al. 2013), independent of

persistent novel communities that may develop as a function of non-analogue climates (Williams and Jackson 2007, Stralberg et al. 2009). This complicates the use of current management targets and highlights the need for adaptive strategies that include intensive long-term monitoring of natural systems as they change over the next century.

2.4.3 *Conservation priorities must complement the current protected areas network*

Our analysis supports findings that the current protected areas network does not adequately represent baseline biodiversity within the boreal region (Andrew et al. 2014), nor will it capture future avian conservation priorities when considering vegetation time lags. Although current protected areas, by virtue of their high-elevation and high-latitude propensity (Cantú-Salazar and Gaston 2010, Andrew et al. 2011), may improve relative to representation of future boreal climates, accompanying biota are likely to lag behind, requiring interim protection elsewhere. Comprehensive conservation priorities will change over time, but macrorefugia that are robust to century-long climate change can provide multi-species benefits now and in 100 years. Transitional protection of near-term conservation priorities could provide “stepping stones” or “temporal corridors” (Rose and Burton 2009) for boreal species migration (Hannah 2011).

Emerging approaches to climate-aware conservation suggest landscapes and major watersheds as planning units (Schindler and Lee 2010, Hilty et al. 2012), and emphasize the need for conservation of areas large enough to sustain dynamic disturbance regimes (Krawchuk et al. 2012). Our consideration of seral-stage habitat associations was intended to guide such broad-scale conservation prioritization. Given the spatial scope of our study, and the lack of comprehensive, fine-scale forest age data, we did not attempt to quantify and map mature forest habitat. However, local land conservation decisions should be informed by knowledge of stand age and disturbance history.

2.4.4 *Conservation priorities minimally sensitive to habitat suitability assumptions*

To some extent, our results were driven by the choice of percentile threshold used to identify the lower age limit of suitable forest habitat for each species. Our bracket of 5th–25th percentiles encompassed a wide range of assumptions about avian habitat requirements. However, the differences in Zonation land rankings were relatively minor between the higher thresholds, which increasingly resembled strict climatic refugia. Thus, if differences in bird densities remain pronounced across forest age classes, then the specific lower-limit threshold has

little influence. Differences were much greater at the lower end, with the 5th percentile yielding rankings more similar to those for unconstrained projections. If boreal birds can readily adapt to breed successfully in younger forests, then a greater emphasis on new climatically-suitable areas may be warranted.

2.4.5 *Model limitations*

Correlative species distribution models depend on the assumption that a state of equilibrium exists between an organism and its environment. We have addressed one aspect of disequilibrium: time lags based on vegetation growth and succession. However, other aspects of the equilibrium assumption may also be violated. For example, at a continental scale, breeding distributions may also be constrained by historical dispersal barriers and by the costs of long-distance migration, such that newly suitable habitats are not readily colonized. In North America, the western Cordillera may provide a natural barrier to range expansion for some species. At a local scale, melting permafrost may also result in time lags as meltwater causes the conversion of forested bogs to open fens (Vitt et al. 2000, Jorgenson et al. 2001). Conversely, in situations where birds are physiologically limited by climate but suitable vegetation already exists, bird species may more readily track climate change in the absence of disturbance, resulting in more rapid distributional shifts. In this case, however, interspecific competition may provide an additional limitation to distributional shifts.

In addition, the demographics of regional and continental populations may result in unsaturated habitats, slowing distributional responses to climate change, especially among declining species, and when wintering-ground changes exceed breeding-ground changes. These circumstances and other change-limiting factors support our conservative refugia-based approach. At the other end of the spectrum, extreme and unanticipated ecological responses to climate change are difficult to anticipate. For well-studied species, mechanistic niche modelling approaches (Kearney and Porter 2009) may provide complementary insights about alternative future outcomes.

There is also great uncertainty about the magnitude and characteristics of change under future climates (Murphy et al. 2004, Kingston et al. 2009). However, our consideration of four complementary GCM projections, and our adoption of a probabilistic approach to core habitat identification accounts for major components of this uncertainty. If the magnitude of change is less than expected, refugia-based approaches remain robust. If the magnitude is greater than

expected, the century-long timeframe for adaptation may be compressed, requiring revised analyses. A seral-stage modified refugia approach must be iterative and adaptive in response to rapid change, and should be supported by a robust monitoring program.

2.4.6 Conclusion

The North American boreal forest region is widely considered among the last global frontiers, with a relatively high proportion of intact and inaccessible areas (Ruckstuhl et al. 2008). However, this status is rapidly changing as industrial development activities expand throughout the region (Bradshaw et al. 2009). Climate change threatens to shrink the overall area of boreal forest, with concomitant shifts northward, upslope, and toward coastal regions (Rehfeldt et al. 2012), and may encourage agricultural expansion and additional timber harvest as primary productivity increases (Nelson et al. 2014). In light of these factors, broad-scale conservation measures that are mindful of climate change are urgently needed (Bradshaw et al. 2009, Schindler and Lee 2010). Although socioeconomic and historical factors influence reserve design outcomes (Powers et al. 2013), climatic conditions constitute important underlying drivers of natural communities, and some areas are more resilient than others to the effects of climate change. Our results for songbirds suggest the presence of key boreal climate refugia that are likely to remain important for a wide range of taxa. Identification, protection and monitoring of these multi-species refugia should be central to any boreal conservation strategy.

2.5 Appendices

([on-line at Diversity and Distributions](#))

[Appendix 2-A.](#) Projected proportional change in core habitat area for 53 boreal forest species under alternative vegetation-lag scenarios by 2071-2100.

[Appendix 2-B.](#) Methods for identification of species' minimum forest age thresholds.

[Appendix 2-C.](#) Alternative distributional assumptions for 53 boreal forest species over the next century.

[Appendix 2-D.](#) R code to calculate core areas, strict refugia, and modified refugia

[Appendix 2-E.](#) Zonation settings and inputs

2.6 Tables

Table 2-1. Proportional change in core habitat area.

Change between the baseline and 2071-2100 time periods, summarized over 53 species under different lag-time assumptions. "Difference" refers to the difference between modified refugia (scenario C) and unconstrained projections (scenario A). Unconstrained = projected core areas without time lags; strict refugia = overlap between baseline and future core areas; modified refugia = species-specific time lags based on seral-stage habitat associations using a 15th percentile threshold. See [Appendix 2-A](#) for species-specific results.

	Scenario A. Unconstrained	Scenario B. Strict refugia	Scenario C. Modified refugia	Difference
mean	0.40	-0.61	-0.22	-0.41
min	-0.81	-0.94	-0.92	-1.69
max	1.56	-0.21	1.31	0

Table 2-2. Sensitivity of Zonation land rankings.

Sensitivity of land rankings to (a) habitat age thresholds for time-lag adjustments; and (b) species weights for each future 30-yr time period. Difference values for habitat age threshold sensitivity were calculated as the sum of the absolute values of pixel-level differences between rankings based on the 15th percentile threshold and rankings based on other thresholds. Difference values for species weight sensitivity were calculated as the sum of the absolute values of pixel-level differences between land rankings based on equally-weighted species and rankings based on species weights determined by the magnitude of climate-change response.

Time period	(a) Habitat age threshold	(b) Species weight	
	sensitivity	sensitivity	
2011-2040	Unconstrained	0.110	0.089
	5 th percentile	0.090	0.054
	15 th percentile	0	0.079
	25 th percentile	0.038	0.048
	Strict refugia	0.044	0.049
2041-2070	Unconstrained	0.208	0.149
	5 th percentile	0.191	0.080
	15 th percentile	0	0.056
	25 th percentile	0.080	0.041
	Strict refugia	0.108	0.037
2071-2100	Unconstrained	0.202	0.117
	5 th percentile	0.192	0.094
	15 th percentile	0	0.054
	25 th percentile	0.131	0.050
	Strict refugia	0.228	0.044

2.7 Figures

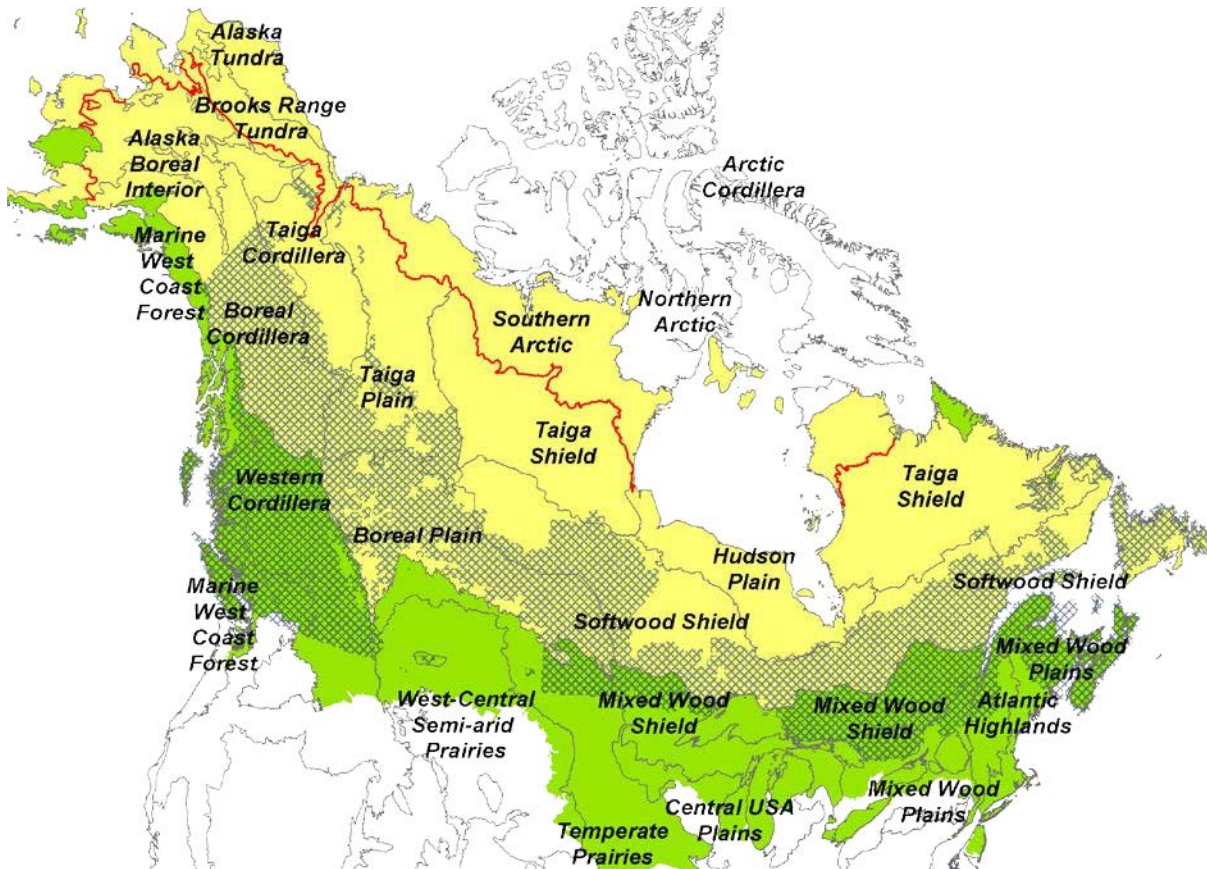


Figure 2-1. Boreal and southern arctic study area.

Study area shown in yellow with boreal/arctic boundary in red. Additional ecoregions projected to move into study area by 2100 are depicted in light green (model-building area). Extent of forest resource inventory data used to determine seral-stage preferences cross-hatched in blue. Level 2 ecoregions within the model-building area are labelled.

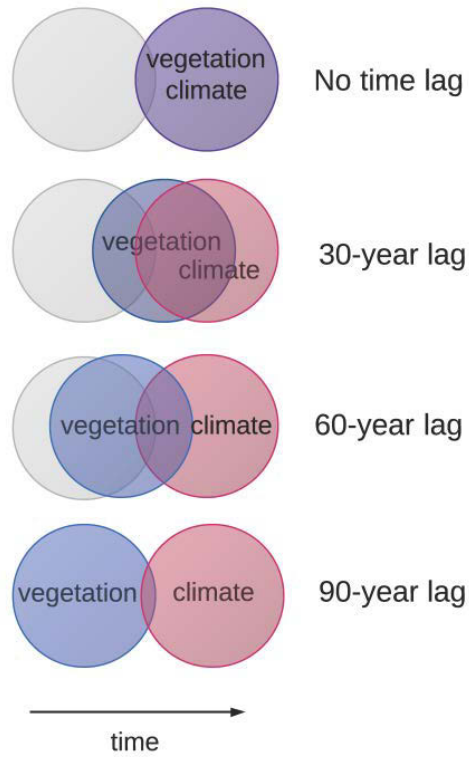


Figure 2-2. Conceptual diagram of assumptions for seral-stage modified refugia approach. Purple intersections represent areas of spatial overlap between suitable climatic conditions and suitable vegetation for an individual species. Time lags can be interpreted as seral-stage preferences for individual species.

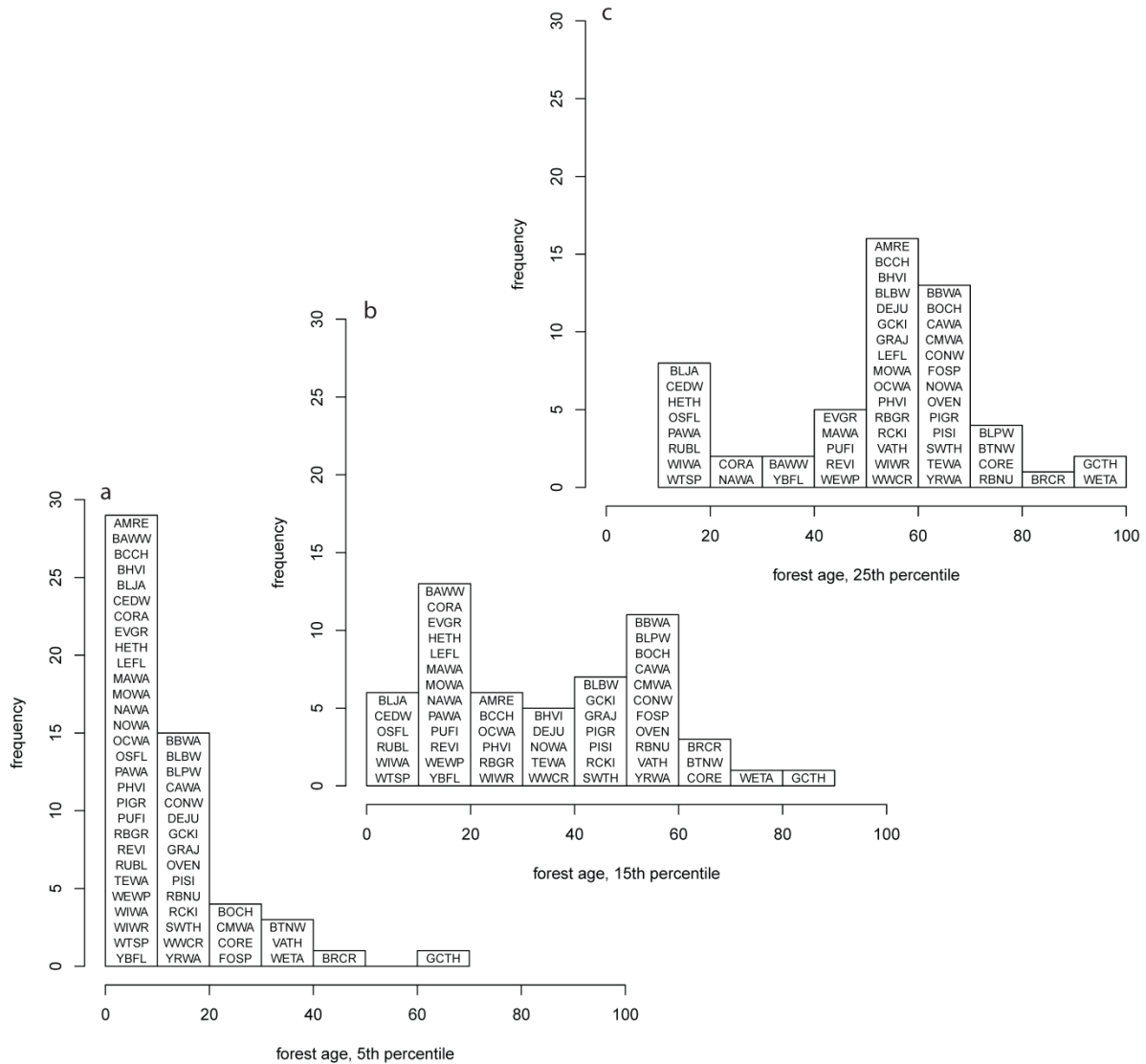


Figure 2-3. Distributions of minimum age thresholds for 53 boreal forest species. Minimum age distributions for based on three different percentile thresholds: (a) 5%, (b) 15%, and (c) 25%. A 15th percentile threshold means that 15% of modelled abundance for a given species occurred in forest habitat that was as young as or younger than the specified age.

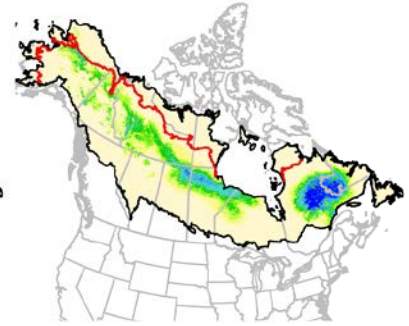
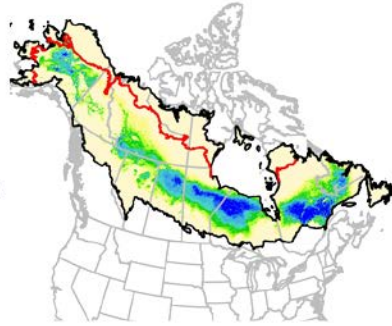
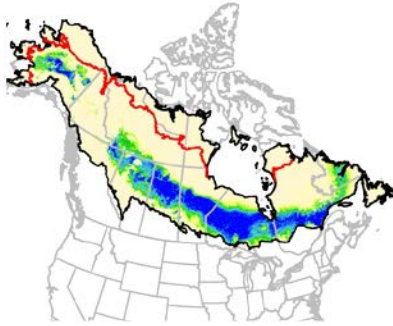
BBWA

a. 2011-2040

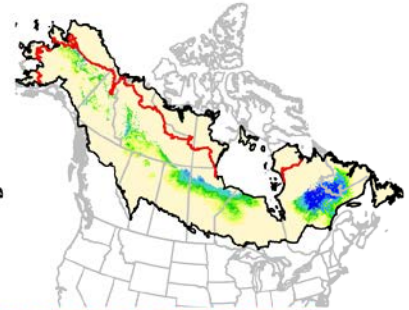
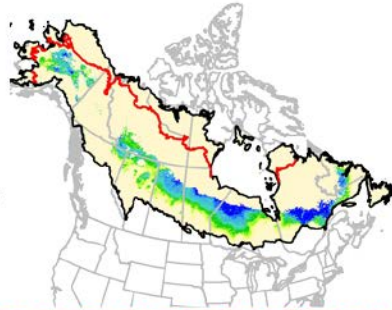
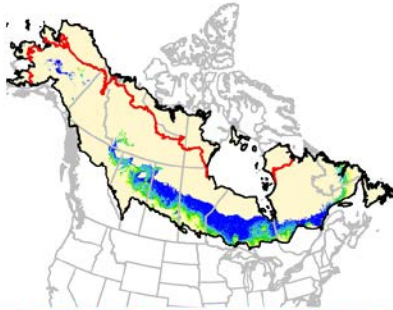
b. 2041-2070

c. 2071-2100

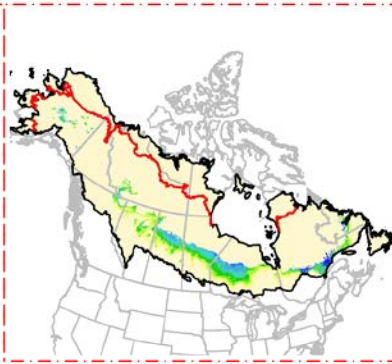
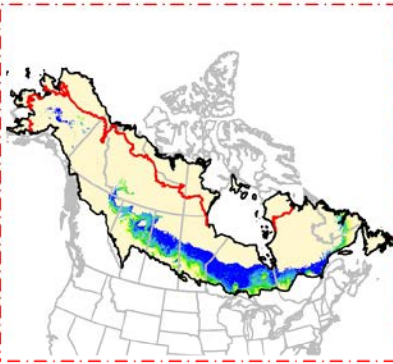
No time lag



30-year lag



60-year lag



90-year lag

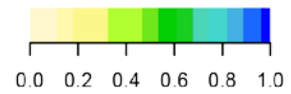
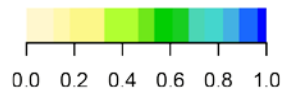
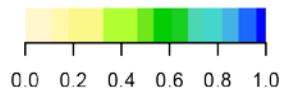
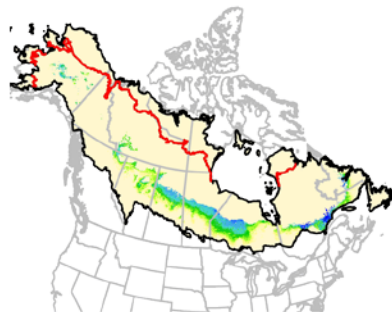
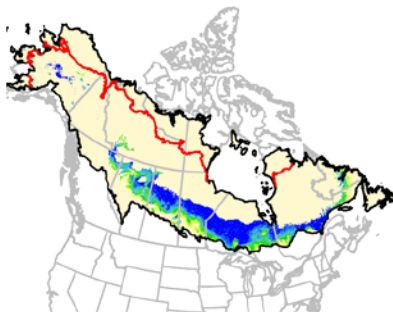


Figure 2-4. Alternative distribution scenarios for an example species.

Alternative scenarios for Bay-breasted Warbler *Setophaga castanea*. The most likely scenario (based on **Figure 2-3**, BBWA) is outlined with red dotted lines. Map values represent the proportion of scenarios (11 bootstrap replicates x 4 GCMs x 2 variable sets) for which a given pixel meets the core area criteria: projected density \geq mean density within model-building study area (including hemiboreal). No lag = projected core areas without constraints; 30-yr lag = core area overlap between future time period of interest and previous 30-yr period; 60-yr lag = core area overlap between future time period of interest and that two time periods earlier (e.g., 2041-2070 and baseline period); 90-yr lag = refugia (overlap between future and baseline core areas).

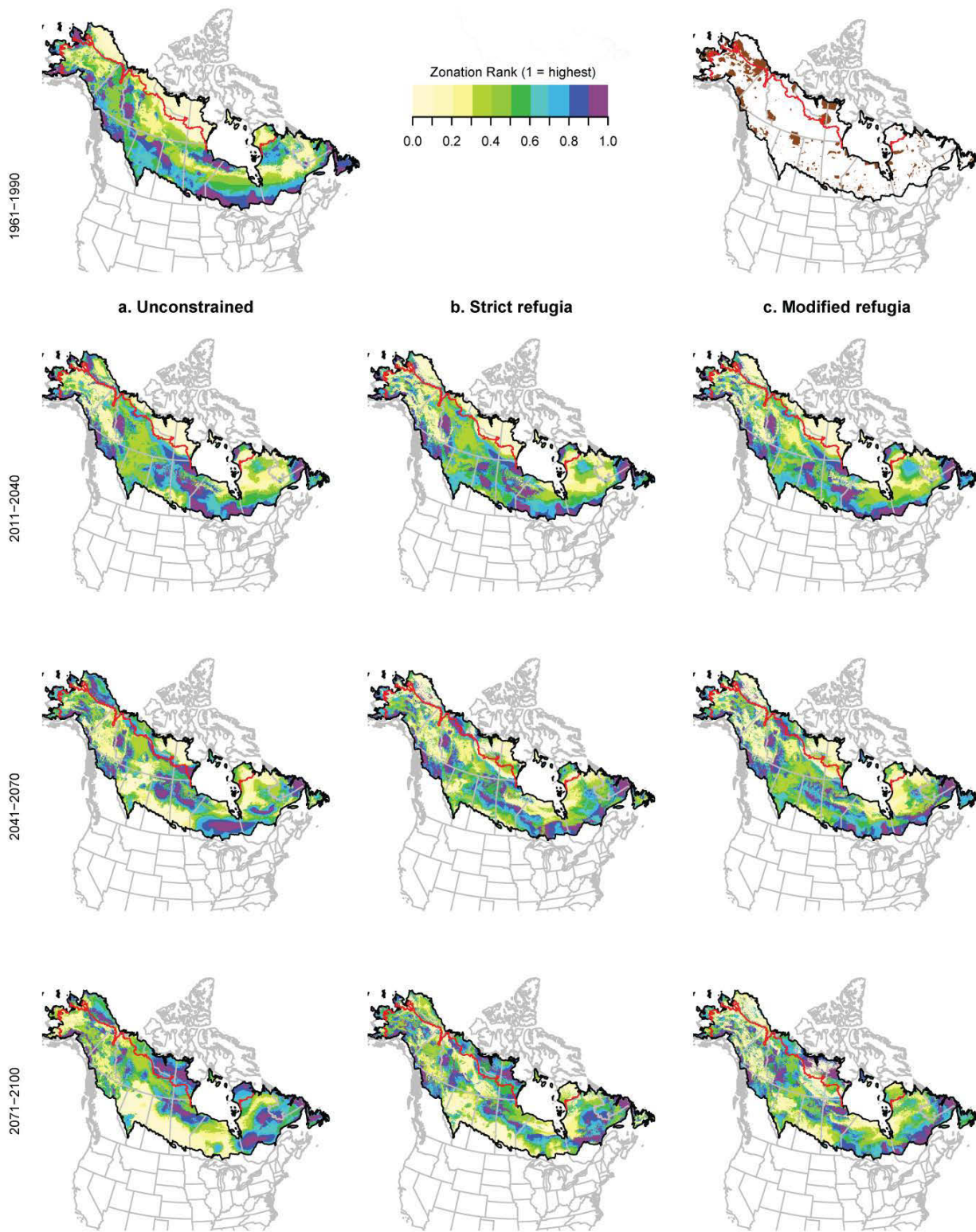


Figure 2-5. Zonation results (land ranking maps).

Land ranking maps based on 53 equally-weighted species for the current period and three future time periods (2011-2040, 2041-2070, 2071-2100). Three scenarios are shown: (a) unconstrained = projected core areas without time lags; (b) strict refugia = overlap between future and baseline core areas; and (c) modified refugia = species-specific time lags based on seral-stage habitat associations using a 15th percentile threshold (see [Appendix 2-B](#)).

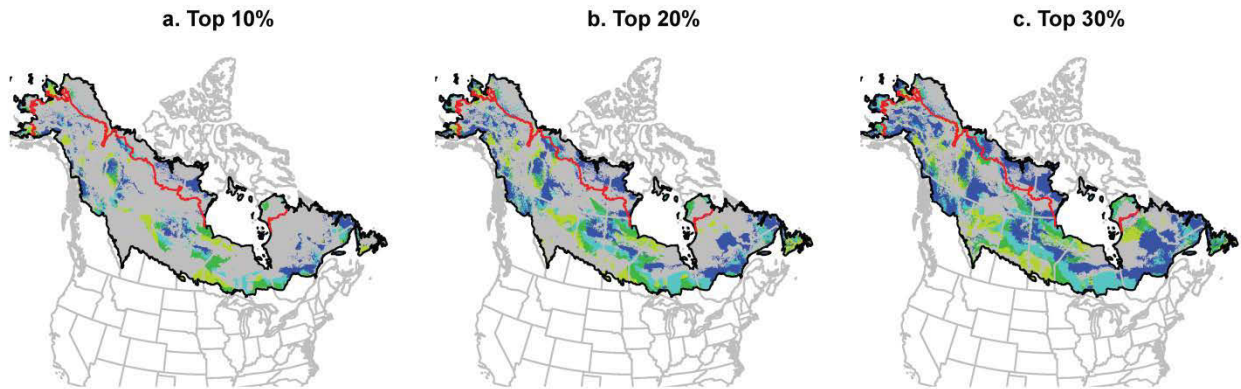


Figure 2-6. Combined Zonation results (land ranking maps) for three future time periods. Results are based on the modified refugia scenario (species-specific time lags for 53 species based on seral-stage habitat associations using a 15th percentile threshold) and three percent thresholds: (a) top-ranked 10%, (b) top-ranked 20%, and (c) top-ranked 30% of study area. Solutions for later time periods shown on top, with non-overlapping solutions from previous time periods also shown. Dark blue = 2071-2100, turquoise = 2041-2070, dark green = 2011-2040, light green = baseline (1961-1990).

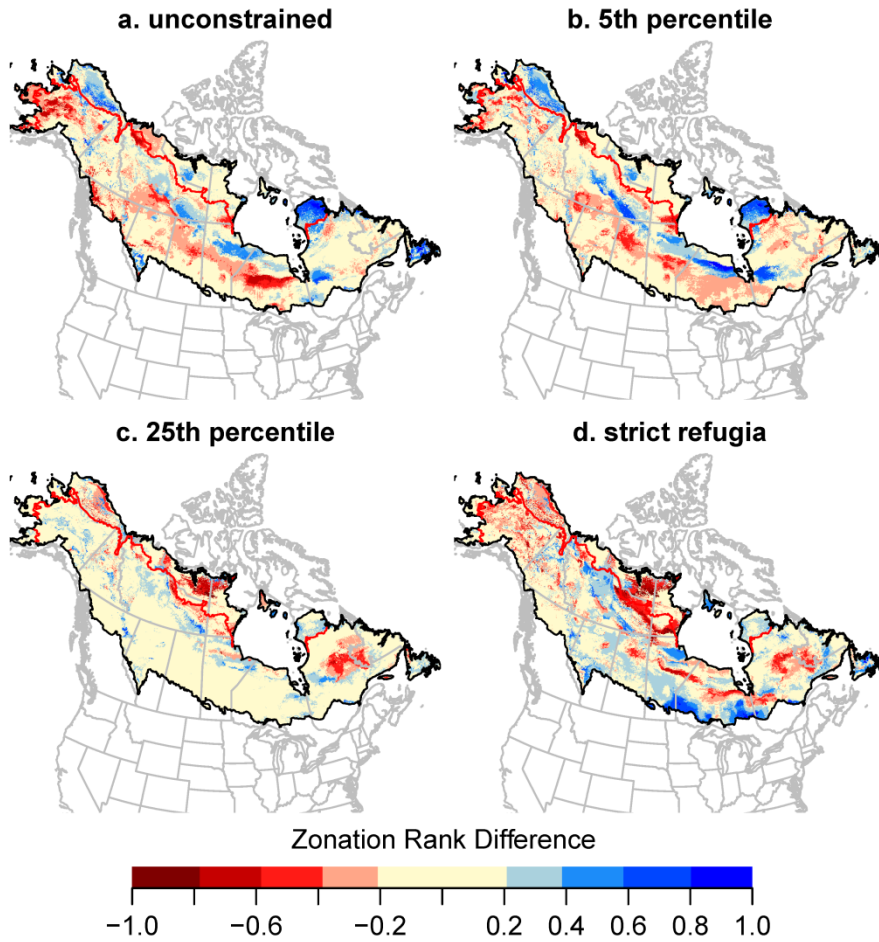
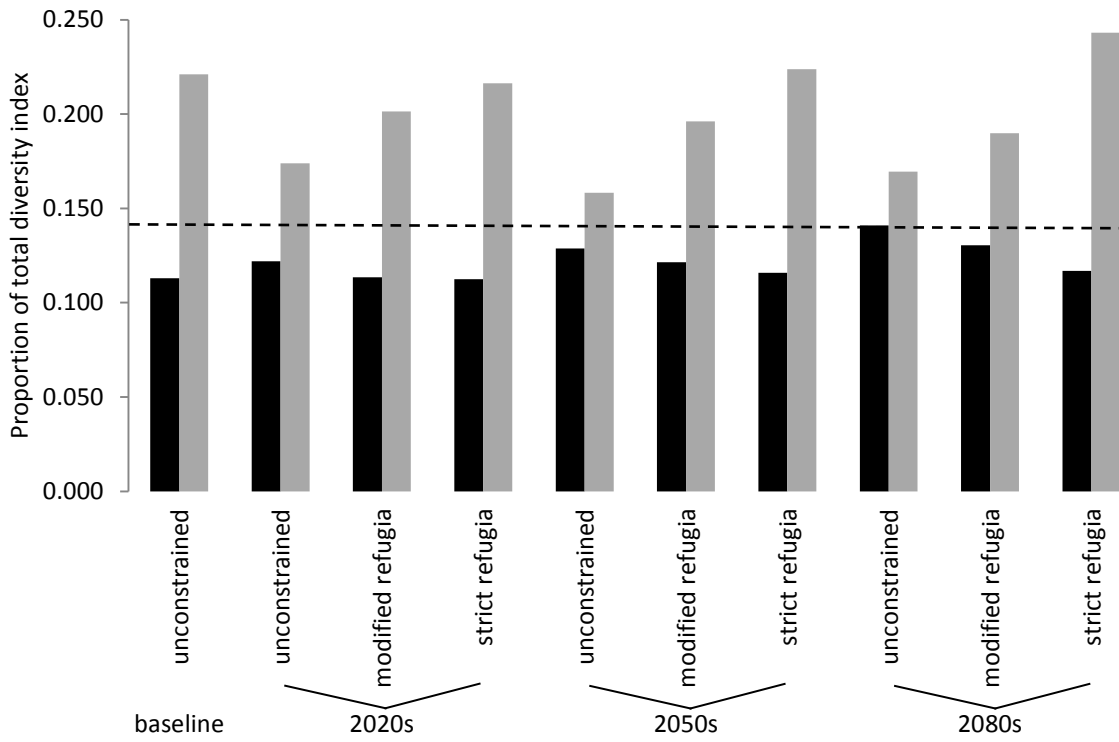


Figure 2-7. Sensitivity of Zonation land rankings to habitat age thresholds. Sensitivity of 2071-2100 land rankings to thresholds for time-lag adjustments. Difference between rankings for the 15th percentile threshold compared to: (a) unconstrained projections, (b) 5th percentile threshold, (c) 25th percentile threshold, and (d) strict refugia. See [Appendix 2-A](#) for habitat age classifications for each species based on each threshold.

(a) WRSCR



(b) MP

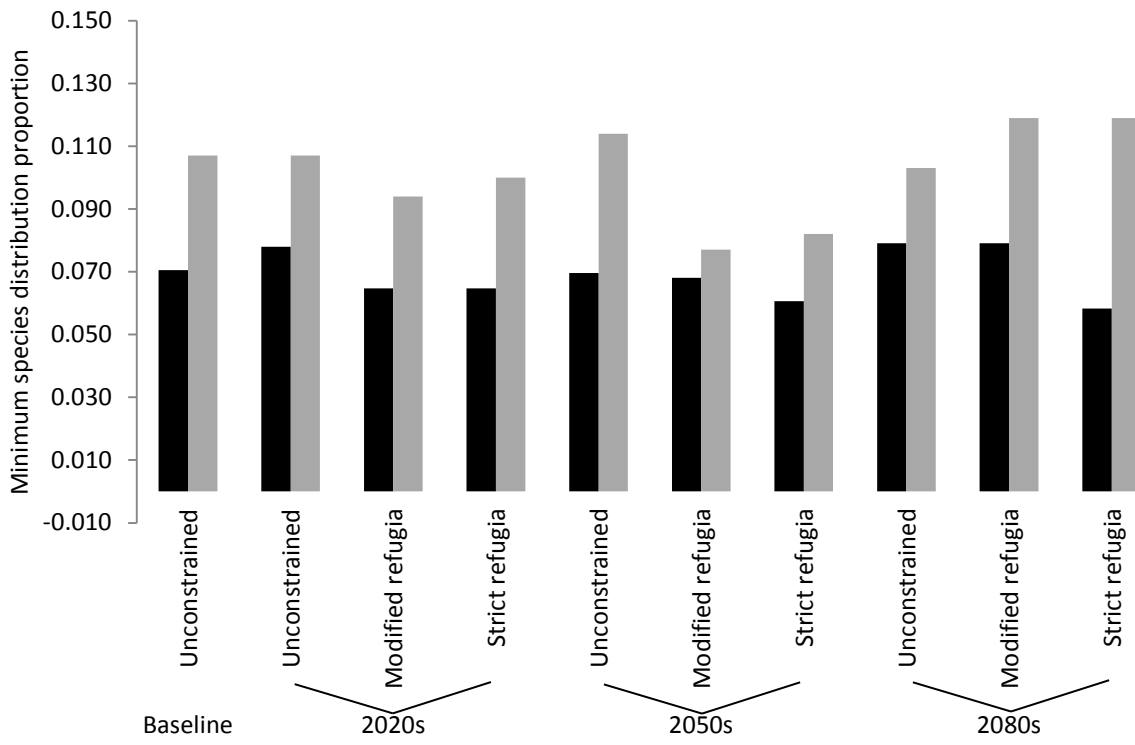


Figure 2-8. Proportion of diversity and minimum species distribution conserved.

(a) Weighted range-size corrected richness index (WRSCR) and (b) Minimum species' distribution proportion (MP). Proportion conserved by the current protected areas network (black, 14% of study area) vs. an optimal network based on Zonation land rankings for the same area (grey). Dotted line represents the percent of diversity expected at random within 14% of study area. Unconstrained = projected core areas without time lags; strict refugia = overlap between baseline and future core areas; modified refugia = species-specific time lags based on seral-stage habitat associations using a 15th percentile threshold.

CHAPTER 3. SCENARIOS OF FUTURE CLIMATE- AND DISTURBANCE-DRIVEN CHANGES FOR THE BOREAL FOREST REGION OF ALBERTA

3.0 Summary

Climate-induced vegetation change may be delayed in the absence of disturbance catalysts. In the western boreal region, a combined increase in wildfires and human activities may accelerate these transitions, also resulting in a younger forest. We developed a hybrid modelling approach based on topo-edaphically constrained projections of climate-driven vegetation change potential, coupled with weather- and fuel-based simulations of future wildfires, and projections of large-scale industrial development activities, to better understand factors influencing decadal-scale upland vegetation change. We simulated scenarios of change in forest composition and structure over the next century, concluding that at least one-third of Alberta's upland mixedwood and conifer forest is likely to be replaced by deciduous woodland and grassland by 2090, with a disproportionate loss of old forest. During this timeframe, the rate of increase in fire probability diminished, suggesting a negative feedback process by which a warmer climate and more extensive near-term fires leads to an increase in deciduous forest that in turn, due to its relatively low flammability, leads to a long-term reduction in area burned.

3.1 Introduction

Global climate change is anticipated to exert biome-scale influences on future vegetation patterns (Hickler et al. 2012, Rehfeldt et al. 2012), with profound influences on terrestrial (Lee and Jetz 2008) and aquatic (Sterling et al. 2013) biota. In the western boreal region of North America, there is evidence that recent anthropogenic climate change has resulted in more frequent and extensive moisture deficits (Peng et al. 2011a), leading in turn to more frequent and larger fires (Kasischke and Turetsky 2006), declines in forest biomass (Ma et al. 2012, Luo and Chen 2013, Chen and Luo 2015), and increased tree mortality (Hogg et al. 2002, Michaelian et al. 2010, Peng et al. 2011a).

Continued warming and increased drought frequency is predicted to result in an eventual conversion of deciduous forest to open woodlands or even grassland (Hogg and Hurdle 1995, Schneider et al. 2009, Mbogga et al. 2010). In mesic upland mixed conifer-deciduous forests, warmer temperatures and increased disturbance frequencies could encourage competitive shifts from conifer-dominated to deciduous-dominated stands (Soja et al. 2007, Johnstone et al. 2010). These major ecosystem changes, which amount to an

eventual shift from the boreal forest biome to a prairie grassland biome (Rehfeldt et al. 2012) will be slowed by the inertia of current forest systems, and the time lags imposed by growth, dispersal, and successional dynamics (Meier et al. 2012, Svenning and Sandel 2013, Wu et al. 2015). In the absence of disturbance, current forest systems may persist for extended periods, as the requirements for mature tree persistence are less restrictive than for seedling establishment (Hogg and Schwarz 1997). However, the boreal forest biome of North America has one of the most active fire regimes in the world (Stocks et al. 2002), and fires are particularly large and frequent in the western boreal region (Parisien et al. 2011a). Across the Canadian boreal forest region, projected future increases in maximum summer temperatures and associated decreases in soil moisture suggest that area burned may increase by as much as five-fold by the end of the 21st century (Flannigan et al. 2005, Balshi et al. 2009, Boulanger et al. 2014).

Consequently, this expected increase in natural disturbance events (i.e., wildfire) will almost certainly accelerate ecosystem shifts, reducing the mismatch between climate conditions and vegetation (Stephens et al. 2013). It should also create a younger forest, a trend that will be exacerbated by continued timber harvest and other industrial development activities (Schneider et al. 2003, Cyr et al. 2009, Hauer et al. 2010). Generalist and early-seral wildlife species may benefit from increased rates of natural disturbance, but late-seral species may face a near-term dual disadvantage as fire- and human-related loss of old-growth habitat is coupled with declines in suitable climate conditions that allow such forests to occur (Stralberg et al. 2015a). Ultimately, such changes in vegetation composition and age structure may be enough to limit populations of some species. Thus, it is critical to understand decadal-scale dynamics of vegetation succession and disturbance in response to climate and land-use change, which are inextricably linked to wildfire dynamics.

Wildfire potential is a function of climate, fuel (vegetation), and ignitions (Parisien et al. 2011a). In the western boreal region, the climate is becoming more fire-conducive, with more extreme fire-weather days already occurring, and projected for the future (Parisien et al. 2011a). In the western boreal region, the climate is becoming more fire-conducive, with more extreme fire-weather days already occurring, and projected for the future (Tymstra et al. 2007, Wang et al. 2015), as well as a longer fire season (Wotton and Flannigan 1993, Flannigan et al. 2009). Lightning-caused ignitions are already numerous and will likely increase with future weather conditions (Krawchuk et al. 2009, Wotton et al. 2010). Fuels (i.e., flammable biomass), however, may decrease over the next century, as forests become younger (Héon et al. 2014) and more aspen- (*Populus tremuloides*) dominated (Johnstone et

al. 2010), and therefore less flammable (Cumming 2001). The grassland systems that are projected to be most suited to southern boreal climate conditions by the end of the 21st century (Schneider et al. 2009, Mbogga et al. 2010), though highly flammable, would represent a further decrease in fuel biomass. Thus, projected increases in fire activity may be relatively short-lived, depending on how quickly fuels change (Terrier et al. 2012, Batllori et al. 2013).

Further complicating the picture is industrial development, which has increased rapidly in recent decades and has already resulted in a substantial human footprint on Alberta's boreal forest landscape (Schneider et al. 2003, Pickell et al. 2015). The combined effects of climate and land-use change have been considered in the context of urban, suburban, and agricultural land conversion (Jongsomjit et al. 2013, Maggini et al. 2014), and in the context of forest harvest (He et al. 2002). Simultaneous recent increases in timber harvest and energy sector expansion in northern Alberta have raised serious concerns about cumulative impacts, leading to the creation of large-scale monitoring and assessment programs, and extensive research on the effects of these cumulative impacts on forests and wildlife (Boutin et al. 2009, Nielsen et al. 2009, Haughland et al. 2010). Cumulative effects research in boreal Canada has a longer history, and has focused on the cumulative impacts of multiple industrial sectors (Schneider et al. 2003, Hervieux et al. 2013, Hobson et al. 2013, Van Wilgenburg et al. 2013), often in consideration of natural disturbance regimes (Sorensen et al. 2008, Mahon et al. 2014), but largely in isolation from climate change (but see Yamasaki et al. 2008).

Due to a real or perceived lack of information, future climate-change effects are still rarely considered in major land-use and conservation planning efforts. Despite the extensive human footprint in Alberta, models suggest that over the long term, impacts of climate change on species and ecosystems may be even greater than those of land use, given anticipated biome-level vegetation shifts (Rehfeldt et al. 2012). The short-term effects of climate change are of much greater relevance to managers and policy-makers, but time-scales of change offered by equilibrium-based bioclimatic distribution model projections are generally unrealistic for a number of species with slower life-history characteristics (e.g., longer lifespans and lower reproductive rates). Dynamic landscape simulation models are needed to address short-term (i.e., decadal scale) vegetation trajectories. Landscape fire simulation models are numerous (see Keane et al. 2004 for a review), but climate-change parameterizations for such models are still fairly rudimentary and system-specific. The landscape simulation models that have been used in boreal or arctic systems are generally

parameterized for specific regions (e.g., Rupp et al. 2000, Perera 2008, Scheller and Mladenoff 2008, Johnstone et al. 2011), or lack spatial detail and climatic vegetation transitions (Schneider et al. 2003, Krawchuk and Cumming 2011). (Schneider et al. 2003, Krawchuk and Cumming 2011). Hybrid modelling approaches that incorporate critical mechanistic processes but also empirically-derived relationships over broad climatic gradients may be best suited for broad-scale ecological inference in a climate-change context (Cushman et al. 2006, Gustafson 2013), or at least most practically implemented. We have developed such an approach for northern Alberta, simultaneously taking advantage of a wealth of systematically surveyed ecosite data (Boutin et al. 2009) and recent developments in extending mechanistic fire behavior simulation to future climates and fire weather (Wang et al. 2014, Wang et al. 2015).

Our objective was to identify decadal-scale risks of climate change on upland boreal forest vegetation, considering (1) topo-edaphic constraints to vegetation change; (2) changes in natural disturbance (wildfire); and (3) large-scale changes in anthropogenic disturbance (primarily timber harvest). Using a scenario evaluation framework and four complementary global climate models (GCM), we addressed the following set of questions for northern Alberta:

1. What are the combined projected impacts of wildfire, anthropogenic disturbance, and climate change on upland vegetation composition and age structure over the next century?
2. How will fire frequency and extent change over time as weather and fuels change? How do disturbance-mediated fuel scenarios (see below) compare with climate-driven and static fuel scenarios?
3. How do disturbance-mediated scenarios of change in upland vegetation differ from direct climate-change projections? How much of the variability across scenarios can be attributed to GCM differences?

To address these questions, we evaluated variations on three alternative scenarios of disturbance and upland vegetation composition and age over a period of 90 years (2001-2090), ranging from highest to lowest impact:

- A. Climate-driven vegetation change:** Upland vegetation types are directly determined by climate (constrained by topo-edaphic conditions), but stand age is altered by natural and anthropogenic disturbance;
- B. Disturbance-mediated vegetation change:** Climate-based upland vegetation transition and stand age dependent on:

- B1. Fire** (simulated for future weather and fuel conditions); or
- B2. Fire + anthropogenic disturbance** (timber harvest and major energy sector development); and
- C. Static vegetation:** Baseline vegetation types remain unchanged, but stand age is altered by natural and anthropogenic disturbance.

Scenarios A and C were considered our less realistic “bookend” scenarios, while scenario B was considered most realistic (scenario B2 in particular).

3.2 Methods

3.2.1 Study Area

Our study area was the boreal forest region within the province of Alberta, Canada (total area = 438,063 km²), ranging from approximately 55 °N to 60 °N latitude at the border with the Northwest Territories. Specifically, we focused our inference on the Boreal Forest and Canadian Shield natural regions, as well as the lower portion of the Foothills natural region (Natural Regions Committee 2006) (Figure 3-1). Although the Alberta Foothills region is included in Brandt’s (2009) North American boreal delineation, it is wetter than the other Alberta boreal regions, with lower seasonal temperature variability. We included it here because it contains many boreal elements and species, some of which may retreat to high-elevation climate refugia in the future (Stralberg et al. 2015a).

Boreal Alberta is characterized by a strongly continental climate. The average annual moisture balance is slightly positive (Hogg 1994), and fire is the predominant natural disturbance. (Hogg 1994), and fire is the predominant natural disturbance. Geologically, the boreal region of Alberta primarily consists of the boreal plain, an area of deep marine sediments, and a small section of the Canadian Shield (eroded Precambrian rock) in the northeastern corner of the province. Upland forests are composed primarily of aspen (*Populus tremuloides*) and white spruce (*Picea glauca*) in various mixtures, with a tendency for the former to dominate on warmer, more exposed sites, and the latter more common on colder and more sheltered sites. Extensive forested wetlands are also found, where sparse black spruce (*P. mariana*) and/or larch (*Larix laricina*) dominate on cold, poor wetland soils. Forests on the granitic expanse of the western Canadian Shield are composed mostly of black spruce and jack pine (*Pinus banksiana*). Foothill forests contain primarily lodgepole pine (*Pinus contorta*), white spruce, and aspen.

Alberta’s wildfire regime is characterized by large, stand-renewing fires primarily initiated by lightning strikes, and a fairly long season, starting early-April and ending late-

September (Tymstra et al. 2005). Most fire activity is in the boreal region, particularly in the northern part of the province, with less activity in the foothills region (Tymstra et al. 2005).

The region contains little urban development (less than 1%), and agricultural activities are climate-limited, covering 10.6% of the boreal region and 3.0% of the foothills region (Schieck et al. 2015). The industrial land-use development footprint is quite extensive, consisting of a combination of timber harvest blocks, oil-and-gas wells, mines, and a network of linear features that includes pipelines, logging roads, seismic lines, and variety of other roads, trails, and cut lines (Schneider et al. 2003). In terms of total area, however, forestry and energy sector footprints are estimated to cover just 2.7% and 1.7%, respectively, of the boreal region (including the Canadian shield portion), and 16.9% and 2.5%, respectively, of the foothills region (Schieck et al. 2015).

3.2.2 *Model and Simulation Overview*

We modelled vegetation as a function of geology, terrain, and climate in a two-stage process and projected future potential vegetation distribution as a function of climate. We assumed that current ecosite types (i.e., relative soil moisture and nutrient conditions) will remain constant over the 90-year study period, and focused our analysis on upland forests, where vegetation transitions are more straightforward than in wetland systems, and more likely to be directly affected by industrial activities such as forestry (Schneider et al. 2015). We first constructed models relating current ecosite type to geology, terrain, and climate, and used those models to predict ecosite type at a 500-m resolution province-wide (Figure 3-2). We then modelled vegetation as a function of ecosite, terrain, and climate, clipped the output prediction to our boreal study area, and converted the output to fuel types that were used as inputs to Burn-P3 (P3 = probability, prediction, and planning), a model that simulates the ignition and growth of individual fires (Parisien et al. 2005). We projected future potential vegetation based on projected future climate variables, holding ecosite type and terrain variables constant. For scenarios C (static vegetation) and A (climate-driven vegetation), we used current and climate-predicted potential future vegetation, respectively, as inputs to Burn-P3, independent of fire simulation results from previous periods. For the disturbance-mediated scenarios (B1 and B2), we used Burn-P3 outputs of simulated fires and spatial projections of anthropogenic disturbance to update disturbed areas based on climate-projected potential future vegetation for three 30-year periods from 2001 to 2090 (Figure 3-2).

3.2.3 *Ecosite and Vegetation Data*

Hierarchical ecosite and vegetation types were based on the ecological land classification system of Alberta, as described in Archibald et al.(1996) and Beckingham and Archibald (1996) but without the natural subregion classification hierarchy (Table 3-1). We omitted this additional hierarchy to ensure that future vegetation was constrained by current soil moisture/nutrient status (i.e., ecosite), but not by current natural subregion climate conditions, which will change in the future. We defined ecosite type as the relative soil moisture and nutrient conditions of a site, as identified by indicator understory species. We defined vegetation type as the combination of understory and overstory species found at a site (referred to as ecosite phase within a specific natural subregion). Vegetation type as we defined it was linked to a specific ecosite type.

In a climate-change context, the moisture component of our ecosite types should be considered relative to other ecosite types in the same climate zone. For example, mesic sites can be found throughout the province, but contain different vegetation depending on local climate conditions (including soil moisture): generally grassland in the prairie region, and aspen or white spruce in the boreal region. A medium-mesic white spruce site could become grassland in the future, but a poor-hydric black spruce bog could not, according to our assumptions.

To avoid propagating vegetation mapping errors, we used ground-based vegetation datasets rather than relying on remotely sensed data products to develop ecosite and vegetation models. In addition, we found substantial discrepancies between ground-based vegetation and remotely-sensed landcover layers, particularly in the wetland classes. We primarily used a terrestrial vegetation (ground cover, site capability) dataset from the Alberta Biodiversity Monitoring Institute (ABMI, <http://www.abmi.ca/home/data/species-habitat-data.html>) consisting of pre-determined sites arranged in a regular grid of 1,656 sites at 20-km intervals across Alberta, each consisting of 9 points arranged in a square grid with adjacent points separated by 300 m (Boutin et al. 2009, Burton et al. 2014). A total of 5,369 points were available for analysis after we excluded highly developed sites without ecosite classifications, and added additional “off-grid” ABMI sites. To improve model power, we also included a dataset collected by Environment Canada in the oil sands monitoring region (Mahon et al. 2016) (n = 3,776), as well as a University of Alberta dataset focused on boreal hill systems (S. Nielsen and E.M. Bayne unpubl.) (n = 115), and the georeferenced portion of the Alberta Government’s Ecological Site Information System (ESIS) database (n = 820), for a total of 10,080 unique point locations used to develop ecosite models (Figure 3-1). Non-

ESIS sites were classified in the field between 2003 and 2014 according to moisture and nutrient categories to derive our ecosite types for analysis.

We used the same dataset for the vegetation models, except for the ESIS dataset, which was not readily converted to classes consistent with the ABMI dataset. Given the large ground-based sample available ($n = 9,260$), we chose to use this consistent, field-derived dataset even though it may mean greater uncertainty in less well-sampled areas than remotely sensed landcover products.

3.2.4 *Climate and Terrain Data*

The climate, terrain, geology, and wetland variables we used as inputs to ecosite and vegetation models are listed in [Table 3-2](#). Climate, terrain, geology, and wetland variables included in random forest models for ecosite and vegetation. Terrain metrics were derived at 100-m raster resolution (S. Nielsen, University of Alberta, species.abmi.ca) and included indices of topographic ruggedness at various scales (VRM, vector ruggedness measure) (Sappington et al. 2007), slope, solar insolation, and terrain wetness (CTI, compound topographic index) (Gessler et al. 1995). Wetland classes were based on the Alberta merged wetland inventory derived from compiled vector polygon GIS layers with a minimum mapping unit of 0.09 ha (AESRD 2014), supplemented by a vegetation map for the Wood Buffalo National Park (Jensen 2003). Surficial geology was based on the surficial geology map of Alberta (map 601), which was derived from vector maps with source scales ranging from 1:50,000 to 1:1,000,000, compiled by the Alberta Geological Survey (2013).

Interpolated climate data for the 1961-1990 normal period based on the parameter-elevation regressions on independent slopes model (PRISM) (Daly et al. 2008) were obtained from Climate WNA at a 500-m resolution (Hamann et al. 2013). We used derived bioclimatic variables relevant to vegetation distributions ([Table 3-2](#)). To represent potential future climates for three consecutive 30-year periods (2011–2040, 2041–2070, and 2071–2100), we used projections from the CMIP3 multi-model dataset, corresponding to the fourth IPCC assessment report (Meehl et al. 2007), also downscaled using Climate WNA. We selected a subset of four complementary GCMs that span a range of projected growing season temperatures and precipitation levels within Alberta (Stralberg 2012): the German MPI ECHAM5, the United States GFDL CM2.1, and the United Kingdom Met Office HadGEM1 model (Stralberg et al. 2015b). We also evaluated the United Kingdom Met Office HadCM3 model, for which future fire weather projections were available (Wang et al. 2015). We adopted a scenario of high and monotonically increasing emissions (SRES A2, IPCC 2001),

reflecting actual emissions during the decade elapsed since the scenario was defined (Raupach et al. 2007).

3.2.5 Fire and Weather Data

A primary input to Burn-P3 is daily fire weather, which consists of daily noon observations of surface air temperature, relative humidity, 10-m open wind speed, and 24-h accumulated precipitation, as well as their corresponding Fire Weather Index (FWI) System (van Wagner 1987) variables, which are used to track daily fuel moisture conditions and fire behavior. Two of the FWI System variables, duff moisture code (DMC, a scaled measure of duff fuel layer moisture content) and fire weather index (FWI, a scaled indicator of overall fire intensity) (van Wagner 1987), were used in the simulations. Only days with a combined $FWI \geq 19$ and $DMC \geq 20$ were used to simulate fire growth, as suggested by Podur and Wotton (2011). Historical daily fire weather data were obtained from an interpolated 3-km resolution grid provided by the Canadian Forest Service based on surface observations taken between April 1 and September 30 from 1981 to 2010 (Wang et al. 2015). One hundred points, separated by at least 40 km, were randomly sampled from the grid to represent baseline fire weather conditions. Future fire weather data were from Wang et al. (2015), who applied monthly change anomalies to daily baseline values to translate future monthly climate projections from GCM simulations into future daily fire weather values for the periods 2001-2030, 2031-2060, and 2061-2090. The same 100 points were randomly sampled from the 3-km resolution grids for both the baseline and future time periods to represent daily fire weather conditions. Among the CMIP3 models, choices for fire weather projection were limited to those that generate future relative humidity values. We used the intermediate United Kingdom Met Office HadCM3 model (4.2 °C increase in mean annual temperature for Alberta by 2071-2100 under A2 emission scenario).

To calibrate Burn-P3 baseline fire simulations, we used fire data from the period 1981-2010 that were obtained from the Canadian National Fire Database (Canadian Forest Service 2015). Fires <200 ha were excluded, as they are inconsistently reported. Large fires (≥ 200 ha) are responsible for ~97% of the area burned in the boreal forest (Stocks et al. 2002).

3.2.6 Anthropogenic Disturbance Data

To represent likely future industrial land-use scenarios, we used spatial projections from the ALCES model (Schneider et al. 2003), as represented by the on-line scenario analysis tool (Carlson et al. 2014). Spatial anthropogenic disturbance projections for each

decade from 2000 to 2060 (latest year available) for the forestry and energy sectors were used to trigger climate-driven vegetation change in our simulations (Figure 3-3). We did not attempt to extrapolate projected disturbance beyond 2060, given the inherent uncertainty. The specific disturbance types included were: cutblocks, cutlines (including seismic lines), roads, oil wells, gas wells, shale gas wells, and in-situ wells. We summed the areas of these human footprint types over the 2.5-km grid cells at which they were estimated, and considered an entire cell disturbed during a given 30-year time period (2001-2030, 2031-2060) if at least half of it was covered by some form of disturbance. If total disturbance within the 2.5-km grid cell was not greater than 0.5, we did not attempt to allocate disturbance to constituent 500-m grid cells. Large disturbances were thereby overestimated, while small disturbances were underestimated. The 2.5-km grid cells were converted to a 500-m resolution layer matching our vegetation projections. Thus our projections reflect large- but not small-scale disturbance (primarily timber harvest) and should be considered an underestimate of total future anthropogenic disturbance. We did not consider projected permanent land conversions such as urban and agricultural development, which were quite small within our study area.

3.2.7 Ecosite and Vegetation Models

Although our approach was similar to that of predictive ecosystem mapping efforts used for resource inventory purposes (Franklin 1995, MacMillan et al. 2007), our climate-change focus meant that we built our model using a larger spatial extent and a coarser spatial resolution than traditional modelling efforts that emphasize high site-level accuracy over model generality. Because we used climate variables as a proxy for traditionally-used ecoregion boundaries, our baseline spatial predicted values should be interpreted with caution in data deficient areas of the province, primarily in the north and in the west (see Figure 3-1).

Although our focus was on boreal Alberta, we used data from throughout the province, including prairie and Rocky mountain regions, to capture the climate conditions that are likely to move northward into the boreal region in the future (Schneider et al. 2009), and to represent climate-vegetation relationships across a wider range of conditions, respectively.

As a basis for identifying topo-edaphic constraints on future projections of vegetation types, we first modelled ecosite as a function of geology, climate, terrain, and mapped wetland class sampled at 100-m grid cell resolution ($n = 10,080$). The influence of these variables can be viewed in a hierarchical manner. Regionally, surficial geology provides the parent material from which soils are created, and influences nutrient availability; climate

determines rates of evapotranspiration and available moisture. At the landscape level, terrain features redistribute solar energy and determine the flow of water and resulting moisture characteristics. Thus, we presumed that terrain, climate, and geology could be used to predict moisture and nutrient conditions at an accuracy level suitable for province-wide analysis. We also included the Alberta merged wetland inventory as a covariate to help improve the predictive power of the model, although accuracy varies by data source across the province.

We used a random forest (Breiman 2001) classification-tree approach to develop predictive models for 12 ecosite types, 5 of which we considered uplands (Table 3-1). Random forest is a powerful ensemble approach based on sophisticated bootstrap sampling and subsequent averaging of the data. It is widely used in vegetation mapping (Evans and Cushman 2009) and species distribution modelling (Iverson et al. 2004, Rehfeldt et al. 2006, Oppel and Huettmann 2010, Drew et al. 2011) due to its high predictive performance (Elith et al. 2006, Prasad et al. 2006, Syphard and Franklin 2009). Models were constructed in 64-bit R v. 3.1.3 (R Core Team 2014) using the ‘randomForest’ package (Liaw 2015). Since random forest is an ensemble model approach, performance was assessed according to out-of-bag (OOB) classification accuracy.

For prediction purposes (vs. model-building), we used 500-m resolution raster layers, even for variables originally sampled at a 100-m resolution, to improve speed and reduce storage requirements, given the boreal scale of the analysis and the focus on regional and landscape-level estimation rather than prediction at individual grid cells.

Because we assumed ecosites would not change state over the next century, we used predicted ecosite types, along with climate and terrain variables, as inputs to random forest models for 32 vegetation types (Table 3-1, Table 3-2). The terrain variables were included again at this stage to allow for local-scale terrain-driven variability within a given ecosite. For example, within the extensive medium-mesic ecosite, the probability of white spruce vs. aspen growth may be related to site exposure (e.g. landform and aspect), as well as temperature and precipitation. In contrast, geology and wetlands were considered first-order classifiers better suited to differentiating among ecosites.

Baseline and future projections of potential vegetation were based on 500-m resolution inputs, with ecosite type and terrain variables held constant while climate variables were based on historical normals (1961-1990) and GCM projections for three future time periods: 2011-2040, 2041-2070, and 2071-2100. Because local negative hydrologic feedbacks are likely to maintain peatland systems in a state of disequilibrium with climate for an unknown length of time (Terrier et al. 2015, Waddington et al. 2015), especially in

permafrost systems (Camill and Clark 2000), we held wetlands (i.e., hydric and hygric moisture classes) constant and only projected changes in upland types.

3.2.8 Fire and Vegetation Change Simulation

To model future fire, we used the Burn-P3 simulation model, which simulates the spatial ignition and growth of fires over multiple stochastic iterations (Parisien et al. 2005). Individual fires are simulated deterministically for one fire year using the Prometheus fire growth model (Tymstra et al. 2010), and this process is repeated for a large number of iterations using variable ignitions and weather. The Prometheus model calculates the growth of each fire based on fuels and terrain according to the Canadian Fire Behaviour Prediction (FBP) System (Forestry Canada Fire Danger Group 1992) and fire spread mechanisms (Richards 1995). We used fire weather data from Wang et al. (2015) and generated corresponding fuel inputs for four time periods: 1981-2000 (baseline), 2001-2030, 2031-2060, and 2061-2090. Only fires ≥ 200 ha were modelled (Parisien et al. 2005).

Although our study area is spatially extensive, we considered it all to be part of the Southern Prairies fire zone (Wang et al. 2014), as delineated by Boulanger et al. (2012), and we did not pursue further spatial stratification. Area burned and fire spread rates are intermediate for this zone in comparison with the northern Great Slave Lake zone (higher) and the Southern Cordillera zone (lower), which overlap the northern and southwestern portions of our study area, respectively. To inform topographic influences on fire spread, we used a 500-m digital elevation model corresponding with the resolution of our fuel inputs (Jarvis et al. 2008).

Each Burn-P3 model iteration represents one realization of parameters for one year of burning. Within this period, two fire seasons were defined to stratify the temporal variability in fire ignition and spread: spring (April 15 – May 24), and summer (May 25 – Sept 15). The start date of the spring season and the end date of the summer season correspond, on average, to the earliest and latest dates at which fires ≥ 200 ha occur. The start date of the summer season corresponds to green-up of broadleaf trees. The fire seasons were determined through summary explorations of fire weather and, in particular, of the distributions of fire numbers and area burned throughout the year. Percent grass curing (dry dead grass) was 80% for the spring season and 65% for the summer season. For both seasons, we assumed spatially random ignitions and 8 hours of potential fire growth per day.

Another Burn-P3 input is the frequency distribution of the number of sequential fire-spread days. A spread day represents a day when a non-negligible area is burned by the fire

and is usually associated with the presence of fire-conducive weather. We determined the FWI-based potential spread days in the baseline period and used the method of Wang et al. (2014) to convert potential (i.e., weather-based) spread days to realized (i.e., actual) days of fire spread via a simple linear regression. As part of the model calibration process, we smoothed and truncated the spread-day distribution at 13 days so that the resulting fire-size distribution and number of fires best matched the observed distribution from historical data.

Fuel inputs were based on our vegetation model, with vegetation types converted to fuel categories as defined by the FBP System, where each fuel type exhibits characteristic fire behavior depending on weather conditions and slope. For the 30-km buffer region required by Burn-P3 to avoid an edge effect, we used a fuel layer derived by reclassifying a national MODIS-based vegetation layer (Beaudoin et al. 2014) into FBP System fuel types (B. Simpson, Canadian Forest Service, unpubl. data). Fuel types can be broadly categorized as coniferous, deciduous, mixedwood, grass, and slash (the latter was not used). The coniferous fuel types are typically viewed as the most conducive to fire ignition and spread. The deciduous (D-1/2) and mixedwood (M-1/2) fuel types have a greater susceptibility to fire growth in the spring, before leaf flush, than later in the season. Fire spread potential in the grass (O-1) fuel type is also more flammable in the spring than in mid-summer because most of its biomass consists of dead material with very low moisture content during this season.

For the baseline period (1981-2010) and for 2001-2030, we used modelled fuels corresponding with historical climate normals from 1961-1990, which reflect the historical growing conditions for Alberta forests better than do current climate conditions. Other than for the static scenario (C), where historical fuels were held constant, we based fuel inputs for future periods on predicted vegetation conditions in an iterative manner (see workflow diagram in [Figure 3-2](#)). For the fire-mediated scenario (B1), fuel inputs to the 2031-2060 fire simulation were derived by updating the historical fuel layer according to the baseline fire simulation. Given the stochastic nature of Burn-P3, we randomly selected one model iteration to reflect each year in the 30-year period. Fire polygon outputs from 30 randomly-selected years were combined to represent the area burned within the baseline period ([Figure 3-3](#)). For these burned areas, we updated the fuels layer based on future projected vegetation for 2011-2040 climate conditions. Elsewhere, baseline fuels were retained. Together with other Burn-P3 inputs, these fuel modifications were the inputs for a single model run. This process was repeated 10 times to capture the stochastic variability across Burn-P3 iterations, and for vegetation projections from four different GCMs (listed in previous section), for a total of 40 runs x 300 iterations = 12,000 individual Burn-P3 iterations for the 2031-2060 time period.

The same process was repeated for inputs to the 2061-2090 fire simulations, with fuels for areas burned in the mid-century (2031-2060) runs updated according to projected 2041-2070 vegetation. Simulated fires from the end-of-century (2061-2090) runs were used to update the mid-century fuels according to 2071-2100 vegetation for areas burned, again for 10 replicates and four GCMs, for a total of 40 additional runs. See [Figure 3-2](#) for workflow diagram.

For the fire- and anthropogenic disturbance-mediated scenario (B2), we repeated the same sequence of methods but also updated fuels based on ALCES anthropogenic disturbance projections (see previous section) for the same time periods as the fire simulations. That is, estimated and projected disturbances from 2001-2030 were combined with 2001-2030 fire simulations to identify disturbed areas where vegetation was updated to reflect corresponding future climate conditions. We did not explicitly factor anthropogenic disturbance into Burn-P3 simulations, given that most disturbances reflected temporary disturbances such as timber harvest, where climatically suitable vegetation should regenerate over time, and effects of cutblocks and seismic lines on burn probability have not been shown to be considerable (Arienti et al. 2006, Krawchuk and Cumming 2011). We considered all industrial development to be renewable even though restoration times may in fact exceed the time frame of this study. The relatively small direct footprint of energy sector development, in comparison with timber harvest and fire, suggested that more realistic regeneration assumptions would not have a discernible influence on results. For the climate-driven scenario (A), fuel inputs were based on climate-based future vegetation projections, assuming that changes in temperature and moisture conditions would be sufficient to initiate vegetation change, generally consisting of the loss of first the coniferous and then the deciduous component of a forest due to drought stress.

This resulted in a total of 255 runs: 3 runs for scenario C, 120 runs (4 GCMs x 10 replicates x 3 time periods) for scenario B1, 120 runs for scenario B2, and 12 runs for scenario A (4 GCMs x 3 time periods). To compare pixel-level burn probability across these four scenarios, we standardized to each to 3,000 iterations per GCM and time period, based on Scenarios B1 and B2, where 10 fuel realizations at 300 iterations each = 3,000 iterations total. For scenarios A, B1, and B2, we had 4 GCMs x 3 time periods x 3,000 iterations for a total of 36,000 iterations each. For scenario C, we had 3 time periods x 3,000 iterations for a total of 9,000 iterations. Thus we simulated a total of 117,000 individual iterations (fire years).

3.2.9 *Fire and Forest Change Analysis*

Projected changes in area burned were evaluated at the 500-m pixel level by calculating the proportion of individual Burn-P3 iterations for which a given pixel was burned within a given time period, and for a given scenario and GCM (scenarios A, B1 and B2 only). For disturbance-mediated scenarios (B1 and B2) we combined results from 300 iterations for each of 10 fuel iterations, resulting in a total of 3,000 iterations. For scenarios A and C we used 3,000 iterations for each time period (and for each GCM in the case of scenario A).

To assess the influence of different sources of variation on simulated burn probability, we sampled a 20-km regular grid of 896 points within the study area and used a full-factorial three-factor ANOVA to partition the variance among the effects of time period, fuel scenario (A, B1, and C), GCM, and residual spatial variation on change in burn probability (difference between baseline and future period). To evaluate the relative contribution of anthropogenic disturbance, we also included scenario B2 (fire + anthropogenic disturbance) in an unbalanced ANOVA using type II sums of squares (Langsrud 2003) with the ‘car’ package for R (Fox and Weisberg 2011).

Projected changes in upland vegetation composition for each scenario were assessed based on a summarization of generalized cover types—grassland, deciduous woodland, mixedwood forest, and coniferous forest (Table 3-1)—by time period and GCM. For scenarios B1 and B2, results were averaged over 10 fuel iterations per time period and GCM.

To assess the importance of different sources of variation in the magnitude of projected changes in vegetation, we conducted a series of ANOVAs with change (compared to baseline) in upland forest area (in km²) by cover type and as the dependent variables, and year, GCM, and scenario as independent variables ($n = 252$). We also included the effect of anthropogenic disturbance and fuel iteration (stochasticity) in the disturbance-mediated scenarios (B1 and B2). We ran an unbalanced ANOVA using type II sums of squares (Langsrud 2003) with the ‘car’ package for R (Fox and Weisberg 2011).

Projected changes in forest age structure were approximated by time-since-fire calculations from 3,000 Burn-P3 runs based on current baseline vegetation and fire weather conditions for each future time period (scenario C). Beginning with an arbitrary baseline age of 300 years, fire polygons resulting from individual Burn-P3 simulations were randomly selected in a sequential manner and used to update vegetation age on an annual basis. That is, the age of each pixel was reset to 0 each time it fell within a simulated fire polygon. The

simulated age distribution was calculated for current areas of upland forest within the study area.

3.3 Results

3.3.1 Ecosite Models

Random forest models for 12 ecosite classes had an out-of-bag (OOB) error rate of 38% (accuracy = 62%). The lowest classification error (11%) was for the medium mesic (MM) upland ecosite type, which was predicted to comprise 50% of the province, including urban and agricultural areas (Table 3-3). The highest classification error (100%) was for the marsh (VG) wetland ecosite type, which had only 26 records and could not be differentiated from other wetland ecosite types. The large majority of misclassified records were correctly classified by either moisture or nutrient status. The OOB error rate for upland vs. wetland classes was 20%. For specific moisture class it was 28% and for nutrient class it was 27%.

The most important explanatory variable in terms of decrease in accuracy was the wetland class variable, followed by growing degree days less than 18 C, surficial geology, summer heat:moisture ratio, and annual heat:moisture ratio (Table 3-2). Predicted ecosite classes are shown in Figure 3-4.

3.3.2 Vegetation Models

Random forest models for 40 vegetation types had an OOB error rate of 19% (accuracy = 81%), with error rates for individual vegetation types ranging from 0% (medium-mesic grassland, rich-mesic grassland, poor-hygic black spruce, poor-hydric black spruce/larch) to 71% (poor-hydric shrub) (Appendix 3-A). Combining vegetation types by FBP System fuel type, the average prediction accuracy was 89% (Table 3-4).

The most important explanatory variable by far in terms of decrease in accuracy was the ecosite class variable, followed by growing degree days less than 18 °C, annual heat:moisture ratio, and summer heat:moisture ratio (Table 3-2). Predicted vegetation classes are shown in Figure 3-5.

3.3.3 Predicted Ecosites and Vegetation

According to our random forest model, 52% of Alberta was predicted to be composed of vegetated natural upland ecosites, after masking out water, agricultural and developed areas, and rocks and ice. Within our study area, 57% (247,895 km²) was composed of vegetated natural uplands and 28% (123,112 km²) was natural wetlands. Of the natural uplands, 83.5% were predicted to be medium-mesic ecosites. Predicted upland vegetation

within the study area amounted to 26.5% conifer, 64.3% boreal mixedwood, 9.0% deciduous, and less than 0.1% grassland. Predicted current and future areas of all upland and wetland ecosite types within the study area are given in [Appendix 3-B](#).

3.3.4 Fire Simulation

Across all scenarios, annual burn probability within the study area increased significantly over time with the frequency of severe fire weather, but with diminishing rates of increase toward the end of the century ([Figure 3-6](#), [Figure 3-7](#)). Scenarios were similar through mid-century, but diverged during the last 30-year period (2061-2090), when burn probability was highest in the climate-driven scenario (C), followed by the static vegetation scenario (A) and the disturbance-mediated scenarios.

The largest source of variation in burn probability was scenario, followed by spatial variation, the interaction between scenario and time period, and time period ([Table 3-5](#)). Other sources of variation were negligible.

3.3.5 Forest Composition

Under the climate-driven change scenario (A), dramatic changes in vegetation types were projected for the next century ([Figure 3-8](#)), with a 198,000-km² increase in grassland area projected by the end of the century on average across GCMs. Climatic potential for upland conifer, mixedwood forest, and deciduous woodland was projected to decrease by ~44,000 km² (67%), ~153,000 km² (96%), and ~5,000 km² (18%) on average, respectively, by the end of the century ([Figure 3-9](#)). Grassland potential increased and mixedwood potential decreased fairly steadily across GCMs, whereas conifer and deciduous projections fluctuated more and were less consistent across GCMs. Most of the upland conifer decline consisted of white spruce, whereas jack pine and lodgepole pine decreases were less dramatic ([Appendix 3-B](#)). Wetland vegetation types were held constant by design and thus did not change. As a function of this, there was little opportunity for upslope or northward movement of upland conifer vegetation types. Instead, change in conifer and mixedwood vegetation types was primarily a matter of contraction in area.

Vegetation projections from the disturbance-mediated scenarios were much less extreme in comparison to the climate-driven scenarios ([Figure 3-9](#)). For the fire-only disturbance-mediated scenario (B1), upland conifer and mixedwood forest were projected to decrease by ~8,200 km² (13%) and ~56,000 km² (35%) on average ([Figure 3-9](#)). Deciduous woodland and grassland were projected to increase by ~19,000 km² (83%) and ~45,000 km² on average. Spatial patterns, averaged over multiple GCMs and fuel iterations, indicated

the greatest likelihood of conifer and mixedwood forest loss in the central and foothill portion of the province, greatest deciduous forest gain in the west-central portion of the province, and greatest grassland gain in the foothills and central province (Figure 3-10).

The largest source of variation in the area of projected upland conifer cover was GCM, followed by time period and the interaction between scenario and time period (Table 3-5). For mixedwood forest, the largest source of variation was scenario, followed by time period. For deciduous forest, the largest source of variation was the interaction between scenario and time period, followed by GCM and time period. Finally, for grassland, the largest source of variation was time period, followed by scenario and the interaction between time period and scenario (Table 3-5). Other sources of variation were relatively small.

3.3.6 Forest Age

Forest age structure was projected to change over time under the static vegetation scenario (C) (Figure 3-11), with simulated median forest age decreasing from 126 years during the baseline period to 101 years during the 2061-2090 period (Table 3-7). The addition of anthropogenic disturbance reduced the median age from 130 to 126 during the 2031-2060 period and from 105 to 98 during the 2061-2090 period.

3.4 Discussion

The speed at which ecosystems will respond to climate change within upcoming decades is a subject of great importance for climate-change adaptation and planning, yet still subject to great uncertainty. We used a novel hybrid modelling approach based on topographically constrained projections of climate-driven vegetation change potential, coupled with weather- and fuel-based simulations of future wildland fire behavior, to address this issue for upland forests in Alberta.

As has been suggested previously (Schneider et al. 2009), our simulations highlighted that climate-driven changes in upland boreal forest vegetation could be substantially delayed if disturbance is necessary to initiate vegetation transitions. Nevertheless, we found that an approximate one-third reduction in the area of mixedwood and conifer forest, accompanied by an increase in deciduous woodland and grassland, should be anticipated at minimum by 2090. This should be considered an underestimate, in that continued future increases in drought-induced tree mortality and limited regeneration will likely result in reduced forest biomass (Girardin et al. 2008) and increased drought-induced tree mortality (Allen et al. 2010, Allen et al. 2015, Zhang et al. 2015), further facilitating ecosystem transitions independent of disturbance.

We observed a projected increase in average burn probability and total area burned over time, consistent with several other boreal studies (Tymstra et al. 2007, Girardin and Mudelsee 2008, Balshi et al. 2009, Krawchuk et al. 2009, Wotton et al. 2010), but also a diminishing rate of increase in burn probability over time for the disturbance-mediated scenarios. This slowdown in fire increase, despite steady increases in extreme fire weather conditions (Wang et al. 2015), partly reflects the importance of vegetation composition (i.e., fuels) to the projection of future wildfire occurrence and spread. Our fuel-dependent wildfire simulations suggest a negative feedback process by which a warmer climate and more extensive near-term fires will lead to an increase in deciduous forest (dominated by trembling aspen, *Populus tremuloides*) that in turn, due to its relatively low flammability, will lead to a long-term reduction in area burned (Terrier et al. 2012). Within the 90-year timeframe that we evaluated, we observed a slower rate of increase, but not a reduction, in average burn probability for the disturbance-mediated scenarios. In our simulations, the large increase in extreme fire weather more than compensated for the gradual reduction in fuel flammability.

As expected, we found that burn probabilities were projected to increase in warmer future climates under a static fuels scenario. However, somewhat surprisingly, we also observed a larger increase in burn probability under the more extreme climate-driven fuel change scenario. This is in contrast with Wang et al. (in press), who found a projected decrease in burn probability over time in the western interior forests of British Columbia, Canada, where increases in fire-conducive weather were modest in comparison with the reduction in fuel flammability. In our study, the increase was apparently driven by the rapid climatic transition to grasslands, which, despite low biomass, provide highly flammable fuels when dry, sometimes referred to as “flashy” fuels. Their contiguous projected future climatic suitability, uninterrupted by low-flammability deciduous forest (Parisien et al. 2011b), suggests that in the absence of fire suppression, eventual grassland vegetation could experience greater rates of fire than parts of the current boreal forest mosaics. Possible current analogs may be found in highly flammable grass-dominated pine forests of the interior western United States (e.g., Idaho and Montana), but such a comparison requires further investigation.

For the static fuel scenario, we found a change in age distribution and a 25-year decrease in median age by 2090, which can be attributed to increases in the annual area burned. The inclusion of projected future anthropogenic disturbance, via industrial development, resulted in an additional 6-year reduction in median forest age by mid-century. The projected loss of old forest has the potential to result in a reduced timber supply

(Bergeron et al. 2006), but also population bottlenecks for late-successional wildlife species, depending on their degree of habitat specialization and capacity for rapid distribution shifts.

Our focus was on upland vegetation, due in part to the additional complexities associated with wetland hydrologic feedbacks (Waddington et al. 2015), and the additional lags expected in these systems (Camill and Clark 2000), especially where permafrost degradation results in additional organic matter deposition (Vitt et al. 2000). Although long-term peatland drying trends (Yu et al. 2003) and shallow peatland depths (Bauer et al. 2003) in some areas suggest that wetland loss could be more imminent, we found that the associated short-term uncertainties were too great to consider in this analysis. Furthermore, upland forests contain most of the merchantable timber and are therefore subject to a larger human footprint, via forestry; they also contain a greater diversity of boreal songbirds compared to wetlands (Mahon et al. 2016). Our generalized ecosite modelling approach allowed us to discriminate among these fundamentally different ecosystems and thereby generate more realistic projections for upland forest types. Although we modelled a finer level of vegetation detail than was presented herein, the thematic resolution was necessary to identify the most appropriate fuel classes, and can also be used to develop more refined projections for forest songbirds and other organisms with variation among ecosite types.

Based on our assumptions, we found that upslope migration of upland conifer and mixedwood forest was constrained by large permafrost wetland complexes at higher elevations (Schneider et al. 2015), although some mixedwood refugia persisted. Thus, in the absence of large-scale rapid permafrost melt and drying of peatlands, upland conifer and mixedwood species may rely heavily on latitudinal shifts into the Northwest Territories and Yukon Territory. The large climate velocity associated with such long-distance shifts may prove challenging for dispersal-limited species (Loarie et al. 2009, Carroll et al. 2015). Thus, in contrast with the traditional paradigm of faster rates of climate-change response on the leading edge of species' distributions where competition is reduced (Ordonez and Williams 2013), the situation may be reversed in the western boreal region. That is, northern and elevational shifts are constrained by wetlands that are likely to persist longer than upland habitats. Meanwhile, southern margins along the boreal-grassland ecotone are most vulnerable to changes in available moisture and associated tree mortality. Thus, retreats along the southern edge may happen faster than advances along northern margins. Long-term monitoring projects are critical to evaluating these rates of change. If wetlands do indeed persist in their current locations, our simulations suggest a novel landscape juxtaposition of

peatlands surrounded by deciduous forest and eventually grasslands over the next century, as discussed by Schneider et al. (2015).

In terms of the influence of natural vs. anthropogenic disturbance (primarily timber harvest), we found that simulated future fires encompassed much greater areas than those subject to anthropogenic disturbance. Although the two disturbance types may result in quite different short-term wildlife communities (Hobson and Schieck 1999, Schieck and Song 2006), our simulations suggest that wildfire in conjunction with climate change will be the largest agent of future change in the boreal forest, especially beyond mid-century. This provides a new perspective for addressing the cumulative effects of human activities on biodiversity, which has generally not previously considered climate change, given the global scale of emissions management and mitigation activities (Burton et al. 2014). However, the relative magnitude of ecosystem change anticipated in direct or indirect response to climate change highlights the need to incorporate this major driver into cumulative effects assessment and monitoring (Bayne et al. 2015).

Our results suggest significant variation in expected vegetation due to GCM, but consistent with other boreal modelling studies (Stralberg et al. 2015b), we did not find this uncertainty greater than the magnitude of expected change. Although we only used one intermediate GCM to drive the Burn-P3 fire simulation, the negative feedback in burn probability that we observed suggests that, although more extreme fire weather conditions would result in more fires early on, changes in fuel flammability could also result in a more rapid negative feedback loop. Additional exploration of sensitivities and thresholds related to this negative feedback loop should be explored in future simulation studies.

3.4.1 Caveats and limitations

Our disturbance-mediated scenarios were relatively conservative in that our industrial development projections only went through 2060, and anthropogenic disturbance was only considered when it affected an area of at least 3.13 km² (half of a 2.5-km x 2.5-km pixel)—but then rounded up to the nearest 6.25 km² pixel. Thus the influences of small-scale disturbances such as linear features were not considered. Furthermore, we considered all disturbances renewable even though many, e.g., mines and wells, are not likely to regenerate to pre-disturbance conditions within the timeframe of this study. We also allowed spatial and temporal overlap of fire and anthropogenic disturbance in our simulations, which likely resulted in an underestimation of the total disturbance footprint, to the extent that land-use activities would be shifted elsewhere rather than overlapping with recent fires.

With respect to Burn-P3 parameterization, our use of a single climate zone meant that spatial patterns of burn probability were de-emphasized, which likely resulted in an overestimation of fires in the Rocky Mountain foothills, and an underestimation in Northern Alberta. To a lesser extent, our use of static “buffer” fuels around the perimeter of the study area may also have resulted in a disproportionately large number of simulated fires occurring outside of the study area, given that mapped buffer fuels in Saskatchewan were generally more flammable than modelled adjacent Alberta fuels, and were assumed to remain that way in the future. In addition, our parameterization of the fire season reflects current conditions and is likely to change in the future; a longer fire season could increase area burned, although this would be partially offset by earlier deciduous leaf flush and thus little overall increase in burn probability of deciduous forest once that forest type begins to dominate.

There was one aspect, however, in which our projections may have been too extreme: the potential for novel climates to affect climate-change projections in the Rocky Mountain foothills and central highlands. Our vegetation model projects a large conversion to grasslands within this region, as do other models specific to Alberta or western North America (Schneider et al. 2009, Mbogga et al. 2010). Yet future climate projections suggest that it will retain a moisture surplus in the future (Schneider et al. 2003); thus an increase in temperature may not result in a conversion to the grassland systems found in warmer portions of Alberta. Other continental-scale analyses suggest that the foothills climate regime could actually more closely resemble that of eastern deciduous forests in terms of vegetation (Rehfeldt et al. 2012) and passerine birds (Stralberg et al. 2015b), but with a high probability that future conditions will have no contemporary analog (Rehfeldt et al. 2012).

3.4.2 Conclusion

While climate-change uncertainty is formidable, the ability to anticipate future change trajectories will be invaluable to climate-change adaptation and conservation planning efforts. Model generality and simplicity are prized in many circumstances. However, the magnitude and scope of anthropogenic climate change, along with the potential for non-analog conditions and prolonged states of disequilibrium, suggests the need for novel, hybrid modelling approaches that address critical local dynamic processes while considering a spatial scale broad enough to capture the range of anticipated future variability (Gustafson 2013). We have developed such an approach for the western boreal region, where it is impossible to consider future climate change in isolation from wildfire, and where topographic legacies have major influences on biota that are not captured with equilibrium

climate models. Our ecosite-based model provides a more realistic view of potential future vegetation in boreal Alberta. Our simulation of individual fire perimeters, combined with comprehensive spatial land-use projections, provides a realistic estimation of future opportunities for large-scale vegetation changes to occur. In light of these constraints, we conservatively concluded that at least one-third of Alberta's upland mixedwood and conifer forest is likely to be replaced by deciduous woodland and grassland by 2090, with a disproportionate loss of both young and old forest classes. Our results provide spatial and temporal refinement of future vegetation change projections, and suggest a template that can be applied to other systems and regions.

3.5 Appendices

[Appendix 3-A](#). Confusion matrix for random forest vegetation predictions.

[Appendix 3-B](#). Vegetation type projections by GCM for scenarios A, B1, B2

3.6 Tables

Table 3-1. Ecosite and vegetation types considered.

FBP = Canadian Forest Fire Behavior Prediction System fuel type for input to Burn-P3.

O = grass fuel; D = deciduous fuel; M = boreal mixedwood fuel; C = conifer fuel. Codes with

* were patched in post-hoc based on remotely sensed 2000 landcover (ABMI 2014).

Code	Ecosite	Vegetation Description	FBP	Cover Type	Upland	Forest
1	PX	Poor-Xeric Grassland	O-1	Grassland	1	0
2	PX	Poor-Xeric Jack Pine	C-1	Conifer	1	1
3	PM	Poor-Mesic Grassland	O-1	Grassland	1	0
4	PM	Poor-Mesic Pine	C-3	Conifer	1	1
5	PM	Poor-Mesic Black Spruce	C-2	Conifer	1	1
6	PG	Poor-Hygric Black Spruce	C-2	Conifer	0	1
7	PD	Poor-Hydric Black Spruce / Larch	C-1	Conifer	0	1
8	PD	Poor-Hydric Shrub	O-1	Shrub	0	0
9	MX	Medium-Xeric Grassland	O-1	Grassland	1	0
10	MX	Medium-Xeric Aspen Mix	M-1/2	Mixedwood	1	1
11	MX	Medium-Xeric Pine	C-1	Conifer	1	1
12	MX	Medium-Xeric Spruce	C-1	Conifer	1	1
13	MM	Medium-Mesic Grassland	O-1	Grassland	1	0
14	MM	Medium-Mesic Aspen	D-1/2	Deciduous	1	1
50	MM	Medium-Mesic Boreal Aspen	M-1/2	Mixedwood	1	1
15	MM	Medium-Mesic Aspen Mix	M-1/2	Mixedwood	1	1
16	MM	Medium-Mesic Pine	C-3	Conifer	1	1
17	MM	Medium-Mesic Pine Mix	C-3	Conifer	1	1
18	MM	Medium-Mesic White Spruce	C-2	Conifer	1	1
19	MG	Medium-Hygric Grassland	O-1	Grassland	0	0
20	MG	Medium-Hygric Poplar Mix	M-1/2	Deciduous	0	1
21	MG	Medium-Hygric Spruce Mix	C-2	Conifer	0	1
22	MG	Medium-Hygric Black Spruce Mix	C-2	Conifer	0	1
25	MD	Medium-Hydric Shrub Fen	O-1	Shrub	0	0
26	MD	Medium-Hydric Black Spruce Fen	O-1	Conifer	0	1
27	RM	Rich-Mesic Grassland	O-1	Grassland	1	0

Code	Ecosite	Vegetation Description	FBP	Cover Type	Upland	Forest
28	RG	Rich-Hygric Shrubland	O-1	Shrub	0	0
29	RG	Rich-Hygric Poplar	D-1/2	Deciduous	0	1
30	RG	Rich-Hygric Lodgepole Pine	C-3	Conifer	0	1
31	RG	Rich-Hygric Spruce	C-2	Conifer	0	1
32	RD	Rich-Hydric Grass Fen	O-1	Grassland	0	0
33	RD	Rich-Hydric Shrub Fen	O-1	Shrub	0	0
34	RD	Rich-Hydric Black Spruce	O-1	Conifer	0	1
35	SD	Marsh	nonfuel	Grassland	0	0
39*	OW	Open Water	nonfuel	None	0	0
41*	AG	Agriculture	nonfuel	None	1	0
42*	UR	Urban	nonfuel	None	1	0
43*	NF	Other Non-Fuel	nonfuel	None	1	0

Table 3-2. Climate, terrain, geology, and wetland variables included in random forest models for ecosite and vegetation.

Variable importance values according to mean decrease in prediction accuracy (higher values = higher importance).

Variable	Definition	Ecosite	Vegetation
ahm	annual heat:moisture ratio	89.73	72.89
shm	summer heat:moisture ratio	93.74	70.00
ddl18	degree days < 18 °C	98.79	73.26
msh	mean summer (May-Sep) precipitation	84.26	69.57
td	temperature difference (summer – winter)	86.39	69.10
emt	extreme minimum temperature	88.66	63.50
slpasp	slope / aspect solar radiation index	47.39	54.85
tpi2km	topographic position index (2-km radius)	65.25	57.42
vrml1x11	vector ruggedness measure (11 x 11 cells)	49.93	58.07
cti	compound topographic index (wetness)	38.10	36.81
slope	slope	49.61	-
landform	landform	31.17	-
geol_surf	surficial geology (parent material)	94.22	-
wetlands	wetland type	107.14	-
ecosite	ecosite type	-	182.43

Table 3-3. Confusion matrix for ecosite classification model.

Upland (X = xeric, M = mesic) grouped separately from lowland (G = hygric, D = hydric) moisture classes. Nutrient class definitions: P = poor, M = medium, R = rich. See [Table 3-1](#) for full ecosite code definitions. Upland classes in bold.

	PX	PM	MX	MM	RM	MG	MD	PG	PD	RG	RD	SD	Class Error
PX	224	54	5	128	0	1	4	0	5	1	6	0	0.48
PM	39	520	5	402	1	11	28	22	63	7	22	0	0.54
MX	13	16	90	29	0	10	6	0	7	1	2	0	0.61
MM	39	127	12	3555	0	69	26	17	43	83	31	0	0.11
RM	0	0	0	12	27	0	0	0	0	0	0	0	0.31
MG	2	31	10	360	1	263	17	9	11	19	40	0	0.66
MD	7	39	0	80	0	11	235	36	58	2	85	0	0.58
PG	1	25	0	94	0	6	60	172	40	6	26	1	0.61
PD	9	73	1	125	0	10	33	33	368	7	34	0	0.51
RG	1	11	0	481	0	16	3	6	11	308	20	0	0.64
RD	9	36	1	102	0	28	72	20	45	11	337	0	0.49
SD	0	0	0	5	0	0	3	5	1	1	11	1	1.00

Table 3-4. Confusion matrix for vegetation classification model, grouped by fuel type.

See [Table 3-1](#) for fuel code correspondence with vegetation types. C-1, C-2 and C-3 represent conifer fuels. D-1/2 is deciduous, M-1/2 is mixedwood, and O-1 is grassland. The only nonfuel vegetation type modelled was marsh (SD).

	C-1	C-2	C-3	D-1/2	M-1/2	O-1	Nonfuel	Class Error
C-1	817	3	0	0	12	15	0	0.04
C-2	5	702	72	16	75	19	0	0.21
C-3	0	46	431	2	38	12	0	0.19
D-1/2	0	41	6	665	25	0	0	0.10
M-1/2	12	156	102	19	1724	5	1	0.15
O-1	5	11	1	1	3	1422	0	0.01
Nonfuel	0	0	0	0	0	0	4	0.00

Table 3-5. Variance partitioning of projected burn probability.

Proportional variance contributions for projected change in burn probability, based on 896 sample points at 20-km intervals. Change in burn probability = difference between baseline and a given time period: 2001-2030, 2031-2060, 2061-2090. (a) Full-factorial three-factor ANOVA with three future time periods, three scenarios, and four complementary global climate models (GCM). Scenarios considered: A = Climate-driven; B = disturbance-mediated; C = static vegetation. (b) Unbalanced ANOVA with additional anthropogenic disturbance factor.

Variance Component	(a)	(b)
Time Period	0.107	0.113
Scenario	0.399	0.377
GCM	0.001	0.000
Scenario*GCM	0.001	0.001
Scenario*Time	0.203	0.210
GCM*Time	0.001	0.002
Scenario*GCM*Time	0.002	0.002
Anthro	N/A	0.000
Remaining	0.286	0.302

Table 3-6. Variance partitioning of projected upland vegetation cover type.

Proportional variance contributions for projected change in total upland vegetation cover within study area. Change in vegetation by cover type = difference in area between baseline and a given time period: 2001-2030, 2031-2060, 2061-2090. Scenarios considered: A = Climate-driven; B = disturbance-mediated. GCM = global climate model (four considered). Anthro = effect of anthropogenic disturbance in disturbance-mediated scenario (B2 vs B1). Stochasticity = variability in Burn-P3 fuel realizations.

Variance Component	Conifer	Mixedwood	Deciduous	Grassland
Time Period	0.295	0.432	0.194	0.389
Scenario	0.049	0.477	0.030	0.377
GCM	0.312	0.051	0.254	0.055
Scenario*GCM	0.063	0.005	0.027	0.022
Scenario*Time	0.170	0.006	0.269	0.112
GCM*Time	0.036	0.001	0.076	0.016
Scenario*GCM*Time	0.044	0.014	0.104	0.016
Anthro	0.001	0.001	0.000	0.001
Stochasticity	0.000	0.000	0.001	0.000
Remaining	0.029	0.012	0.045	0.012

Table 3-7. Simulated changes in median upland forest stand age within study area.

Age distributions approximated by time-since-fire calculations from 3,000 Burn-P3 runs based on current baseline vegetation (scenario C) and fire weather conditions for each future time period. 25th and 75th percentile values shown in parentheses.

Year	Fire only	Fire + Anthropogenic
2010	126 (46, 285)	N/A
2030	130 (54, 269)	126 (48, 266)
2060	105 (47, 216)	98 (38, 215)
2090	101 (45, 218)	N/A

3.7 Figures

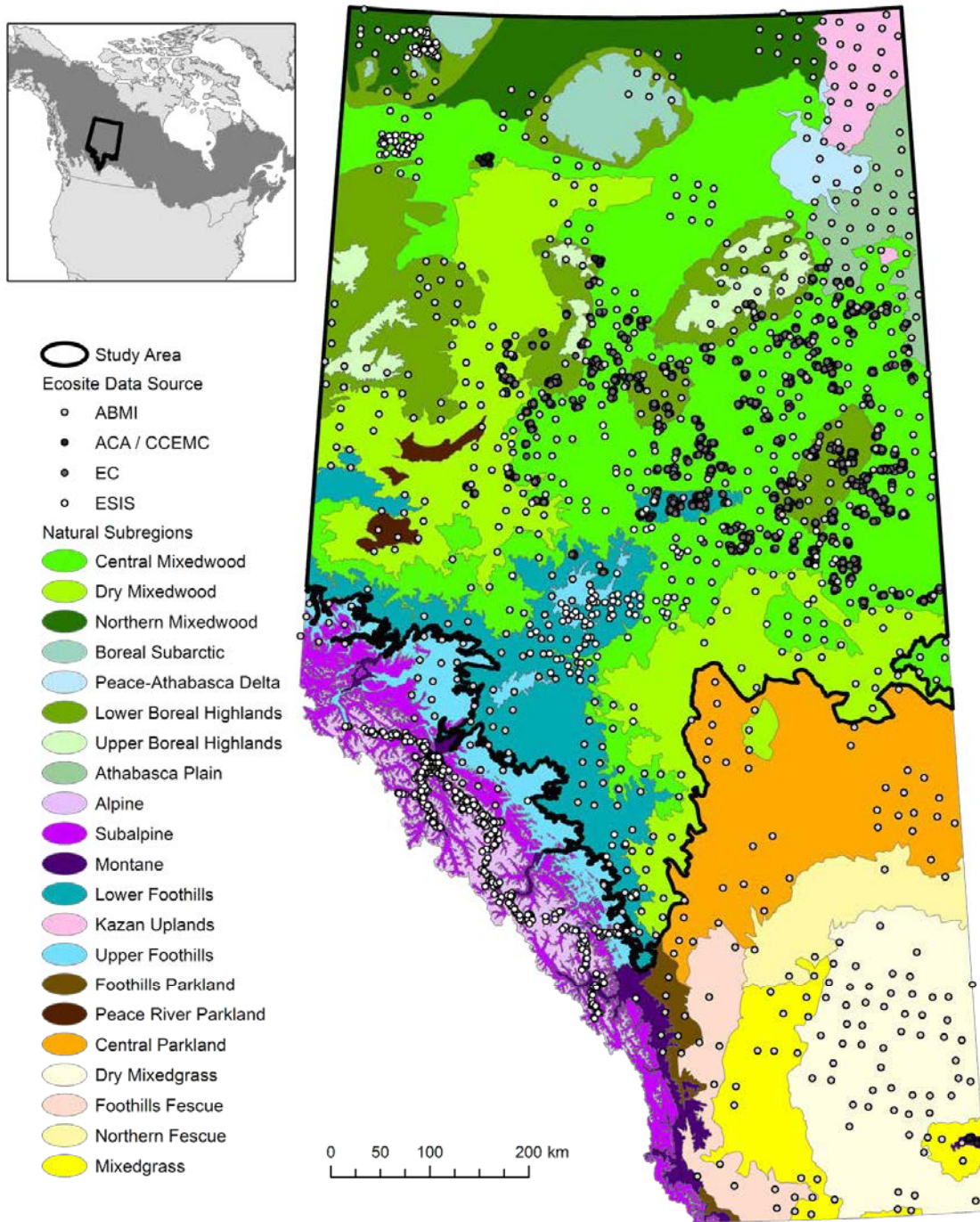
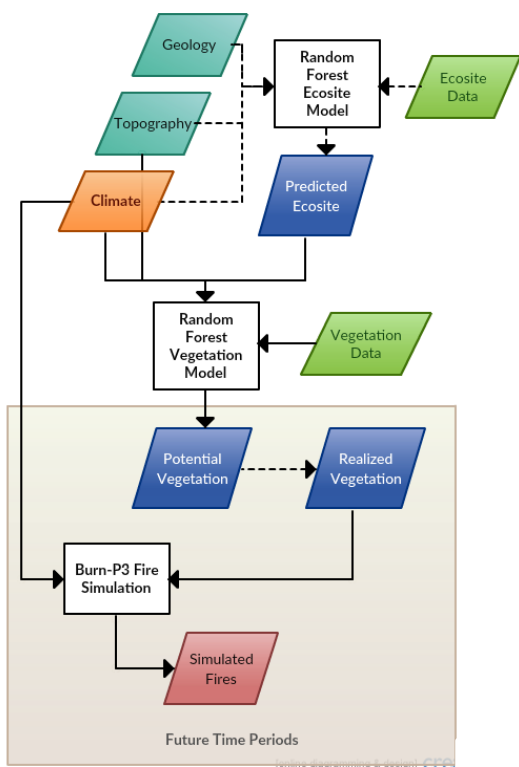
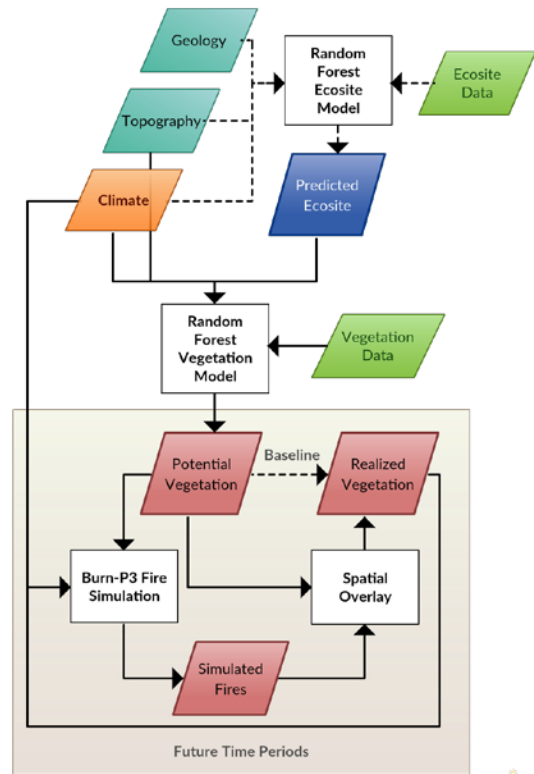


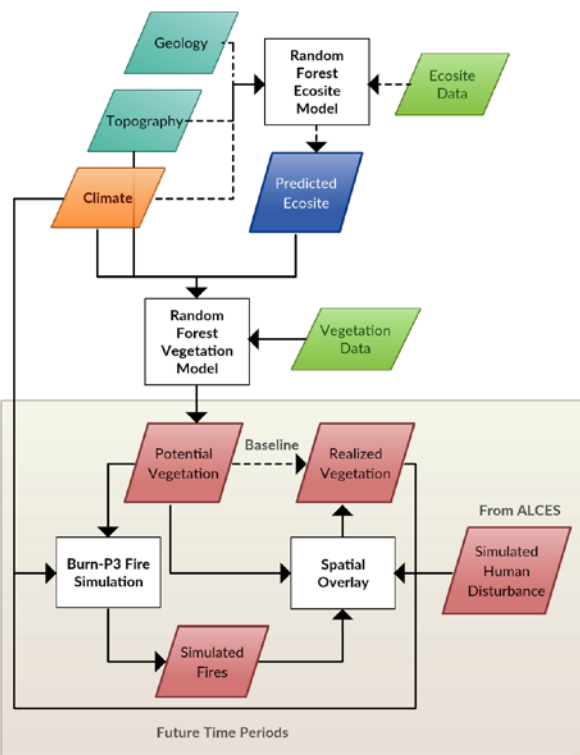
Figure 3-1. Study area and data locations with data source / project funding information. ABMI = Alberta Biodiversity Monitoring Institute; ACA = Alberta Conservation Association; CCEMC = Climate Change Emissions Management Corporation; EC = Environment Canada; ESIS = Ecological Site Information System



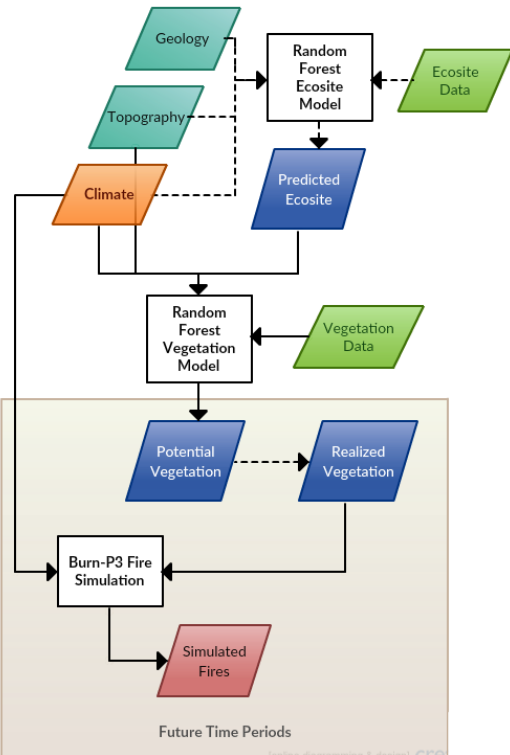
A



B1



B2



C

Figure 3-2. Workflow diagram for modelling process.

Scenario A = climate-driven, B1 = fire-mediated; B2 = fire- and anthropogenic disturbance-mediated; C = static vegetation. Green parallelograms represent point-level data inputs; turquoise parallelograms are static raster data inputs; orange parallelograms are dynamic raster data inputs; blue parallelograms are static raster data outputs; red parallelograms are dynamic raster data outputs. White boxes are model processes. The elements outside the brown box represent the ecosite and vegetation modelling components of the modelling process; the elements within the brown box represent the iterative fire simulation and vegetation update components, which are repeated for three time periods: 2001-2031, 2031-2060, and 2061-2090.

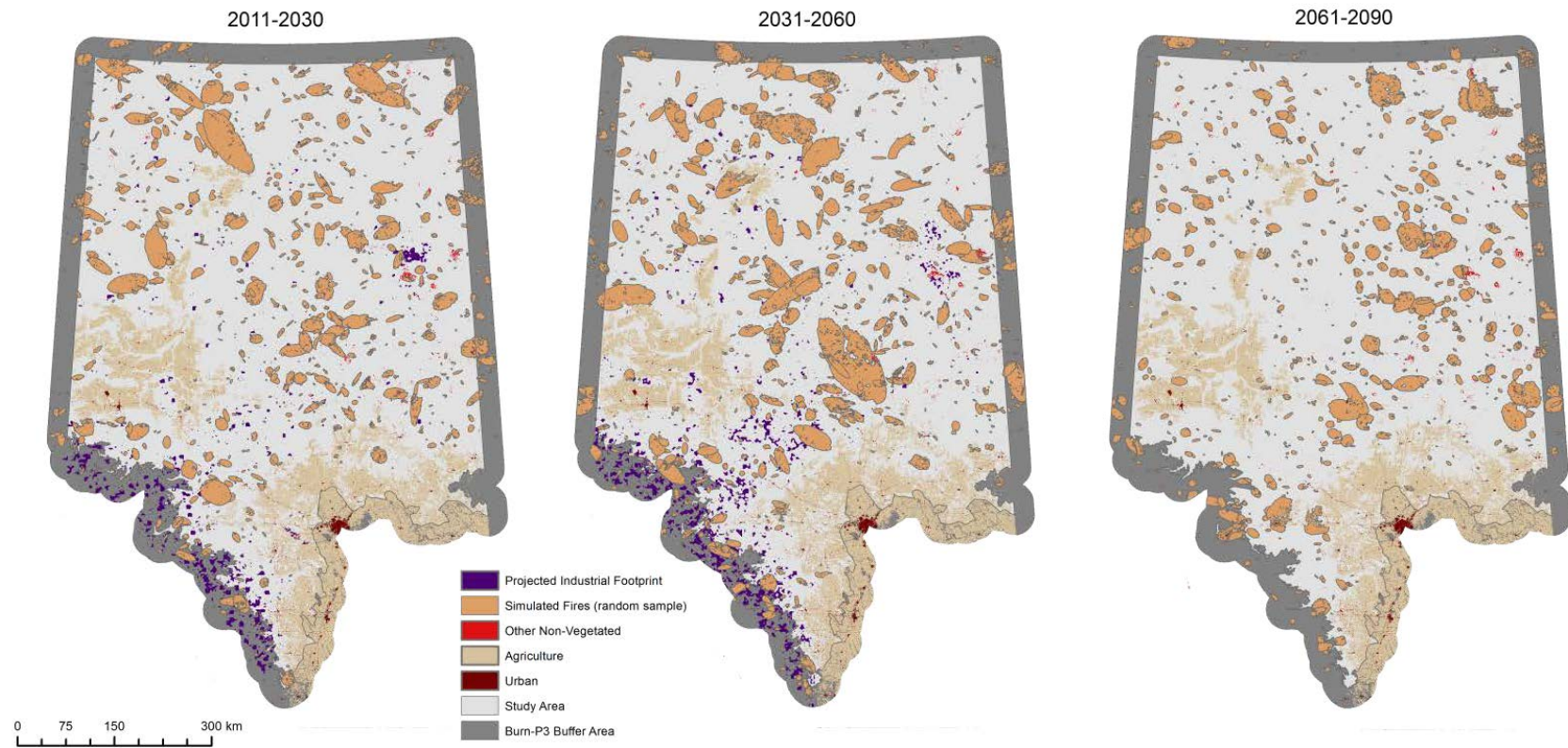


Figure 3-3. Disturbance footprints, study area, and Burn-P3 buffer area.

Anthropogenic disturbance projections (Carlson et al. 2014) were only available through 2060. Burn-P3 simulated fires represent a random sample for a single fuel realization (10 total) and for a single GCM (MPI ECHAM5, four total).

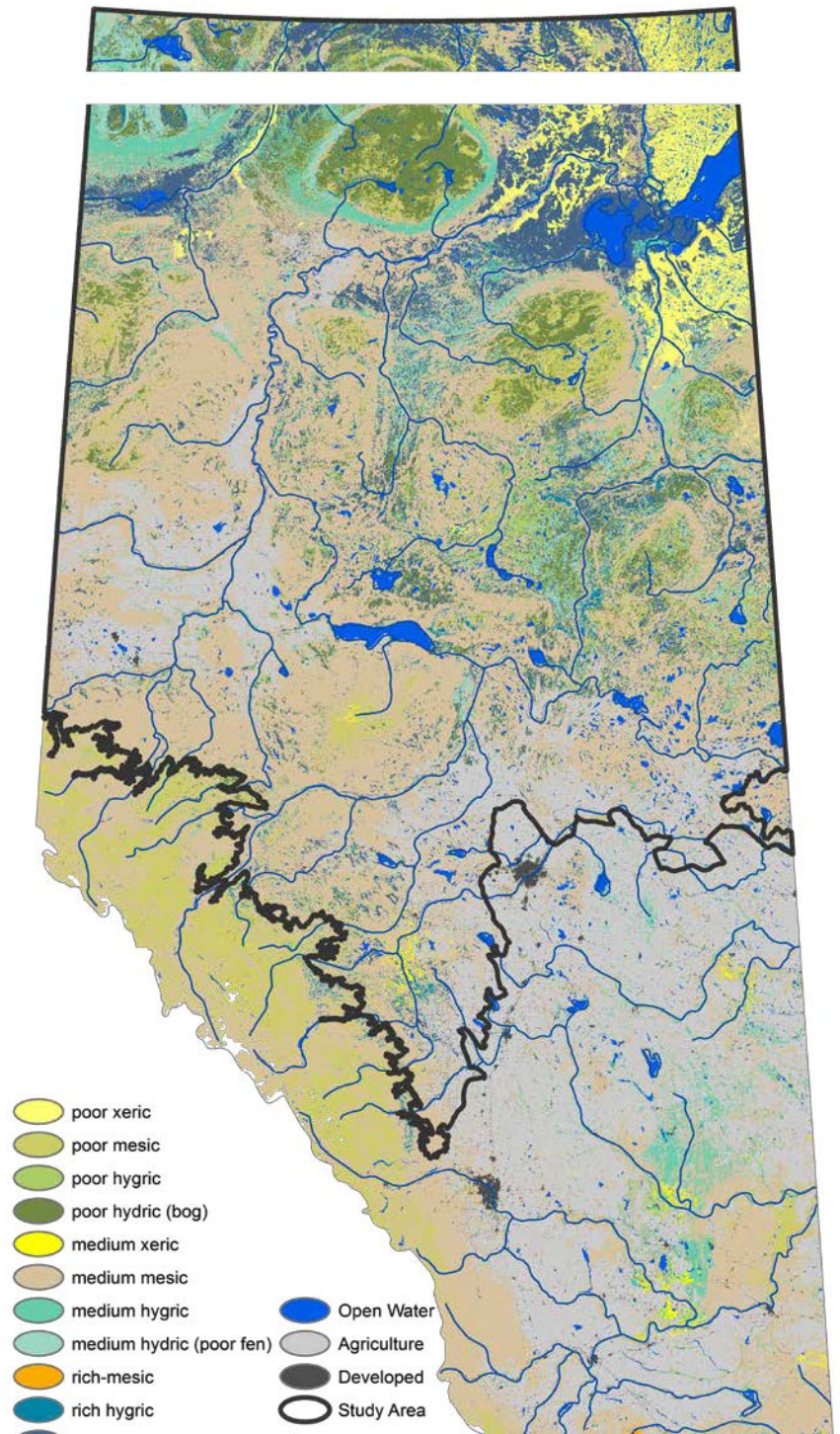


Figure 3-4. Predicted ecosite type (relative soil moisture/nutrient combination). Open water, agriculture, and developed areas are taken from ABMI's wall-to-wall landcover layer.

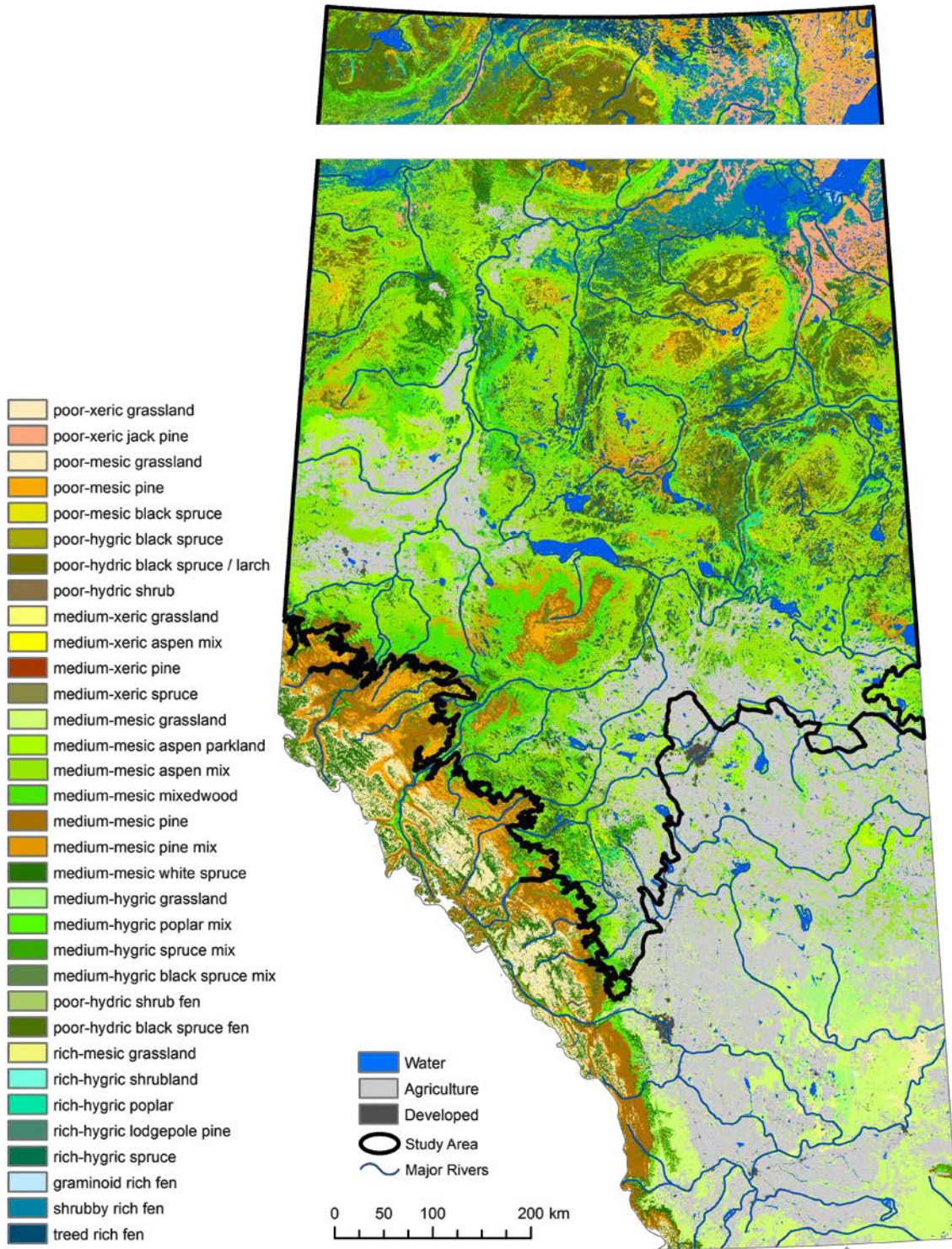


Figure 3-5. Predicted current vegetation type as a function of ecosite, terrain, and climate.

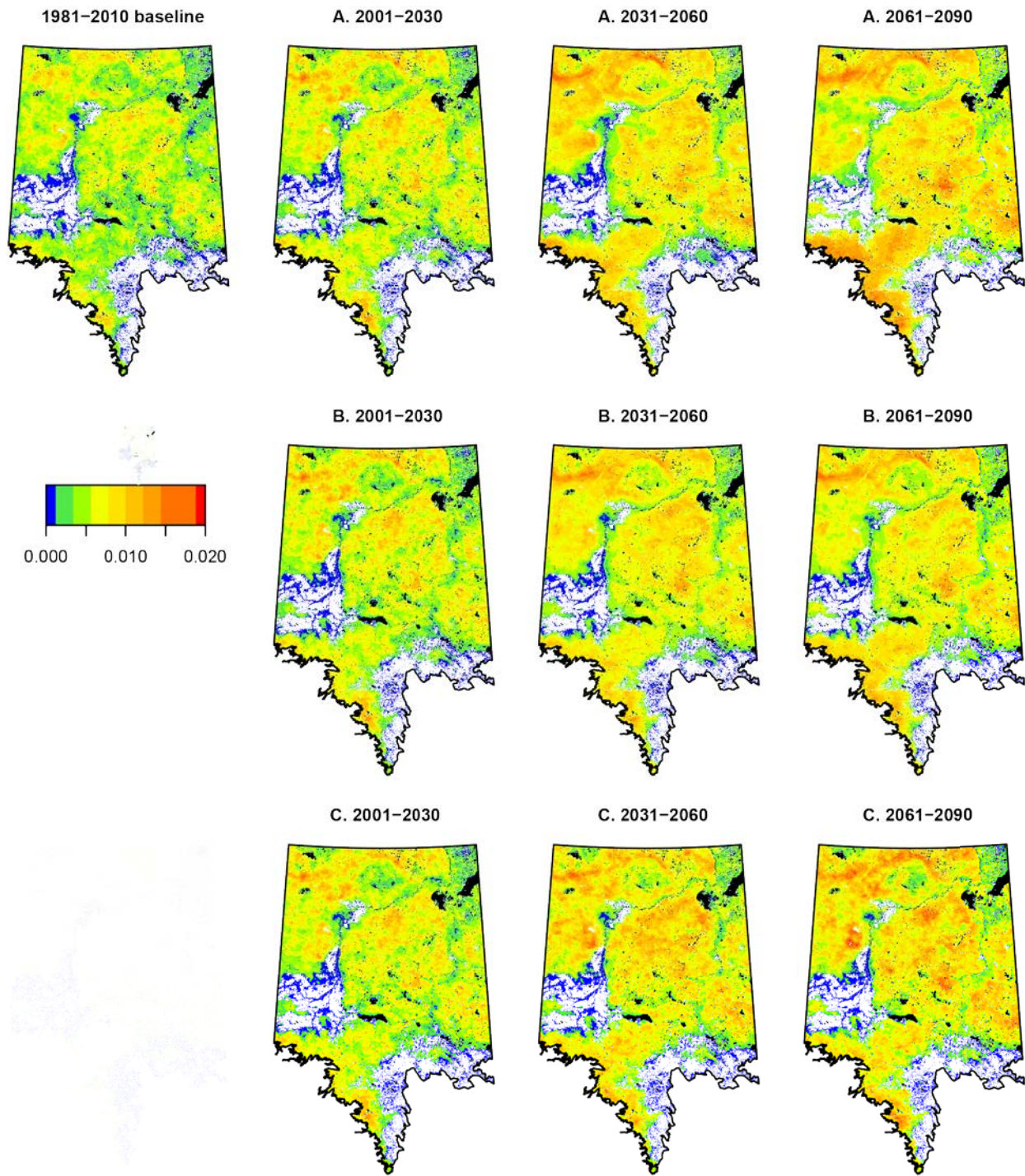


Figure 3-6. Mean burn probability for each time period and scenario under the HadCM3 model. Burn probabilities were averaged across 3000 iterations (10 fuel inputs x 300 runs for scenario B). White areas represent non-fuel types. A = Climate-driven; B = disturbance-mediated; C = static fuels.

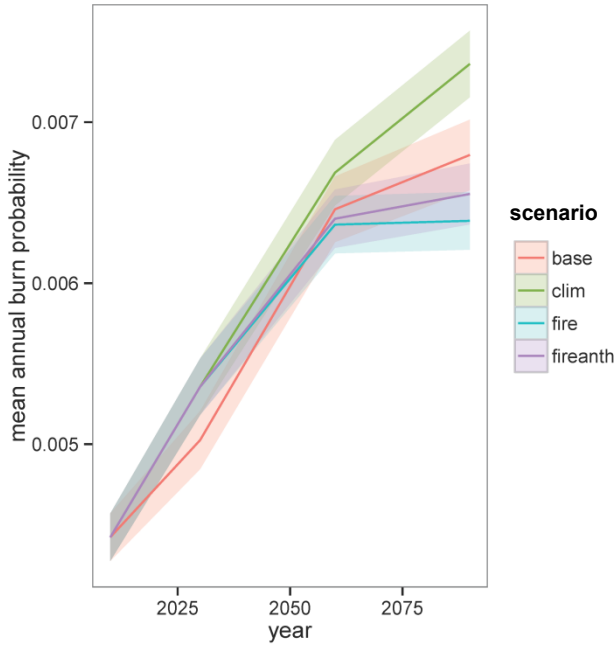


Figure 3-7. Projected change in mean annual burn probability by scenario within study area. base = scenario C, fire = scenario B1, fireanthro = scenario B2, clim = scenario A. The total forest area remains constant only in scenario C. Water and other non-fuel pixels are included in this summary. Confidence intervals represent spatial variability, as well as GCM variability for scenarios B1, B2, and A, and fuel stochasticity for scenarios B1 and B2.

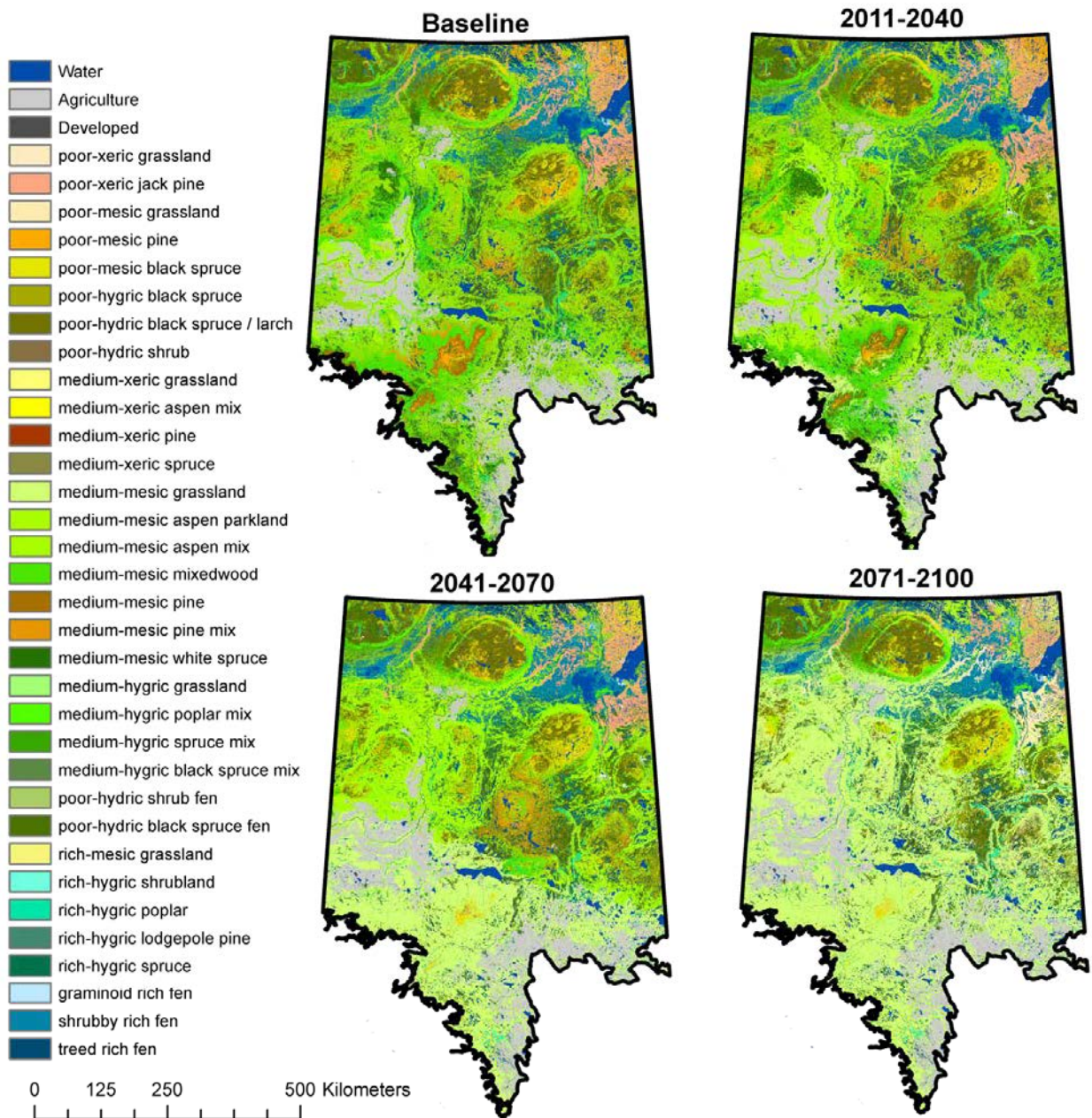


Figure 3-8. Projected climate-driven vegetation potential for current and future time periods. Predicted vegetation potential based on the MPI-ECHAM5 model under scenario A (climate-driven).

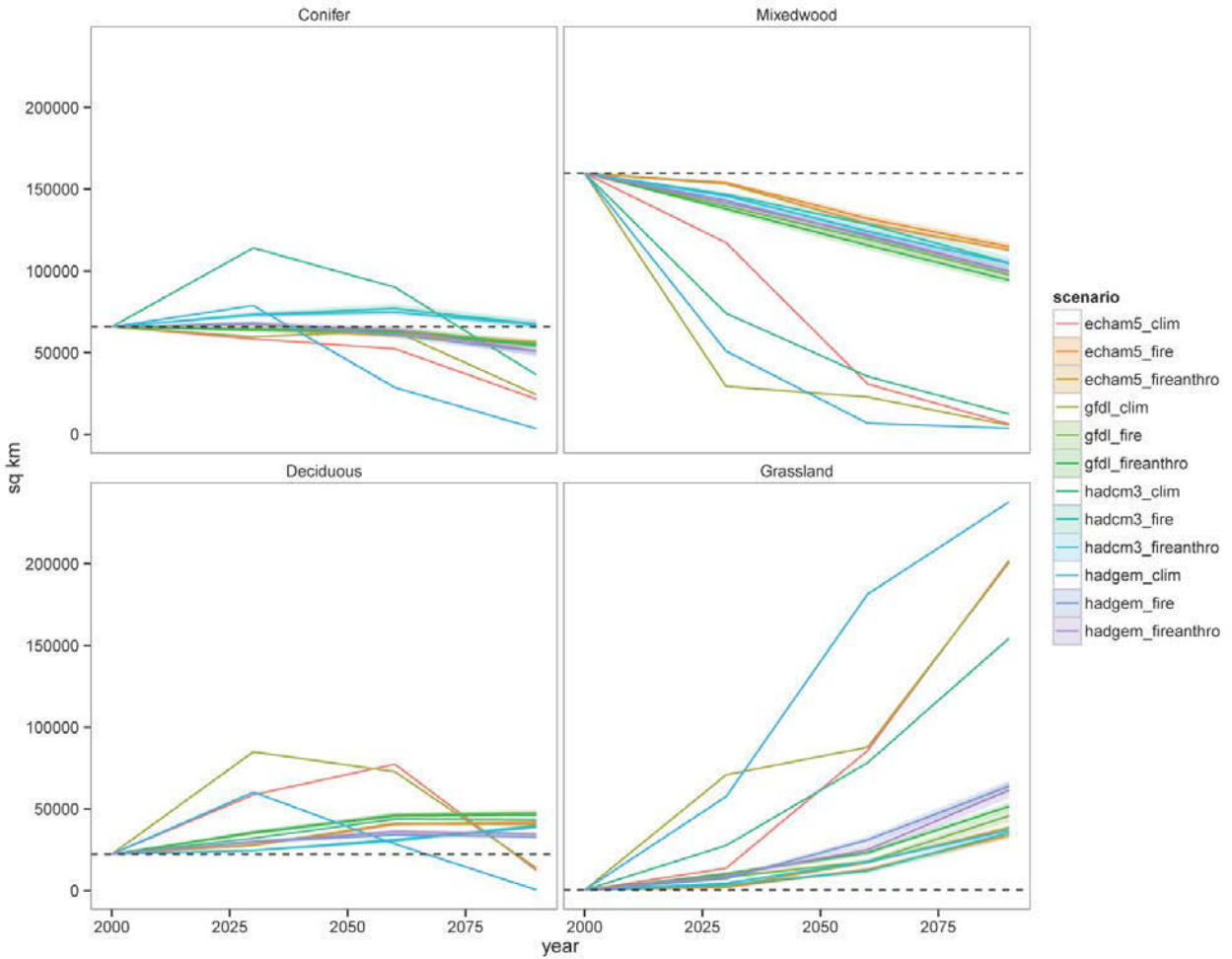


Figure 3-9. Projected change in upland vegetation cover type over time by GCM and scenario. clim = climate-driven (scenario A), fire = fire-mediated (scenario B1), fireanthro = fire- and anthropogenic disturbance-mediated (scenario B2). Scenario C = no change (dashed line). Forest area units are km²

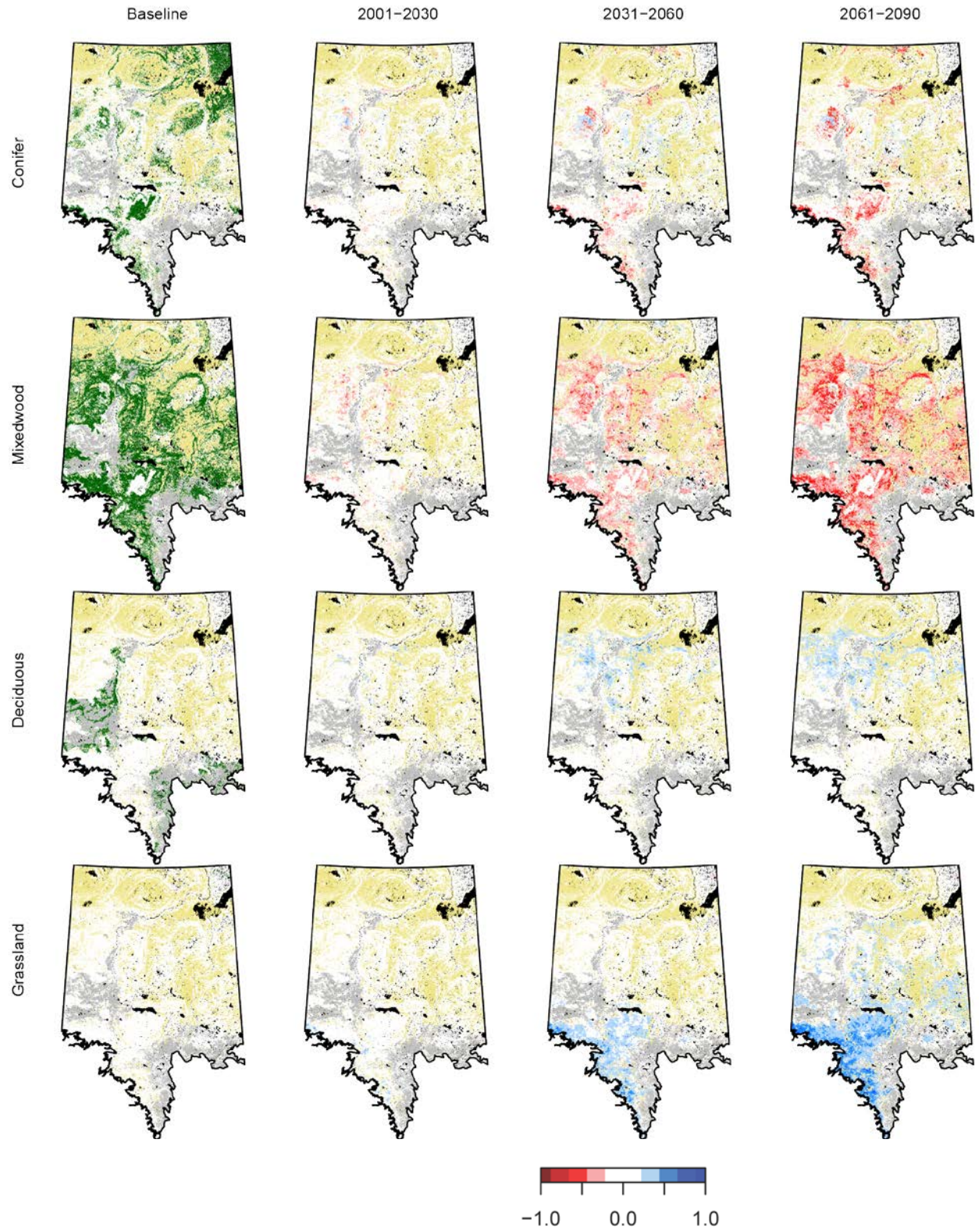


Figure 3-10. Predicted proportional change in conifer, mixedwood, deciduous, and grassland vegetation types for current and three future time periods.

Generalized vegetation proportions summarized across Burn-P3 runs under scenario B1 (fire-mediated) for 10 fuel realizations x 4 GCMs. Baseline modelled vegetation shown in green in first column. Black = open water; gray = non-fuel; beige = lowland vegetation.

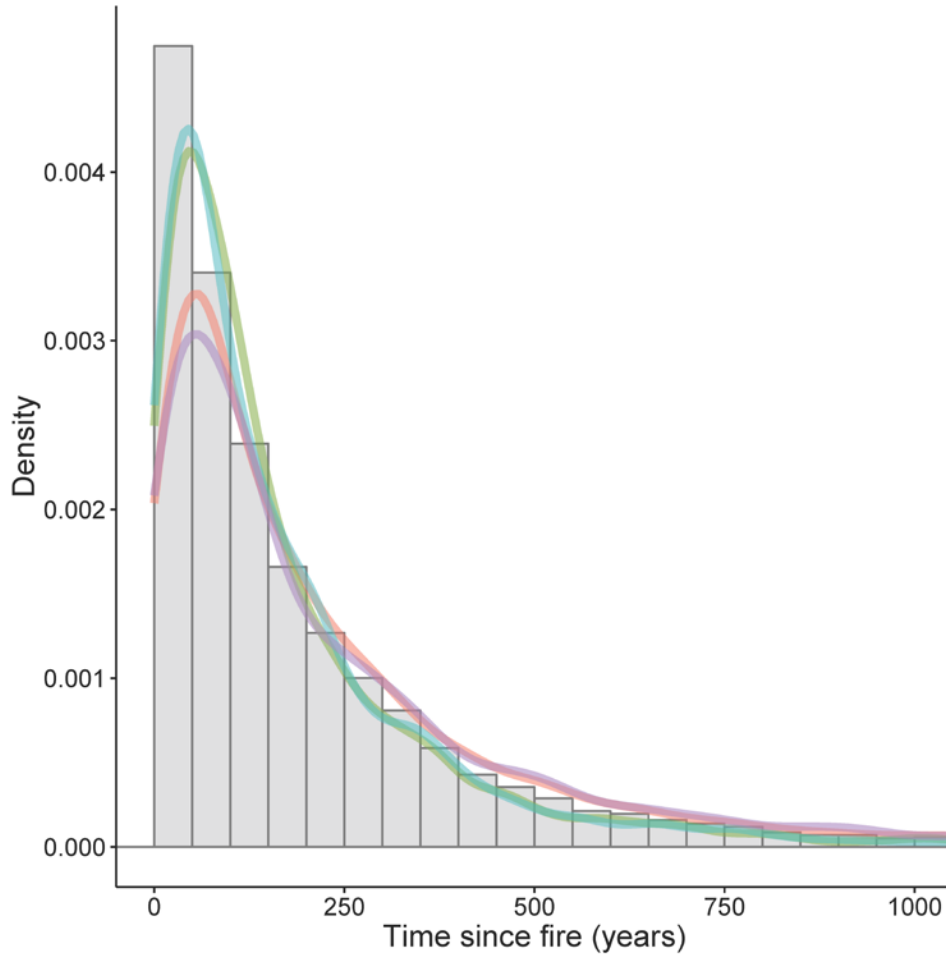


Figure 3-11. Projected change in age class distribution for upland forest fuel types. Density functions based on Gaussian smoothing kernels (3*default bandwidth), overlaid on combined histogram, were derived from time-since-fire calculations from 3,000 Burn-P3 runs based on current baseline vegetation and fire weather conditions for each future time period (scenario C). Purple = baseline; pink = 2001-2030; green = 2031-2060; blue = 2061-2090.

CHAPTER 4. BIOGEOGRAPHY OF BOREAL PASSERINE RANGE DYNAMICS IN WESTERN NORTH AMERICA: PAST, PRESENT, AND FUTURE

4.0 Summary

Many of the Neotropical migrant bird species that breed throughout the Canadian boreal region are not found in the Alaskan boreal region, separated by the northwestern cordillera mountains, despite the presence of climatically suitable habitat. We asked whether biological or climatic factors constrain certain species from crossing this geographic barrier. Logistic phylogenetic regression analysis was used to evaluate the relative importance of physical, migratory and competition metrics versus current and paleoclimatic suitability factors. Controlling for current climatic suitability within boreal Alaska, we found that species with the greatest climatic suitability across the northwestern cordillera, presently and also during the mid-Holocene period, were most likely to be regular breeders in the Alaskan boreal region. Migratory strategy also played a role, but could not be disentangled from its strong phylogenetic basis. Our analysis of a comprehensive dataset for 80 boreal passerines suggests that the perceived barrier of the northwestern cordillera may be easily weakened as climate change improves conditions there for many forest species.

4.1 Introduction

4.1.1 *Glaciation history shapes boreal bird distributions*

Physiographic barriers to recolonization post glaciation often restrict current species distributions and diversity patterns at high latitudes, especially in Europe (Svenning and Skov 2004, Fløjgaard et al. 2011, Hortal et al. 2011). Distribution in North America is generally less constrained, in that major mountain ranges have a north-south rather than east-west orientation, thus facilitating post-glacial northward expansion of species. However, portions of the western cordillera, a series of mountain ranges stretching across western North America, may have served as barriers to longitudinal expansion for some species. During glacial periods of the Pleistocene epoch, widespread North American temperate and boreal bird species are presumed to have retracted their ranges into geographically-isolated refugia, leading to the divergence of sister taxa and ultimately to speciation (Mengel 1964, Johnson and Cicero 2004, Weir and Schluter 2004, Lovette 2005). During alternating interglacial periods, the western cordillera has

served to further isolate many species' populations, contributing to the formation of distinct eastern and western subspecies (Milot et al. 2000).

The current North American boreal biome is geographically extensive, spanning from Alaska to Newfoundland, but it is disrupted by the northern portion of the western cordillera, hereafter referred to as the “northwestern cordillera” (Figure 4-1). Although most boreal tree species (with the exception of *Abies balsamea*) and many bird species occur on both sides of the cordilleran mountain ranges, passerine diversity is higher on the Canadian side of the cordillera than in the Alaskan boreal region (Distler et al. 2015). Many of the Neotropical migrant species that breed throughout the Canadian boreal region are not found in Alaska, despite the presence of climatically suitable habitat, e.g., Tennessee Warbler (*Oreothlypis peregrina*), Palm Warbler (*Setophaga palmarum*), Cape May Warbler (*S. tigrina*), and Bay-breasted Warbler (*S. castanaea*) (Stralberg et al. 2015b). Predicted suitable Alaskan habitats for these and other species are largely discontinuous with current Canadian boreal breeding ranges (Figure 4-2). Presumably, geographic barriers to movement or competition from closely related taxa have prevented some species of eastern origins from crossing the northwestern cordillera into the Alaskan boreal region (Figure 4-3).

At the last glacial maximum (LGM) ~20,000 years before present (YBP), boreal forest tree species (e.g., *Picea glauca*, *Picea mariana*, *Pinus banksiana*, *Abies balsamea*, *Populus tremuloides*, *Betula papyrifera*) were displaced to a contiguous refugium in the southeastern United States, according to vegetation reconstructions based on pollen data from sediment cores (Overpeck et al. 1992, Jackson et al. 2000, Dyke 2005). Trees that recolonized the North American boreal region during the early Holocene epoch are generally assumed to have originated from this single refugium. Thus, if boreal birds require those tree species as habitat, it is plausible that most birds colonized the boreal forest from this eastern refugium post glaciation. That many migratory birds seem to follow an eastern migration route supports this hypothesis. However, genetic evidence suggests that small pockets of white spruce (*Picea glauca*) and other boreal tree species may have persisted as cryptic refugia in Beringia (Anderson et al. 2006). Furthermore, many boreal bird species have wide-ranging distributions and are capable of using a wide variety of boreal and non-boreal tree species as habitat. Thus, today's boreal bird species may have had multiple geographically isolated refugia across North America during the Pleistocene epoch. Genetic evidence from a few species like Swainson's Thrush (*Catharus*

ustulatus), Wilson's Warbler (*Cardellina pusilla*), and Yellow Warbler (*Setophaga petechia*) support a multiple refugia hypothesis (Milot et al. 2000, Clegg et al. 2003, Ruegg et al. 2006).

If avian distributions are largely climate-driven, as evidence suggests (Jiménez-Valverde et al. 2011, Cumming et al. 2014), paleoclimate reconstructions can be used in a niche modelling framework to hindcast species' distributions (Kerr and Dobrowski 2013). LGM hindcasts identify locations of probable glacial refugia for extant species (Huntley et al. 2013, Levinsky et al. 2013). These can then be used to generate hypotheses about migratory route origins (Ruegg et al. 2006) or about the current population structure of individual species (Ralston and Kirchman 2012). Such hypotheses are often tested by evaluating how genetic structure and current distribution relate to past climatic suitability. In this study, we hypothesize that species with very distant eastern LGM refugia would have been less likely to colonize the Alaskan boreal region than those with western refugia. Furthermore, species with possible Beringian LGM refugia, based on hindcasted climate conditions, should be more likely to presently occur in boreal Alaska, compared to species with no possible Beringian refugia.

Also of interest is the relatively warm Holocene climatic optimum (mid-Holocene) ~6,000 YBP, which may have allowed some species to cross the cordillera via short-term connections of climatically suitable habitat. The mid-Holocene warm period may have been similar to future projected conditions under increased CO₂ levels (Strong and Hills 2003). Therefore, species with projected mid-Holocene climatic suitability across the northwestern cordillera should have been more likely to colonize the Alaskan boreal region than species with no such historical opportunities.

4.1.2 Migratory habits reinforce geographic segregation

Despite the tremendous mobility of migratory birds, their ties to southern wintering grounds and fidelity to migratory routes may reinforce geographic separation. Long-distance migrants have been shown to exhibit less longitudinal variation in their ranges than resident species, despite greater mobility (Böhning-Gaese et al. 1998). Strong genetic programming of migration timing (Both et al. 2006, Stanley et al. 2012) also suggests greater dispersal constraints on long-distance migrants, and the added energetic costs of longer migration routes may limit resources required for the exploration of new suitable habitat.

Indeed, among passerines, almost all resident species in the North American boreal region have broad distributions and occur on both the Alaskan and Canadian sides of the

cordillera—e.g., Boreal Chickadee (*Poecile hudsonicus*) and Gray Jay (*Perisoreus canadensis*). They also tend to occupy high-elevation habitats, providing range contiguity across the northwestern cordillera. Many cold-adapted winter residents such as chickadees (Paridae) and nuthatches (Sittidae) have pan-boreal (i.e., Eurasian) origins and a long evolutionary history in cold climates (Mayr 1946). Conversely, many migratory species of the Canadian boreal forest do not occur west of the cordillera in boreal Alaska. Most of these belong to the New World warblers (family Parulidae), a group that has experienced fairly recent (Pliocene) diversification from its Neotropical origins, especially within the *Setophaga* (formerly *Dendroica*) genus (Lovette and Bermingham 1999).

Passerine species that breed predominantly in Nearctic boreal regions tend to migrate to wintering grounds in Central or South America. Those that breed regularly in boreal Alaska, e.g., Blackpoll Warbler (*Setophaga striata*), Alder Flycatcher (*Empidonax alnorum*), and Gray-cheeked Thrush (*Catharus minimus*), all have boreal distributions across the northwestern cordillera, and are thought to migrate along eastern migratory corridors (Lowther 1999, Lowther et al. 2001, DeLuca et al. 2013), suggesting eastern distributional origins. Alaskan boreal populations of widespread migratory species such as Swainson's Thrush and Yellow Warbler are also thought to follow eastern migratory routes to Central and South American wintering sites, even though coastal populations use western migratory routes, which are shorter for Alaskan migrants (Ruegg et al. 2006). Other migratory species in boreal Alaska generally have shorter migration routes, wintering in the United States and/or northern Mexico—e.g., Townsend's Warbler (*Setophaga townsendi*), Ruby-crowned Kinglet (*Regulus calendula*), and Yellow-rumped Warbler (*Setophaga coronata*). Thus the passerine avifauna of boreal Alaska appears to lack western long-distance migrants.

Passage across the northwestern cordillera between Alaska and Canada involves environmentally harsh landscapes at high elevations and/or northern latitudes. Although the likelihood that individuals breed at or near their place of origin (natal philopatry) is relatively low in migratory species compared to resident species, isolated populations are thought to exhibit higher rates of natal philopatry (Weatherhead and Forbes 1994), suggesting that a species may fill spatially contiguous suitable habitats first and may be less likely to colonize areas that are spatially disjunct at a broad spatial extent. The relatively young age of the boreal forest also translates into fewer opportunities for chance colonization events of habitat west of the

cordilleras to occur. For many species with refugia in the eastern U.S. at the end of the LGM, environmentally suitable connections across the cordillera may not yet have developed, or enough time may not yet have elapsed for birds to disperse across them.

4.1.3 Will climate-projected range shifts be impeded by the northwestern cordillera?

Given the magnitude of past climatically driven changes in avian distributions, substantial future climate warming can be expected to result in extensive changes to boreal bird distribution patterns. An important spatial pattern of projected change across multiple passerine species is that of range expansion from the Canadian boreal region into the Alaskan boreal region, including newly contiguous climatically suitable habitats across the northwestern cordillera (Stralberg et al. 2015b). Almost all Canadian boreal species that are not currently found in the Alaskan boreal region are projected to experience increased climatic suitability in Alaska within the next 30–90 years, e.g., Tennessee Warbler (*Oreothlypis peregrina*, [Figure 4-2](#)). This raises several questions: How likely are these projected distributional shifts to occur for different species? Will the northwestern cordillera provide an effective barrier to range shifts? Or will increased connectivity of suitable climates facilitate northwestern migration of Canadian boreal species into Alaska?

We proposed that for each boreal species not currently found in the Alaskan boreal region there are two potential explanations for their exclusion, with contrasting implications for future climate-change outcomes:

1. The northwestern cordillera constitutes a long-term barrier to birds as a function of life-history characteristics, including (a) migratory strategy or distance; (b) physical traits; or (c) competition from recently diverged congeneric species. That is, suitable habitat in Alaska is not occupied due to evolutionary constraints that may or may not respond to changing selection pressures in the future.
2. The northwestern cordillera constitutes a temporary barrier to birds as a function of climate and glaciation history. That is, suitable habitat in Alaska is not occupied by many migratory species due to climate factors during and after the last glacial maximum, including (a) a current lack of suitable habitat connectivity across the northwestern cordillera connecting Canada and Alaska; (b) a lack of mid-Holocene habitat suitability within boreal Alaska or across the northwestern cordillera; and/or (c) distance from LGM glacial refugia (i.e., eastern vs. western U.S. or Beringia).

To the extent that migratory strategy, competition or physical physical factors constrain species from crossing the cordillera, this could result in major range constrictions among boreal specialists in the future, as southern range boundaries shift northward without compensation in the north. If it is simply a matter of climatic habitat connectivity, however, distributional shifts could occur in the future as soon as contiguous suitable climates become available. In some cases, this may involve a time lag due to the time required for forest growth and succession to catch up with the altered climate (Stralberg et al. 2015a). The relative importance of these various constraints is likely to vary by species and phylogenetic origin. This paper contributes a phylogenetic logistic regression analysis to analyze the relative importance of life-history characteristics versus post-glaciation climatic factors on the distributions of North American boreal-breeding species west of the northwestern cordillera in the Alaskan boreal region, and we used this information to predict which species are most likely to shift their distributions from Canada into boreal Alaska in the future.

4.2 Methods

4.2.1 Study area and species

We evaluated potential drivers of breeding population occurrence within the Alaskan boreal region for 80 boreal forest songbird species for which density offsets (Sólymos et al. 2013) and species distribution models (Sólymos et al. 2013, Stralberg et al. 2015b) and species distribution models (Stralberg et al. 2015b) were available. All of these species were predicted to have suitable climates for breeding within the approximately 400,000 km² Alaskan boreal region (Table 4-1). We defined the Alaskan boreal region as the Alaska Boreal Interior (3.1) level II ecoregion, an ecological region that is separated from the Western Taiga Plain (3.3) and Boreal Plain (5.4) by the northwestern cordillera, defined as adjacent Taiga Cordillera (3.2) and Boreal Cordillera (6.1) ecoregions (CEC 1997) (Figure 4-1). We used recently compiled information on breeding distribution of birds in Alaska (Gibson 2011, Gibson and Withrow 2015) to determine which of the 80 species are currently considered regular breeders in the Alaska Boreal Interior region (Table 4-1). To quantify climatically suitable areas for each species, we used density-based boosted regression tree (BRT) species distribution models (SDM) that we had previously developed using a standardized avian survey dataset from across northern North America. These models included boreal, hemi-boreal and other sub-boreal regions containing climates projected to move northward into the current boreal region within the next century (Stralberg et al. 2015b).

SDM-predicted density estimates were used to project the amount of suitable habitat estimated to occur within the Alaska Boreal Interior ecoregion (see below).

4.2.2 *Paleo-hindcasting*

To represent paleoclimate conditions, we obtained temperature and precipitation anomalies for 6,000 (mid-Holocene, MH) and 21,000 YBP (last glacial maximum, LGM) based on millennial equilibrium projections from two U.S. global climate models (GCM) that were part of the Paleoclimate Modelling Intercomparison Project, Phase II: (1) the Community Climate Model (CCM1) developed by the National Center for Atmospheric Research (Kutzbach et al. 1998) and (2) the Geophysical Fluid Dynamics Laboratory (GFDL) model, from the National Oceanic and Atmospheric Administration. Monthly temperature and precipitation anomalies were combined with 4-km 1961-1990 baseline interpolated climate data (<http://www.ualberta.ca/~ahamann/data/climatena.html>) to develop millennial-scale hindcasts for average monthly climate conditions (Roberts and Hamann 2015). We converted these monthly variables to bioclimatic indices (Table 4-2) and used them as inputs to existing SDMs of avian density developed from current climate data (Stralberg et al. 2015b). Eleven bootstrap replicates were averaged to create a single mean density map for each period. For cross-species comparisons, we converted density estimates within 4 km x 4 km grid cells for each species to binary estimates of its suitable core habitat, defined as areas where the species' predicted density exceeded its mean baseline predicted density within the boreal and sub-boreal model-building area (Stralberg et al. 2015a). Maps of current predictions and hindcasts for each species and GCM are provided in Appendix 4-A (CCM1) and Appendix 4-B (GFDL).

4.2.3 *Climate suitability variables*

To compare modern connectivity of suitable climates across the northwestern cordillera to that of the mid-Holocene period, we calculated the total model-predicted core area for current and mid-Holocene periods within the Taiga Cordillera (3.2) and Boreal Cordillera (6.1) ecoregions combined (Figure 4-1, Appendix 4-C). We deemed traditional landscape connectivity metrics (sensu McGarigal and Marks 1995) inappropriate to address the broad temporal and spatial scales of interest and used a simple metric for climatic connectivity. We assessed climatic connectivity with a one-sided paired *t*-test to determine whether the mean total amount (log-transformed) of suitable core habitat available for 80 species of boreal passerines within the cordillera during the mid-Holocene was significantly greater than that currently available, and

found that it was not ($p > 0.05$ for both CCM1 and GFDL). However, the amount of mid-Holocene suitable core habitat was greater than current suitable core habitat for some species and GCMs (Appendix 4-C). Thus we retained these variables for modelling purposes.

To test the potential effects of the location of LGM refugia on the likelihood of a species' currently occurring in the Alaskan boreal region, we first used BRT model projections to estimate for each species the area of LGM suitable core habitat available as glacial refugia in eastern U.S. ecoregions: Eastern Temperate Forests (ecoregion numbers 8.2 – 8.5) and Great Plains (9.2 – 9.4), versus western U.S. ecoregions: Western Cordillera (6.2), Marine West Coast Forest (7.1), Cold Deserts (10.1), and Mediterranean California (11.1) (Figure 4-1, Appendix 4-C). We then calculated a log-transformed ratio of the area in eastern versus western refugia, which ranged from -0.84 (strongly western LGM distribution) to 4.24 (strongly eastern). We also calculated the (log-transformed) area of LGM suitable core habitat contained in the ice-free Alaska Boreal Interior (Beringian refugia) (Anderson et al. 2006). See Table 4-2 for a list of all climate suitability variables.

4.2.4 Life-history variables

We summarized life history characteristics, taken from Birds of North America species accounts (Poole 2005) for each species related to migratory strategy, physical traits, and feeding and habitat guilds (Table 4-3). To address congeneric exclusion, we calculated an index of competition from related taxa currently occupying the Alaska Boreal Interior region. For our 80 study species and closely related taxa, we downloaded a random subset of 500 equally likely phylogenetic trees, compiled in a Bayesian framework (birdtree.org, Jetz et al. 2012) based on full trees from the Hackett (2008) backbone (see example tree in Figure 4-4). Using the 'ape' package (Paradis et al. 2004) for R version 3.1.2 (R Core Team 2014), we calculated correlations among species pairs based on the lengths of shared branches (Garland and Ives 2000), and then averaged those resulting phylogenetic correlation matrices (Martins and Hansen 1997). (Martins and Hansen 1997). For each of our 80 study species, the maximum pairwise correlation between that species and other species defined as regular breeders in the Alaskan boreal region (Gibson 2011, Gibson and Withrow 2015) (Gibson 2011, Gibson and Withrow 2015) was used as an index of competition pressure (see Appendix 4-D). We did this rather than restricting our focus to sister species because we found no true boreal sister species that do not already co-occur in the Canadian boreal region. The closest geographically separated pair, Black-throated Green and

Townsend's Warbler (*Setophaga virens* and *S. townsendi*) are no longer considered sister taxa based on molecular data (Johnson and Cicero 2004).

4.2.5 Phylogenetic logistic regression analysis

We used phylogenetic logistic regression analysis (Ives and Garland 2010) to evaluate the relative influence of each climate suitability and life-history variable on current presence/absence of species considered regular breeders in the Alaska boreal interior while accounting for trait covariance among related species. We included log-transformed area of current suitable core habitat within the Alaska Boreal Interior as an offset in the models to account for current climatic suitability for each species. Correlation matrices for 500 phylogenetic trees, as described above, were used to conduct a series of phylogenetic logistic regression analyses using the 'phylolm' package (Tung Ho and Ané 2014) for R, which uses an iterative penalized quasi-likelihood approach to estimate the phylogenetic parameter or transition rate, α , and covariate coefficients, β . Results from the 500 models were averaged for interpretation.

We used a stepped approach for testing models. We first developed a phylogenetic logistic regression model for each subcategory of life-history and climate covariates (Table 4-3) to assess the relative explanatory power of each, including log-transformed current predicted Alaska Boreal Interior core area for each species as an offset. Continuous independent variables were standardized to a mean of zero and standard deviation of 1 to allow for comparison of resulting model coefficients. We then combined variables from top individual climatic and life-history models (based on AICc scores), dropped non-explanatory variables, and evaluated support for alternative combined models compared with the offset-only null model (based on AICc and Pseudo-R²). We also evaluated the importance of individual coefficients and α values, and calculated the area under the curve (AUC) of the receiver operating characteristics (ROC) plot for the average model using the 'AUC' package for R (Ballings and Van den Poel 2013).

Finally, to evaluate the influence of phylogenetic correlation, we compared coefficients from phylogenetic logistic regression models with those from standard logistic regression models containing the same terms.

4.2.6 Evaluating future habitat potential

We used AICc and AICc differences (Δ_i) to identify the top-ranking combined models for current species occurrence and assign weights to each model. To predict future occupancy, we replaced current estimated Cordilleran habitat suitability values with mean future climate-

change projected values, where applicable, for three future time periods: 2011-2040, 2041-2070, and 2071-2100, based on projections from Stralberg et al. (2015b). Projections from each model were multiplied by AICc weights ($\exp(-1/2*\Delta_i)$) and then summed together to obtain an AICc-weighted model-averaged projection. We used current mean prevalence (in our case, 38/80 species currently in Alaska, or $p > 0.475$) as the presence/absence threshold as recommended by Freeman and Moisen (2008).

4.3 Results

4.3.1 Model fit and variable importance

Among phylogenetic logistic regression models that used a single set of climatic factors or life-history traits to explain the current occurrence of species regularly breeding in the Alaskan boreal region, we found greatest support for the model based on current northwestern cordillera climate suitability (mean AIC_c difference (Δ_i) = 0; Table 4-4). The second-ranked model, based on mid-Holocene cordilleran climate suitability (according to the GFDL projection), had much lower support ($\Delta_i = 7.9$). The next three models, which also included past climatic condition variables (mid-Holocene cordilleran climate (CCM1), LGM eastern refugia (CCM1), and LGM Alaska refugia (GFDL)), had about equal but less support than the top two models ($\Delta_i = 16.6$ – 18.8) (Table 4-4). Other models that performed better than the null model were (in order): LGM Alaska refugia (CCM1), migratory strategy, and LGM eastern refugia (GFDL). The models based on competition and physical trait variables did not perform better than the null model.

Phylogenetic correlation was highest (i.e., α was lowest) for the model based on mid-Holocene cordilleran climate suitability (GFDL), followed by models based on current and mid-Holocene (CCM1) cordilleran climate suitability, respectively. Other models had α values greater than 5, indicating that no meaningful phylogenetic correlation remained after accounting for migratory strategy, physical traits, competition, LGM refugia, or current climatic suitability of the Alaskan boreal region (null model). In other words, the current and mid-Holocene (GFDL and CCM1) cordilleran climate suitability models were the only models that were not confounded with phylogeny. Other models represent alternative explanations for patterns that could also be driven by phylogeny.

Among the candidate models that combined both climatic and life-history variables, the model that best ($\Delta_i = 0$) predicted occupancy of the Alaskan boreal region included current

cordilleran climate suitability (with a positive association, +), the ratio of mid-Holocene (GFDL) to current cordilleran climate suitability (+), winter resident status (+), and use of South American wintering grounds (+) (Table 4-5). Current cordilleran climate suitability had the largest effect size by threefold. In other words, the best model predicted that, controlling for current climatic suitability within boreal Alaska, species with the greatest climatic suitability across the northwestern cordillera, now and during the mid-Holocene period, were most likely to currently occupy the Alaskan boreal region. Winter resident species were the most likely to occupy the Alaska Boreal Interior, followed by long-distance migrants with South American wintering grounds. That is, among long-distance migrants, those that winter in South America have been the most successful at colonizing the Alaska Boreal Interior.

The second-ranked model ($\Delta_i = 4.5$) included similar coefficients for the variables in the top model, but included CCM1-predicted instead of GFDL-predicted mid-Holocene climate suitability (+/-), and also included a positive association with short-distance migrant status (Table 4-5). Other models contained different combinations of these variables with similar coefficient values. Higher-AIC_c models also included the CCM1-predicted eastern LGM refugia variable (-). The magnitude of proportion of variance explained (Pseudo-R²) and area-under-the-curve (AUC) values generally coincided with rankings based on AIC_c (i.e., the top-ranked AIC_c model also had the largest Pseudo-R² (0.64) and largest AUC (0.97).

Compared with standard logistic regression models, the phylogenetic models had smaller coefficients for variables related to migratory strategy, highlighting the strong phylogenetic component to these variables (Table 4-5). The climatic suitability effects were smaller in the top two phylogenetic models, compared with the non-phylogenetic versions, but larger in some of the other models with negligible phylogenetic correlation.

4.3.2 Model predictions for current and future climate

Using the current mean prevalence (0.475) as a threshold, we identified six species that were predicted to occur in boreal Alaska but are not yet considered regularly breeding species there (Table 4-6). Breeding has, however, recently been documented for two of these six species within boreal-adjacent south-central Alaska (Table 4-7). There were only three species that currently breed regularly in the Alaskan boreal region but for which the averaged models predicted probabilities below the threshold: American Pipit (*Anthus rubescens*), Horned Lark

(*Eremophila alpestris*), Red-winged Blackbird (*Agelaius phoeniceus*), all of which were either tundra- or wetland-associated (Appendix 4-E).

Model-averaged projections for future periods suggested that up to 31 new species could occur as regular breeders in the Alaska Boreal Interior by the 2020s, up to 38 by the 2050s, and up to 40 by the 2080s (Table 4-6, Table 4-7, Appendix 4-E). Among these, the Yellow-bellied Flycatcher (*Empidonax flaviventris*) has just recently been recorded breeding within the Alaska boreal region and seven other species have recently been documented either exhibiting territorial behavior in the boreal interior or breeding in south-central Alaska (Gibson, 2011; Gibson & Withrow, 2015). The models also predict, however, that among the 38 species that now regularly breed in the Alaskan boreal region, northwest cordilleran climate suitability will remain for as few as 31 of these by the 2080s (Table 4-6, Appendix 4-E).

4.4 Discussion

4.4.1 Past and present climatic suitability account for barrier effect

Despite the demonstrated influence of western cordillera mountain ranges as barriers leading to vicariance of several wide-ranging North American passerine species (Milot et al. 2000, Kimura et al. 2002, Clegg et al. 2003), our analysis of boreal-breeding passerines suggests that the northwestern portion of this prominent geographic feature has not generally been a barrier for boreal species. Although many boreal species do not yet occupy climatically suitable habitat within the Alaskan boreal region, these species appear to be primarily those without climatically suitable habitat connections across the northwestern cordillera region that bridges Canadian and Alaskan portions of the boreal forest biome. We found that, controlling for Alaskan climatic suitability, the quantity of cordilleran suitable habitat was a strong predictor of regular breeding in the Alaskan boreal region. Furthermore, our analysis suggested that species that had more suitable habitat connections during the warmer mid-Holocene period are even more likely to breed in the Alaskan boreal region. These species may have had improved chances for colonization approximately 6,000 YBP, supporting the hypothesis that Alaskan boreal occupancy may be a matter of both connectivity and time.

We also found a relatively weak relationship between Alaskan boreal occupancy and predicted LGM refugia south of the ice sheet. Paleoclimate hindcast projections for ~21,000 YBP indicated that species with mostly eastern refugia were less likely to have colonized the Alaskan boreal region than those with mostly western refugia, suggesting that the relatively

longer distance from eastern refugia may have deterred or delayed some species, and that the Alaskan boreal region may have been colonized from both western and eastern LGM refugia. In general, however, species that are strictly boreal in their current distribution had largely eastern projected LGM refugia, whereas western refugia were associated with wide-ranging species that occur outside the boreal region (Figure 4-5). Thus, it is also possible that all species colonized the Alaskan boreal region from eastern refugia, and that western forested refugia were sources of coastal or non-boreal interior populations. Species with western refugia could have been more successful at colonizing the Alaskan boreal region due to greater mobility or other factors not directly related to LGM refugia *per se*.

We also found some support for a relationship between potential climatic refugia in Alaska (Beringia) and current occupancy of the Alaskan boreal region, but only for one of the GCMs that we evaluated (GFDL). Resident boreal species that were able to persist in Alaska during the Pleistocene period should still occur there today. However, due to the underrepresentation of arctic sites in our model-building dataset (Stralberg et al. 2015b), as well as the non-analog conditions that occurred in Beringia at the LGM (Roberts and Hamann 2012), our confidence in model projections for this time period and region is relatively low. It is also unknown whether migratory species would have crossed major ice sheets. Thus predicted Beringian refugia may only be realistic for a handful of cold-tolerant resident species—primarily those associated with tundra habitats, but potentially a few forest-dependent species that were able to survive in small boreal refugia (Anderson et al. 2006).

4.4.2 Migratory strategy also influences Alaskan boreal occupancy

Although past and present cordilleran climatic suitability were the strongest predictors of Alaskan boreal occupancy, we also found that migratory strategy, which has a strong phylogenetic component (Helbig 2003), is an important factor in determining which species have successfully colonized the Alaskan boreal region post glaciation. Most northern resident species are already found there, some of which may have persisted in Beringian refugia. Our results suggest that resident species with more southerly climate associations, such as Blue Jay (*Cyanocitta cristata*), are likely to occur in the Alaskan boreal region by mid-century; the recent urbanization-driven westward expansion of this species (Smith 1978) suggests that further expansion is possible. Short-distance migrants were also more likely to occupy boreal Alaska and thus more likely to colonize in the near future than long-distance migrants, with exception of

migrants with South American wintering grounds. The latter is consistent with leapfrog migration, documented within a number of northern species (Boland 1990, Bell 1997, Kelly et al. 2002), whereby individuals with more southerly wintering grounds often breed farther north and have longer migration routes, either to optimize resource utilization (Greenberg 1980, Pienkowski et al. 1985) or reduce competition (Lundberg and Alerstam 1986). This, combined with the lack of importance of any of the migration distance metrics we evaluated, suggests that migration distance *per se* is not a limiting factor for breeding range expansion, although strong genetic control of migration routes may limit the capacity of a species to alter its migration route, timing, and destination in the face of rapid climate change (Both et al. 2010).

We did not find any evidence that competitive exclusion or physical traits such as body size or clutch size affect a species' ability to colonize boreal Alaska. With respect to body size, it may be that migration counters the trend toward larger-bodied individuals and species in colder climates predicted by Bergmann's rule. Both body size and clutch size may also vary substantially across the range of a species (Hussell 1972, Dunn et al. 2000, Ashton 2002), reducing the reliability of general literature-derived values for wide-ranging species. With respect to competition, it is possible that we did not adequately quantify competition pressure. However, the generally low diversity of this region and relatively short time since glaciation suggests that lack of niche saturation is a more likely explanation for the small effect of competitive exclusion.

4.4.3 Perceived cordilleran barrier may easily be weakened

Our results generally suggest that the northwestern Cordillera can be considered a “weak” barrier, with a capacity for many additional species to disperse into Alaska once climatic connectivity is achieved in the future. Indeed, in recent years, the first breeding record has been documented for Yellow-bellied Flycatcher. Of the eight species we considered that were classified by Gibson (2011) or (Gibson and Withrow 2015) as most likely to be added to the region's breeding avifauna, all were predicted by at least one model to be present in 2011-2040 climate conditions. These climate conditions are now being experienced in Alaska, especially given that warming has occurred faster there than elsewhere in North America (ACIA 2005, Wendler and Shulksi 2009). Thus, it is possible that we are already seeing a change in cordilleran habitat suitability in response to recent anthropogenic climate change, and that some migratory species are already in the process of adjusting their distributions to track climate (Figure 4-2).

Of course several (four) of the species for which our model predicts current Alaskan boreal occupancy have not been detected there, which is not surprising given the plethora of factors that may contribute to successful range expansion, and the large stochastic component (Pielou 1991). For example, the absence of American Redstart (*Setophaga ruticilla*) and Warbling Vireo (*Vireo gilvus*) may be explained by their strong association with deciduous habitats, particularly along riparian corridors (Sherry & Holmes, 1997; Gardali & Ballard, 2000), which are largely discontinuous across the northwestern cordillera into boreal Alaska—but do connect with southeastern Alaska, where these species are found. Indeed, several other species—e.g., Song Sparrow (*Melospiza melodia*) and Brown-headed Cowbird (*Molothrus ater*)—are known to breed in southern Alaska but not in boreal (interior) Alaska, suggesting that the east-west running Alaska Range, which contains Mount Denali, the highest peak in North America, may be as important a barrier as the north-south running MacKenzie, Selwyn, and northern Rocky Mountain ranges (Figure 4-3).

4.4.4 Range expansions may lead to community reshuffling

The ecological implications of relatively rapid range expansions and consequent community reshuffling are difficult to anticipate (Stralberg et al. 2009). On the one hand, the lower passerine species diversity in boreal Alaska compared with boreal Canada, and its relatively long distance from presumed LGM boreal refugia, suggest that niches may not yet be saturated, such that new species could “invade” without major ecological ramifications. In general, northern range limits are thought to be more constrained by climate than by competition and other species interactions, compared with southern range limits (MacArthur 1972, Root 1988). This may explain the relative rapidity of documented range expansions, compared with range contractions (Parmesan et al. 1999). On the other hand, novel species communities may bring ecological surprises (Schneider and Root 1996, Williams and Jackson 2007), and warmer conditions may increase competition and predation pressures. Among the passerine species we examined that are not yet breeding in the Alaskan boreal region, the two corvids—American Crow (*Corvus brachyrhynchos*) and Blue Jay—are documented nest predators (Yahner and Scott 1988, Vander Haegen and Degraaf 1996) and could increase predation pressure for northern forest birds, altering population demographics. Although we did not find evidence of competitive exclusion currently keeping species out of Alaska, it is possible that expanding species may have detrimental competitive effects on closely related species, for example Black-throated Green

Warbler in Canada and Townsend's Warbler in Alaska. With the exception of this example, however, most of these closely related species pairs already co-occur elsewhere. A few unique species combinations may arise where Old World species such as Arctic Warbler (*Phylloscopus borealis*) and Bluethroat (*Luscinia svecica*) occupy niches that could also be occupied by New World species.

4.4.5 Conclusion

Our analysis of life-history traits and paleoclimate suitability suggests that the perceived barrier of the northwestern cordillera may be easily weakened as climate change improves conditions for many forest species across this region. This demonstrates yet another way in which the anticipated climate-change impacts of the upcoming century and beyond may cause major changes in systems that are traditionally perceived as constant. Conservationists and land managers must prepare to reconsider conservation policies and strategies in light of evolving ecological communities.

4.5 Appendices

[Appendix 4-A](#). Projected current and paleo-historical core area distributions based on the CCM1 global climate model.

[Appendix 4-B](#). Projected current and paleo-historical core area distributions based on the GFDL global climate model.

[Appendix 4-C](#). Values of climate suitability variables for each species.

[Appendix 4-D](#). Values of calculated competition indices.

[Appendix 4-E](#). Predicted probability of occurrence within Alaska Boreal Interior ecoregion.

4.6 Tables

Table 4-1. Range characteristics of 80 boreal study species.

Species currently occurring as regular breeders in the Alaska Boreal Interior (AKBreed) according to Gibson (2011) or Gibson and Withrow (2015) are indicated by ‘1.’ Breeding ranges are characterized as boreal/arctic (BA), boreal + western (BW), boreal + eastern (BE), or WR (wide-ranging), and migratory strategy is characterized as R (winter resident), LD (long-distance migrant), or SD (short-distance migrant).

	Common name (<i>Scientific name</i>)	AK Breed	Breed Range	Mig Strat
ALFL	Alder Flycatcher (<i>Empidonax alnorum</i>)	1	BE	LD
AMCR	American Crow (<i>Corvus brachyrhynchos</i>)	0	WR	SD
AMGO	American Goldfinch (<i>Spinus tristis</i>)	0	WR	SD
AMPI	American Pipit (<i>Anthus rubescens</i>)	1	BW	SD
AMRE	American Redstart (<i>Setophaga ruticilla</i>)	0	WR	LD
AMRO	American Robin (<i>Turdus migratorius</i>)	1	WR	SD
ATSP	American Tree Sparrow (<i>Spizella arborea</i>)	1	BA	SD
BAWW	Black-and-white Warbler (<i>Mniotilta varia</i>)	0	BE	LD
BBWA	Bay-breasted Warbler (<i>Setophaga castanea</i>)	0	BA	LD
BCCH	Black-capped Chickadee (<i>Poecile atricapillus</i>)	1	WR	R
BHCO	Brown-headed Cowbird (<i>Molothrus ater</i>)	0	WR	SD
BHVI	Blue-headed Vireo (<i>Vireo solitarius</i>)	0	BE	SD
BLBW	Blackburnian Warbler (<i>Setophaga fusca</i>)	0	BE	LD
BLJA	Blue Jay (<i>Cyanocitta cristata</i>)	0	BE	R
BLPW	Blackpoll Warbler (<i>Setophaga striata</i>)	1	BA	LD
BOCH	Boreal Chickadee (<i>Poecile hudsonicus</i>)	1	BA	R
BRBL	Brewer’s Blackbird (<i>Euphagus cyanocephalus</i>)	0	WR	SD
BRCR	Brown Creeper (<i>Certhia americana</i>)	1	WR	R
BTNW	Black-throated Green Warbler (<i>Setophaga virens</i>)	0	BE	LD
CAWA	Canada Warbler (<i>Cardellina canadensis</i>)	0	BE	LD
CCSP	Clay-colored Sparrow (<i>Spizella pallida</i>)	0	BE	LD
CEDW	Cedar Waxwing (<i>Bombycilla cedrorum</i>)	0	WR	SD

	Common name (<i>Scientific name</i>)	AK Breed	Breed Range	Mig Strat
CHSP	Chipping Sparrow (<i>Spizella passerina</i>)	1	WR	SD
CMWA	Cape May Warbler (<i>Setophaga tigrina</i>)	0	BE	LD
COGR	Common Grackle (<i>Quiscalus quiscula</i>)	0	BE	SD
CONW	Connecticut Warbler (<i>Oporornis agilis</i>)	0	BE	LD
CORA	Common Raven (<i>Corvus corax</i>)	1	WR	R
CORE	Common Redpoll (<i>Acanthis flammea</i>)	1	BA	R
COYE	Common Yellowthroat (<i>Geothlypis trichas</i>)	0	WR	SD
CSWA	Chestnut-sided Warbler (<i>Setophaga pensylvanica</i>)	0	BE	LD
DEJU	Dark-eyed Junco (<i>Junco hyemalis</i>)	1	WR	SD
EAKI	Eastern Kingbird (<i>Tyrannus tyrannus</i>)	0	BE	LD
EAPH	Eastern Phoebe (<i>Sayornis phoebe</i>)	0	BE	SD
EVGR	Evening Grosbeak (<i>Coccothraustes vespertinus</i>)	0	BW	R
FOSP	Fox Sparrow (<i>Passerella iliaca</i>)	1	BW	SD
GCKI	Golden-crowned Kinglet (<i>Regulus satrapa</i>)	1	WR	SD
GCTH	Gray-cheeked Thrush (<i>Catharus minimus</i>)	1	BA	LD
GRAJ	Gray Jay (<i>Perisoreus canadensis</i>)	1	BW	R
HETH	Hermit Thrush (<i>Catharus guttatus</i>)	1	WR	SD
HOLA	Horned Lark (<i>Eremophila alpestris</i>)	1	WR	SD
LCSP	Le Conte's Sparrow (<i>Ammodramus leconteii</i>)	0	BE	SD
LEFL	Least Flycatcher (<i>Empidonax minimus</i>)	0	WR	LD
LISP	Lincoln's Sparrow (<i>Melospiza lincolni</i>)	1	WR	SD
MAWA	Magnolia Warbler (<i>Setophaga magnolia</i>)	0	BE	LD
MOWA	Mourning Warbler (<i>Geothlypis philadelphia</i>)	0	BE	LD
NAWA	Nashville Warbler (<i>Oreothlypis ruficapilla</i>)	0	WR	LD
NOWA	Northern Waterthrush (<i>Parkesia noveboracensis</i>)	1	WR	LD
OCWA	Orange-crowned Warbler (<i>Oreothlypis celata</i>)	1	WR	SD
OSFL	Olive-sided Flycatcher (<i>Contopus cooperi</i>)	1	WR	LD
OVEN	Ovenbird (<i>Seiurus aurocapilla</i>)	0	BE	LD
PAWA	Palm Warbler (<i>Setophaga palmarum</i>)	0	BE	LD

	Common name (<i>Scientific name</i>)	AK Breed	Breed Range	Mig Strat
PHVI	Philadelphia Vireo (<i>Vireo philadelphicus</i>)	0	BE	LD
PIGR	Pine Grosbeak (<i>Pinicola enucleator</i>)	1	BW	R
PISI	Pine Siskin (<i>Spinus pinus</i>)	1	BW	SD
PUFI	Purple Finch (<i>Haemorhous purpureus</i>)	0	WR	SD
RBGR	Rose-breasted Grosbeak (<i>Pheucticus ludovicianus</i>)	0	BE	LD
RBNU	Red-breasted Nuthatch (<i>Sitta canadensis</i>)	1	WR	R
RCKI	Ruby-crowned Kinglet (<i>Regulus calendula</i>)	1	WR	SD
REVI	Red-eyed Vireo (<i>Vireo olivaceus</i>)	0	BE	LD
RUBL	Red-winged Blackbird (<i>Agelaius phoeniceus</i>)	1	WR	SD
RWBL	Rusty Blackbird (<i>Euphagus carolinus</i>)	1	BA	SD
SAVS	Savannah Sparrow (<i>Passerculus sandwichensis</i>)	1	WR	SD
SOSP	Song Sparrow (<i>Melospiza melodia</i>)	0	WR	SD
SWSP	Swamp Sparrow (<i>Melospiza georgiana</i>)	0	BE	SD
SWTH	Swainson's Thrush (<i>Catharus ustulatus</i>)	1	WR	LD
TEWA	Tennessee Warbler (<i>Oreothlypis peregrina</i>)	0	BE	LD
TRES	Tree Swallow (<i>Tachycineta bicolor</i>)	1	WR	LD
VATH	Varied Thrush (<i>Ixoreus naevius</i>)	1	BW	SD
VESP	Vesper Sparrow (<i>Pooecetes gramineus</i>)	0	WR	SD
WAVI	Warbling Vireo (<i>Vireo gilvus</i>)	0	WR	LD
WCSP	White-crowned Sparrow (<i>Zonotrichia leucophrys</i>)	1	WR	SD
WETA	Western Tanager (<i>Piranga ludoviciana</i>)	0	BW	LD
WEWP	Western Wood-Pewee (<i>Contopus sordidulus</i>)	1	BW	SD
WIWA	Wilson's Warbler (<i>Cardellina pusilla</i>)	1	WR	LD
WIWR	Winter Wren (<i>Troglodytes hiemalis</i>)	0	WR	SD
WTSP	White-throated Sparrow (<i>Zonotrichia albicollis</i>)	0	BE	SD
WWCR	White-winged Crossbill (<i>Loxia leucoptera</i>)	1	BW	R
YBFL	Yellow-bellied Flycatcher (<i>Empidonax flaviventris</i>)	0	BE	LD
YRWA	Yellow-rumped Warbler (<i>Setophaga coronata</i>)	1	WR	SD
YWAR	Yellow Warbler (<i>Setophaga petechia</i>)	1	WR	LD

Table 4-2. Mean bioclimatic variable values by time period, boreal ecoregion, and GCM. Northwestern Cordillera = Taiga Cordillera + Boreal Cordillera. MH = Mid-Holocene. GFDL and CCM1 are global climate models (GCM).

Variable	Northwestern Cordillera			Alaska Boreal Interior		
	Current	MHGFDL	MHCCM1	Current	MHGFDL	MHCCM1
Mean cold month temperature (°C)	-20.5	-21.1	-15.6	-21.7	-22.3	-14.6
Mean warm month temperature (°C)	11.5	13.1	12.7	14.8	16.0	15.8
Chilling degree days (< 0 °C)	2945	2986	2628	3164	3188	2716
Growing degree days (> 5 °C)	630	682	743	967	995	1102
Extreme minimum temperature (°C)	-50.0	-47.1	-49.8	-51.8	-48.7	-54.0
Annual temperature difference (°C)	32.1	34.1	28.3	36.5	38.3	30.4
Annual climatic moisture index (mm)	41.5	41.5	48.6	14.0	16.9	12.8
Summer climatic moisture index (mm)	5.2	4.8	5.5	-2.3	1.6	-2.1
Mean summer precipitation (mm)	358	364	406	257	309	277

Table 4-3. Climate and life-history variables included in phylogenetic logistic regression analysis. See [Figure 4-1](#) for ecoregion definitions. GCM = general circulation model: CCM1 = Community Climate System Model, GFDL = Geophysical Fluid Dynamics Laboratory Model. Model ID relates variables to candidate models in [Table 4-4](#).

Category	Sub-category	Variable abbreviation	Model ID	Variable description		
Climatic suitability	Current	CurrCordillera	A	Log-transformed area of current suitable habitat contained in the Boreal and Taiga Cordillera ecoregions		
		MHCordilleraCCM1	B	Log-transformed area of GCM-predicted mid-Holocene suitable habitat contained in the Boreal and Taiga Cordillera ecoregions		
		MHCordilleraGFDL	C			
	Mid-Holocene (MH, 6kBP)	MHCordDiffCCM1	N/A	Log-transformed difference between area of current suitable habitat and GCM-predicted mid-Holocene suitable habitat (used only in combined model with CurrCordillera)		
		MHCordDiffGFDL				
		Last Glacial Maximum (LGM, 21kBP)	LGMEastCCM1		D	Ratio of log-transformed area of GCM-predicted LGM suitable habitat (glacial refugia) contained in eastern U.S. ecoregions to area of LGM suitable habitat contained in western U.S. ecoregions
			LGMEastGFDL		E	
Last Glacial Maximum (LGM, 21kBP)	LGMAAlaskaCCM1	F	Log-transformed area of LGM suitable habitat contained in the Alaska Boreal Interior ecoregion			
	LGMAAlaskaGFDL	G				

Category	Sub-category	Variable abbreviation	Model ID	Variable description	
Life history	Migratory strategy	Resident	H	Migratory status (LDMigrant as contrast)	
		SDMigrant			
		LatMean	H	Mean and maximum latitude, and mean longitude of species' wintering range (courtesy of S. Crawford and T. Rich)	
		LatMax			
	LonMean				
		SAWinter	H	Approximate proportion of wintering grounds in South America (0 / 0.5 / 1) (Poole 2005)	
	Physical traits and habitat		Mass	I	Log-transformed mean body size (g) (Poole 2005)
			ClutchSize	I	Mean clutch size (Poole 2005)
			Insectivore Frugivore	I	Primary feeding guild (omnivore as contrast) (Poole 2005)
			Forest Woodland Shrub Wetland	I	Primary habitat association (grassland as contrast) (Poole 2005)
Competition			Compet	J	Maximum phylogenetic correlation coefficient with species currently in Alaska Boreal Interior

Table 4-4. AICc scores for candidate phylogenetic logistic regression models.

Phylogenetic regression models for species core area within the Alaska Boreal Interior ecoregion were developed for 500 trees; AIC scores and α values (lower value = higher phylogenetic correlation) were averaged across 500 models. Variables included in each model are identified by model ID in [Table 4-3](#).

Rank	ID	Model	AICc mean	AICc SD	α mean	α SD
1	A	Current northwestern cordilleran climate	59.47	0.113	1.307	1.941
2	C	Mid-Holocene cordilleran climate (GFDL)	67.39	1.767	0.508	1.524
3	B	Mid-Holocene cordilleran climate (CCM1)	76.08	3.741	1.536	2.440
4	D	Last glacial maximum eastern refugia (CCM1)	77.69	0.057	5.025	0.955
5	G	Last glacial maximum Alaska refugia (GFDL)	78.23	0.000	5.279	0.801
6	F	Last glacial maximum Alaska refugia (CCM1)	102.72	0.001	5.643	0.600
7	H	Migratory strategy	108.48	0.001	5.637	0.513
8	E	Last Glacial Maximum eastern refugia (GFDL)	109.47	0.002	5.697	0.580
9		Null model (offset only)	114.70	0.002	5.802	0.494
10	J	Competition	115.50	0.002	5.772	0.519
11	I	Physical traits (+ habitat)	119.41	0.002	5.742	0.543

Table 4-5. Mean logistic regression model coefficients and model diagnostics.

Model coefficients and diagnostics for 7 candidate phylogenetic (P) and standard (non-phylogenetic, NP) logistic regression models of occurrence as a regular breeder in the Alaska Boreal Interior (see [Figure 4-1](#)) for 80 boreal-breeding species (see [Table 4-1](#)). AICc scores, pseudo-R² values, and standardized regression coefficients for phylogenetic models were averaged across 100 models, each based on a different phylogenetic tree. Area-under-the-curve (AUC) was derived from mean model predictions.

Rank/ Model	Model	AICc mean	AICc sd	Pseudo- R ² mean	AUC
1	P -0.87 + 5.04 * CurrCordillera + 1.70 * MHCordDiffGFDL + 0.66 * Resident + 0.29 * SAWinter	50.79	0.000	0.64	0.97
	NP -1.01 + 5.35 * CurrCordillera + 1.95 * MHCordDiffGFDL + 0.99 * Resident + 0.34 * SAWinter	51.39		0.52	
2	P -0.76 + 4.37 * CurrCordillera + 1.37 * MHCordDiffCCM1 + 0.97 * Resident + 0.71 * SDMigrant + 0.78 * SAWinter	55.32	0.002	0.63	0.96
	NP -0.87 + 4.66 * CurrCordillera + 1.59 * MHCordDiffCCM1 + 1.44 * Resident + 1.00 * SDMigrant + 1.03 * SAWinter	52.79		0.53	
3	P -0.86 + 3.45 * CurrCordillera + 0.96 * Resident + 0.66 * SDMigrant + 1.09 * SAWinter	58.88	0.001	0.58	0.94
	NP -0.97 + 3.44 * CurrCordillera + 1.39 * Resident + 0.87 * SDMigrant + 1.34 * SAWinter	56.78		0.46	
4	P -0.36 + 1.53 * MHCordilleraCMM1 - 1.20 * LGMEastCCM1 + 0.74 * Resident + 0.97 * SDMigrant + 0.76 * SAWinter	68.31	0.531	0.52	0.94
	NP -0.52 + 1.37 * MHCordilleraCCM1 - 1.44 * LGMEastCCM1 + 1.03 * Resident + 1.11 * SDMigrant + 1.06 * SAWinter	60.00		0.45	
5	P -0.30 + 1.01 * MHCordilleraGFDL + 1.01 * Resident + 0.98 * SDMig + 0.58 * SAWinter	69.77	0.009	0.48	0.91
	NP -0.39 + 1.69 * MHCordilleraGFDL + 1.31 * Resident + 1.13 * SDMigrant + 0.72 * SAWinter	63.12		0.39	
6	P -0.30 + 1.80 * MHCordilleraCCM1 + 0.99 * Resident + 1.17 * SDMig + 0.57 * SAWinter	76.11	0.002	0.43	0.91
	NP -0.30 + 1.45 * MHCordilleraCCM1 + 1.26 * Resident + 1.27 * SDMig + 0.75 * SAWinter	66.78		0.35	
7	P -0.40 - 1.49 * LGMEastCCM1 + 0.72 * Resident + 0.53 * SDMigrant + 0.56 * SAWinter	91.08	0.002	0.29	0.84
	NP -0.42 - 1.25 * LGMEastCCM1 + 1.02 * Resident + 0.72 * SDMigrant + 0.77 * SAWinter	72.90		0.27	

Table 4-6. Numbers of species projected to breed regularly in the Alaska Boreal Interior currently and during future 30-year periods, based on a mean predicted prevalence threshold ($p > 0.475$) for AICc-weighted model-averaged predictions (see [Table 4-5](#)).

(a)	Actual	Projected			
	Current	Current	2011-2040	2041-2070	2071-2100
Entire boreal	80	41	67	74	71
In Alaskan boreal	38	35	36	36	31
Not in Alaskan boreal	42	6	31	38	40

Table 4-7. Species most likely to move into the Alaska Boreal Interior currently and during future 30-year periods.

Classifications are according to AICc-weighted model-averaged predictions using a threshold of $p > 0.475$ (Table 4-5). Species shown in bold have had recently documented breeding or territorial behavior in the Alaskan interior or in adjacent south-central Alaska (Gibson 2011, Gibson and Withrow 2015). See Appendix 4-E for scientific names and probabilities across species and models.

Rank	Baseline (1961-1990)	2011-2040	2041-2070	2071-2100
1	Common Grackle	Common Grackle	Tennessee Warbler	Red-eyed Vireo
2	Brown-headed Cowbird	Tennessee Warbler	Cedar Waxwing	Blue Jay
3	Evening Grosbeak	Evening Grosbeak	Evening Grosbeak	Cedar Waxwing
4	Warbling Vireo	American Redstart	American Redstart	Blackburnian Warbler
5	American Redstart	Cedar Waxwing	Red-eyed Vireo	Mourning Warbler
6	Song Sparrow	Brown-headed Cowbird	White-throated Sparrow	Common Yellowthroat
7		Warbling Vireo	Common Yellowthroat	Evening Grosbeak
8		White-throated Sparrow	Common Grackle	American Redstart
9		Song Sparrow	Mourning Warbler	White-throated Sparrow
10		Purple Finch	Least Flycatcher	Chestnut-sided Warbler
11		Common Yellowthroat	Blackburnian Warbler	Black-and-white Warbler
12		Western Tanager	Warbling Vireo	Ovenbird
13		Least Flycatcher	Song Sparrow	Common Grackle
14		Red-eyed Vireo	Blue Jay	Canada Warbler
15		Black-throated Green Warbler	Canada Warbler	American Goldfinch
16		Palm Warbler	Brown-headed Cowbird	Least Flycatcher
17		American Goldfinch	Black-throated Green Warbler	Tennessee Warbler
18		Philadelphia Vireo	Purple Finch	Black-throated Green Warbler

Rank	Baseline (1961-1990)	2011-2040	2041-2070	2071-2100
19		American Crow	Ovenbird	Red-breasted Grosbeak
20		Vesper Sparrow	Black-and-white Warbler	Blue-headed Vireo
21		Cape May Warbler	American Goldfinch	Song Sparrow
22		Winter Wren	Western Tanager	Purple Finch
23		Ovenbird	Cape May Warbler	Magnolia Warbler
24		Mourning Warbler	Chestnut-sided Warbler	Warbling Vireo
25		Magnolia Warbler	Magnolia Warbler	Eastern Phoebe
26		Swamp Sparrow	Bay-breasted Warbler	Bay-breasted Warbler
27		Brewer's Blackbird	Blue-headed Vireo	American Crow
28		Black-and-white Warbler	Philadelphia Vireo	Winter Wren
29		Blue-headed Vireo	Winter Wren	Nashville Warbler
30		Clay-colored Sparrow	American Crow	Cape May Warbler
31		Yellow-bellied Flycatcher	Red-breasted Grosbeak	Brown-headed Cowbird
32			Nashville Warbler	Philadelphia Vireo
33			Yellow-bellied Flycatcher	Connecticut Warbler
34			Vesper Sparrow	Western Tanager
35			Connecticut Warbler	Yellow-bellied Flycatcher
36			Palm Warbler	Vesper Sparrow
37			Brewer's Blackbird	Eastern Kingbird
38			Clay-colored Sparrow	Swamp Sparrow
39				Brewer's Blackbird
40				Clay-colored Sparrow

4.7 Figures



Figure 4-1. North American ecoregions.

CEC Level II ecoregions used in analysis: 3.1 Alaska Boreal Interior (study area); 3.2 Taiga Cordillera; 3.3 Taiga Plain; 5.4 Boreal Plain; 6.1 Boreal Cordillera. Additional ecoregions evaluated for last glacial maximum projections (portions above 30 degrees N latitude): 6.2, 7.1, 10.1-2, 11.1 (western); 8.1-5, 9.2-4 (eastern). Northwestern cordillera ecoregions (3.2 and 6.1) are shown with stippled pattern. Boreal ecoregions are shown in gray. Map projection is Lambert azimuthal equal-area.

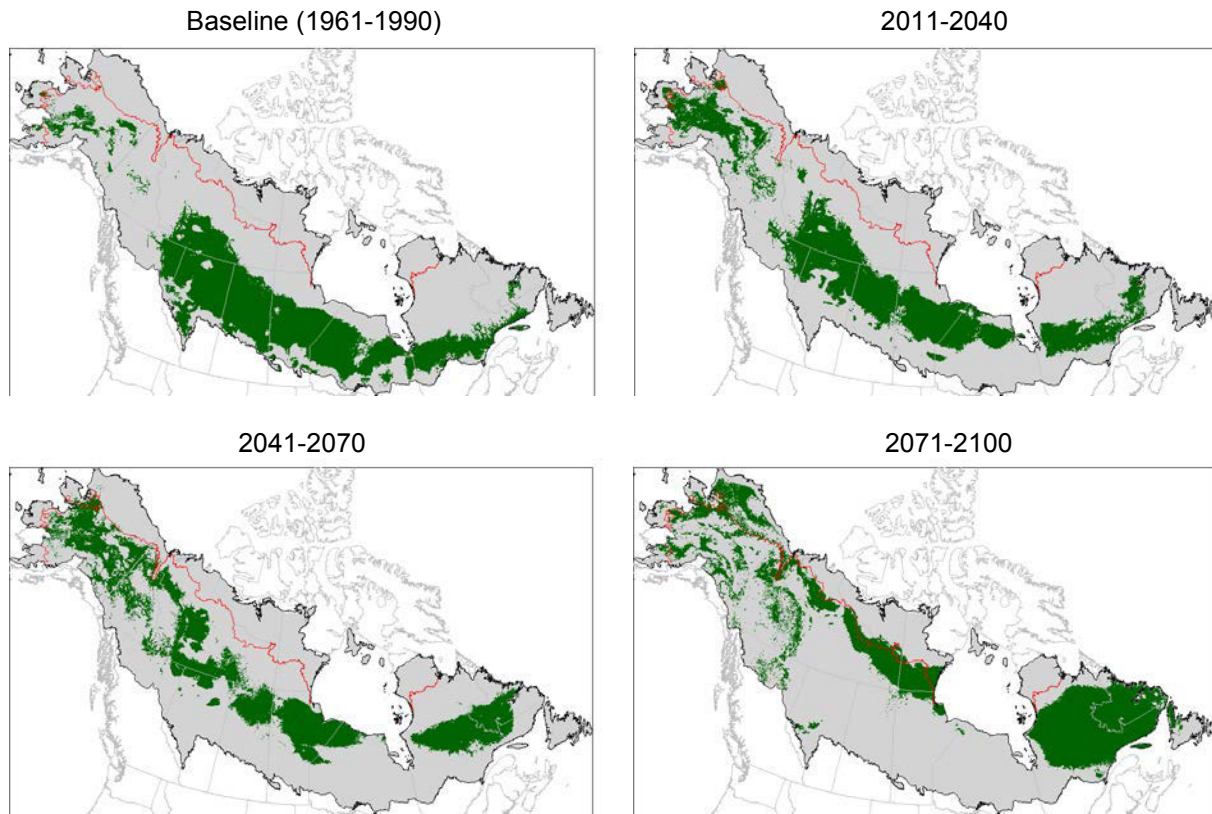


Figure 4-2. Climatically suitable core habitat for an example species in current and future time periods.

Climatically suitable habitat (green) for Tennessee Warbler, *Oreothlypis peregrina*. Data are from Stralberg et al. (2015b). Discontinuous patches of suitable habitat with the Alaska Boreal Interior are currently unoccupied by regularly breeding birds although territorial singing males have recently been documented there (Gibson 2011).

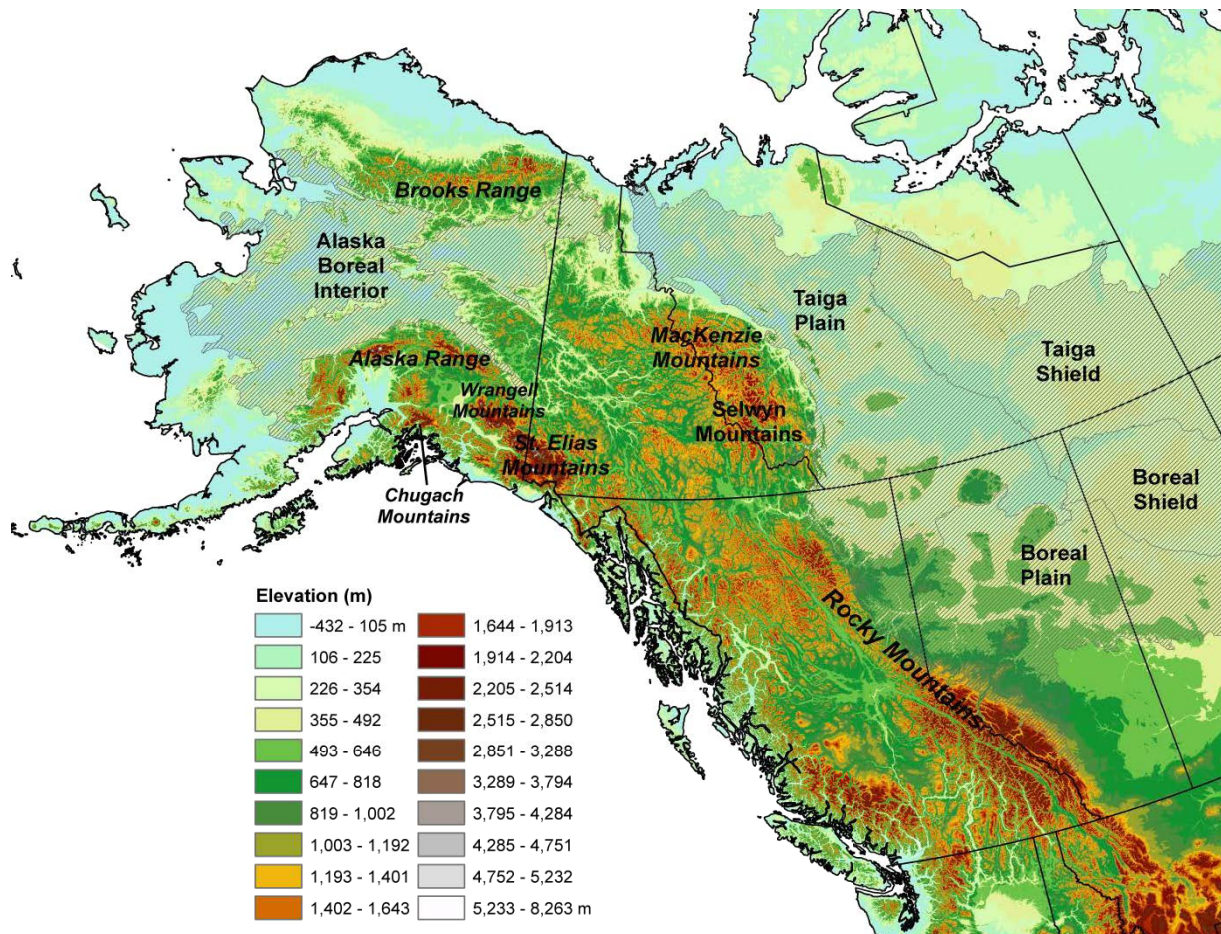


Figure 4-3. Northwestern cordillera mountain ranges that present potential barriers between non-mountain boreal ecoregions in Canada and Alaska.

Non-mountain boreal ecoregions, as mapped by the Commission for Environmental Cooperation (1997), are indicated by cross-hatching: Alaska Boreal Interior, Taiga Plain, Taiga Shield, Boreal Plain, and Boreal Shield. Only the northernmost portion of the Rocky Mountains was considered in our analysis (see [Figure 4-1](#)). Map projection is Yukon Albers equal-area conic.

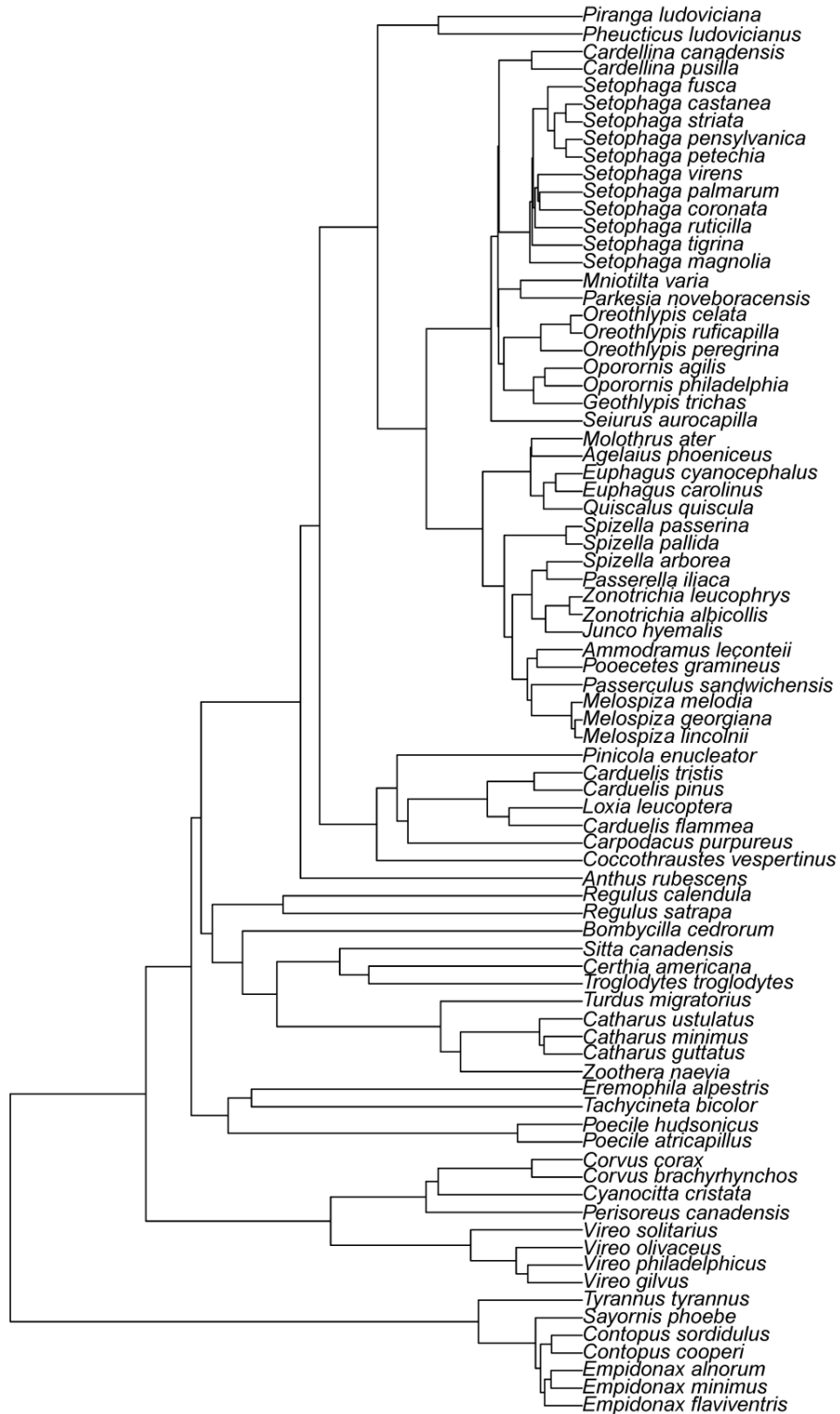


Figure 4-4. Sample phylogeny for the 80 boreal-breeding species analyzed.

One of 500 phylogenies (each considered equally likely) obtained from bird.tree.org (Jetz et al. 2012).

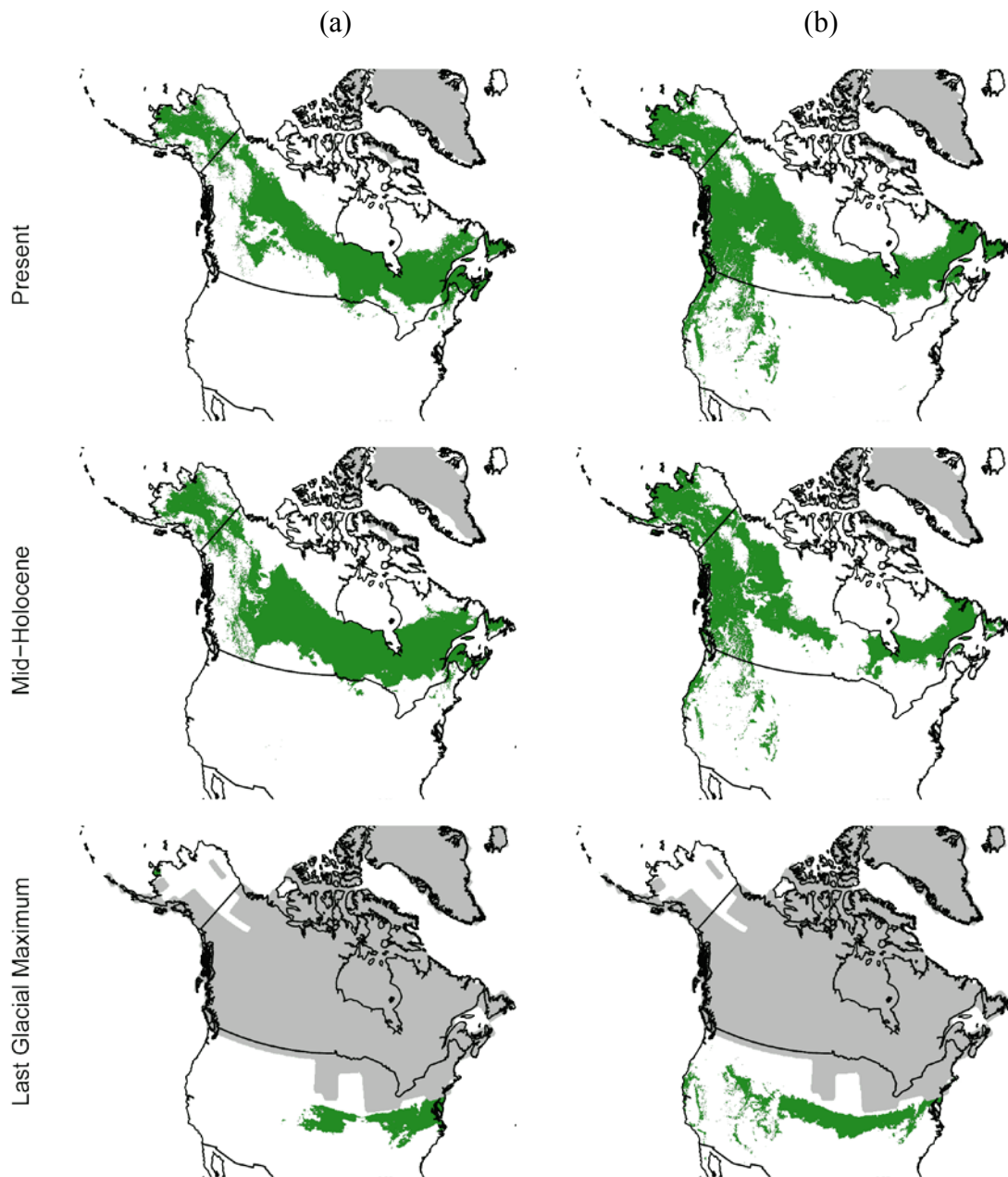


Figure 4-5. Climatically suitable core habitat in current, mid-Holocene, and LGM periods for two example species.

Climatically suitable habitat (green) for (a) Alder Flycatcher (*Empidonax alnorum*), a largely boreal species, and (b) Swainson's Thrush (*Catharus ustulatus*), a wide-ranging species. Both are regular breeders in the Alaska boreal region with substantial climatically suitable habitat within the northwestern cordillera. Hindcasts are based on the CCM1 global climate model. Ice sheet extent shown in dark gray. See [Appendix 4-A](#) and [Appendix 4-B](#) for remaining species.

CONCLUSION

The research presented in this thesis improves scientific understanding of controls on boreal passerine distribution and abundance, and suggests anticipated boreal bird and vegetation responses to anthropogenic climate change. As with most SDM-based predictive modelling research, much of my work can be considered hypothesis-generating. Spatio-temporally extensive datasets are lacking for retrospective analysis of avian distributional responses to historic climate change, and relatively small climate-change effects have thus far been observed, in comparison with expected future changes. Thus, data-driven forecasts with appropriate caveats and uncertainty bounds provide some of the most useful planning tools (Silver 2012). Herein, I have perhaps provided more questions than answers, but these questions can and will guide future research on the topic of boreal ecosystem responses to climate change. Some specific questions and research directions are discussed below by chapter.

In Chapter 1, [Projecting boreal bird responses to climate change: the signal exceeds the noise](#) (Stralberg et al. 2015b), I used information-rich point-count abundance data to identify the climatic drivers of distributions for 80 boreal-breeding passerine species, and to quantify and attribute the uncertainty associated with current and future species distribution model (SDM) projections. I concluded that future habitat potential would decrease due to climate change for a majority of boreal species, and that despite uncertainties, primarily in global climate model projections, the “signal” of climate change was greater than the model “noise” for most species, indicating that with best modelling practices and reasonable data, models useful for conservation planning can be developed, and that uncertainty information should be used to frame results. My models and predictions are somewhat unique, however, in their incorporation of abundance information, and a preliminary investigation suggested that density models are more accurate and more spatially refined than data-equivalent presence/absence models (Stralberg et al. 2012), as others have since also demonstrated (Veloz et al. 2015). The inclusion of the [Boreal Avian Modelling Project](#)'s (BAM) comprehensive off-road dataset for the boreal region should also make for more accurate predictions within the boreal region and to the north, compared with similar continental-scale efforts that are based on roadside breeding bird survey data (Distler et al. 2015, Schuetz et al. 2015).

Current and future predicted density layers from this paper are publicly available at [BAM's DataBasin web portal](#), and have been used for several Environment Canada planning

projects, including the quantification of boreal ecosystem services, the evaluation of boreal bird conservation priorities, and species-at-risk assessment. Conservation organizations such as The Canadian BEACONS Project, Nature Conservancy Canada, and the Canadian Parks and Wilderness Society may also use the models. Current distribution predictions can also be used to refine range maps and identify data gaps, especially for species-at-risk and at northern range limits, which I plan to pursue as part of my future work with BAM. The data products may also be used to explore a number of macro-ecological questions related to the climatic drivers and life-history correlates of climate-change response and uncertainty—areas that have been well-studied, but with inconsistent results across regions and taxa (Stockwell 2002, McPherson et al. 2004, Segurado and Araújo 2004, McPherson and Jetz 2007, Kharouba et al. 2013). My preliminary (unpublished) analyses suggest that in the boreal region, future prediction uncertainty and change magnitude are driven primarily by soil moisture availability, as represented by the climatic moisture index. Thus the relative balance between deciduous forest and grassland in the western boreal interior will have a great influence on associated bird species, and may determine the population-level fate of deciduous forest-associated species in particular. I also found an influence of niche breadth, with relative habitat specialists demonstrating higher prediction uncertainty. This analysis should be revisited in light of the seral-stage associations and modified refugia projections identified in the subsequent chapter.

In light of expected time lags in vegetation responses to climate, Chapter 2, [Conservation of future boreal forest bird communities considering lags in vegetation response to climate change: a modified refugia approach](#) (Stralberg et al. 2015a), built on the SDM projections from Chapter 1 to identify multi-species conservation priorities for a subset of 53 strictly forest species in the face of climate change. To do so, I analyzed these species' forest age associations and quantified boreal species' vulnerability to climate change in light of their seral-stage habitat associations. These results can be used for species-at-risk planning, as well as species vulnerability assessments. I used the information to modify individual species' projections and identify the location of common boreal macrorefugia, where boreal species are most likely to persist in the future. Although some obvious descriptors emerged from visual inspection (mountain and coastal regions, ecotonal boundaries), further analysis of environmental correlates is warranted, and is planned as part of my future work with the [AdaptWest](#) climate adaptation project.

My results suggested that the locations of these multi-species refugia were fairly robust to different species weighting schemes, and were strongly terrain driven. It also happens that many of these areas, because of their correspondence with relatively steep terrain in remote areas, are relatively poorly surveyed. Thus they are prime candidates for climate-change monitoring efforts. In collaboration with Erin M. Bayne and Scott E. Nielsen at the University of Alberta, I have initiated new field research in four of Alberta's hill systems. We have collected data on birds, vegetation, and temperature, and preliminary results suggest strong and intuitive elevation gradients in bird diversity compared to latitudinal gradients (Bayne and Stralberg 2015), reinforcing the idea that Alberta's climatic refugia potential may be found in these and other minor hill systems. Planned future data analyses will provide additional insights into the importance of local terrain and topo-climate variability on vegetation and bird communities.

In Chapter 3, [Scenarios of future climate- and disturbance-driven changes for the boreal forest region of Alberta](#), I took a closer look at near-term forest change projections, focusing on boreal Alberta. Considering anticipated climate-vegetation disequilibrium, I pursued a dynamic fire simulation approach coupled with empirical ecosite-based models of vegetation distribution, as a way to bridge the gap between broad climate gradient controls and local mechanistic controls on short-term dynamics (Cushman et al. 2006, Gustafson 2013). This hybrid approach is similar to one I employed for climate-change projection based on sea-level rise in San Francisco Bay tidal marshes (Stralberg et al. 2011). While the two systems and drivers are very different, they both involved identifying key processes of short-term change in dynamic systems (sediment deposition in tidal marshes, wildfire regimes in boreal forests) and incorporating mechanistic simulations of those key processes in an empirical model framework.

Results indicated that despite lags in vegetation response to climate change, the combination of fire, human disturbance and climate change will reduce the area of young and old forest, creating challenges for both early- and late-seral wildlife species. More research on patterns and drivers of inter-annual variability in bird abundance, including annual life cycle analysis and modelling (Hostetler et al. 2015), will be invaluable to evaluating population responses of boreal birds to climate change. My ongoing and future work with BAM is addressing this by analyzing the relative importance of breeding vs. wintering ground climate and disturbance factors on multi-species inter-annual variability.

Simulation models also suggested that area burned will increase in the future, but should slow towards the end of the century, as new climate-suitable forests become dominated by deciduous trees and create a less flammable landscape. In the long-term, if and when vegetation catches up with changes in climate, a future grass-dominated landscape could again have high rates of fire. This emphasizes the transient nature of decadal-scale projections, and calls for adaptive conservation planning and management paradigms that can detect and respond to short-term change (Kellomäki et al. 2008, Oliver et al. 2012)

This as-yet unpublished chapter also leads to ample future research opportunities. The next step is to develop bird density models based on ecosite/vegetation and forest age, in order to extend vegetation projections to bird abundance and assess potential future population bottlenecks. Preliminary investigations suggest that climatic differences between lower foothill and boreal regions pose challenges for projecting bird densities as a direct function of vegetation, especially in light of the novel future climates expected in the Rocky Mountain foothills.

In addition, the ecosite modelling framework can be used to develop ongoing updates to current and future ecosite and vegetation predictions, as new data are collected, and additional existing datasets are assembled. The subregion-independent approach to predictive mapping is more flexible in a climate-change context, and also more robust to sampling inadequacies in that larger datasets may be used in a machine-learning framework. The broad focus on Northern Alberta may easily be scaled down to specific regions, such as the data-rich and energy-sector-affected Lower Athabasca watershed, potentially at a finer 100-m spatial resolutions corresponding with input data. Local climate refugia may emerge at this scale, both as a function of topo-climate effects on vegetation (Ackerly et al. 2010), and as a result of fire refugia, i.e., areas that burn less as a function of nearby water bodies and terrain characteristics (Keppel et al. 2012). Fire zone stratification within northern Alberta may provide more spatially refined outputs toward this end. Vegetation trajectories in the foothill regions also need to be re-evaluated within a larger geographic context, in light of no-analog conditions.

Finally, Chapter 4, [Biogeography of boreal passerine range dynamics in western North America: past, present, and future](#), provided an opportunity to evaluate the apparent climate disequilibrium in the Alaskan boreal region, as well as range shift hypotheses generated by distribution models developed in Chapter 1. I took the long view of climate change by investigating paleoclimate conditions for boreal songbirds and evaluating the factors determining

which passerine species have been able to colonize the boreal region of Alaska since the last glacial maximum. Given the lack of a passerine fossil record, I used paleo-hindcasting combined with phylogenetic analysis to identify common characteristics of species that have colonized the Alaskan boreal region post-glaciation. I found that climatic suitability of the northwestern cordillera, now and during the mid-Holocene warm period 6,000 years BP, was the strongest predictor of boreal Alaska occupancy, controlling for climatic suitability and phylogeny. This suggests that the northwestern cordillera mountains present a weak barrier to bird dispersal, determined primarily by suitable climate connectivity now and in the mid-Holocene period. Indeed, many of the species we identified as candidates for near-term colonization of the Alaskan boreal region have in fact been identified as potential new breeders already (Gibson 2011, Gibson and Withrow 2015). Thus, as climatically suitable passageways across the northwestern cordillera increase in upcoming decades, additional new breeding records should be expected. Standardized surveys at regular intervals should be used to detect changes in composition and abundance of the Alaskan boreal avifauna. Experimental assisted migration (McLane and Aitken 2011) could also be explored as a way to assist these transitions and evaluate model-predicted habitat suitability.

For passerine birds, this work suggests that the primary barrier to a species occupying its fundamental niche may be distance, or lack of suitable habitat connectivity, rather than mountains *per se*, although topography certainly affects habitat connectivity, as can human disturbance in more densely populated regions. In the future, climate change may also create new barriers within the otherwise mostly contiguous boreal biome. For example, I observed in Chapter 1 that climatically suitable habitat for many species will become separated by James Bay and Hudson Bay over time, leading to vicariance and potential genetic divergence among populations.

In conclusion, a rapidly changing world is sure to include disequilibria that challenge the persistence of species and ecosystems. Admittedly, the correlative SDM approach that I have pursued in this thesis has clear limitations, given the equilibrium assumption that will increasingly be violated in the future. My work has addressed historical and anticipated disequilibria directly, however, as well as the uncertainties associated with climate change. By quantifying and controlling prediction uncertainty, focusing on climatic refugia as conservation priorities, and simulating realistic rates of vegetation change based on simulated fire dynamics, I

have provided well-defined bounds and caveats for future projections, as well as testable hypotheses for future research.

REFERENCES

- ABMI. 2014. 2000 Alberta Backfilled Wall-to-Wall Land Cover Version 2.5 - Metadata.
- ACIA. 2005. Arctic Climate Impact Assessment. ACIA Overview report. Cambridge University Press, New York.
- Ackerly, D. D., S. R. Loarie, W. K. Cornwell, S. B. Weiss, H. Hamilton, R. Branciforte, and N. J. B. Kraft. 2010. The geography of climate change: implications for conservation biogeography. *Diversity and Distributions* **16**:476-487.
- AESRD. 2014. Alberta Merged Wetland Inventory. Alberta Environment and Sustainable Resource Development. Edmonton, AB.
- Alberta Geological Survey. 2013. Surficial Geology Map of Alberta *in* A. G. Survey, editor., Edmonton, Alberta.
- Allen, C. D., D. D. Breshears, and N. G. McDowell. 2015. On underestimation of global vulnerability to tree mortality and forest die-off from hotter drought in the Anthropocene. *Ecosphere* **6**:art129.
- Allen, C. D., A. K. Macalady, H. Chenchouni, D. Bachelet, N. McDowell, M. Vennetier, T. Kitzberger, A. Rigling, D. D. Breshears, E. H. Hogg, P. Gonzalez, R. Fensham, Z. Zhang, J. Castro, N. Demidova, J.-H. Lim, G. Allard, S. W. Running, A. Semerci, and N. Cobb. 2010. A global overview of drought and heat-induced tree mortality reveals emerging climate change risks for forests. *Forest Ecology and Management* **259**:660-684.
- Anderson, L. L., F. S. Hu, D. M. Nelson, R. J. Petit, and K. N. Paige. 2006. Ice-age endurance: DNA evidence of a white spruce refugium in Alaska. *Proceedings of the National Academy of Sciences* **103**:12447-12450.
- Anderson, M. G., and C. E. Ferree. 2010. Conserving the stage: Climate change and the geophysical underpinnings of species diversity. *PLoS ONE* **5**:e11554.
- Andrew, M. E., M. A. Wulder, and J. A. Cardille. 2014. Protected areas in boreal Canada: a baseline and considerations for the continued development of a representative and effective reserve network¹. *Environmental Reviews* **22**:1-26.

- Andrew, M. E., M. A. Wulder, and N. C. Coops. 2011. Patterns of protection and threats along productivity gradients in Canada. *Biological Conservation* **144**:2891-2901.
- Araújo, M. B., M. Cabeza, W. Thuiller, L. Hannah, and P. H. Williams. 2004. Would climate change drive species out of reserves? An assessment of existing reserve-selection methods. *Global Change Biology* **10**:1618-1626.
- Araújo, M. B., and M. New. 2007. Ensemble forecasting of species distributions. *Trends in Ecology & Evolution* **22**:42-47.
- Araújo, M. B., and R. G. Pearson. 2005. Equilibrium of species' distributions with climate. *Ecography* **28**:693-695.
- Araújo, M. B., and A. T. Peterson. 2012. Uses and misuses of bioclimatic envelope modeling. *Ecology* **93**:1527-1539.
- Araújo, M. B., W. Thuiller, and N. G. Yoccoz. 2009. Reopening the climate envelope reveals macroscale associations with climate in European birds. *Proceedings of the National Academy of Sciences of the United States of America* **106**:E45-E46.
- Araújo, M. B., R. J. Whittaker, R. J. Ladle, and M. Erhard. 2005. Reducing uncertainty in projections of extinction risk from climate change. *Global Ecology and Biogeography* **14**:529-538.
- Archibald, J. H., G. D. Klapstein, and I. G. W. Corns. 1996. Field guide to ecosites of Southwestern Alberta. Natural Resources Canada, Canadian Forest Service, Edmonton, Alberta.
- Arienti, M. C., S. G. Cumming, and S. Boutin. 2006. Empirical models of forest fire initial attack success probabilities: the effects of fuels, anthropogenic linear features, fire weather, and management. *Canadian Journal of Forest Research* **36**:3155-3166.
- Arponen, A., A. Moilanen, and S. Ferrier. 2008. A successful community-level strategy for conservation prioritization. *Journal of Applied Ecology* **45**:1436-1445.
- Ashcroft, M. B. 2010. Identifying refugia from climate change. *Journal of Biogeography* **37**:1407-1413.
- Ashton, K. G. 2002. Patterns of within-species body size variation of birds: strong evidence for Bergmann's rule. *Global Ecology and Biogeography* **11**:505-523.
- Badiou, P., R. Baldwin, M. Carlson, M. Darveau, P. Drapeau, K. Gaston, J. Jacobs, J. Kerr, S. Levin, M. Manseau, G. Orians, S. Pimm, H. Possingham, P. Raven, F. Reid, D. Roberts,

- T. Root, N. Roulet, J. Schaefer, D. Schindler, J. Strittholt, N. Turner, and J. Wells. 2013. Conserving the World's Last Great Forest Is Possible: Here's How. International Boreal Conservation Science Panel.
- Bahn, V., R. J. O'Connor, and W. B. Krohn. 2006. Importance of spatial autocorrelation in modeling bird distributions at a continental scale. *Ecography* **29**:835-844.
- Balling, R. C., P. J. Michaels, and P. C. Knappenberger. 1998. Analysis of winter and summer warming rates in gridded temperature time series. *Climate Research* **9**:175-181.
- Ballings, M., and D. Van den Poel. 2013. Package 'AUC'. Available on-line at <http://cran.r-project.org/web/packages/AUC/index.html>.
- Balshi, M. S., A. D. McGuire, P. Duffy, M. Flannigan, J. Walsh, and J. Melillo. 2009. Assessing the response of area burned to changing climate in western boreal North America using a Multivariate Adaptive Regression Splines (MARS) approach. *Global Change Biology* **15**:578-600.
- Barbet-Massin, M., W. Thuiller, and F. Jiguet. 2012. The fate of European breeding birds under climate, land-use and dispersal scenarios. *Global Change Biology* **18**:881-890.
- Barker, N. K. S., P. C. Fontaine, S. G. Cumming, D. Stralberg, A. Westwood, E. M. Bayne, P. Sólymos, F. K. A. Schmiegelow, S. J. Song, and D. J. Rugg. 2015. Ecological monitoring through harmonizing existing data: Lessons from the boreal avian modelling project. *Wildlife Society Bulletin* **39**:480-487.
- Barnagaud, J.-Y., W. Daniel Kissling, B. Sandel, W. L. Eiserhardt, Ç. H. Şekercioğlu, B. J. Enquist, C. Tsirogiannis, and J.-C. Svenning. 2014. Ecological traits influence the phylogenetic structure of bird species co-occurrences worldwide. *Ecology Letters* **17**:811–820.
- Batllori, E., M.-A. Parisien, M. A. Krawchuk, and M. A. Moritz. 2013. Climate change-induced shifts in fire for Mediterranean ecosystems. *Global Ecology and Biogeography* **22**:1118–1129.
- Bauer, I. E., L. D. Gignac, and D. H. Vitt. 2003. Development of a peatland complex in boreal western Canada: lateral site expansion and local variability in vegetation succession and long-term peat accumulation. *Canadian Journal of Botany* **81**:833-847.
- Bayne, E., and D. Stralberg. 2015. Bird community composition along elevation and latitudinal gradients in Alberta's mixedwood forest: analogues for our future climate? *Progress*

- report prepared for the Biodiversity Management and Climate Change Adaptation Project. Alberta Biodiversity Monitoring Institute, Edmonton, Alberta.
- Bayne, E. M., D. Stralberg, and A. Nixon. 2015. Adapting monitoring to more effectively assess the impacts of climate change on Alberta's biodiversity. Report prepared for the Biodiversity Management and Climate Change Adaptation Project. Alberta Biodiversity Monitoring Institute, Edmonton, AB.
- Beale, C. M., J. J. Lennon, and A. Gimona. 2008. Opening the climate envelope reveals no macroscale associations with climate in European birds. *Proceedings of the National Academy of Sciences of the United States of America* **105**:14908-14912.
- Beaudoin, A., P. Y. Bernier, L. Guindon, P. Villemaire, X. J. Guo, G. Stinson, T. Bergeron, S. Magnussen, and R. J. Hall. 2014. Mapping attributes of Canada's forests at moderate resolution through kNN and MODIS imagery. *Canadian Journal of Forest Research* **44**:521-532.
- Beckingham, J. D., and J. H. Archibald. 1996. Field guide to ecosites of Northern Alberta. Natural Resources Canada, Canadian Forest Service, Edmonton, AB.
- Bell, C. P. 1997. Leap-frog migration in the Fox Sparrow: Minimizing the cost of Spring migration. *The Condor* **99**:470-477.
- Bergeron, Y., D. Cyr, C. R. Drever, M. Flannigan, S. Gauthier, D. Kneeshaw, È. Lauzon, A. Leduc, H. L. Goff, D. Lesieur, and K. Logan. 2006. Past, current, and future fire frequencies in Quebec's commercial forests: implications for the cumulative effects of harvesting and fire on age-class structure and natural disturbance-based management. *Canadian Journal of Forest Research* **36**:2737-2744.
- Bierwagen, B. G., D. M. Theobald, C. R. Pyke, A. Choate, P. Groth, J. V. Thomas, and P. Morefield. 2010. National housing and impervious surface scenarios for integrated climate impact assessments. *Proceedings of the National Academy of Sciences* **107**:20887-20892.
- Blancher, P. J. 2003. The Importance of Canada's Boreal Forest to Landbirds. BSC, Port Rowan, ON.
- Blois, J. L., P. L. Zarnetske, M. C. Fitzpatrick, and S. Finnegan. 2013. Climate change and the past, present, and future of biotic interactions. *Science* **341**:499-504.

- Böhning-Gaese, K., L. González-Guzmán, and J. Brown. 1998. Constraints on dispersal and the evolution of the avifauna of the Northern Hemisphere. *Evolutionary Ecology* **12**:767-783.
- Boland, J. M. 1990. Leapfrog migration in North American shorebirds: Intra- and interspecific examples. *The Condor* **92**:284-290.
- Both, C., S. Bouwhuis, C. M. Lessells, and M. E. Visser. 2006. Climate change and population declines in a long-distance migratory bird. *Nature* **441**:81-83.
- Both, C., C. A. M. Van Turnhout, R. G. Bijlsma, H. Siepel, A. J. Van Strien, and R. P. B. Foppen. 2010. Avian population consequences of climate change are most severe for long-distance migrants in seasonal habitats. *Proceedings of the Royal Society B: Biological Sciences* **277**:1259-1266.
- Boulanger, Y., S. Gauthier, and P. J. Burton. 2014. A refinement of models projecting future Canadian fire regimes using homogeneous fire regime zones. *Canadian Journal of Forest Research* **44**:365-376.
- Boulanger, Y., S. Gauthier, P. J. Burton, and M.-A. Vaillancourt. 2012. An alternative fire regime zonation for Canada. *International Journal of Wildland Fire* **21**:1052-1064.
- Boutin, S., D. L. Haughland, J. Schieck, J. Herbers, and E. Bayne. 2009. A new approach to forest biodiversity monitoring in Canada. *Forest Ecology and Management* **258**, **Supplement**:S168-S175.
- Bradshaw, C. J. A., I. G. Warkentin, and N. S. Sodhi. 2009. Urgent preservation of boreal carbon stocks and biodiversity. *Trends in Ecology & Evolution* **24**:541-548.
- Brandt, J. P. 2009. The extent of the North American boreal zone. *Environmental Reviews* **17**:101-161.
- Braunisch, V., J. Coppes, R. Arlettaz, R. Suchant, H. Schmid, and K. Bollmann. 2013. Selecting from correlated climate variables: a major source of uncertainty for predicting species distributions under climate change. *Ecography* **36**:971-983.
- Breiman, L. 2001. Random Forests. *Machine Learning* **45**:5-32.
- Brotons, L., W. Thuiller, M. B. Araújo, and A. H. Hirzel. 2004. Presence-absence versus presence-only modelling methods for predicting bird habitat suitability. *Ecography* **27**:437-448.
- Buckland, S. T., D. R. Anderson, K. P. Burnham, J. L. Laake, D. L. Borchers, and L. Thomas. 2001. *Introduction to Distance Sampling*. Oxford University Press, Oxford.

- Buisson, L., W. Thuiller, N. Casajus, S. Lek, and G. Grenouillet. 2009. Uncertainty in ensemble forecasting of species distribution. *Global Change Biology* **16**:1145-1157.
- Burton, A. C., D. Huggard, E. Bayne, J. Schieck, P. Sóllymos, T. Muhly, D. Farr, and S. Boutin. 2014. A framework for adaptive monitoring of the cumulative effects of human footprint on biodiversity. *Environmental Monitoring and Assessment*:1-13.
- Burton, P. J., and S. G. Cumming. 1995. Potential effects of climatic change on some western Canadian forests, based on phenological enhancements to a patch model of forest succession. *Water, Air, & Soil Pollution* **82**:401-414.
- Calmé, S., and A. Desrochers. 2000. Biogeographic aspects of the distribution of bird species breeding in Québec's peatlands. *Journal of Biogeography* **27**:725-732.
- Camill, P., and J. S. Clark. 2000. Long-term perspectives on lagged ecosystem responses to climate change: permafrost in boreal peatlands and the grassland/woodland boundary. *Ecosystems* **3**:534-544.
- Canadian Forest Service. 2015. Canadian National Fire Database. Natural Resources Canada, Canadian Forest Service, Northern Forestry Centre, Edmonton, Alberta. Available at: http://cwfis.cfs.nrcan.gc.ca/en_CA/nfdb.
- Cantú-Salazar, L., and K. J. Gaston. 2010. Very large protected areas and their contribution to terrestrial biological conservation. *BioScience* **60**:808-818.
- Carlson, M., B. Stelfox, N. Purves-Smith, J. Straker, S. Berryman, T. Barker, and B. Wilson. 2014. ALCES Online: Web-delivered Scenario Analysis to Inform Sustainable Land-use Decisions. *in* International Environmental Modelling and Software Society (iEMSs) 7th Intl. Congress on Env. Modelling and Software, San Diego, USA.
- Carroll, C., J. R. Dunk, and A. Moilanen. 2010. Optimizing resiliency of reserve networks to climate change: multispecies conservation planning in the Pacific Northwest, USA. *Global Change Biology* **16**:891-904.
- Carroll, C., J. J. Lawler, D. R. Roberts, and A. Hamann. 2015. Biotic and Climatic Velocity Identify Contrasting Areas of Vulnerability to Climate Change. *PLoS ONE* **10**:e0140486.
- Carvalho, S. B., J. C. Brito, E. G. Crespo, M. E. Watts, and H. P. Possingham. 2011. Conservation planning under climate change: Toward accounting for uncertainty in predicted species distributions to increase confidence in conservation investments in space and time. *Biological Conservation* **144**:2020-2030.

- CEC. 2010. Terrestrial Protected Areas of North America. Commission for Environmental Cooperation, Montreal, Canada.
- Chapin, F. S., T. V. Callaghan, Y. Bergeron, M. Fukuda, J. F. Johnstone, G. Juday, and S. A. Zimov. 2004. Global change and the boreal forest: thresholds, shifting states or gradual change? *AMBIO: A Journal of the Human Environment* **33**:361-365.
- Chen, H. Y. H., and Y. Luo. 2015. Net aboveground biomass declines of four major forest types with forest ageing and climate change in western Canada's boreal forests. *Global Change Biology* **21**:3675–3684.
- Clavero, M., D. Villero, and L. Brotons. 2011. Climate change or land use dynamics: do we know what climate change indicators indicate? *PLoS ONE* **6**:e18581.
- Clegg, S. M., J. F. Kelly, M. Kimura, and T. B. Smith. 2003. Combining genetic markers and stable isotopes to reveal population connectivity and migration patterns in a Neotropical migrant, Wilson's warbler (*Wilsonia pusilla*). *Molecular Ecology* **12**:819-830.
- Cohen, J. 1992. A power primer. *Psychological Bulletin* **112**:155-159.
- Commission for Environmental Cooperation. 1997. Ecological Regions of North America: Toward a Common Perspective, Montreal, Canada.
- Cumming, S. 2001. Forest type and wildfire in the Alberta boreal mixedwood: what do fires burn? . *Ecological Applications* **11**:97-110.
- Cumming, S. G., C. R. Drever, M. Houle, J. Cosco, P. Racine, E. Bayne, and F. K. A. Schmiegelow. 2015. A gap analysis of tree species representation in the protected areas of the Canadian boreal forest: applying a new assemblage of digital Forest Resource Inventory data. *Canadian Journal of Forest Research* **45**:163-173.
- Cumming, S. G., K. L. Lefevre, E. Bayne, T. Fontaine, F. K. A. Schmiegelow, and S. J. Song. 2010. Toward conservation of Canada's boreal forest avifauna: design and application of ecological models at continental extents. *Avian Conservation and Ecology* **5**:8.
- Cumming, S. G., D. Stralberg, K. L. Lefevre, P. Sólomos, E. M. Bayne, S. Fang, T. Fontaine, D. Mazerolle, F. K. A. Schmiegelow, and S. J. Song. 2014. Climate and vegetation hierarchically structure patterns of songbird distribution in the Canadian boreal region. *Ecography* **37**:137-151.

- Cushman, S. A., D. McKenzie, D. L. Peterson, J. Littell, and K. S. McKelvey. 2006. Research Agenda for Integrated Landscape Modeling. USDA Forest Service Gen. Tech. Rep. RMRS-194. Rocky Mountain Research Station, Fort Collins, CO.
- Cyr, D., S. Gauthier, Y. Bergeron, and C. Carcaillet. 2009. Forest management is driving the eastern North American boreal forest outside its natural range of variability. *Frontiers in Ecology and the Environment* **7**:519-524.
- Daly, C., M. Halbleib, J. I. Smith, W. P. Gibson, M. K. Doggett, G. H. Taylor, J. Curtis, and P. P. Pasteris. 2008. Physiographically sensitive mapping of climatological temperature and precipitation across the conterminous United States. *International Journal of Climatology* **28**:2031-2064.
- Danby, R. K., and D. S. Hik. 2007. Variability, contingency and rapid change in recent subarctic alpine tree line dynamics. *Journal of Ecology* **95**:352-363.
- David, B. L., and B. B. Marshall. 2008. Why are agricultural impacts of climate change so uncertain? The importance of temperature relative to precipitation. *Environmental Research Letters* **3**:034007.
- De'ath, G. 2007. Boosted trees for ecological modeling and prediction. *Ecology* **88**:243-251.
- DeLuca, W., R. Holberton, P. D. Hunt, and B. C. Eliason. 2013. Blackpoll Warbler (*Setophaga striata*), The Birds of North America Online (A. Poole, Ed.). Ithaca: Cornell Lab of Ornithology; Retrieved from the Birds of North America Online: <http://bna.birds.cornell.edu/bna/species/431/>.
- Devictor, V., R. Julliard, D. Couvet, and F. Jiguet. 2008. Birds are tracking climate warming, but not fast enough. *Proceedings of the Royal Society B: Biological Sciences* **275**:2743.
- Diniz-Filho, J. A. F., L. M. Bini, T. F. Rangel, R. D. Loyola, C. Hof, D. Nogués-Bravo, and M. B. Araújo. 2009. Partitioning and mapping uncertainties in ensembles of forecasts of species turnover under climate change. *Ecography* **32**:897-906.
- Distler, T., J. G. Schuetz, J. Velásquez-Tibatá, and G. M. Langham. 2015. Stacked species distribution models and macroecological models provide congruent projections of avian species richness under climate change. *Journal of Biogeography* **42**:976–988.
- Dobrowski, S. Z. 2010. A climatic basis for microrefugia: the influence of terrain on climate. *Global Change Biology* **17**:1022-1035.

- Dobrowski, S. Z., J. H. Thorne, J. A. Greenberg, H. D. Safford, A. R. Mynsberge, S. M. Crimmins, and A. K. Swanson. 2011. Modeling plant ranges over 75 years of climate change in California, USA: temporal transferability and species traits. *Ecological Monographs* **81**:241-257.
- Dormann, C. F., J. Elith, S. Bacher, C. Buchmann, G. Carl, G. Carré, J. R. G. Marquéz, B. Gruber, B. Lafourcade, P. J. Leitão, T. Münkemüller, C. McClean, P. E. Osborne, B. Reineking, B. Schröder, A. K. Skidmore, D. Zurell, and S. Lautenbach. 2013. Collinearity: a review of methods to deal with it and a simulation study evaluating their performance. *Ecography* **36**:27–46.
- Dormann, C. F., O. Purschke, J. R. G. Márquez, S. Lautenbach, and B. Schröder. 2008a. Components of uncertainty in species distribution analysis: a case study of the great gray shrike. *Ecology* **89**:3371-3386.
- Dormann, C. F., O. Schweiger, P. Arens, I. Augenstein, S. Aviron, D. Bailey, J. Baudry, R. Billeter, R. Bugter, R. Bukáček, F. Burel, M. Cerny, R. D. Cock, G. D. Blust, R. DeFilippi, T. Diekötter, J. Dirksen, W. Durka, P. J. Edwards, M. Frenzel, R. Hamersky, F. Hendrickx, F. Herzog, S. Klotz, B. Koolstra, A. Lausch, D. L. Coeur, J. Liira, J. P. Maelfait, P. Opdam, M. Roubalova, A. Schermann-Legionnet, N. Schermann, T. Schmidt, M. J. M. Smulders, M. Speelmans, P. Simova, J. Verboom, W. v. Wingerden, and M. Zobel. 2008b. Prediction uncertainty of environmental change effects on temperate European biodiversity. *Ecology Letters* **11**:235-244.
- Drapeau, P., A. Leduc, J.-F. Giroux, J.-P. L. Savard, Y. Bergeron, and W. L. Vickery. 2000. Landscape-scale disturbances and changes in bird communities of boreal mixed-wood forests. *Ecological Monographs* **70**:423-444.
- Drew, C. A., Y. F. Wiersma, and F. Huettman. 2011. *Predictive modeling in landscape ecology*. Springer, New York.
- Dunn, P. O., K. J. Thusius, K. Kimber, and D. W. Winkler. 2000. Geographic and ecological variation in clutch size of Tree Swallows. *The Auk* **117**:215-221.
- Dyke, A. S. 2005. Late Quaternary vegetation history of northern North America based on pollen, macrofossil, and faunal remains. *Géographie physique et Quaternaire* **59**:211-262.
- Elith, J., M. A. Burgman, and H. M. Regan. 2002. Mapping epistemic uncertainties and vague concepts in predictions of species distribution. *Ecological Modelling* **157**:313-329.

- Elith, J., and C. H. Graham. 2009. Do they? How do they? WHY do they differ? On finding reasons for differing performances of species distribution models. *Ecography* **32**:66-77.
- Elith, J., C. H. Graham, R. P. Anderson, M. Dudik, S. Ferrier, A. Guisan, R. J. Hijmans, F. Huettmann, J. R. Leathwick, A. Lehmann, J. Li, L. G. Lohmann, B. A. Loiselle, G. Manion, C. Moritz, M. Nakamura, Y. Nakazawa, J. McC. M. Overton, A. Townsend Peterson, S. J. Phillips, K. Richardson, R. Scachetti-Pereira, R. E. Schapire, J. Soberón, S. Williams, M. S. Wisz, and N. E. Zimmermann. 2006. Novel methods improve prediction of species' distributions from occurrence data. *Ecography* **29**:129-151.
- Elith, J., J. R. Leathwick, and T. Hastie. 2008. A working guide to boosted regression trees. *Journal of Animal Ecology* **77**:802-813.
- Erskine, A. J. 1977. *Birds in boreal Canada: communities, densities, and adaptations*. CWS, Ottawa, ON.
- Eskildsen, A., P. C. le Roux, R. K. Heikkinen, T. T. Høye, W. D. Kissling, J. Pöyry, M. S. Wisz, and M. Luoto. 2013. Testing species distribution models across space and time: high latitude butterflies and recent warming. *Global Ecology and Biogeography* **22**:1293-1303.
- Evans, J., and S. Cushman. 2009. Gradient modeling of conifer species using random forests. *Landscape Ecology* **24**:673-683.
- Fasullo, J. T., and K. E. Trenberth. 2012. A less cloudy future: the role of subtropical subsidence in climate sensitivity. *Science* **338**:792-794.
- Flannigan, M., K. Logan, B. Amiro, W. Skinner, and B. Stocks. 2005. Future Area Burned in Canada. *Climatic Change* **72**:1-16-16.
- Flannigan, M. D., M. A. Krawchuk, W. J. de Groot, B. M. Wotton, and L. M. Gowman. 2009. Implications of changing climate for global wildland fire. *International Journal of Wildland Fire* **18**:483-507.
- Fløjgaard, C., S. Normand, F. Skov, and J.-C. Svenning. 2011. Deconstructing the mammal species richness pattern in Europe – towards an understanding of the relative importance of climate, biogeographic history, habitat heterogeneity and humans. *Global Ecology and Biogeography* **20**:218-230.
- Fordham, D. A., C. Mellin, B. D. Russell, R. H. Akçakaya, C. J. A. Bradshaw, M. E. Aiello-Lammens, J. M. Caley, S. D. Connell, S. Mayfield, S. A. Shepherd, and B. W. Brook.

2013. Population dynamics can be more important than physiological limits for determining range shifts under climate change. *Global Change Biology* **19**:3224-3237.
- Forestry Canada Fire Danger Group. 1992. Development and structure of the Canadian Forest Fire Behavior Prediction System. Forestry Canada, Information Report ST-X-3 Ottawa, ON.
- Fox, J., and S. Weisberg. 2011. An {R} Companion to Applied Regression, Second Edition. Sage, Thousand Oaks, CA.
- Franklin, J. 1995. Predictive vegetation mapping: geographic modelling of biospatial patterns in relation to environmental gradients. *Progress in Physical Geography* **19**:474-499.
- Freeman, E. A., and G. G. Moisen. 2008. A comparison of the performance of threshold criteria for binary classification in terms of predicted prevalence and kappa. *Ecological Modelling* **217**:48-58.
- Frelich, L. E., and P. B. Reich. 2009. Will environmental changes reinforce the impact of global warming on the prairie–forest border of central North America? *Frontiers in Ecology and the Environment* **8**:371-378.
- Friedman, J. H. 2001. Greedy Function Approximation: A Gradient Boosting Machine. *Annals of Statistics* **29**:1189-1232.
- Friend, A. D., W. Lucht, T. T. Rademacher, R. Keribin, R. Betts, P. Cadule, P. Ciais, D. B. Clark, R. Dankers, P. D. Falloon, A. Ito, R. Kahana, A. Kleidon, M. R. Lomas, K. Nishina, S. Ostberg, R. Pavlick, P. Peylin, S. Schaphoff, N. Vuichard, L. Warszawski, A. Wiltshire, and F. I. Woodward. 2014. Carbon residence time dominates uncertainty in terrestrial vegetation responses to future climate and atmospheric CO₂. *Proceedings of the National Academy of Sciences of the United States of America* **111**:3280-3285.
- Fuller, T., D. P. Morton, and S. Sarkar. 2008. Incorporating uncertainty about species' potential distributions under climate change into the selection of conservation areas with a case study from the Arctic Coastal Plain of Alaska. *Biological Conservation* **141**:1547-1559.
- Garcia, R. A., N. D. Burgess, M. Cabeza, C. Rahbek, and M. B. Araújo. 2012. Exploring consensus in 21st century projections of climatically suitable areas for African vertebrates. *Global Change Biology* **18**:1253-1269.
- Gardali, T., N. E. Seavy, R. T. DiGaudio, and L. A. Comrack. 2012. A climate change vulnerability assessment of California's at-risk birds. *PLoS ONE* **7**:e29507.

- Garland, Jr., and A. R. Ives. 2000. Using the past to predict the present: confidence intervals for regression equations in phylogenetic comparative methods. *The American Naturalist* **155**:346-364.
- Gauthier, S., P. Bernier, T. Kuuluvainen, A. Z. Shvidenko, and D. G. Schepaschenko. 2015. Boreal forest health and global change. *Science* **349**:819-822.
- Gessler, P. E., I. D. Moore, M. N.J., and R. P.J. 1995. Soil-landscape modeling and spatial prediction of soil attributes. *International Journal of GIS* **9**:421-432.
- Gibson, D. D. 2011. Nesting shorebirds and landbirds of interior Alaska. Report to USGS. Ester, Alaska.
- Gibson, D. D., and J. J. Withrow. 2015. Inventory of the species and subspecies of Alaska birds, second edition. *Western Birds* **46**:94-185.
- Gillett, N. P., A. J. Weaver, F. W. Zwiers, and M. D. Flannigan. 2004. Detecting the effect of climate change on Canadian forest fires. *Geophysical Research Letters* **31**:L18211.
- Gilman, S. E., M. C. Urban, J. Tewksbury, G. W. Gilchrist, and R. D. Holt. 2010. A framework for community interactions under climate change. *Trends in Ecology & Evolution* **25**:325-331.
- Girardin, M. P., and M. Mudelsee. 2008. Past and future changes in Canadian boreal wildfire activity. *Ecological Applications* **18**:391-406.
- Girardin, M. P., F. Raulier, P. Y. Bernier, and J. C. Tardif. 2008. Response of tree growth to a changing climate in boreal central Canada: A comparison of empirical, process-based, and hybrid modelling approaches. *Ecological Modelling* **213**:209-228.
- Greenberg, R. S. 1980. Demographic aspects of long-distance migration. Pages 493-504 *in* A. Keast and E. S. Morton, editors. *Migrant Birds in the Neotropics*. Smithsonian Institution Press, Washington, DC.
- Greenwood, P. J., and P. H. Harvey. 1982. The natal and breeding dispersal of birds. *Annual Review of Ecology and Systematics* **13**:1-21.
- Grinnell, J. 1917. The niche-relationships of the California Thrasher. *Auk* **34**:427-434.
- Guisan, A., and N. E. Zimmermann. 2000. Predictive habitat distribution models in ecology. *Ecological Modelling* **135**:147-186.

- Gustafson, E. 2013. When relationships estimated in the past cannot be used to predict the future: using mechanistic models to predict landscape ecological dynamics in a changing world. *Landscape Ecology* **28**:1429-1437.
- Haché, S., M.-A. Villard, and E. M. Bayne. 2013. Experimental evidence for an ideal free distribution in a breeding population of a territorial songbird. *Ecology* **94**:861-869.
- Hackett, S. J., R. T. Kimball, S. Reddy, R. C. K. Bowie, E. L. Braun, M. J. Braun, J. L. Chojnowski, W. A. Cox, K.-L. Han, J. Harshman, C. J. Huddleston, B. D. Marks, K. J. Miglia, W. S. Moore, F. H. Sheldon, D. W. Steadman, C. C. Witt, and T. Yuri. 2008. A phylogenomic study of birds reveals their evolutionary history. *Science* **320**:1763-1768.
- Halpin, P. N. 1997. Global climate change and natural-area protection: management responses and research directions. *Ecological Applications* **7**:828-843.
- Hamann, A., and S. N. Aitken. 2013. Conservation planning under climate change: accounting for adaptive potential and migration capacity in species distribution models. *Diversity and Distributions* **19**:268–280.
- Hamann, A., D. Roberts, Q. Barber, C. Carroll, and S. Nielsen. 2014. Velocity of climate change algorithms for guiding conservation and management. *Global Change Biology* **21**:997–1004.
- Hamann, A., and T. Wang. 2006. Potential effects of climate change on ecosystem and tree species distribution in British Columbia. *Ecology* **87**:2773-2786.
- Hamann, A., T. Wang, D. L. Spittlehouse, and T. Q. Murdock. 2013. A comprehensive, high-resolution database of historical and projected climate surfaces for western North America. *Bulletin of the American Meteorological Society* **94**:1307–1309.
- Hannah, K. C., F. K. Schmiegelow, and K. E. Aitken. 2008. White-throated sparrow response to forest harvesting in north-central Alberta: results not so clear-cut? *Avian Conservation and Ecology* **3**:6.
- Hannah, L. 2011. Climate change, connectivity, and conservation success. *Conservation Biology* **25**:1139-1142.
- Hannah, L., G. Midgley, S. Andelman, M. Araujo, G. Hughes, E. Martinez-Meyer, R. Pearson, and P. Williams. 2007. Protected area needs in a changing climate. *Frontiers in Ecology and the Environment* **5**:131-138.

- Hanowski, J. M., and G. J. Niemi. 1995. Experimental design considerations for establishing an off-road, habitat-specific bird monitoring program using point-counts. USDA Forest Service General Technical Report: PSW-GTR-149. Pages 145-150 in C. J. Ralph, J. R. Sauer, and S. Droege, editors. *Monitoring Bird Populations by Point Counts*. USDA Forest Service, Pacific Southwest Research Station, Albany, CA.
- Hansen, J., P. Kharecha, M. Sato, V. Masson-Delmotte, F. Ackerman, D. J. Beerling, P. J. Hearty, O. Hoegh-Guldberg, S.-L. Hsu, C. Parmesan, J. Rockstrom, E. J. Rohling, J. Sachs, P. Smith, K. Steffen, L. Van Susteren, K. von Schuckmann, and J. C. Zacher. 2013. Assessing “Dangerous Climate Change”: Required Reduction of Carbon Emissions to Protect Young People, Future Generations and Nature. *PLoS ONE* **8**:e81648.
- Hauer, G., S. Cumming, F. Schmiegelow, W. Adamowicz, M. Weber, and R. Jagodzinski. 2010. Tradeoffs between forestry resource and conservation values under alternate policy regimes: A spatial analysis of the western Canadian boreal plains. *Ecological Modelling* **221**:2590-2603.
- Haughland, D. L., J.-M. Hero, J. Schieck, J. G. Castley, S. Boutin, P. Solyomos, B. E. Lawson, G. Holloway, and W. E. Magnusson. 2010. Planning forwards: biodiversity research and monitoring systems for better management. *Trends in Ecology & Evolution* **25**:199-200.
- Hawkins, B. A., and E. E. Porter. 2003. Relative influences of current and historical factors on mammal and bird diversity patterns in deglaciated North America. *Global Ecology and Biogeography* **12**:475-481.
- He, H. S., D. J. Mladenoff, and E. J. Gustafson. 2002. Study of landscape change under forest harvesting and climate warming-induced fire disturbance. *Forest Ecology and Management* **155**:257-270.
- Helbig, A. 2003. Evolution of Bird Migration: A Phylogenetic and Biogeographic Perspective. Pages 3-20 in P. Berthold, E. Gwinner, and E. Sonnenschein, editors. *Avian Migration*. Springer Berlin Heidelberg.
- Héon, J., D. Arseneault, and M.-A. Parisien. 2014. Resistance of the boreal forest to high burn rates. *Proceedings of the National Academy of Sciences of the United States of America* **11**:13888–13893.

- Hernandez, P. A., C. H. Graham, L. L. Master, and D. L. Albert. 2006. The effect of sample size and species characteristics on performance of different species distribution modeling methods. *Ecography* **29**:773-785.
- Hervieux, D., M. Hebblewhite, N. J. DeCesare, M. Russell, K. Smith, S. Robertson, and S. Boutin. 2013. Widespread declines in woodland caribou (*Rangifer tarandus caribou*) continue in Alberta. *Canadian Journal of Zoology* **91**:872-882.
- Hickler, T., K. Vohland, J. Feehan, P. A. Miller, B. Smith, L. Costa, T. Giesecke, S. Fronzek, T. R. Carter, W. Cramer, I. Kühn, and M. T. Sykes. 2012. Projecting the future distribution of European potential natural vegetation zones with a generalized, tree species-based dynamic vegetation model. *Global Ecology and Biogeography* **21**:50-63.
- Hijmans, R. J., and C. H. Graham. 2006. The ability of climate envelope models to predict the effect of climate change on species distributions. *Global Change Biology* **12**:2272-2281.
- Hijmans, R. J., S. Phillips, J. Leathwick, and J. Elith. 2011. Package 'dismo'. Available online at <http://cran.r-project.org/web/packages/dismo/index.html>.
- Hijmans, R. J., and J. van Etten. 2012. Package 'raster'. Available on-line at <http://cran.r-project.org/web/packages/raster/index.html>.
- Hilty, J. A., C. C. Chester, and M. S. Cross, editors. 2012. *Climate and Conservation: Landscape and Seascape Science, Planning, and Action*. Island Press, Washington, DC.
- Hitch, A. T., and P. L. Leberg. 2007. Breeding distributions of North American bird species moving north as a result of climate change. *Conservation Biology* **21**:534-539.
- Hobson, K. A., and E. Bayne. 2000. Breeding bird communities in boreal forests of western Canada: consequences of "unmixing" the mixedwoods *Condor* **102**:759-769.
- Hobson, K. A., and J. Schieck. 1999. Changes in bird communities in boreal mixedwood forest: harvest and wildfire effects over 30 years. *Ecological Applications* **9**:849-863.
- Hobson, K. A., A. G. Wilson, S. L. Van Wilgenburg, and E. M. Bayne. 2013. An estimate of nest loss in Canada due to industrial forestry operations. *Avian Conservation and Ecology* **8**.
- Hodgson, J. A., C. D. Thomas, B. A. Wintle, and A. Moilanen. 2009. Climate change, connectivity and conservation decision making: back to basics. *Journal of Applied Ecology* **46**:964-969.
- Hof, C., M. B. Araujo, W. Jetz, and C. Rahbek. 2011. Additive threats from pathogens, climate and land-use change for global amphibian diversity. *Nature* **480**:516-519.

- Hogg, E. H. 1994. Climate and the southern limit of the western Canadian boreal forest. *Canadian Journal of Forest Research* **24**:1835-1845.
- Hogg, E. H., and P. Y. Bernier. 2005. Climate change impacts on drought-prone forests in western Canada. *Forestry Chronicle* **81**:675-682.
- Hogg, E. H., J. P. Brandt, and B. Kochtubajda. 2002. Growth and dieback of aspen forests in northwestern Alberta, Canada, in relation to climate and insects. *Canadian Journal of Forest Research* **32**:823–832.
- Hogg, E. H., and P. A. Hurdle. 1995. The aspen parkland in western Canada: A dry-climate analogue for the future boreal forest? *Water, Air, & Soil Pollution* **82**:391-400.
- Hogg, E. H., and A. G. Schwarz. 1997. Regeneration of planted conifers across climatic moisture gradients on the Canadian prairies: implications for distribution and climate change. *Journal of Biogeography* **24**:527-534.
- Holm, S. 1979. A simple sequentially rejective multiple test procedure. *Scandinavian Journal of Statistics* **6**:65-70.
- Hortal, J., J. A. F. Diniz-Filho, L. M. Bini, M. Á. Rodríguez, A. Baselga, D. Nogués-Bravo, T. F. Rangel, B. A. Hawkins, and J. M. Lobo. 2011. Ice age climate, evolutionary constraints and diversity patterns of European dung beetles. *Ecology Letters* **14**:741-748.
- Hostetler, J. A., T. S. Sillett, and P. P. Marra. 2015. Full-annual-cycle population models for migratory birds. *The Auk* **132**:433-449.
- Huntley, B., J. R. M. Allen, P. Barnard, Y. C. Collingham, and P. R. Holliday. 2013. Species distribution models indicate contrasting late-Quaternary histories for Southern and Northern Hemisphere bird species. *Global Ecology and Biogeography* **22**:277-288.
- Huntley, B., Y. C. Collingham, S. G. Willis, and R. E. Green. 2008. Potential impacts of climatic change on European breeding birds. *PLoS ONE* **3**:e1439.
- Huntley, B., R. E. Green, Y. C. Collingham, J. K. Hill, S. G. Willis, P. J. Bartlein, W. Cramer, W. J. M. Hagemeijer, and C. J. Thomas. 2004. The performance of models relating species geographical distributions to climate is independent of trophic level. *Ecology Letters* **7**:417-426.
- Huntley, B., R. A. Spicer, W. G. Chaloner, and E. A. Jarzembowski. 1993. The use of climate response surfaces to reconstruct palaeoclimate from Quaternary pollen and plant

- macrofossil data [and discussion]. *Philosophical Transactions of the Royal Society of London. Series B: Biological Sciences* **341**:215-224.
- Hussell, D. J. T. 1972. Factors affecting clutch size in Arctic passerines. *Ecological Monographs* **42**:317-364.
- Hutchinson, G. E. 1957. Concluding remarks. *Cold Spring Harbor Symposium on Quantitative Biology* **22**:415-427.
- IPCC. 2001. *Climate Change 2001. Third Assessment Report of the Intergovernmental Panel on Climate Change*. Cambridge University Press, Cambridge.
- IPCC. 2013. Summary for Policymakers. In: *Climate Change 2013: The Physical Science Basis. Contribution of Working Group I to the Fifth Assessment Report of the Intergovernmental Panel on Climate Change*.
- Iverson, L. R., and A. M. Prasad. 1998. Predicting abundance of 80 tree species following climate change in the eastern United States. *Ecological Monographs* **68**:465-485.
- Iverson, L. R., M. W. Schwartz, and A. M. Prasad. 2004. How fast and far might tree species migrate in the eastern United States due to climate change? *Global Ecology and Biogeography* **13**:209-219.
- Ives, A. R., and T. Garland. 2010. Phylogenetic logistic regression for binary dependent variables. *Systematic Biology* **59**:9-26.
- Jackson, S. T., R. S. Webb, K. H. Anderson, J. T. Overpeck, T. I. Webb, J. W. Williams, and B. C. S. Hansen. 2000. Vegetation and environment in eastern North America during the last glacial maximum. *Quaternary Science Reviews* **19**:489-508.
- Jarvis, A., H. I. Reuter, A. Nelson, and E. Guevara. 2008. Hole-filled seamless SRTM data V4, International Centre for Tropical Agriculture (CIAT). Available from <http://srtm.csi.cgiar.org>.
- Jensen, O. 2003. *Wood Buffalo National Park Vegetation Classification Final Report*.
- Jetz, W., G. H. Thomas, J. B. Joy, K. Hartmann, and A. O. Mooers. 2012. The global diversity of birds in space and time. *Nature* **491**:444-448.
- Jetz, W., D. Wilcove, and A. Dobson. 2007. Projected impacts of climate and land-use change on the global diversity of birds. *PLoS Biology* **5**:e157.

- Jiménez-Valverde, A., N. Barve, A. Lira-Noriega, S. P. Maher, Y. Nakazawa, M. Papeş, J. Soberón, J. Sukumaran, and A. T. Peterson. 2011. Dominant climate influences on North American bird distributions. *Global Ecology and Biogeography* **20**:114-118.
- Johnson, N. K., and C. Cicero. 2004. New mitochondrial DNA data affirm the importance of Pleistocene speciation in North American birds. *Evolution* **58**:1122-1130.
- Johnstone, J., T. Rupp, M. Olson, and D. Verbyla. 2011. Modeling impacts of fire severity on successional trajectories and future fire behavior in Alaskan boreal forests. *Landscape Ecology* **26**:487-500-500.
- Johnstone, J. F., T. N. Hollingsworth, F. S. Chapin, and M. C. Mack. 2010. Changes in fire regime break the legacy lock on successional trajectories in Alaskan boreal forest. *Global Change Biology* **16**:1281-1295.
- Jongsomjit, D., D. Stralberg, T. Gardali, L. Salas, and J. A. Wiens. 2013. Between a rock and a hard place: the impacts of climate change and development on breeding birds in California. *Landscape Ecology* **28**:187-200.
- Jorgenson, M. T., C. Racine, J. Walters, and T. Osterkamp. 2001. Permafrost degradation and ecological changes associated with a warming climate in central Alaska. *Climatic Change* **48**:551-579.
- Jun, M., R. Knutti, and D. W. Nychka. 2008. Spatial Analysis to Quantify Numerical Model Bias and Dependence. *Journal of the American Statistical Association* **103**:934-947.
- Kang, E. L., and N. Cressie. 2013. Bayesian hierarchical ANOVA of regional climate-change projections from NARCCAP phase II. *International Journal of Applied Earth Observation and Geoinformation* **22**.
- Kasischke, E. S., and M. R. Turetsky. 2006. Recent changes in the fire regime across the North American boreal region—Spatial and temporal patterns of burning across Canada and Alaska. *Geophysical Research Letters* **33**:L09703.
- Keane, R. E., G. J. Cary, I. D. Davies, M. D. Flannigan, R. H. Gardner, S. Lavorel, J. M. Lenihan, C. Li, and T. S. Rupp. 2004. A classification of landscape fire succession models: spatial simulations of fire and vegetation dynamics. *Ecological Modelling* **179**:3-27.
- Kearney, M., and W. Porter. 2009. Mechanistic niche modelling: combining physiological and spatial data to predict species' ranges. *Ecology Letters* **12**:334-350.

- Keith, D. A., H. R. Akçakaya, W. Thuiller, G. F. Midgley, R. G. Pearson, S. J. Phillips, H. M. Regan, M. B. Araújo, and T. G. Rebelo. 2008. Predicting extinction risks under climate change: coupling stochastic population models with dynamic bioclimatic habitat models. *Biology Letters* **4**:560-563.
- Kellomäki, S., H. Peltola, T. Nuutinen, K. T. Korhonen, and H. Strandman. 2008. Sensitivity of managed boreal forests in Finland to climate change, with implications for adaptive management. *Philosophical Transactions of the Royal Society of London B: Biological Sciences* **363**:2339-2349.
- Kelly, J., V. Atudorei, Z. Sharp, and D. Finch. 2002. Insights into Wilson's Warbler migration from analyses of hydrogen stable-isotope ratios. *Oecologia* **130**:216-221.
- Keppel, G., K. P. Van Niel, G. W. Wardell-Johnson, C. J. Yates, M. Byrne, L. Mucina, A. G. T. Schut, S. D. Hopper, and S. E. Franklin. 2012. Refugia: identifying and understanding safe havens for biodiversity under climate change. *Global Ecology and Biogeography* **21**:393-404.
- Kerr, J. T., and S. Z. Dobrowski. 2013. Predicting the impacts of global change on species, communities and ecosystems: it takes time. *Global Ecology and Biogeography* **22**:261-263.
- Kharouba, H. M., A. C. Algar, and J. T. Kerr. 2009. Historically calibrated predictions of butterfly species' range shift using global change as a pseudo-experiment. *Ecology* **90**:2213-2222.
- Kharouba, H. M., J. L. McCune, W. Thuiller, and B. Huntley. 2013. Do ecological differences between taxonomic groups influence the relationship between species' distributions and climate? A global meta-analysis using species distribution models. *Ecography* **36**:657-664.
- Kimura, M., S. M. Clegg, I. J. Lovette, K. R. Holder, D. J. Girman, B. Milá, P. Wade, and T. B. Smith. 2002. Phylogeographical approaches to assessing demographic connectivity between breeding and overwintering regions in a Nearctic–Neotropical warbler (*Wilsonia pusilla*). *Molecular Ecology* **11**:1605-1616.
- Kingston, D. G., M. C. Todd, R. G. Taylor, J. R. Thompson, and N. W. Arnell. 2009. Uncertainty in the estimation of potential evapotranspiration under climate change. *Geophysical Research Letters* **36**:L20403.

- Klein, E., E. E. Berg, and R. Dial. 2005. Wetland drying and succession across the Kenai Peninsula Lowlands, south-central Alaska. *Canadian Journal of Forest Research* **35**:1931-1941.
- Krawchuk, M., and S. Cumming. 2011. Effects of biotic feedback and harvest management on boreal forest fire activity under climate change. *Ecological Applications* **21**:122–136.
- Krawchuk, M., S. Cumming, and M. Flannigan. 2009. Predicted changes in fire weather suggest increases in lightning fire initiation and future area burned in the mixedwood boreal forest. *Climatic Change* **92**:83-97-97.
- Krawchuk, M., K. Lisgo, S. Leroux, P. Vernier, S. Cumming, and F. Schmiegelow. 2012. Boreal Forest, Canada. Pages 69-79 in J. A. Hilty, C. C. Chester, and M. S. Cross, editors. *Climate and Conservation: Landscape and Seascape Science, Planning, and Action*. Island Press, Washington, DC.
- Kujala, H., A. Moilanen, M. B. Araújo, and M. Cabeza. 2013. Conservation planning with uncertain climate change projections. *PLoS ONE* **8**:e53315.
- Kutzbach, J., R. Gallimore, S. Harrison, P. Behling, R. Selin, and F. Laarif. 1998. Climate and biome simulations for the past 21,000 years. *Quaternary Science Reviews* **17**:473-506.
- La Sorte, F. A., T. M. Lee, H. Wilman, and W. Jetz. 2009. Disparities between observed and predicted impacts of climate change on winter bird assemblages. *Proceedings of the Royal Society B: Biological Sciences* **276**:3167-3174.
- Langsrud, Ø. 2003. ANOVA for unbalanced data: Use Type II instead of Type III sums of squares. *Statistics and Computing* **13**:163-167.
- Lawler, J. J., D. D. Ackerly, C. M. Albano, M. G. Anderson, S. Z. Dobrowski, J. L. Gill, N. E. Heller, R. L. Pressey, E. W. Sanderson, and S. B. Weiss. 2015. The theory behind, and the challenges of, conserving nature's stage in a time of rapid change. *Conservation Biology* **29**:618-629.
- Lawler, J. J., A. S. Ruesch, J. D. Olden, and B. H. McRae. 2013. Projected climate-driven faunal movement routes. *Ecology Letters* **16**:1014-1022.
- Lawler, J. J., D. White, R. P. Neilson, and A. R. Blaustein. 2006. Predicting climate-induced range shifts: model differences and model reliability. *Global Change Biology* **12**:1568-1584.

- Lee, P., J. D. Gysbers, and Z. Stanojevic. 2006. Canada's Forest Landscape Fragments: A First Approximation. Global Forest Watch Canada, Edmonton, Canada.
- Lee, T. M., and W. Jetz. 2008. Future battlegrounds for conservation under global change. *Proceedings of the Royal Society B: Biological Sciences* **275**:1261-1270.
- Lenihan, J. M. 1993. Ecological response surfaces for North American boreal tree species and their use in forest classification. *Journal of Vegetation Science* **4**:667-680.
- Leroux, S. J., F. K. A. Schmiegelow, R. B. Lessard, and S. G. Cumming. 2007. Minimum dynamic reserves: A framework for determining reserve size in ecosystems structured by large disturbances. *Biological Conservation* **138**:464-473.
- Levinsky, I., M. B. Araújo, D. Nogués-Bravo, A. M. Haywood, P. J. Valdes, and C. Rahbek. 2013. Climate envelope models suggest spatio-temporal co-occurrence of refugia of African birds and mammals. *Global Ecology and Biogeography* **22**:351-363.
- Liaw, A. 2015. Package 'randomForest'. Available on-line at <http://cran.r-project.org/web/packages/randomForest/index.html>.
- Loarie, S. R., P. B. Duffy, H. Hamilton, G. P. Asner, C. B. Field, and D. D. Ackerly. 2009. The velocity of climate change. *Nature* **462**:1052-1055.
- Lovette, I. J. 2005. Glacial cycles and the tempo of avian speciation. *TRENDS in Ecology and Evolution* **20**:57-58.
- Lovette, I. J., and E. Bermingham. 1999. Explosive speciation in the New World Dendroica warblers. *Proceedings of the Royal Society of London. Series B: Biological Sciences* **266**:1629-1636.
- Lovette, I. J., and W. M. Hochachka. 2006. Simultaneous effects of phylogenetic niche conservatism and competition on avian community structure. *Ecology* **87**:S14-S28.
- Lowther, P. E. 1999. Alder Flycatcher (*Empidonax alnorum*), *The Birds of North America Online* (A. Poole, Ed.). Ithaca: Cornell Lab of Ornithology; Retrieved from the Birds of North America Online: <http://bna.birds.cornell.edu/bna/species/446/>.
- Lowther, P. E., C. C. Rimmer, B. Kessel, S. L. Johnson, and W. G. Ellison. 2001. Gray-cheeked Thrush (*Catharus minimus*), *The Birds of North America Online* (A. Poole, Ed.). Ithaca: Cornell Lab of Ornithology; Retrieved from the Birds of North America Online: <http://bna.birds.cornell.edu/bna/species/591/>.

- Loyola, R., P. Lemes, J. Nabout, J. Trindade-Filho, M. Sagnori, R. Dobrovolski, and J. Diniz-Filho. 2013. A straightforward conceptual approach for evaluating spatial conservation priorities under climate change. *Biodiversity & Conservation* **22**:483-495.
- Lundberg, S., and T. Alerstam. 1986. Bird migration patterns: Conditions for stable geographical population segregation. *Journal of Theoretical Biology* **123**:403-414.
- Luo, Y., and H. Y. H. Chen. 2013. Observations from old forests underestimate climate change effects on tree mortality. *Nat Commun* **4**:1655.
- Ma, Z., C. Peng, Q. Zhu, H. Chen, G. Yu, W. Li, X. Zhou, W. Wang, and W. Zhang. 2012. Regional drought-induced reduction in the biomass carbon sink of Canada's boreal forests. *Proceedings of the National Academy of Sciences* **109**:2423-2427.
- MacArthur, R. H. 1972. *Geographical Ecology*. Harper & Row, New York.
- MacMillan, R. A., D. E. Moon, and R. A. Coupé. 2007. Automated predictive ecological mapping in a Forest Region of B.C., Canada, 2001–2005. *Geoderma* **140**:353-373.
- Maggini, R., A. Lehmann, N. Zbinden, N. E. Zimmermann, J. Bolliger, B. Schröder, R. Foppen, H. Schmid, M. Beniston, and L. Jenni. 2014. Assessing species vulnerability to climate and land use change: the case of the Swiss breeding birds. *Diversity and Distributions* **20**:708–719.
- Mahon, C. L., E. M. Bayne, P. Sólymos, S. M. Matsuoka, M. Carlson, E. Dzus, F. K. A. Schmiegelow, and S. J. Song. 2014. Does expected future landscape condition support proposed population objectives for boreal birds? *Forest Ecology and Management* **312**:28-39.
- Mahon, C. L., G. H. Holloway, P. Solymos, S. G. Cumming, E. M. Bayne, F. K. A. Schmiegelow, and S. J. Song. 2016. Community structure and niche characteristics of upland and lowland western boreal birds at multiple spatial scales. *Forest Ecology and Management* **361**:99-116.
- Margules, C. R., and R. L. Pressey. 2000. Systematic conservation planning. *Nature* **405**:243-253.
- Martins, E. P., and T. F. Hansen. 1997. Phylogenies and the comparative method: A general approach to incorporating phylogenetic information into the analysis of interspecific data. *The American Naturalist* **149**:646-667.

- Masson, D., and R. Knutti. 2011. Climate model genealogy. *Geophysical Research Letters* **38**:L08703.
- Matthews, S. N., L. R. Iverson, A. M. Prasad, and M. P. Peters. 2011. Changes in potential habitat of 147 North American breeding bird species in response to redistribution of trees and climate following predicted climate change. *Ecography* **34**:933-945.
- Mayr, E. 1946. History of the North American bird fauna. *The Wilson Bulletin* **58**:3-41.
- Mbogga, M. S., X. Wang, and A. Hamann. 2010. Bioclimate envelope model predictions for natural resource management: dealing with uncertainty. *Journal of Applied Ecology* **47**:731-740.
- McClure, C. J. W., B. W. Rolek, K. McDonald, and G. E. Hill. 2012. Climate change and the decline of a once common bird. *Ecology & Evolution* **2**:370-378.
- McGarigal, K., and B. J. Marks. 1995. FRAGSTATS: spatial pattern analysis program for quantifying landscape structure. USDA For. Serv. Gen. Tech. Rep. PNW-351.
[URL: <http://www.umass.edu/landeco/research/fragstats/fragstats.html>].
- McInerny, G. J., and D. W. Purves. 2011. Fine-scale environmental variation in species distribution modelling: regression dilution, latent variables and neighbourly advice. *Methods in Ecology and Evolution* **2**:248-257.
- McKenney, D. W., M. F. Hutchinson, J. L. Kesteven, and L. A. Venier. 2001. Canada's plant hardiness zones revisited using modern climate interpolation techniques. *Canadian Journal of Plant Science* **81**:129-143.
- McKenney, D. W., J. H. Pedlar, K. Lawrence, K. Campbell, and M. F. Hutchinson. 2007a. Beyond traditional hardiness zones: Using climate envelopes to map plant range limits. *BioScience* **57**:929-937.
- McKenney, D. W., J. H. Pedlar, K. Lawrence, K. Campbell, and M. F. Hutchinson. 2007b. Potential impacts of climate change on the distribution of North American trees. *BioScience* **57**:939-948.
- McLane, S. C., and S. N. Aitken. 2011. Whitebark pine (*Pinus albicaulis*) assisted migration potential: testing establishment north of the species range. *Ecological Applications* **22**:142-153.
- McPherson, J. M., and W. Jetz. 2007. Effects of species' ecology on the accuracy of distribution models. *Ecography* **30**:135-151.

- McPherson, J. M., W. Jetz, and D. J. Rogers. 2004. The effects of species' range sizes on the accuracy of distribution models: ecological phenomenon or statistical artefact? *Journal of Applied Ecology* **41**:811-823.
- Meehl, G. A., C. Covey, T. Delworth, M. Latif, B. McAvaney, J. F. B. Mitchell, R. J. Stouffer, and K. E. Taylor. 2007. The WCRP CMIP3 multi-model dataset: a new era in climate change research. *Bulletin of the American Meteorological Society* **88**:1383-1394.
- Meehl, G. A., R. Moss, K. E. Taylor, V. Eyring, R. J. Stouffer, S. Bony, and B. Stevens. 2014. Climate Model Intercomparisons: Preparing for the Next Phase. *Eos, Transactions American Geophysical Union* **95**:77-78.
- Mehta, V., G. Meehl, L. Goddard, J. Knight, A. Kumar, M. Latif, T. Lee, A. Rosati, and D. Stammer. 2010. Decadal climate predictability and prediction: Where are we? *Bulletin of the American Meteorological Society* **92**:637-640.
- Meier, E. S., H. Lischke, D. R. Schmatz, and N. E. Zimmermann. 2012. Climate, competition and connectivity affect future migration and ranges of European trees. *Global Ecology and Biogeography* **21**:164-178.
- Mengel, R. M. 1964. The probable history of species formation in some northern wood warblers (Parulidae). *Living Bird* **3**:9-43.
- Meynard, C. N., A. Migeon, and M. Navajas. 2013. Uncertainties in predicting species distributions under climate change: a case study using *Tetranychus evansi* (Acari: Tetranychidae), a widespread agricultural pest. *PLoS ONE* **8**:e66445.
- Michaelian, M., E. H. Hogg, R. J. Hall, and E. Arsenault. 2010. Massive mortality of aspen following severe drought along the southern edge of the Canadian boreal forest. *Global Change Biology* **17**:2084–2094.
- Milot, E., H. L. Gibbs, and K. A. Hobson. 2000. Phylogeography and genetic structure of northern populations of the Yellow Warbler (*Dendroica petechia*). *Molecular Ecology* **9**:667-681.
- Moilanen, A. 2007. Landscape Zonation, benefit functions and target-based planning: Unifying reserve selection strategies. *Biological Conservation* **134**:571-579.
- Moilanen, A., L. Meller, J. Leppanen, F. M. Pouzols, A. Arponen, and H. Kujala. 2012. Zonation version 3.1 user manual. Biodiversity Conservation Informatics Group, Department of Biosciences, University of Helsinki, Helsinki, Finland.

- Murphy, J. M., D. M. H. Sexton, D. N. Barnett, G. S. Jones, M. J. Webb, M. Collins, and D. A. Stainforth. 2004. Quantification of modelling uncertainties in a large ensemble of climate change simulations. *Nature* **430**:768-772.
- Natural Regions Committee. 2006. Natural Regions and Subregions of Alberta. Compiled by D.J. Downing and W.W. Pettapiece. Government of Alberta. Pub. No. T/852.
- Nelson, T. A., N. C. Coops, M. A. Wulder, L. Perez, J. Fitterer, R. Powers, and F. Fontana. 2014. Predicting climate change impacts to the Canadian boreal forest. *Diversity* **6**:133-157.
- Nielsen, S., D. Haughland, E. Bayne, and J. Schieck. 2009. Capacity of large-scale, long-term biodiversity monitoring programmes to detect trends in species prevalence. *Biodiversity & Conservation* **18**:2961-2978.
- North American Bird Conservation Initiative Canada. 2012. The State of Canada's Birds, 2012. Environment Canada, Ottawa, Canada.
- Noss, R. F. 2001. Beyond Kyoto: Forest management in a time of rapid climate change. *Conservation Biology* **15**:578-590.
- Oliver, T. H., R. J. Smithers, S. Bailey, C. A. Walmsley, and K. Watts. 2012. A decision framework for considering climate change adaptation in biodiversity conservation planning. *Journal of Applied Ecology* **49**:1247-1255.
- Oppel, S., and F. Huettmann. 2010. Using a Random Forest Model and Public Data to Predict the Distribution of Prey for Marine Wildlife Management. Pages 151-163 *in* S. Cushman and F. Huettmann, editors. *Spatial Complexity, Informatics, and Wildlife Conservation*. Springer Japan.
- Ordonez, A., and J. W. Williams. 2013. Climatic and biotic velocities for woody taxa distributions over the last 16 000 years in eastern North America. *Ecology Letters* **16**:773-781.
- Overpeck, J. T., R. S. Webb, and T. Webb III. 1992. Mapping eastern North American vegetation change over the past 18,000 years: no analogs and the future. *Geology* **20**:1071-1074.
- Paradis, E., J. Claude, and K. Strimmer. 2004. APE: analyses of phylogenetics and evolution in R language. *Bioinformatics* **20**:289-290.

- Parisien, M.-A., S. Parks, M. Krawchuk, M. Flannigan, L. Bowman, and M. Moritz. 2011a. Scale-dependent controls on the area burned in the boreal forest of Canada, 1980-2005. *Ecological Applications* **21**:789-805.
- Parisien, M.-A., S. Parks, C. Miller, M. Krawchuk, M. Heathcott, and M. Moritz. 2011b. Contributions of ignitions, fuels, and weather to the spatial patterns of burn probability of a boreal landscape. *Ecosystems* **14**:1141-1155.
- Parisien, M. A., V. G. Kafka, K. G. Hirsch, J. B. Todd, S. G. Lavoie, and P. D. Maczek. 2005. Using the Burn-P3 simulation model to map wildfire susceptibility. Information Rep. NOR-X-405. Edmonton, AB: Natural Resources Canada, Canadian Forest Service, Northern Forestry Centre. 36 p. .
- Parmesan, C., N. Ryrholm, C. Stefanescu, J. K. Hill, C. D. Thomas, H. Descimon, B. Huntley, L. Kaila, J. Kullberg, T. Tammaru, W. J. Tennent, J. A. Thomas, and M. Warren. 1999. Poleward shifts in geographical ranges of butterfly species associated with regional warming. *Nature* **399**:579-583.
- Pasher, J., E. Seed, and J. Duffe. 2013. Development of boreal ecosystem anthropogenic disturbance layers for Canada based on 2008 to 2010 Landsat imagery. *Canadian Journal of Remote Sensing* **39**:42-58.
- Pearson, R. G., and T. P. Dawson. 2003. Predicting the impacts of climate change on the distribution of species: are bioclimate envelope models useful? *Global Ecology and Biogeography* **12**:361-371.
- Pearson, R. G., and T. P. Dawson. 2004. Bioclimate envelope models: what they detect and what they hide - response to Hampe (2004). *Global Ecology and Biogeography* **13**:471-473.
- Peng, C., Z. Ma, X. Lei, Q. Zhu, H. Chen, W. Wang, S. Liu, W. Li, X. Fang, and X. Zhou. 2011a. A drought-induced pervasive increase in tree mortality across Canada's boreal forests. *Nature Clim. Change* **1**:467-471.
- Peng, C. H., Z. H. Ma, X. D. Lei, Q. Zhu, H. Chen, W. F. Wang, S. R. Liu, W. Z. Li, X. Q. Fang, and X. L. Zhou. 2011b. A drought-induced pervasive increase in tree mortality across Canada's boreal forests. *Nature Climate Change* **1**:467-471.
- Pennell, C., and T. Reichler. 2011. On the effective number of climate models. *Journal of Climate* **24**:2358-2367.

- Perera, A. H., Marc Ouellette, Wenbin Cui, Michael Drescher, and Den Boychuk. 2008. BFOLDS 1.0 A spatial simulation model for exploring large scale fire regimes and succession in boreal forest landscapes. Ontario Forest Research Institute, Sault Ste. Marie, Ontario, Canada.
- Peterson, A. T. 2001. Predicting species' geographic distributions based on ecological niche modeling. *Condor* **103**:599-605.
- Peterson, A. T., M. A. Ortega-Huerta, J. Bartley, V. Sanchez-Cordero, J. Soberón, R. H. Buddemeier, and D. R. B. Stockwell. 2002. Future projections for Mexican faunas under global climate change scenarios. *Nature* **41**:626-629.
- Pickell, P. D., D. W. Andison, N. C. Coops, S. E. Gergel, and P. L. Marshall. 2015. The spatial patterns of anthropogenic disturbance in the western Canadian boreal forest following oil and gas development. *Canadian Journal of Forest Research* **45**:732-743.
- Pielou, E. C. 1991. *After the Ice Age: The Return of Life to Glaciated North America*. University of Chicago Press, Chicago, IL.
- Pienkowski, M., P. Evans, and D. Townshend. 1985. Leap-frog and other migration patterns of waders: a critique of the Alerstam and Högstedt hypothesis, and some alternatives. *Ornis Scandinavica* **16**:61-70.
- Podur, J., D. L. Martell, and K. Knight. 2002. Statistical quality control analysis of forest fire activity in Canada. *Canadian Journal of Forest Research* **32**:195-205.
- Podur, J. J., and B. M. Wotton. 2011. Defining fire spread event days for fire-growth modeling. *International Journal of Wildland Fire* **20**:497-507.
- Poole, A., editor. 2005. *The Birds of North America Online*: <http://bna.birds.cornell.edu/BNA/>. Cornell Laboratory of Ornithology, Ithaca, NY.
- Powers, R. P., N. C. Coops, T. Nelson, M. A. Wulder, and C. Ronnie Drever. 2013. Integrating accessibility and intactness into large-area conservation planning in the Canadian boreal forest. *Biological Conservation* **167**:371-379.
- Prasad, A. M., L. R. Iverson, and A. Liaw. 2006. Newer classification and regression tree techniques: bagging and random forests for ecological prediction. *Ecosystems* **9**:181-199.
- Prentice, I. C., J. Bartlein, and W. Thompson. 1991. Vegetation and climate change in eastern North America since the last glacial maximum. *Ecology* **72**:2038-2056.

- Price, D. T., R. I. Alfaro, K. J. Brown, M. D. Flannigan, R. A. Fleming, E. H. Hogg, M. P. Girardin, T. Lakusta, M. Johnston, D. W. McKenney, J. H. Pedlar, T. Stratton, R. N. Sturrock, I. D. Thompson, J. A. Trofymow, and L. A. Venier. 2013. Anticipating the consequences of climate change for Canada's boreal forest ecosystems. *Environmental Reviews* **21**:322-365.
- Price, D. T., D. W. McKenney, L. A. Joyce, R. M. Siltanen, P. Papadopol, and K. Lawrence. 2011. High resolution interpolation of IPCC AR4 GCM climate scenarios for Canada. Natural Resources Canada, Northern Forestry Centre, Edmonton, Alberta, Canada.
- R Core Team. 2012. R: A Language and Environment for Statistical Computing. <http://www.R-project.org>. R Foundation for Statistical Computing, Vienna, Austria.
- R Core Team. 2014. R: A language and environment for statistical computing. R Foundation for Statistical Computing, Vienna, Austria. <http://www.R-project.org/>.
- Radeloff, V. C., E. Nelson, A. J. Plantinga, D. J. Lewis, D. Helmers, J. J. Lawler, J. C. Withey, F. Beaudry, S. Martinuzzi, V. Butsic, E. Lonsdorf, D. White, and S. Polasky. 2011. Economic-based projections of future land use in the conterminous United States under alternative policy scenarios. *Ecological Applications* **22**:1036-1049.
- Rahbek, C., and G. R. Graves. 2001. Multiscale assessment of patterns of avian species richness. *Proceedings of the National Academy of Sciences of the United States of America* **98**:4534-4539.
- Räisänen, J. 2007. How reliable are climate models? *Tellus A* **59**:2-29.
- Ralph, C. J., J. R. Sauer, and S. Droege. 1995. Monitoring bird populations by point count. USDA Forest Service General Technical Report PSW-GTR-149.
- Ralston, J., and J. J. Kirchman. 2012. Continent-scale genetic structure in a boreal forest migrant, the Blackpoll Warbler (*Setophaga striata*). *The Auk* **129**:467-478.
- Raupach, M. R., G. Marland, P. Ciais, C. Le Quéré, J. G. Canadell, G. Klepper, and C. B. Field. 2007. Global and regional drivers of accelerating CO₂ emissions. *Proceedings of the National Academy of Sciences* **104**:10288-10293.
- Regan, H. M., Y. Ben-Haim, B. Langford, W. G. Wilson, P. Lundberg, S. J. Andelman, and M. A. Burgman. 2005. Robust decision making under severe uncertainty for conservation management. *Ecological Applications* **15**:1471-1477.

- Rehfeldt, G. E., N. L. Crookston, C. Sáenz-Romero, and E. M. Campbell. 2012. North American vegetation model for land-use planning in a changing climate: a solution to large classification problems. *Ecological Applications* **22**:119-141.
- Rehfeldt, G. E., N. L. Crookston, M. V. Warwell, and J. S. Evans. 2006. Empirical analyses of plant-climate relationships for the western United States. *International Journal of Plant Sciences* **167**:1123-1150.
- Rich, T. D., C. J. Beardmore, H. Berlanga, P. J. Blancher, M. S. W. Bradstreet, G. S. Butcher, D. W. Demarest, E. H. Dunn, W. C. Hunter, E. E. Iñigo-Elias, J. A. Kennedy, A. M. Martell, A. O. Panjabi, D. N. Pashley, K. V. Rosenberg, C. M. Rustay, J. S. Wendt, and T. C. Will. 2004. Partners in Flight North American Landbird Conservation Plan. Cornell Lab of Ornithology, Ithaca, NY.
- Richards, G. D. 1995. A general mathematical framework for modeling two-dimensional wildland fire spread. *International Journal of Wildland Fire* **5**:63-72.
- Ridgely, R. S., T. F. Allnutt, T. Brooks, D. K. McNicol, D. W. Mehlman, B. E. Young, and J. R. Zook. 2005. Digital distribution maps of the birds of the western hemisphere, version 2.1. NatureServe.
- Ridgeway, G. 2012. Package 'gbm'. Available on-line at <http://cran.r-project.org/web/packages/gbm/index.html>.
- Roberts, D. R., and A. Hamann. 2012. Predicting potential climate change impacts with bioclimate envelope models: a palaeoecological perspective. *Global Ecology and Biogeography* **21**:121-133.
- Roberts, D. R., and A. Hamann. 2015. Glacial refugia and modern genetic diversity of 22 western North American tree species. *Proceedings of the Royal Society B: Biological Sciences* **282**.
- Rohling, E. J., A. Sluijs, H. A. Dijkstra, P. Köhler, R. S. W. v. d. Wal, A. S. v. d. Heydt, D. J. Beerling, A. Berger, P. K. Bijl, M. Crucifix, R. DeConto, S. S. Drijfhout, A. Fedorov, G. L. Foster, A. Ganopolski, J. Hansen, B. Hönlisch, H. Hooghiemstra, M. Huber, P. Huybers, R. Knutti, D. W. Lea, L. J. Lourens, D. Lunt, V. Masson-Demotte, M. Medina-Elizalde, B. Otto-Bliesner, M. Pagani, H. Pälike, H. Renssen, D. L. Royer, M. Siddall, P. Valdes, J. C. Zachos, and R. E. Zeebe. 2012. Making sense of palaeoclimate sensitivity. *Nature* **491**:683-691.

- Root, T. 1988. Environmental factors associated with avian distributional boundaries. *Journal of Biogeography* **15**:489-505.
- Rose, N.-A., and P. J. Burton. 2009. Using bioclimatic envelopes to identify temporal corridors in support of conservation planning in a changing climate. *Forest Ecology and Management* **258S**:S64–S74.
- Rubidge, E. M., W. B. Monahan, J. L. Parra, S. E. Cameron, and J. S. Brashares. 2011. The role of climate, habitat, and species co-occurrence as drivers of change in small mammal distributions over the past century. *Global Change Biology* **17**:696-708.
- Ruckstuhl, K. E., E. A. Johnson, and K. Miyanishi. 2008. Introduction. The boreal forest and global change. *Philosophical Transactions of the Royal Society of London B Biological Sciences* **363**:2243-2247.
- Ruegg, K. C., R. J. Hijmans, and C. Moritz. 2006. Climate change and the origin of migratory pathways in the Swainson's Thrush, *Catharus ustulatus*. *Journal of Biogeography* **33**:1172-1182.
- Rupp, T. S., A. M. Starfield, and F. S. Chapin. 2000. A frame-based spatially explicit model of subarctic vegetation response to climatic change: comparison with a point model. *Landscape Ecology* **15**:383-400-400.
- Sandel, B., L. Arge, B. Dalsgaard, R. G. Davies, K. J. Gaston, W. J. Sutherland, and J.-C. Svenning. 2011. The Influence of Late Quaternary Climate-Change Velocity on Species Endemism. *Science* **334**:660-664.
- Sappington, J. M., K. M. Longshore, and D. B. Thompson. 2007. Quantifying Landscape Ruggedness for Animal Habitat Analysis: A Case Study Using Bighorn Sheep in the Mojave Desert. *The Journal of Wildlife Management* **71**:1419-1426.
- Sauer, J. R., J. E. Hines, and J. Fallon. 2011. The North American Breeding Bird Survey, Results and Analysis 1966-2010. Version 5.15.2011. USGS Patuxent Wildlife Research Center, Laurel, MD.
- Scheffer, M., M. Hirota, M. Holmgren, E. H. Van Nes, and F. S. Chapin. 2012. Thresholds for boreal biome transitions. *Proceedings of the National Academy of Sciences* **109**:21384-21389.

- Scheller, R. M., and D. J. Mladenoff. 2008. Simulated effects of climate change, fragmentation, and inter-specific competition on tree species migration in northern Wisconsin, USA. *Climate Research* **36**:191-202.
- Scherrer, S. C. 2011. Present-day interannual variability of surface climate in CMIP3 models and its relation to future warming. *International Journal of Climatology* **31**:1518-1529.
- Schieck, J., P. Solyomos, and D. Huggard. 2015. Human Footprint in Alberta. ABMI Science Letters. Available online: http://ftp.public.abmi.ca/home/publications/documents/364_Schieck_etal_2014_LetterHFInAlberta_ABMI.pdf.
- Schieck, J., and S. J. Song. 2006. Changes in bird communities throughout succession following fire and harvest in boreal forests of western North America: literature review and meta-analyses. *Canadian Journal of Forest Research* **36**:1299-1318.
- Schindler, D. W., and P. G. Lee. 2010. Comprehensive conservation planning to protect biodiversity and ecosystem services in Canadian boreal regions under a warming climate and increasing exploitation. *Biological Conservation* **143**:1571-1586.
- Schloss, C. A., T. A. Nuñez, and J. J. Lawler. 2012. Dispersal will limit ability of mammals to track climate change in the Western Hemisphere. *Proceedings of the National Academy of Sciences* **109**:8606-8611.
- Schmiegelow, F. K. A., S. G. Cumming, K. A. Lisgo, S. J. Leroux, and M. A. Krawchuk. 2014. Catalyzing Large Landscape Conservation in Canada's Boreal Systems: The BEACONS Project Experience. Pages 97-122 in J. N. Levitt, editor. *Conservation Catalysts*. Lincoln Institute of Land Policy, Cambridge, MA.
- Schmiegelow, F. K. A., C. S. Machtans, and S. J. Hannon. 1997. Are boreal birds resilient to forest fragmentation? An experimental study of short-term community responses. *Ecology* **78**:1914-1932.
- Schneider, R., E. Bayne, and K. DeVito. 2015. Moving beyond bioclimatic envelope models: integrating upland forest and peatland processes to predict ecosystem transitions under climate change in the western Canadian boreal plain. *Ecohydrology*. DOI: 10.1002/eco.1707

- Schneider, R. J., B. Stelfox, S. Boutin, and S. Wasel. 2003. Managing the cumulative impacts of land uses in the Western Canadian Sedimentary Basin: a modeling approach. *Conservation Ecology* **7**:8.
- Schneider, R. R., A. Hamann, D. Farr, X. Wang, and S. Boutin. 2009. Potential effects of climate change on ecosystem distribution in Alberta. *Canadian Journal of Forest Research* **39**:1001-1010.
- Schneider, S. H., and T. L. Root. 1996. Ecological implications of climate change will include surprises. *Biodiversity & Conservation* **5**:1109-1119.
- Schuetz, J. G., G. M. Langham, C. U. Soykan, C. B. Wilsey, T. Auer, and C. C. Sanchez. 2015. Making spatial prioritizations robust to climate change uncertainties: a case study with North American birds. *Ecological Applications*.
- Scott, D., J. R. Malcolm, and C. Lemieux. 2002. Climate change and modelled biome representation in Canada's national park system: implications for system planning and park mandates. *Global Ecology and Biogeography* **11**:475-484.
- Scott, P. A., R. I. C. Hansell, and D. C. F. Fayle. 1987. Establishment of White Spruce Populations and Responses to Climatic Change at the Treeline, Churchill, Manitoba, Canada. *Arctic and Alpine Research* **19**:45-51.
- Screen, J. A., and I. Simmonds. 2010. The central role of diminishing sea ice in recent Arctic temperature amplification. *Nature* **464**:1334-1337.
- Segurado, P., and M. B. Araújo. 2004. An evaluation of methods for modelling species distributions. *Journal of Biogeography* **31**:1555-1568.
- Shaw, M. R., K. Klausmeyer, D. R. Cameron, J. Mackenzie, and P. Roehrdanz. 2012. Economic costs of achieving current conservation goals in the future as climate changes. *Conservation Biology*:no-no.
- Siegel, R. B., P. Pyle, J. H. Thorne, A. J. Holguin, C. A. Howell, S. Stock, and M. W. Tingley. 2014. Vulnerability of birds to climate change in California's Sierra Nevada. *Avian Conservation and Ecology* **9**.
- Silver, N. 2012. *The Signal and the Noise: Why So Many Predictions Fail-but Some Don't*. Penguin Books, London, UK.

- Siriwardena, G. M., H. Q. P. Crick, S. R. Baillie, and J. D. Wilson. 2000. Agricultural land-use and the spatial distribution of granivorous lowland farmland birds. *Ecography* **23**:702-719.
- Smith, K. G. 1978. Range extension of the Blue Jay into western North America. *Bird-Banding* **49**:208-214.
- Soberón, J. 2007. Grinnellian and Eltonian niches and geographic distributions of species. *Ecology Letters* **10**:1115-1123.
- Soberón, J., and M. Nakamura. 2009. Niches and distributional areas: Concepts, methods, and assumptions. *Proceedings of the National Academy of Sciences of the United States of America* **106**:19644-19650.
- Soja, A. J., N. M. Tchebakova, N. H. F. French, M. D. Flannigan, H. H. Shugart, B. J. Stocks, A. I. Sukhinin, E. I. Parfenova, F. S. Chapin Iii, and J. P. W. Stackhouse. 2007. Climate-induced boreal forest change: predictions versus current observations. *Global and Planetary Change* **56**:274-296.
- Sólymos, P., S. M. Matsuoka, E. M. Bayne, S. R. Lele, P. Fontaine, S. G. Cumming, D. Stralberg, F. K. A. Schmiegelow, and S. J. Song. 2013. Calibrating indices of avian density from non-standardized survey data: making the most of a messy situation. *Methods in Ecology and Evolution* **4**:1047-1058.
- Sorensen, T., P. D. McLoughlin, D. Hervieux, E. Dzus, J. Nolan, B. O. B. Wynes, and S. Boutin. 2008. Determining sustainable levels of cumulative effects for boreal caribou. *The Journal of Wildlife Management* **72**:900-905.
- Stanley, C. Q., M. MacPherson, K. C. Fraser, E. A. McKinnon, and B. J. M. Stutchbury. 2012. Repeat tracking of individual songbirds reveals consistent migration timing but flexibility in route. *PLoS ONE* **7**:e40688.
- Stephens, S. L., J. K. Agee, P. Z. Fulé, M. P. North, W. H. Romme, T. W. Swetnam, and M. G. Turner. 2013. Managing Forests and Fire in Changing Climates. *Science* **342**:41-42.
- Sterling, S. M., A. Ducharme, and J. Polcher. 2013. The impact of global land-cover change on the terrestrial water cycle. *Nature Clim. Change* **3**:385-390.
- Stocks, B. J., J. A. Mason, J. B. Todd, E. M. Bosch, B. M. Wotton, B. D. Amiro, M. D. Flannigan, K. G. Hirsch, K. A. Logan, D. L. Martell, and W. R. Skinner. 2002. Large

- forest fires in Canada, 1959–1997. *Journal of Geophysical Research: Atmospheres* **107**:FFR 5-1-FFR 5-12.
- Stockwell, D. R. B., and A. T. Peterson. 2002. Effects of sample size on accuracy of species distribution models. *Ecological Modelling* **148**:1-13.
- Stralberg, D. 2012. GCM Recommendations for Alberta. Report to the Alberta Biodiversity Monitoring Institute.
- Stralberg, D., E. M. Bayne, S. G. Cumming, P. Sólymos, S. J. Song, and F. K. A. Schmiegelow. 2015a. Conservation of future boreal forest bird communities considering lags in vegetation response to climate change: a modified refugia approach. *Diversity and Distributions* **21**:1112-1128.
- Stralberg, D., M. Brennan, J. C. Callaway, J. K. Wood, L. M. Schile, D. Jongsomjit, M. Kelly, V. T. Parker, and S. Crooks. 2011. Evaluating tidal marsh sustainability in the face of sea-level rise: A hybrid modeling approach applied to San Francisco Bay. *PLoS ONE* **6**:e27388.
- Stralberg, D., D. Jongsomjit, C. A. Howell, M. A. Snyder, J. D. Alexander, J. A. Wiens, and T. L. Root. 2009. Re-shuffling of species with climate disruption: a no-analog future for California birds? *PLoS ONE* **4**:e6825.
- Stralberg, D., S. M. Matsuoka, A. Hamann, E. M. Bayne, P. Sólymos, F. K. A. Schmiegelow, X. Wang, S. G. Cumming, and S. J. Song. 2015b. Projecting boreal bird responses to climate change: the signal exceeds the noise. *Ecological Applications* **25**:52–69.
- Stralberg, D., P. Solymos, E. Bayne, S. Matsuoka, F. Schmiegelow, S. Cumming, Trish Fontaine, and S. Song. 2012. Beyond distribution: Projecting climate-change effects on boreal bird density patterns. National American Ornithological Conference, Vancouver, BC.
- Strong, W. L., and L. V. Hills. 2003. Post-Hypsithermal plant disjunctions in western Alberta, Canada. *Journal of Biogeography* **30**:419–430.
- Summers, D. M., B. A. Bryan, N. D. Crossman, and W. S. Meyer. 2012. Species vulnerability to climate change: impacts on spatial conservation priorities and species representation. *Global Change Biology* **18**:2335-2348.
- Svenning, J.-C., and B. Sandel. 2013. Disequilibrium vegetation dynamics under future climate change. *American Journal of Botany* **100**:1266-1286.

- Svenning, J.-C., and F. Skov. 2004. Limited filling of the potential range in European tree species. *Ecology Letters* **7**:565-573.
- Synes, N. W., and P. E. Osborne. 2011. Choice of predictor variables as a source of uncertainty in continental-scale species distribution modelling under climate change. *Global Ecology and Biogeography* **20**:904–914.
- Syphard, A. D., and J. Franklin. 2009. Differences in spatial predictions among species distribution modeling methods vary with species traits and environmental predictors. *Ecography* **32**:907-918.
- Tebaldi, C., R. L. Smith, D. Nychka, and L. O. Mearns. 2005. Quantifying uncertainty in projections of regional climate change: a Bayesian approach to the analysis of multimodel ensembles. *Journal of Climate* **18**:1524-1540.
- Terrier, A., M. P. Girardin, A. Cantin, W. J. de Groot, K. A. Anyomi, S. Gauthier, and Y. Bergeron. 2015. Disturbance legacies and paludification mediate the ecological impact of an intensifying wildfire regime in the Clay Belt boreal forest of eastern North America. *Journal of Vegetation Science* **26**:588-602.
- Terrier, A., M. P. Girardin, C. Périé, P. Legendre, and Y. Bergeron. 2012. Potential changes in forest composition could reduce impacts of climate change on boreal wildfires. *Ecological Applications* **23**:21-35.
- Thomas, C. D. 2010. Climate, climate change and range boundaries. *Diversity and Distributions* **16**:488-495.
- Thomas, C. D., and J. L. Lennon. 1999. Birds extend their ranges northwards. *Nature* **399**:213.
- Thuiller, W. 2004. Patterns and uncertainties of species' range shifts under climate change. *Global Change Biology* **10**:2020-2027.
- Thuiller, W., B. Lafourcade, R. Engler, and M. B. Araújo. 2009. BIOMOD - a platform for ensemble forecasting of species distributions. *Ecography* **32**:369-373.
- Thuiller, W., S. Lavorel, M. B. Araújo, M. T. Sykes, and I. C. Prentice. 2005. Climate change threats to plant diversity in Europe. *Proceedings of the National Academy of Sciences of the United States of America* **102**:8245-8250.
- Tingley, M. W., W. B. Monahan, S. R. Beissinger, and C. Moritz. 2009. Birds track their Grinnellian niche through a century of climate change. *Proceedings of the National Academy of Sciences of the United States of America* **106**:19637–19643.

- Tung Ho, L. s., and C. Ané. 2014. A linear-time algorithm for Gaussian and non-Gaussian trait evolution models. *Systematic Biology* **63**:397-408.
- Tymstra, C., R. Bryce, B. Wotton, and O. Armitage. 2010. Development and structure of Prometheus: the Canadian wildland fire growth simulation Model. Northern Forestry Centre.
- Tymstra, C., M. D. Flannigan, O. B. Armitage, and K. Logan. 2007. Impact of climate change on area burned in Alberta's boreal forest. *International Journal of Wildland Fire* **16**:153-160.
- Tymstra, C., D. Wang, and M.-P. Rogeau. 2005. Alberta wildfire regime analysis. Alberta Sustainable Resource Development, Forest Protection Division Wildfire Science and Technology Report PFFC-01-05, Edmonton, AB, Canada.
- van Wagner, C. E. 1987. Development and Structure of the Canadian Forest Fire Weather Index System. Forestry Technical Report 35. Canadian Forest Service, Ottawa, Canada.
- Van Wilgenburg, S. L., K. A. Hobson, E. M. Bayne, and N. Koper. 2013. Estimated avian nest loss associated with oil and gas exploration and extraction in the western Canadian sedimentary basin. *Avian Conservation and Ecology* **8**.
- Vander Haegen, W. M., and R. M. Degraaf. 1996. Predation on artificial nests in forested riparian buffer strips. *Journal Of Wildlife Management* **60**:542-550.
- Veloz, S., L. Salas, B. Altman, J. Alexander, D. Jongsomjit, N. Elliott, and G. Ballard. 2015. Improving effectiveness of systematic conservation planning with density data. *Conservation Biology*:n/a-n/a.
- Veloz, S. D., N. Nur, L. Salas, D. Jongsomjit, J. Wood, D. Stralberg, and G. Ballard. 2013. Modeling climate change impacts on tidal marsh birds: Restoration and conservation planning in the face of uncertainty. *Ecosphere* **4**:art49.
- Vitt, D. H., L. A. Halsey, and S. C. Zoltai. 2000. The changing landscape of Canada's western boreal forest: the current dynamics of permafrost. *Canadian Journal of Forest Research* **30**:283-287.
- Waddington, J. M., P. J. Morris, N. Kettridge, G. Granath, D. K. Thompson, and P. A. Moore. 2015. Hydrological feedbacks in northern peatlands. *Ecohydrology* **8**:113-127.
- Wang, M., J. E. Overland, V. Kattsov, J. E. Walsh, X. Zhang, and T. Pavlova. 2007. Intrinsic versus forced variation in coupled climate model simulations over the Arctic during the twentieth century. *Journal of Climate* **20**:1093-1107.

- Wang, T., A. Hamann, D. L. Spittlehouse, and T. Q. Murdock. 2012. ClimateWNA—high-resolution spatial climate data for western North America. *Journal of Applied Meteorology and Climatology* **51**:16-29.
- Wang, X., M.-A. Parisien, M. D. Flannigan, S. A. Parks, K. R. Anderson, J. M. Little, and S. W. Taylor. 2014. The potential and realized spread of wildfires across Canada. *Global Change Biology* **20**:2518-2530.
- Wang, X., M.-A. Parisien, S. W. Taylor, D. D. B. Perrakis, J. Little, and M. D. Flannigan. in press. Future burn probability in south-central British Columbia. *International Journal of Wildland Fire*.
- Wang, X., D. K. Thompson, G. A. Marshall, C. Tymstra, R. Carr, and M. D. Flannigan. 2015. Increasing frequency of extreme fire weather in Canada with climate change. *Climatic Change* **130**:573-586.
- Warren, M. S., J. K. Hill, J. A. Thomas, J. Asher, R. Fox, B. Huntley, D. B. Roy, M. G. Telfer, S. Jeffcoate, P. Harding, G. Jeffcoate, S. G. Willis, J. N. Greatorex-Davies, D. Moss, and C. D. Thomas. 2001. Rapid responses of British butterflies to opposing forces of climate and habitat change. *Nature* **414**:65-69.
- Watson, J. E. M., T. Iwamura, and N. Butt. 2013. Mapping vulnerability and conservation adaptation strategies under climate change. *Nature Clim. Change* **3**:989-994.
- Weatherhead, P. J., and M. R. L. Forbes. 1994. Natal philopatry in passerine birds: genetic or ecological influences? *Behavioral Ecology* **5**:426-433.
- Weir, J. T., and D. Schluter. 2004. Ice sheets promote speciation in boreal birds. *Philosophical Transactions of the Royal Society of London B Biological Sciences* **271**:1881-1887.
- Wells, J., and P. Blancher. 2011. Global role for sustaining bird populations. *in* J. Wells, editor. *Boreal Birds of North America: A Hemispheric View of their Conservation Links and Significance*. Studies in Avian Biology, no. 41. UC Press, Berkeley, CA.
- Wendler, G., and M. Shulksi. 2009. A century of climate change for Fairbanks, Alaska. *Arctic* **62**:295-300.
- Wiens, J. A., D. Stralberg, D. Jongsomjit, C. A. Howell, and M. A. Snyder. 2009. Niches, models, and climate change: Assessing the assumptions and uncertainties. *Proceedings of the National Academy of Sciences of the United States of America* **106**:19729-19736.

- Wiens, J. J., D. D. Ackerly, A. P. Allen, B. L. Anacker, L. B. Buckley, H. V. Cornell, E. I. Damschen, T. J. Davies, J.-A. Grytnes, S. P. Harrison, B. A. Hawkins, R. D. Holt, C. M. McCain, and P. R. Stephens. 2010. Niche conservatism as an emerging principle in ecology and conservation biology. *Ecology Letters* **13**:1310-1324.
- Wiens, J. J., and C. H. Graham. 2005. Niche conservatism: integrating evolution, ecology, and conservation biology. *Annual Review of Ecology Evolution and Systematics* **36**:519-539.
- Williams, J. W., and S. T. Jackson. 2007. Novel climates, no-analog communities, and ecological surprises. *Frontiers in Ecology and the Environment* **5**:475-482.
- Williams, J. W., S. T. Jackson, and J. E. Kutzbach. 2007. Projected distributions of novel and disappearing climates by 2100 AD. *Proceedings of the National Academy of Sciences of the United States of America* **104**:5738-5742.
- Wisz, M. S., R. J. Hijmans, J. Li, A. T. Peterson, C. H. Graham, and A. Guisan. 2008. Effects of sample size on the performance of species distribution models. *Diversity and Distributions* **14**:763-773.
- Wotton, B. M., and M. D. Flannigan. 1993. Length of the fire season in a changing climate. *The Forestry Chronicle* **69**:187-192.
- Wotton, B. M., C. A. Nock, and M. D. Flannigan. 2010. Forest fire occurrence and climate change in Canada. *International Journal of Wildland Fire* **19**:253-271.
- Wu, D., X. Zhao, S. Liang, T. Zhou, K. Huang, B. Tang, and W. Zhao. 2015. Time-lag effects of global vegetation responses to climate change. *Global Change Biology* **21**:3520-3531.
- Yahner, R. D. H., and D. P. Scott. 1988. Effects of forest fragmentation on depredation of artificial nests. *Journal Of Wildlife Management* **52**:158-161.
- Yamasaki, S. H., R. Duchesneau, F. Doyon, J. S. Russell, and T. Gooding. 2008. Making the case for cumulative impacts assessment: Modelling the potential impacts of climate change, harvesting, oil and gas, and fire. *The Forestry Chronicle* **84**:349-368.
- Yu, Z., D. H. Vitt, I. D. Campbell, and M. J. Apps. 2003. Understanding Holocene peat accumulation pattern of continental fens in western Canada. *Canadian Journal of Botany* **81**:267-282.
- Zhang, J., S. Huang, and F. He. 2015. Half-century evidence from western Canada shows forest dynamics are primarily driven by competition followed by climate. *Proceedings of the National Academy of Sciences of the United States of America* **112**:4009-4014.

- Zuckerberg, B., A. M. Woods, and W. F. Porter. 2009. Poleward shifts in breeding bird distributions in New York State. *Global Change Biology* **15**:1866-1883.
- Zurell, D., J. Elith, and B. Schröder. 2012. Predicting to new environments: tools for visualizing model behaviour and impacts on mapped distributions. *Diversity and Distributions* **18**:628-634.
- Zurell, D., F. Jeltsch, C. F. Dormann, and B. Schröder. 2009. Static species distribution models in dynamically changing systems: how good can predictions really be? *Ecography* **32**:733-744.

APPENDICES

Appendix 1-A. Global climate model summary and downscaling methods

Downscaling Methods

Global climate model (GCM) projections were obtained from the Intergovernmental Panel on Climate Change (IPCC) 4th Assessment Report (AR4) (IPCC 2007) as part of the World Climate Research Programme's Coupled Model Intercomparison Project phase 3 (WCRP CMIP) multi-model dataset [http://www-pcmdi.llnl.gov/ipcc/info_for_analysts.php] (Meehl et al. 2007). Historical projections were taken from the 20th century simulation, which were generally initiated between 1850 and 1880 and run through 1999 or 2000. Future projections were taken from three emission scenarios (IPCC 2000)—SRESA2 (high), SRESA1B (intermediate), and SRESB2 (low)—run from 2000 or 2001 through at least 2099 or 2100. Projections of monthly temperature and total precipitation were averaged across multiple GCM runs (if available) for each thirty-year period. A total of 24 GCM simulations were used, 17 of which were run for all three future scenarios, with grid cell resolutions ranging from 1.125° to 5° (Table A2). Temperature values were converted to degrees Celsius and precipitation values were converted to mm/day.

For each future time period, we calculated climate anomalies as the absolute change in temperature and the percent change in precipitation between the projected values for each future period and the projected climate normals for the baseline period. Projected precipitation anomalies were capped at 500% of the projected normal to prevent unrealistic values stemming from chance differences at the low end of the precipitation spectrum. We clipped the projected climate anomalies to North America, downscaled them to a 0.5° resolution using a thin-plate spline interpolation, and then added the downscaled anomalies to the 4-km interpolated climate normals (described above). We did not have future projections for minimum and maximum temperature for 13 of the 19 GCMs. We therefore used the average temperature anomalies in place of minimum and maximum temperature anomalies to calculate future projected minimum and maximum temperature averaged across GCMs. Mean monthly projections of monthly temperature and precipitation were used to calculate derived bioclimatic variables (Table A1) for each 4-km grid cell in each future time period. Projections for each variable and each time period (including current baseline) were converted to separate raster layers for GIS analysis and mapping purposes.

Technical Details

GCM projections in NetCDF format were imported into R and manipulated into a tabular format using the 'ncdf' (Pierce 2013) package. Due to inconsistent time periods across GCMs, the starting year for each simulation was included in the NetCDF file name for parsing purposes. For each GCM run and for each variable (tmin, tmax, tavg, prec), a separate .csv file for each simulation year was created, with one record per grid cell (as given by x-y coordinates) and one column per month. Annual monthly means were then averaged across 30-year time periods, creating a single .csv file for each 30-year time period. In this step, longitude coordinates were converted from a scale of 0-360 to a standard geographic coordinate system (central meridian at Greenwich) ranging from -180 to 180.

Anomalies were converted to raster format using the 'raster' package, and clipped to the North American land boundary. Remaining points were interpolated with a thin-plate spline algorithm using the 'fields' (Fields Development Team 2006) and 'raster' (Hijmans and van Etten 2012) packages. Interpolated monthly anomalies for each future period were added to the baseline (1961-1990) monthly means to create .csv files containing monthly mean projections for centerpoints of a 4-km grid for North America. These monthly projections were then used to calculate a separate csv file containing derived bioclimatic variables for each future period.

Finally, decimal-degree-based projections for monthly and derived bioclimatic variables were joined with a base file containing Lambert Conformal Conic coordinates using a unique identifier field. Points outside of the 4-km grid (small protected areas) were filtered out, and separate .asc raster layers (4-km grid cell resolution) were generated for each variable using the 'raster' package.

We performed all climate data manipulations using the program R, version 2.12.1 (R Development Core Team 2010).

References

- Chen, W., Z. Jiang, and L. Li. 2011. Probabilistic projections of climate change over China under the SRES A1B scenario using 28 AOGCMs. *Journal of Climate* 24:4741-4756.
- Fasullo, J. T. and K. E. Trenberth. 2012. A less cloudy future: the role of subtropical subsidence in climate sensitivity. *Science* 338:792-794.
- Fields Development Team. 2006. fields: Tools for Spatial Data. National Center for Atmospheric Research, Boulder, CO. Available on-line at <http://www.cgd.ucar.edu/Software/Fields>.
- Gleckler, P. J., K. E. Taylor, and C. Doutriaux. 2008. Performance metrics for climate models. *Journal of Geophysical Research* 113:D06104.
- Hijmans, R. J. and J. van Etten. 2012. Package 'raster'. Available on-line at <http://cran.r-project.org/web/packages/raster/index.html>.
- Hogg, E. H. 1997. Temporal scaling of moisture and the forest-grassland boundary in western Canada. *Agricultural and Forest Meteorology* 84:115-122.
- IPCC. 2000. Special Report on Emissions Scenarios. Summary for Policymakers. A Special Report of IPCC Working Group III.
- IPCC. 2007. Climate Change 2007: The Physical Science Basis. Contribution of Working Group I to the Fourth Assessment Report of the Intergovernmental Panel on Climate Change. Cambridge University Press, Cambridge.
- Meehl, G. A., C. Covey, T. Delworth, M. Latif, B. McAvaney, J. F. B. Mitchell, R. J. Stouffer, and K. E. Taylor. 2007. The WCRP CMIP3 multi-model dataset: a new era in climate change research. *Bulletin of the American Meteorological Society* 88:1383-1394.
- Pierce, D. 2013. Package 'ncdf'. Available on-line at <http://cran.r-project.org/web/packages/ncdf/index.html>.
- R Development Core Team. 2010. R: A language and environment for statistical computing. R Foundation for Statistical Computing, Vienna, Austria.
- Scherrer, S. C. 2011. Present-day interannual variability of surface climate in CMIP3 models and its relation to future warming. *International Journal of Climatology* 31:1518-1529.
- Walsh, J. E., W. L. Chapman, V. Romanovsky, J. H. Christensen, and M. Stendel. 2008. Global climate model performance over Alaska and Greenland. *Journal of Climate* 21:6156-6174.
- Wang, M., J. E. Overland, V. Kattsov, J. E. Walsh, X. Zhang, and T. Pavlova. 2007. Intrinsic versus forced variation in coupled climate model simulations over the Arctic during the twentieth century. *Journal of Climate* 20:1093-1107.

Table A1. Summary of derived bioclimatic variables calculated for 24 GCMs, three emission scenarios, and four time periods.

Variable	Definition
MAP	mean annual precipitation
MSP	mean summer (May-Sep) precipitation
PPT_WT	winter (Dec/Jan/Feb) precipitation
PPT_SM	summer (Jun/Jul/Aug) precipitation
PAS	precipitation as snow
MAT	mean annual temperature
MCMT	mean cold month (Jan) temperature
MWMT	mean warm month (Jul) temperature
TD	temperature difference (mwmt – mcmt)
FFP	frost-free period
NFFD	number of frost-free days
EMT	extreme minimum temperature
DD51	degree days above 5 C
DD01	degree days below 0 C
PET	potential evapotranspiration ¹
CMI	climate moisture index (map – pet) ¹
CMIJJA	climate moisture index (Jun/Jul/Aug) ¹

¹ Calculated using Hogg's (1997) modified Penman-Monteith method. Values were calculated separately for each month and then summed across months of interest.

Table A2. General circulation models (GCM) and country of origin, their spatial resolution, and their associated number of runs for each century and climate variable. The projected climate variables include monthly precipitation (precip) and monthly average (tavg), minimum (tmin), and maximum (tmax) temperature. The four climate models in bold are compared herein. Models below the dotted line were not candidates for selection.

GCM, Country	x (°)	y (°)	Resolution	Walsh et al. 2008 ¹	Wang et al. 2007 ²	Gleckler et al. 2008 ¹	Chen et al. 2011 ⁴	Scherrer 2011 ⁵	Fasullo & Trenberth 2012 ⁶	Overall rank
INGV-ECHAM4, Italy/Germany	1.12500	1.12500	1.5				1			0.83
CCSM3, USA	1.40625	1.40625	3	5	3	9	6	9	9	4.40
ECHAM5/MPI-OM, Germany	1.87500	1.87500	6	1	6.5	2	14	9	7	4.55
UKMO-HadGEM1, UK	1.87500	1.24138	4			1	13.5	9	2.5	5.00
CSIRO-Mk3.5, Australia	1.87500	1.87500	6				5	9		5.00
UKMO-HadCM3, UK	3.75000	2.46575	17	8.5	9.5	3	3	9	4.5	5.45
ECHO-G, Germany/Korea	3.75000	3.75000	20		3		10			5.50
MIROC3.2(hires), Japan	1.12500	1.12500	1.5		16.5	5	6.5	9	1	5.64
GFDL-CM2.1, USA	2.50000	2.00000	8.5	2	12	4	11	9	10.5	5.70
CSIRO-Mk3.0, Australia	1.87500	1.87500	6	15	3	7	8	9	13	6.10
GFDL-CM2.0, USA	2.50000	2.00000	8.5	3	6.5	11	11.5	9	12	6.15
MIROC3.2(medres), Japan	2.81250	2.81250	12.5	4	16.5	10	8	9	6	6.60
CGCM3.1(T47), Canada	3.75000	3.75000	19	10.5	9.5	6	15.5	9	2.5	7.20
CGCM3.1(T63), Canada	2.81250	2.81250	12.5		9.5	8	8.5	9	4.5	7.43
MRI-CGCM2.3.2, Japan	2.81250	2.81250	12.5	7	16.5	12	11	9	10.5	7.85
CNRM-CM3, France	2.81250	2.81250	12.5	6	9.5	13	25.5	9		8.28
PCM, USA	2.81250	2.81250	12.5	10.5	3	16	23	9	14	8.80
IPSL-CM4, France	3.75000	2.50000	18	12.5	16.5	19	15	9	8	9.80
INM-CM3.0, Russia	5.00000	4.00000	24	14	3	14	23	9	15	10.20
GISS-ER, USA	5.00000	3.91305	23	12.5	16.5	18		19.5		12.05
FGOALS-g1.0, China	2.81250	3.00000	16	8.5	16.5	20	24	19.5	16	12.17
GISS-AOM, USA	4.00000	3.00000	21		16.5	17		19.5		12.79
BCCR-BCM2.0, Norway	2.81250	2.81250	12.5				24			16.75
GISS-EH, USA	5.00000	3.91305	22		16.5	15	27.5	19.5		18.50

¹ 20°–90°N: precipitation, temperature, sea level pressure

² Arctic: inter-annual variability

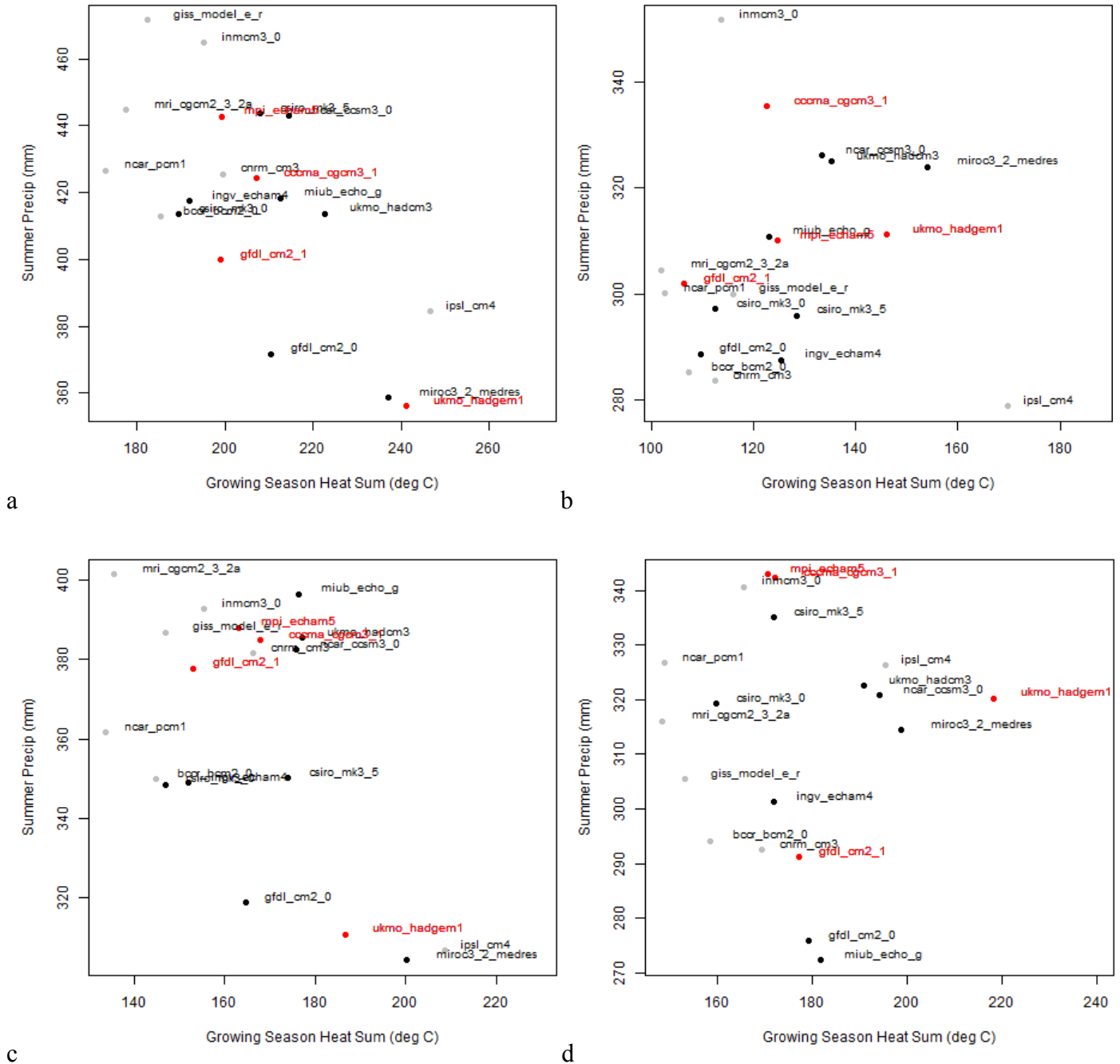
³ 20°–90°N

⁴ China: spatial accuracy, inter-annual variability

⁵ Inter-annual variability

⁶ Subtropics: cloud dynamics, moisture

Figure A1. Global climate model (GCM) differences: growing season heat sum (growing degree days above 5 °C) vs. mean summer precipitation (mm) for 19 GCMs based on the A2 emissions scenario for 2071-2100. Values are summarized by level 1 ecoregions as defined by the Commission for Environmental Cooperation: (a) Northern Forests, (b) Taiga, (c) Hudson Plains, (d) Northwest Forested Mountains. GCMs chosen for analysis are shown in red. Models not considered are shown in gray.



Appendix 1-B. Covariate correlations

Table B1. Pearson correlation coefficients between climate, topographic, and land-use variables for (a) model-building dataset, averaged across 11 bootstrap samples; (b) current period (1961-1990) within boreal and subarctic study area; (c) 2011-2040 within study area; (d) 2041-2070 within prediction area; (e) 2071-2100 within prediction area . See Table 1 for climate variable definitions.

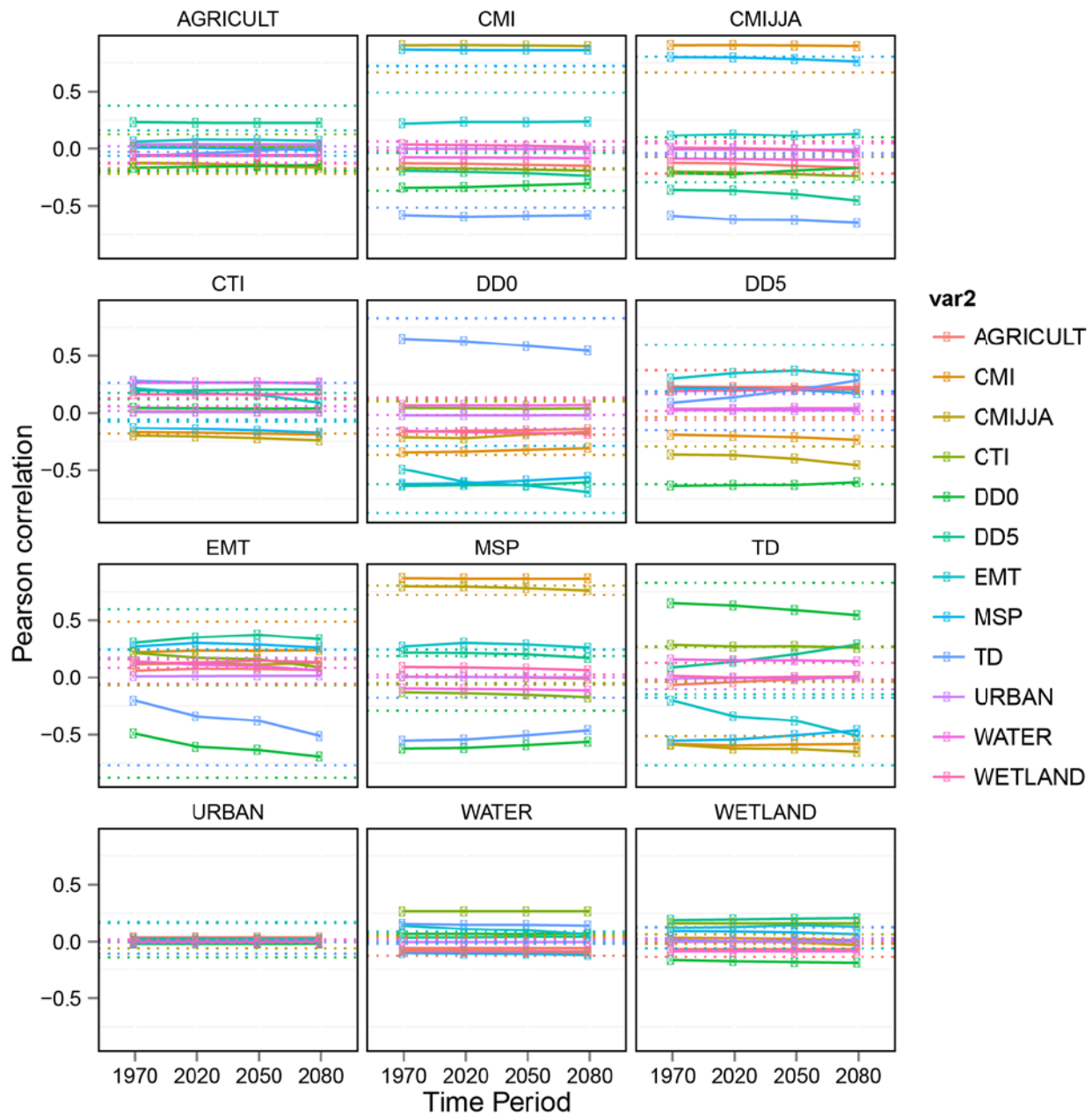
(a) model-building dataset, averaged across 11 bootstrap samples

	CMI	CMIJJA	DD0	DD5	EMT	MSP	TD	CTI	WETLAND	AGRICULT	URBAN	WATER
CMI	1.000	0.664	-0.367	-0.036	0.489	0.721	-0.513	-0.180	-0.016	-0.168	0.009	0.061
CMIJJA	0.664	1.000	0.099	-0.294	-0.063	0.803	-0.041	-0.073	0.065	-0.216	-0.057	0.045
DD0	-0.367	0.099	1.000	-0.621	-0.876	-0.288	0.827	0.119	0.133	-0.191	-0.135	-0.015
DD5	-0.036	-0.294	-0.621	1.000	0.596	0.186	-0.150	0.175	-0.058	0.375	0.167	0.020
EMT	0.489	-0.063	-0.876	0.596	1.000	0.243	-0.771	-0.072	-0.056	0.159	0.173	0.086
MSP	0.721	0.803	-0.288	0.186	0.243	1.000	-0.177	-0.054	0.028	-0.063	-0.003	0.001
TD	-0.513	-0.041	0.827	-0.150	-0.771	-0.177	1.000	0.267	0.129	-0.028	-0.104	-0.017
CTI	-0.180	-0.073	0.119	0.175	-0.072	-0.054	0.267	1.000	0.128	0.125	0.020	0.059
WETLAND	-0.016	0.065	0.133	-0.058	-0.056	0.028	0.129	0.128	1.000	-0.129	0.007	0.026
AGRICULT	-0.168	-0.216	-0.191	0.375	0.159	-0.063	-0.028	0.125	-0.129	1.000	0.020	-0.122
URBAN	0.009	-0.057	-0.135	0.167	0.173	-0.003	-0.104	0.020	0.007	0.020	1.000	0.017
WATER	0.061	0.045	-0.015	0.020	0.086	0.001	-0.017	0.059	0.026	-0.122	0.017	1.000

(b) current period (1961-1990) within boreal and subarctic study area

	CMI	CMIJJA	DD0	DD5	EMT	MSP	TD	CTI	WETLAND	AGRICULT	URBAN	WATER
CMI	1.000	0.905	-0.344	-0.191	0.219	0.867	-0.581	-0.168	0.035	-0.127	-0.002	-0.076
CMIJJA	0.905	1.000	-0.213	-0.362	0.115	0.797	-0.587	-0.198	0.007	-0.123	-0.008	-0.087
DD0	-0.344	-0.213	1.000	-0.637	-0.492	-0.621	0.647	0.045	-0.158	-0.166	-0.019	0.067
DD5	-0.191	-0.362	-0.637	1.000	0.303	0.216	0.089	0.194	0.190	0.233	0.025	0.036
EMT	0.219	0.115	-0.492	0.303	1.000	0.269	-0.202	0.213	0.122	0.060	0.011	0.141
MSP	0.867	0.797	-0.621	0.216	0.269	1.000	-0.553	-0.131	0.092	0.008	0.005	-0.098
TD	-0.581	-0.587	0.647	0.089	-0.202	-0.553	1.000	0.283	0.015	-0.067	-0.011	0.157
CTI	-0.168	-0.198	0.045	0.194	0.213	-0.131	0.283	1.000	0.163	0.015	0.009	0.267
WETLAND	0.035	0.007	-0.158	0.190	0.122	0.092	0.015	0.163	1.000	-0.064	-0.002	-0.084
AGRICULT	-0.127	-0.123	-0.166	0.233	0.060	0.008	-0.067	0.015	-0.064	1.000	0.037	-0.055
URBAN	-0.002	-0.008	-0.019	0.025	0.011	0.005	-0.011	0.009	-0.002	0.037	1.000	-0.003
WATER	-0.076	-0.087	0.067	0.036	0.141	-0.098	0.157	0.267	-0.084	-0.055	-0.003	1.000

Figure B1. Changes in mean Pearson correlation coefficients between climate, topographic, and land-use variables over time (solid lines) within the boreal and southern arctic study area, averaged over 19 GCMs for scenario A1. 1970 = current period (1961-1990); 2020 = 2011-2040; 2050 = 2041-2070; 2080 = 2071-2100. Compared with correlation coefficients within the model-building dataset averaged across 11 bootstrap samples (dotted lines). See Table 1 for climate variable definitions.



Appendix 1-C. Individual species model evaluation

Table C1. Mean cross-validation statistics for climate-only vs. climate + land use + topography models across 11 bootstrap iterations containing 10 cross-validation runs each. Significantly greater cross-validation statistics (n=11) based on pairwise t-tests with a multiple comparison correction ($n = 80$) are indicated in bold (* $p < 0.05$, ** $p < 0.005$). ‡ symbols denote the 38 species currently breeding in the Alaskan boreal region.

Species Code	Common name (<i>Scientific name</i>)	Climate-only		Climate + Land Use + Topo	
		Deviance Explained	Correlation Coefficient	Deviance Explained	Correlation Coefficient
ALFL	Alder Flycatcher (<i>Empidonax alnorum</i>) ‡	0.123	0.230	0.115	0.233
AMCR	American Crow (<i>Corvus brachyrhynchos</i>)	0.108	0.196	0.158	** 0.246
AMGO	American Goldfinch (<i>Spinus tristis</i>)	0.253	0.333	0.267	** 0.339
AMPI	American Pipit (<i>Anthus rubescens</i>) ‡	0.152	0.205	0.134	0.188
AMRE	American Redstart (<i>Setophaga ruticilla</i>)	0.164	0.329	0.153	0.314
AMRO	American Robin (<i>Turdus migratorius</i>) ‡	0.085	0.250	0.105	** 0.275
ATSP	American Tree Sparrow (<i>Spizella arborea</i>) ‡	0.638	0.511	0.634	0.518
BAWW	Black-and-white Warbler (<i>Mniotilta varia</i>)	0.152	0.216	0.143	0.217
BBWA	Bay-breasted Warbler (<i>Setophaga castanea</i>)	0.218	0.229	0.221	0.229
BCCH	Black-capped Chickadee (<i>Poecile atricapillus</i>) ‡	0.120	0.200	0.119	0.202
BHCO	Brown-headed Cowbird (<i>Molothrus ater</i>)	0.303	0.324	0.324	** 0.326
BHVI	Blue-headed Vireo (<i>Vireo solitarius</i>)	0.176	0.252	0.173	0.251
BLBW	Blackburnian Warbler (<i>Setophaga fusca</i>)	0.217	0.276	0.222	0.271
BLJA	Blue Jay (<i>Cyanocitta cristata</i>)	0.202	0.240	0.197	0.238
BLPW	Blackpoll Warbler (<i>Setophaga striata</i>) ‡	0.198	0.250	0.193	0.236
BOCH	Boreal Chickadee (<i>Poecile hudsonicus</i>) ‡	0.140	0.157	0.130	0.151
BRBL	Brewer's Blackbird (<i>Euphagus cyanocephalus</i>)	0.294	0.203	0.292	0.207
BRCR	Brown Creeper (<i>Certhia americana</i>) ‡	0.040	0.104	0.043	0.108
BTNW	Black-throated Green Warbler (<i>Setophaga virens</i>)	0.223	0.292	0.219	0.293
CAWA	Canada Warbler (<i>Cardellina canadensis</i>)	0.126	0.206	0.122	0.200
CCSP	Clay-colored Sparrow (<i>Spizella pallida</i>)	0.530	0.497	0.532	0.484
CEDW	Cedar Waxwing (<i>Bombycilla cedrorum</i>)	0.069	0.110	0.067	0.110
CHSP	Chipping Sparrow (<i>Spizella passerina</i>) ‡	0.082	0.185	0.085	0.187
CMWA	Cape May Warbler (<i>Setophaga tigrina</i>)	0.196	0.195	0.183	0.189
COGR	Common Grackle (<i>Quiscalus quiscula</i>)	0.338	0.322	0.352	** 0.335

Species Code	Common name (<i>Scientific name</i>)	Climate-only		Climate + Land Use + Topo	
		Deviance Explained	Correlation Coefficient	Deviance Explained	Correlation Coefficient
CONW	Connecticut Warbler (<i>Oporornis agilis</i>)	0.244	0.180	0.239	0.177
CORA	Common Raven (<i>Corvus corax</i>) ‡	0.003	0.060	-0.003	0.050
CORE	Common Redpoll (<i>Acanthis flammea</i>) ‡	0.361	0.260	0.355	0.257
COYE	Common Yellowthroat (<i>Geothlypis trichas</i>)	0.136	0.246	0.142	0.254 *
CSWA	Chestnut-sided Warbler (<i>Setophaga pensylvanica</i>)	0.267	0.333	0.273	0.341
DEJU	Dark-eyed Junco (<i>Junco hyemalis</i>) ‡	0.197	0.297	0.204	0.298
EAKI	Eastern Kingbird (<i>Tyrannus tyrannus</i>)	0.216	0.222	0.225	0.224
EAPH	Eastern Phoebe (<i>Sayornis phoebe</i>)	0.162	0.172	0.149	0.166
EVGR	Evening Grosbeak (<i>Coccothraustes vespertinus</i>)	0.069	0.115	0.078	0.117
FOSP	Fox Sparrow (<i>Passerella iliaca</i>) ‡	0.419	0.434	0.406	0.421
GCKI	Golden-crowned Kinglet (<i>Regulus satrapa</i>) ‡	0.114	0.171	0.127 **	0.181 **
GCTH	Gray-cheeked Thrush (<i>Catharus minimus</i>) ‡	0.415	0.342	0.417	0.346
GRAJ	Gray Jay (<i>Perisoreus canadensis</i>) ‡	0.237	0.295	0.211	0.286
HETH	Hermit Thrush (<i>Catharus guttatus</i>) ‡	0.112	0.241	0.119 *	0.250 **
HOLA	Horned Lark (<i>Eremophila alpestris</i>) ‡	0.467	0.413	0.482	0.409
LCSP	Le Conte's Sparrow (<i>Ammodramus leconteii</i>)	0.207	0.184	0.178	0.157
LEFL	Least Flycatcher (<i>Empidonax minimus</i>)	0.092 *	0.162 *	0.080	0.150
LISP	Lincoln's Sparrow (<i>Melospiza lincolni</i>) ‡	0.186	0.254	0.189	0.253
MAWA	Magnolia Warbler (<i>Setophaga magnolia</i>)	0.298	0.412	0.300	0.416
MOWA	Mourning Warbler (<i>Geothlypis philadelphia</i>)	0.166	0.226	0.167	0.230
NAWA	Nashville Warbler (<i>Oreothlypis ruficapilla</i>)	0.354	0.428	0.359	0.436
NOWA	Northern Waterthrush (<i>Parkesia noveboracensis</i>) ‡	0.140	0.201	0.137	0.195
OCWA	Orange-crowned Warbler (<i>Oreothlypis celata</i>) ‡	0.273	0.298	0.271	0.297
OSFL	Olive-sided Flycatcher (<i>Contopus cooperi</i>) ‡	0.078	0.126	0.077	0.131
OVEN	Ovenbird (<i>Seiurus aurocapilla</i>)	0.301	0.453	0.309	0.461 *
PAWA	Palm Warbler (<i>Setophaga palmarum</i>)	0.226	0.251	0.210	0.239
PHVI	Philadelphia Vireo (<i>Vireo philadelphicus</i>)	0.255	0.271	0.252	0.268
PIGR	Pine Grosbeak (<i>Pinicola enucleator</i>) ‡	0.052	0.084	0.052	0.088
PISI	Pine Siskin (<i>Spinus pinus</i>) ‡	0.168	0.181	0.185	0.195
PUFI	Purple Finch (<i>Carpodacus purpureus</i>)	0.095	0.129	0.071	0.114

Species Code	Common name (<i>Scientific name</i>)	Climate-only		Climate + Land Use + Topo	
		Deviance Explained	Correlation Coefficient	Deviance Explained	Correlation Coefficient
RBGR	Rose-breasted Grosbeak (<i>Pheucticus ludovicianus</i>)	0.159	0.210	0.169	0.220
RBNU	Red-breasted Nuthatch (<i>Sitta canadensis</i>) ‡	0.097	0.178	0.107 *	0.187
RCKI	Ruby-crowned Kinglet (<i>Regulus calendula</i>) ‡	0.276	0.419	0.285	0.426
REVI	Red-eyed Vireo (<i>Vireo olivaceus</i>)	0.286	0.437	0.287	0.442 **
RUBL	Red-winged Blackbird (<i>Agelaius phoeniceus</i>) ‡	0.156	0.166	0.157	0.171
RWBL	Rusty Blackbird (<i>Euphagus carolinus</i>) ‡	0.307	0.370	0.332 **	0.374
SAVS	Savannah Sparrow (<i>Passerculus sandwichensis</i>) ‡	0.195	0.320	0.252 **	0.341
SOSP	Song Sparrow (<i>Melospiza melodia</i>)	0.227	0.372	0.263 **	0.408 **
SWSP	Swamp Sparrow (<i>Melospiza georgiana</i>)	0.156	0.194	0.149	0.181
SWTH	Swainson's Thrush (<i>Catharus ustulatus</i>) ‡	0.227	0.423	0.245	0.429 **
TEWA	Tennessee Warbler (<i>Oreothlypis peregrina</i>)	0.429	0.535	0.442	0.543
TRES	Tree Swallow (<i>Tachycineta bicolor</i>) ‡	0.070	0.115	0.098 *	0.139
VATH	Varied Thrush (<i>Ixoreus naevius</i>) ‡	0.373	0.376	0.378	0.375
VESP	Vesper Sparrow (<i>Pooecetes gramineus</i>)	0.462	0.457	0.474	0.460
WAVI	Warbling Vireo (<i>Vireo gilvus</i>)	0.274	0.340	0.267	0.342
WCSP	White-crowned Sparrow (<i>Zonotrichia leucophrys</i>) ‡	0.558	0.527	0.556	0.528
WETA	Western Tanager (<i>Piranga ludoviciana</i>)	0.333	0.336	0.331	0.339
WEWP	Western Wood-Pewee (<i>Contopus sordidulus</i>) ‡	0.278	0.295	0.272	0.295
WIWA	Wilson's Warbler (<i>Cardellina pusilla</i>) ‡	0.291	0.357	0.288	0.354
WIWR	Winter Wren (<i>Troglodytes hiemalis</i>)	0.244	0.340	0.254 **	0.350 **
WTSP	White-throated Sparrow (<i>Zonotrichia albicollis</i>)	0.279	0.434	0.276	0.434
WWCR	White-winged Crossbill (<i>Loxia leucoptera</i>) ‡	0.106	0.118	0.102	0.116
YBFL	Yellow-bellied Flycatcher (<i>Empidonax flaviventris</i>)	0.243	0.303	0.252	0.310
YRWA	Yellow-rumped Warbler (<i>Setophaga coronata</i>) ‡	0.155	0.304	0.178 **	0.318
YWAR	Yellow Warbler (<i>Setophaga petechia</i>) ‡	0.143	0.271	0.144	0.260
Mean		0.222	0.274	0.225	0.276
5%		0.069	0.115	0.071	0.114
95%		0.462	0.459	0.474	0.462

Table C2. Variable importance (across bootstrap iterations) in climate-only models, as measured by the proportion of overall deviance explained by each variable. See Table C1 for species code definitions. See Table 1 for climate variable definitions.

species	dd01	dd51	emt	td	cmi	cmijja	msp
ALFL	0.019	0.026	0.017	0.023	0.012	0.011	0.013
AMCR	0.015	0.037	0.009	0.008	0.012	0.011	0.016
AMGO	0.032	0.121	0.031	0.03	0.015	0.011	0.014
AMPI	0.004	0.092	0.036	0.004	0.002	0.008	0.006
AMRE	0.035	0.04	0.019	0.024	0.019	0.009	0.018
AMRO	0.018	0.013	0.032	0.008	0.008	0.003	0.004
ATSP	0.128	0.193	0.175	0.06	0.032	0.013	0.036
BAWW	0.015	0.047	0.01	0.018	0.018	0.012	0.034
BBWA	0.048	0.048	0.013	0.045	0.025	0.012	0.028
BCCH	0.014	0.036	0.029	0.005	0.008	0.019	0.008
BHCO	0.024	0.101	0.017	0.025	0.083	0.019	0.036
BHVI	0.021	0.043	0.01	0.012	0.035	0.02	0.035
BLBW	0.029	0.072	0.015	0.027	0.022	0.014	0.037
BLJA	0.008	0.108	0.01	0.008	0.013	0.019	0.034
BLPW	0.035	0.042	0.032	0.029	0.021	0.012	0.027
BOCH	0.034	0.031	0.011	0.004	0.015	0.017	0.029
BRBL	0.037	0.047	0.035	0.039	0.082	0.031	0.023
BRCR	0.01	0.002	0.004	0.004	0.003	0.002	0.016
BTNW	0.039	0.045	0.03	0.028	0.037	0.012	0.031
CAWA	0.029	0.041	0.012	0.014	0.01	0.004	0.016
CEDW	0.015	0.009	0.019	0.009	0.01	0.003	0.004
CHSP	0.007	0.011	0.005	0.016	0.021	0.011	0.011
CMWA	0.077	0.035	0.011	0.032	0.008	0.012	0.021
COGR	0.014	0.182	0.02	0.023	0.049	0.015	0.036
CONW	0.066	0.044	0.028	0.03	0.018	0.021	0.039
CORA	0.001	0.001	0	0.001	0	0	0
CORE	0.123	0.062	0.123	0.02	0.009	0.008	0.017
COYE	0.02	0.048	0.008	0.012	0.015	0.012	0.021
CSWA	0.066	0.072	0.02	0.033	0.039	0.012	0.025
DEJU	0.025	0.046	0.02	0.038	0.029	0.012	0.028
EAKI	0.019	0.045	0.033	0.022	0.055	0.007	0.035
EAPH	0.019	0.048	0.017	0.01	0.027	0.006	0.034
EVGR	0.004	0.004	0.009	0.011	0.024	0.01	0.006
FOSP	0.059	0.107	0.06	0.042	0.033	0.076	0.043
GCKI	0.013	0.018	0.018	0.023	0.018	0.01	0.015
GCTH	0.105	0.156	0.086	0.051	0.005	0.003	0.009
GRAJ	0.041	0.031	0.019	0.01	0.018	0.01	0.027
HETH	0.017	0.019	0.011	0.024	0.009	0.015	0.016
HOLA	0.049	0.056	0.039	0.068	0.194	0.015	0.046
LCSP	0.033	0.048	0.012	0.029	0.033	0.011	0.042

species	dd01	dd51	emt	td	cmi	cmijja	msp
LEFL	0.026	0.02	0.008	0.014	0.008	0.004	0.012
LISP	0.036	0.053	0.03	0.033	0.006	0.012	0.016
MAWA	0.035	0.072	0.02	0.035	0.048	0.023	0.064
MOWA	0.044	0.039	0.006	0.033	0.016	0.003	0.025
NAWA	0.064	0.046	0.023	0.091	0.029	0.015	0.085
NOWA	0.024	0.038	0.021	0.02	0.013	0.006	0.017
OCWA	0.035	0.057	0.033	0.05	0.032	0.025	0.041
OSFL	0.009	0.017	0.011	0.013	0.014	0.005	0.009
OVEN	0.054	0.083	0.024	0.045	0.029	0.03	0.036
PAWA	0.039	0.019	0.022	0.086	0.036	0.009	0.014
PHVI	0.064	0.03	0.018	0.062	0.008	0.012	0.06
PIGR	0.004	0.007	0.005	0.007	0.005	0.004	0.02
PISI	0.024	0.031	0.02	0.046	0.017	0.01	0.021
PUFI	0.01	0.021	0.008	0.01	0.021	0.005	0.019
RBGR	0.041	0.032	0.005	0.03	0.015	0.009	0.028
RBNU	0.013	0.014	0.008	0.016	0.015	0.022	0.009
RCKI	0.034	0.087	0.012	0.032	0.014	0.063	0.034
REVI	0.035	0.114	0.023	0.029	0.017	0.037	0.031
RUBL	0.039	0.017	0.021	0.049	0.012	0.004	0.015
RWBL	0.027	0.121	0.024	0.026	0.038	0.008	0.063
SAVS	0.034	0.036	0.044	0.025	0.023	0.011	0.023
SOSP	0.017	0.12	0.035	0.012	0.011	0.018	0.014
SWSP	0.02	0.026	0.014	0.035	0.037	0.006	0.019
SWTH	0.027	0.081	0.018	0.023	0.047	0.013	0.018
TEWA	0.141	0.101	0.079	0.045	0.023	0.015	0.024
TOWA	0.019	0.039	0.032	0.151	0.079	0.019	0.057
TRES	0.007	0.037	0.004	0.005	0.003	0.008	0.006
VATH	0.014	0.053	0.016	0.06	0.099	0.033	0.099
VESP	0.041	0.048	0.029	0.018	0.272	0.021	0.034
WAVI	0.01	0.041	0.012	0.084	0.057	0.029	0.041
WCSP	0.23	0.087	0.145	0.037	0.008	0.01	0.041
WETA	0.026	0.035	0.02	0.076	0.05	0.071	0.056
WEWP	0.021	0.028	0.019	0.072	0.049	0.035	0.054
WIWA	0.044	0.122	0.041	0.036	0.024	0.01	0.014
WIWR	0.066	0.033	0.009	0.033	0.02	0.029	0.054
WTSP	0.055	0.045	0.009	0.034	0.023	0.064	0.049
WWCR	0.025	0.027	0.01	0.015	0.006	0.008	0.014
YBFL	0.042	0.022	0.013	0.037	0.032	0.045	0.051
YRWA	0.028	0.05	0.014	0.013	0.021	0.012	0.018
YWAR	0.03	0.026	0.025	0.017	0.016	0.01	0.02
Mean	0.037	0.053	0.025	0.031	0.030	0.016	0.028
5%	0.007	0.009	0.005	0.005	0.005	0.003	0.006
95%	0.106	0.121	0.079	0.076	0.082	0.046	0.060

Table C3. Mean variable importance (across bootstrap iterations) in climate + land use + topography models, as measured by the proportion of overall deviance explained by each variable. See Table C1 for species code definitions. See Table 1 for climate variable definitions; cti = compound topographic index; wetland/agricult/urban/water = wetland/agricultural/urban/water proportion within 4-km grid cell. Species with a clear negative response to agriculture and/or urban development are highlighted in bold.

Species	DD01	DD51	EMT	TD	CMI	CMIJJA	MSP	CTI	WETLAND	AGRICULT	URBAN	WATER
ALFL	0.013	0.016	0.011	0.016	0.009	0.008	0.010	0.012	0.007	0.003	0.000	0.009
AMCR	0.010	0.028	0.008	0.006	0.014	0.009	0.005	0.011	0.004	0.057	0.003	0.005
AMGO	0.016	0.073	0.016	0.019	0.015	0.009	0.010	0.019	0.019	0.045	0.008	0.017
AMPI	0.004	0.082	0.030	0.003	0.002	0.004	0.005	0.003	0.000	0.000	0.000	0.001
AMRE	0.018	0.037	0.012	0.015	0.013	0.008	0.011	0.008	0.005	0.006	0.000	0.019
AMRO	0.013	0.008	0.025	0.006	0.007	0.003	0.004	0.001	0.001	0.012	0.006	0.018
ATSP	0.113	0.186	0.159	0.036	0.021	0.008	0.026	0.070	0.012	0.000	0.000	0.003
BAWW	0.008	0.035	0.004	0.008	0.012	0.008	0.025	0.014	0.003	0.018	0.001	0.007
BBWA	0.039	0.042	0.012	0.035	0.017	0.006	0.015	0.016	0.012	0.005	0.000	0.022
BCCH	0.008	0.023	0.019	0.002	0.007	0.014	0.006	0.005	0.002	0.013	0.017	0.003
BHCO	0.018	0.075	0.015	0.017	0.068	0.016	0.025	0.015	0.000	0.066	0.006	0.002
BHVI	0.007	0.033	0.006	0.006	0.040	0.014	0.027	0.009	0.017	0.005	0.000	0.009
BLBW	0.021	0.054	0.009	0.021	0.017	0.006	0.026	0.019	0.008	0.016	0.000	0.023
BLJA	0.005	0.095	0.007	0.006	0.008	0.017	0.028	0.005	0.004	0.012	0.008	0.003
BLPW	0.029	0.038	0.019	0.018	0.010	0.010	0.014	0.018	0.024	0.000	0.000	0.012
BOCH	0.028	0.025	0.007	0.002	0.010	0.019	0.026	0.003	0.003	0.000	0.000	0.006
BRBL	0.018	0.019	0.020	0.040	0.060	0.018	0.021	0.015	0.000	0.037	0.005	0.039
BRCR	0.009	0.003	0.003	0.002	0.001	0.001	0.006	0.001	0.001	0.000	0.016	0.001
BTNW	0.019	0.030	0.021	0.013	0.041	0.008	0.022	0.012	0.004	0.021	0.000	0.026
CAWA	0.016	0.030	0.009	0.010	0.006	0.003	0.007	0.015	0.002	0.005	0.000	0.020
CCSP	0.040	0.030	0.104	0.020	0.073	0.005	0.026	0.016	0.000	0.218	0.000	0.000
CEDW	0.004	0.004	0.008	0.012	0.002	0.001	0.001	0.011	0.000	0.019	0.001	0.003
CHSP	0.006	0.008	0.005	0.014	0.018	0.009	0.009	0.004	0.002	0.004	0.003	0.003
CMWA	0.053	0.028	0.007	0.016	0.005	0.007	0.011	0.005	0.018	0.000	0.000	0.033
COGR	0.006	0.133	0.009	0.010	0.043	0.005	0.025	0.005	0.002	0.054	0.001	0.057
CONW	0.055	0.028	0.025	0.025	0.017	0.016	0.025	0.009	0.004	0.021	0.000	0.014
CORA	0.000	0.000	0.000	0.000	0.000	0.000	0.000	0.003	0.000	0.000	0.000	0.000

Species	DD01	DD51	EMT	TD	CMI	CMIJJA	MSP	CTI	WETLAND	AGRICULT	URBAN	WATER
CORE	0.071	0.030	0.082	0.008	0.009	0.007	0.012	0.020	0.113	0.000	0.000	0.004
COYE	0.016	0.038	0.006	0.013	0.013	0.009	0.017	0.008	0.002	0.016	0.001	0.002
CSWA	0.058	0.068	0.014	0.035	0.025	0.008	0.016	0.012	0.008	0.021	0.001	0.007
DEJU	0.016	0.051	0.015	0.030	0.026	0.011	0.020	0.006	0.014	0.006	0.004	0.004
EAKI	0.012	0.037	0.022	0.018	0.051	0.003	0.029	0.009	0.000	0.034	0.000	0.009
EAPH	0.011	0.037	0.014	0.006	0.011	0.002	0.021	0.008	0.012	0.013	0.012	0.002
EVGR	0.004	0.004	0.009	0.012	0.026	0.013	0.006	0.004	0.000	0.001	0.000	0.000
FOSP	0.038	0.101	0.047	0.032	0.022	0.070	0.029	0.021	0.040	0.000	0.000	0.006
GCKI	0.012	0.012	0.019	0.023	0.014	0.009	0.014	0.004	0.007	0.006	0.000	0.007
GCTH	0.082	0.138	0.084	0.046	0.010	0.002	0.008	0.027	0.019	0.000	0.000	0.001
GRAJ	0.036	0.024	0.015	0.010	0.013	0.009	0.023	0.009	0.024	0.001	0.000	0.002
HETH	0.014	0.015	0.010	0.023	0.006	0.012	0.014	0.008	0.005	0.008	0.002	0.003
HOLA	0.043	0.025	0.037	0.045	0.203	0.006	0.029	0.035	0.001	0.053	0.000	0.006
LCSP	0.011	0.016	0.002	0.031	0.017	0.002	0.015	0.003	0.000	0.068	0.000	0.012
LEFL	0.019	0.016	0.004	0.009	0.005	0.003	0.006	0.010	0.001	0.007	0.000	0.001
LISP	0.026	0.050	0.021	0.025	0.005	0.009	0.011	0.011	0.020	0.003	0.000	0.008
MAWA	0.022	0.072	0.009	0.032	0.046	0.017	0.065	0.011	0.007	0.013	0.001	0.006
MOWA	0.033	0.029	0.003	0.035	0.013	0.003	0.016	0.011	0.011	0.004	0.000	0.009
NAWA	0.048	0.033	0.015	0.109	0.012	0.008	0.085	0.004	0.006	0.023	0.000	0.015
NOWA	0.014	0.029	0.010	0.011	0.007	0.004	0.008	0.021	0.020	0.001	0.000	0.010
OCWA	0.025	0.051	0.021	0.051	0.026	0.020	0.033	0.021	0.005	0.007	0.000	0.010
OSFL	0.008	0.014	0.009	0.011	0.011	0.003	0.006	0.005	0.005	0.000	0.000	0.004
OVEN	0.024	0.080	0.013	0.049	0.014	0.037	0.021	0.013	0.005	0.043	0.001	0.009
PAWA	0.028	0.011	0.015	0.071	0.029	0.006	0.010	0.016	0.016	0.000	0.000	0.008
PHVI	0.031	0.009	0.006	0.043	0.004	0.007	0.028	0.008	0.002	0.000	0.000	0.114
PIGR	0.004	0.005	0.005	0.004	0.005	0.004	0.020	0.005	0.000	0.000	0.000	0.001
PISI	0.023	0.027	0.018	0.050	0.014	0.010	0.017	0.023	0.000	0.001	0.000	0.001
PUFI	0.002	0.008	0.002	0.002	0.011	0.002	0.011	0.013	0.017	0.001	0.000	0.002
RBGR	0.038	0.025	0.007	0.030	0.013	0.008	0.028	0.007	0.002	0.008	0.000	0.003
RBNU	0.013	0.010	0.007	0.013	0.013	0.026	0.008	0.006	0.002	0.008	0.000	0.001
RCKI	0.027	0.077	0.013	0.028	0.011	0.061	0.031	0.007	0.014	0.012	0.000	0.004
REVI	0.034	0.109	0.019	0.024	0.009	0.035	0.026	0.004	0.002	0.020	0.001	0.003

Species	DD01	DD51	EMT	TD	CMI	CMIJJA	MSP	CTI	WETLAND	AGRICULT	URBAN	WATER
RUBL	0.033	0.012	0.020	0.045	0.009	0.002	0.011	0.004	0.003	0.000	0.000	0.018
RWBL	0.020	0.058	0.017	0.027	0.013	0.011	0.021	0.010	0.007	0.106	0.000	0.041
SAVS	0.025	0.029	0.035	0.012	0.009	0.012	0.007	0.010	0.035	0.077	0.000	0.001
SOSP	0.011	0.060	0.016	0.007	0.029	0.017	0.020	0.003	0.007	0.081	0.003	0.009
SWSP	0.011	0.014	0.007	0.030	0.035	0.004	0.013	0.014	0.004	0.000	0.000	0.016
SWTH	0.025	0.076	0.019	0.019	0.034	0.012	0.014	0.008	0.004	0.030	0.000	0.003
TEWA	0.122	0.091	0.081	0.037	0.023	0.011	0.020	0.013	0.018	0.015	0.000	0.009
TRES	0.003	0.010	0.002	0.005	0.001	0.003	0.010	0.012	0.006	0.023	0.001	0.022
VATH	0.012	0.051	0.011	0.054	0.097	0.030	0.094	0.015	0.004	0.000	0.000	0.010
VESP	0.034	0.038	0.025	0.025	0.201	0.020	0.026	0.022	0.000	0.081	0.000	0.004
WAVI	0.006	0.035	0.008	0.078	0.046	0.027	0.037	0.014	0.002	0.010	0.000	0.005
WCSP	0.223	0.083	0.139	0.032	0.007	0.008	0.039	0.006	0.011	0.001	0.003	0.005
WETA	0.019	0.020	0.016	0.053	0.036	0.060	0.037	0.069	0.004	0.008	0.002	0.007
WEWP	0.014	0.022	0.017	0.063	0.044	0.031	0.045	0.010	0.002	0.021	0.000	0.003
WIWA	0.038	0.113	0.033	0.032	0.021	0.009	0.011	0.025	0.001	0.000	0.000	0.004
WIWR	0.063	0.021	0.007	0.035	0.018	0.025	0.051	0.011	0.004	0.017	0.000	0.002
WTSP	0.052	0.039	0.007	0.028	0.022	0.059	0.040	0.011	0.012	0.004	0.000	0.004
WCCR	0.011	0.017	0.013	0.008	0.004	0.007	0.009	0.013	0.017	0.000	0.000	0.001
YBFL	0.032	0.015	0.011	0.035	0.030	0.039	0.039	0.008	0.026	0.003	0.000	0.013
YRWA	0.024	0.046	0.020	0.011	0.016	0.010	0.017	0.008	0.002	0.016	0.000	0.008
YWAR	0.015	0.017	0.015	0.011	0.011	0.006	0.009	0.015	0.009	0.019	0.001	0.016
Mean	0.028	0.041	0.021	0.024	0.024	0.013	0.021	0.012	0.009	0.019	0.001	0.010
5%	0.004	0.005	0.003	0.002	0.002	0.002	0.005	0.003	0.000	0.000	0.000	0.001
95%	0.072	0.109	0.082	0.054	0.068	0.040	0.045	0.025	0.024	0.077	0.008	0.033

Appendix 1-D. Individual species climate-change projections

Table D1. Projected changes in potential abundance (mean and 95% confidence intervals) as determined by climatic suitability for 80 species across three future time periods. Means and standard errors are based on 11 bootstrap runs, two models, and four GCMs. See [Appendix 1-C](#), Table C1 for species code definitions. Current abundance estimates should not be used for population estimation purposes without consultation.

Species	Current period (1961-1990)		2011-2040		2041-2070		2071-2100	
	Mean	(5 th , 95 th percentiles)	Mean	(5 th , 95 th percentile)	Mean	(5 th , 95 th percentile)	Mean	(5 th , 95 th percentile)
ALFL	56.34	(51.87, 62.19)	-8.9%	(-17.2%, -1.8%)	-16.8%	(-28.3%, -7.3%)	-29.4%	(-44.9%, -16%)
AMCR	3.28	(2.4, 4.41)	51.8%	(15.6%, 97.2%)	122.3%	(47.2%, 250.5%)	230.4%	(96%, 427.4%)
AMGO	14.37	(10.92, 18.1)	43.6%	(21%, 67%)	159.9%	(76.3%, 335.4%)	362.2%	(170.2%, 618.5%)
AMPI	1.61	(0.65, 2.92)	-19.0%	(-54%, -0.9%)	-38.1%	(-109.3%, -2.6%)	-56.0%	(-143.6%, -4%)
AMRE	36.92	(31.39, 44.59)	42.2%	(20.8%, 84.5%)	76.4%	(53.6%, 126.6%)	110.5%	(70%, 176.1%)
AMRO	94.70	(87.86, 97.11)	6.8%	(0.4%, 15.3%)	18.1%	(5.2%, 34.7%)	49.7%	(25.4%, 110.6%)
ATSP	54.02	(42.9, 68.85)	-31.2%	(-48.8%, -18.8%)	-54.8%	(-88%, -32.8%)	-80.8%	(-115%, -54.8%)
BAWW	13.98	(12.25, 16.54)	34.3%	(14.8%, 57%)	70.8%	(47.3%, 99.9%)	82.9%	(39.5%, 128%)
BBWA	31.79	(25.97, 35.29)	4.0%	(-10.2%, 26%)	-9.5%	(-37.3%, 12%)	-37.0%	(-68.8%, -3.8%)
BCCH	22.77	(20.03, 25.02)	40.8%	(17.4%, 71.7%)	103.7%	(63.9%, 155.5%)	187.5%	(132.8%, 261.7%)
BHCO	19.74	(16.15, 24.16)	9.1%	(0.8%, 26.8%)	46.7%	(6.5%, 168.8%)	171.5%	(45.9%, 448%)
BHVI	12.89	(11.4, 14.51)	23.5%	(6%, 35.9%)	30.3%	(11%, 49.5%)	35.5%	(6%, 66.1%)
BLBW	9.24	(6.83, 11.63)	85.4%	(45.5%, 127.4%)	132.0%	(80.5%, 186.2%)	130.8%	(53.1%, 216.8%)
BLJA	2.24	(1.83, 2.62)	59.6%	(36.3%, 90.3%)	207.7%	(142.3%, 287.1%)	347.6%	(231.6%, 511.2%)
BLPW	123.39	(90.06, 183.34)	-30.0%	(-67.1%, -7.1%)	-43.5%	(-92.8%, -15.5%)	-49.4%	(-102.1%, -13.5%)
BOCH	54.49	(44.85, 66)	2.2%	(-3.7%, 8.5%)	-1.6%	(-21.2%, 14.2%)	-26.6%	(-58.1%, -4.5%)
BRBL	3.14	(2.14, 3.98)	20.1%	(4.4%, 57.6%)	63.2%	(11.5%, 197.1%)	159.0%	(26.5%, 323.6%)
BRCR	15.10	(11.15, 18.3)	-0.5%	(-9.8%, 7.3%)	-5.1%	(-20.9%, 11.7%)	-20.4%	(-45.2%, -0.2%)
BTNW	8.52	(6.57, 10.69)	42.0%	(19.3%, 71.1%)	84.1%	(59.2%, 112.3%)	133.7%	(73%, 178.1%)
CAWA	4.77	(3.06, 10.94)	35.6%	(4.2%, 61.1%)	52.9%	(6.8%, 86.5%)	65.1%	(9.8%, 133.5%)
CCSP	6.89	(5.4, 8.05)	33.6%	(-26%, 110.7%)	47.9%	(-41.8%, 175.5%)	51.8%	(-42.9%, 208.9%)
CEDW	43.67	(38.05, 50.89)	22.5%	(10.7%, 37.1%)	54.7%	(36.1%, 77.9%)	96.2%	(62.3%, 137.9%)
CHSP	109.05	(104.17, 15.45)	0.6%	(-4.7%, 6.4%)	6.1%	(-2.6%, 14.8%)	8.8%	(2.4%, 17.8%)
CMWA	20.68	(16.4, 27.6)	-1.9%	(-12.2%, 16.4%)	-10.5%	(-36.3%, 18.7%)	-40.0%	(-67.9%, -15.1%)
COGR	18.63	(14.5, 22.71)	14.8%	(6.4%, 28.1%)	72.5%	(26.2%, 173%)	427.5%	(175.2%, 1131.8%)
CONW	2.05	(1.56, 2.48)	2.1%	(-31.7%, 42.2%)	-16.1%	(-49.6%, 22.2%)	-41.7%	(-88.9%, 5.1%)

Species	Current period (1961-1990) Singing male abundance x 10 ⁶		2011-2040 % change		2041-2070 % change		2071-2100 % change	
	Mean	(5 th , 95 th percentiles)	Mean	(5 th , 95 th percentile)	Mean	(5 th , 95 th percentile)	Mean	(5 th , 95 th percentile)
CORA	10.77	(9.01, 12.39)	1.4%	(-2.7%, 7.4%)	2.9%	(-5%, 10.7%)	-3.2%	(-13.5%, 9.2%)
CORE	122.75	(74.99, 207.68)	-28.7%	(-59.4%, -12.1%)	-40.1%	(-103.3%, -14.5%)	-60.6%	(-139%, -22.7%)
COYE	19.48	(16.52, 21.9)	29.3%	(13.7%, 46.1%)	79.4%	(54.4%, 115.5%)	134.2%	(79.6%, 198.8%)
CSWA	7.50	(6.2, 8.48)	121.7%	(69.1%, 180%)	257.2%	(193.2%, 357.1%)	265.7%	(155.8%, 385.3%)
DEJU	104.06	(88.18, 118.76)	-12.0%	(-19.5%, -5.9%)	-22.8%	(-36.7%, -11.9%)	-38.1%	(-55.1%, -24.2%)
EAKI	2.37	(1.92, 3.26)	11.8%	(1.2%, 38.4%)	107.6%	(17%, 376.7%)	400.3%	(128.2%, 1021.3%)
EAPH	1.30	(0.94, 1.84)	16.9%	(5.2%, 31.1%)	107.7%	(44%, 186.4%)	289.7%	(172.2%, 411.4%)
EVGR	5.15	(3.74, 7.07)	28.8%	(11.9%, 55.6%)	55.8%	(27.9%, 96.7%)	93.1%	(50.2%, 163.2%)
FOSP	50.67	(41.09, 64.46)	-20.1%	(-34.6%, -8.5%)	-44.5%	(-63.2%, -30.8%)	-60.1%	(-87.3%, -40%)
GCKI	58.79	(50.13, 64.92)	15.9%	(5%, 29.8%)	26.7%	(11.2%, 38.9%)	23.3%	(0.3%, 43.2%)
GCTH	14.60	(9.97, 20.38)	-38.5%	(-68.4%, -10.1%)	-50.0%	(-95.4%, -22.7%)	-73.4%	(-118%, -43.6%)
GRAJ	83.40	(78.1, 89.86)	-10.2%	(-17.9%, -3%)	-24.5%	(-40.9%, -12%)	-46.5%	(-69.9%, -33.4%)
HETH	40.05	(35.64, 42.82)	-1.5%	(-9.1%, 6%)	-7.0%	(-20.7%, 3%)	-22.0%	(-39.3%, -9.1%)
HOLA	7.86	(3.69, 16.34)	-7.6%	(-43.8%, 13.1%)	-10.3%	(-92.5%, 38.2%)	48.1%	(-52.9%, 228.5%)
LCSP	1.98	(1.31, 3.11)	0.7%	(-15.5%, 22.6%)	-4.0%	(-28.9%, 37.3%)	-23.8%	(-63.5%, 10.8%)
LEFL	33.64	(28.81, 39.04)	19.3%	(10.1%, 29.8%)	36.9%	(20.9%, 54.2%)	33.0%	(9.9%, 53.7%)
LISP	44.39	(40.28, 48.2)	-15.4%	(-22.2%, -7.8%)	-28.6%	(-44.8%, -18%)	-45.1%	(-65.9%, -29.8%)
MAWA	65.94	(56.52, 74.25)	17.3%	(-7.3%, 36.5%)	25.4%	(10.3%, 39.9%)	9.5%	(-12.4%, 31%)
MOWA	7.53	(6.65, 8.28)	70.2%	(37.9%, 109%)	100.4%	(54.1%, 140.8%)	75.9%	(18.5%, 138%)
NAWA	32.10	(28.35, 35.29)	45.8%	(8.2%, 77%)	71.5%	(17.8%, 103.6%)	20.1%	(-17.4%, 63.9%)
NOWA	23.78	(19.15, 25.99)	-9.8%	(-21%, 3%)	-18.2%	(-29.4%, -7.1%)	-29.9%	(-47.8%, -13.4%)
OCWA	56.35	(50.23, 65.52)	-14.2%	(-24.6%, -6%)	-18.7%	(-30.4%, -8.5%)	-26.1%	(-40.3%, -9.7%)
OSFL	4.14	(2.96, 5.52)	-3.1%	(-9.6%, 6.1%)	-10.3%	(-26.6%, 3.7%)	-18.5%	(-39.3%, -1%)
OVEN	27.87	(25.82, 30.36)	33.8%	(8.3%, 51.1%)	62.3%	(34.6%, 95.5%)	63.5%	(16.6%, 123.7%)
PAWA	23.22	(18.72, 28.06)	-35.8%	(-54%, -16.7%)	-51.9%	(-74.3%, -30.9%)	-70.7%	(-96.2%, -49.2%)
PHVI	10.28	(8.97, 11.41)	22.9%	(-1.9%, 62.8%)	23.3%	(0.4%, 46.5%)	-10.7%	(-38.5%, 19.5%)
PIGR	7.96	(3.67, 13.7)	-8.2%	(-33.3%, 4.3%)	-17.1%	(-65%, 5.1%)	-31.0%	(-101.1%, 1.6%)
PISI	56.64	(50.07, 66.09)	9.3%	(-11.2%, 30.6%)	27.2%	(8.4%, 51.1%)	61.5%	(21.2%, 120.2%)
PUFI	7.74	(5.51, 12.42)	25.6%	(10.3%, 43.9%)	54.9%	(31.7%, 78.9%)	101.4%	(65%, 136.2%)
RBGR	3.25	(2.57, 4.22)	38.6%	(9.5%, 58.6%)	91.2%	(46.8%, 145.9%)	132.5%	(58.6%, 251.3%)

Species	Current period (1961-1990) Singing male abundance x 10 ⁶		2011-2040 % change		2041-2070 % change		2071-2100 % change	
	Mean	(5 th , 95 th percentiles)	Mean	(5 th , 95 th percentile)	Mean	(5 th , 95 th percentile)	Mean	(5 th , 95 th percentile)
RBNU	22.07	(21, 23.52)	31.5%	(19.6%, 45.4%)	56.2%	(43.9%, 78.8%)	74.5%	(50.8%, 105.8%)
RCKI	109.36	(103.74, 13.93)	-4.7%	(-12.3%, 2.4%)	-17.1%	(-31.8%, -5.6%)	-39.4%	(-59.1%, -28.3%)
REVI	34.17	(31.97, 37.14)	49.7%	(24.8%, 77.7%)	95.7%	(73.1%, 122.4%)	109.2%	(60.6%, 152.7%)
RUBL	9.61	(5.44, 17.38)	-17.6%	(-57%, 1.1%)	-36.7%	(-120.8%, -5.9%)	-55.3%	(-149.7%, -17.9%)
RWBL	12.11	(9.38, 14.87)	29.5%	(0.2%, 92.3%)	112.9%	(19.8%, 376.6%)	307.0%	(82.3%, 835.8%)
SAVS	86.13	(64.09, 108.7)	-27.7%	(-46.2%, -13.2%)	-44.1%	(-70.7%, -17.3%)	-51.2%	(-84.3%, -13.6%)
SOSP	13.50	(11.1, 15.92)	43.1%	(18.6%, 69.7%)	128.9%	(61.7%, 263.1%)	265.9%	(114.7%, 537.6%)
SWSP	20.15	(16.8, 23.81)	-7.5%	(-22.8%, 12.4%)	-6.9%	(-21.2%, 8%)	-14.0%	(-35.5%, -0.5%)
SWTH	122.20	(114.51, 28.93)	4.7%	(0.5%, 9.7%)	1.5%	(-6.9%, 9.1%)	-11.5%	(-26.2%, -0.2%)
TEWA	112.07	(104.01, 19.12)	-8.3%	(-23.4%, 12.4%)	-24.6%	(-49.5%, 1.4%)	-55.2%	(-87.2%, -32.9%)
TRES	22.89	(19.32, 29.02)	4.2%	(0.2%, 10.6%)	16.5%	(3.8%, 41.3%)	65.5%	(24%, 166%)
VATH	14.22	(11.44, 17.24)	0.7%	(-17.3%, 16%)	8.3%	(-5.7%, 24%)	19.2%	(-8.8%, 63.6%)
VESP	3.21	(2.71, 3.69)	45.9%	(1.7%, 154.9%)	112.5%	(15.7%, 337.8%)	248.2%	(41.5%, 497%)
WAVI	15.62	(11.85, 18.87)	21.1%	(3.9%, 42.4%)	61.0%	(34.8%, 99.3%)	131.6%	(81.4%, 207.8%)
WCSP	92.08	(82.25, 106.29)	-34.4%	(-46.6%, -21.5%)	-49.8%	(-71.1%, -33.4%)	-73.9%	(-96.4%, -55.2%)
WETA	7.73	(5.96, 9.76)	2.4%	(-13.6%, 18.8%)	5.6%	(-4.2%, 19.3%)	15.4%	(-1.4%, 34.6%)
WEWP	4.34	(3.29, 5.3)	5.3%	(-10.1%, 24.9%)	11.9%	(-2.8%, 32.8%)	25.9%	(-2.5%, 56.1%)
WIWA	67.55	(58.73, 76.12)	-3.5%	(-15.1%, 8.1%)	-13.8%	(-30%, 6.1%)	-29.5%	(-53.1%, -0.9%)
WIWR	15.40	(14.18, 17.87)	12.0%	(-9.4%, 33.9%)	12.3%	(-3%, 23.3%)	-19.5%	(-44%, 3.1%)
WTSP	82.52	(77.02, 87.53)	11.4%	(-0.8%, 22.3%)	11.6%	(-3.6%, 25.3%)	-6.8%	(-31.3%, 11.7%)
WOCR	81.39	(68.09, 96.2)	-13.1%	(-24.4%, -2%)	-29.2%	(-46%, -13.9%)	-49.8%	(-71.3%, -34.1%)
YBFL	22.31	(19.62, 24.99)	-4.7%	(-19.8%, 6.9%)	-9.8%	(-36.7%, 5.8%)	-32.4%	(-58.3%, -18%)
YRWA	173.15	(157.02, 97.43)	-1.7%	(-19.7%, 9.1%)	-6.3%	(-23.2%, 4.6%)	-23.8%	(-43.7%, -9.2%)
YWAR	58.18	(47.86, 72.2)	-4.3%	(-23.7%, 11.8%)	-0.2%	(-26.4%, 24.9%)	26.0%	(-12.4%, 101.4%)

Table D2. Signal-to-noise ratio (Cohen’s *d*) for projected change in bird abundance of 80 species over three future time periods. Prediction uncertainty (“noise”) was calculated based on four complementary global climate models (GCM), two variable sets, and 11 bootstrap sampling iterations. See Appendix C, Table C1 for species code definitions.

species	2011-2040	2041-2070	2071-2100	species	2011-2040	2041-2070	2071-2100	species	2011-2040	2041-2070	2071-2100
ALFL	1.35	2.49	4.01	COYE	2.48	5.58	5.31	RBNU	4.35	6.50	4.84
AMCR	2.31	3.15	2.91	CSWA	3.92	6.67	4.69	RCKI	0.97	2.53	4.98
AMGO	2.76	3.01	3.70	DEJU	1.52	2.87	4.26	REVI	3.48	8.18	4.91
AMPI	0.49	1.06	1.61	EAKI	0.62	1.20	1.95	RUBL	0.59	1.36	2.05
AMRE	2.42	4.60	5.19	EAPH	0.74	2.60	4.15	RWBL	1.41	1.53	1.89
AMRO	1.62	2.65	2.53	EVGR	1.29	2.27	2.84	SAVS	1.73	2.87	3.12
ATSP	2.20	3.60	6.09	FOSP	1.46	3.54	4.35	SOSP	3.31	3.31	2.98
BAWW	2.48	4.80	3.73	GCKI	1.84	3.47	2.48	SWSP	0.54	0.56	1.17
BBWA	0.33	0.68	2.25	GCTH	1.73	2.43	3.68	SWTH	1.02	0.32	1.77
BCCH	2.69	4.61	6.31	GRAJ	1.79	3.17	4.98	TEWA	0.82	1.81	4.23
BHCO	0.57	1.12	1.86	HETH	0.22	0.91	2.65	TRES	0.29	0.97	2.00
BHVI	2.50	2.88	2.46	HOLA	0.16	0.25	0.72	VATH	0.04	0.54	0.97
BLBW	3.43	4.61	3.12	LCSP	0.02	0.13	0.82	VESP	1.30	1.54	2.49
BLJA	3.46	5.31	4.88	LEFL	2.22	3.83	3.04	WAVI	1.26	3.36	4.34
BLPW	1.51	2.33	2.31	LISP	2.47	3.97	5.23	WCSP	3.66	4.88	7.57
BOCH	0.16	0.10	1.88	MAWA	1.38	2.53	0.73	WETA	0.16	0.41	1.01
BRBL	0.78	1.24	2.15	MOWA	3.77	4.56	2.45	WEWP	0.34	0.78	1.43
BRCR	0.03	0.37	1.53	NAWA	2.36	3.27	0.91	WIWA	0.31	1.20	2.11
BTNW	1.88	3.80	4.64	NOWA	1.07	2.25	3.36	WIWR	0.97	1.36	1.52
CAWA	0.78	1.17	1.32	OCWA	1.58	2.20	2.81	WTSP	1.71	1.44	0.64
CCSP	1.11	0.92	0.85	OSFL	0.20	0.71	1.34	WWCR	1.18	2.60	4.58
CEDW	2.02	4.08	5.04	OVEN	3.03	4.47	2.53	YBFL	0.48	0.81	2.78
CHSP	0.13	1.15	1.75	PAWA	2.53	3.69	5.74	YRWA	0.20	0.71	2.36
CMWA	0.11	0.53	2.33	PHVI	1.45	1.56	0.69	YWAR	0.34	0.01	1.08
COGR	0.99	1.95	1.79	PIGR	0.23	0.50	0.96				
CONW	0.11	0.76	1.94	PISI	0.71	1.89	2.59	Mean	1.42	2.38	2.87
CORA	0.15	0.33	0.36	PUFI	1.04	2.35	4.04	5 th percentile	0.11	0.31	0.73
CORE	0.82	1.22	1.68	RBGR	2.04	3.74	2.96	95 th percentile	3.49	5.32	5.33

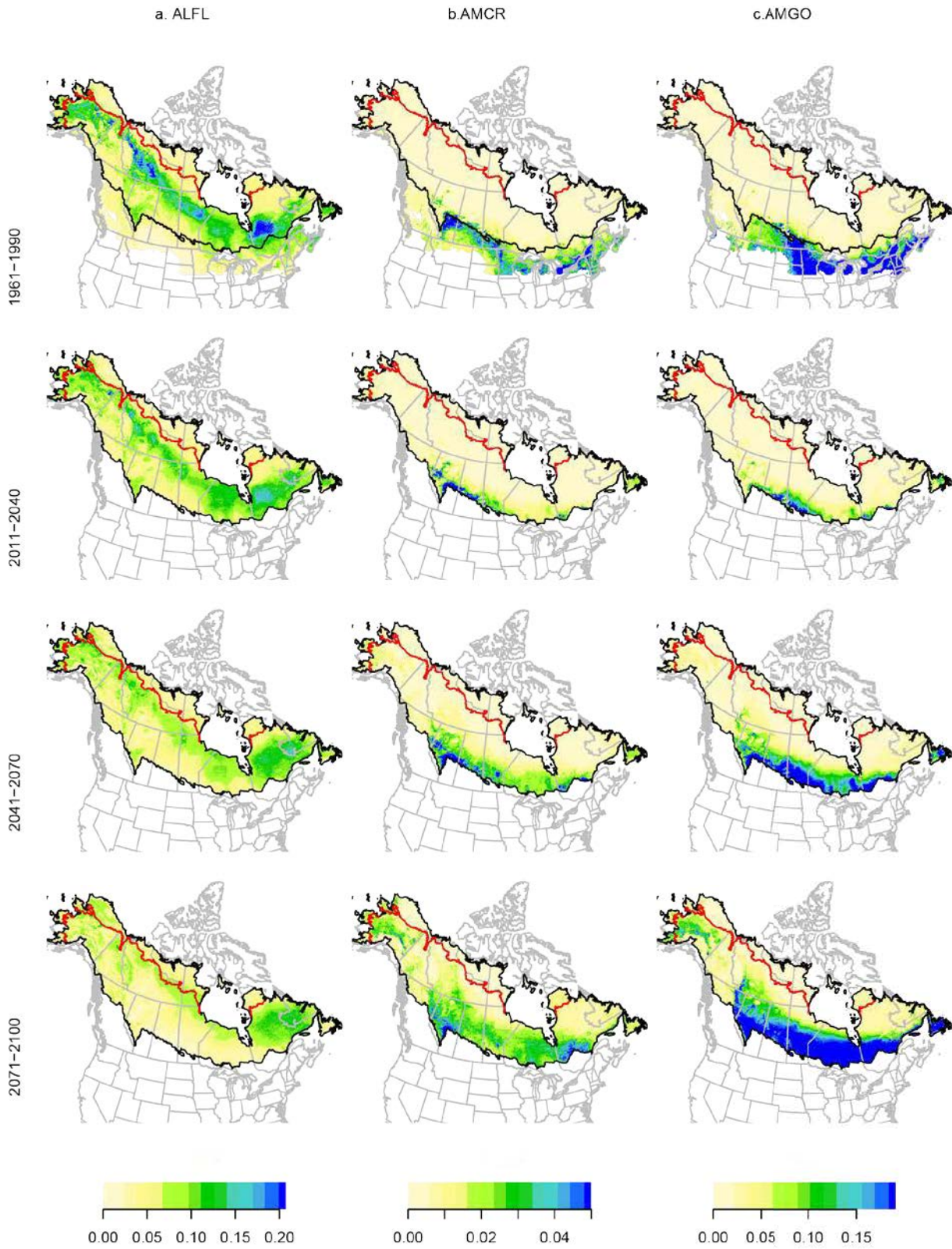
Table D3. Variance component attributed to time (climate change effect) and each source of prediction uncertainty, based on an analysis of variance with three future time periods, four complementary global climate models (GCM), two variable sets, and 11 bootstrap sampling iterations. Greatest source of uncertainty in last column. Values in bold represent species for which land use + topography variables performed better than climate-only models based on at least one cross-validation statistic (see [Appendix 1-C](#), Table C1).

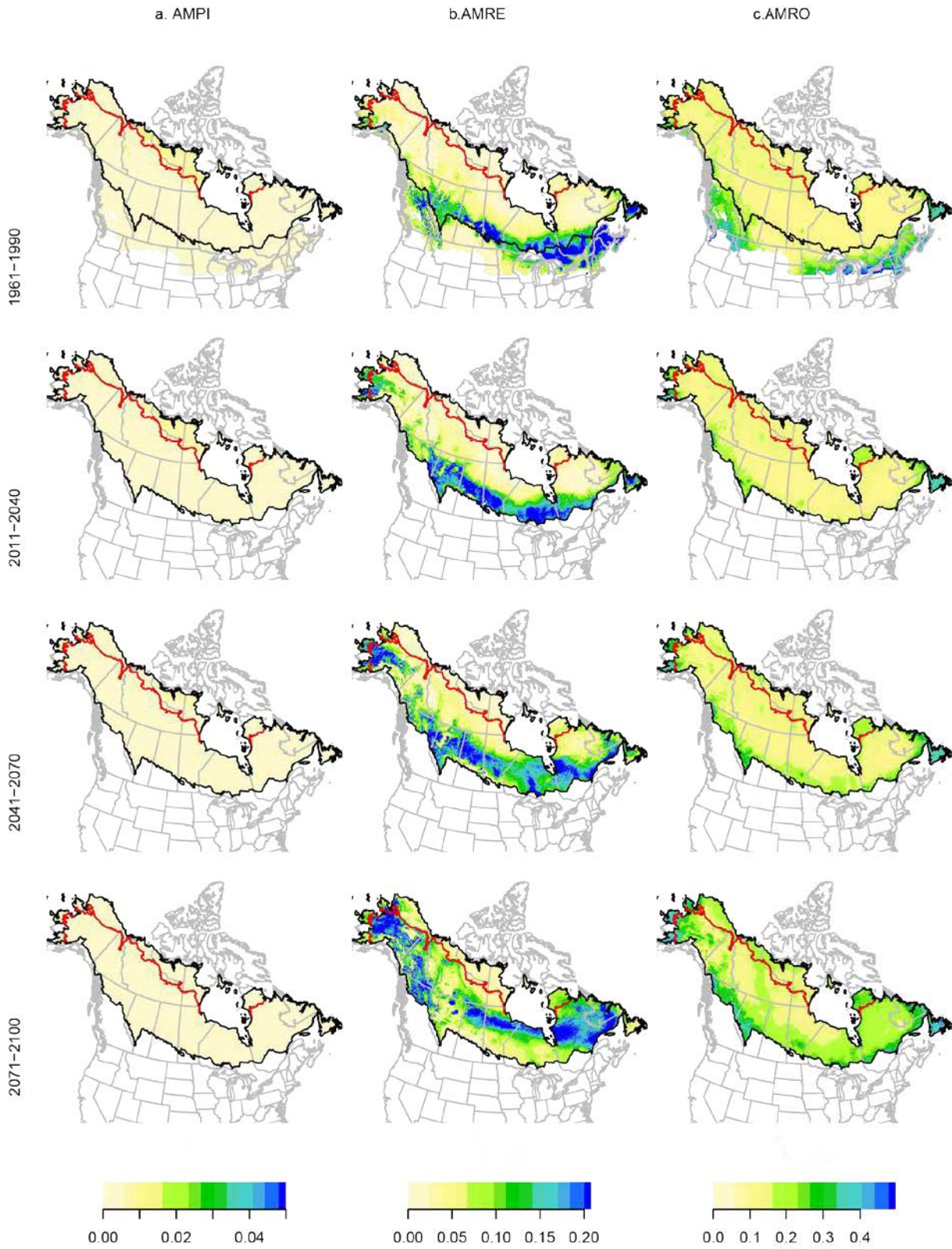
Species	Time	Sampling	GCM	Variable	GCM*	Variable*	Error	Greatest Source
ALFL	0.577	0.057	0.217	0.032	0.082	0.006	0.028	GCM
AMCR	0.441	0.008	0.103	0.245	0.051	0.074	0.078	Variable
AMGO	0.656	0.004	0.103	0.098	0.056	0.060	0.023	GCM
AMPI	0.163	0.644	0.029	0.018	0.005	0.002	0.139	Sampling
AMRE	0.548	0.021	0.280	0.057	0.018	0.009	0.066	GCM
AMRO	0.536	0.003	0.245	0.027	0.148	0.018	0.022	GCM
ATSP	0.635	0.171	0.097	0.001	0.032	0.002	0.062	Sampling
BAWW	0.514	0.048	0.228	0.042	0.078	0.031	0.058	GCM
BBWA	0.524	0.030	0.276	0.026	0.078	0.008	0.059	GCM
BCCH	0.791	0.006	0.150	0.001	0.038	0.000	0.014	GCM
BHCO	0.443	0.006	0.182	0.084	0.145	0.063	0.078	GCM
BHVI	0.117	0.077	0.351	0.145	0.154	0.046	0.109	GCM
BLBW	0.231	0.137	0.249	0.074	0.115	0.056	0.138	GCM
BLJA	0.761	0.005	0.119	0.001	0.104	0.001	0.009	GCM
BLPW	0.111	0.553	0.059	0.051	0.073	0.008	0.146	Sampling
BOCH	0.521	0.077	0.137	0.022	0.080	0.004	0.158	GCM
BRBL	0.426	0.042	0.235	0.025	0.175	0.009	0.087	GCM
BRCR	0.397	0.336	0.035	0.003	0.040	0.001	0.188	Sampling
BTNW	0.714	0.012	0.173	0.000	0.048	0.000	0.053	GCM
CAWA	0.144	0.210	0.258	0.080	0.094	0.026	0.188	GCM
CCSP	0.011	0.034	0.023	0.745	0.053	0.052	0.081	Variable
CEDW	0.754	0.013	0.164	0.008	0.038	0.002	0.021	GCM
CHSP	0.340	0.135	0.235	0.049	0.088	0.020	0.133	GCM
CMWA	0.550	0.042	0.239	0.001	0.080	0.000	0.089	GCM
COGR	0.463	0.006	0.174	0.019	0.212	0.027	0.099	GCM
CONW	0.333	0.050	0.463	0.005	0.074	0.000	0.074	GCM
CORA	0.183	0.341	0.022	0.052	0.087	0.006	0.309	Sampling
CORE	0.184	0.344	0.119	0.001	0.050	0.000	0.302	Sampling
COYE	0.737	0.022	0.108	0.047	0.034	0.020	0.034	GCM
CSWA	0.558	0.038	0.243	0.004	0.107	0.016	0.033	GCM
DEJU	0.657	0.111	0.110	0.007	0.071	0.003	0.041	Sampling
EAKI	0.453	0.024	0.160	0.070	0.112	0.068	0.112	GCM
EAPH	0.782	0.013	0.043	0.002	0.066	0.009	0.085	GCM
EVGR	0.479	0.155	0.114	0.052	0.033	0.031	0.137	Sampling
FOSP	0.628	0.134	0.118	0.001	0.065	0.007	0.048	Sampling
GCKI	0.156	0.298	0.038	0.164	0.159	0.066	0.119	Sampling

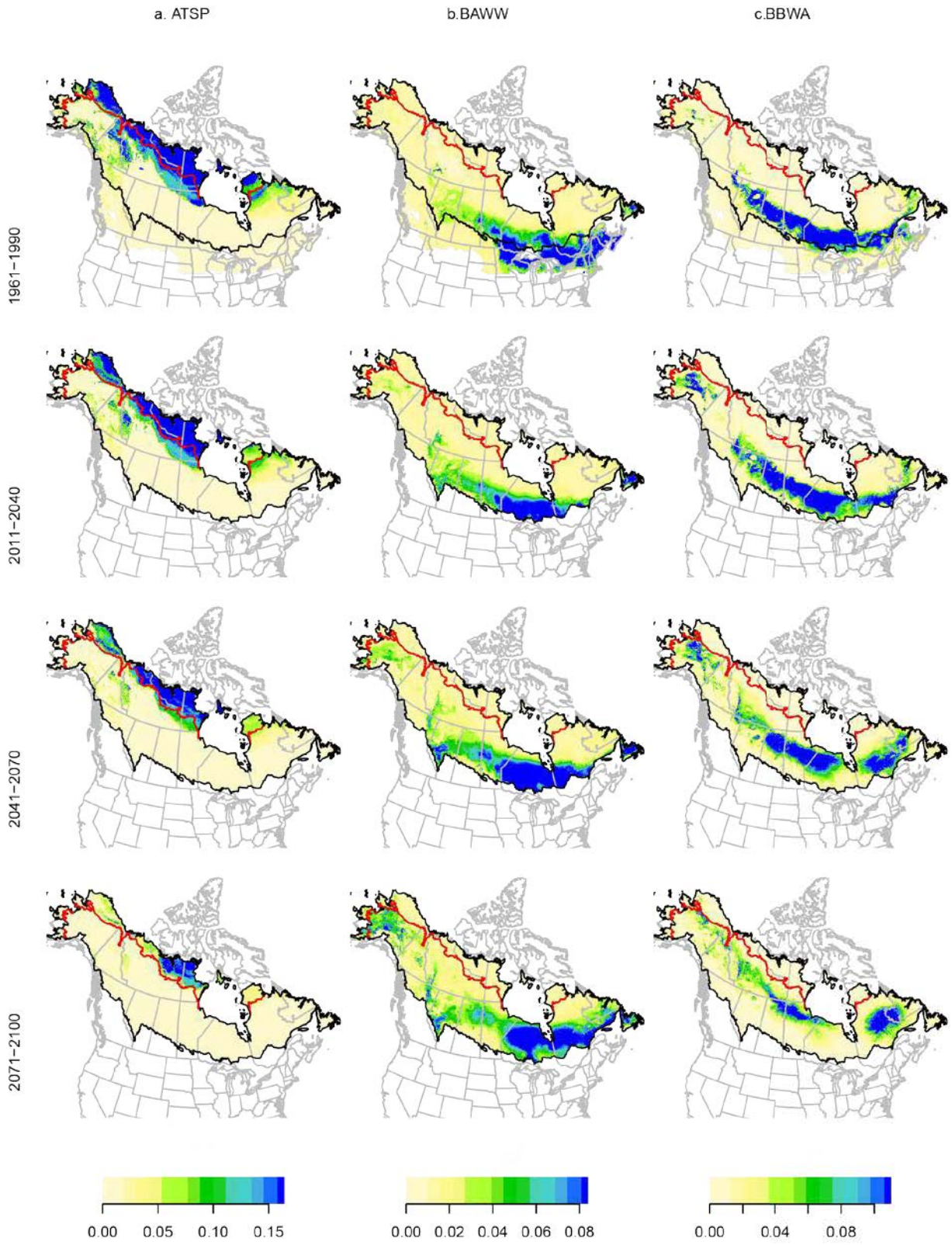
Species	Time	Sampling	GCM	Variable	GCM* Time	Variable* Time	Error	Greatest Source
GCTH	0.328	0.418	0.121	0.001	0.029	0.000	0.103	Sampling
GRAJ	0.721	0.030	0.185	0.002	0.051	0.000	0.012	GCM
HETH	0.566	0.065	0.091	0.016	0.204	0.006	0.051	GCM
HOLA	0.185	0.240	0.168	0.007	0.231	0.011	0.157	Sampling
LCSP	0.241	0.163	0.145	0.134	0.065	0.009	0.243	Sampling
LEFL	0.334	0.148	0.150	0.125	0.124	0.009	0.110	GCM
LISP	0.670	0.058	0.171	0.007	0.066	0.001	0.027	GCM
MAWA	0.207	0.071	0.370	0.042	0.201	0.026	0.083	GCM
MOWA	0.142	0.045	0.401	0.011	0.339	0.004	0.058	GCM
NAWA	0.390	0.009	0.153	0.084	0.309	0.025	0.030	GCM
NOWA	0.496	0.184	0.029	0.016	0.141	0.000	0.135	Sampling
OCWA	0.289	0.139	0.371	0.010	0.063	0.005	0.123	GCM
OSFL	0.313	0.275	0.238	0.000	0.032	0.000	0.142	Sampling
OVEN	0.240	0.011	0.426	0.102	0.154	0.036	0.033	GCM
PAWA	0.546	0.225	0.113	0.000	0.045	0.000	0.071	Sampling
PHVI	0.470	0.066	0.053	0.000	0.300	0.001	0.109	Time*GCM
PIGR	0.135	0.523	0.087	0.039	0.016	0.006	0.194	Sampling
PISI	0.513	0.074	0.234	0.000	0.099	0.000	0.080	GCM
PUFI	0.760	0.039	0.120	0.003	0.020	0.001	0.058	GCM
RBGR	0.465	0.052	0.283	0.003	0.141	0.000	0.055	GCM
RBNU	0.608	0.030	0.048	0.141	0.024	0.083	0.065	Variable
RCKI	0.760	0.007	0.117	0.007	0.096	0.000	0.012	GCM
REVI	0.547	0.012	0.288	0.000	0.129	0.010	0.015	GCM
RUBL	0.207	0.626	0.020	0.001	0.015	0.000	0.131	Sampling
RWBL	0.373	0.005	0.096	0.224	0.078	0.131	0.092	Variable
SAVS	0.262	0.413	0.041	0.065	0.015	0.047	0.158	Sampling
SOSP	0.543	0.006	0.135	0.129	0.066	0.059	0.062	GCM
SWSP	0.062	0.275	0.052	0.026	0.209	0.003	0.374	Sampling
SWTH	0.590	0.042	0.108	0.000	0.191	0.005	0.064	GCM
TEWA	0.591	0.004	0.290	0.001	0.101	0.000	0.013	GCM
TRES	0.515	0.045	0.142	0.031	0.116	0.023	0.129	GCM
VATH	0.185	0.059	0.548	0.000	0.121	0.001	0.086	GCM
VESP	0.391	0.005	0.212	0.118	0.178	0.040	0.055	GCM
WAVI	0.733	0.020	0.092	0.015	0.113	0.004	0.023	GCM
WCSP	0.661	0.076	0.163	0.000	0.042	0.000	0.059	GCM
WETA	0.250	0.151	0.009	0.015	0.240	0.001	0.333	Error
WEWP	0.280	0.205	0.168	0.007	0.259	0.001	0.080	Sampling
WIWA	0.402	0.066	0.387	0.000	0.066	0.001	0.078	GCM
WIWR	0.558	0.034	0.103	0.012	0.232	0.010	0.051	GCM
WTSP	0.381	0.014	0.287	0.003	0.283	0.000	0.032	GCM
WWCR	0.681	0.044	0.125	0.007	0.040	0.000	0.103	GCM

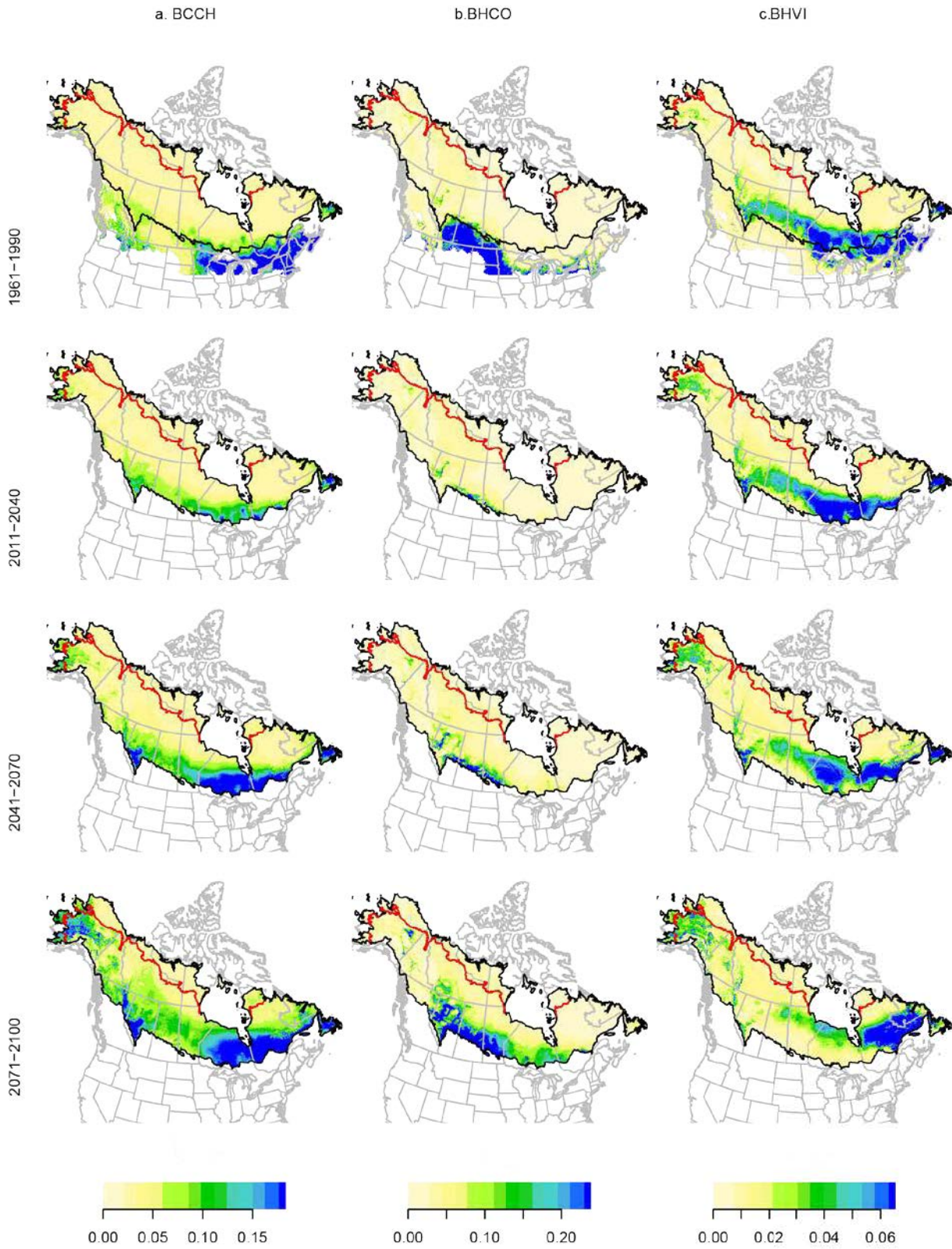
Species	Time	Sampling	GCM	Variable	GCM*	Variable*	Error	Greatest Source
YBFL	0.502	0.040	0.226	0.014	0.183	0.000	0.034	GCM
YRWA	0.506	0.061	0.242	0.000	0.072	0.017	0.102	GCM
YWAR	0.281	0.125	0.198	0.092	0.134	0.046	0.123	GCM
Mean	0.442	0.118	0.174	0.047	0.107	0.017	0.095	
5%	0.134	0.005	0.028	0.000	0.018	0.000	0.014	
95%	0.760	0.424	0.388	0.146	0.260	0.066	0.246	

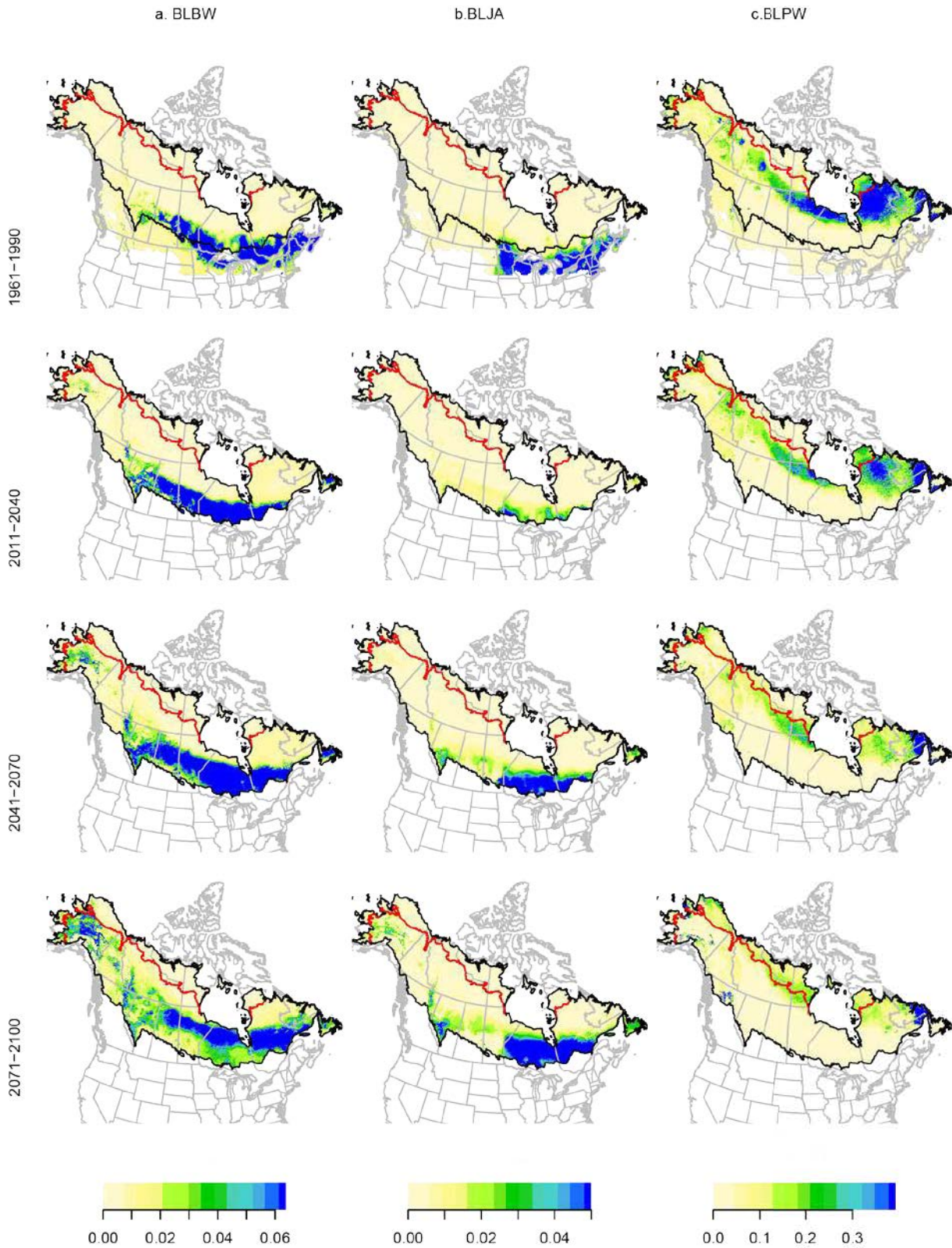
Figure D1. Spatial predictions and projection of breeding density (males/ha) for 80 boreal passerine species. Spatial predictions for the current period (1961-1990) are based on density models developed from point-count data. Future projections from models are presented for three time periods (2011-2040, 2041-2070, 2071-2100), averaged across 11 bootstrap samples, two variable sets (climate-only and climate + land use + topography), and four global climate models. Boreal and southern arctic regions are divided by the red line. Ranges in density values are relative within individual species, and colors cannot be compared directly across species. [Appendix 1-C](#), Table C1 provides the common and scientific names associated with the 4-letter species codes. Interactive maps available at <http://borealbirds.databasin.org/>.

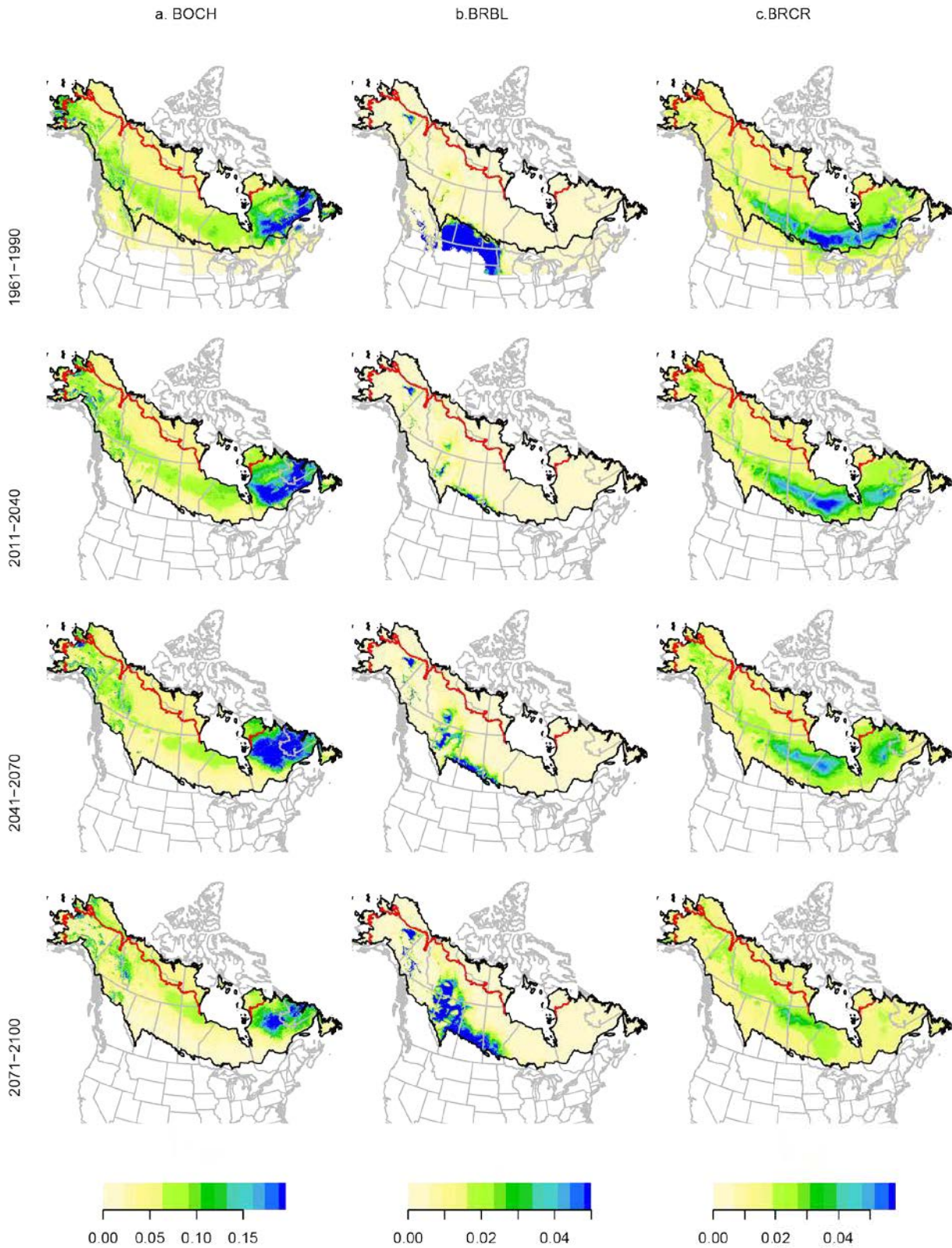


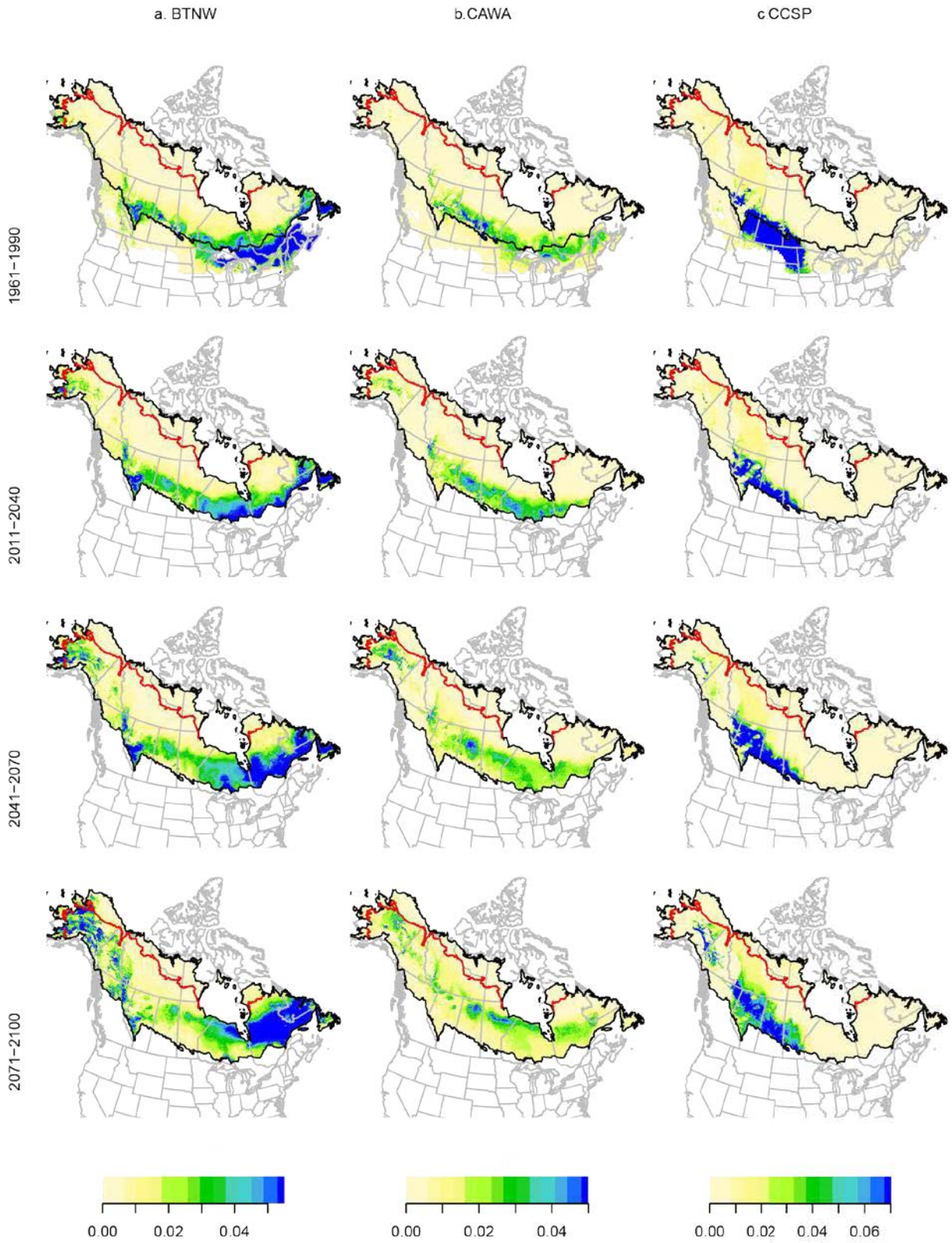


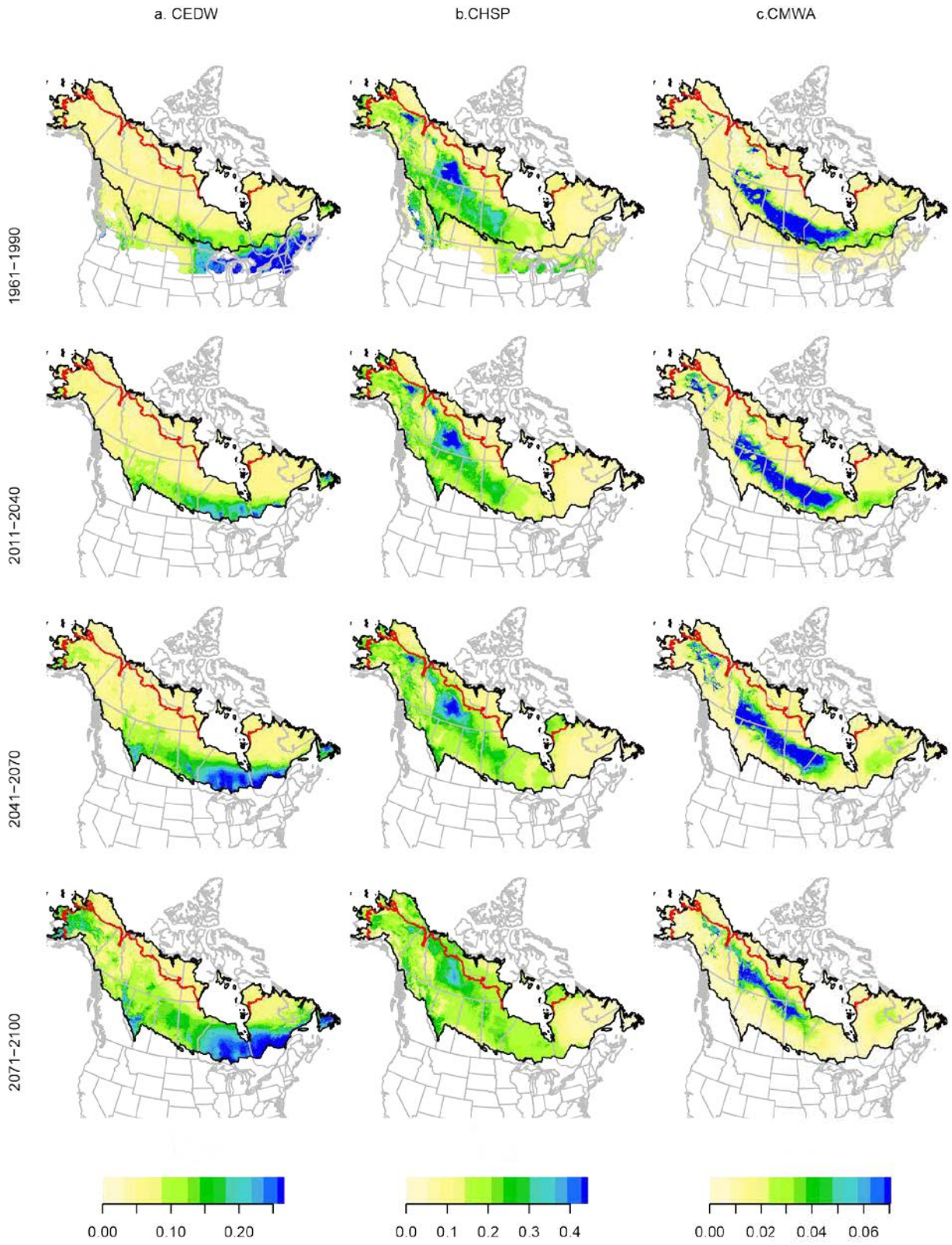


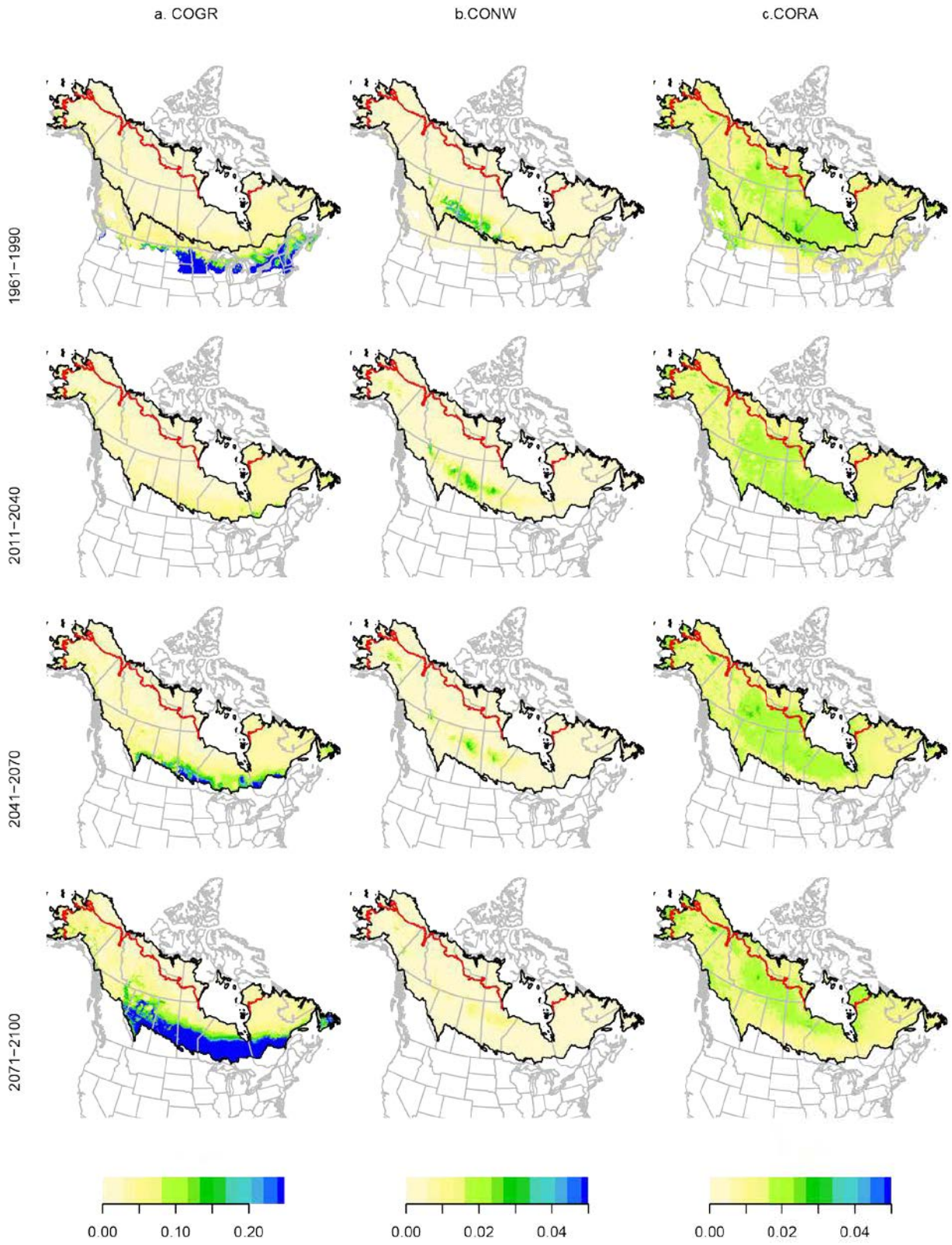


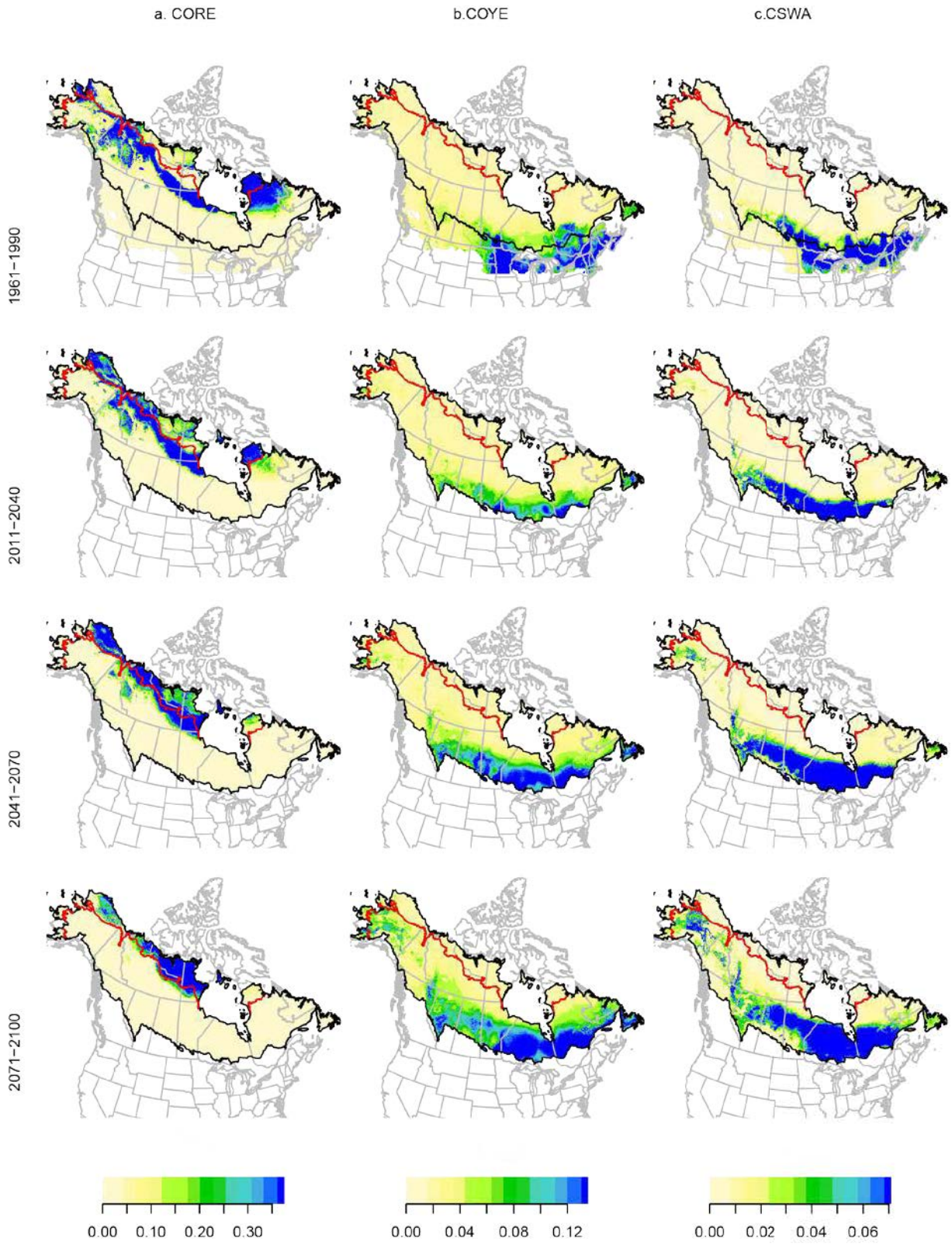


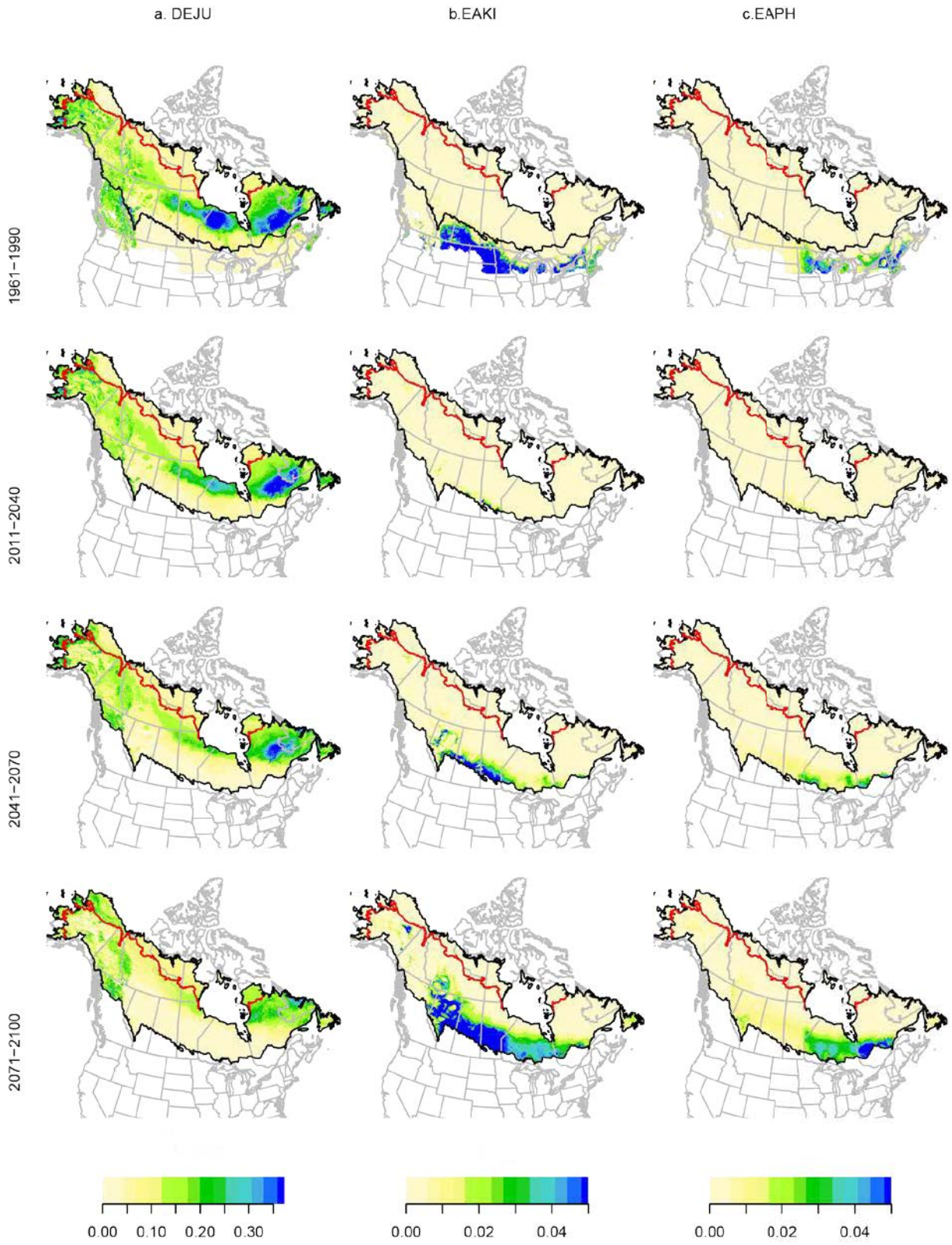


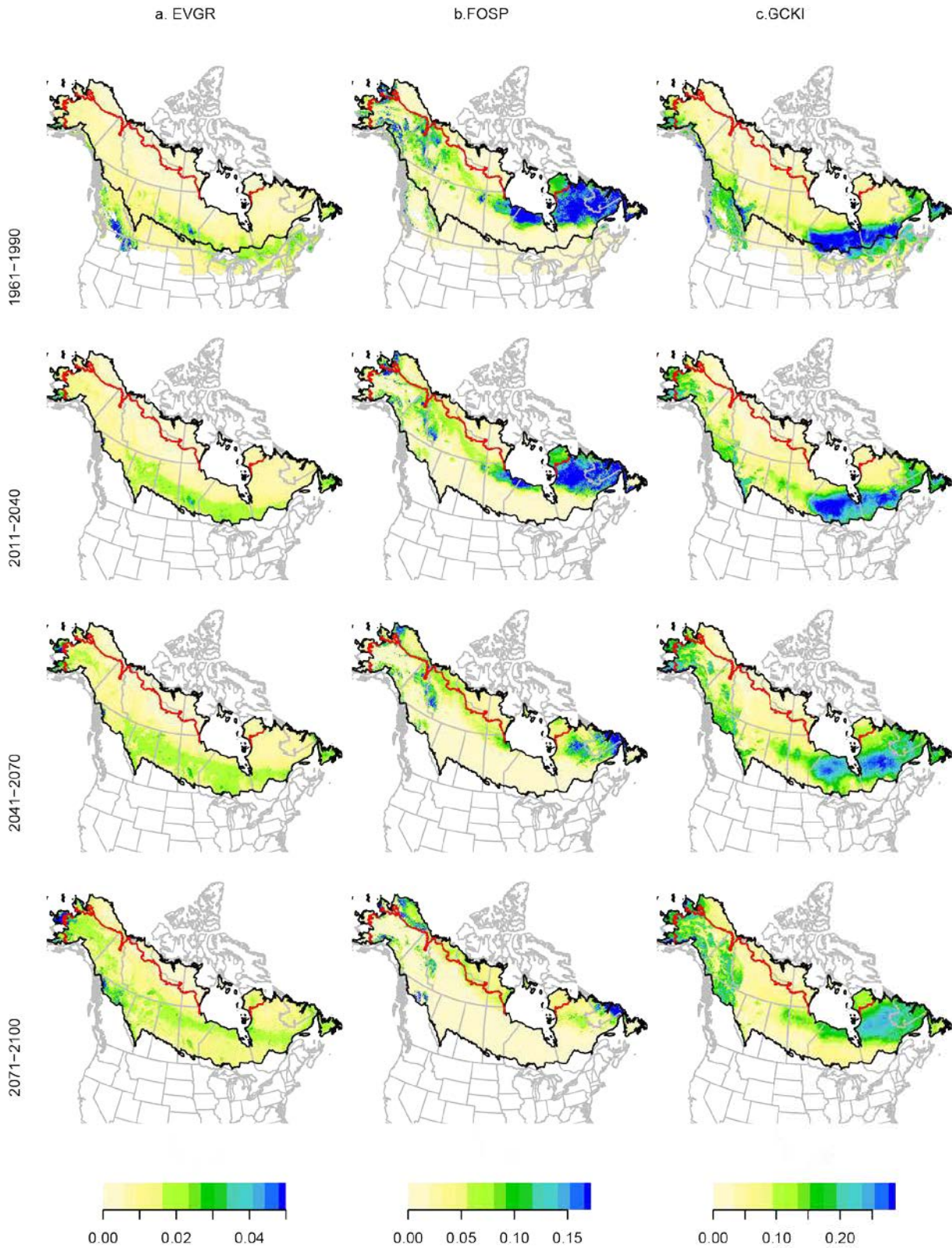


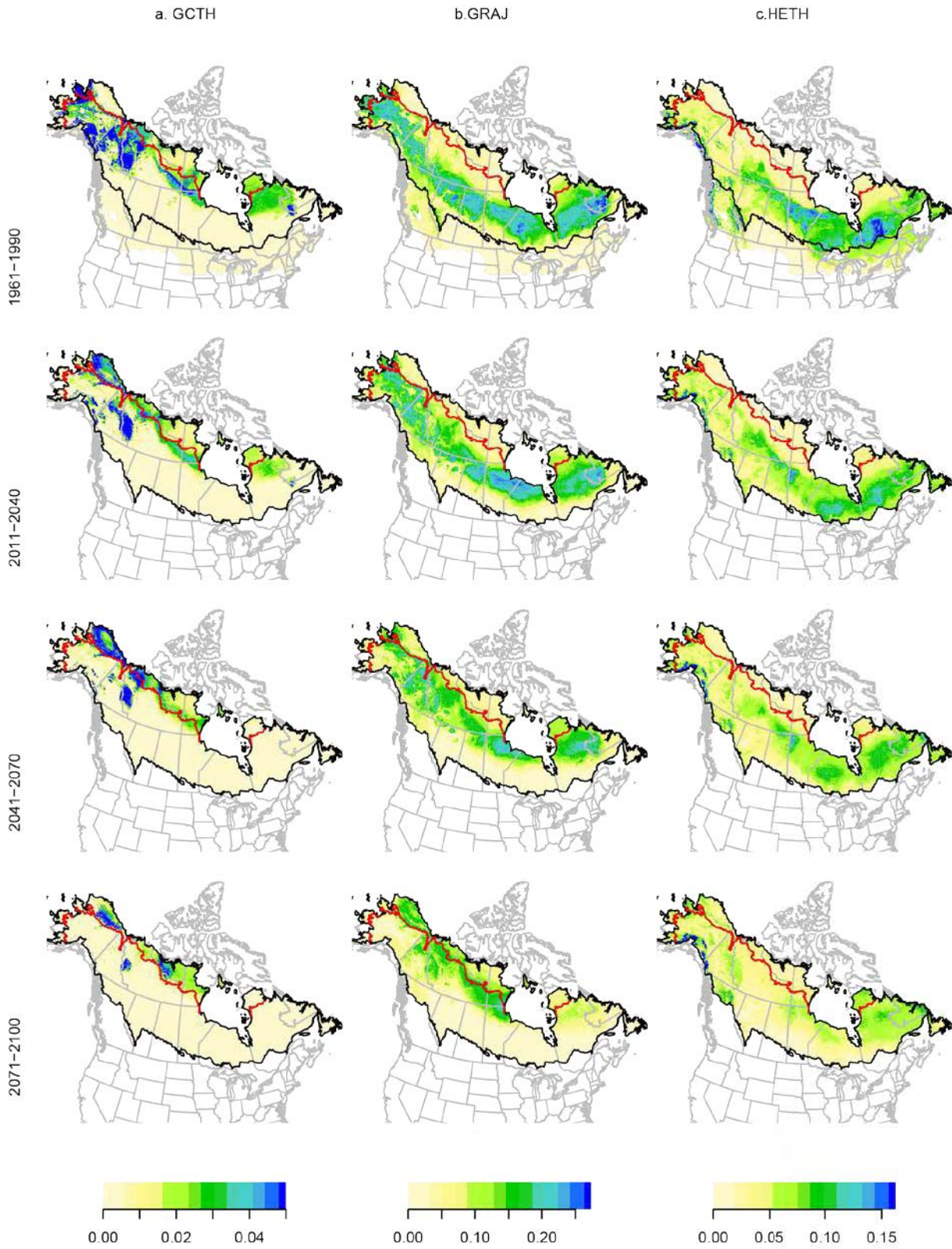


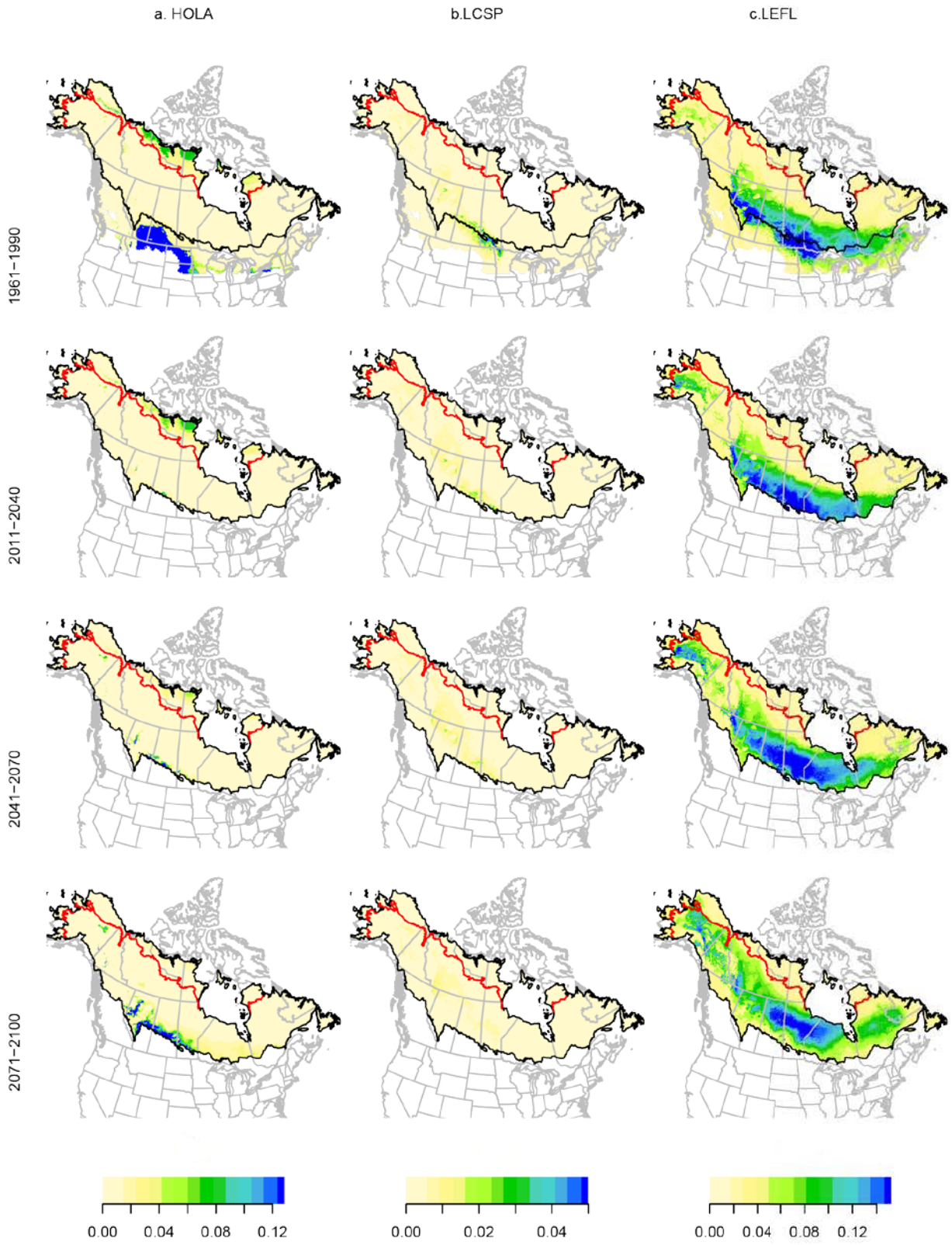


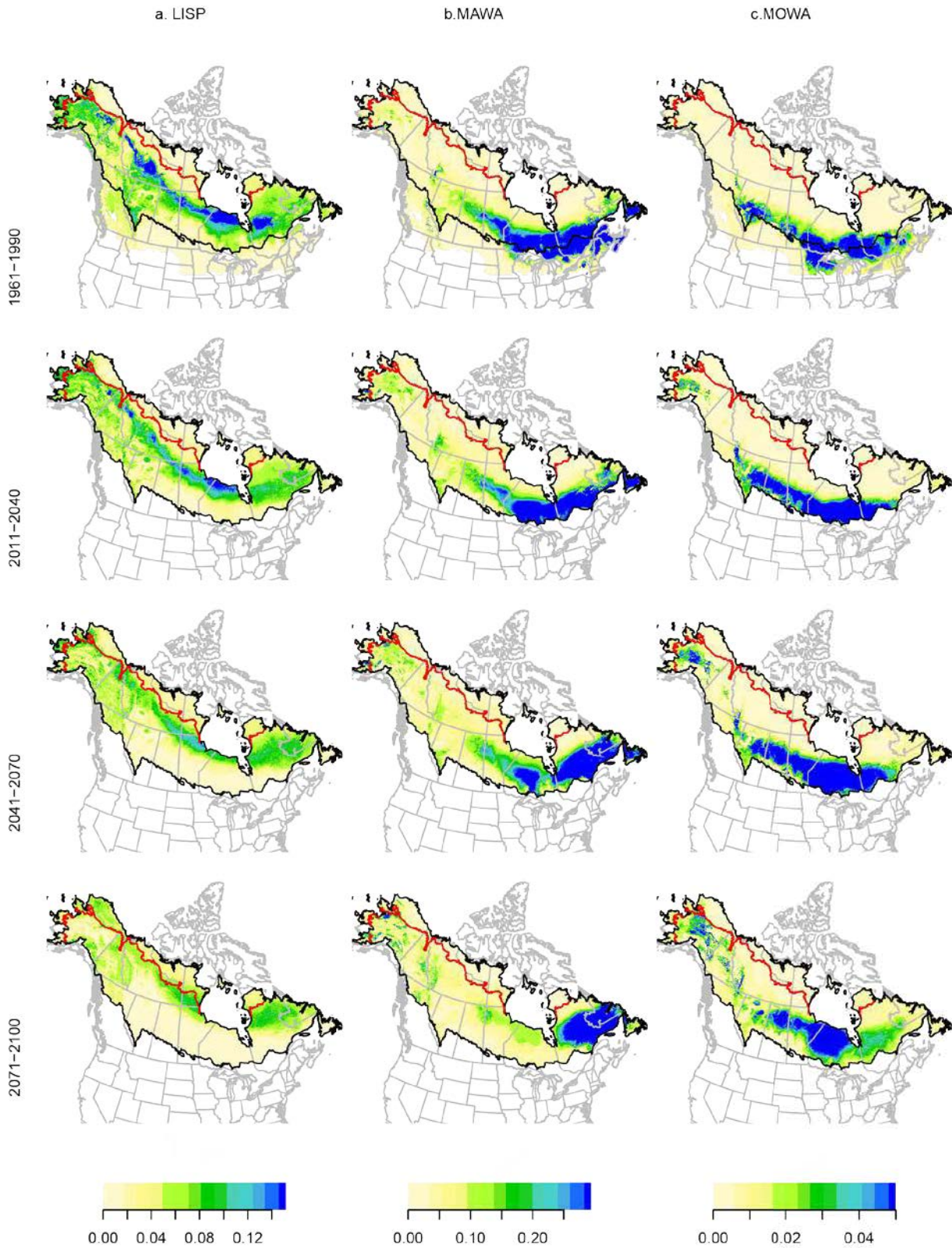


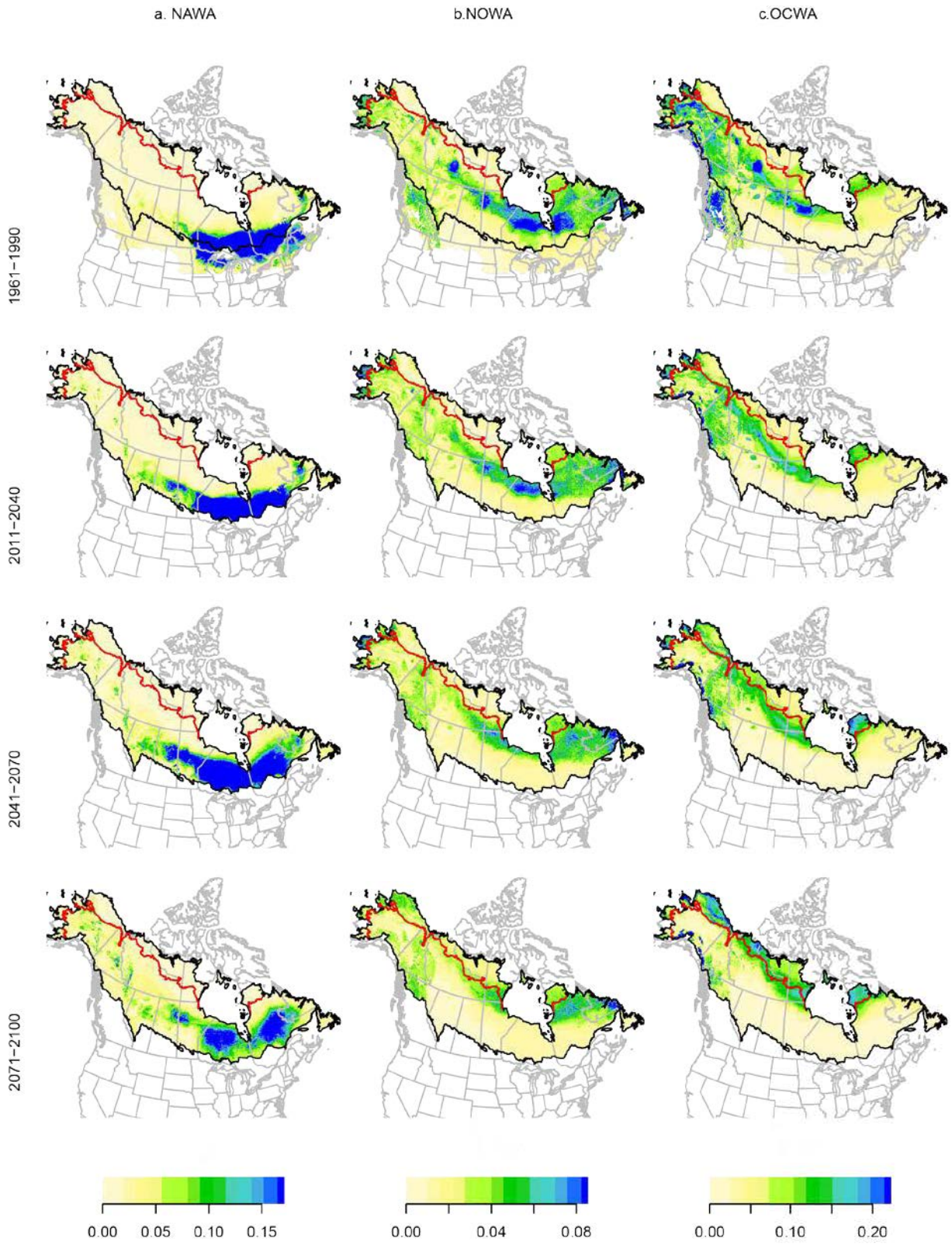


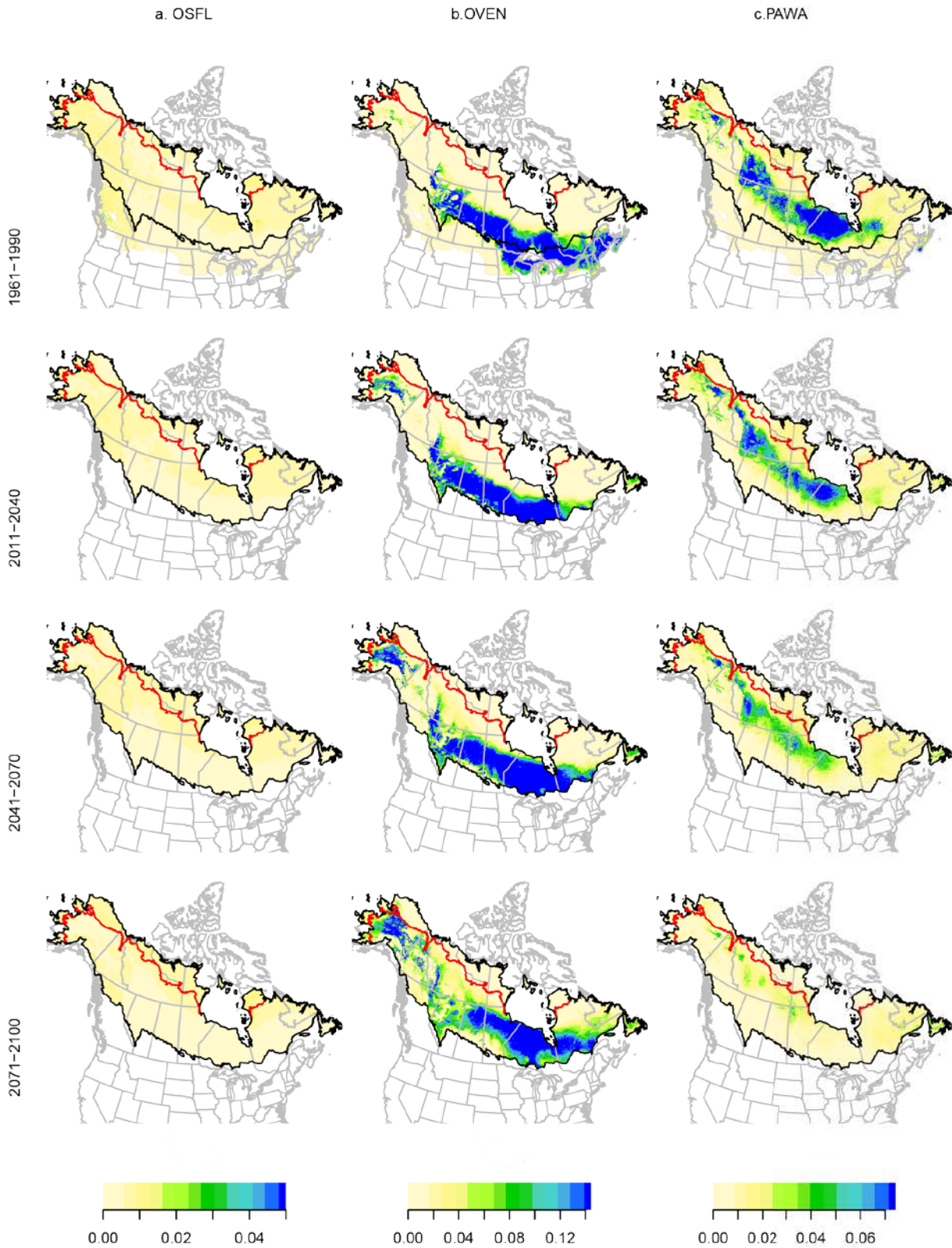


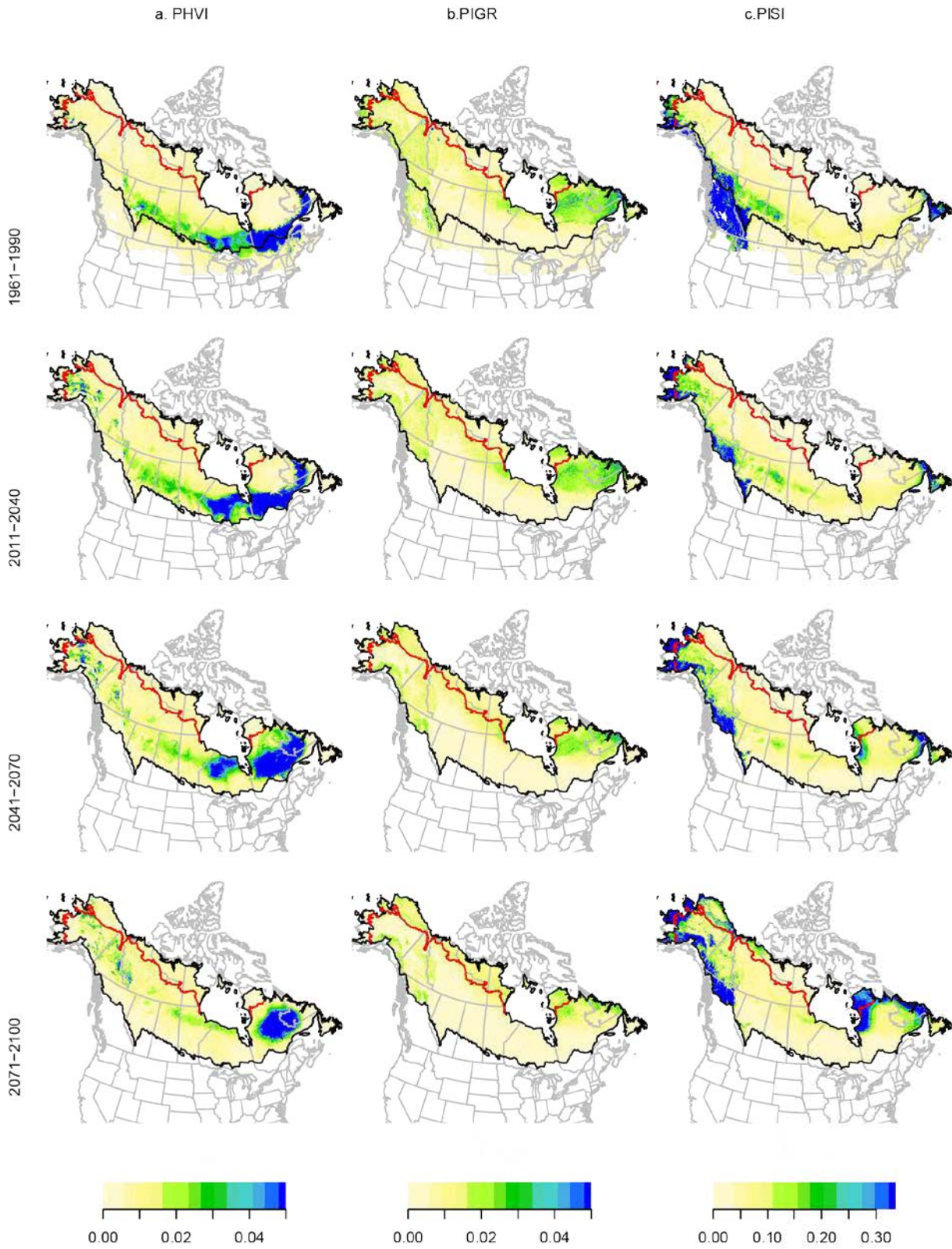


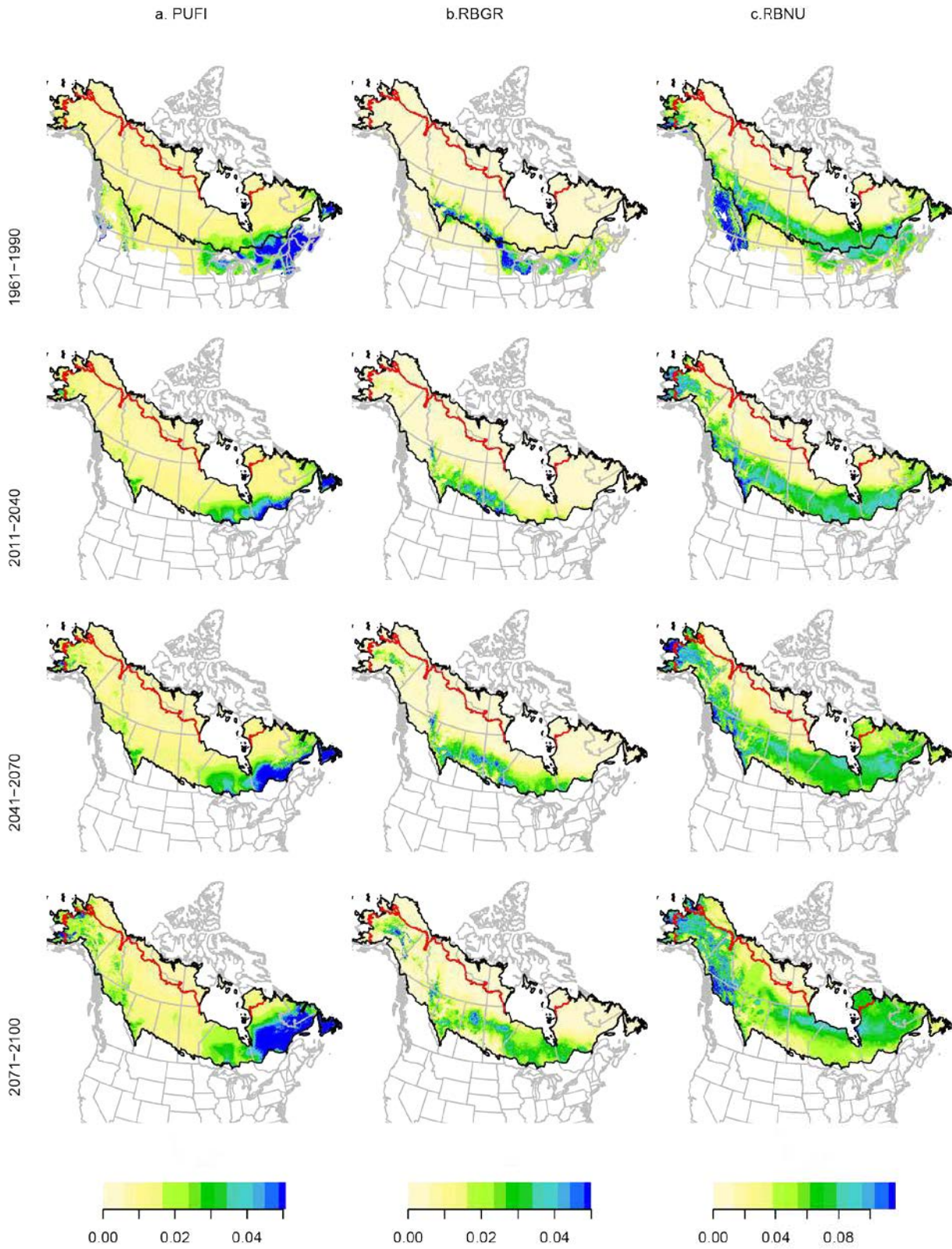


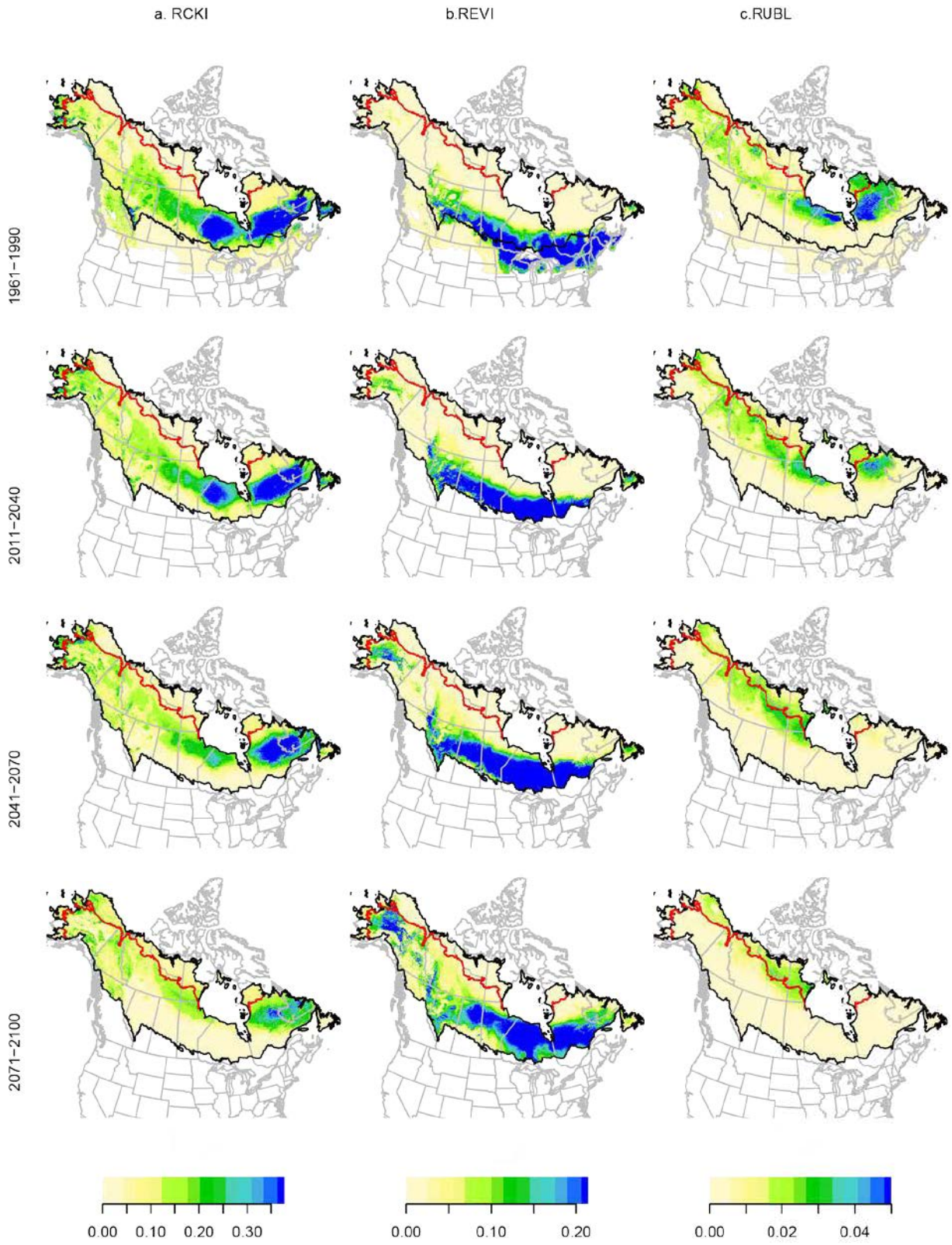


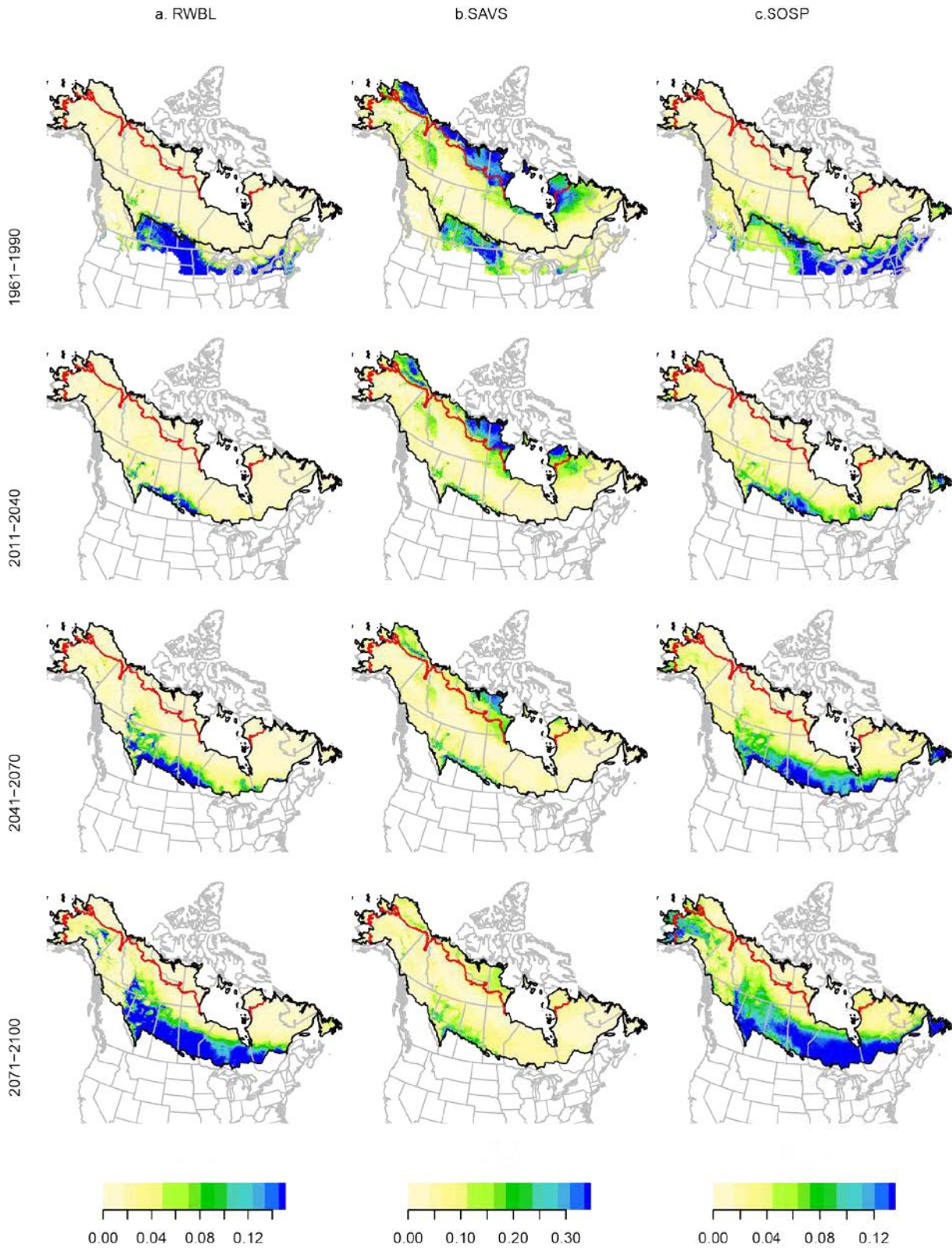


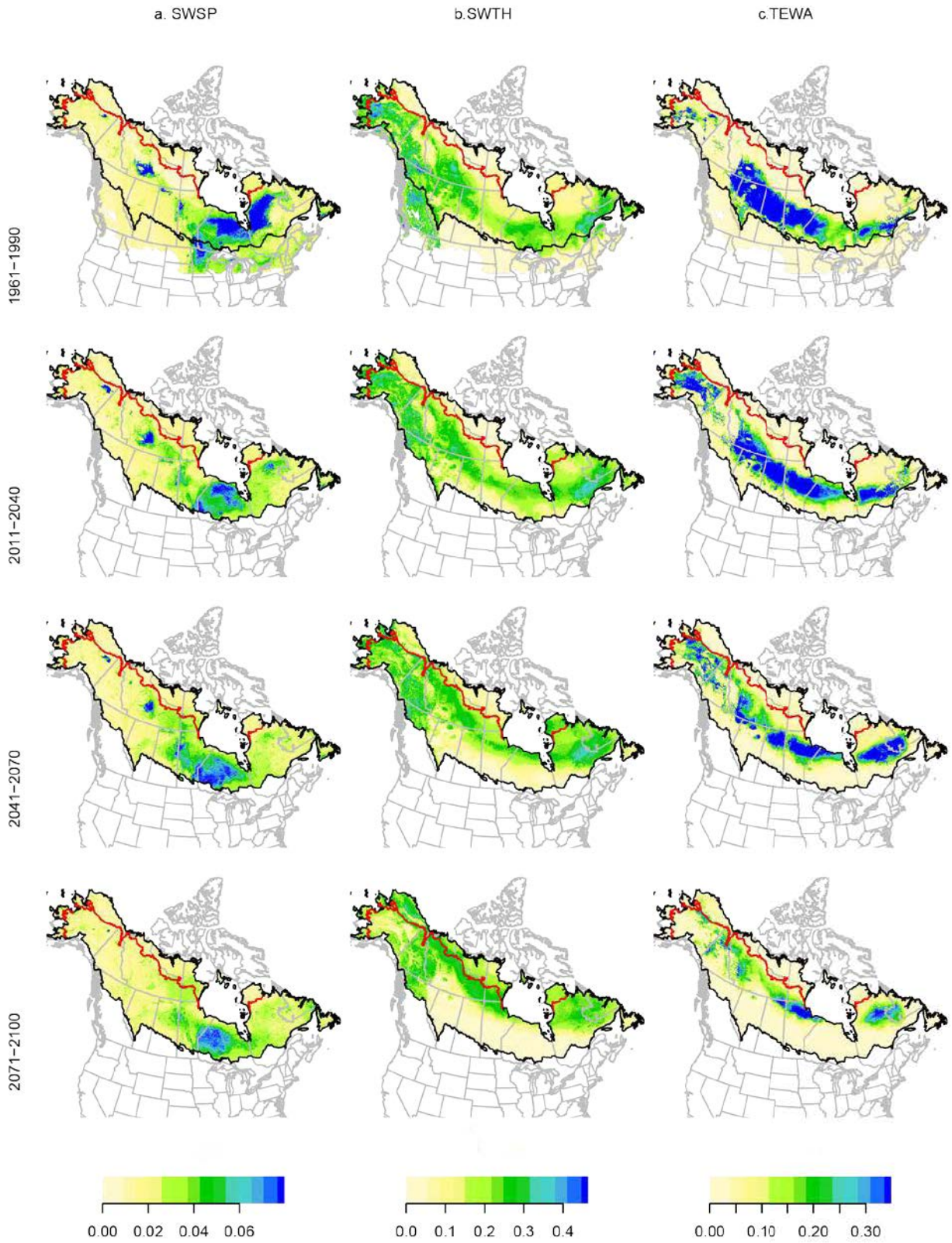


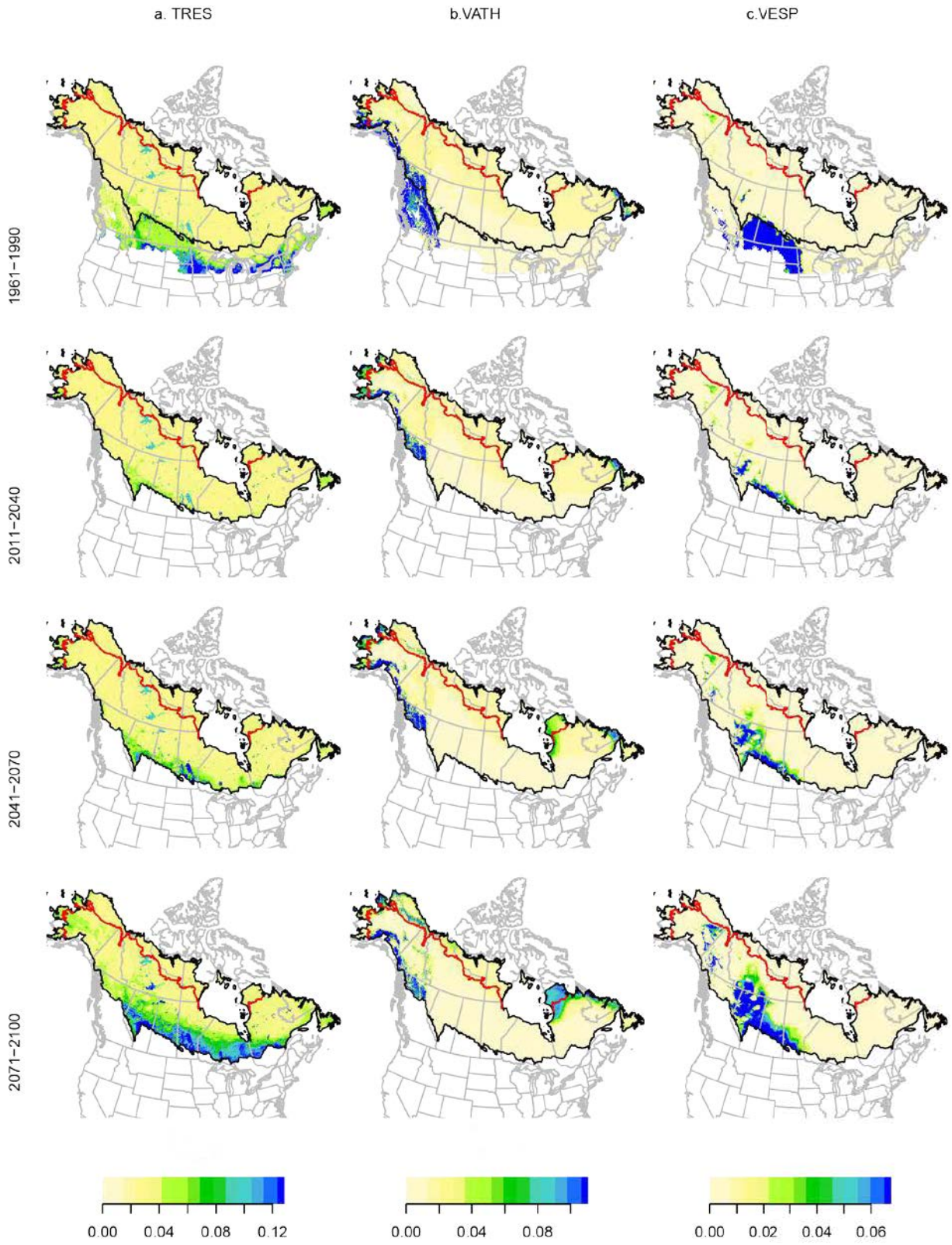


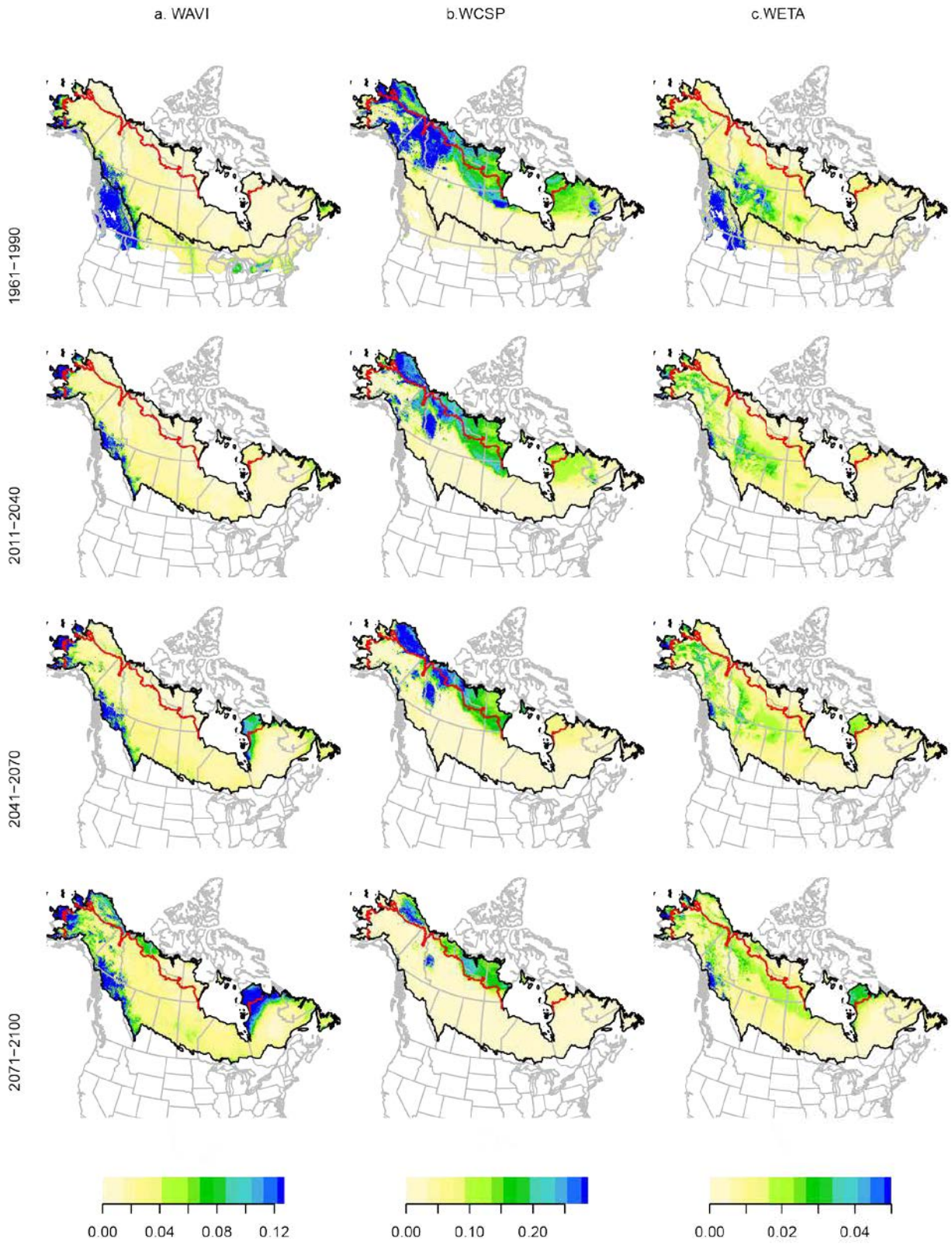


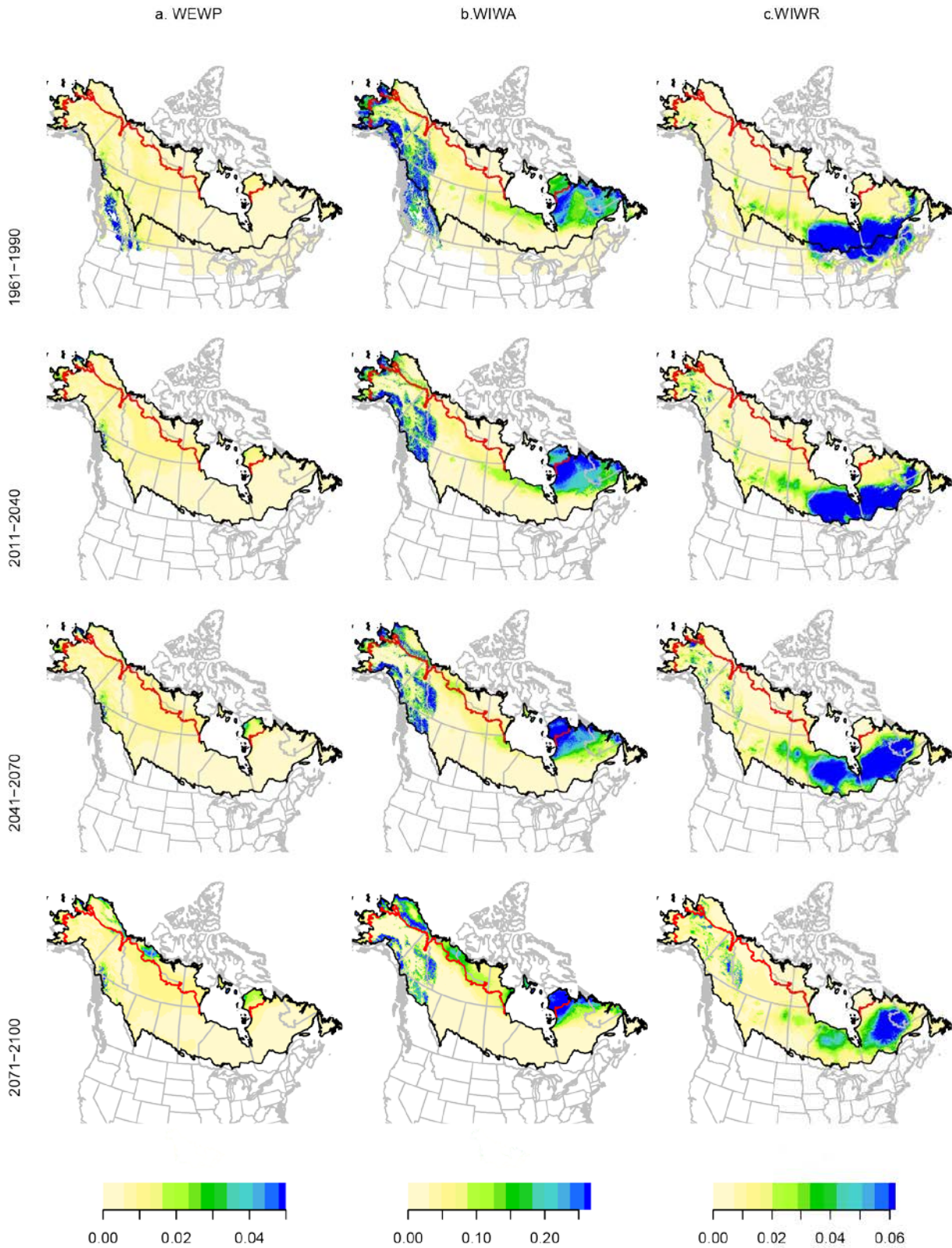


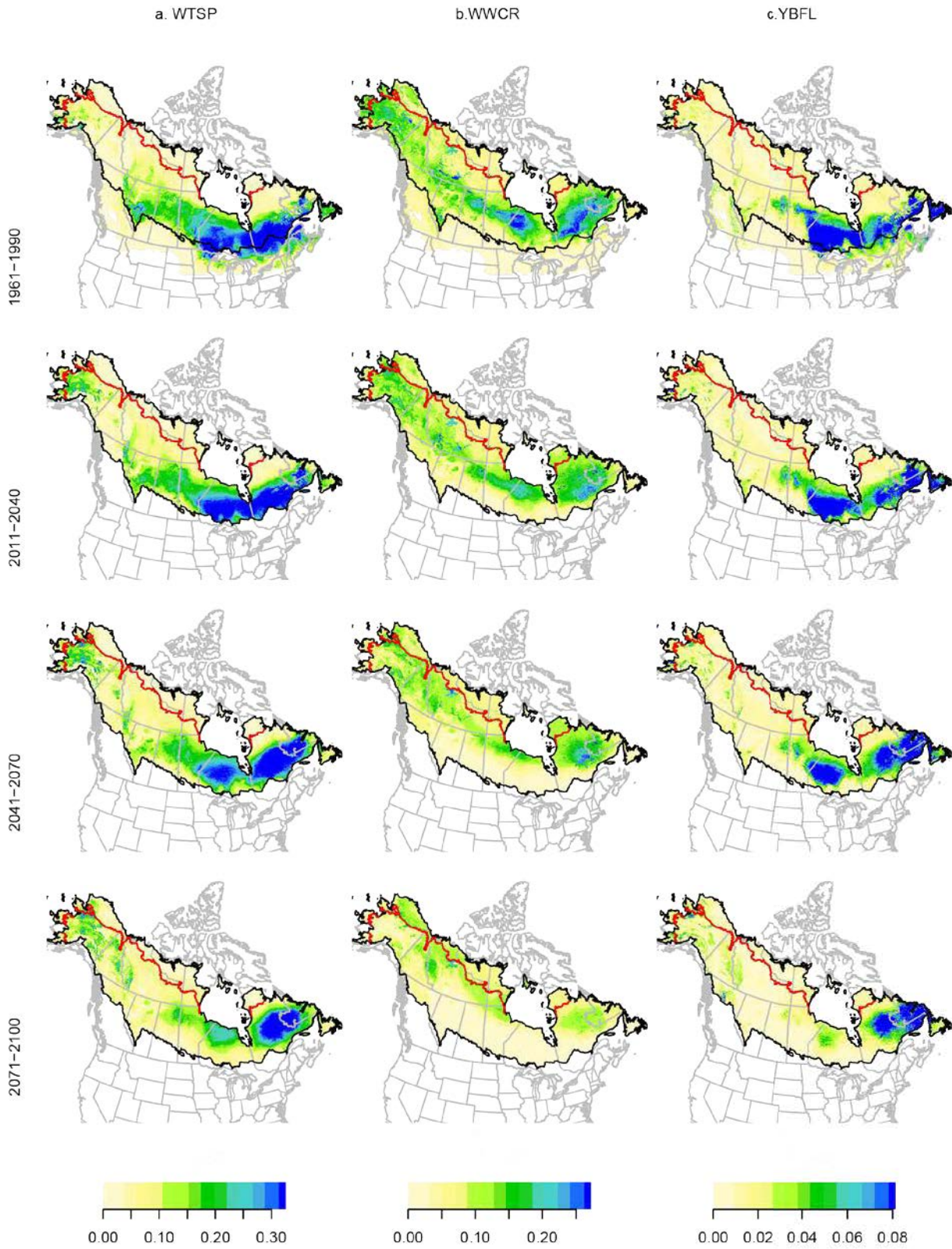












a. YRWA

b. YWAR

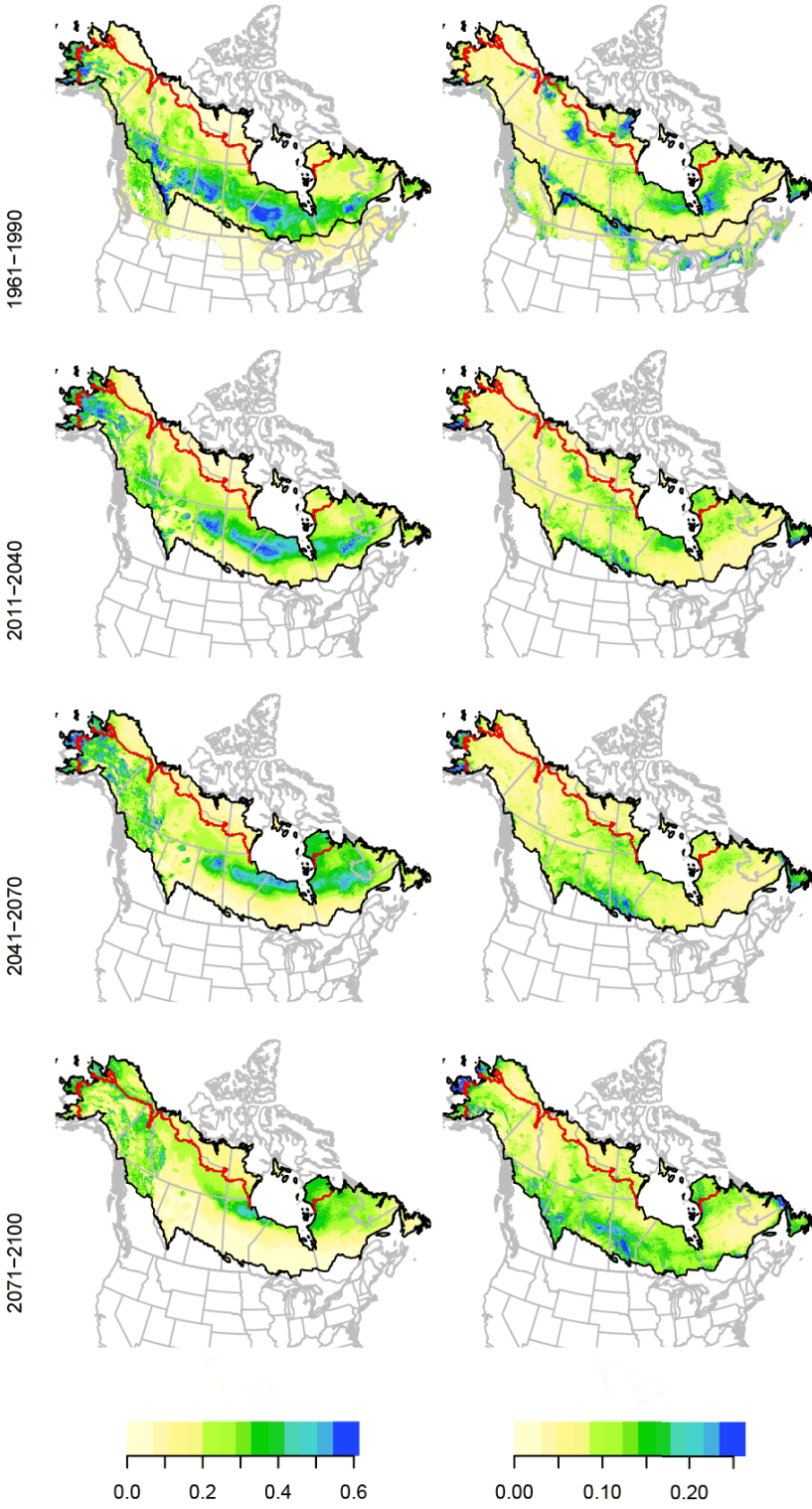
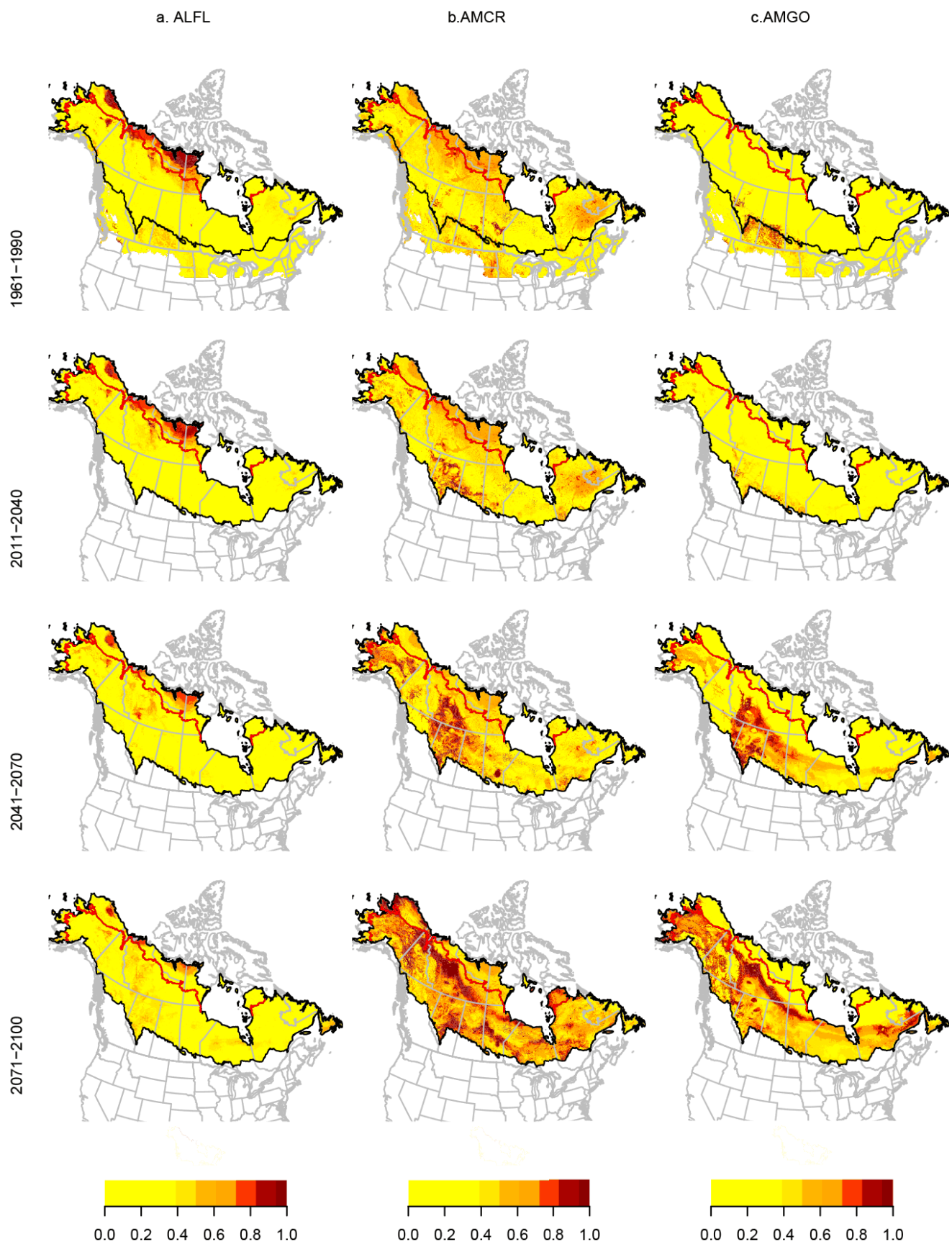
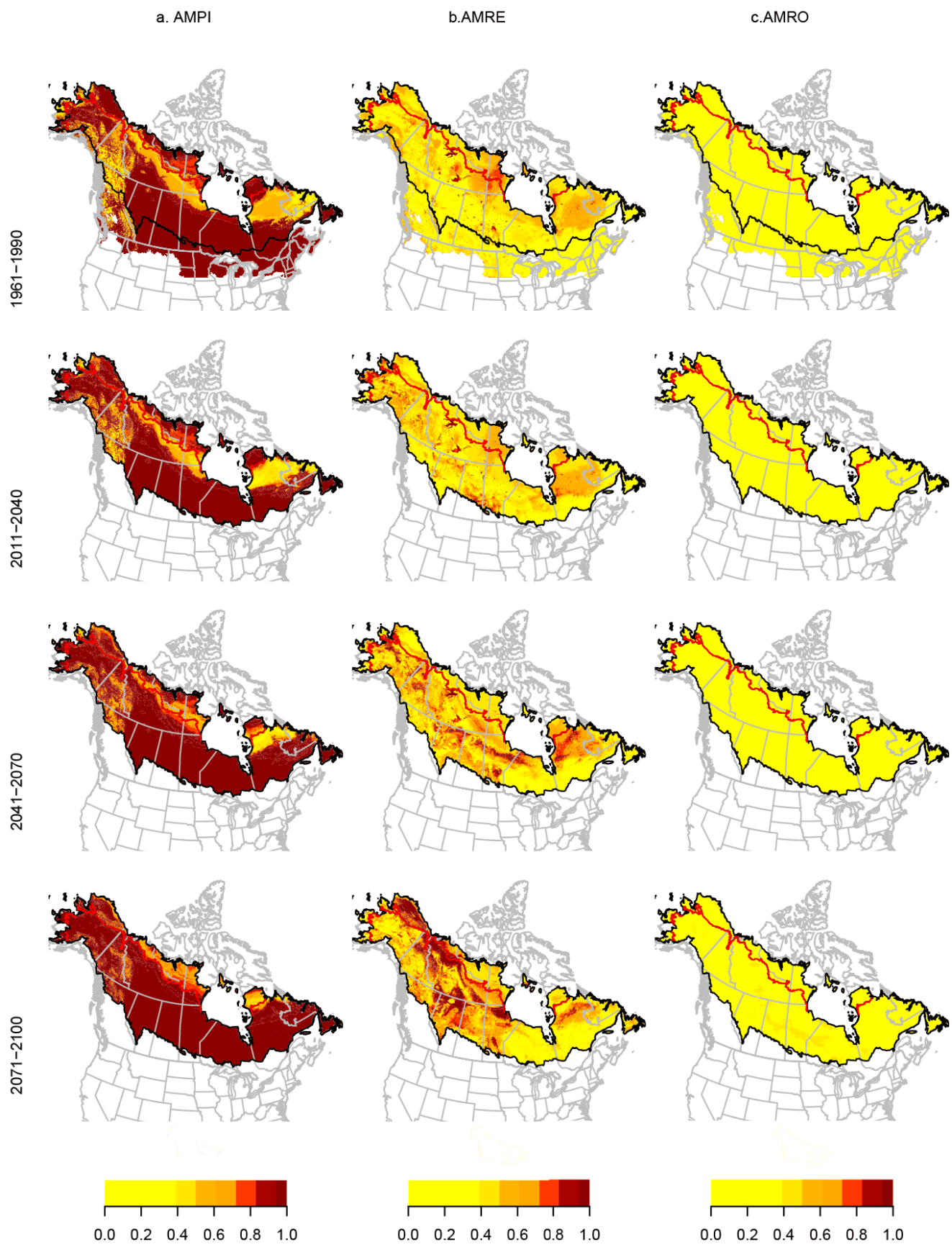
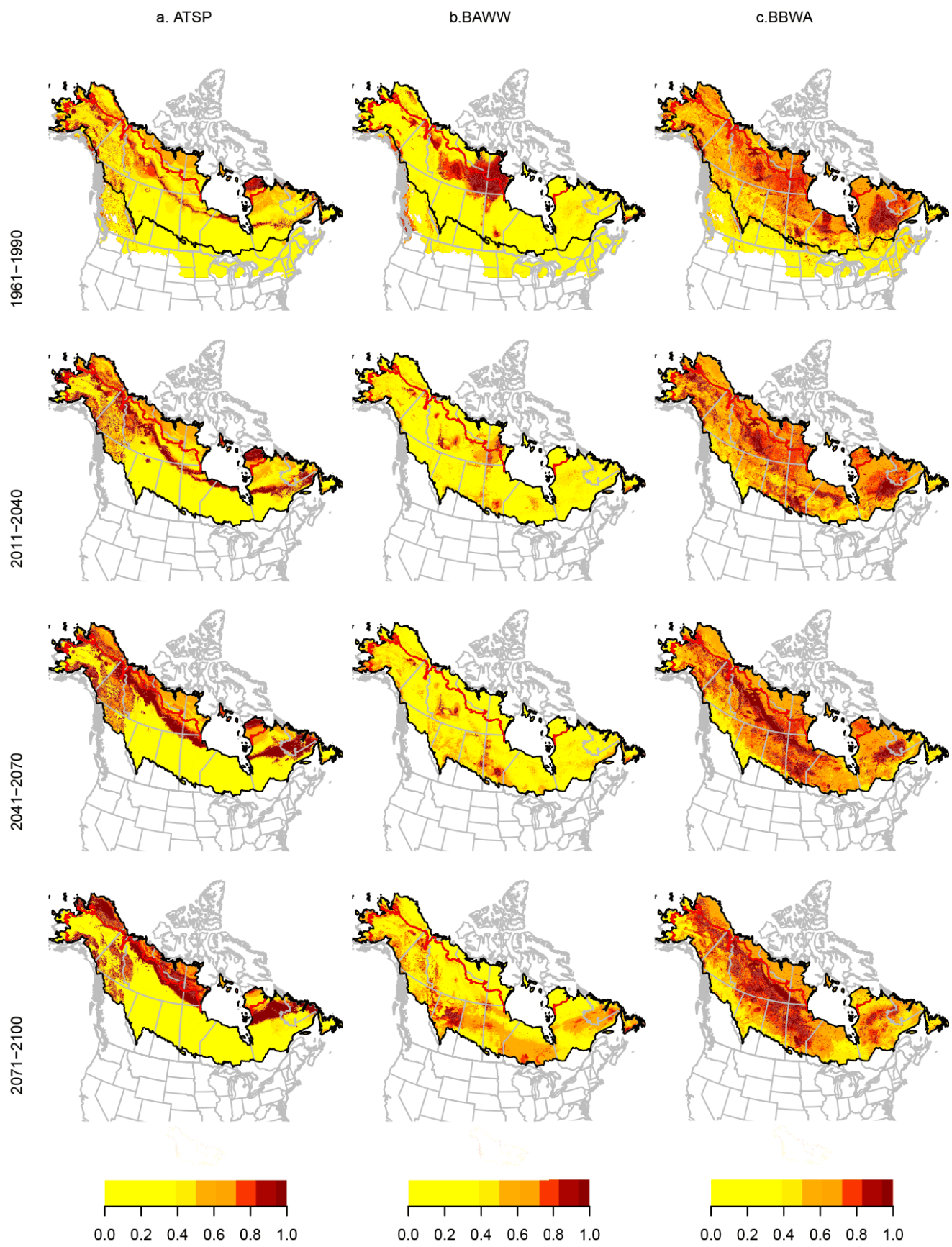
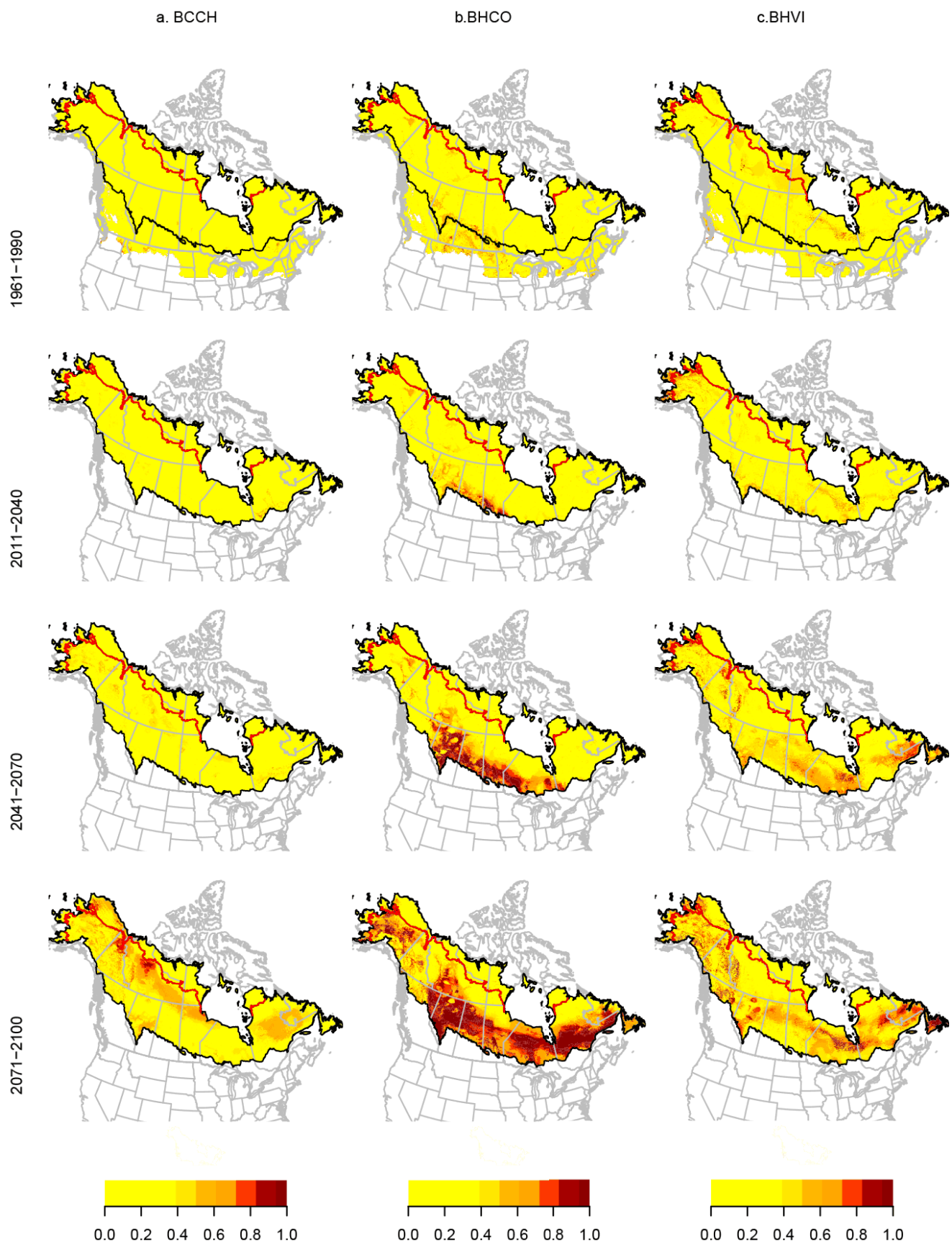


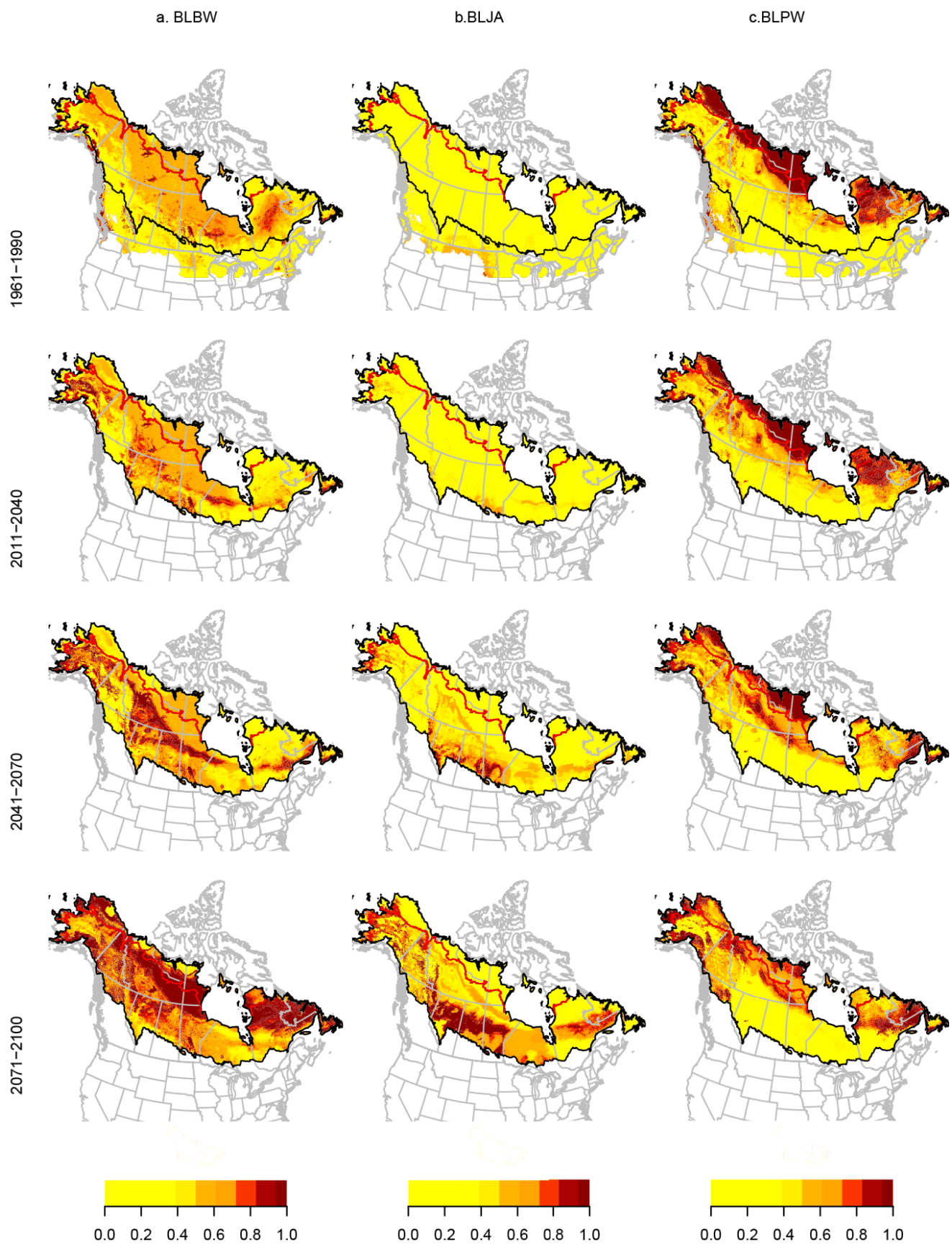
Figure D2. Spatial and temporal representations of coefficient of variation in projected abundance for the current period (1961-1990) and three future time periods (2011-2040, 2041-2070, 2071-2100). Sources of uncertainty include: sampling uncertainty due to variation across 11 bootstrap samples; model uncertainty due to variation between climate-only and climate + land use + topography models; and GCM uncertainty due to variation across 4 global climate models. Boreal and southern arctic regions are divided by the red line. [Appendix 1-C](#), Table C1 provides the common and scientific names associated with the 4-letter species codes. Interactive maps available at <http://borealbirds.databasin.org/>.

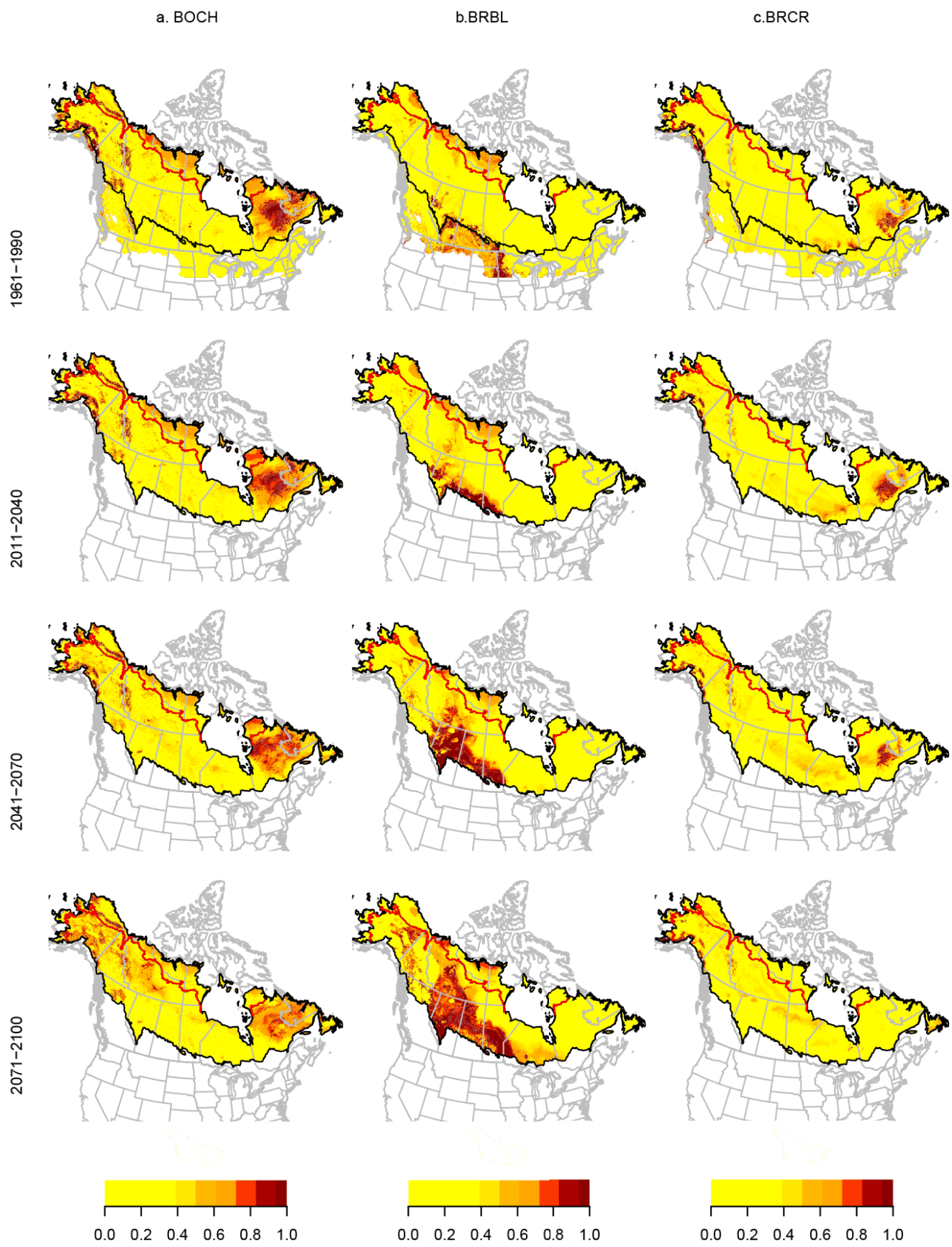


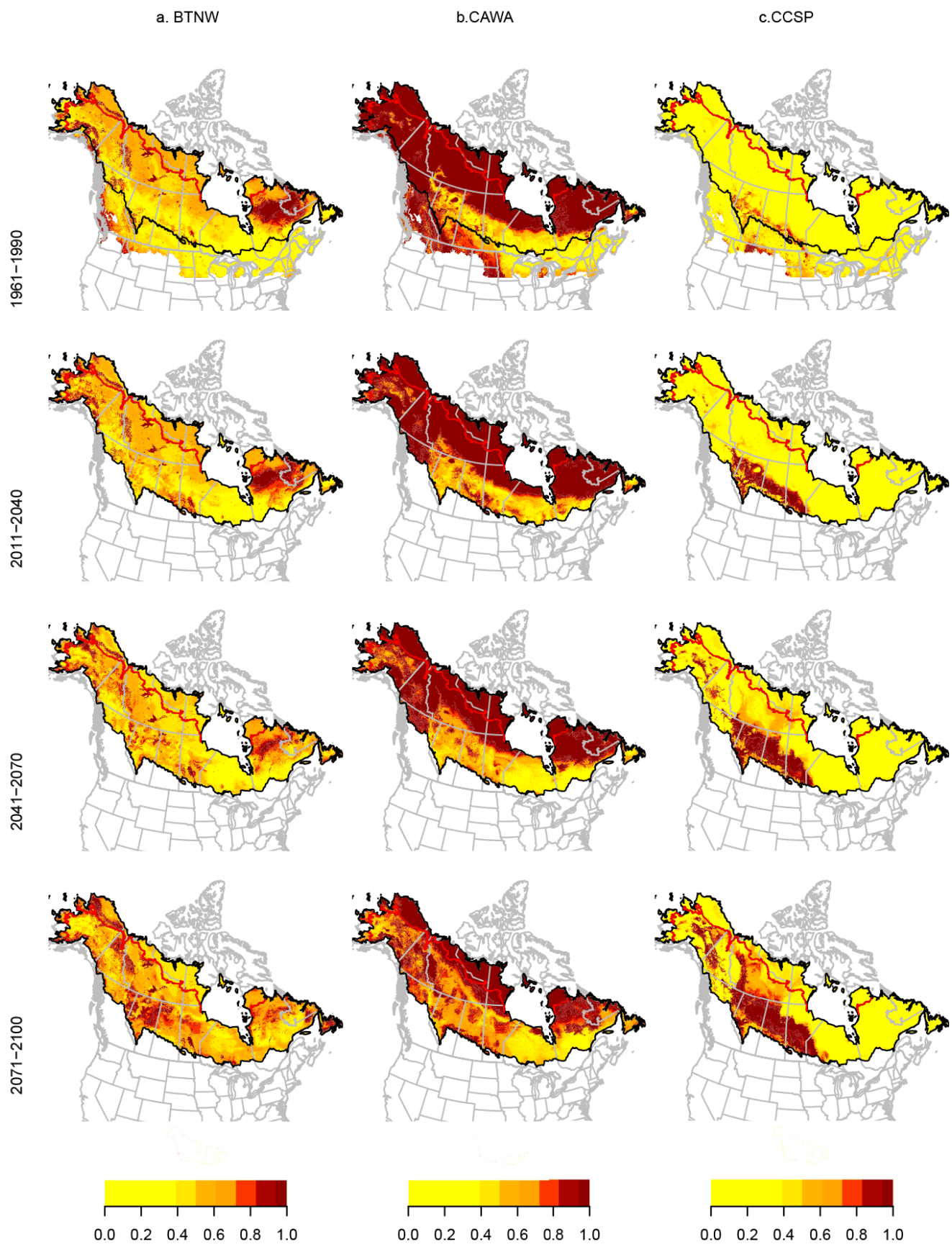


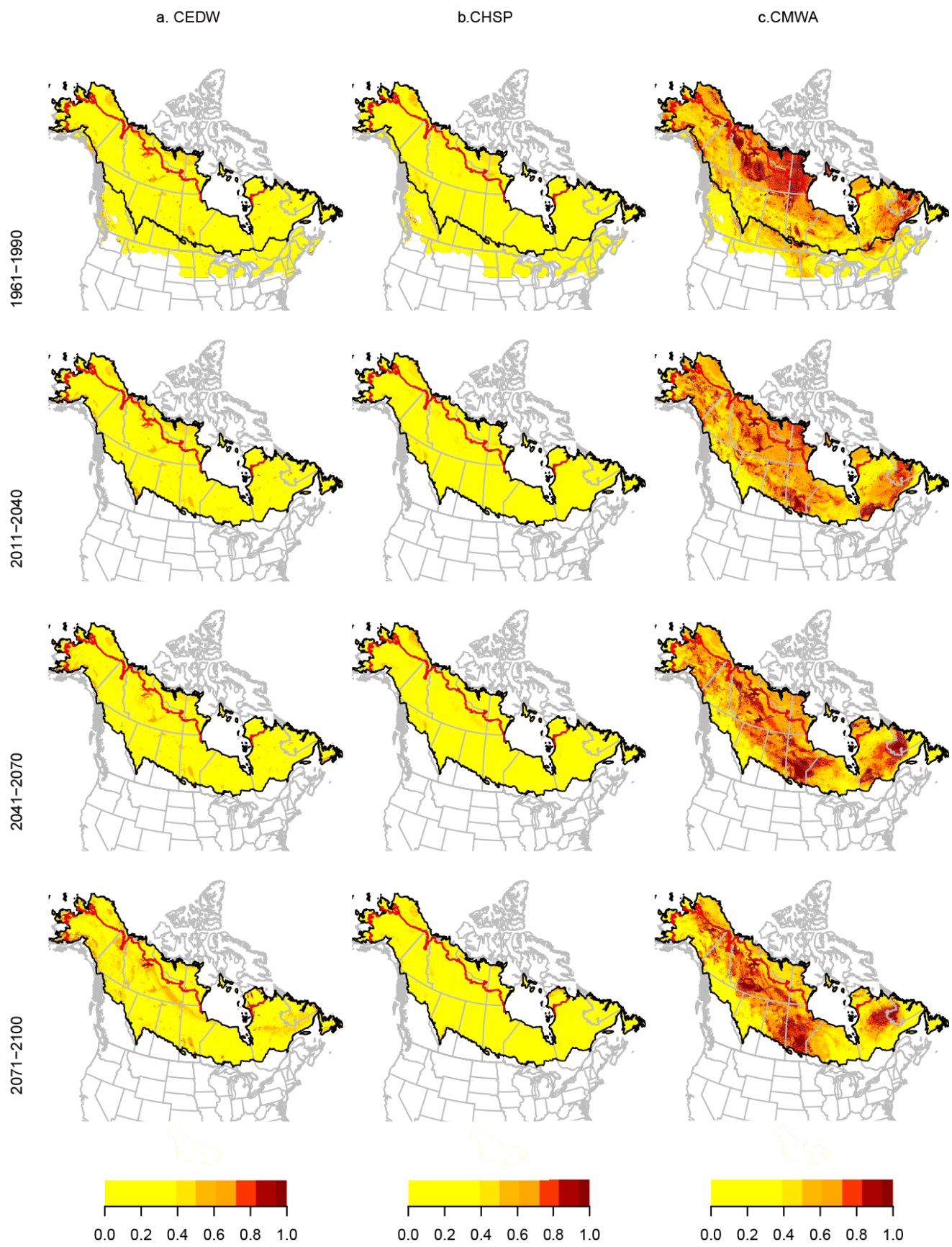


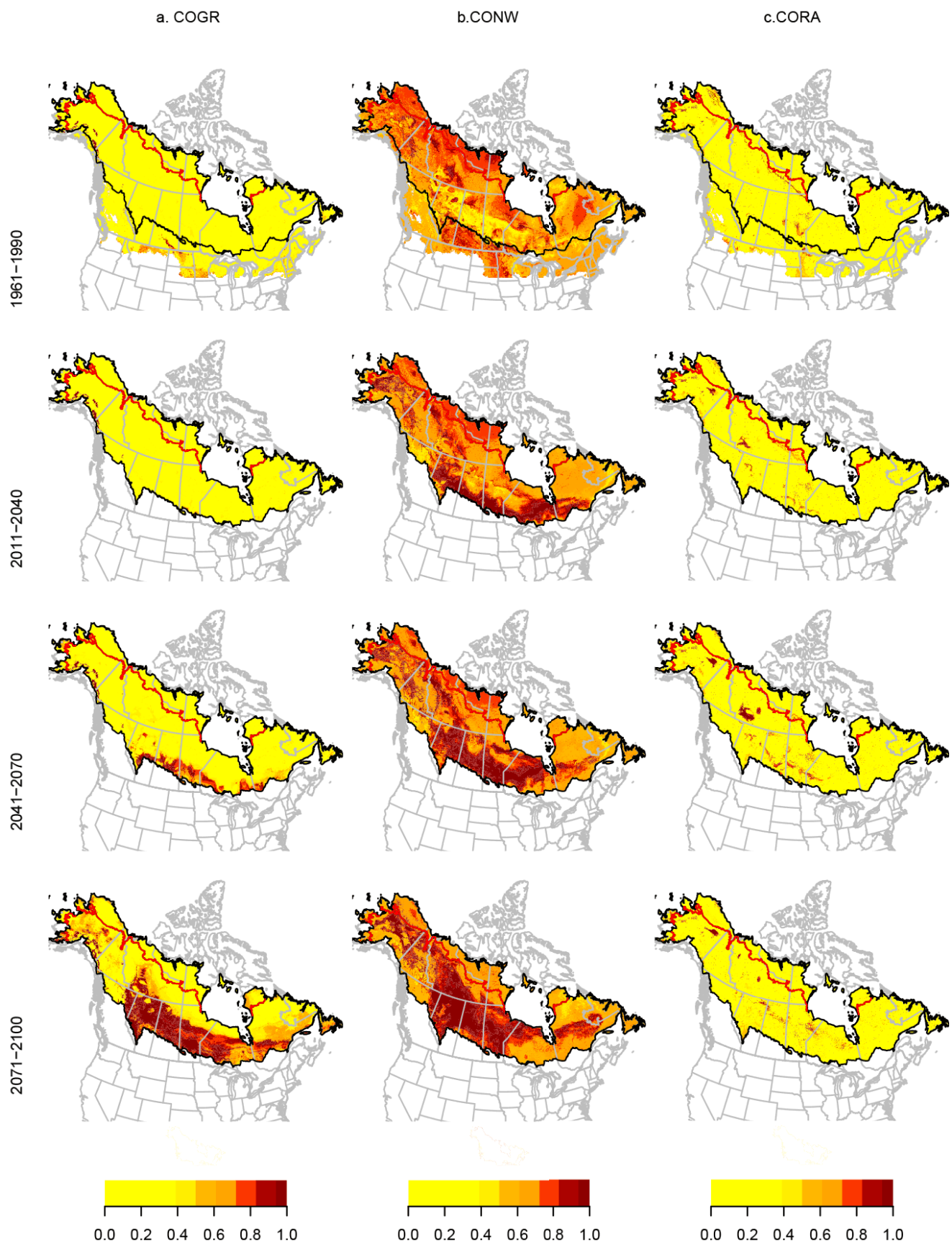


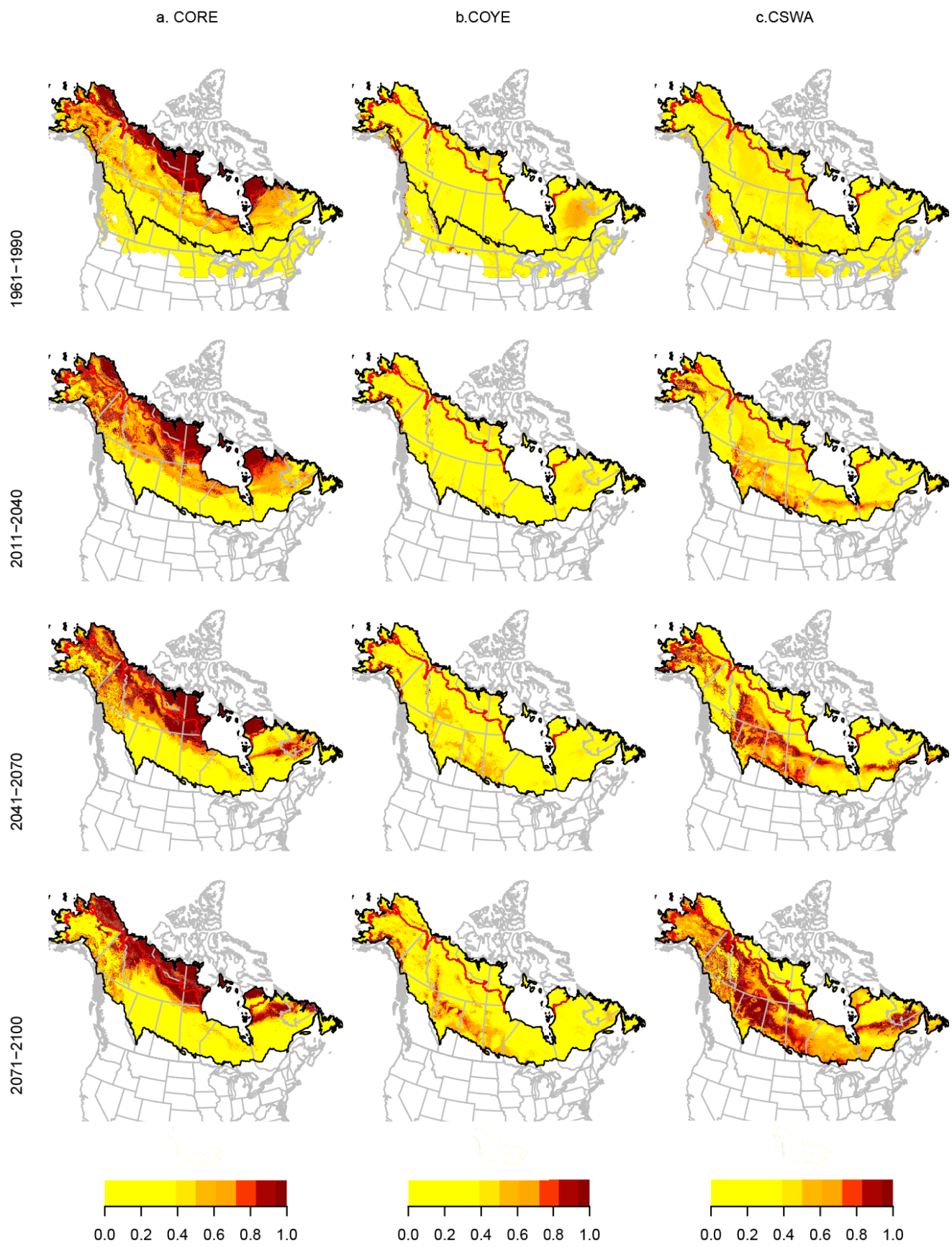


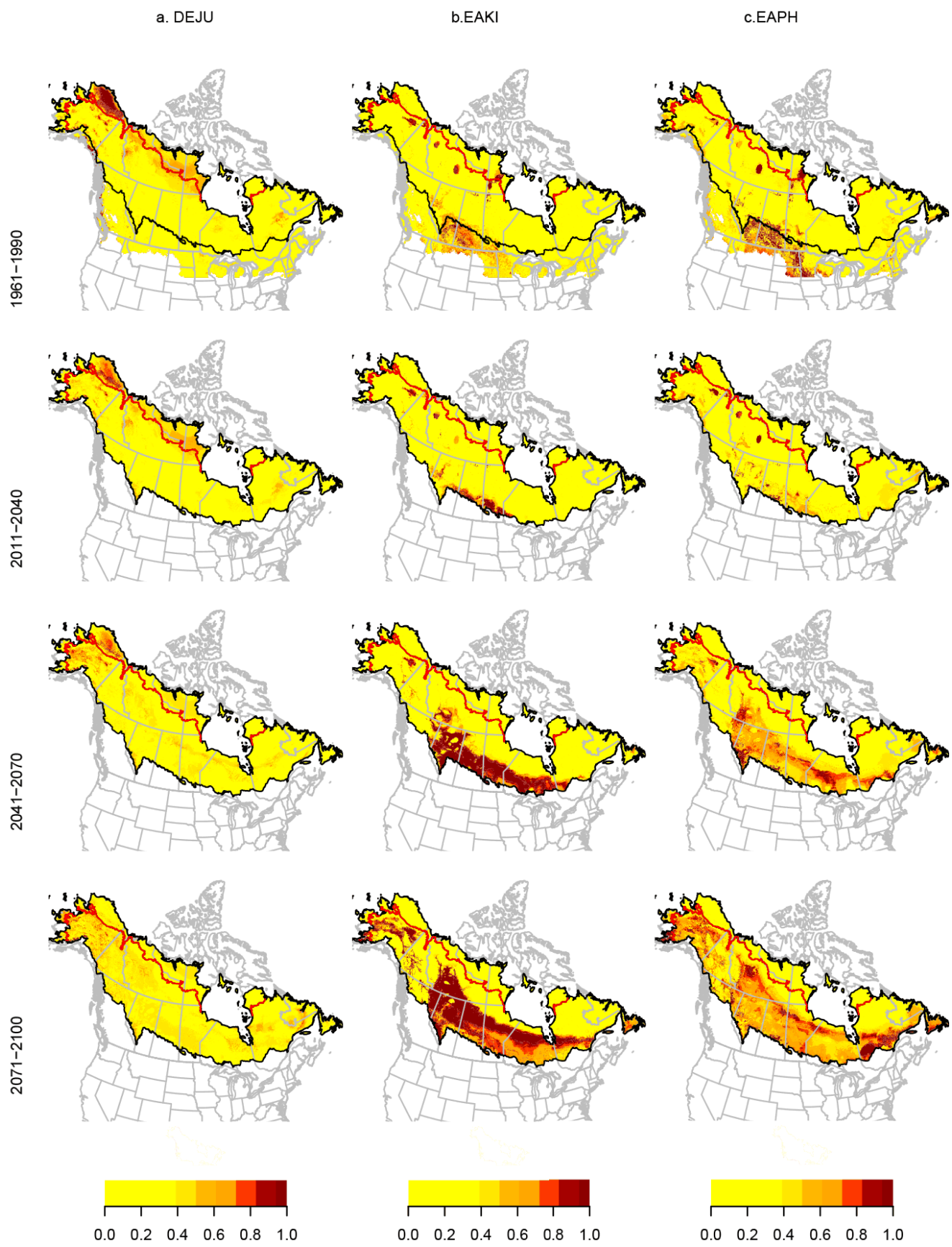


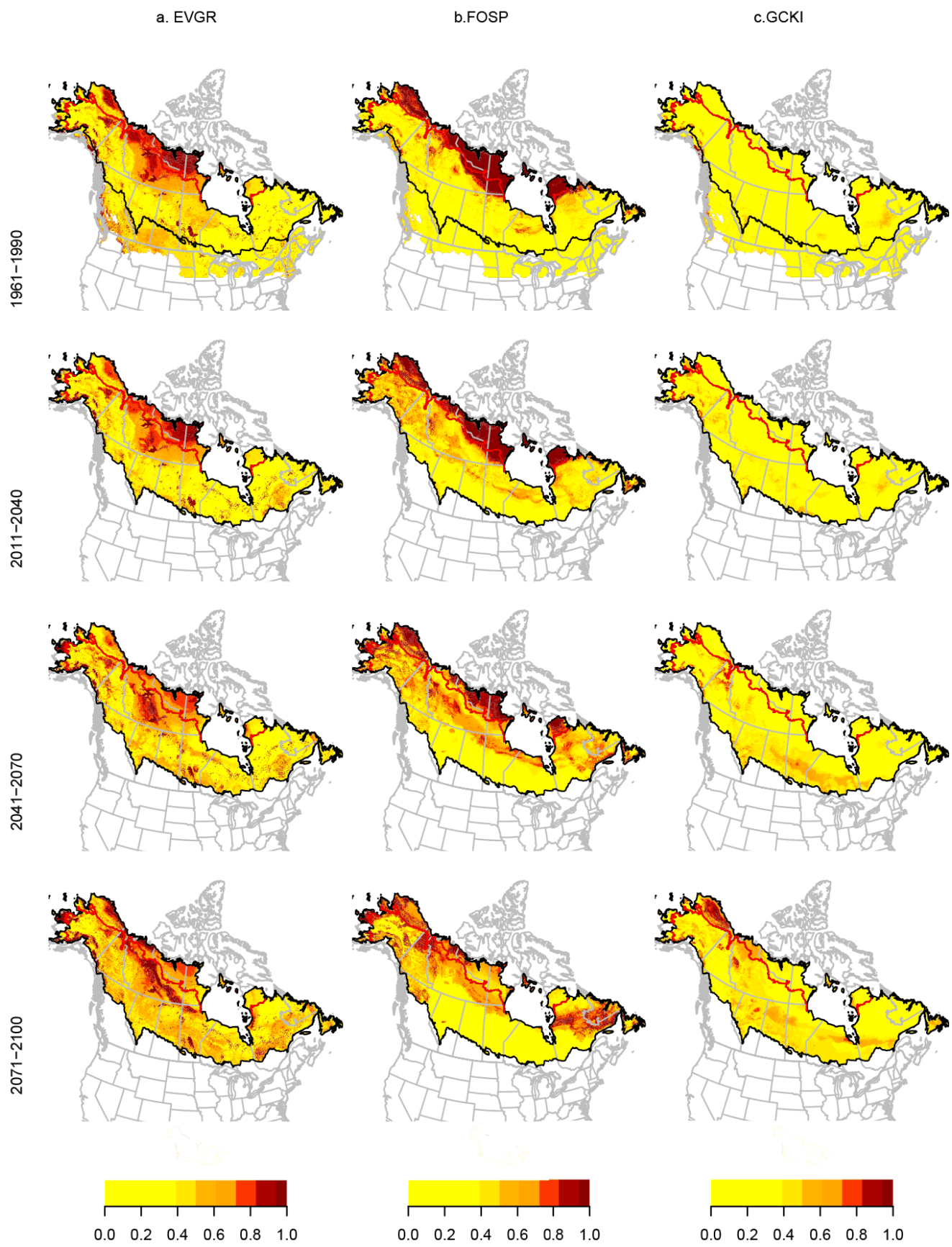


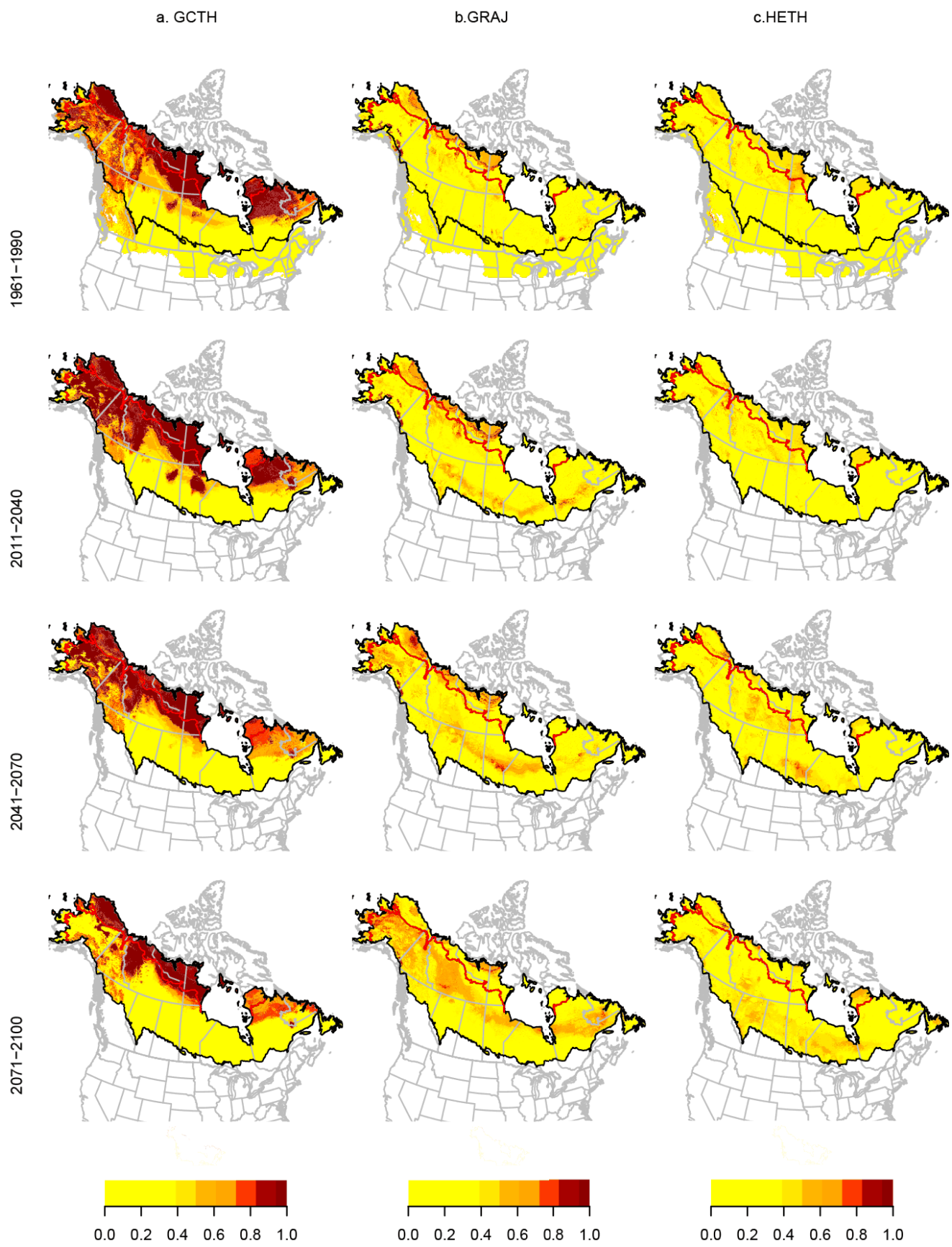


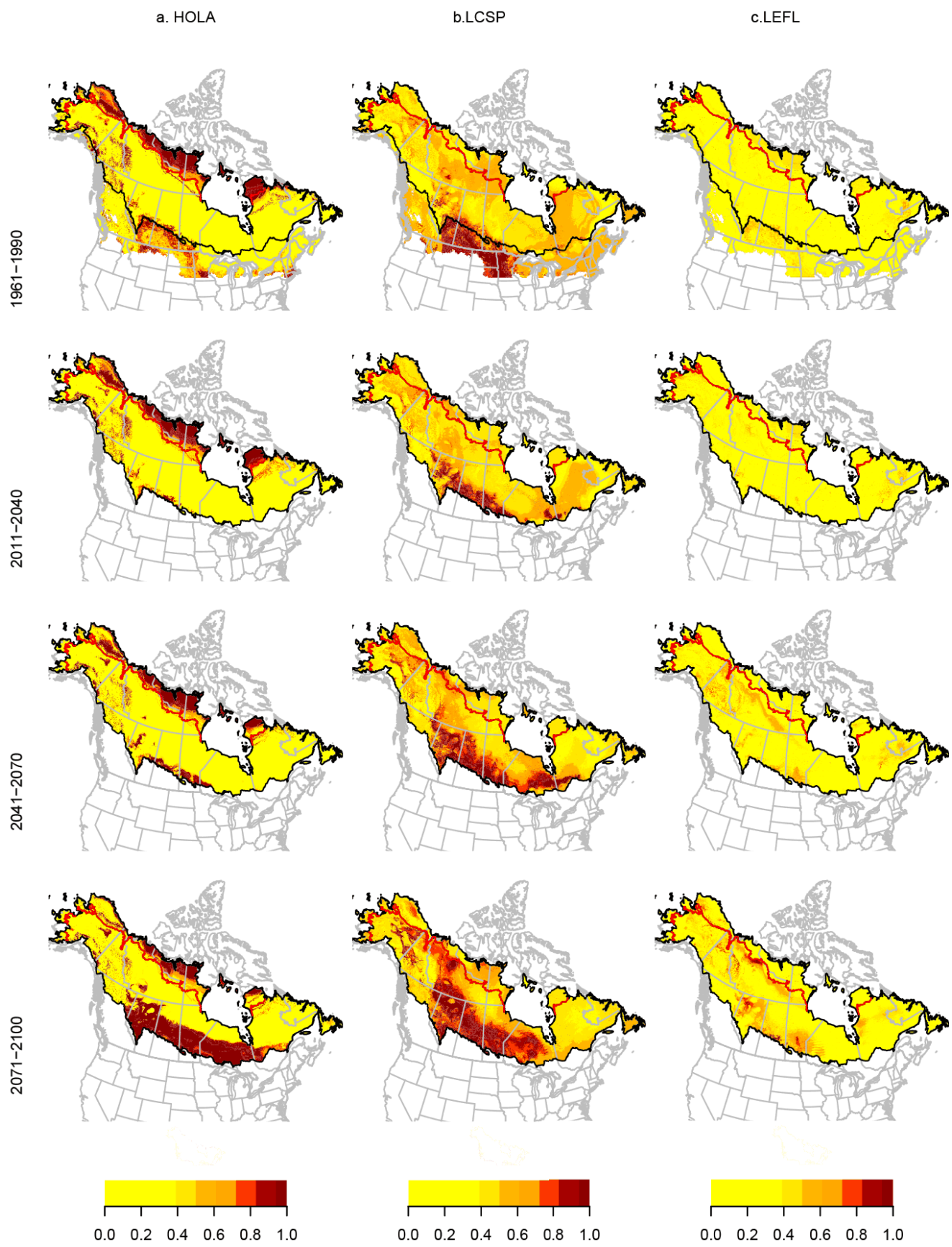


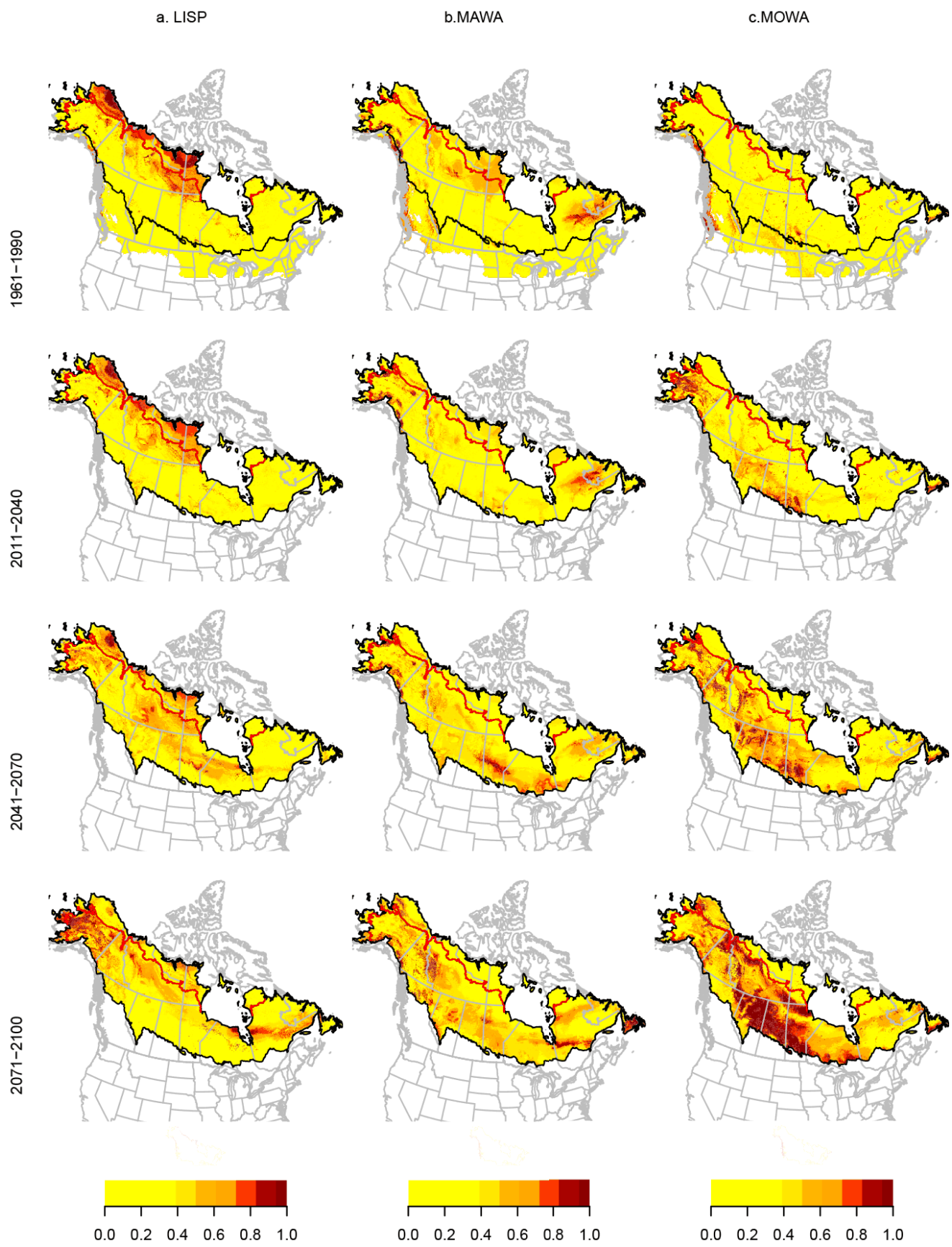


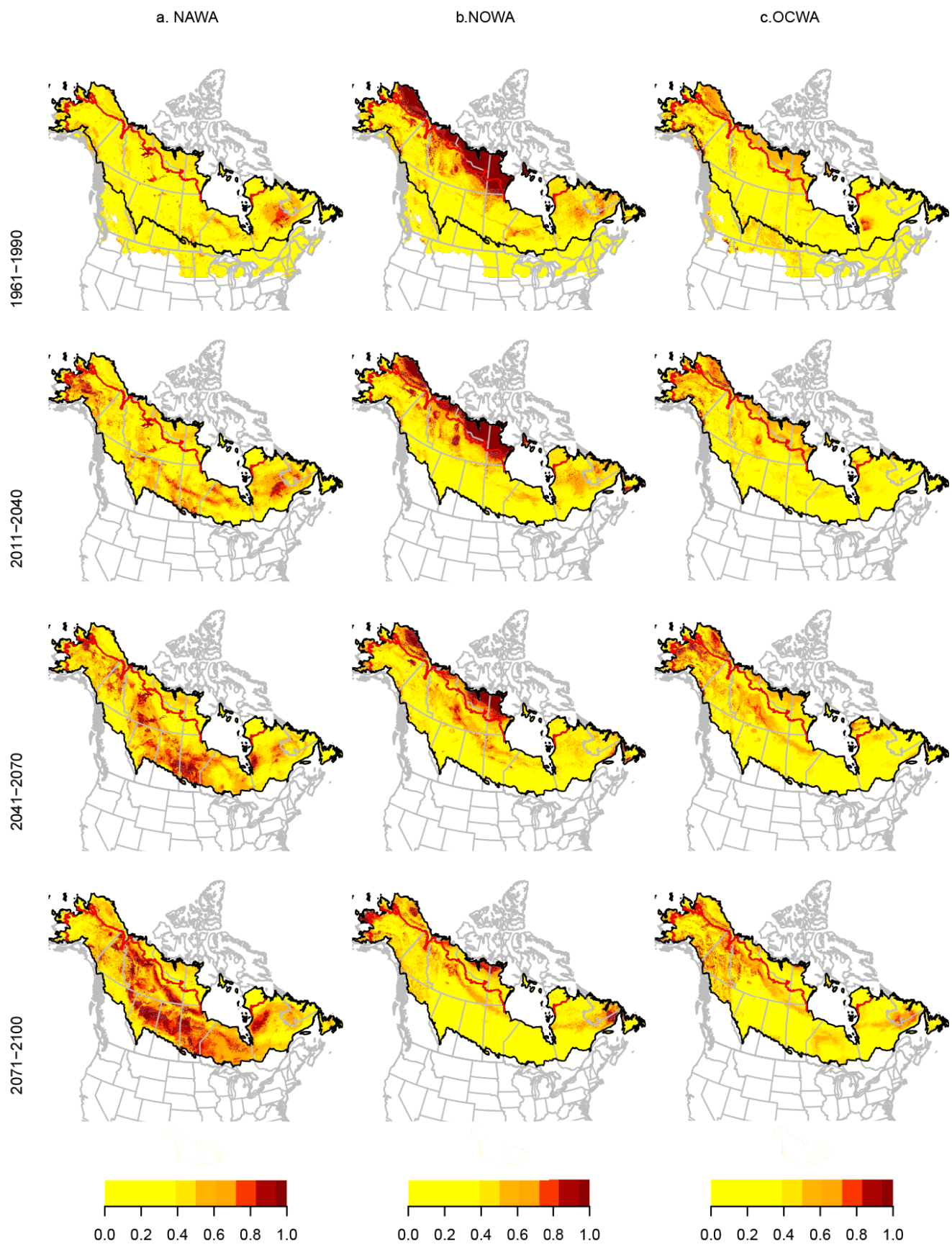


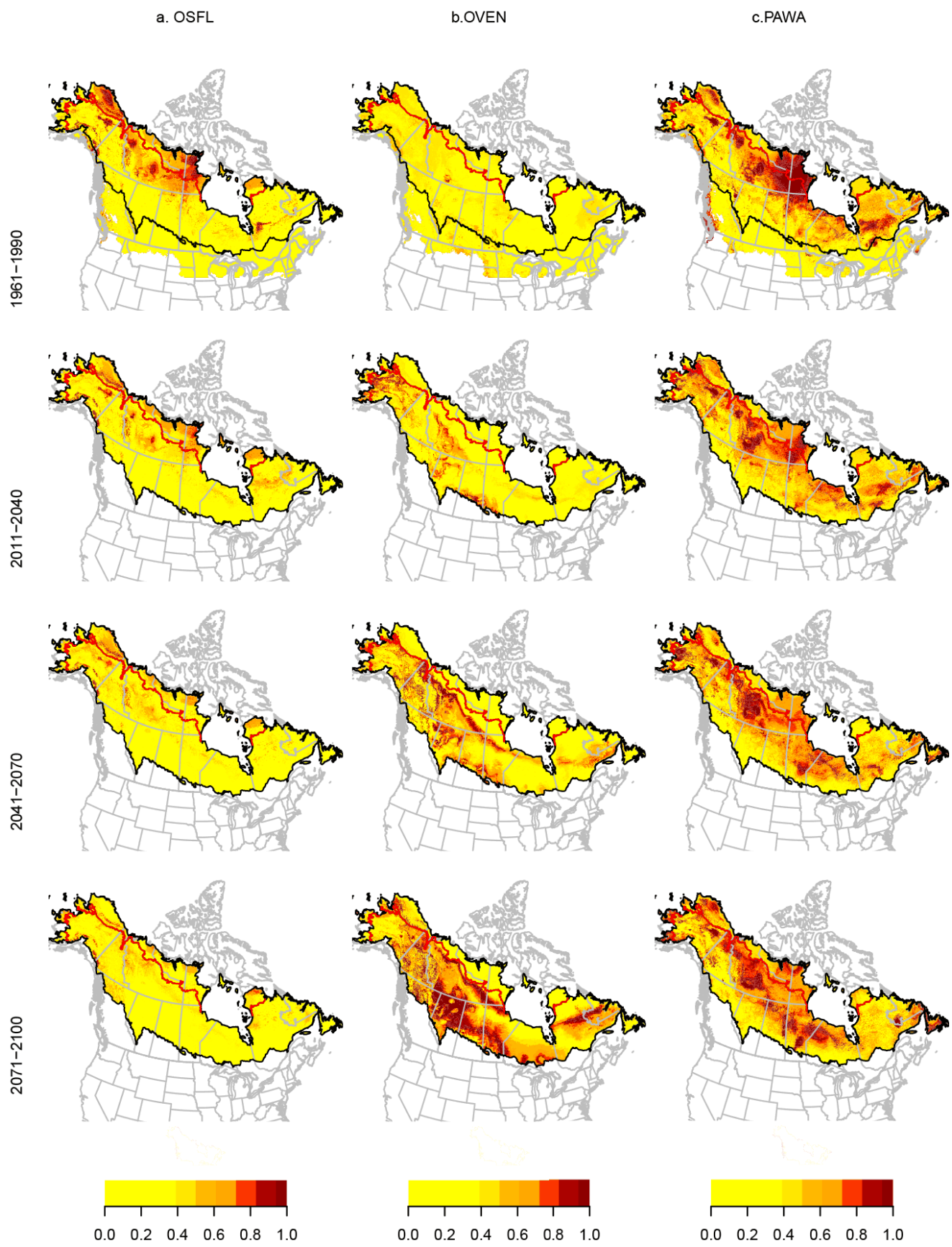


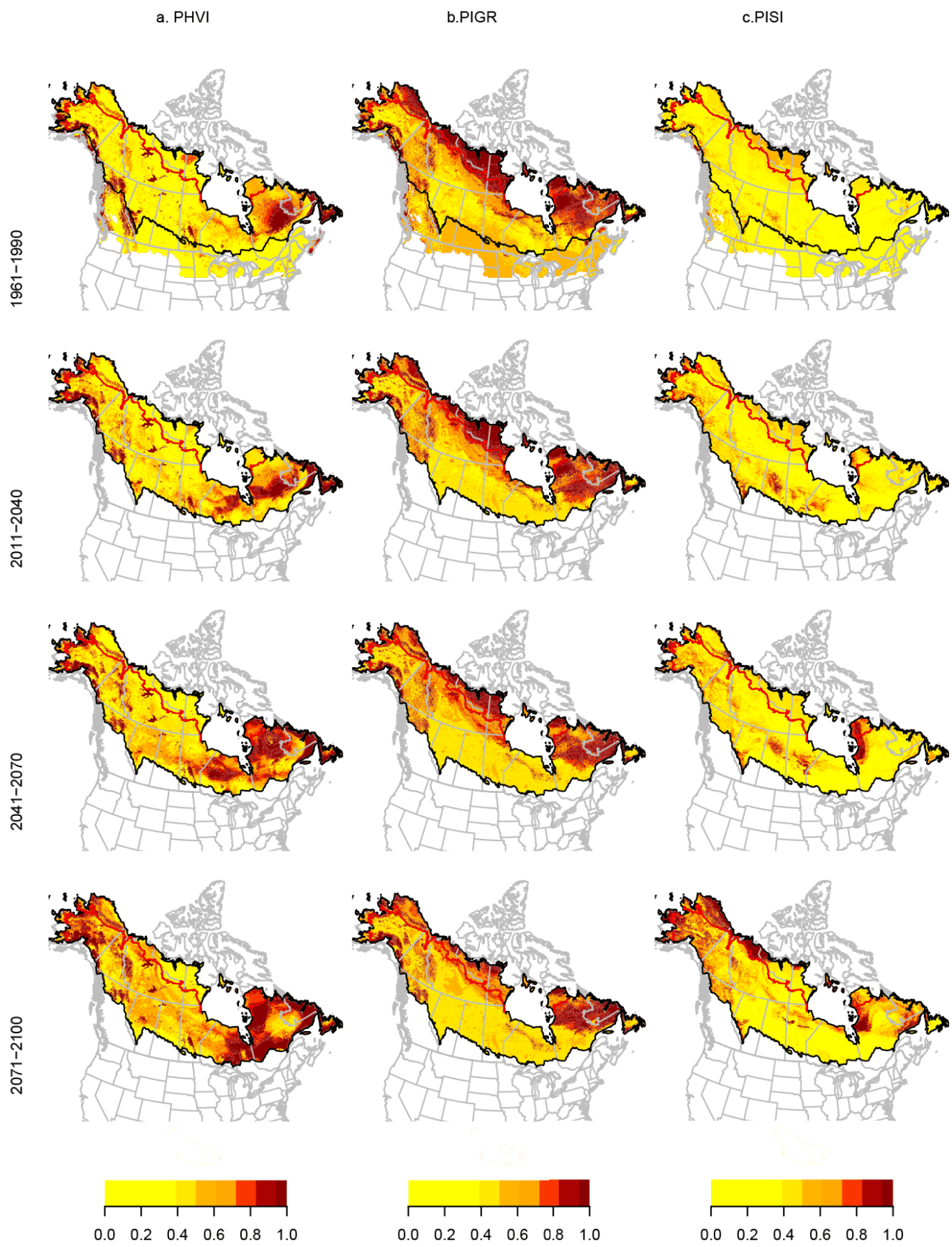


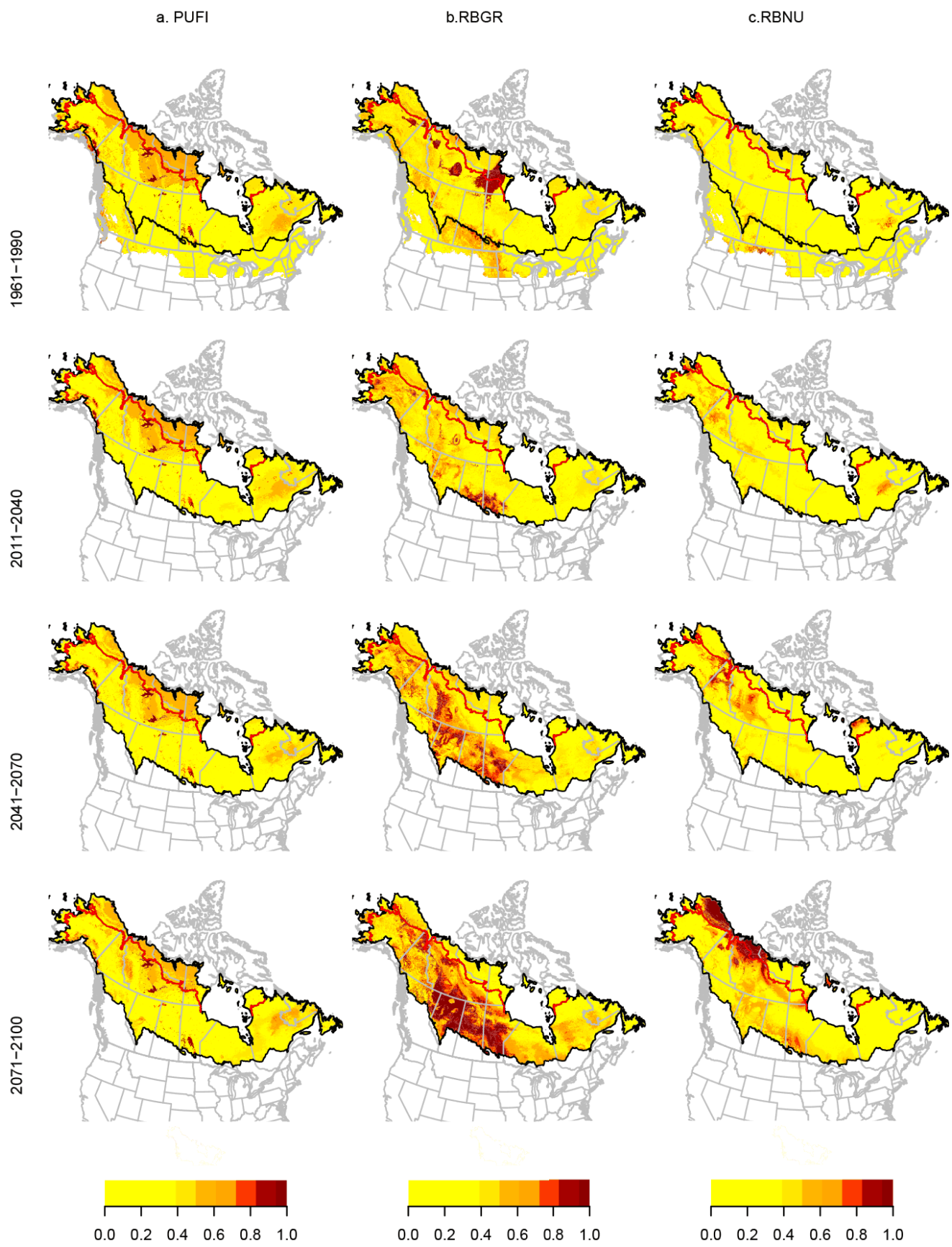


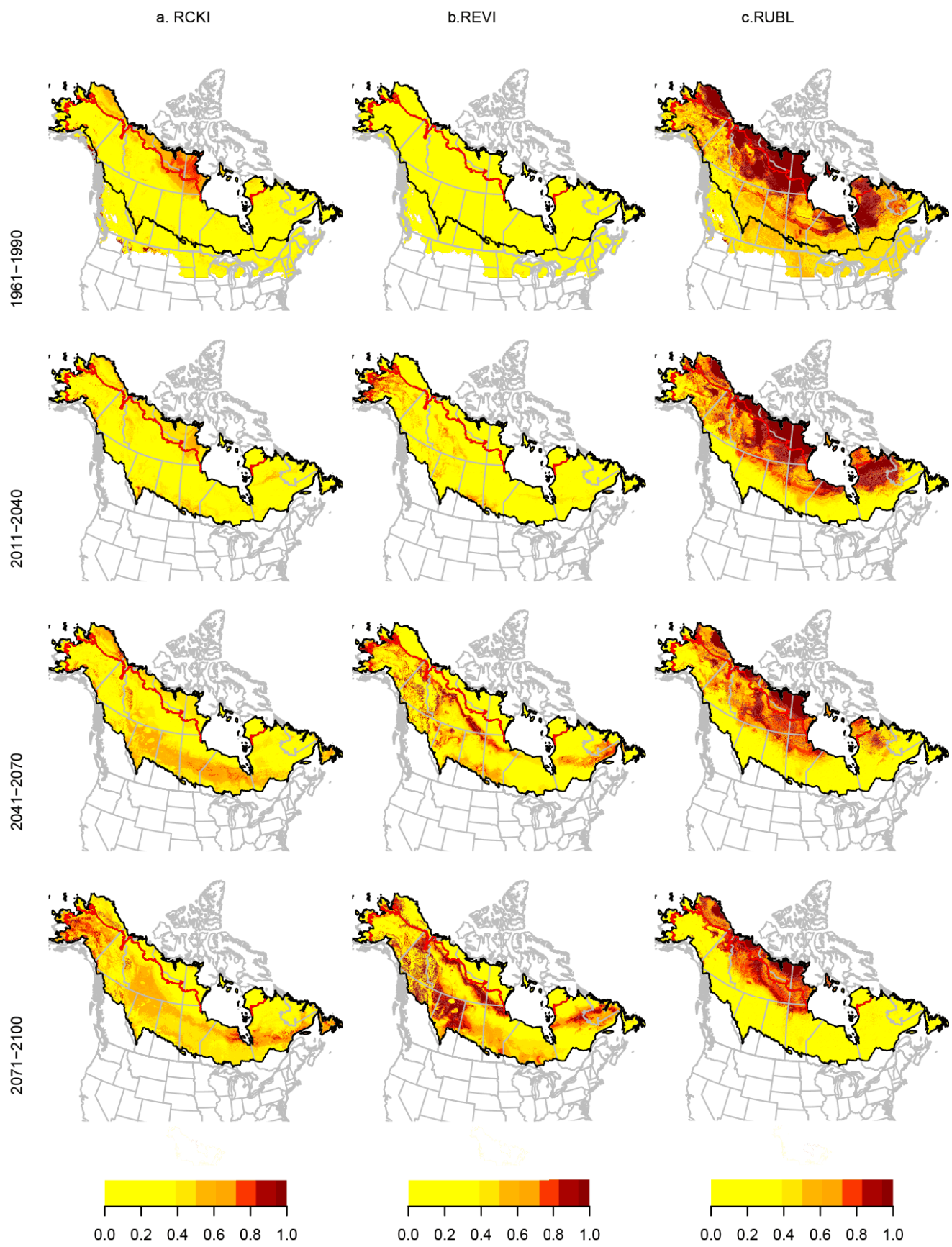


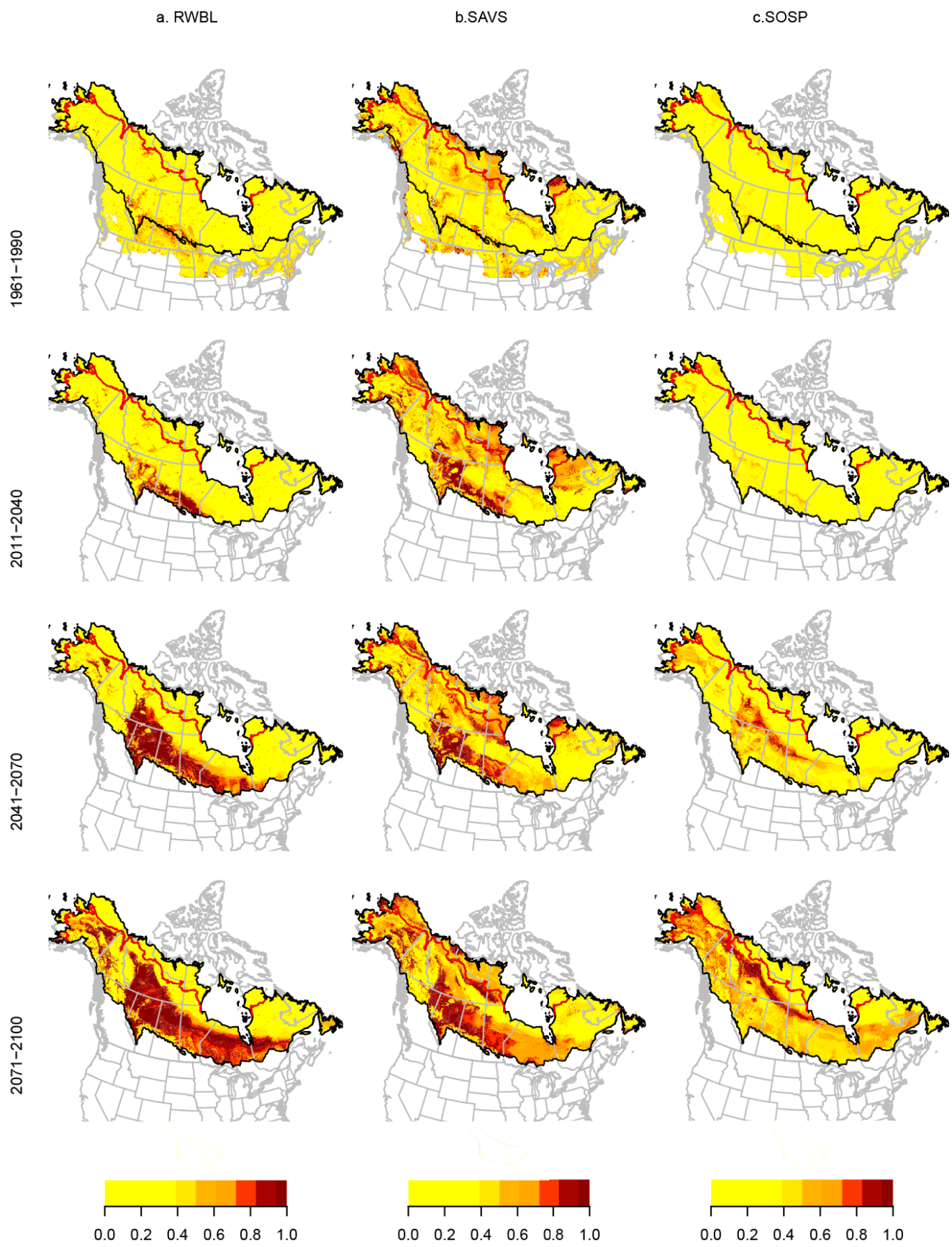


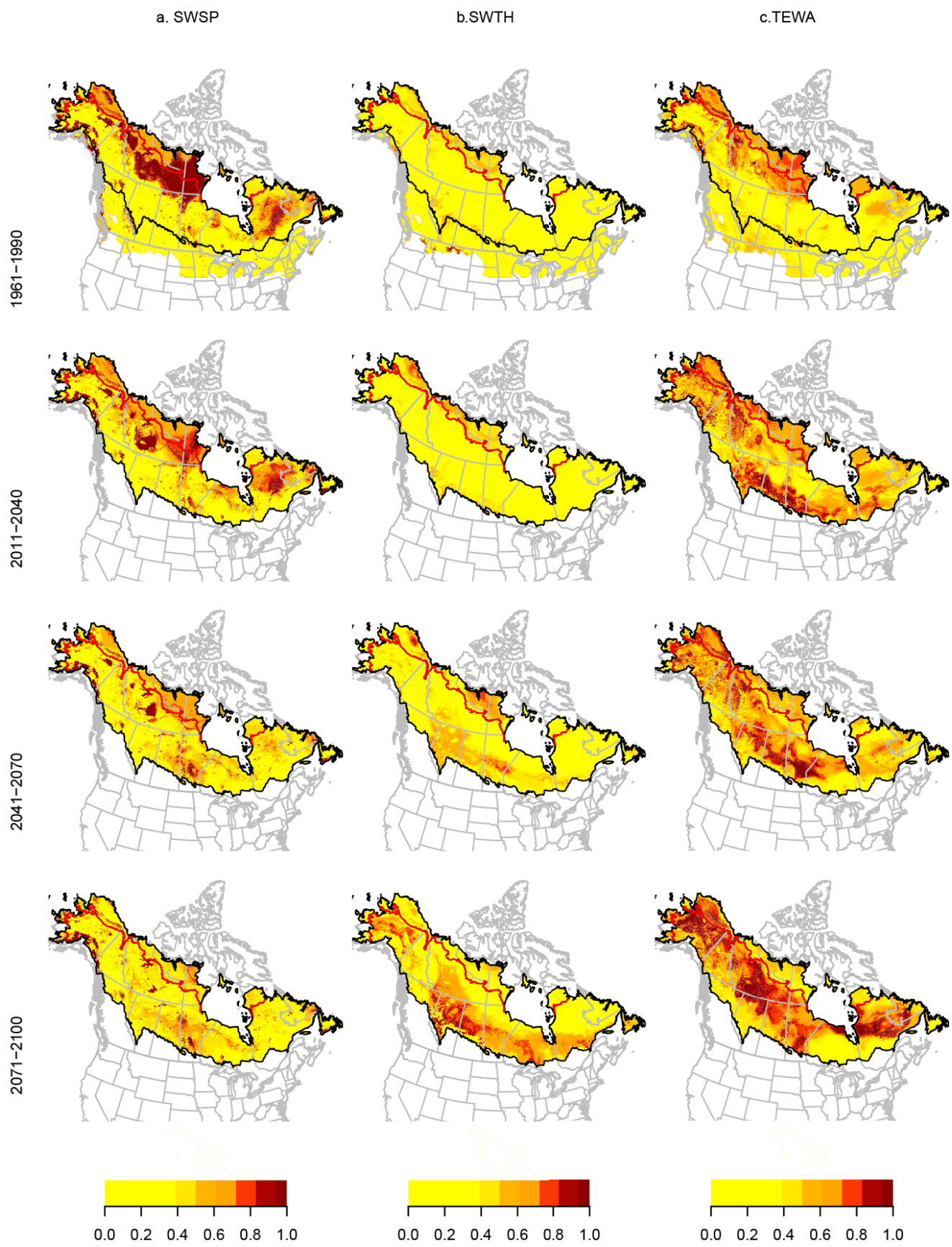


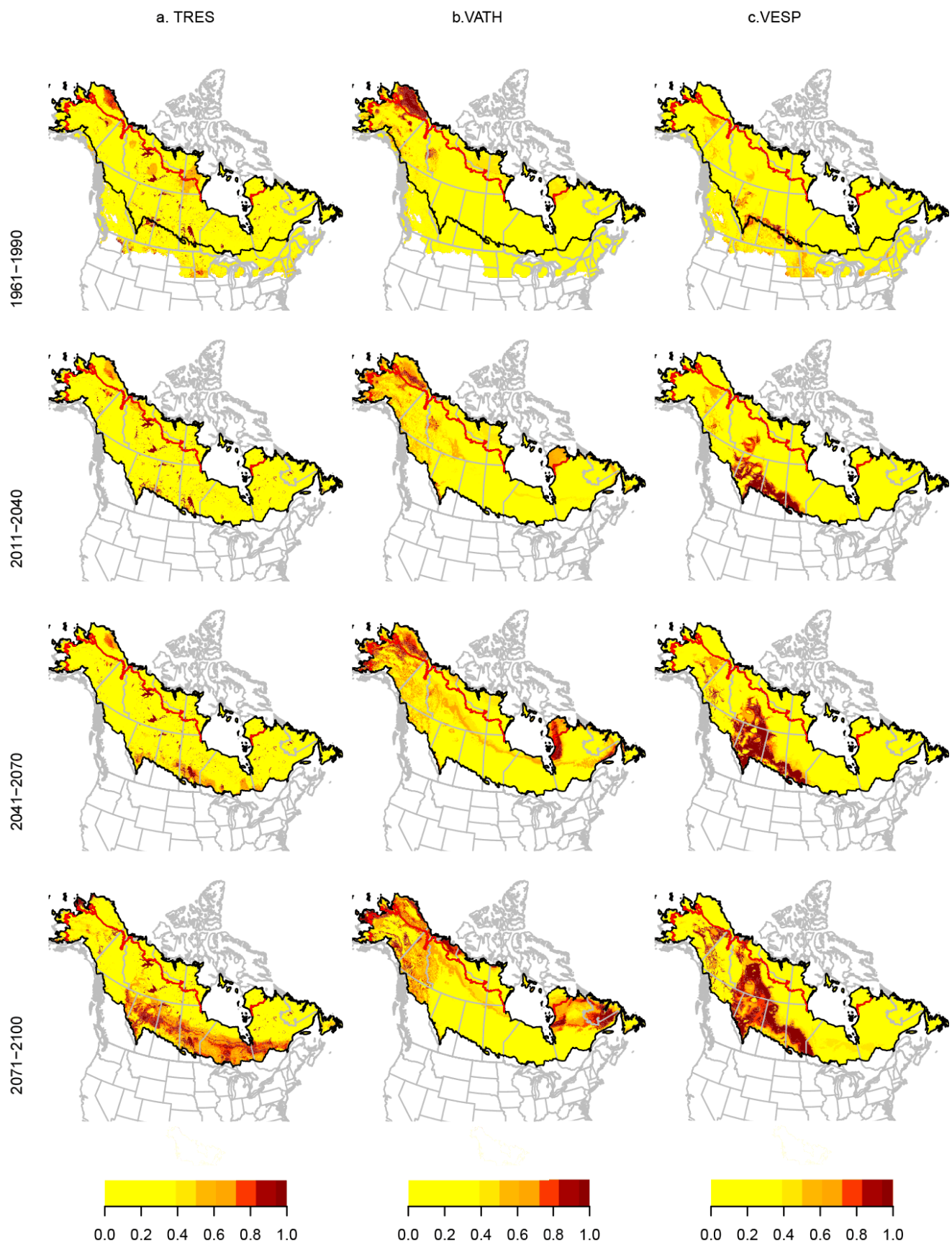


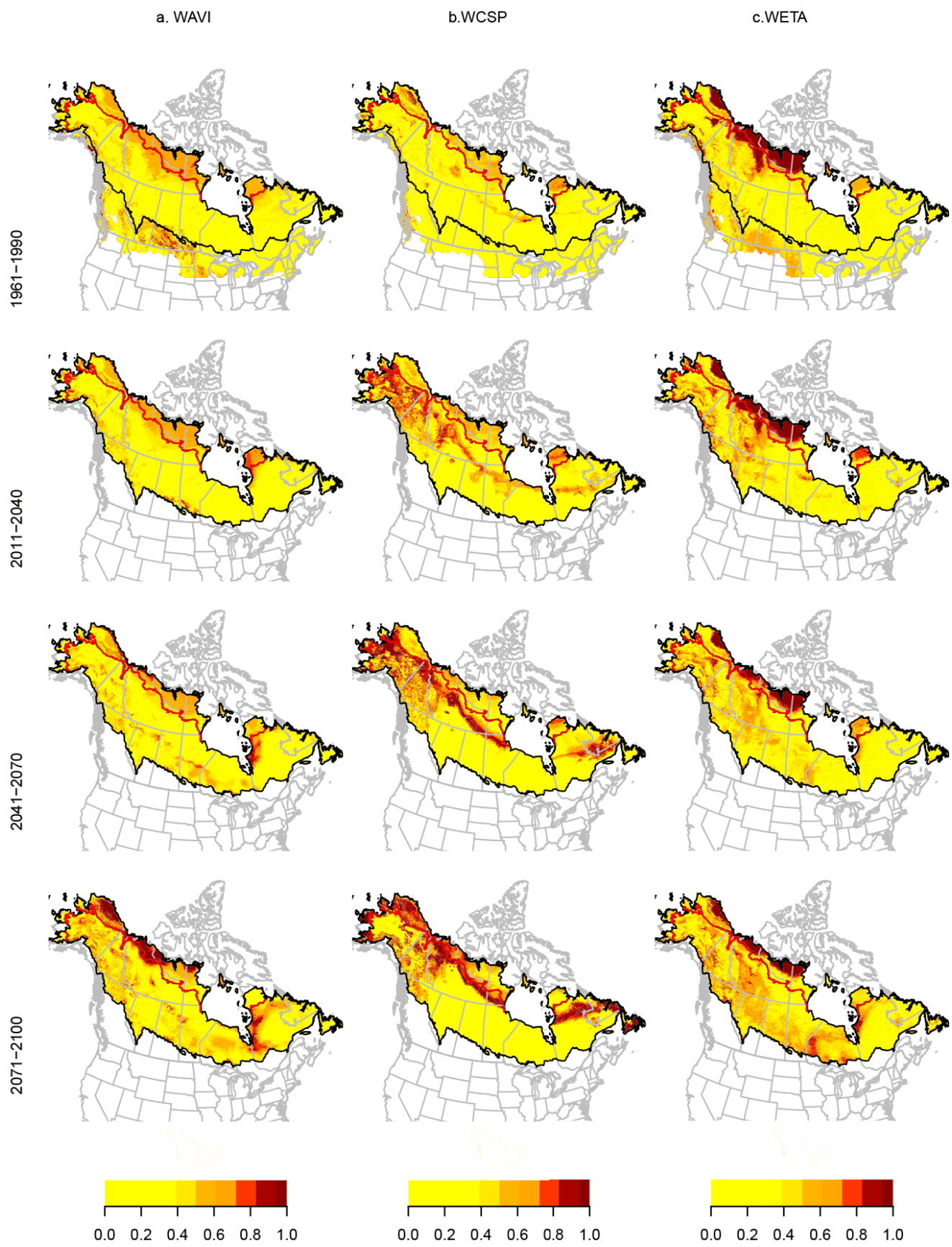


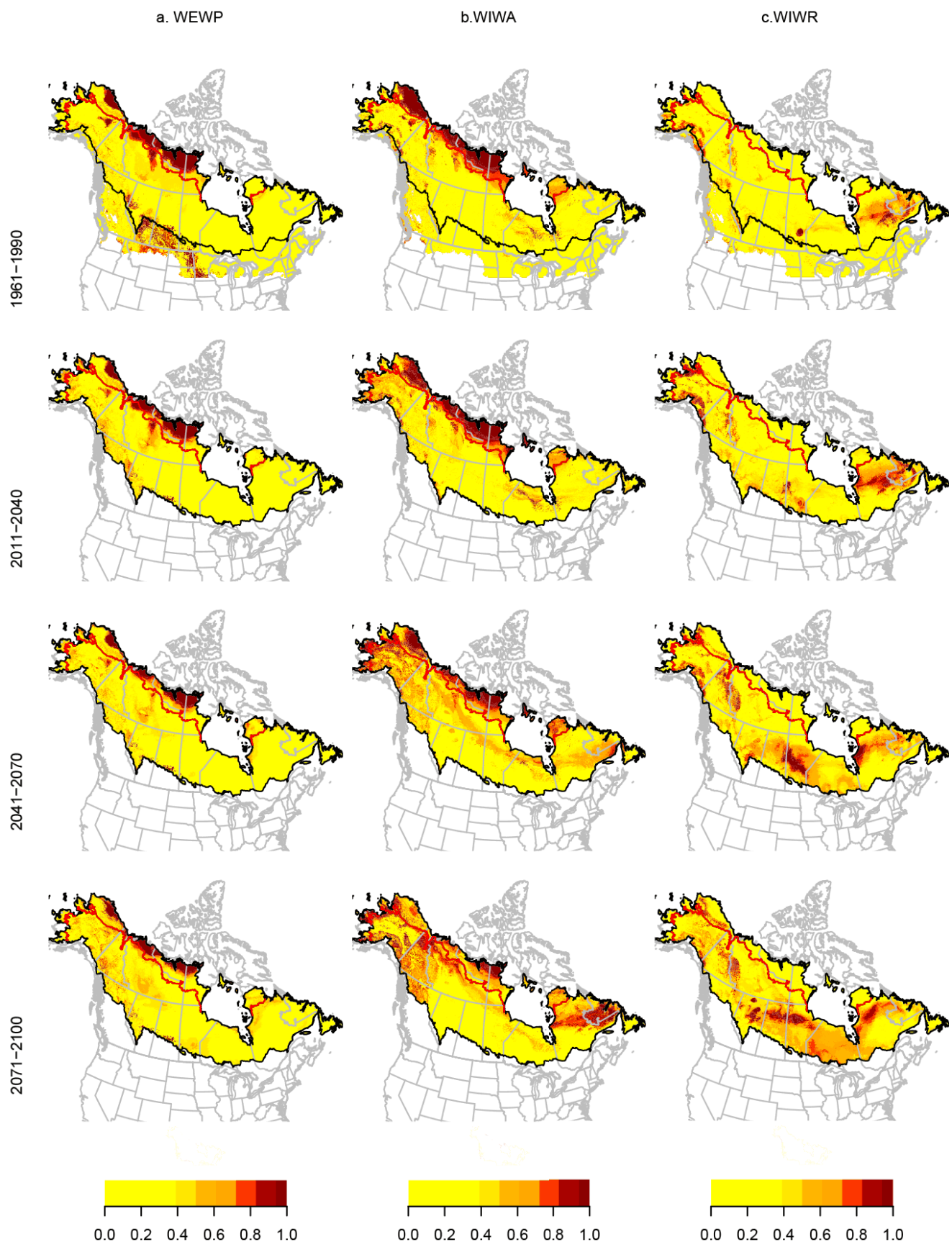












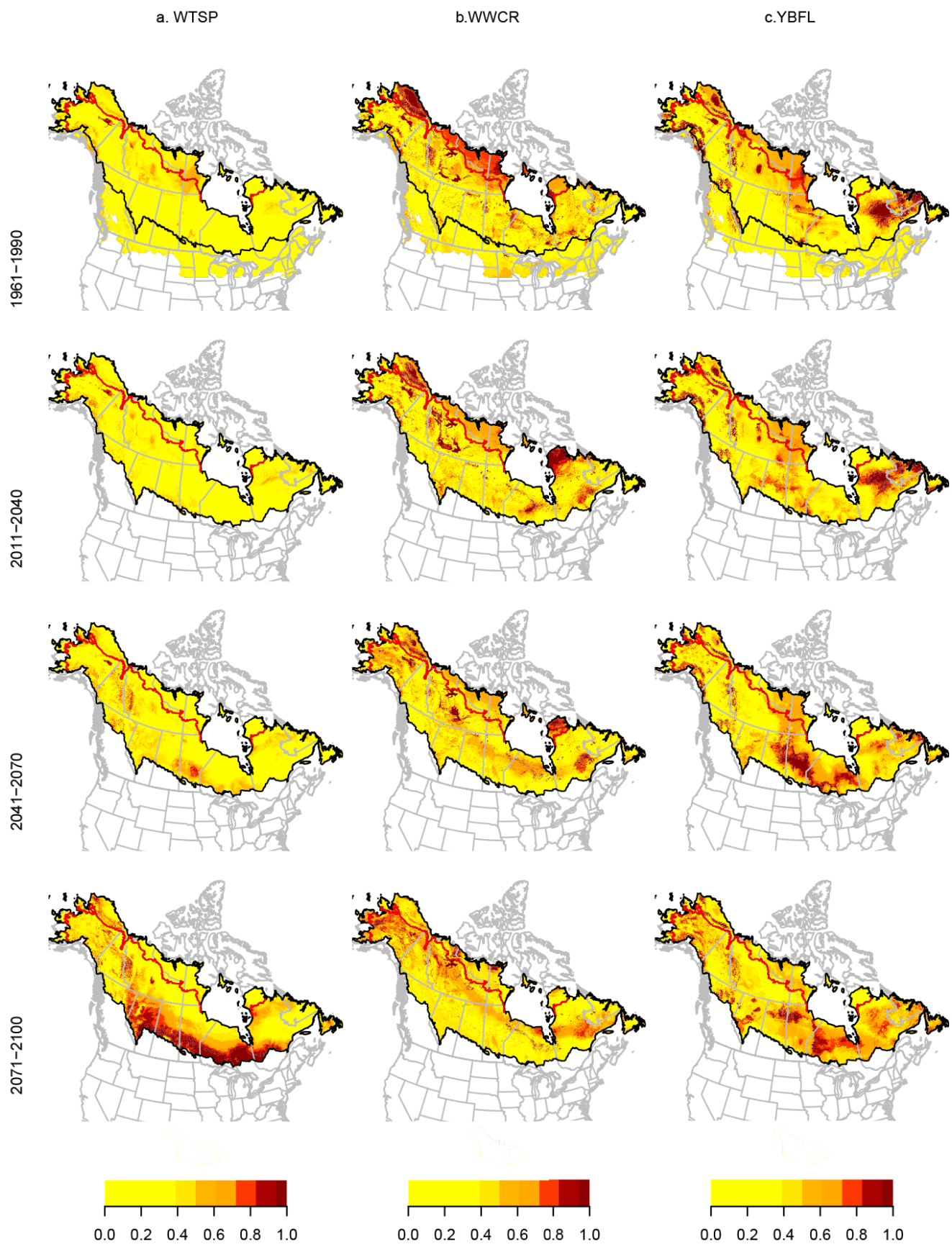
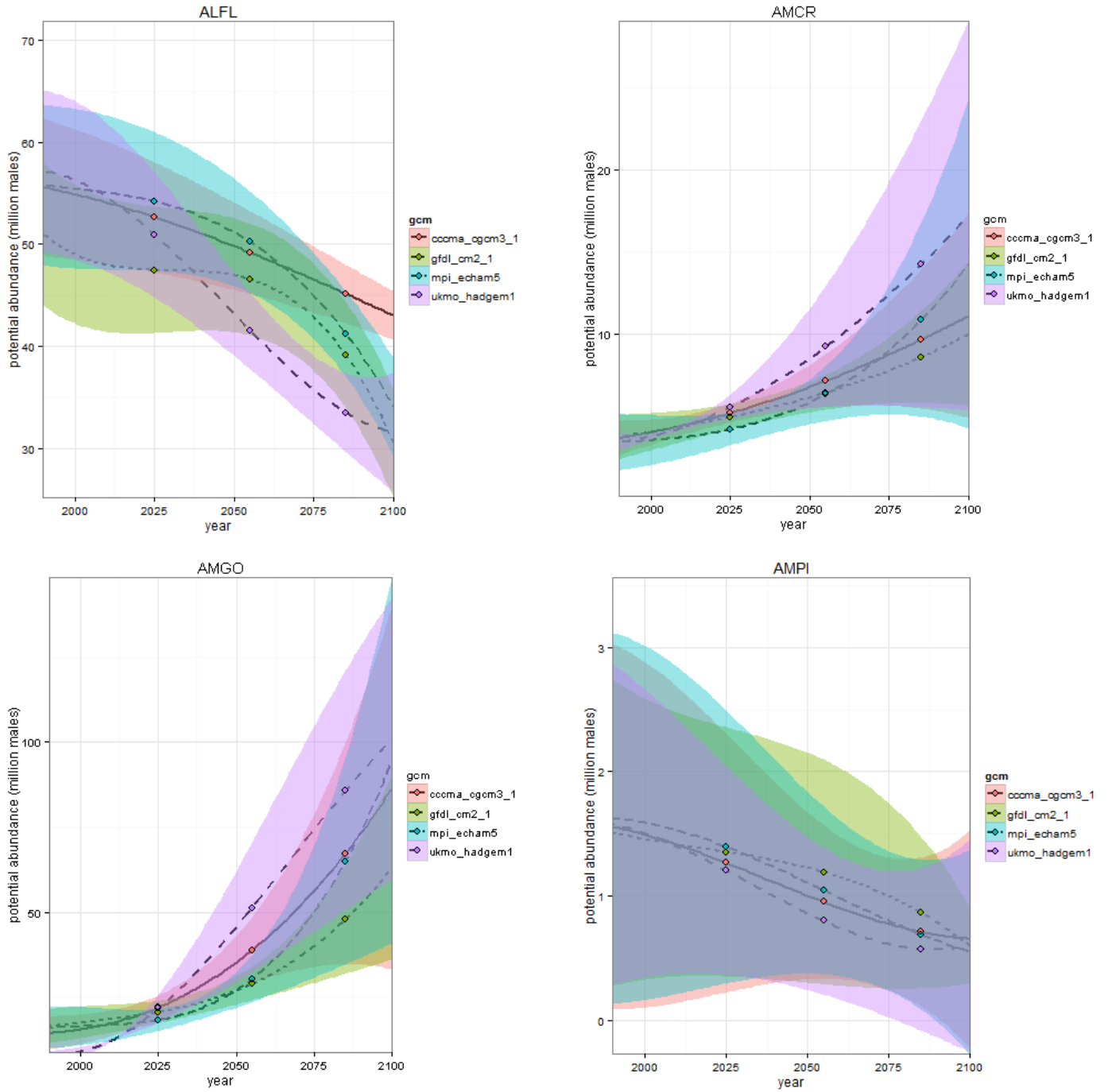
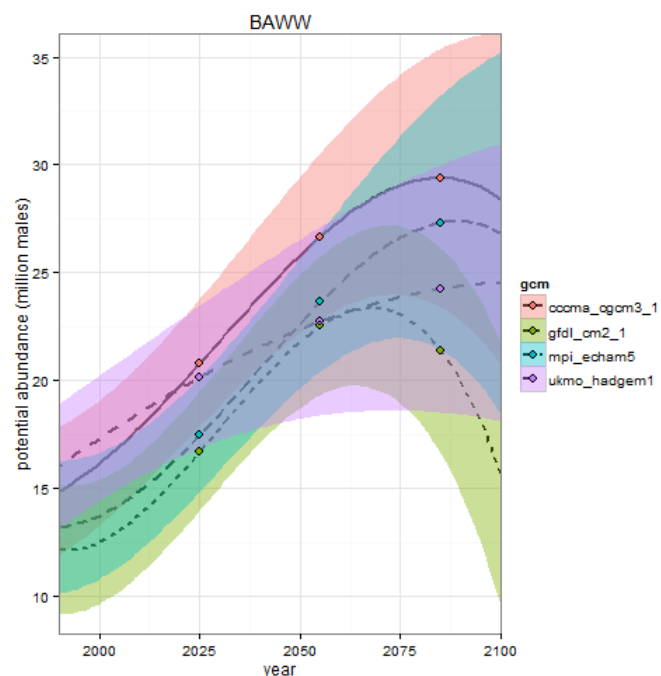
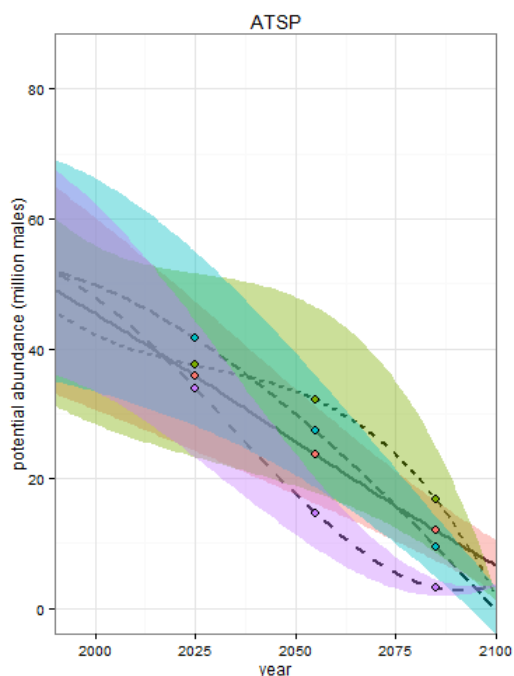
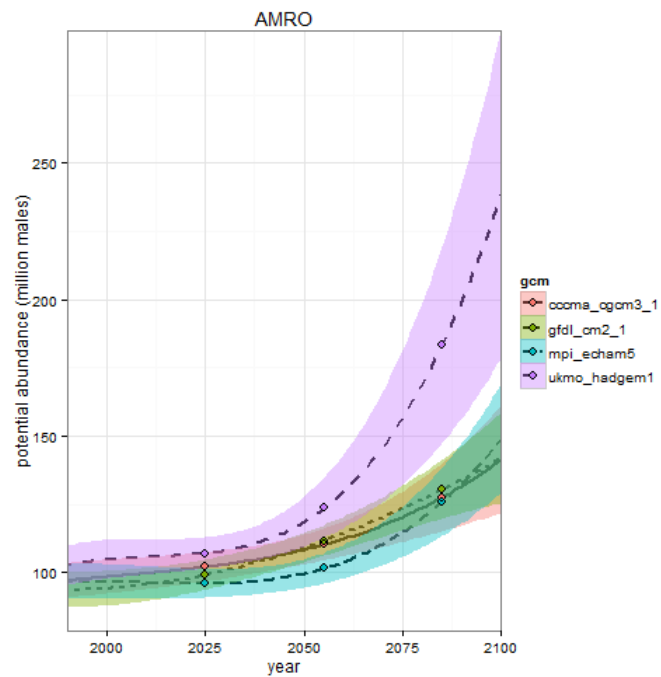
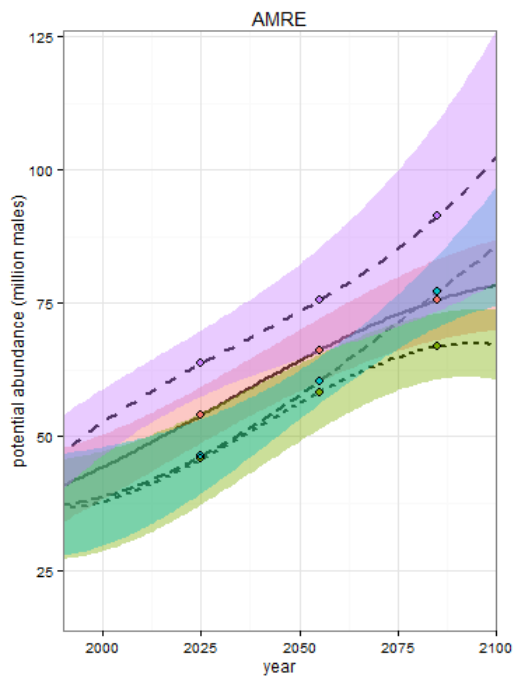
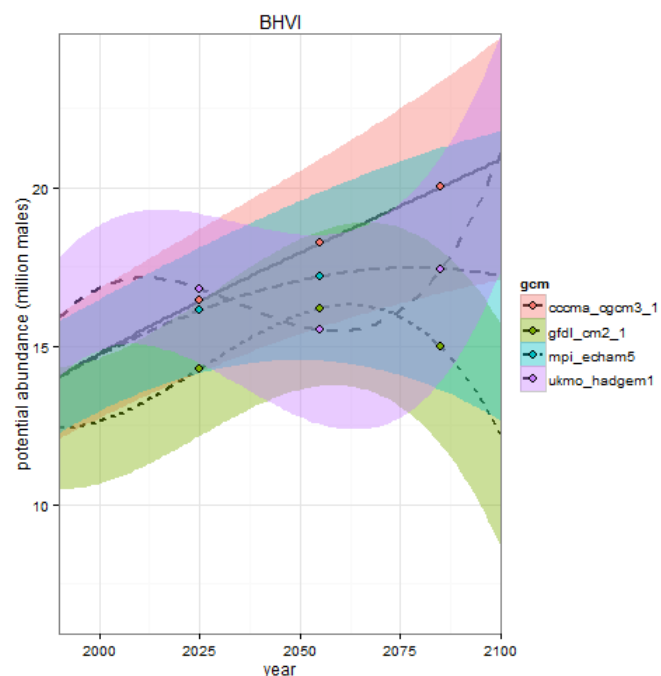
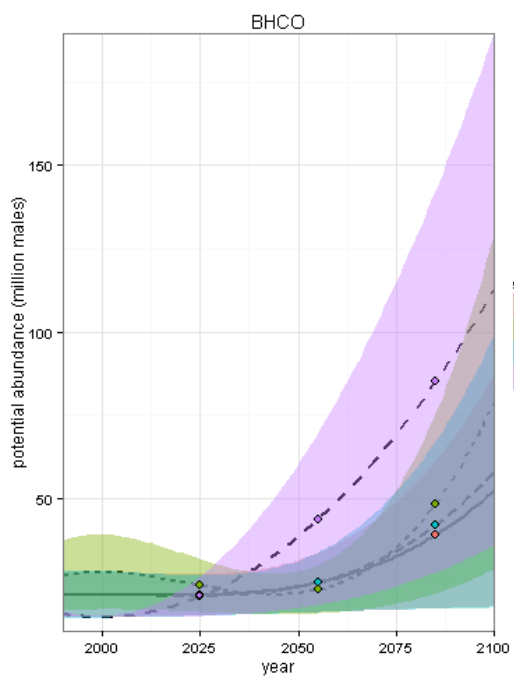
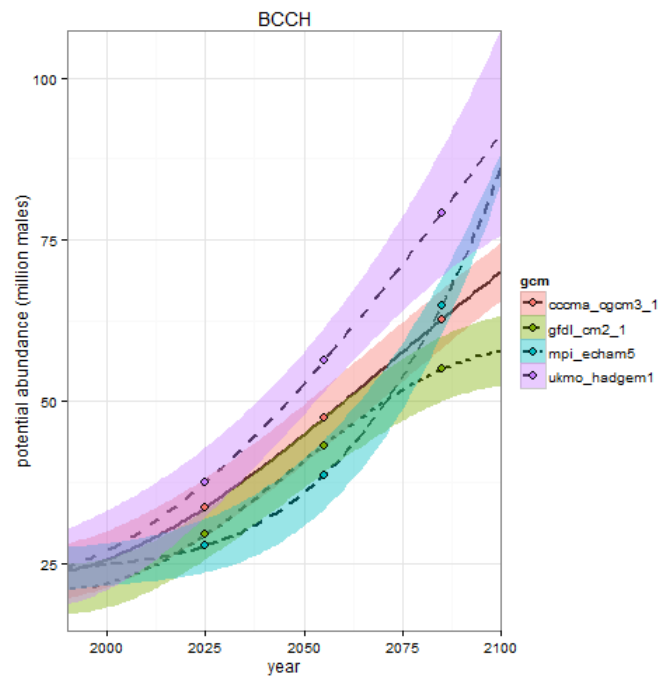
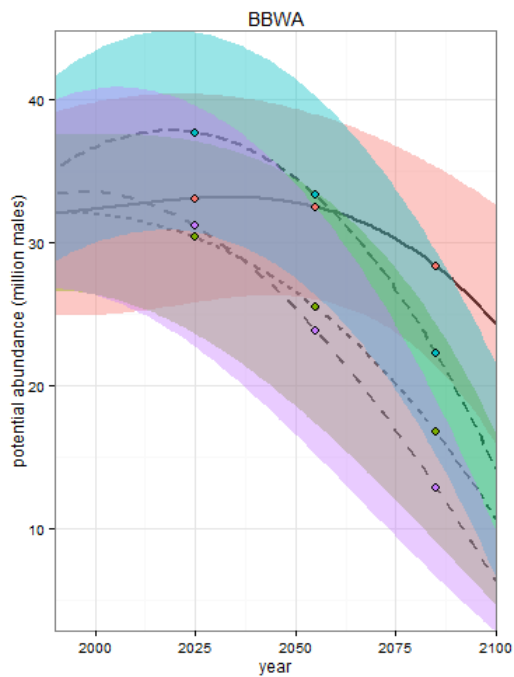
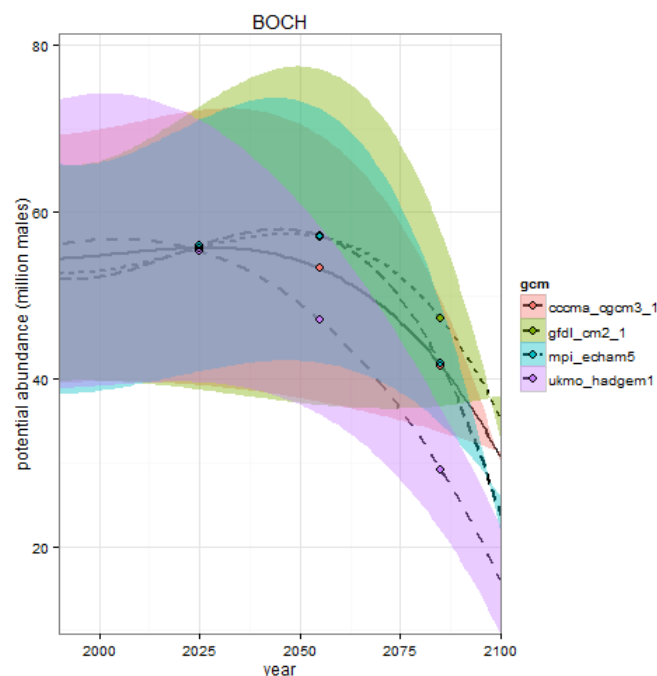
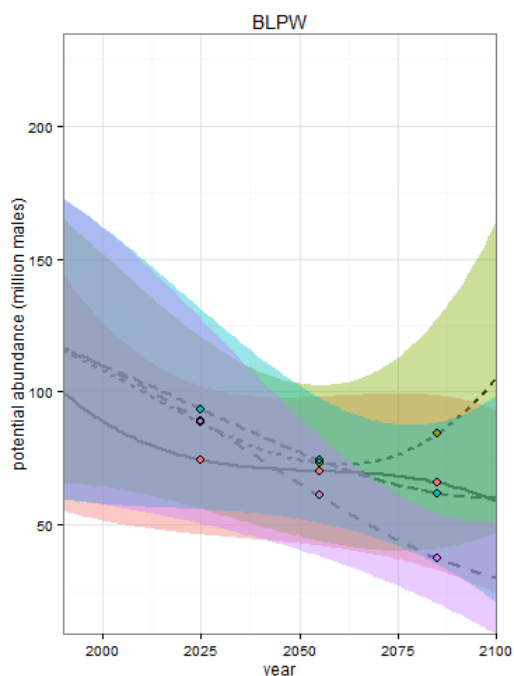
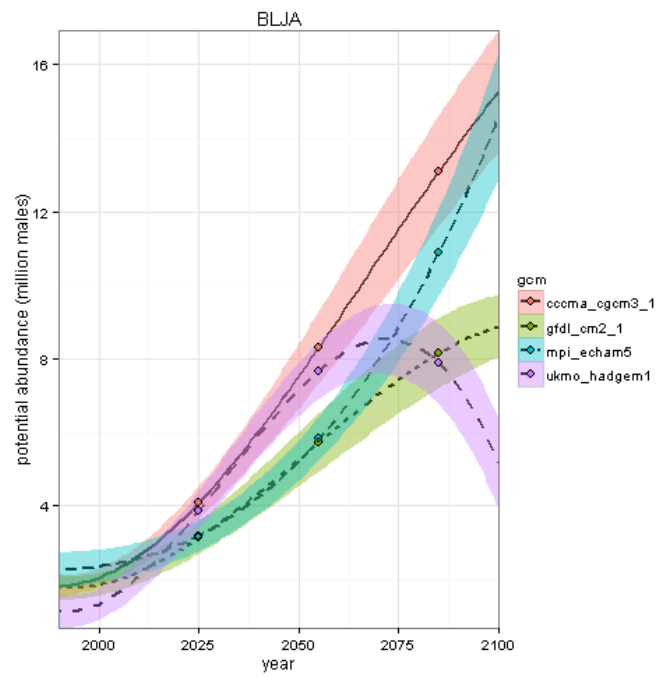
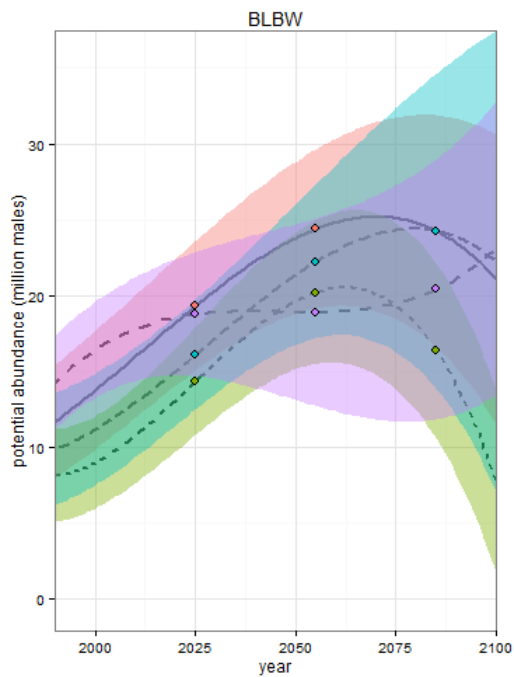


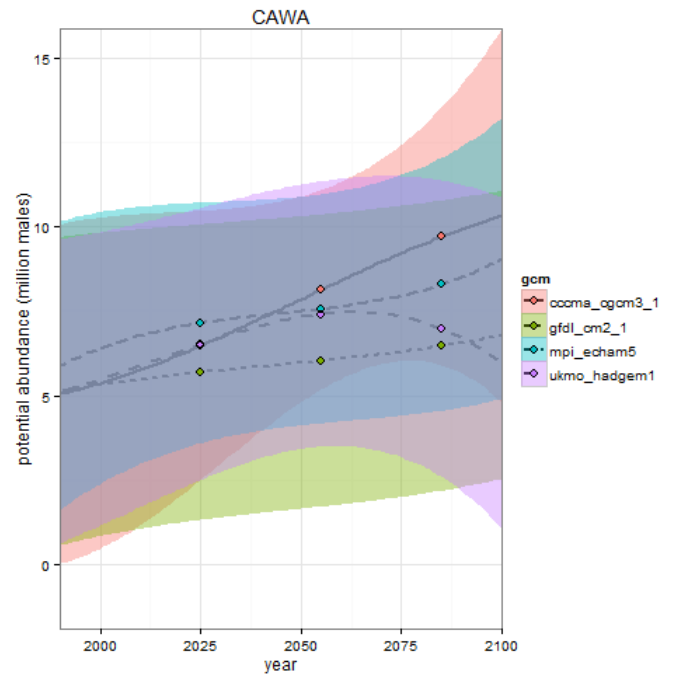
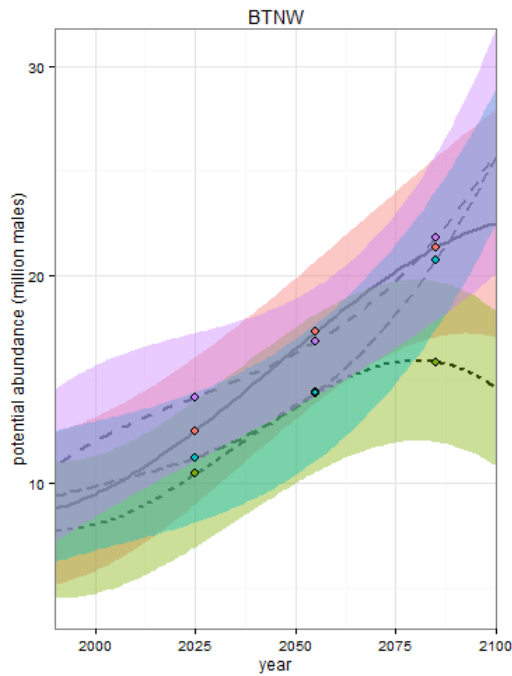
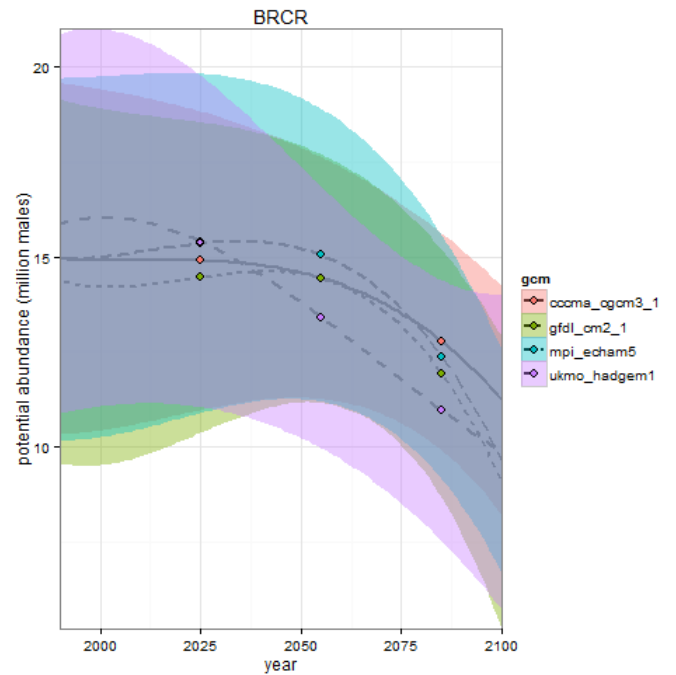
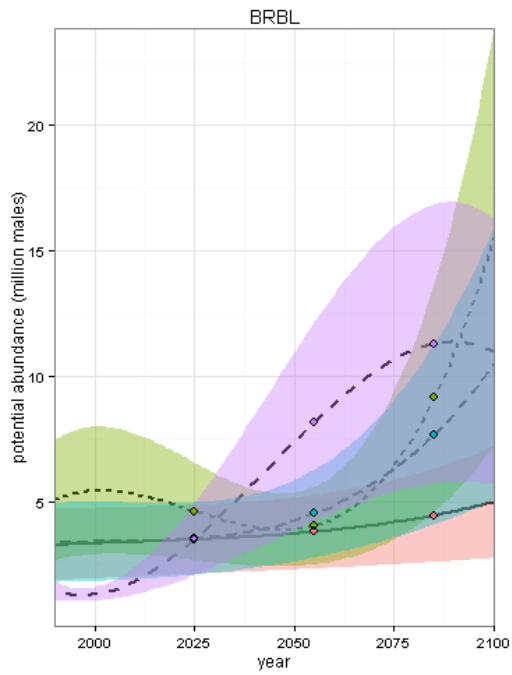
Figure D3. Projected changes over time according to four different climate-change trajectories. Projections are thirty-year averages (represented by points) interpolated with a third-order polynomial function for each of four global climate models. Lines = mean values; colored bands = 2 SE. [Appendix 1-C](#), Table C1 provides the common and scientific names associated with the 4-letter species codes.

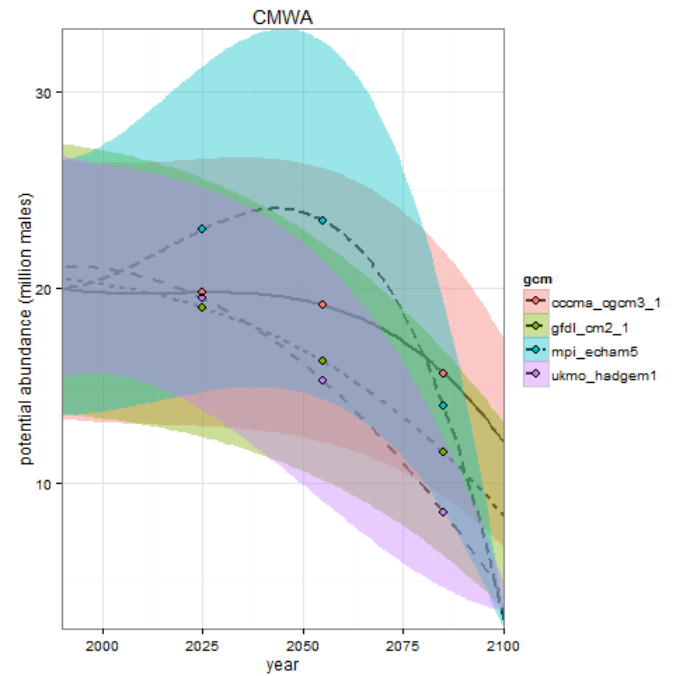
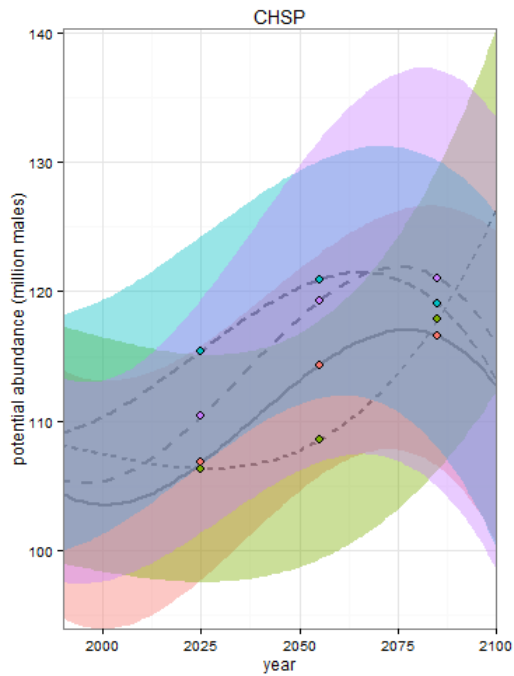
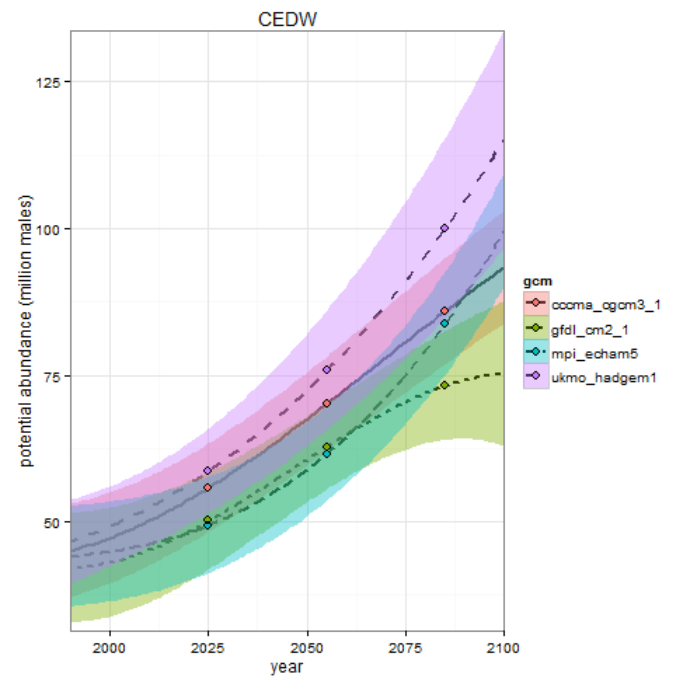
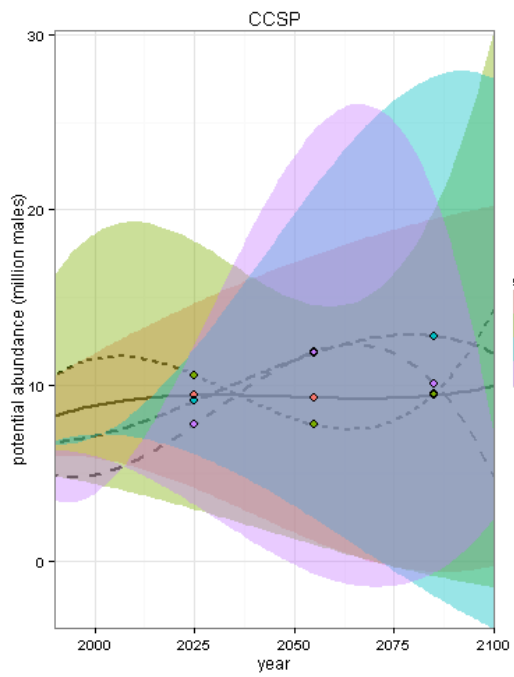


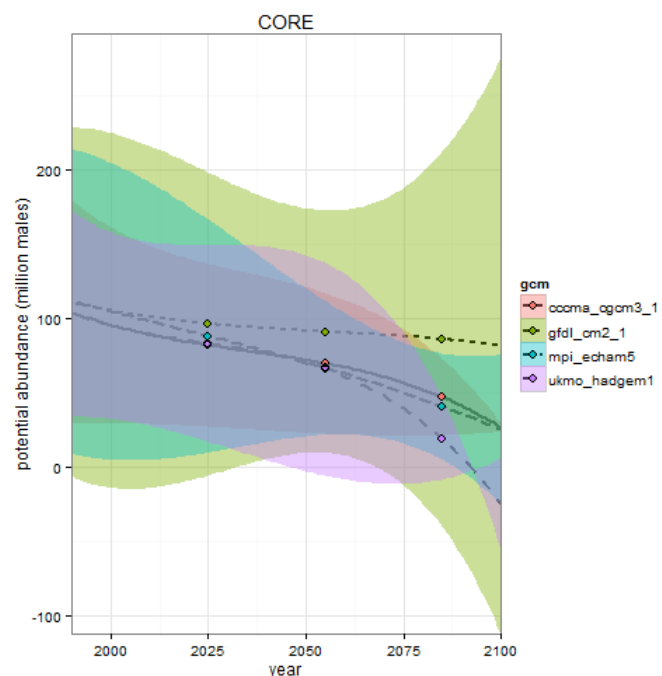
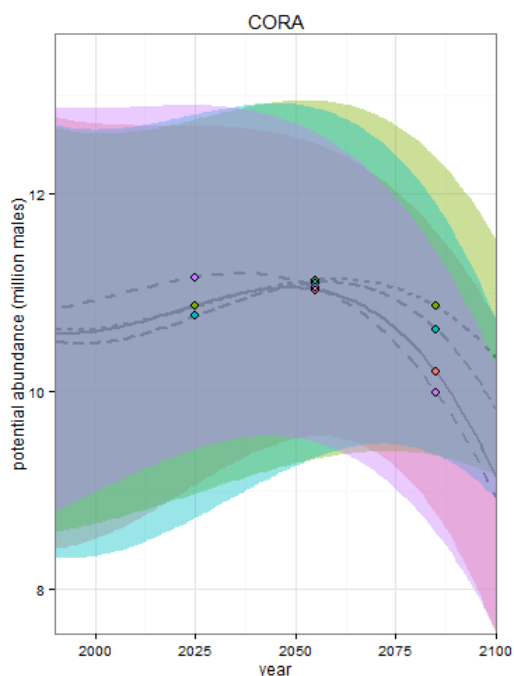
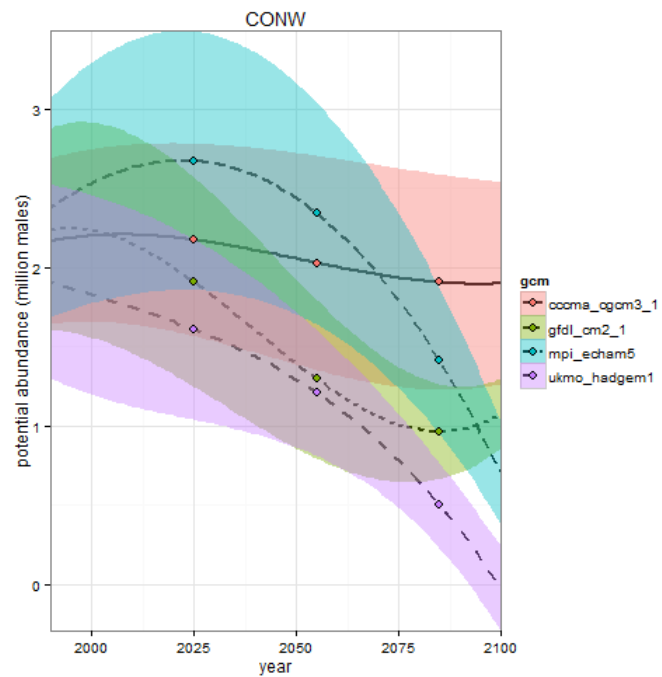
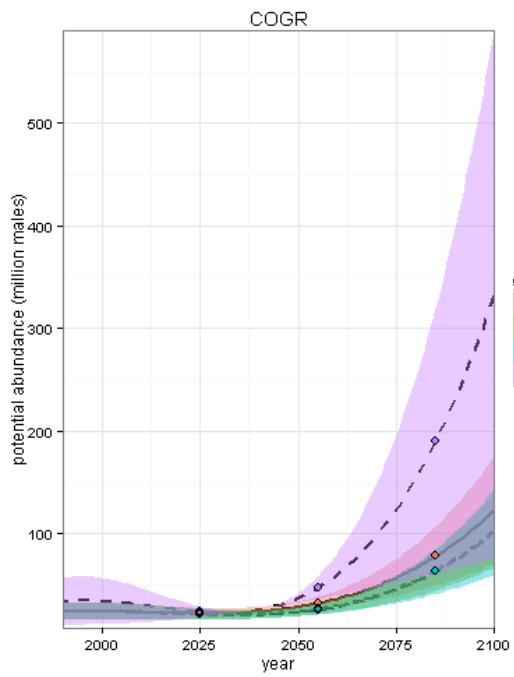


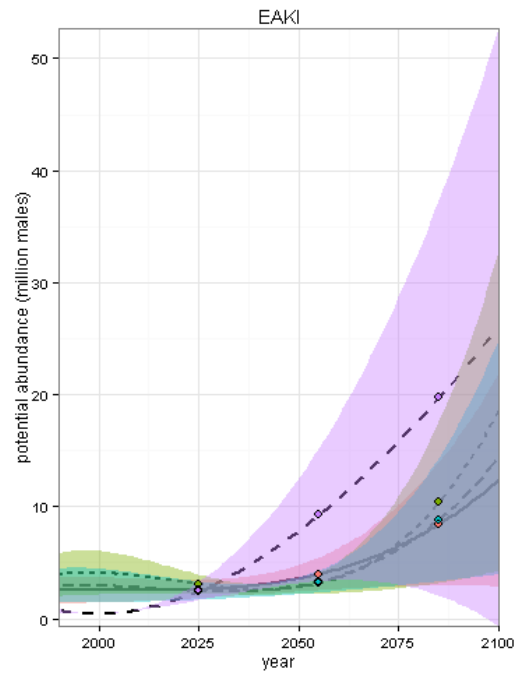
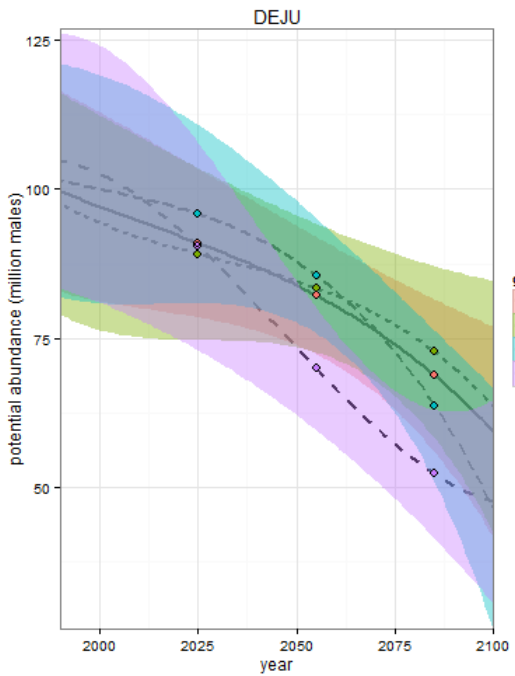
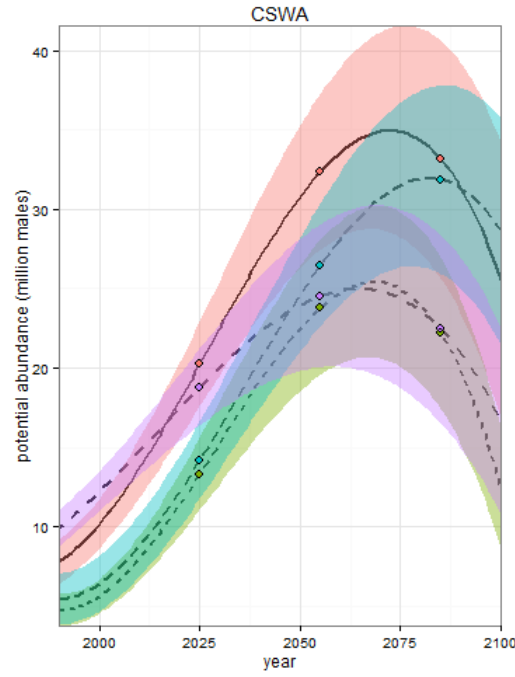
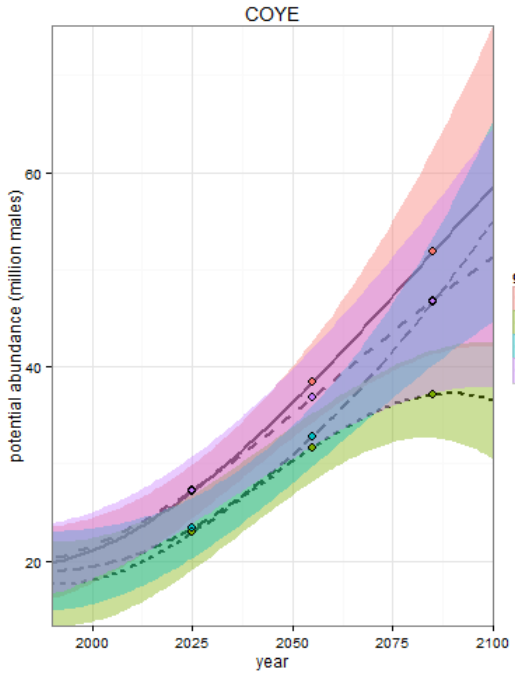


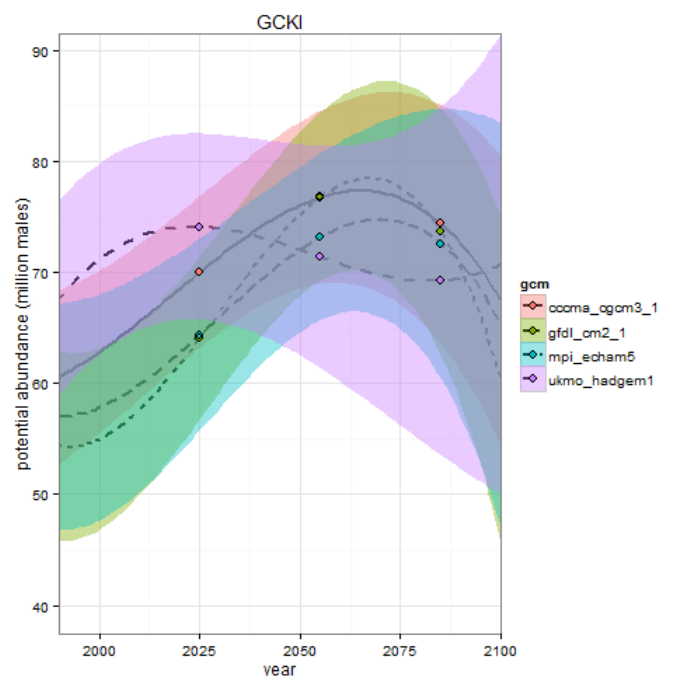
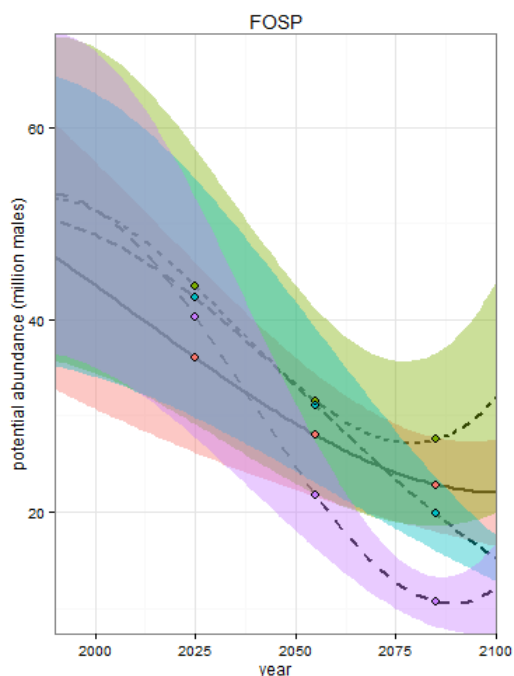
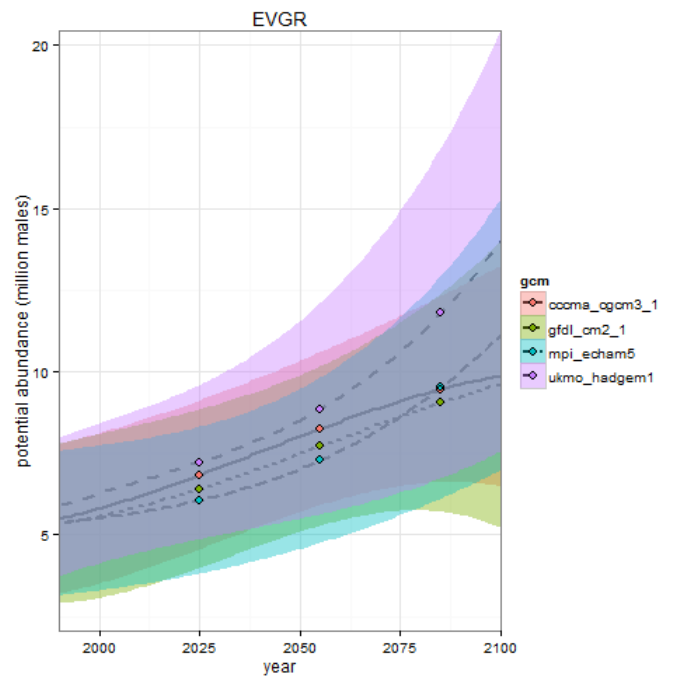
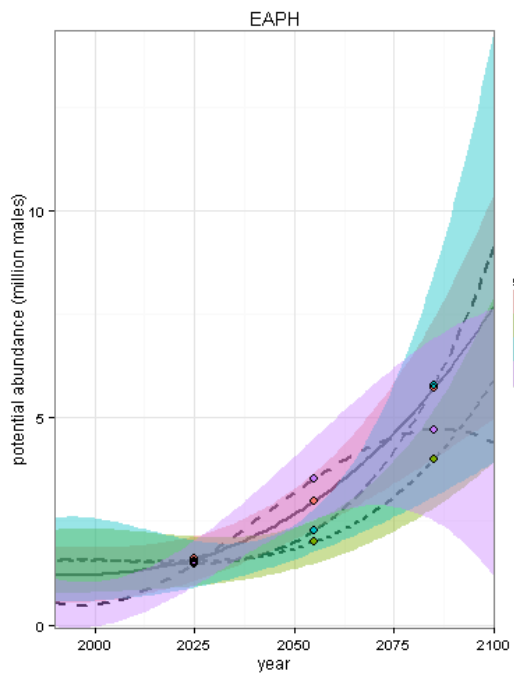


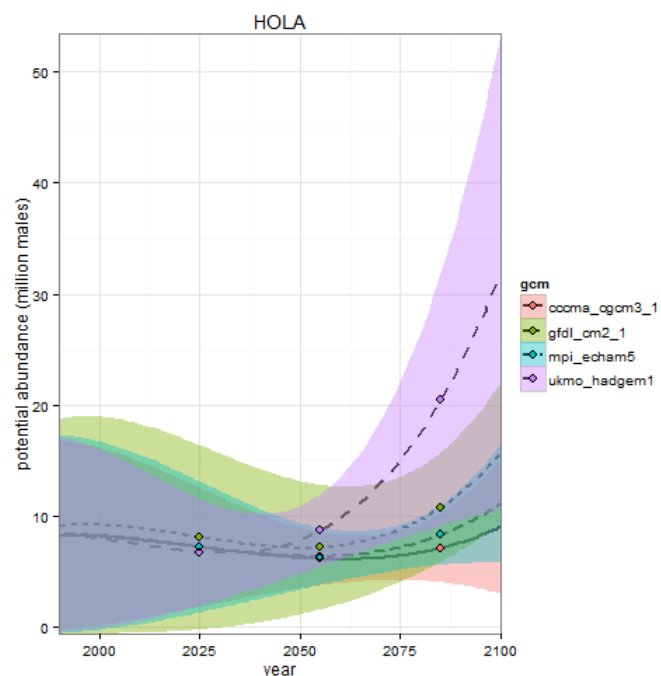
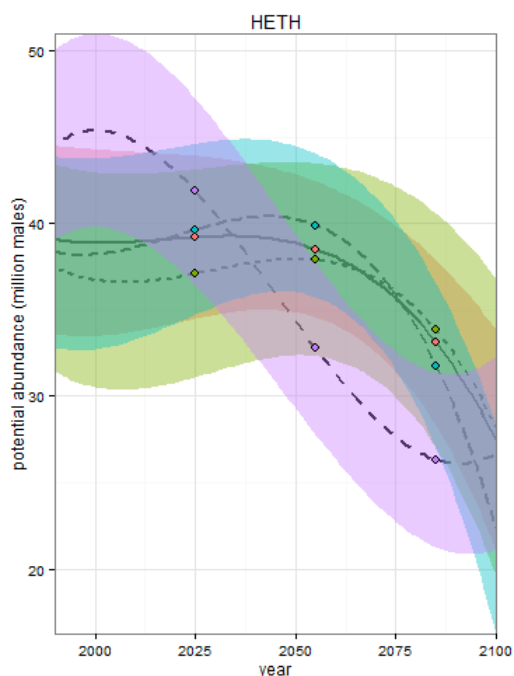
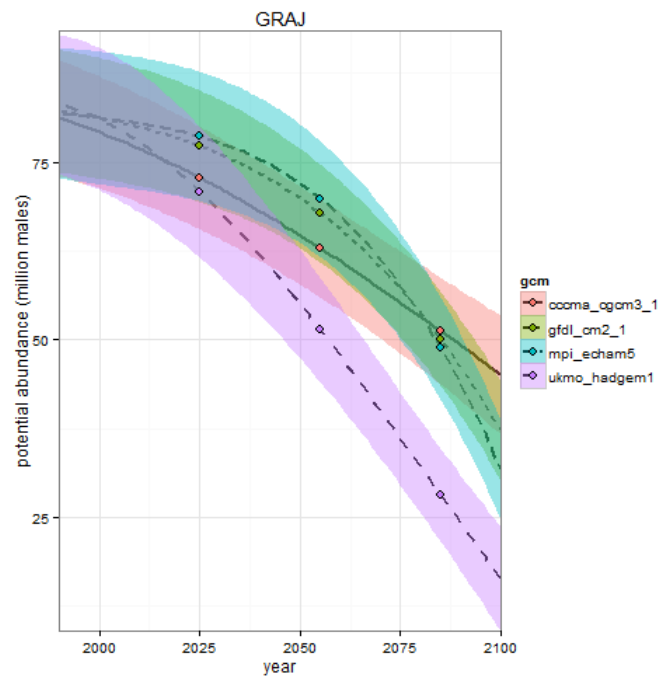
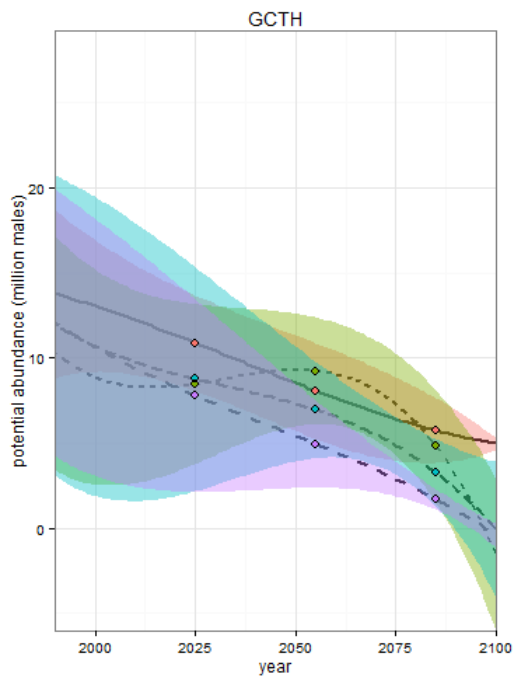


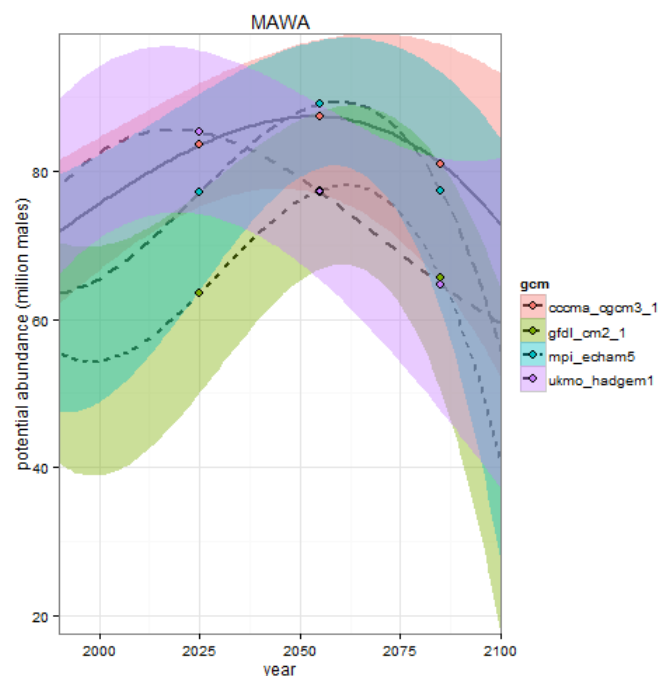
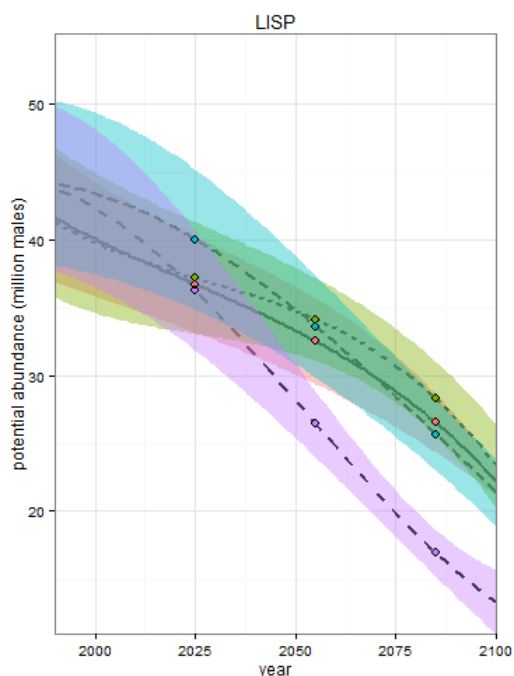
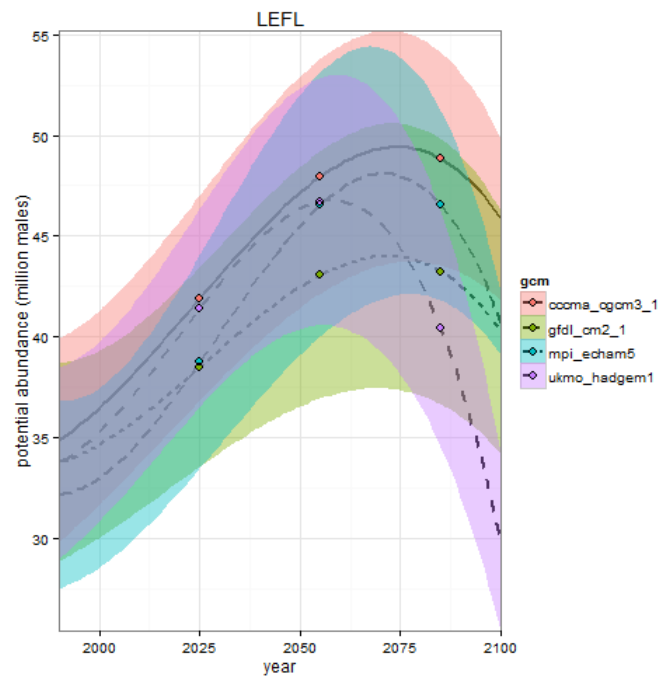
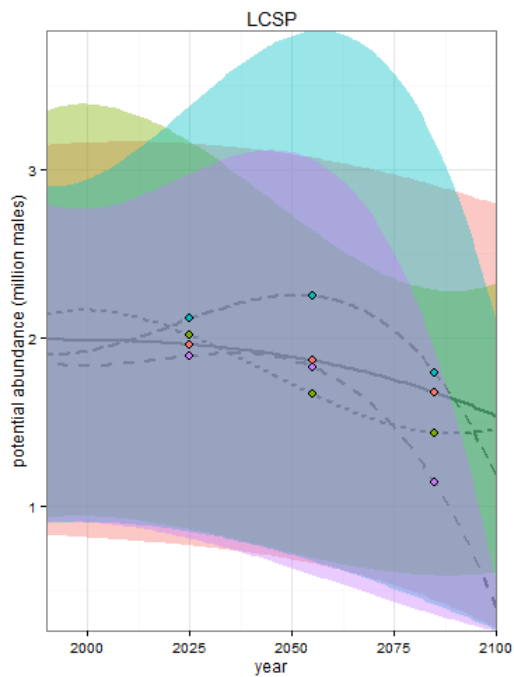


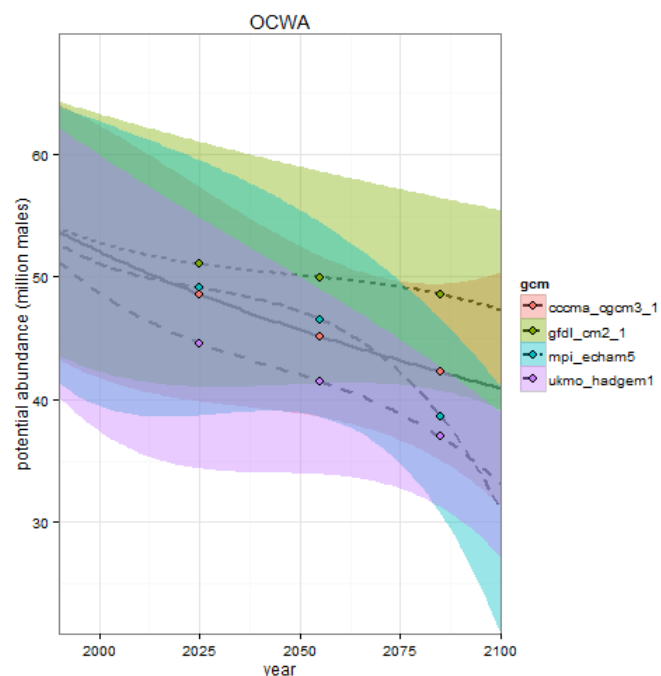
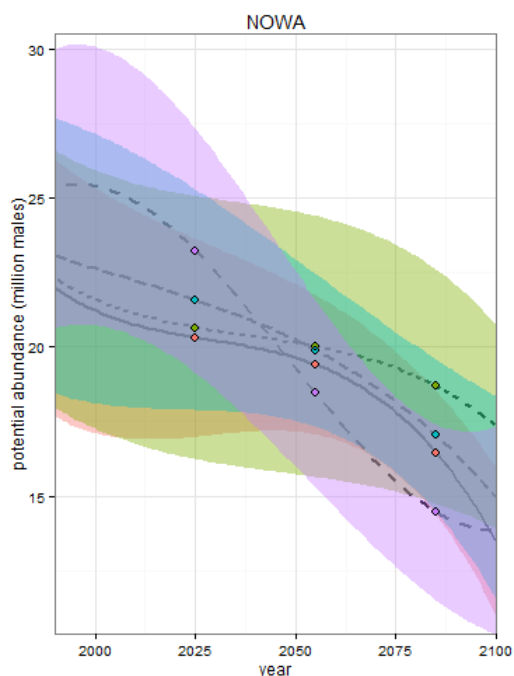
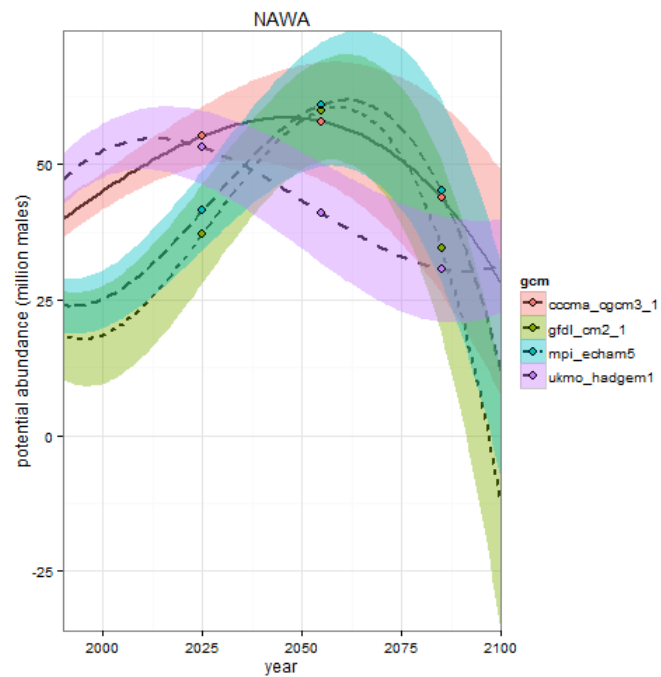
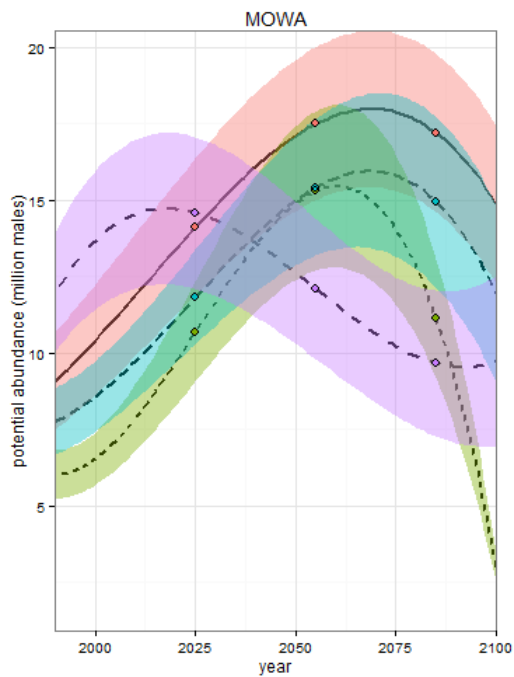


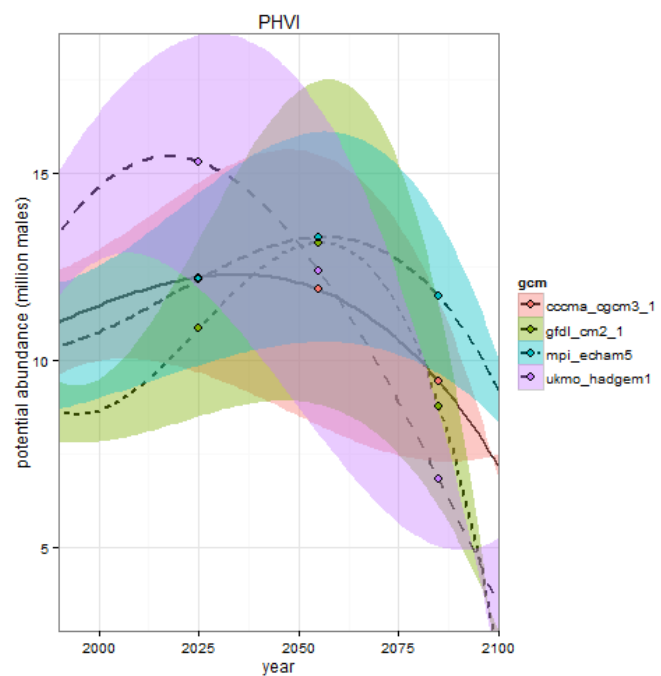
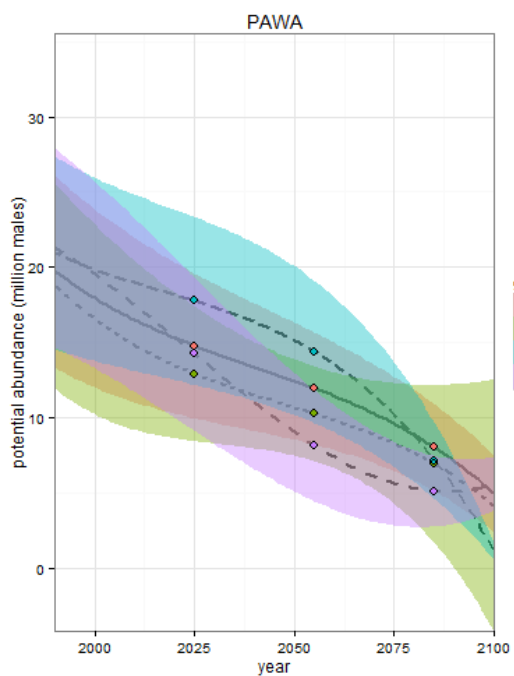
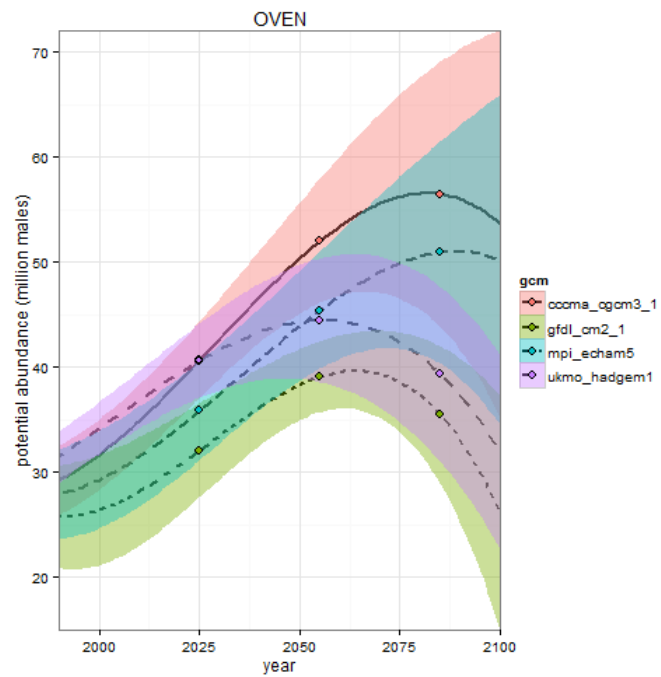
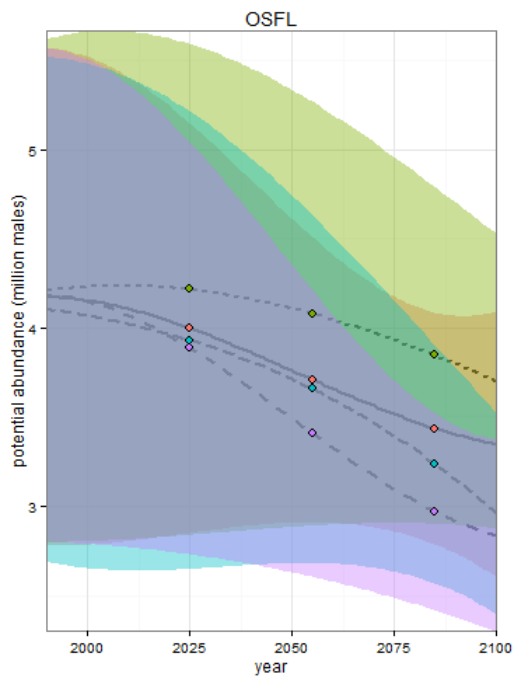


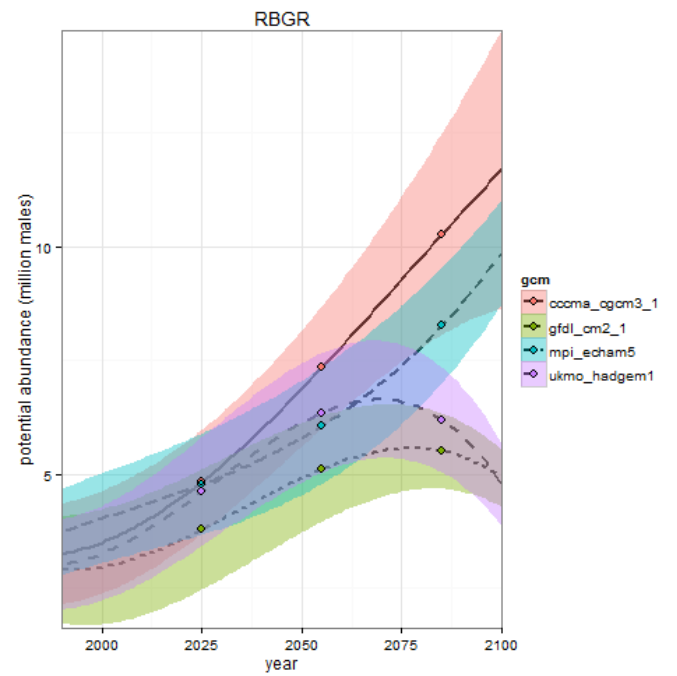
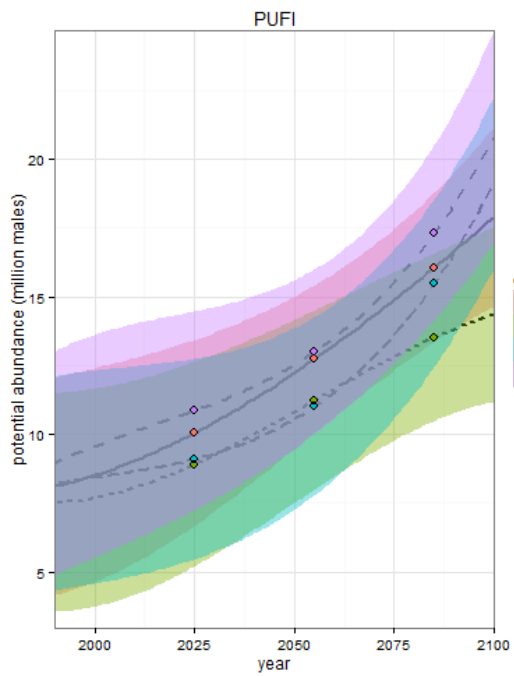
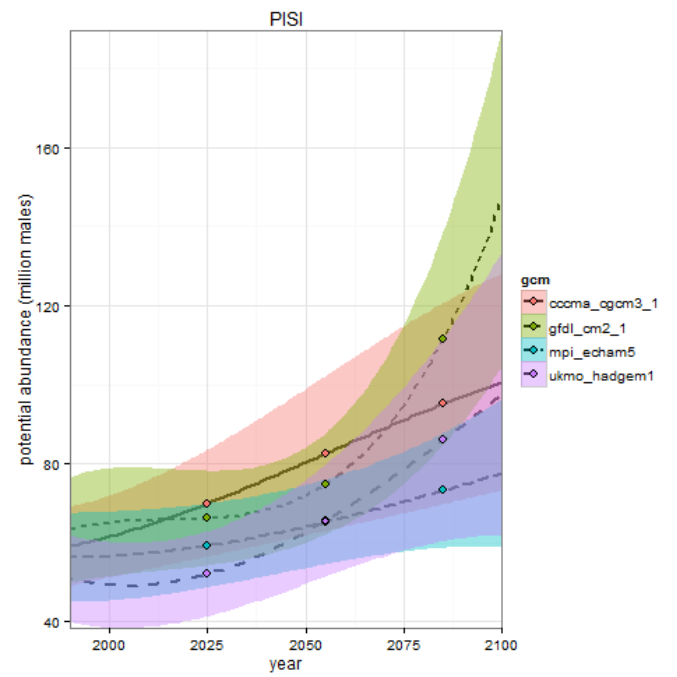
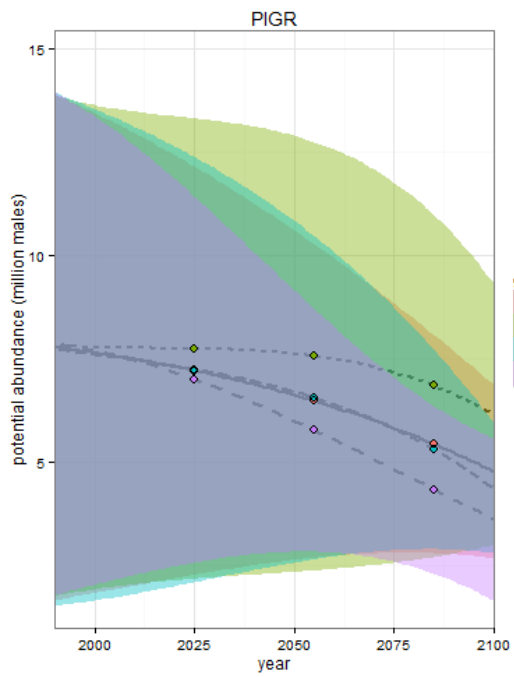


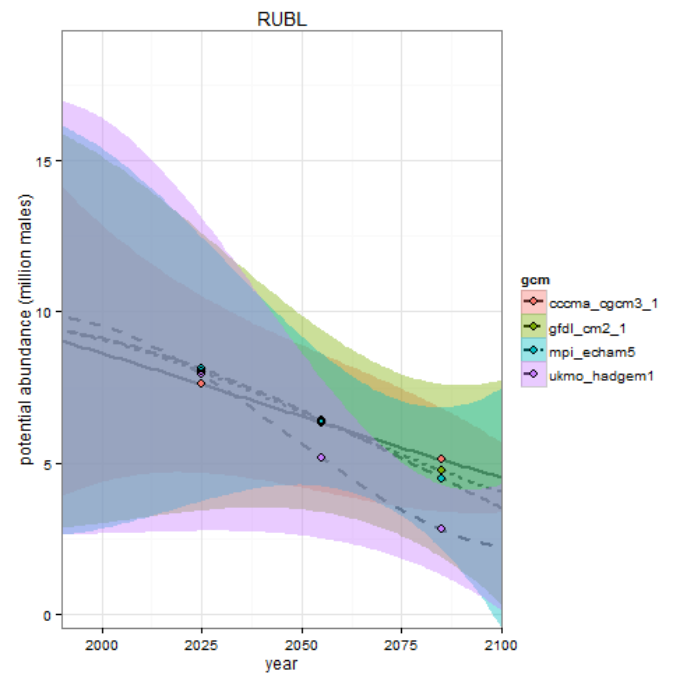
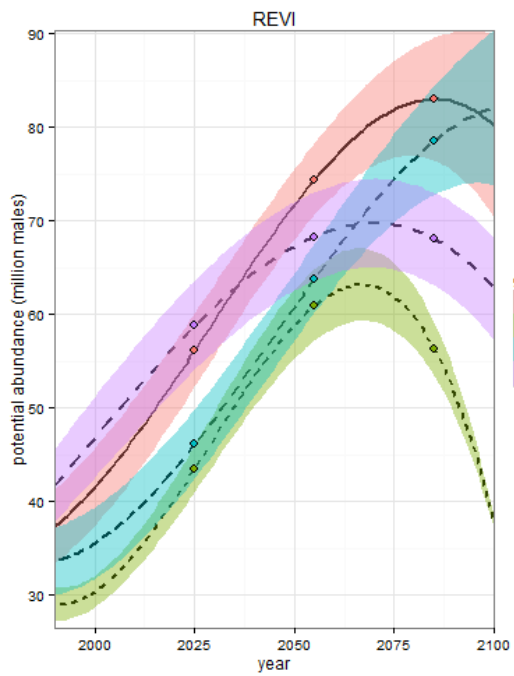
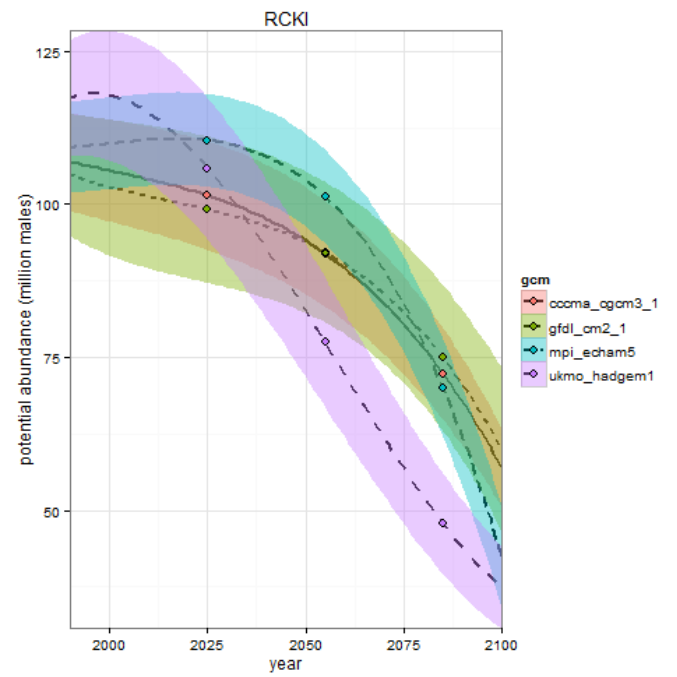
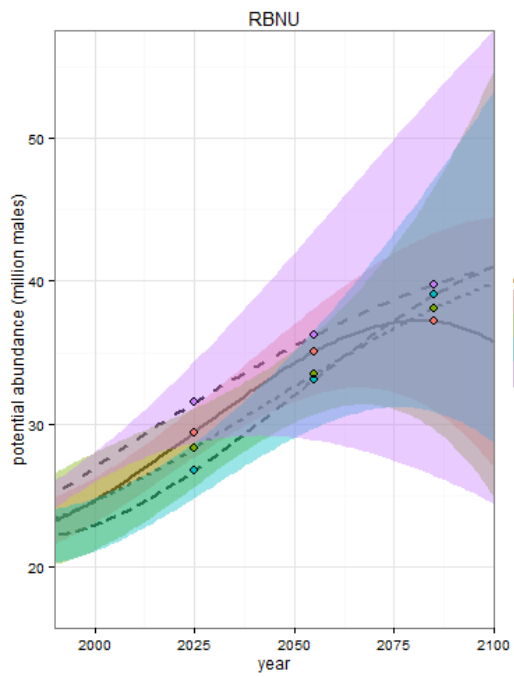


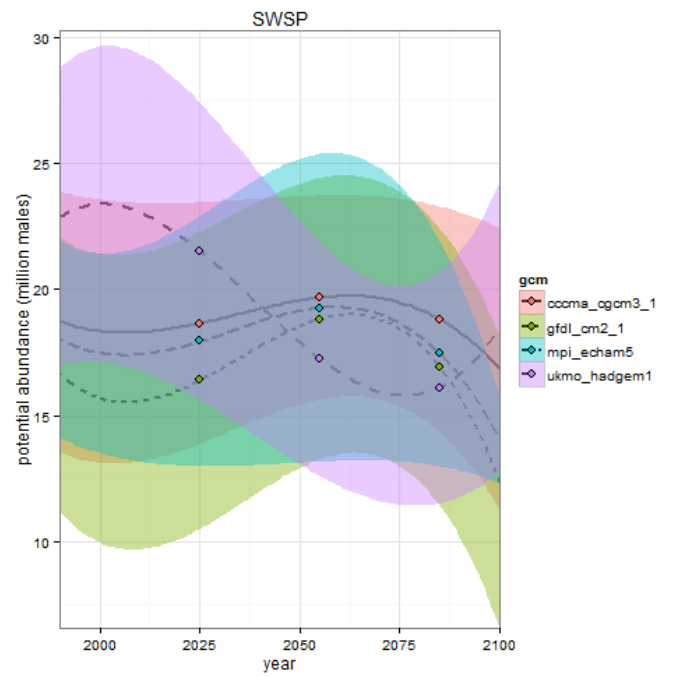
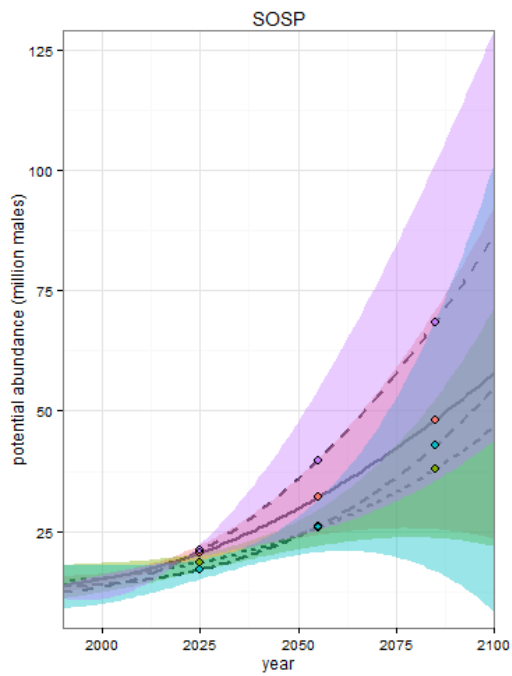
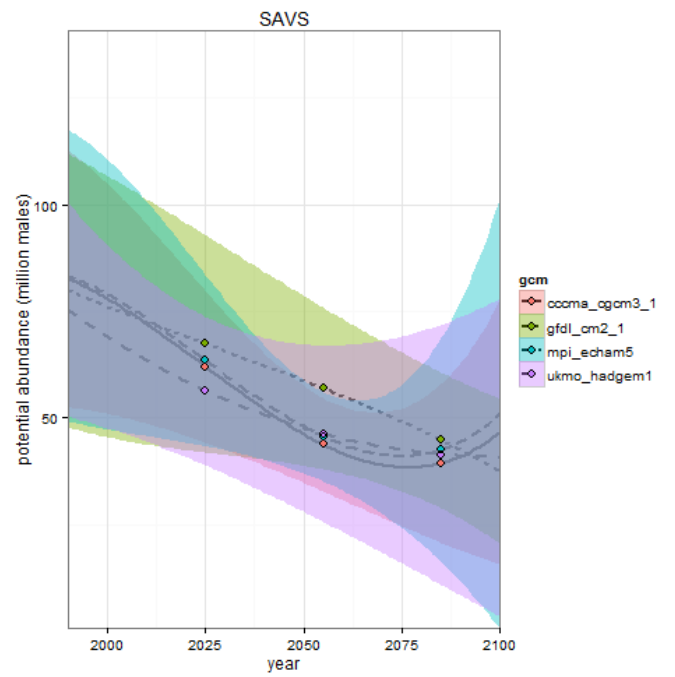
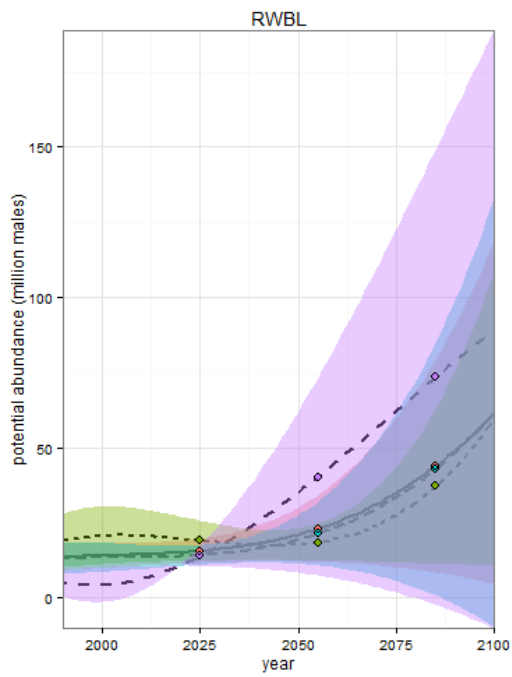


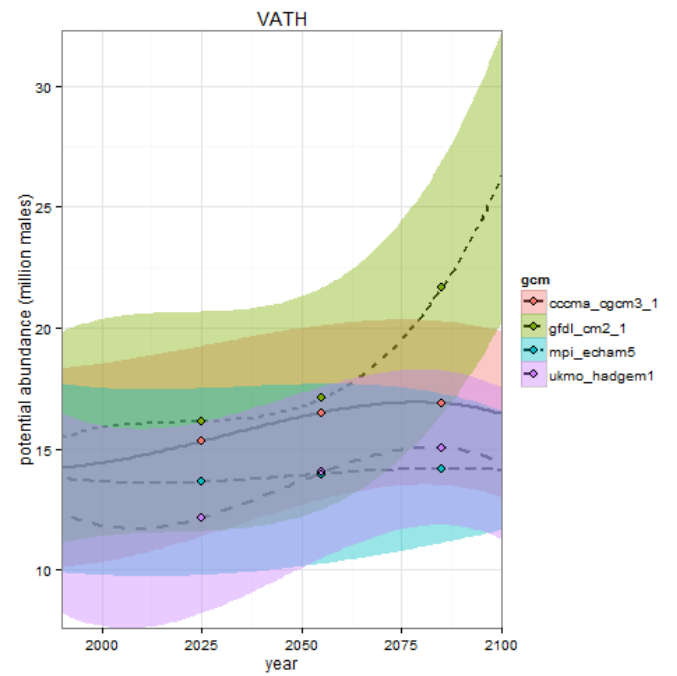
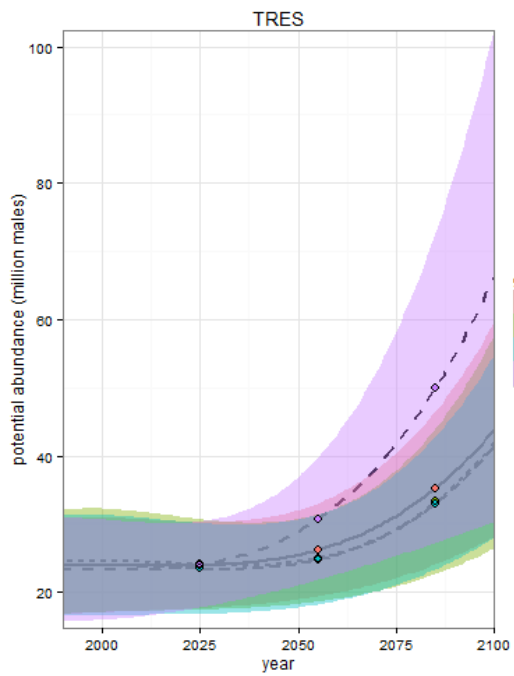
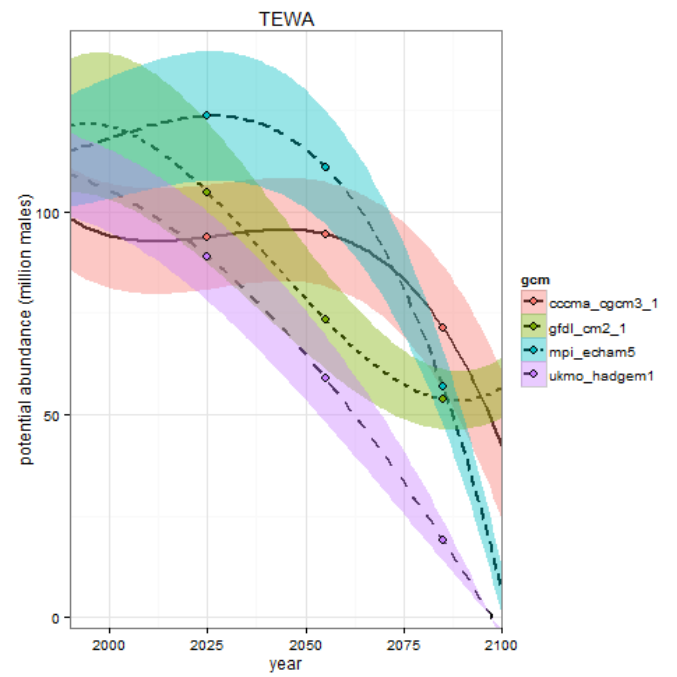
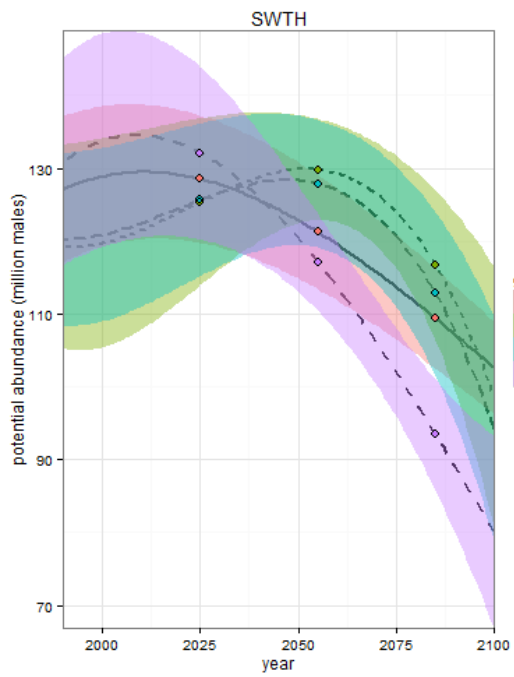


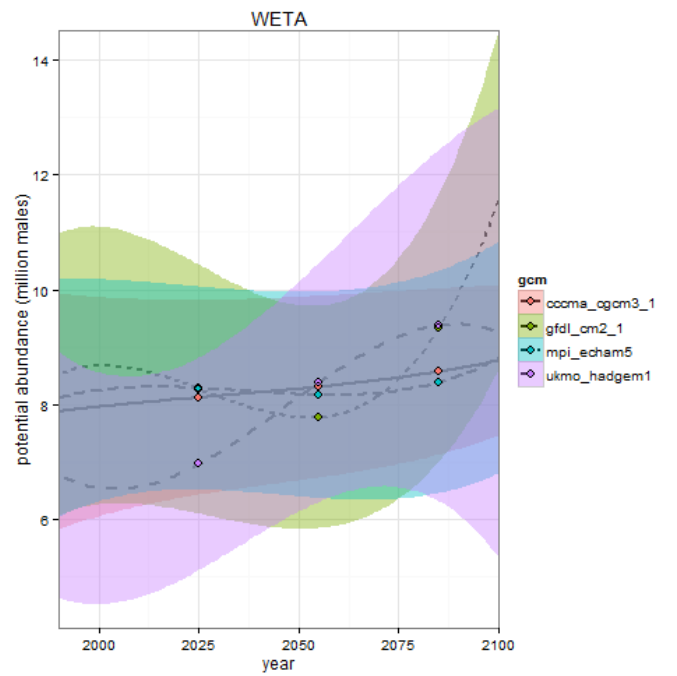
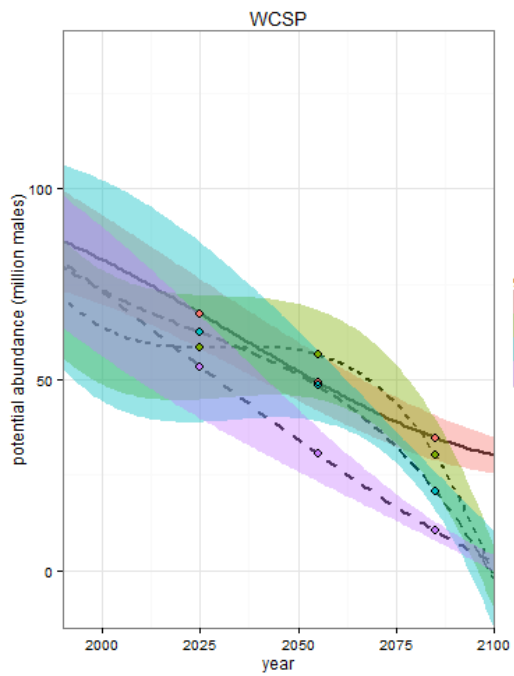
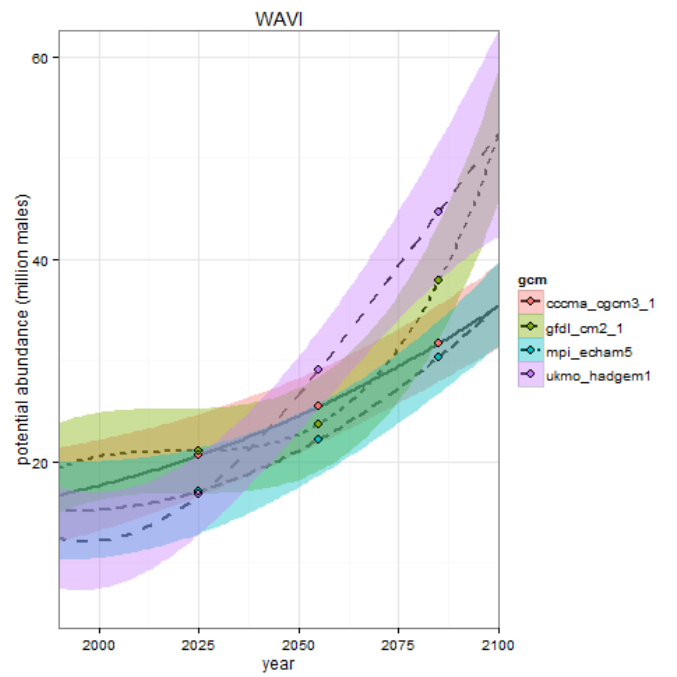
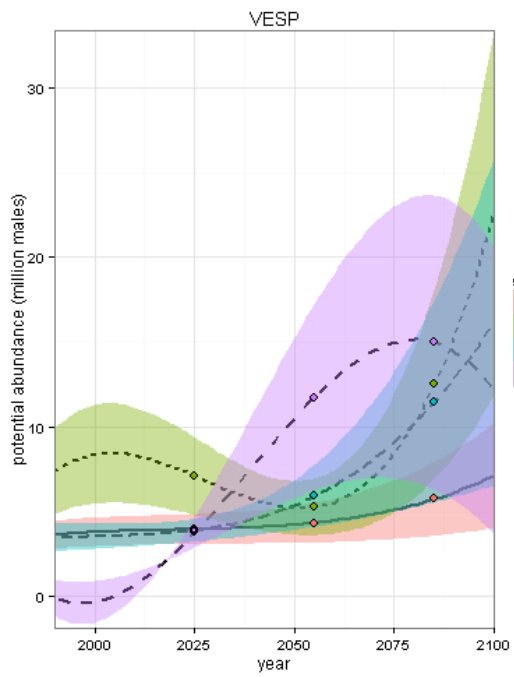


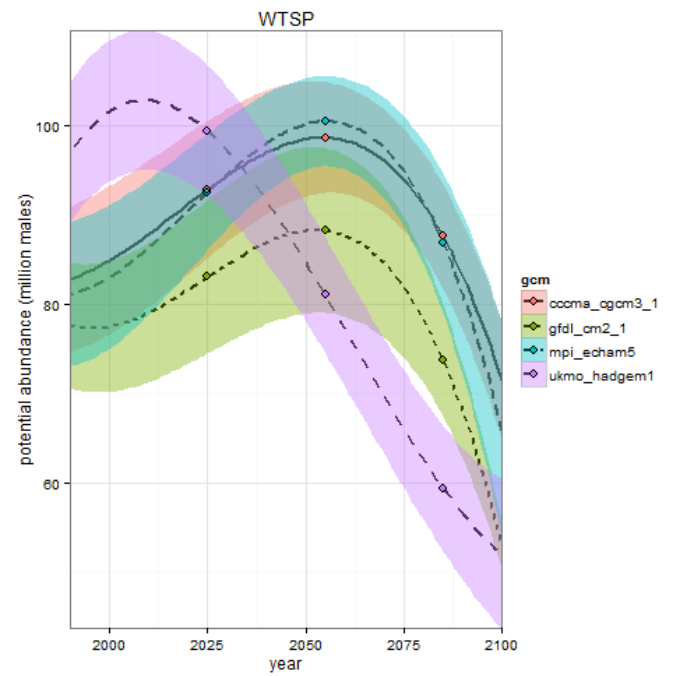
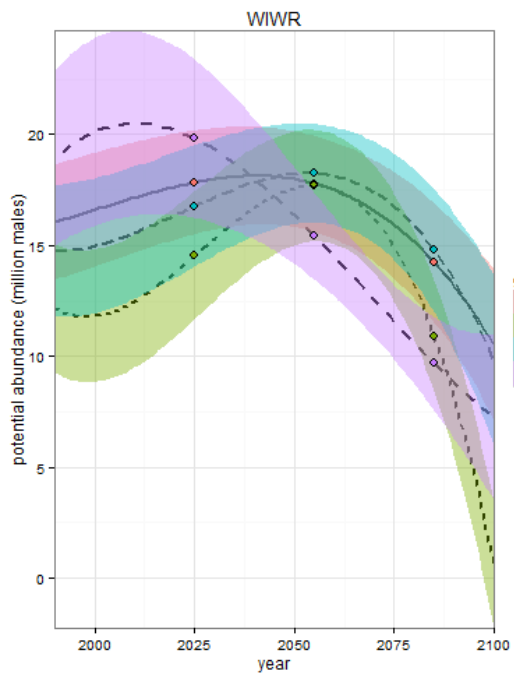
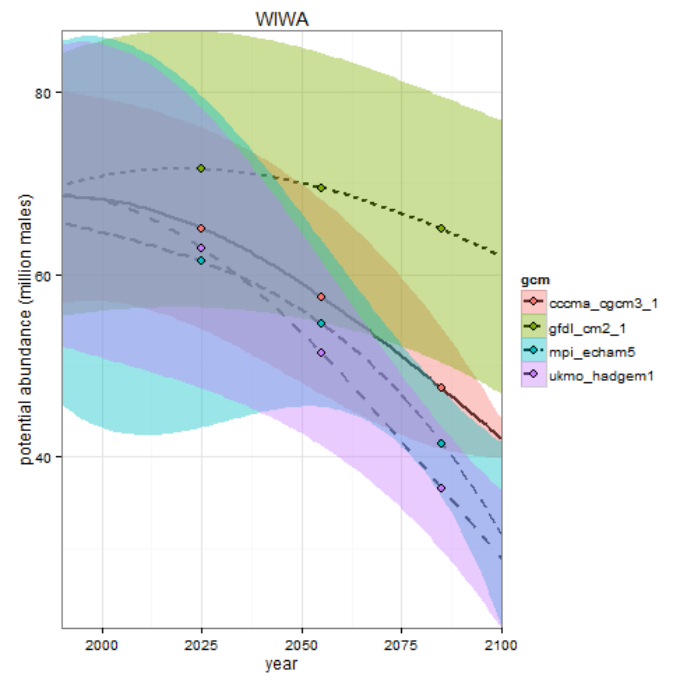
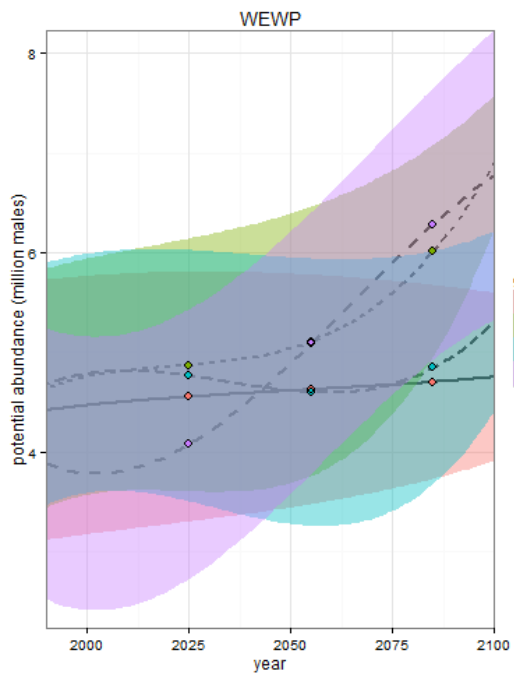


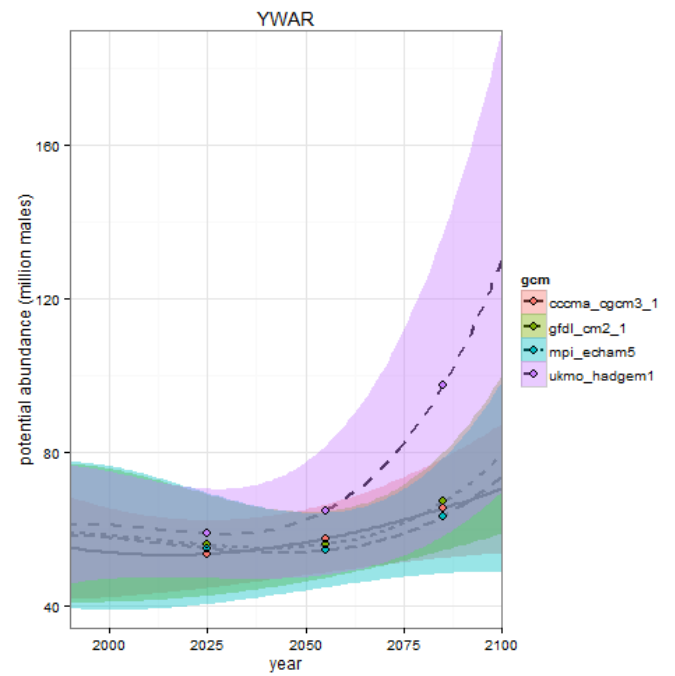
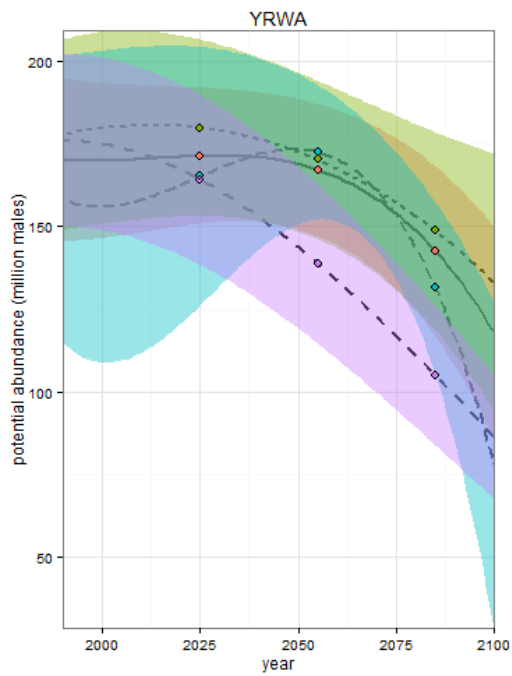
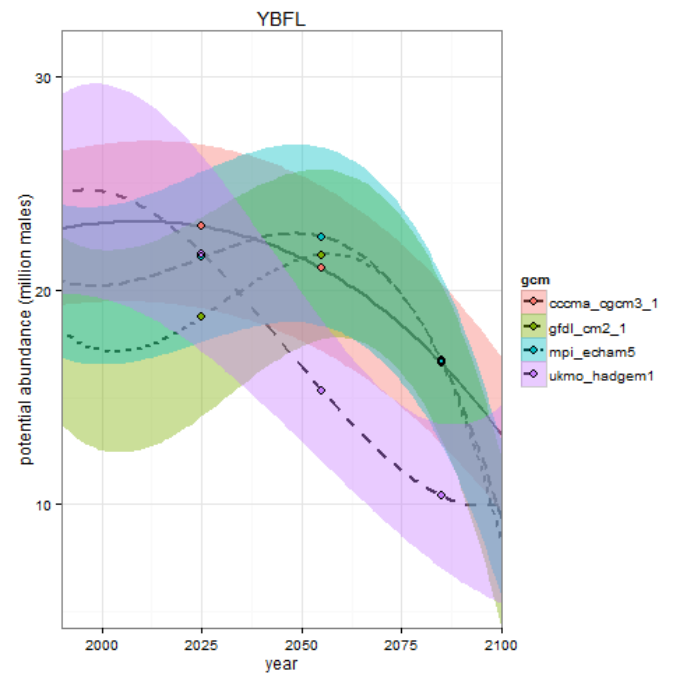
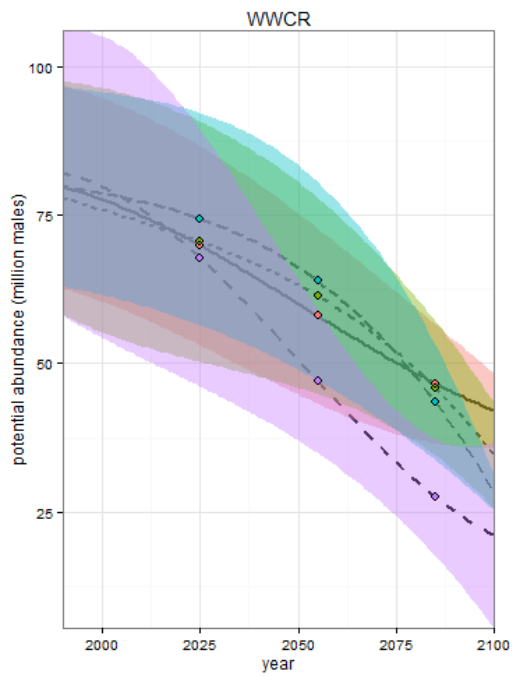












Appendix 1-E. R Code for boosted regression tree models

```
#####  
# R code to develop boosted regression tree models and generate current  
# predictions  
library(raster) #Reading, writing, manipulating, analyzing and modeling of  
# gridded spatial data  
library(dismo) #Species distribution modeling  
library(gbm) #Generalized boosted regression models  
library(sampling) #Functions for drawing and calibrating samples  
  
#####  
#Data Preparation  
  
#Bird data compiled by Boreal Avian Modelling Project, availability subject  
# to data agreements with individual providers  
#(http://www.borealbirds.ca/user/contact.php)  
#speclist: species list (by four-letter code)  
#PC: point-count dataframe  
#xx: survey attributes dataframe  
#RES: list of dataframes with offsets for each species (see QPAD estimation  
# in 'detect' package, https://github.com/psolymos/QPAD)  
#XY: Point-count coordinate dataframe  
  
#Field definitions  
#ABUND = raw count for a given species and survey  
#SPEC = 4-letter species code  
#PKEY = unique survey ID  
#SS = unique point location ID  
#PCODE = unique project code  
#SITE = unique site code (collection of points locations)  
#YEAR = survey year  
#A = estimated area surveyed (QPAD offset component)  
#p = estimated singing rate (QPAD offset component)  
#q = estimated probability of detection (QPAD offset component)  
  
surveydate <- aggregate(PC$ABUND,  
by=list("PKEY"=PC$PKEY, "YEAR"=PC$YEAR, "SS"=PC$SS, "PCODE"=PC$PCODE, "SITE"=PC$S  
ITE), FUN=sum)  
  
#Load current climate raster layers (requires raster package)  
setwd(curclimate) #set current climate directory  
clim <- list.files(curclimate, pattern=".asc$")  
curclim<-stack(raster(clim[1]), raster(clim[2]))  
i<-3  
while (i <= length(clim)) {  
  curclim <- addLayer(curclim,raster(clim[i]))  
  i<-i+1  
}  
  
#Load landcover raster layers (requires raster package)  
setwd(landcover) #set landcover directory  
curlc <- list.files(landcover, pattern=".asc$")  
lcstack <- stack(raster(curlc[1]), raster(curlc[2]))  
i<-3  
while (i <= length(curlc)) {
```

```

    lcstack <- addLayer(lcstack,raster(curlc[i]))
    i<-i+1
  }

#Load topoedaphic raster layers (requires raster package)
setwd(topo) #set topoedaphic directory
topoedaphic <- list.files(topo, pattern=".asc$")
topostack <- stack(raster(topoedaphic[1]), raster(topoedaphic[2]))
i<-3
while (i <= length(topoedaphic)) {
  topostack <- addLayer(topostack,raster(topoedaphic[i]))
  i<-i+1
}

#Combine climate, landcover, and topoedaphic raster layers in a single stack
(requires raster package)
climstack <- curclim
climstack <- addLayer(climstack, topostack,lcstack)

#Extract climate, landcover, and topography data by XY coordinates
sites <- aggregate(PC$ABUND, by = list("SITE" = PC$SITE, "PCODE"=PC$PCODE,
"SS"=PC$SS), FUN = sum)
XY <- merge(XY, sites[,1:3], by="SS")
climxy <- cbind(XY,extract(climstack,as.matrix(cbind(XY[,2],XY[,3]))))
climxy<-cbind(climxy,extract(nalc,as.matrix(cbind(climxy[,2],climxy[,3]))))
#Extract NALCMS landcover class for point filtering
names(climxy)[ncol(climxy)] <- "LCC"
climxy <- na.omit(climxy)
climxy$ID <- as.factor(climxy$ID)
#####

#####
#Bootstrap sampling of data locations, repeated 11 times to create 11
different resampled datasets
#Requires raster and sampling packages
#Additional field definitions
#LCC = landcover class code from NALCMS landcover dataset
#YearGuess = earliest possible year of mapped disturbance

#Define sampling strata as intersection between SITE and PCODE
survey <- xx[1:2]
survey$ID <- row.names(survey)
dat1 <- merge(survey[,1:2],climxy,by="SS")
dat1$group <- paste(dat1$PCODE, dat1$SITE, dat1$ID, sep="-")

#Remove urban, agricultural, and open water points
dat1 <- dat1[(dat1$LCC %in% c(15,16,17)) == FALSE,]

#Remove points with surveys conducted after disturbance event
disturb <- read.csv("Disturb.csv") #Intersection of X-Y coordinates with
anthropogenic disturbance from Global Forest Watch data
dat2 <- merge(dat1, disturb[,c(1,65)])
dat3 <- merge(dat2, surveydate[,1:5], by=c("SS","PKEY","PCODE","SITE"))
dat3$YearGuess <- ifelse(dat3$YearGuess == 0,9999,dat3$YearGuess)
dat3$keep <- ifelse(dat3$YearGuess < dat3$YEAR, 0, 1)
dat4 <- dat3[dat3$keep == 1,]

```

```

#Count number of surveys within group (SITE x PCODE)
dat4$count <- 1
count <- aggregate(dat4$count, by=list("group" = dat4$group), FUN = sum)
names(count)[2] <- "count"
dat4 <- merge(dat4[,1:ncol(dat4)-1],count)

set.seed(72189) #Set seed for repeatability (different in each iteration)

#Sample one point from each group with more than 10 surveys
datmany <- dat4[dat4$count>10,]
datsamp <- stratified(datmany, 1, 1)

#Sample one point from a third of the groups with fewer than 10 surveys
datfew <- dat4[dat4$count<11,]
datfew1 <- aggregate(datfew$count, by=list("group"=datfew$group), FUN = sum)
datsamp1 <- as.data.frame(sample(datfew1$group, size=nrow(datfew1)/3,
replace=FALSE))
names(datsamp1)[1] <- "group"
datsamp2 <- merge(datfew,datsamp1)
datsamp3 <- stratified(datsamp2, 1, 1)

#Assign weights to sampled points based on inverse of total number of surveys
#within a 20 km x 20 km (5 pixel by 5 pixel) area
datsamp4 <- rbind(datsamp[,c(1:62,64:66,69)],datsamp3[,c(1:62,64:66,69)])
r2 <- raster(clim[1])
samprast <- rasterize(datsamp4[,6:7], r2, field=1)
sampsam25 <- focal(samprast, w=5, na.rm=TRUE)
datsamp5 <-
  cbind(datsamp4,extract(sampsam25,as.matrix(cbind(datsamp4[,6],datsamp4[,7]
))))
names(datsamp5)[ncol(datsamp5)] <- "sampsam25"
datsamp5$wt <- 1/datsamp5$sampsam25

datsampx <- datsamp5 #where is x is the iteration
#####

#####
#Build and save models, predict and export rasters
#Requires dismo, gbm, and raster packages
setwd(w) #set working directory

for (j in 1:length(specieslist)) {
  specdat <- PC[PC$SPECIES == as.character(specieslist[j]),]
  dat1 <-
    merge(datsamp5,specdat[,1:6],by=c("SS","PKEY","SITE","PCODE"),all.x=TRUE)
  dat1$SPECIES <- as.character(specieslist[j])
  dat1$ABUND <- as.integer(ifelse(is.na(dat1$ABUND),0,dat1$ABUND))
  off <- as.data.frame(cbind(xx[1],RES[spp==specieslist[j]])
  off$Species <- specieslist[j]
  names(off) <- c("PKEY","A","p","q","SPECIES")
  off$offset <- off$A * off$p * off$q
  dat2 <- merge(dat1,off[,c(1,5:6)])
  dat2$logoffset <- log(dat2$offset)

  #Build and predict climate-only models

```

```

bird.brt.step1 <- gbm.step(dat2, gbm.y = (ncol(dat2)-2), gbm.x =
  c(11,12,14,16,19,25,37), family = "poisson", tree.complexity = 3,
  learning.rate = 0.001, bag.fraction = 0.5, offset=dat2$logoffset,
  site.weights=dat2$wt)
save(bird.brt.step1, file=paste(w,speclist[j],"_brt_clim1.RData",sep=""))
pdf(paste(w,speclist[j],"_brtplotclim1.pdf",sep=""))
gbm.plot(bird.brt.step1)
gbm.plot.fits(bird.brt.step1, v=1:7)
dev.off()
rast <- predict(climstack, bird.brt.step1, type="response",
  n.trees=bird.brt.step1$n.trees)
writeRaster(rast,
  filename=paste(w,speclist[j],"_brtpredclim_1.asc",sep=""),
  format="ascii",overwrite=TRUE)

#Build and predict climate + land-use + topography models
bird.brt.step2 <- gbm.step(dat2, gbm.y = (ncol(dat2)-2), gbm.x =
  c(11,12,14,16,19,25,37,41,53,54,56,57), family = "poisson",
  tree.complexity = 3, learning.rate = 0.001, bag.fraction = 0.5,
  offset=dat2$logoffset, site.weights=dat2$wt)
save(bird.brt.step2,
  file=paste(w,speclist[j],"_brt_climtop1.RData",sep=""))
pdf(paste(w,speclist[j],"_brtplotclimtop1.pdf",sep=""))
gbm.plot(bird.brt.step2)
gbm.plot.fits(bird.brt.step2, v=1:12)
dev.off()
rast <- predict(climstack, bird.brt.step2, type="response",
  n.trees=bird.brt.step2$n.trees)
writeRaster(rast,
  filename=paste(w,speclist[j],"_brtpredclimtop_1.asc",sep=""),
  format="ascii",overwrite=TRUE)
}
#####

#####
#Generate future projections

#Load landcover raster layers (requires raster package)
setwd(landcover) #set landcover directory
curlc <- list.files(landcover, pattern=".asc$")
lcstack <- stack(raster(curlc[1]), raster(curlc[2]))
i<-3
while (i <= length(curlc)) {
  lcstack <- addLayer(lcstack,raster(curlc[i]))
  i<-i+1
}

#Load topoedaphic raster layers (requires raster package)
setwd(topo) #set topoedaphic directory
topoedaphic <- list.files(topo, pattern=".asc$")
topostack <- stack(raster(topoedaphic[1]), raster(topoedaphic[2]))
i<-3
while (i <= length(topoedaphic)) {
  topostack <- addLayer(topostack,raster(topoedaphic[i]))
  i<-i+1
}

```

```

setwd(ft) #set future climate directory (time period / senario)
#Future climate rasters organized in sub-directories named according to GCM
#Very time consuming; only 4/20 GCMs + ensembles predicted
gcms <- read.csv("gcms.csv") #List of GCMs for A2 scenario
gcms <- as.factor(as.character(gcms[1:20,1]))

for (i in 1:length(gcms)) {
  fclimtop <- list.files(paste(ft,gcms[i],sep=""), pattern=".asc$")
  setwd(paste(ft,gcms[i],sep="")) #set working directory to GCM
  futclimtop <- stack(raster(fclimtop[1]), raster(fclimtop[2]))
  k<-3
  while (k <= length(fclimtop)) {
    futclimtop <- addLayer(futclimtop,raster(fclimtop[k]))
    k<-k+1
  }
  climstack <- futclimtop
  climstack <- addLayer(climstack, topostack,lcstack

  setwd(w) #Set working directory
  models <- list.files(w, pattern=".RData")
  try(rm(bird.brt.step1))
  try(rm(bird.brt.step2))
  for (j in 1:length(models)) {
    base <- gsub(".RData","",models[j])
    if(file.exists(paste(w,"gcms/",base,"_",gcms[i],".asc",sep=""))) ==
FALSE) {
      load(paste(w,models[j],sep=""))
      try(rast <- predict(climstack, bird.brt.step2, type="response",
n.trees=bird.brt.step2$n.trees))
      try(rast <- predict(climstack, bird.brt.step1, type="response",
n.trees=bird.brt.step1$n.trees))
      writeRaster(rast,
filename=paste(w,"gcms/",base,"_",gcms[i],".asc",sep=""),
format="ascii",overwrite=TRUE)
      png(paste(w,"gcms/",base,"_",gcms[i],".png",sep=""))
      plot(rast, zlim=c(0,1))
      dev.off()
      try(rm(bird.brt.step1))
      try(rm(bird.brt.step2))
    }
  }
}
#####

```

Appendix 2-A. Projected proportional change in core habitat area for 53 boreal forest species under alternative vegetation-lag scenarios by 2071-2100.

Most likely seral-stage adjusted scenario based on 15th percentile habitat age thresholds emboldened. “Difference” refers to the difference between seral-stage adjusted (modified refugia) and unconstrained scenarios.

Species common name (<i>scientific name</i>)	Scenario A. Unconstrained	30-year lag	60-year lag	Scenario B. Strict refugia	Scenario C. Modified refugia	Difference
American Redstart (<i>Setophaga ruticilla</i>)	1.22	0.44	-0.15	-0.60	0.44	-0.78
Black-and-white Warbler (<i>Mniotilta varia</i>)	0.63	0.01	-0.34	-0.60	0.01	-0.62
Bay-breasted Warbler (<i>Setophaga castanea</i>)	0.02	-0.37	-0.77	-0.93	-0.77	-0.79
Black-capped Chickadee (<i>Poecile atricapillus</i>)	1.05	0.18	-0.27	-0.73	0.18	-0.87
Blue-headed Vireo (<i>Vireo solitarius</i>)	0.17	-0.27	-0.58	-0.79	-0.27	-0.44
Blackburnian Warbler (<i>Setophaga fusca</i>)	1.56	0.56	-0.13	-0.65	-0.13	-1.69
Blue Jay (<i>Cyanocitta cristata</i>)	1.31	0.34	-0.27	-0.82	1.31	0
Blackpoll Warbler (<i>Setophaga striata</i>)	-0.47	-0.75	-0.78	-0.81	-0.78	-0.31
Boreal Chickadee (<i>Poecile hudsonicus</i>)	-0.28	-0.53	-0.59	-0.69	-0.59	-0.31
Brown Creeper (<i>Certhia americana</i>)	0.03	-0.48	-0.56	-0.64	-0.56	-0.59
Black-throated Green Warbler (<i>Setophaga virens</i>)	0.90	0.31	-0.16	-0.55	-0.16	-1.06
Canada Warbler (<i>Cardellina canadensis</i>)	1.38	0.53	0.02	-0.40	0.02	-1.36
Cedar Waxwing (<i>Bombycilla cedrorum</i>)	0.84	0.13	-0.29	-0.63	0.84	0
Cape May Warbler (<i>Setophaga tigrina</i>)	-0.13	-0.46	-0.71	-0.86	-0.71	-0.58
Connecticut Warbler (<i>Oporornis agilis</i>)	-0.13	-0.44	-0.68	-0.86	-0.68	-0.55
Common Raven (<i>Corvus corax</i>)	0.45	0.05	-0.09	-0.21	0.45	0
Common Redpoll (<i>Acanthis flammea</i>)	-0.64	-0.65	-0.72	-0.91	-0.72	-0.08
Dark-eyed Junco (<i>Junco hyemalis</i>)	-0.27	-0.46	-0.55	-0.62	-0.46	-0.19
Evening Grosbeak (<i>Coccothraustes vespertinus</i>)	1.21	0.45	-0.06	-0.49	0.45	-0.76
Fox Sparrow (<i>Passerella iliaca</i>)	-0.59	-0.75	-0.79	-0.82	-0.79	-0.20
Golden-crowned Kinglet (<i>Regulus satrapa</i>)	0.53	0.19	-0.25	-0.58	-0.19	-0.34
Gray-cheeked Thrush (<i>Catharus minimus</i>)	-0.81	-0.85	-0.88	-0.92	-0.92	-0.11
Gray Jay (<i>Perisoreus canadensis</i>)	-0.45	-0.63	-0.73	-0.85	-0.63	-0.28

Species common name (<i>scientific name</i>)	Scenario A. Unconstrained	30-year lag	60-year lag	Scenario B. Strict refugia	Scenario C. Modified refugia	Difference
Hermit Thrush (<i>Catharus guttatus</i>)	-0.31	-0.50	-0.56	-0.65	-0.31	0
Least Flycatcher (<i>Empidonax minimus</i>)	0.63	0.23	-0.10	-0.36	0.23	-0.40
Magnolia Warbler (<i>Setophaga magnolia</i>)	0.00	-0.31	-0.55	-0.75	-0.31	-0.31
Mourning Warbler (<i>Geothlypis philadelphia</i>)	0.87	0.22	-0.19	-0.56	0.87	0
Nashville Warbler (<i>Oreothlypis ruficapilla</i>)	0.80	0.27	-0.18	-0.53	0.80	0
Northern Waterthrush (<i>Parkesia noveboracensis</i>)	-0.23	-0.44	-0.54	-0.64	-0.44	-0.21
Orange-crowned Warbler (<i>Oreothlypis celata</i>)	-0.28	-0.42	-0.60	-0.64	-0.42	-0.14
Olive-sided Flycatcher (<i>Contopus cooperi</i>)	0.06	-0.01	-0.23	-0.37	0.06	0
Ovenbird (<i>Seiurus aurocapilla</i>)	0.72	0.16	-0.18	-0.52	-0.18	-0.90
Palm Warbler (<i>Setophaga palmarum</i>)	-0.77	-0.86	-0.88	-0.91	-0.77	0
Philadelphia Vireo (<i>Vireo philadelphicus</i>)	-0.01	-0.39	-0.77	-0.94	-0.39	-0.38
Pine Grosbeak (<i>Pinicola enucleator</i>)	-0.53	-0.60	-0.67	-0.73	-0.60	-0.07
Pine Siskin (<i>Spinus pinus</i>)	0.02	-0.44	-0.64	-0.76	-0.64	-0.66
Purple Finch (<i>Carpodacus purpureus</i>)	1.01	0.09	-0.27	-0.53	0.09	-0.92
Rose-breasted Grosbeak (<i>Pheucticus ludovicianus</i>)	1.26	0.50	-0.04	-0.53	0.50	-0.76
Red-breasted Nuthatch (<i>Sitta canadensis</i>)	0.87	0.46	0.00	-0.39	0.00	-0.87
Ruby-crowned Kinglet (<i>Regulus calendula</i>)	-0.19	-0.44	-0.60	-0.75	-0.44	-0.25
Red-eyed Vireo (<i>Vireo olivaceus</i>)	0.87	0.23	-0.14	-0.48	0.23	-0.64
Rusty Blackbird (<i>Euphagus carolinus</i>)	-0.64	-0.67	-0.74	-0.90	-0.64	0
Swainson's Thrush (<i>Catharus ustulatus</i>)	0.04	-0.15	-0.35	-0.59	-0.35	-0.39
Tennessee Warbler (<i>Oreothlypis peregrina</i>)	-0.41	-0.60	-0.78	-0.92	-0.60	-0.19
Varied Thrush (<i>Ixoreus naevius</i>)	0.21	-0.28	-0.58	-0.69	-0.58	-0.79
Western Tanager (<i>Piranga ludoviciana</i>)	0.19	-0.32	-0.45	-0.78	-0.78	-0.97
Western Wood-Pewee (<i>Contopus sordidulus</i>)	-0.05	-0.30	-0.38	-0.50	-0.30	-0.25
Wilson's Warbler (<i>Cardellina pusilla</i>)	-0.33	-0.52	-0.58	-0.62	-0.33	0
Winter Wren (<i>Troglodytes hiemalis</i>)	0.06	-0.12	-0.32	-0.57	-0.12	-0.18
White-throated Sparrow (<i>Zonotrichia albicollis</i>)	-0.12	-0.30	-0.41	-0.55	-0.12	0

Species common name (<i>scientific name</i>)	Scenario A. Unconstrained	30-year lag	60-year lag	Scenario B. Strict refugia	Scenario C. Modified refugia	Difference
White-winged Crossbill (<i>Loxia leucoptera</i>)	-0.50	-0.68	-0.73	-0.77	-0.68	-0.18
Yellow-bellied Flycatcher (<i>Empidonax flaviventris</i>)	-0.11	-0.32	-0.45	-0.60	-0.32	-0.21
Yellow-rumped Warbler (<i>Setophaga coronata</i>)	-0.07	-0.30	-0.43	-0.65	-0.43	-0.36

Appendix 2-B. Methods for identification of species' minimum forest age thresholds

Standardized aerial-photo-derived forest inventory polygon data (Cumming et al. 2015) (Fig. 1) were intersected with an updated set of BAM point-count locations surveyed between 1993 and 2011 to determine the tree-species composition and apparent age of forested stands, and the year and type of known recent disturbances. Surveys of coniferous, deciduous and mixed forest stands were combined for analysis. Pre-disturbance surveys (48,113) were excluded. Of the remaining 52,125 survey locations, 1,231 were in cutblocks. Thus, approximately 2% of age-class designations were post-harvest; natural stand origins were assumed for the remaining surveys. For each bird species and habitat class, we fit generalized additive models of mean species density, with forest age as the predictor variable and raw counts as the response variable. We used the *mgcv* package (Wood 2011) for R (R Core Team 2013) with a reduced df ($k = 5$) spline function, Poisson error distribution, and logarithmic link function with detectability offsets (Sólymos *et al.*, 2013). Using the fitted models, we predicted density for each bird species across integer values of forest age ranging from 1 to 240, and multiplied these values by the corresponding proportion of available habitat to obtain a within-sample abundance estimate for each age. Year-specific abundance values were divided by the sum over all ages to generate a cumulative distribution of proportional abundance as a function of age.

For each species, cumulative predicted density distributions were analysed to obtain minimum forest age thresholds (y) corresponding with percentile values (x) of predicted avian density ranging from 1% to 50%. The 18th percentile yielded the highest variance in forest age threshold across species ($\bar{y} = 40.0$, $SD = 21.2$), indicating a peak in discrimination potential. To be conservative, we selected the 15th percentile of predicted density for identifying minimum forest age thresholds, bracketed by values of 5th and 25th percentiles to determine sensitivity. Species-specific minimum forest ages based on these percentiles were then used to assign species-specific time lags corresponding with the three 30-year intervals encompassed by our future projections, based on the midpoint of each 30-year period. That is, a species with a minimum forest age of 15 years or less was considered to have no time lag, a species with a minimum forest age of 16-45 years had a 30-year lag period, 46-75 years or less had a 60-year lag period, and 76 years or more had a 90-year lag period.

References

- Cumming, S.G., Drever, C.R., Houle, M., Cosco, J., Racine, P., Bayne, E. & Schmiegelow, F.K.A. 2015. A gap analysis of tree species representation in the protected areas of the Canadian boreal forest: applying a new assemblage of digital Forest Resource Inventory data. *Canadian Journal of Forest Research* **45**, 163-173.
- R Core Team. 2013. R: A language and environment for statistical computing. <http://www.R-project.org/>. R Foundation for Statistical Computing.
- Sólymos, P., Matsuoka, S.M., Bayne, E.M., Lele, S.R., Fontaine, P., Cumming, S.G., Stralberg, D., Schmiegelow, F.K.A. & Song, S.J. 2013. Calibrating indices of avian density from non-standardized survey data: making the most of a messy situation. *Methods in Ecology and Evolution* **4**, 1047-1058.
- Wood, S.N. 2011. Fast stable restricted maximum likelihood and marginal likelihood estimation of semiparametric generalized linear models. *Journal of the Royal Statistical Society: Series B (Statistical Methodology)* **73**, 3-36.

Appendix 2-C. Alternative distributional assumptions for 53 boreal species.

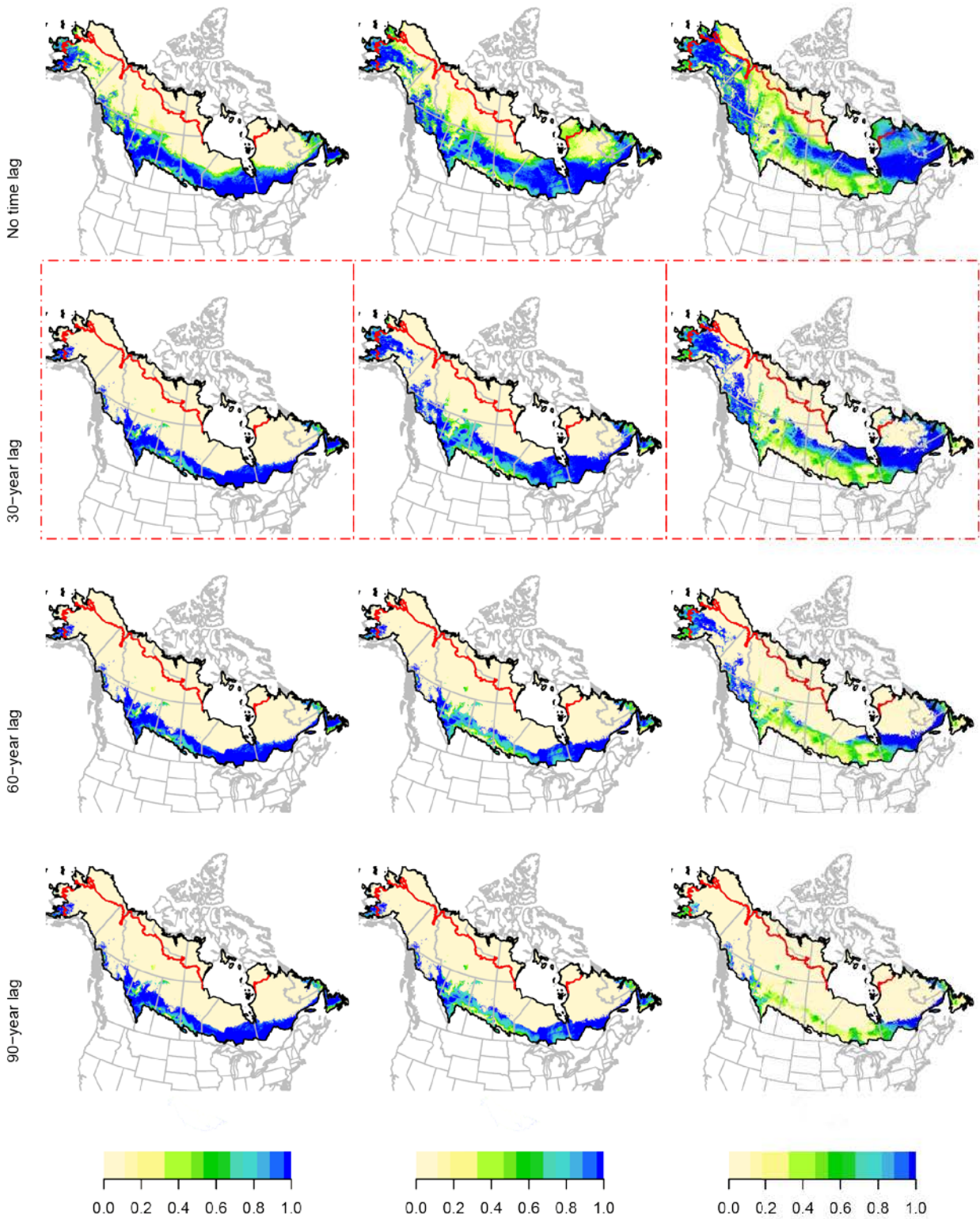
Most likely scenarios according to analysis of forest inventory data outlined with red dotted lines. See species code definitions in Appendix 2-A.

AMRE

a. 2011-2040

b. 2041-2070

c. 2071-2100

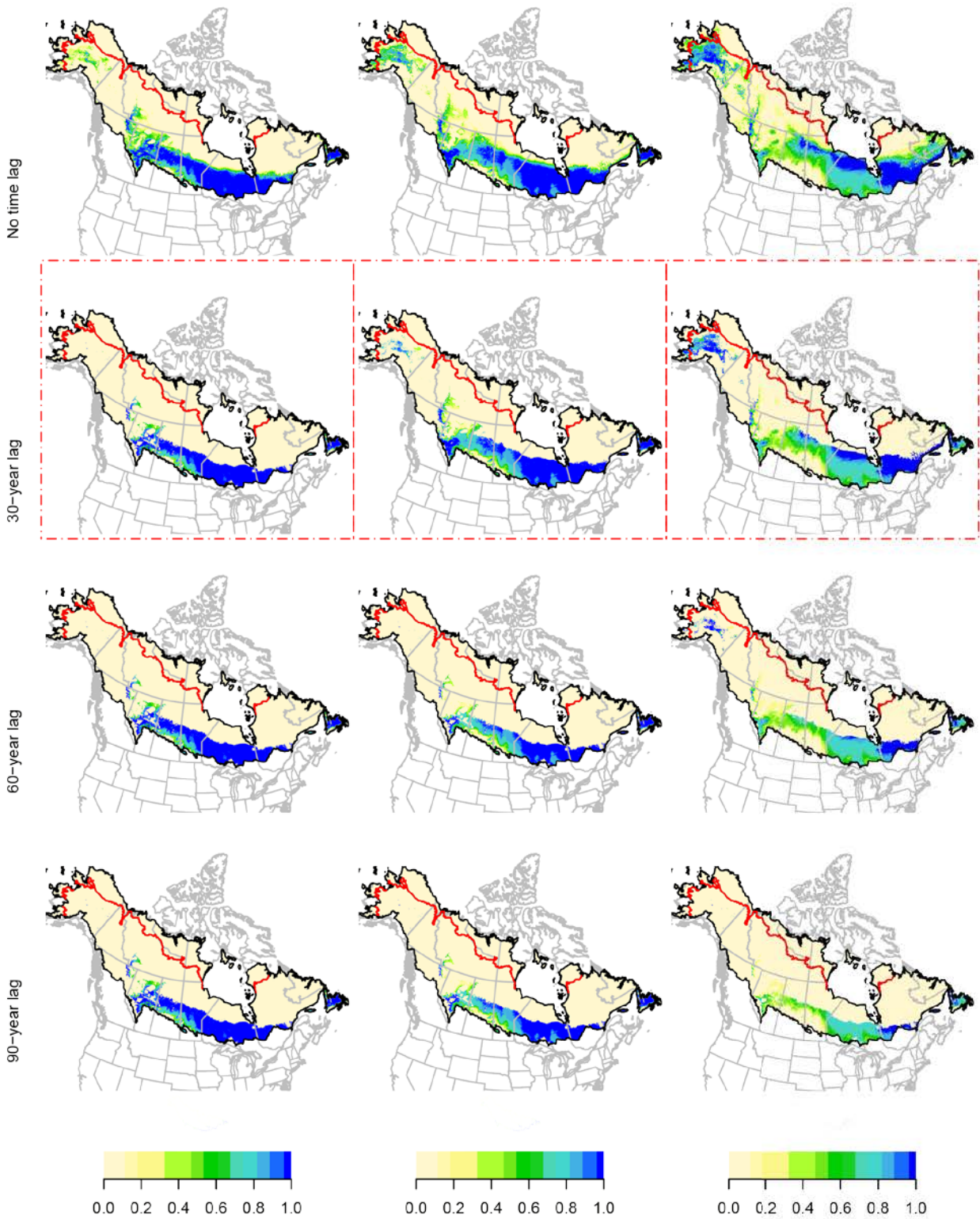


BAWW

a. 2011-2040

b. 2041-2070

c. 2071-2100

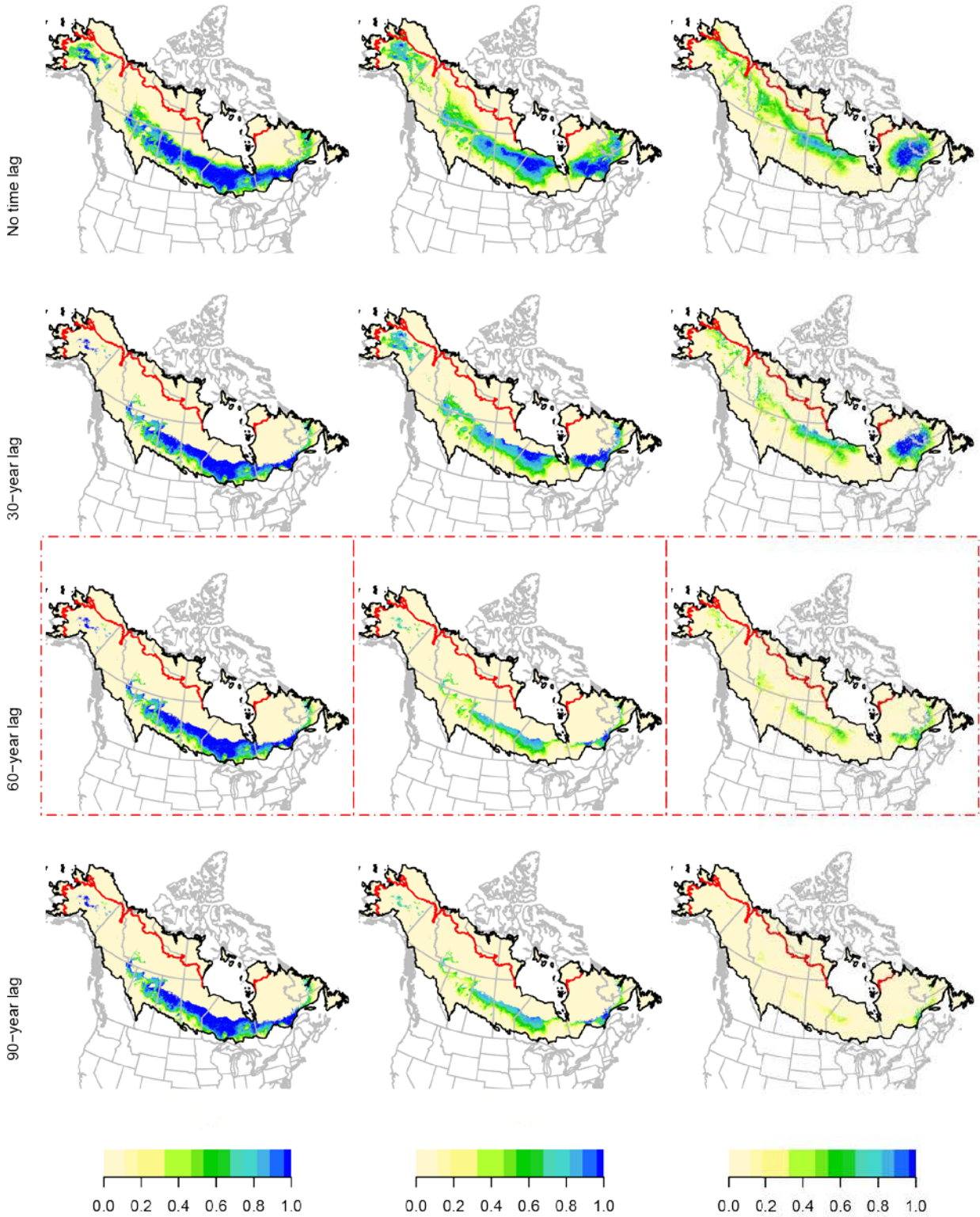


BBWA

a. 2011-2040

b. 2041-2070

c. 2071-2100

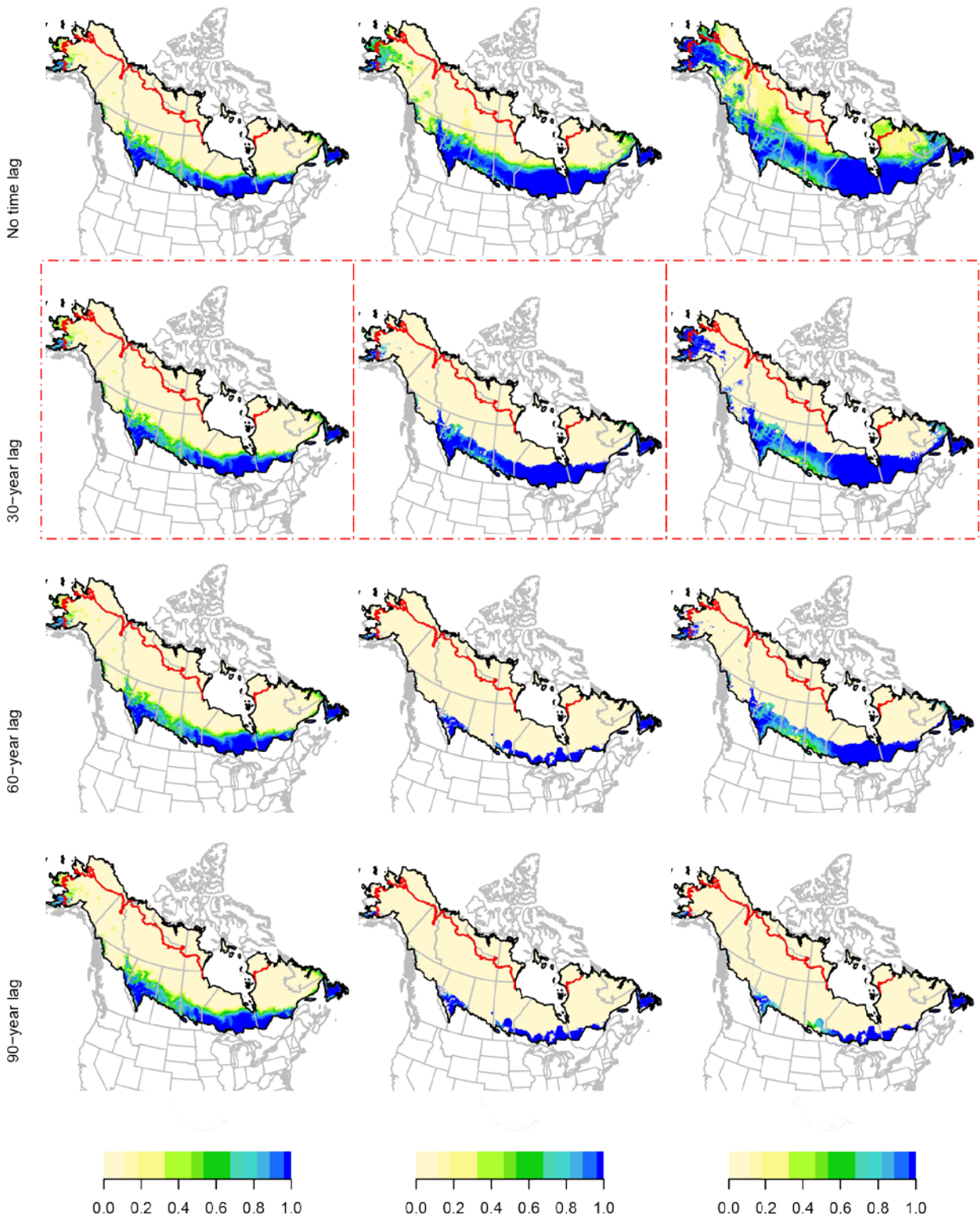


BCCH

a. 2011-2040

b. 2041-2070

c. 2071-2100

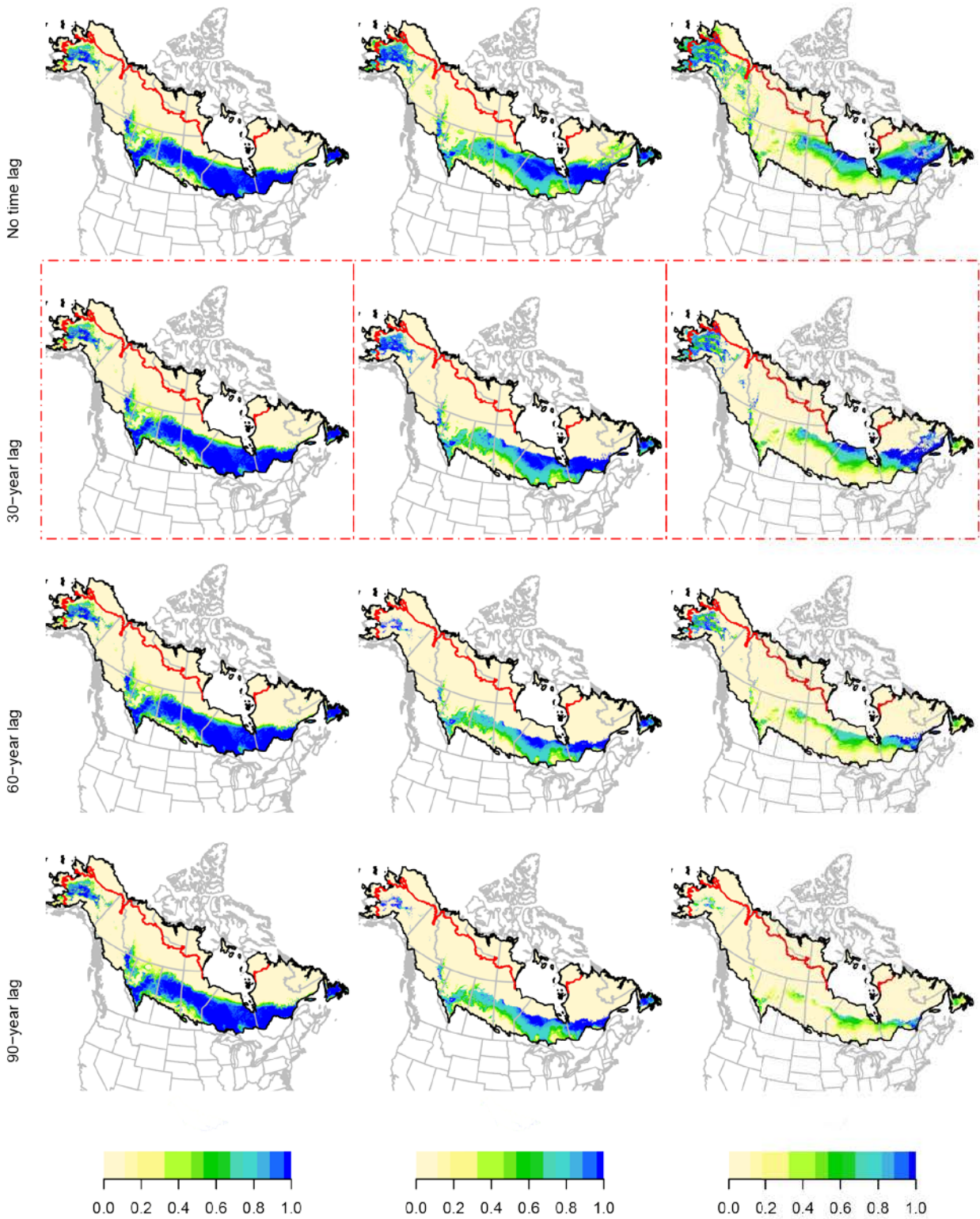


BHVI

a. 2011-2040

b. 2041-2070

c. 2071-2100

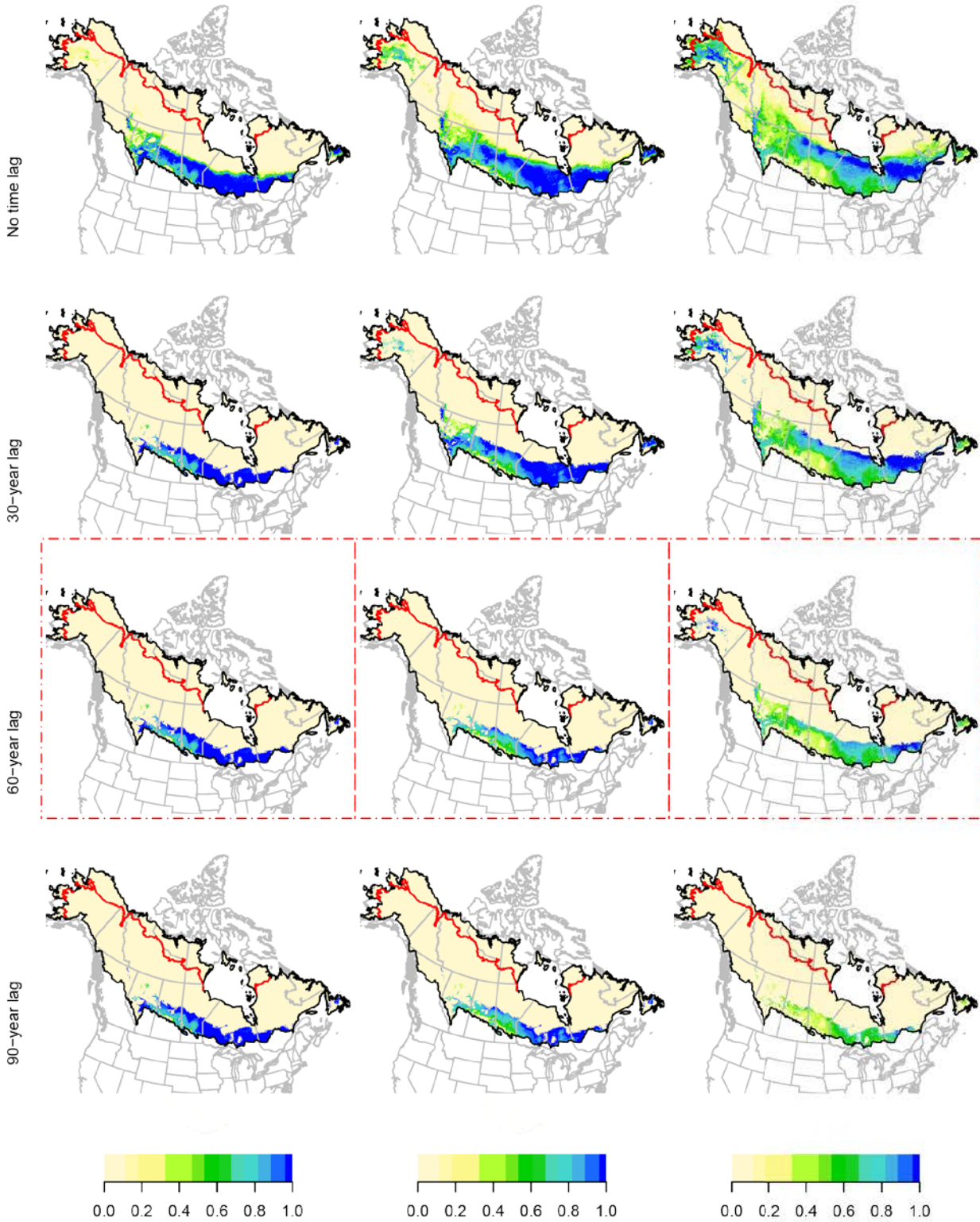


BLBW

a. 2011-2040

b. 2041-2070

c. 2071-2100

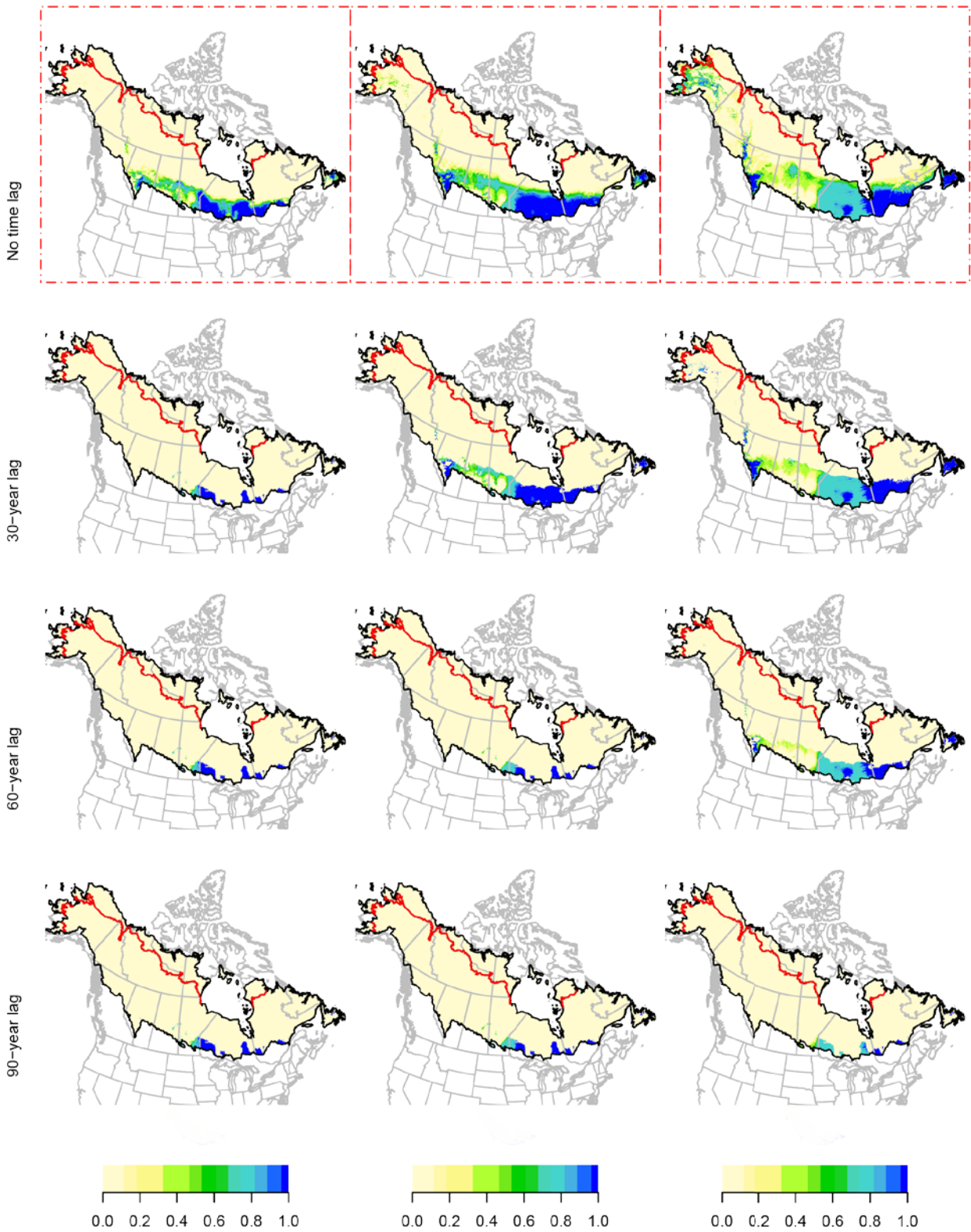


BLJA

a. 2011-2040

b. 2041-2070

c. 2071-2100

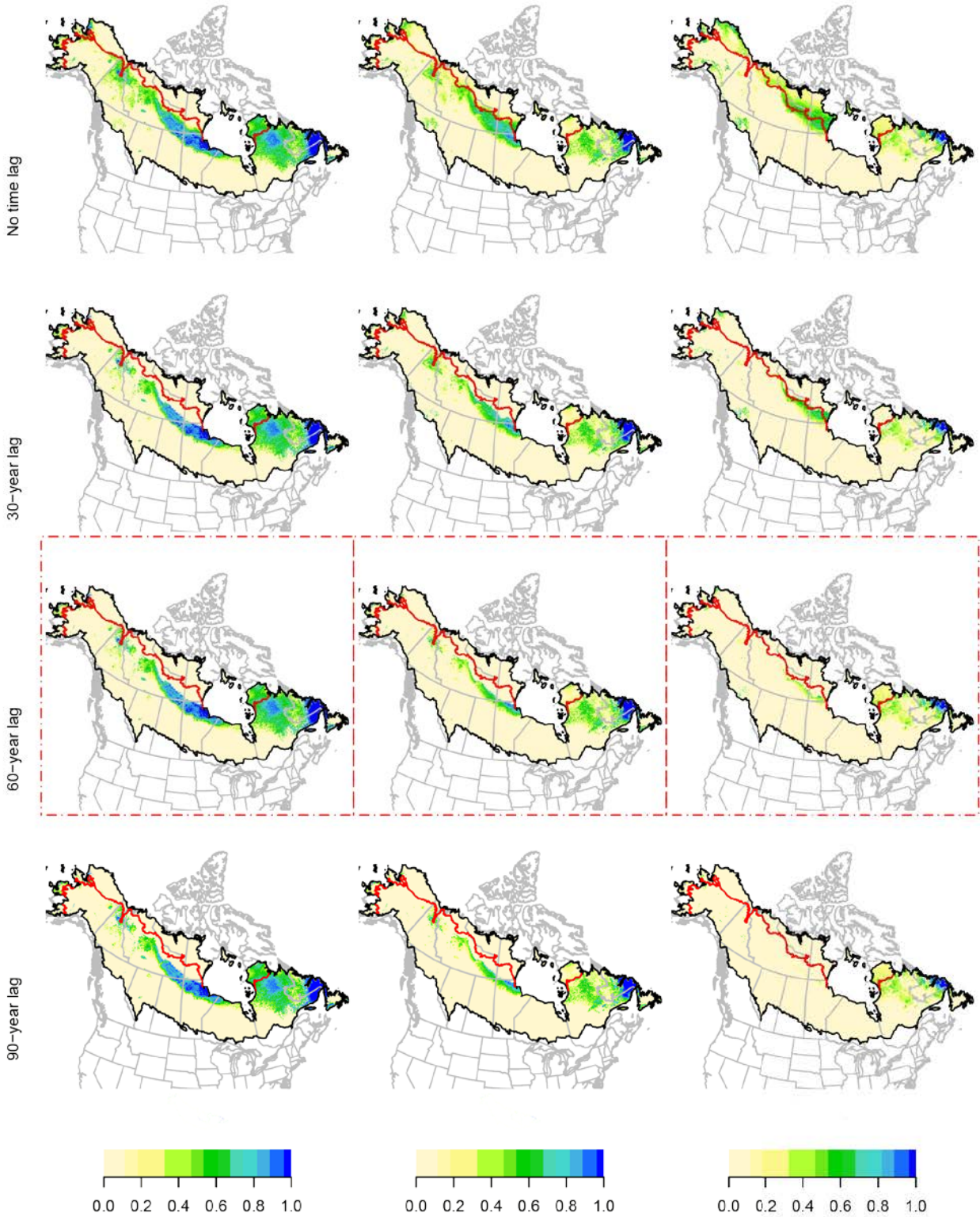


BLPW

a. 2011-2040

b. 2041-2070

c. 2071-2100

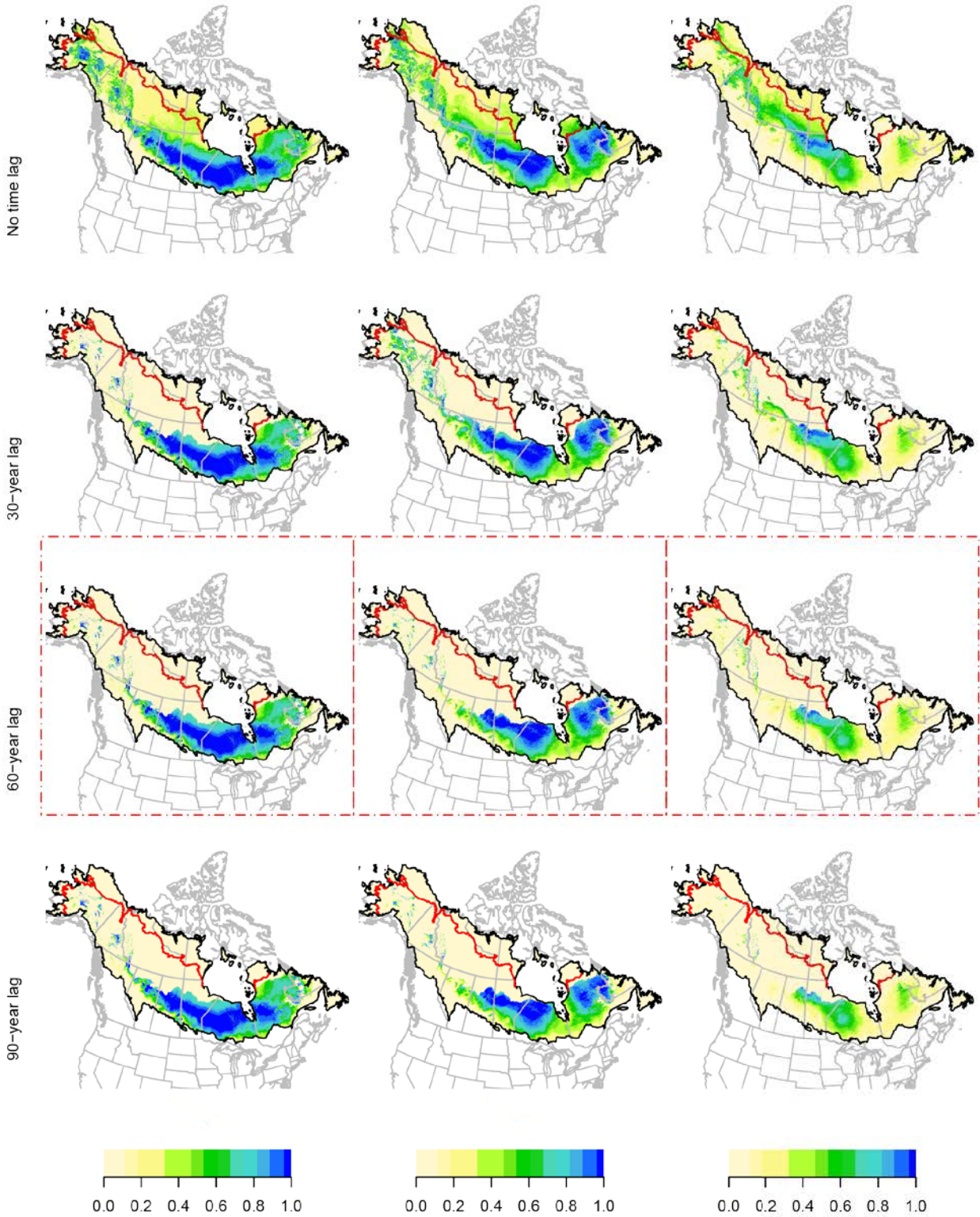


BRCR

a. 2011-2040

b. 2041-2070

c. 2071-2100

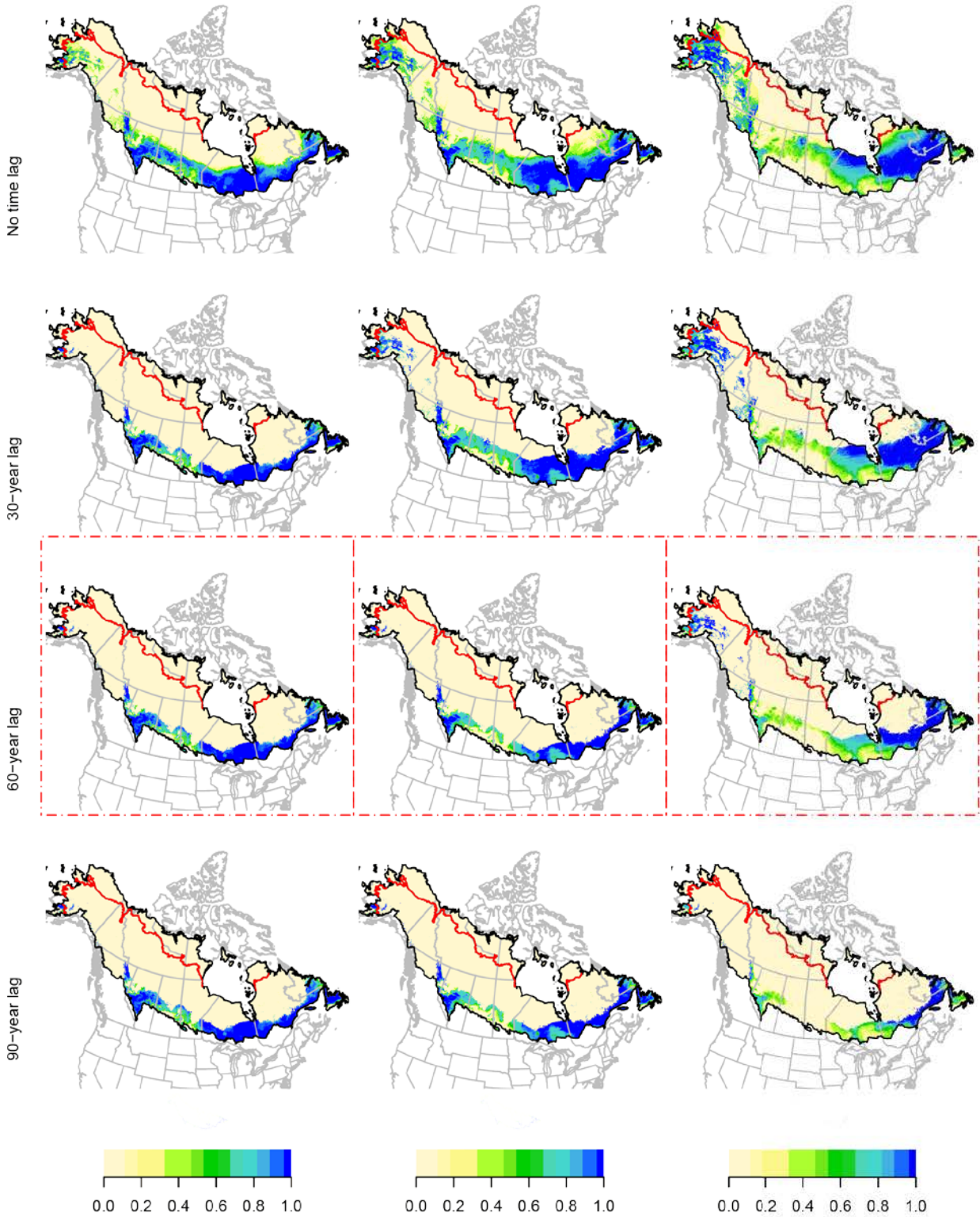


BTNW

a. 2011-2040

b. 2041-2070

c. 2071-2100

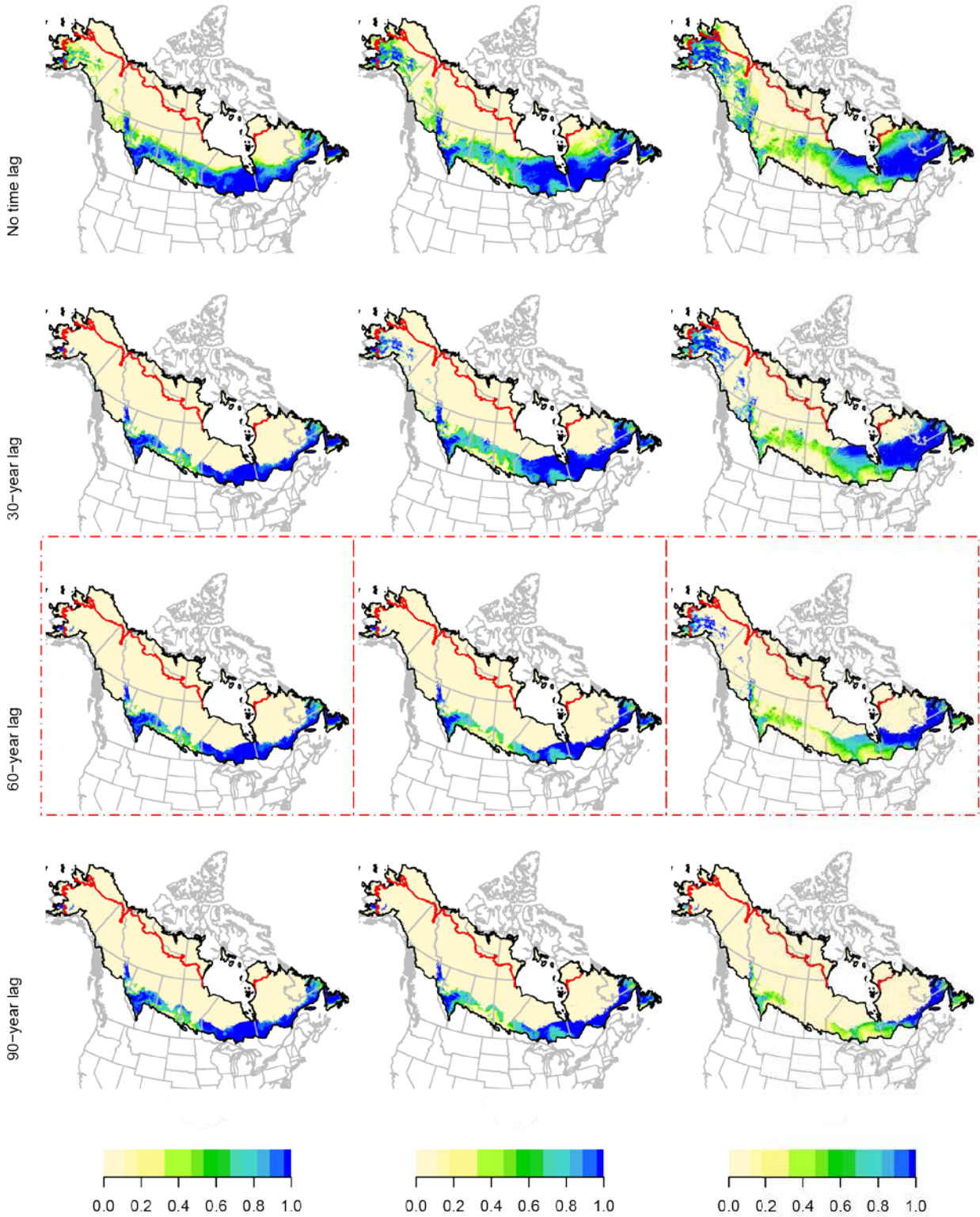


BTNW

a. 2011-2040

b. 2041-2070

c. 2071-2100

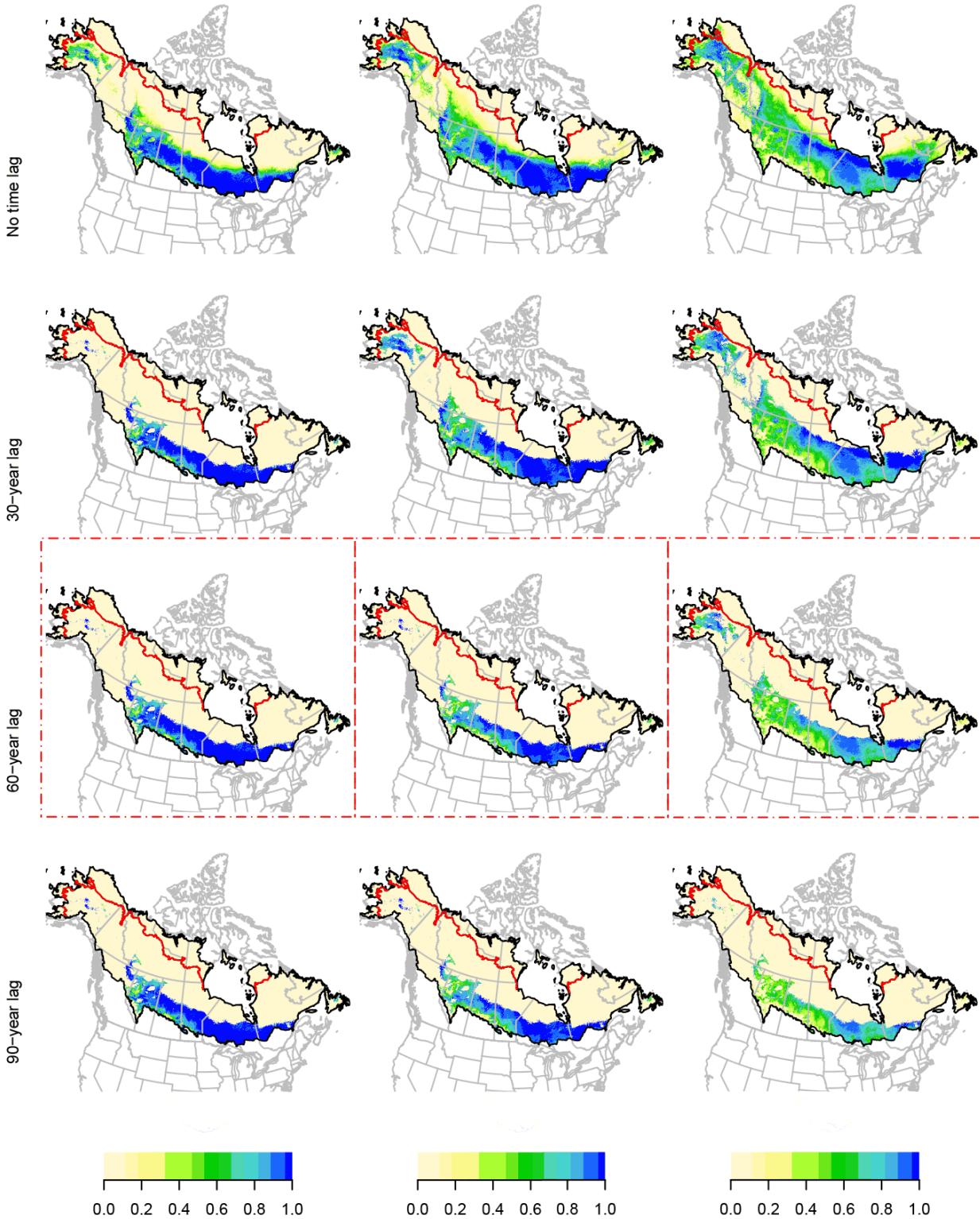


CAWA

a. 2011-2040

b. 2041-2070

c. 2071-2100

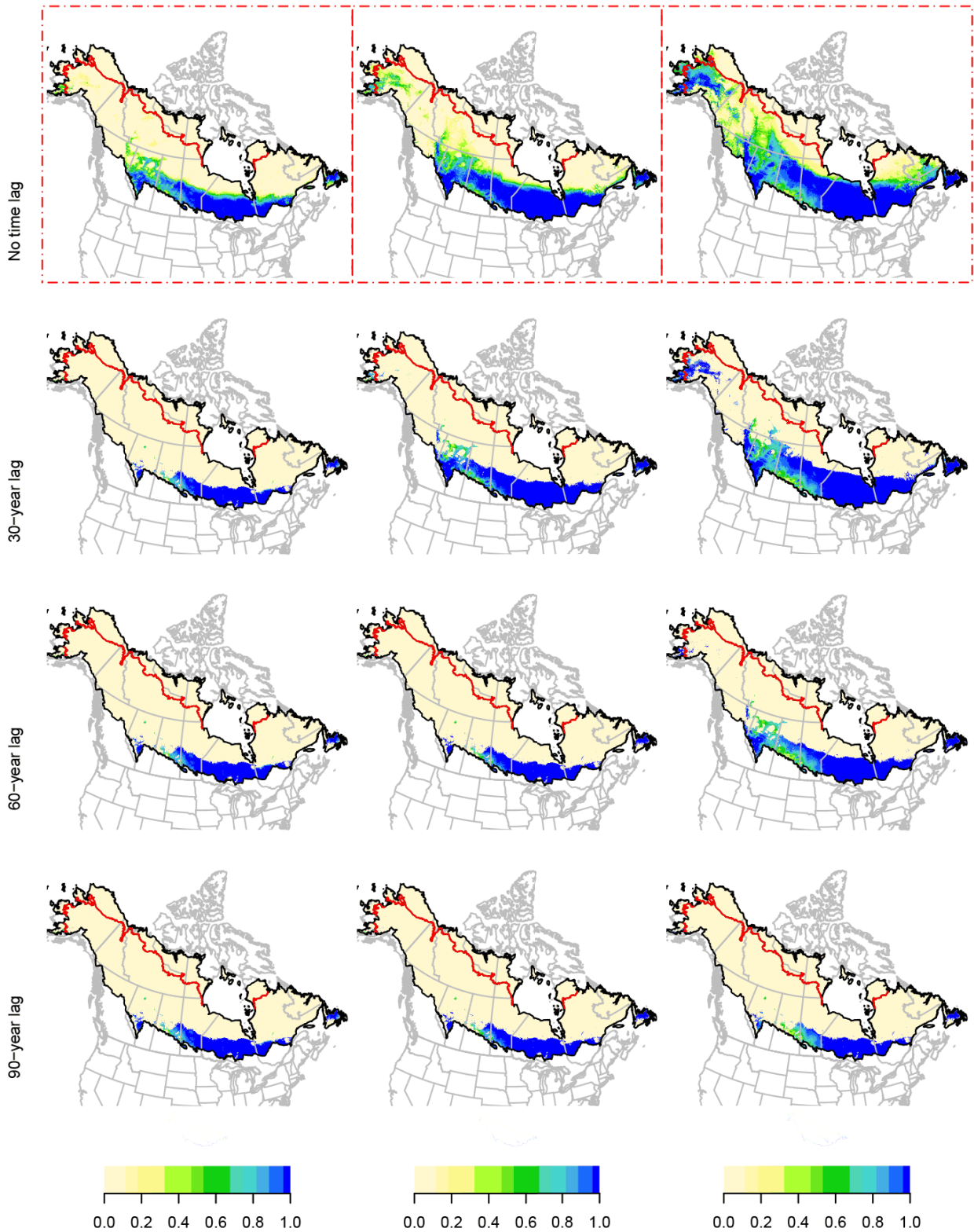


CEDW

a. 2011-2040

b. 2041-2070

c. 2071-2100

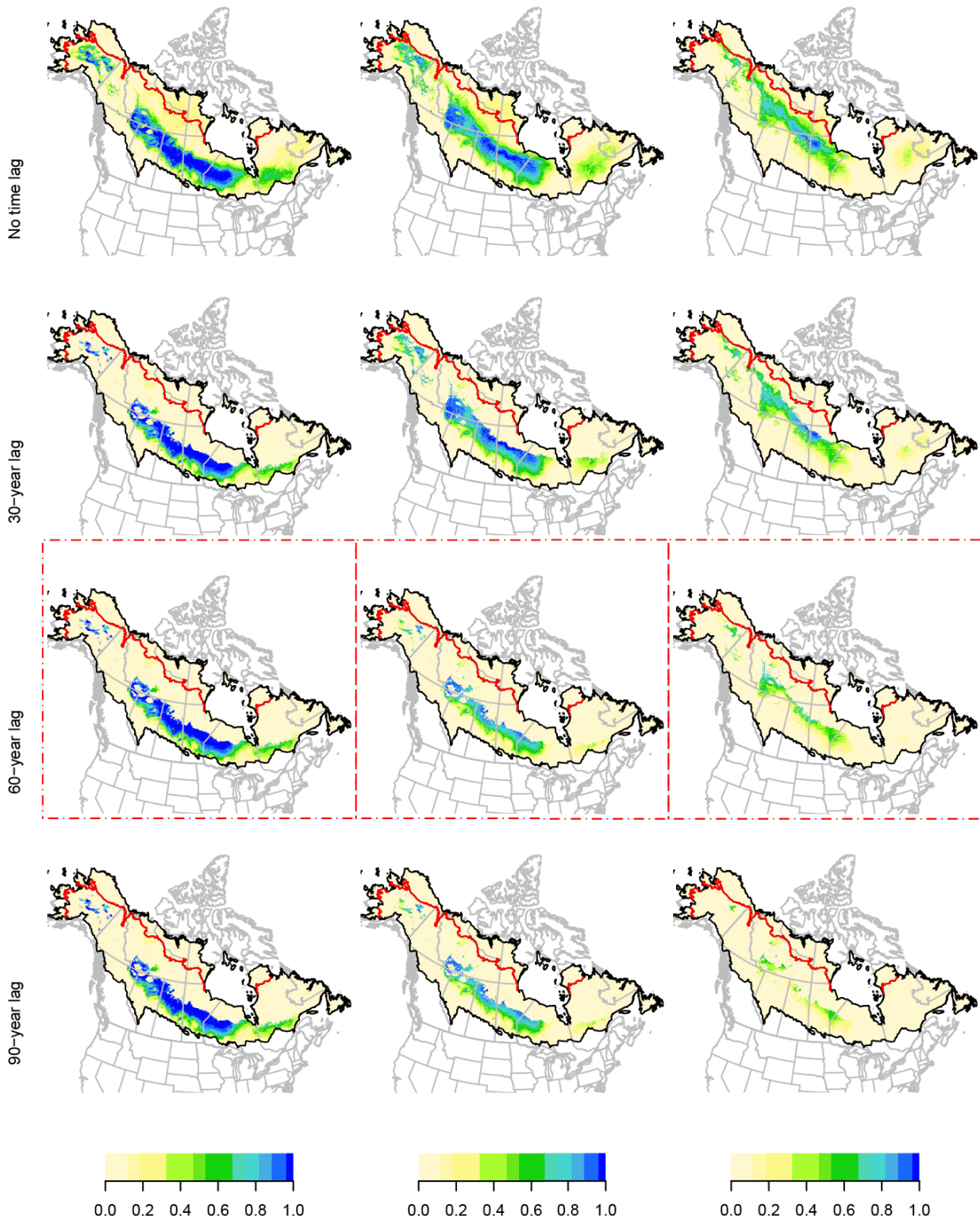


CMWA

a. 2011-2040

b. 2041-2070

c. 2071-2100

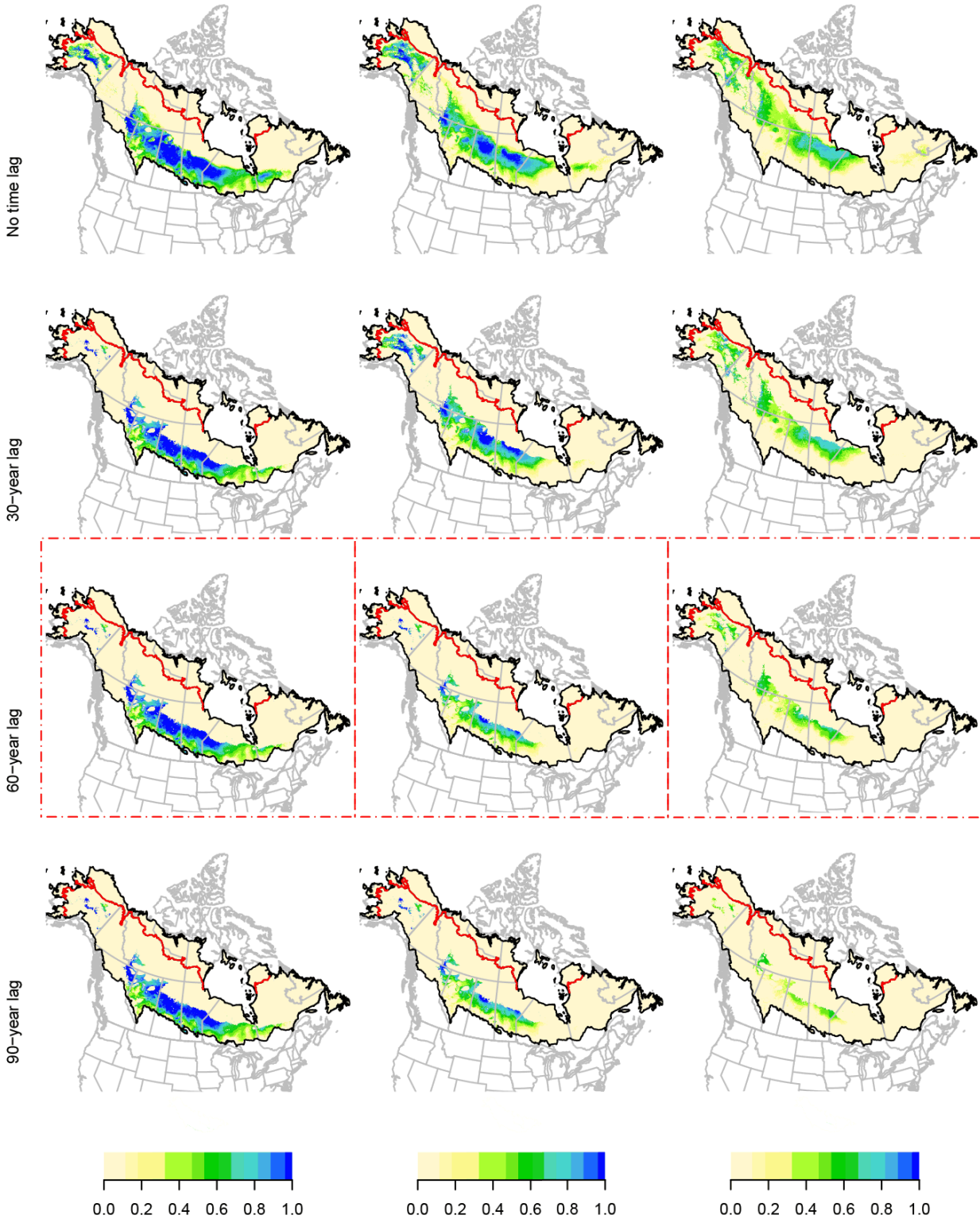


CONW

a. 2011-2040

b. 2041-2070

c. 2071-2100

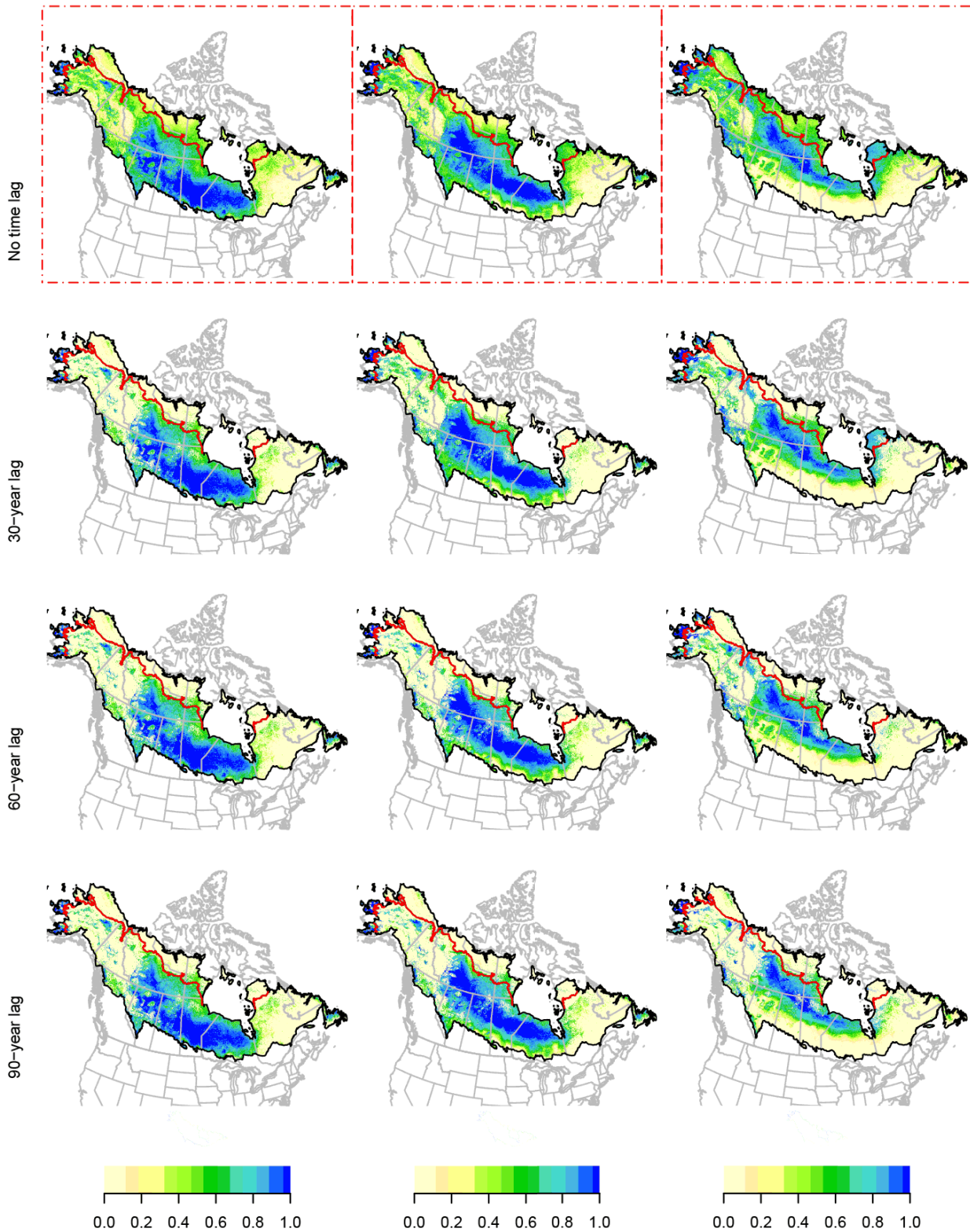


CORA

a. 2011-2040

b. 2041-2070

c. 2071-2100

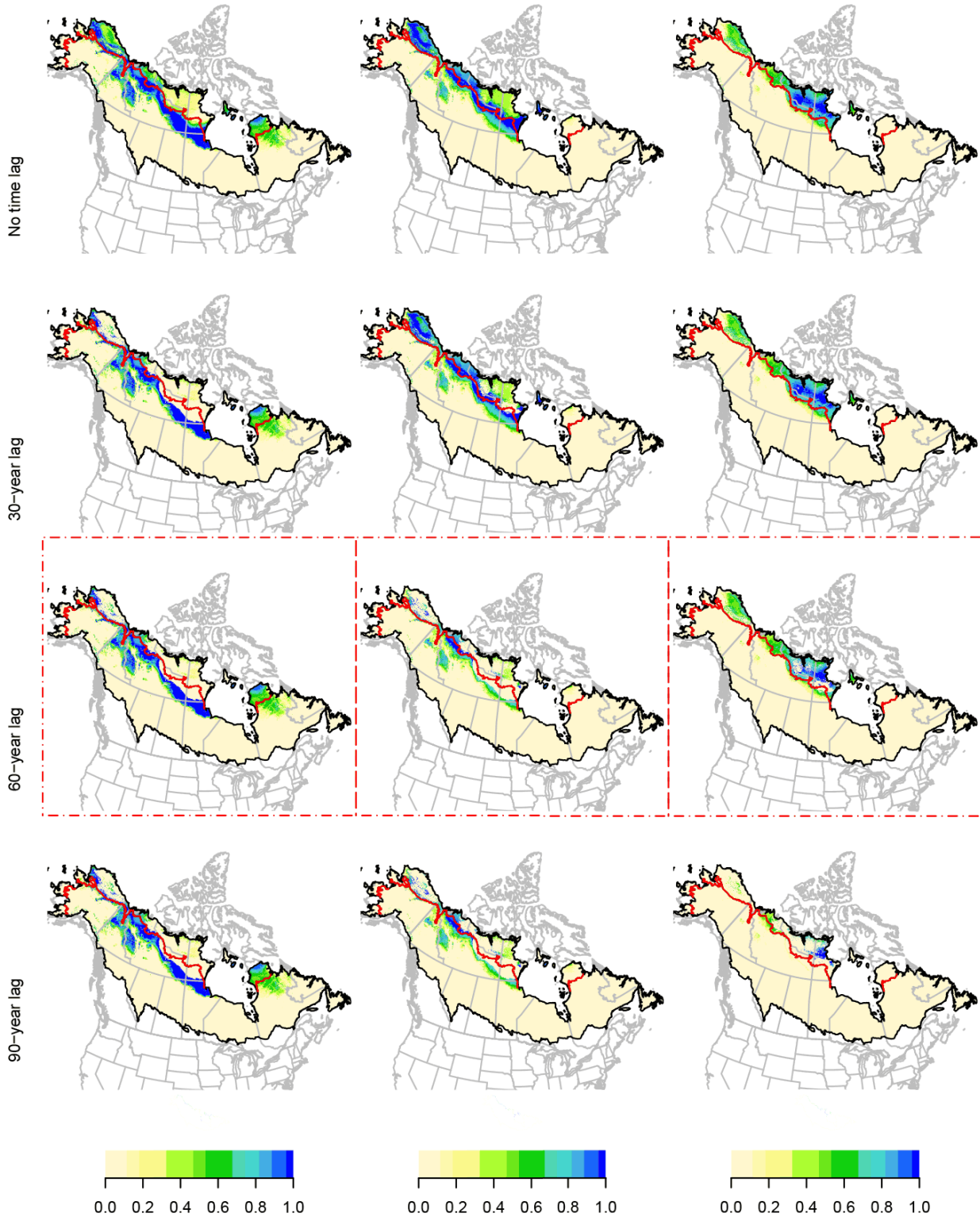


CORE

a. 2011-2040

b. 2041-2070

c. 2071-2100

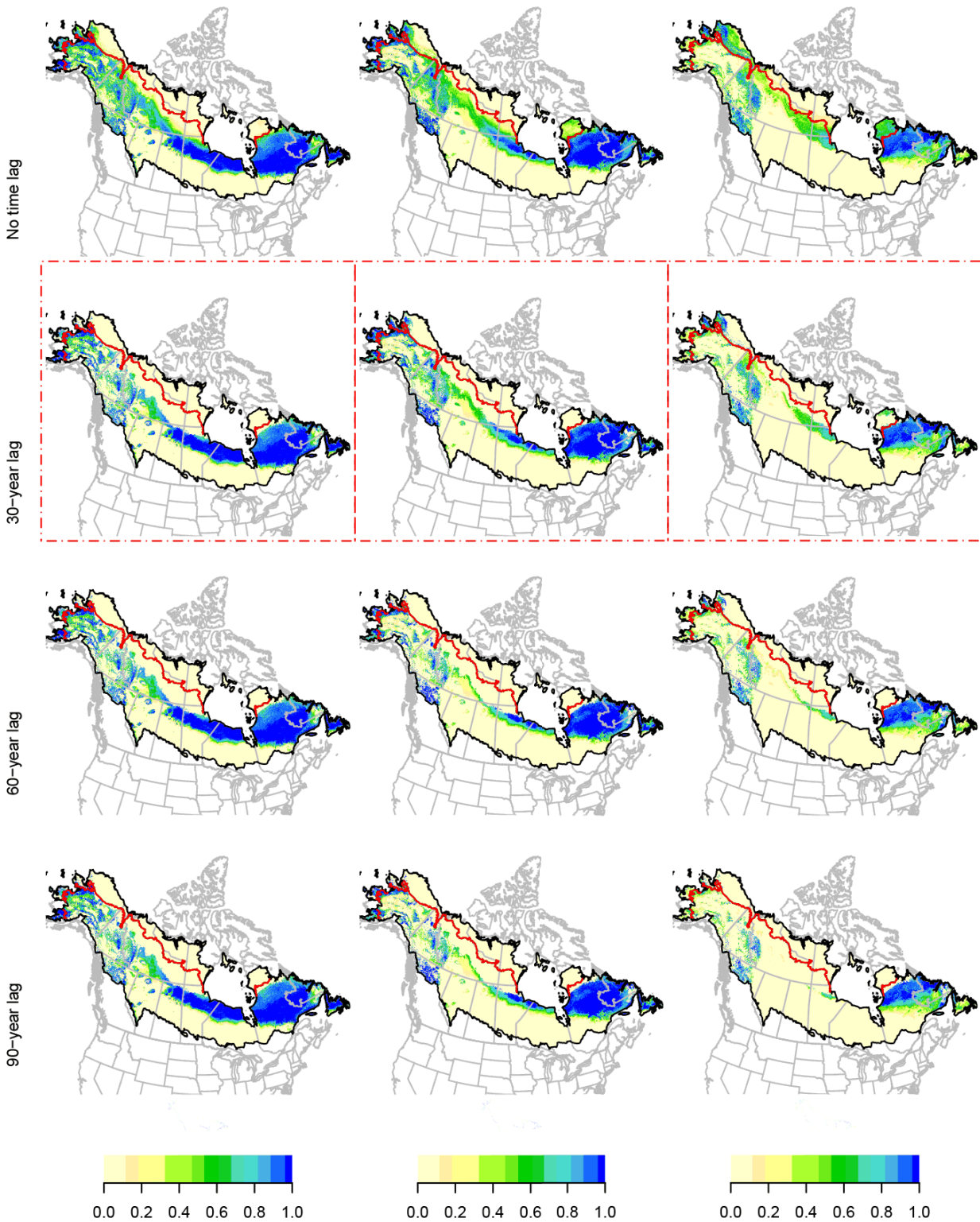


DEJU

a. 2011-2040

b. 2041-2070

c. 2071-2100

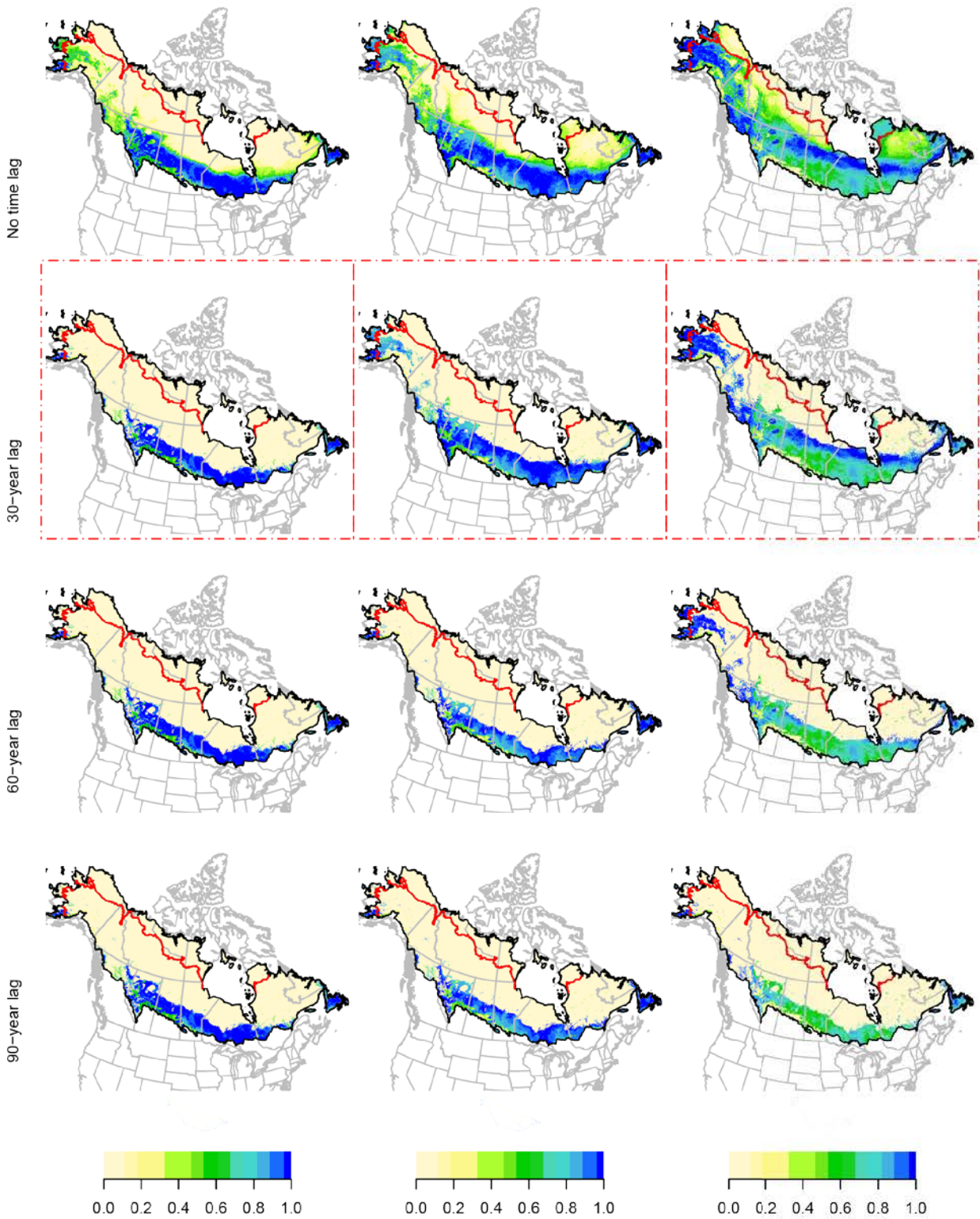


EVGR

a. 2011-2040

b. 2041-2070

c. 2071-2100

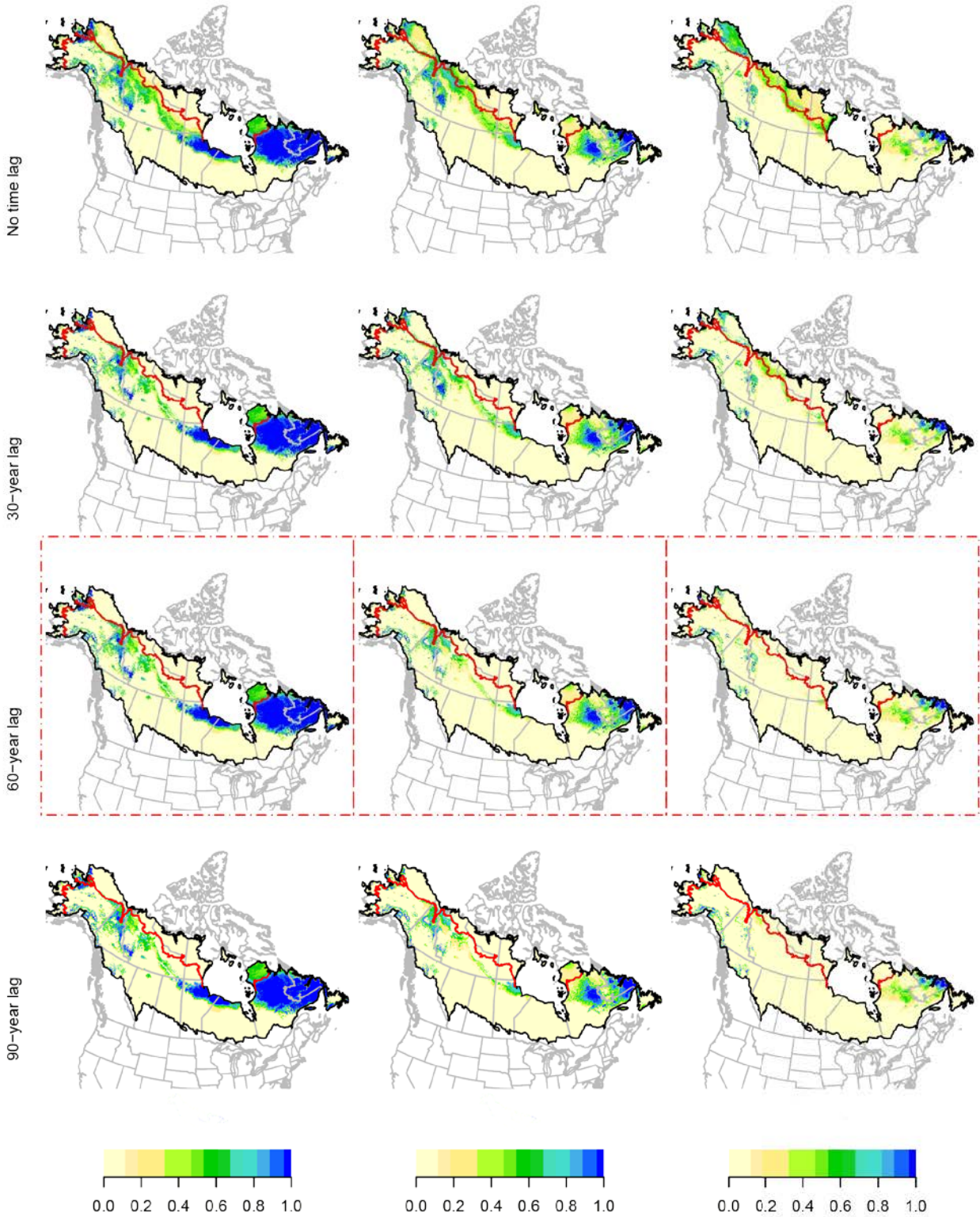


FOSP

a. 2011-2040

b. 2041-2070

c. 2071-2100

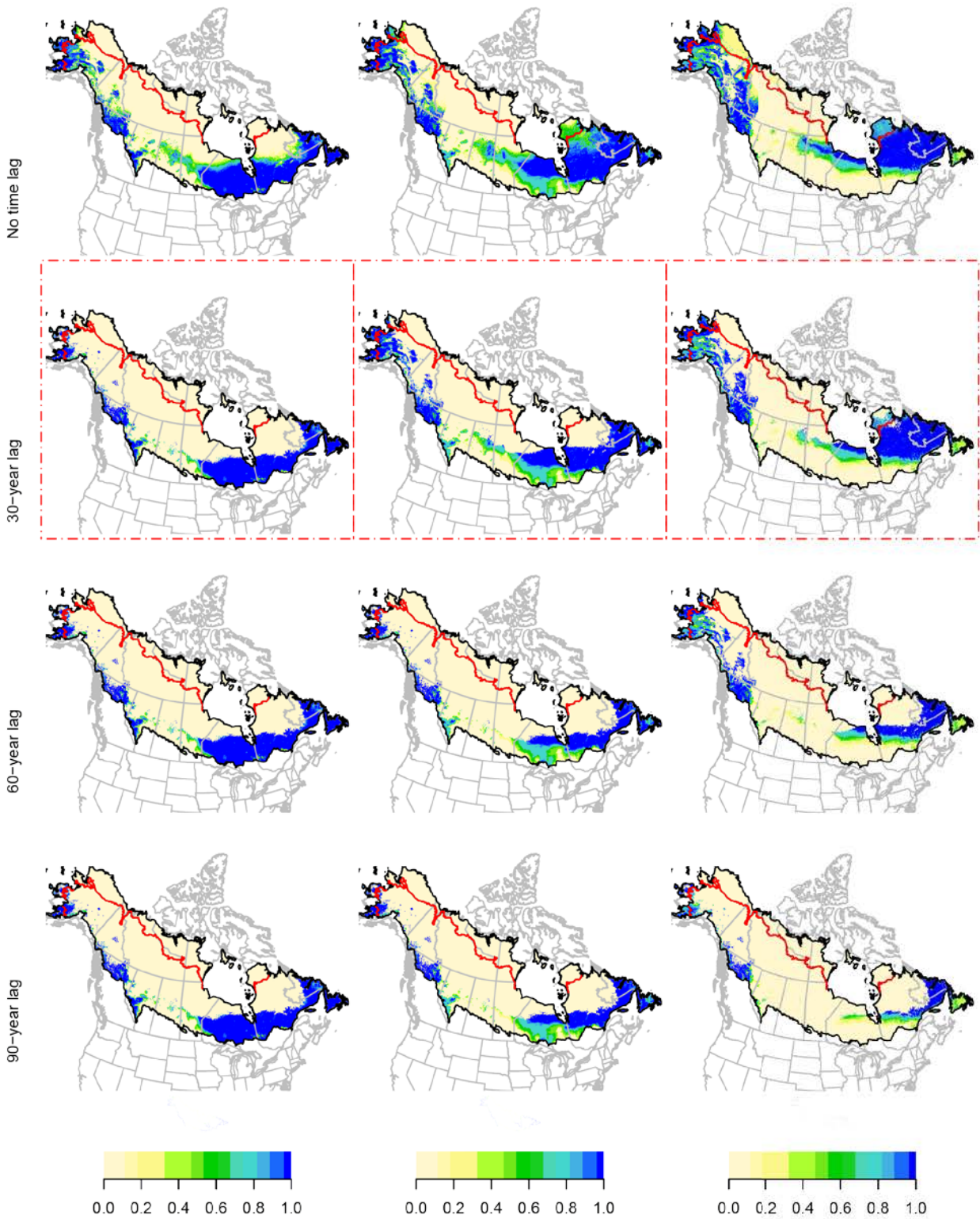


GCKI

a. 2011-2040

b. 2041-2070

c. 2071-2100



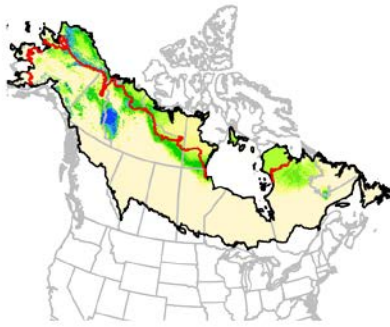
GCTH

a. 2011-2040

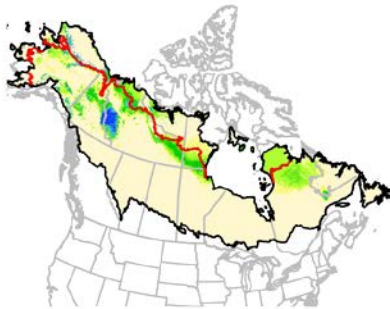
b. 2041-2070

c. 2071-2100

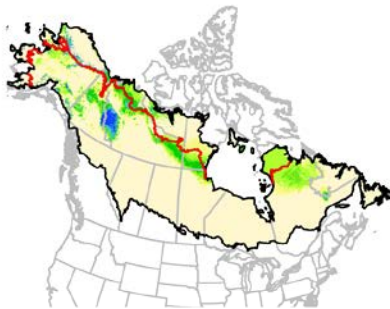
No time lag



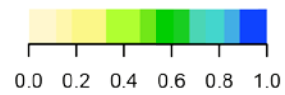
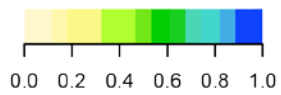
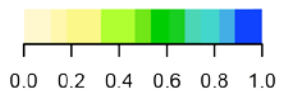
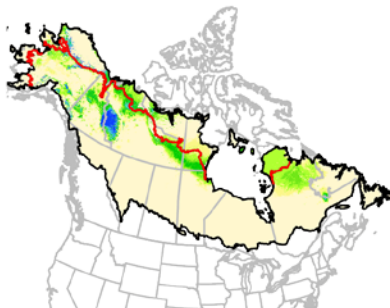
30-year lag



60-year lag



90-year lag

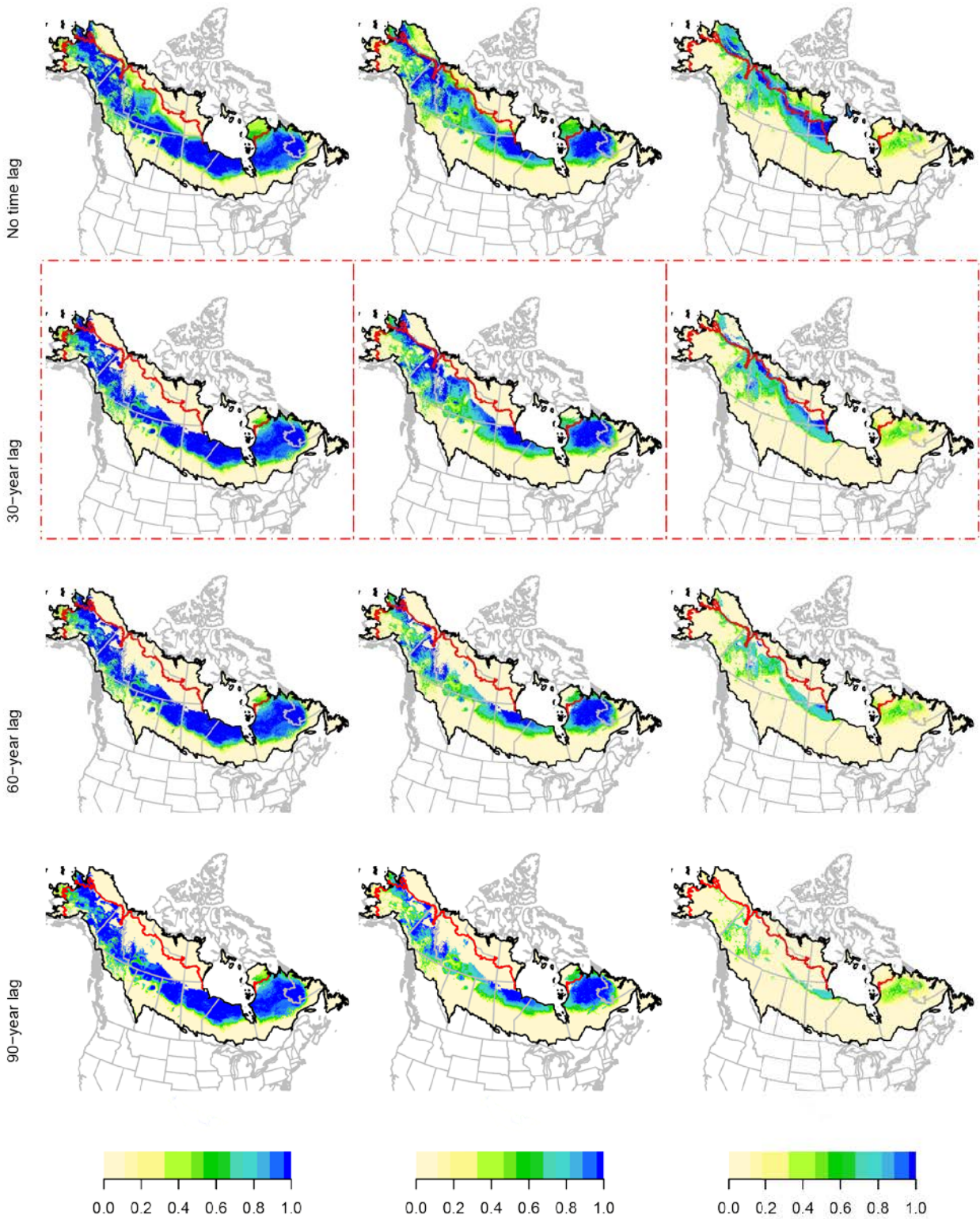


GRAJ

a. 2011-2040

b. 2041-2070

c. 2071-2100

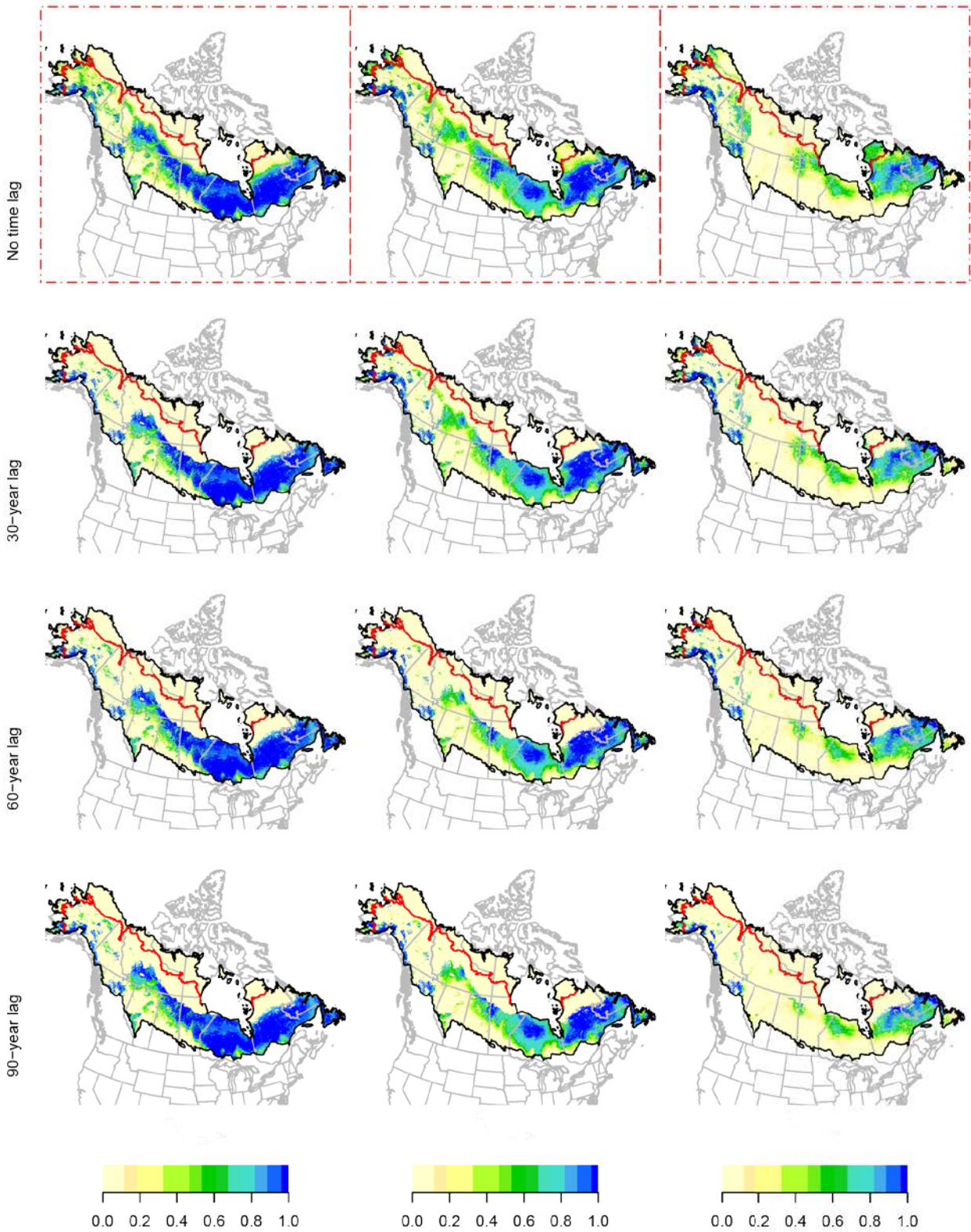


HETH

a. 2011-2040

b. 2041-2070

c. 2071-2100

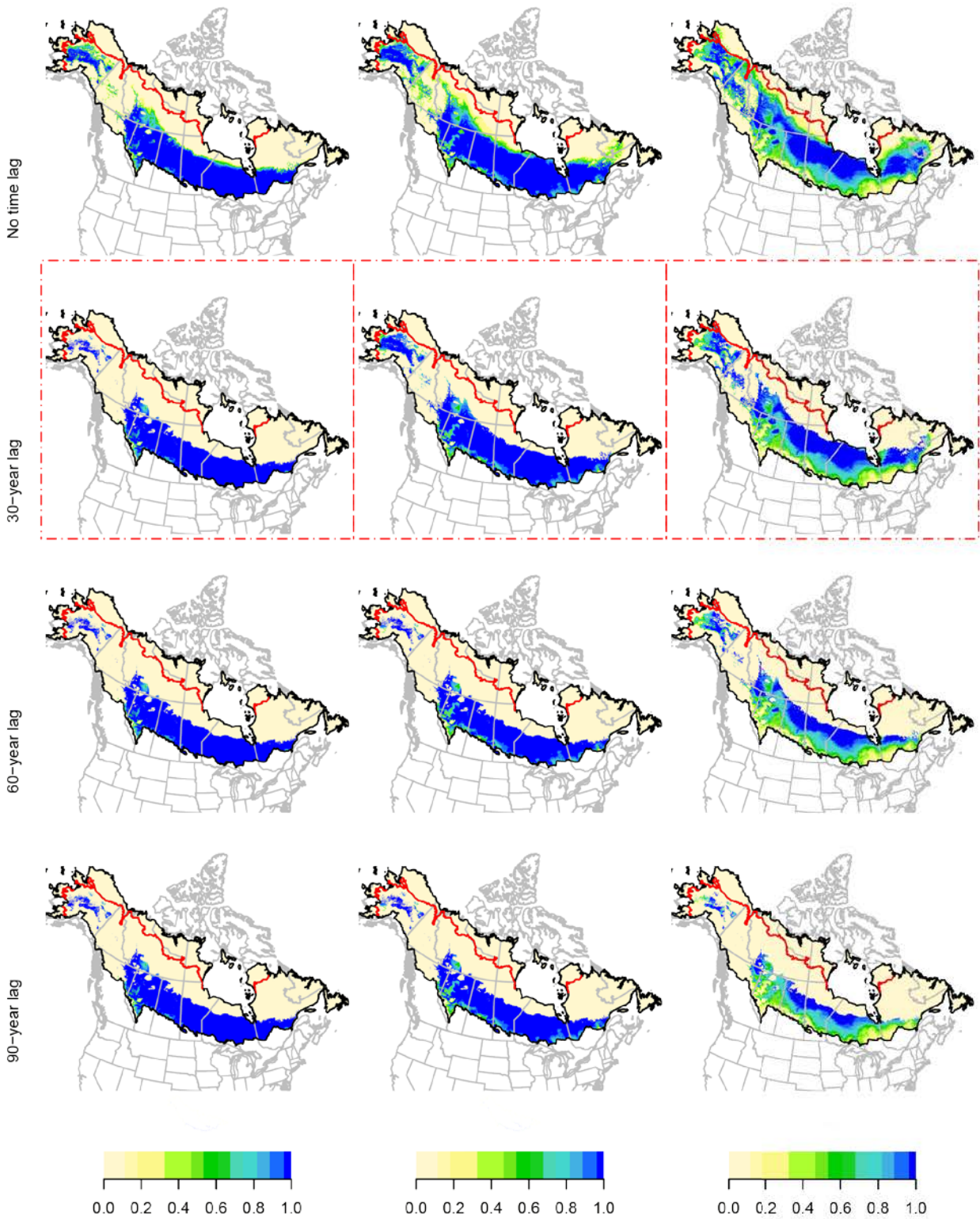


LEFL

a. 2011-2040

b. 2041-2070

c. 2071-2100

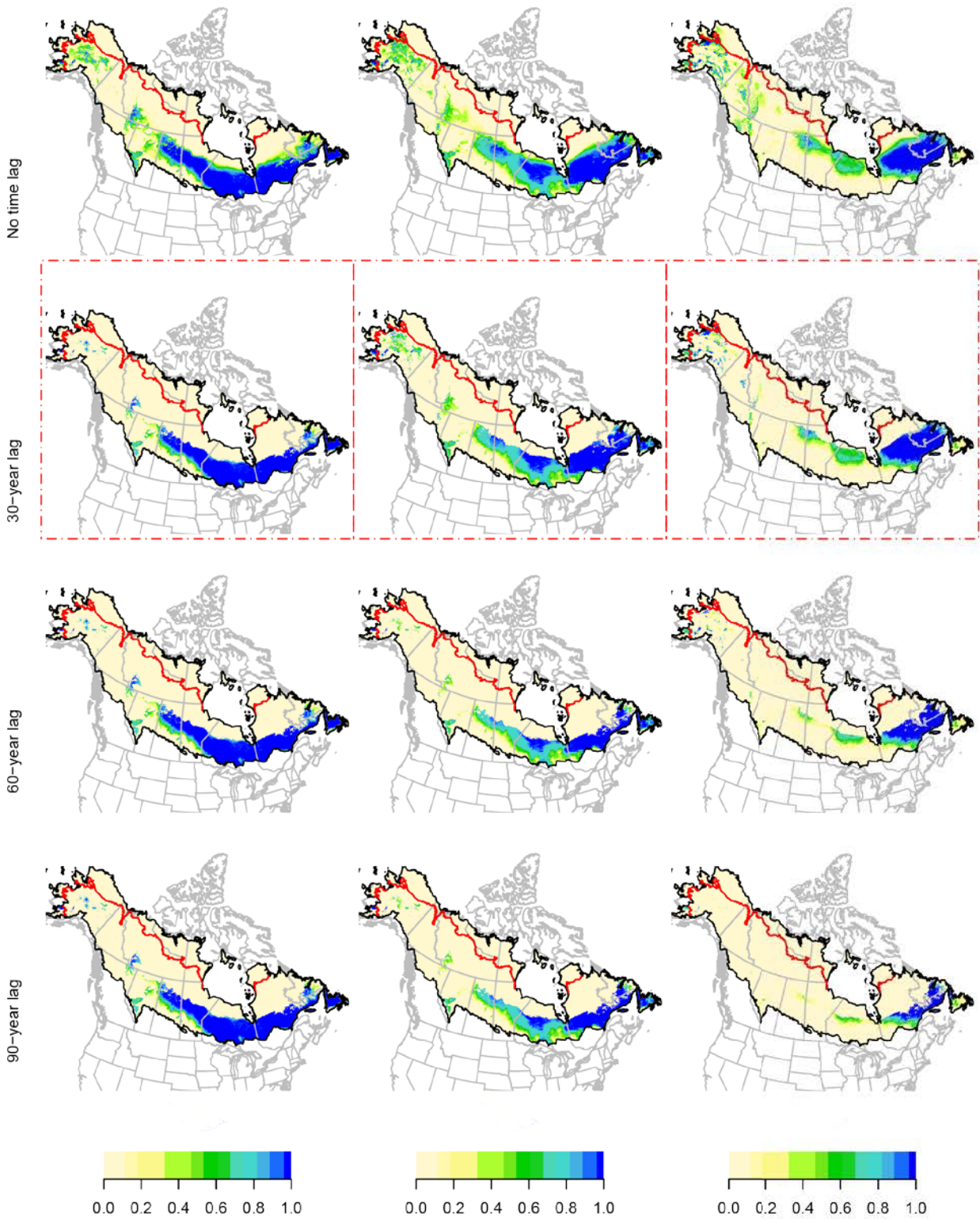


MAWA

a. 2011-2040

b. 2041-2070

c. 2071-2100

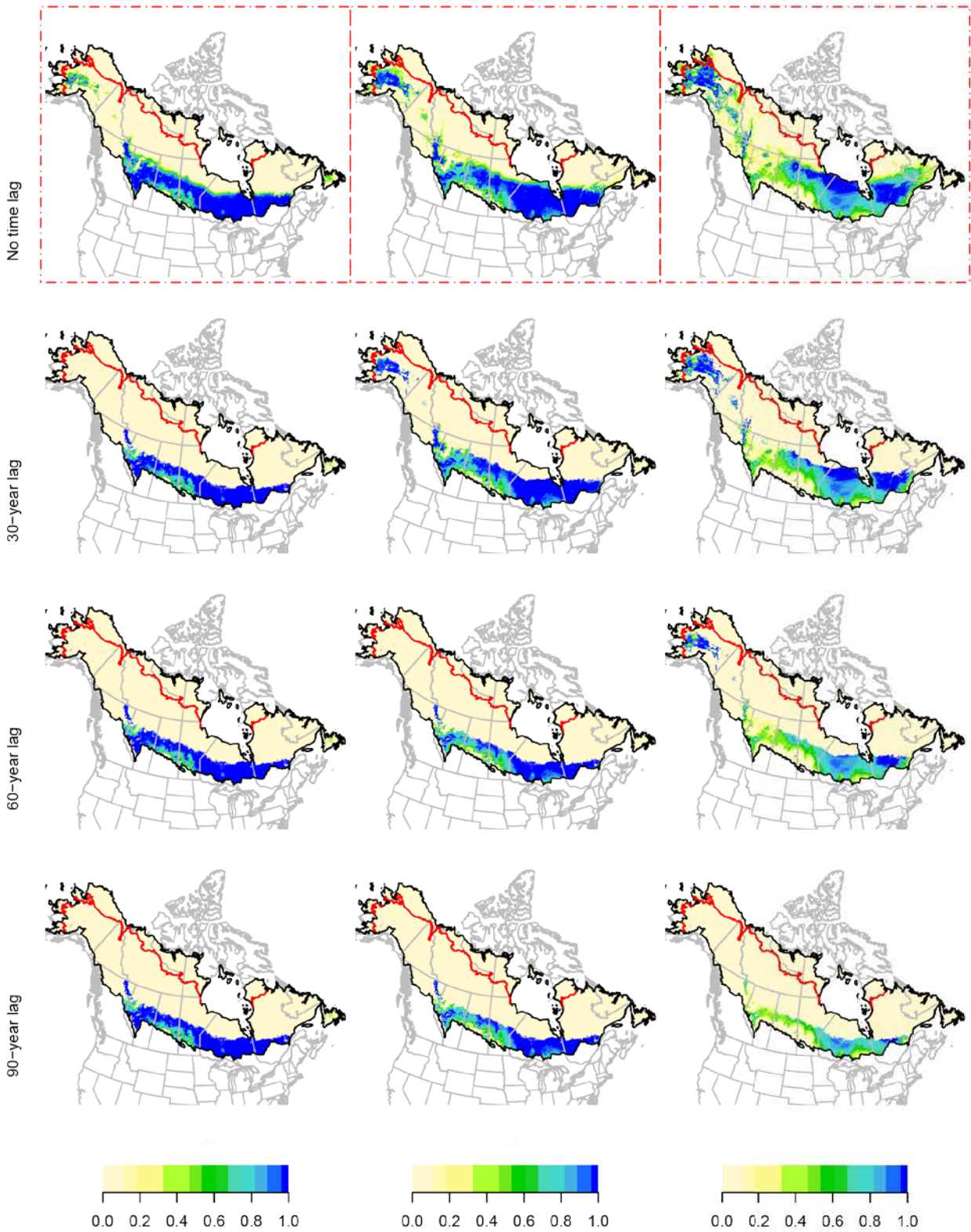


MOWA

a. 2011-2040

b. 2041-2070

c. 2071-2100

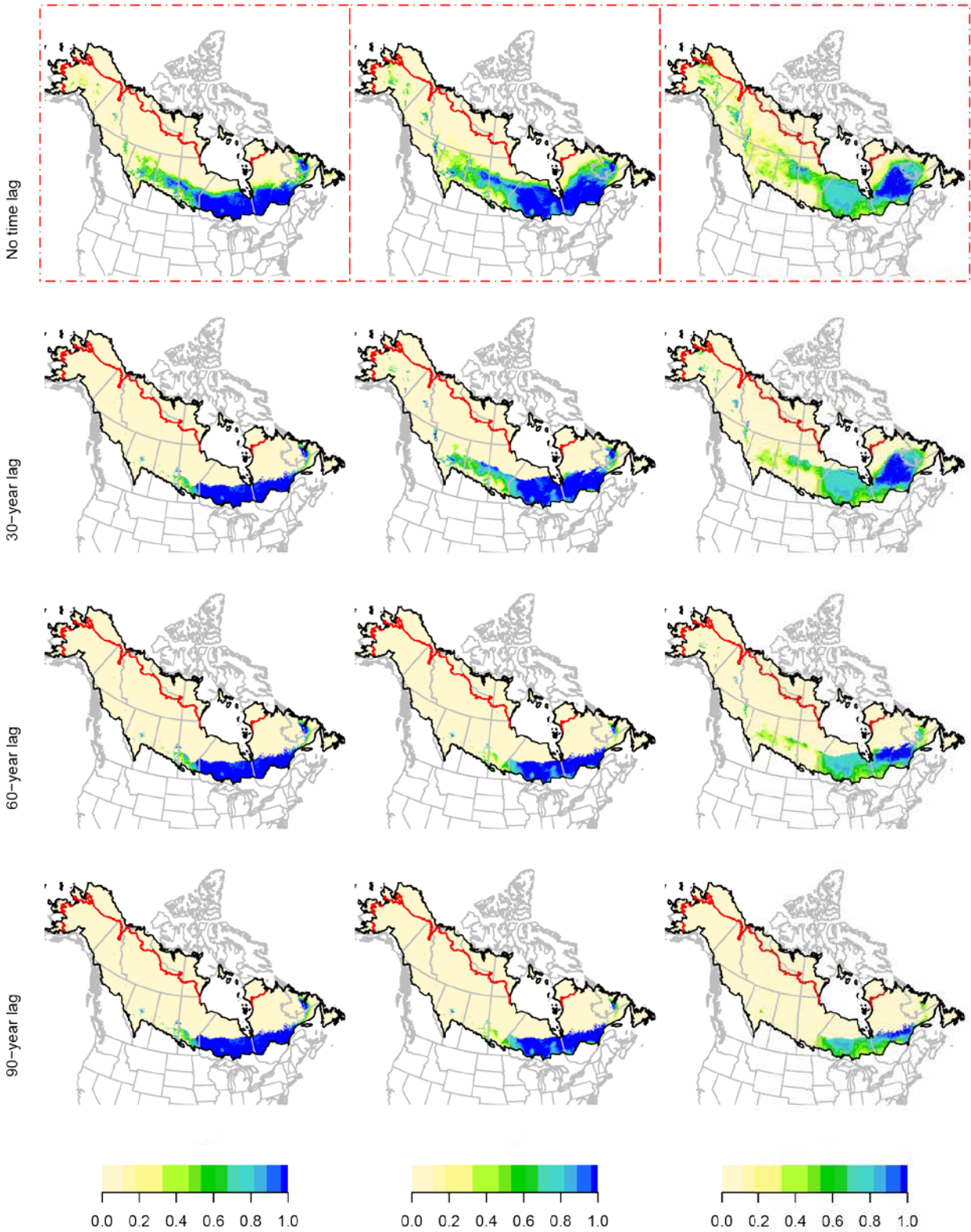


NAWA

a. 2011-2040

b. 2041-2070

c. 2071-2100

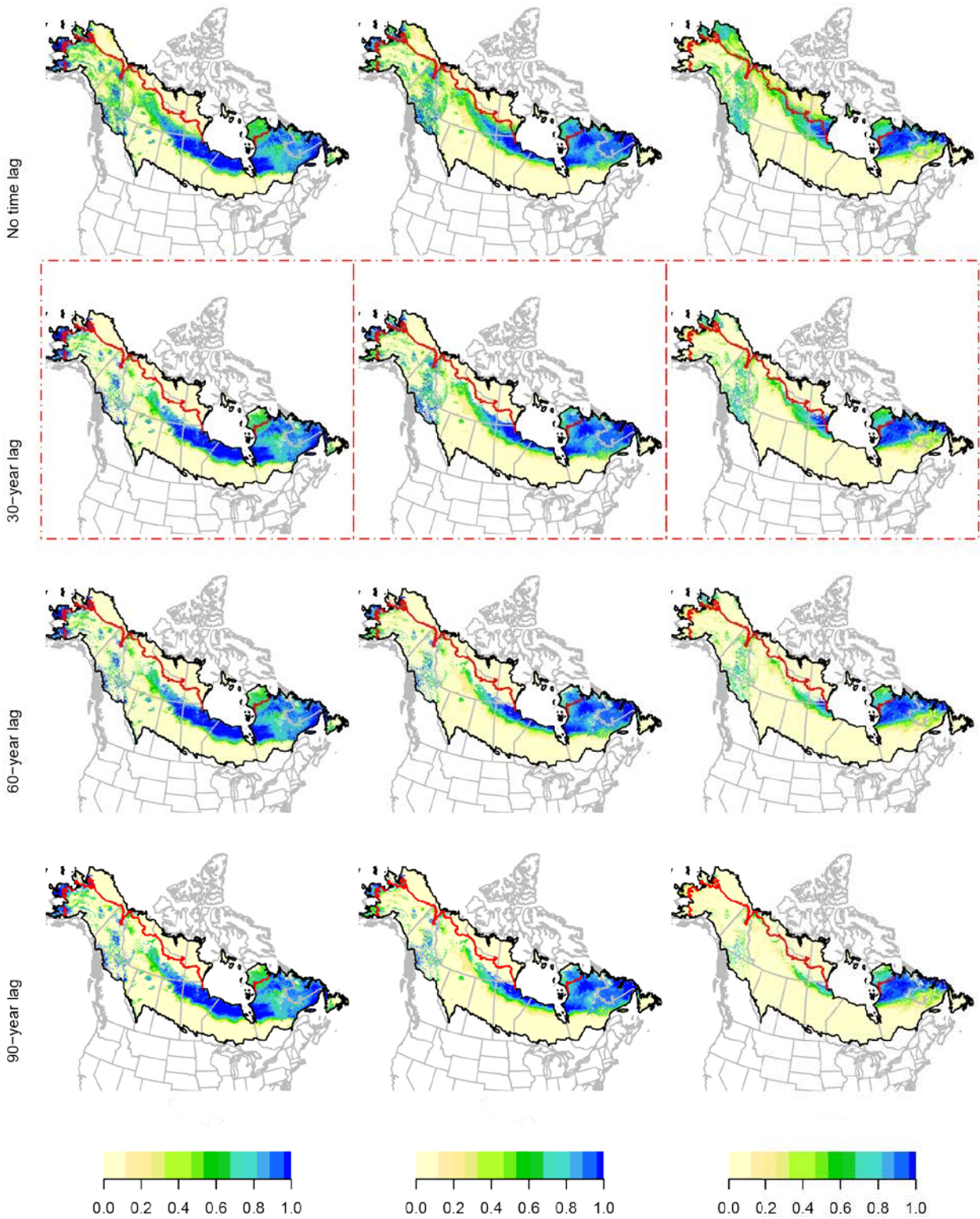


NOWA

a. 2011-2040

b. 2041-2070

c. 2071-2100

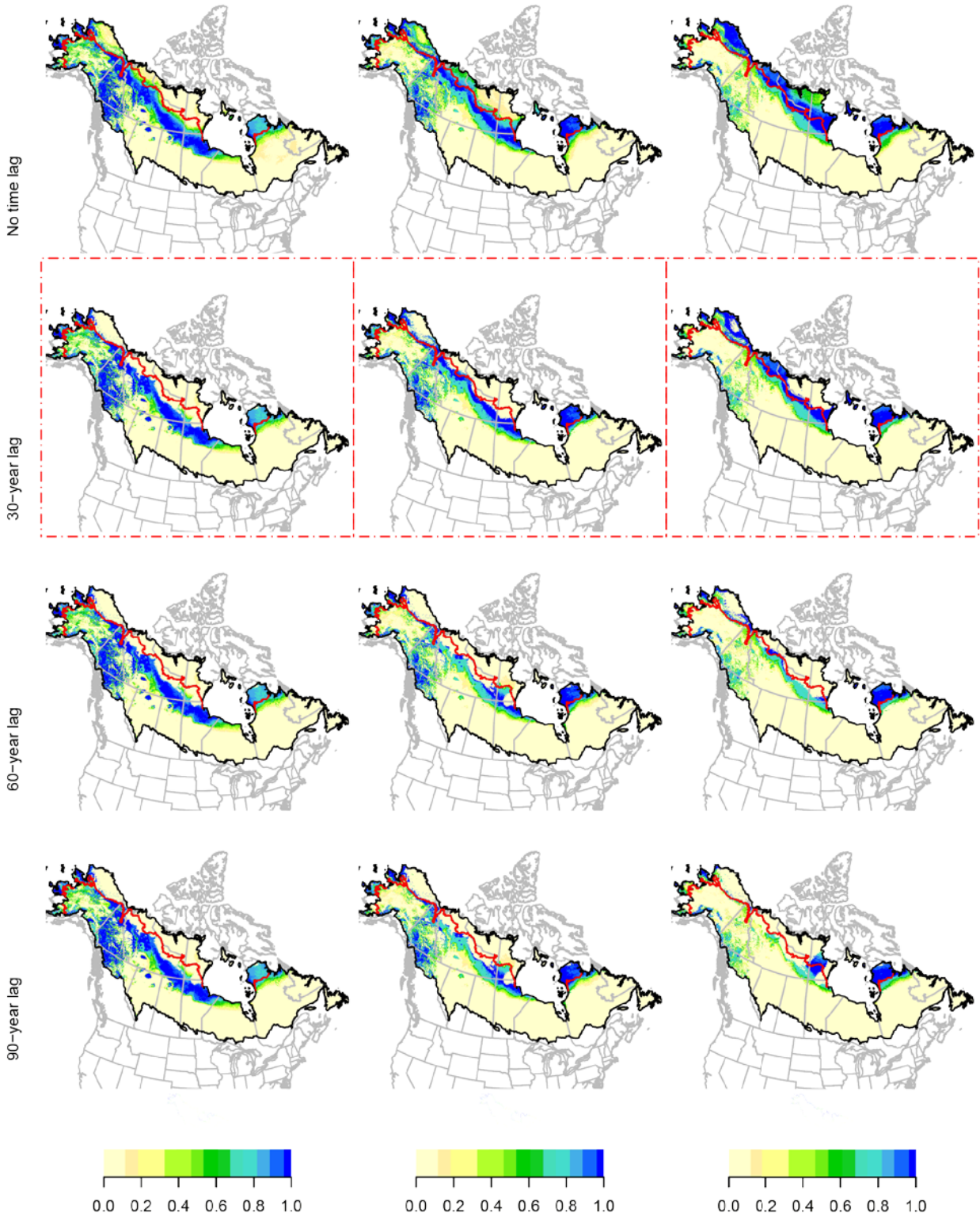


OCWA

a. 2011-2040

b. 2041-2070

c. 2071-2100

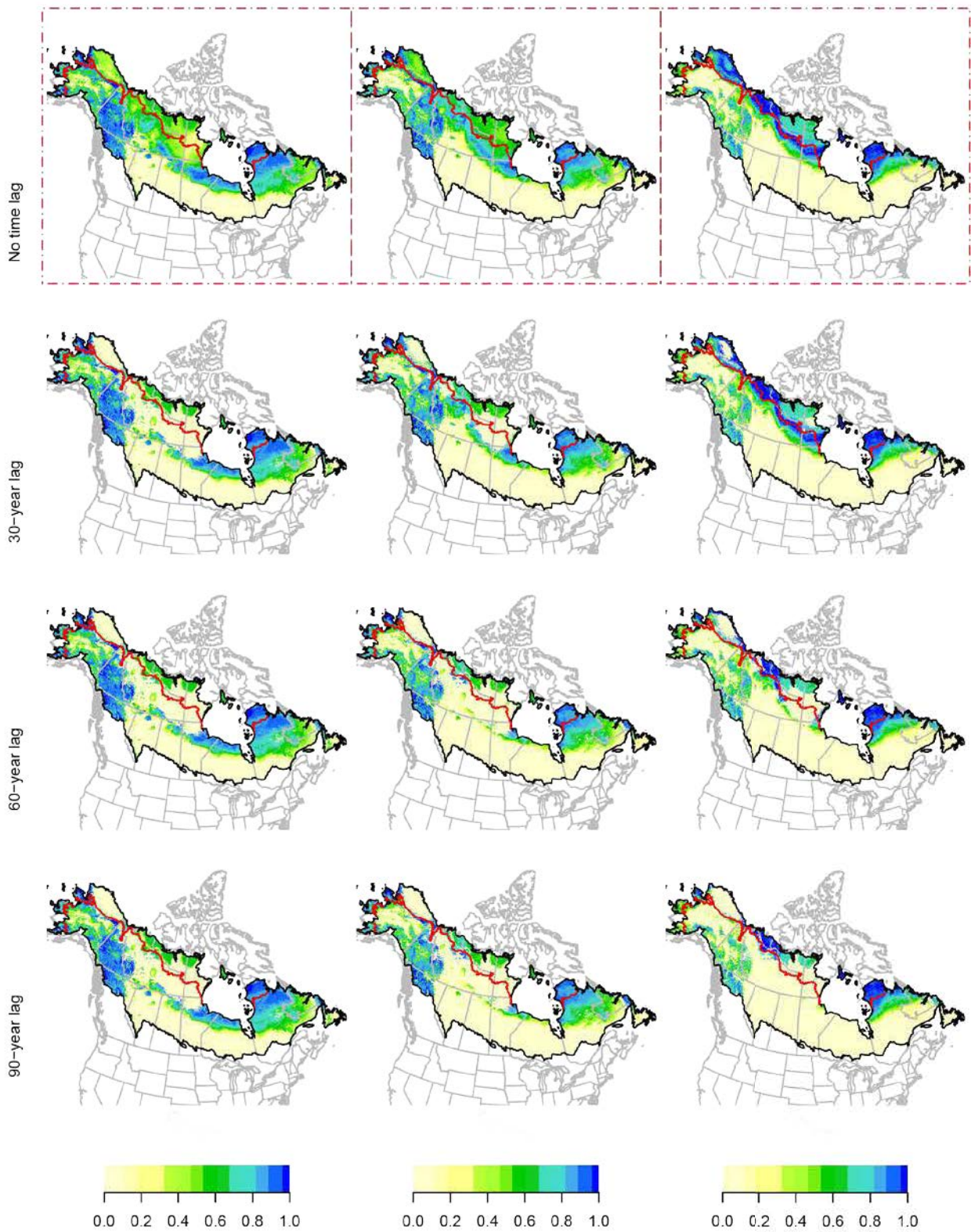


OSFL

a. 2011-2040

b. 2041-2070

c. 2071-2100

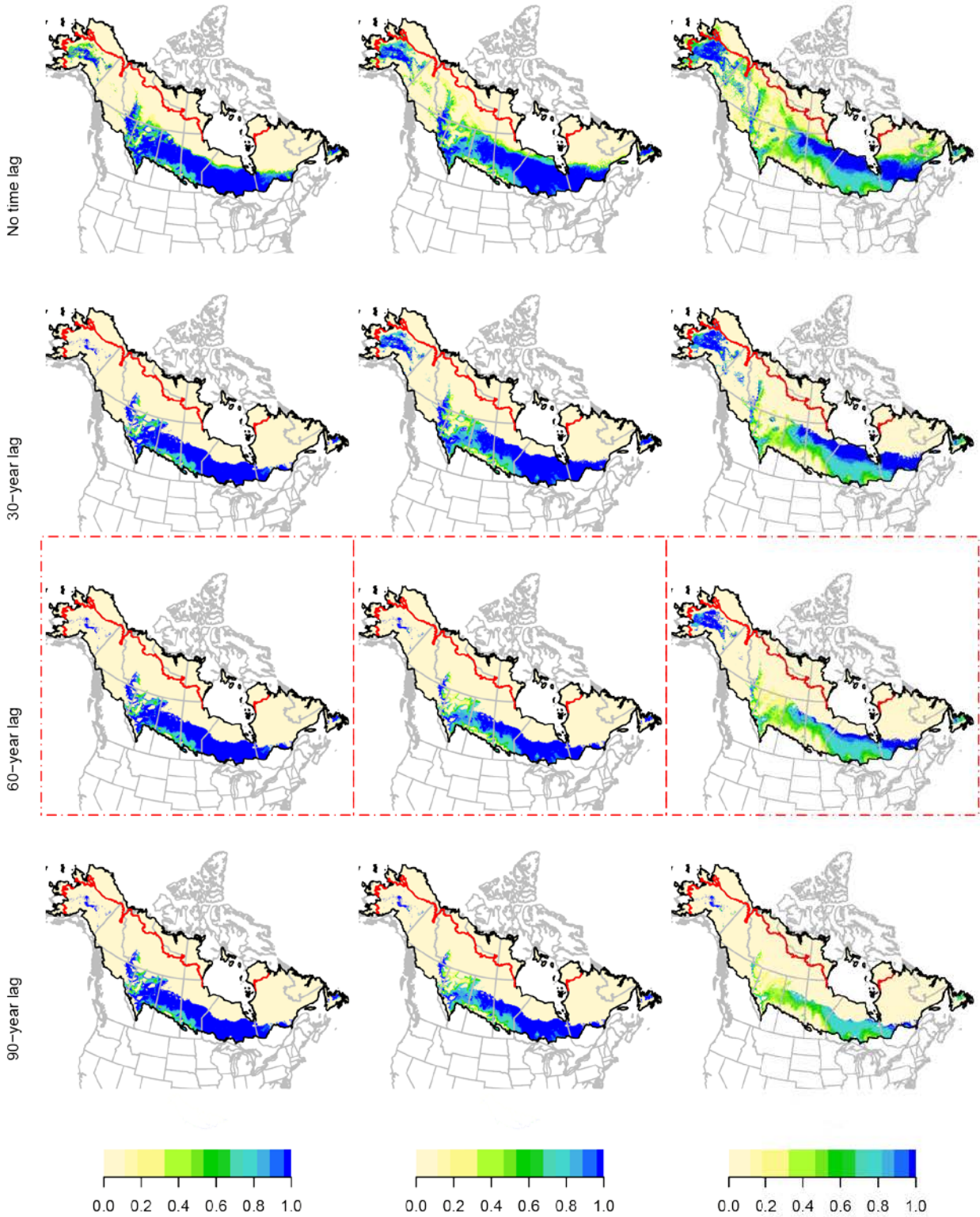


OVEN

a. 2011-2040

b. 2041-2070

c. 2071-2100

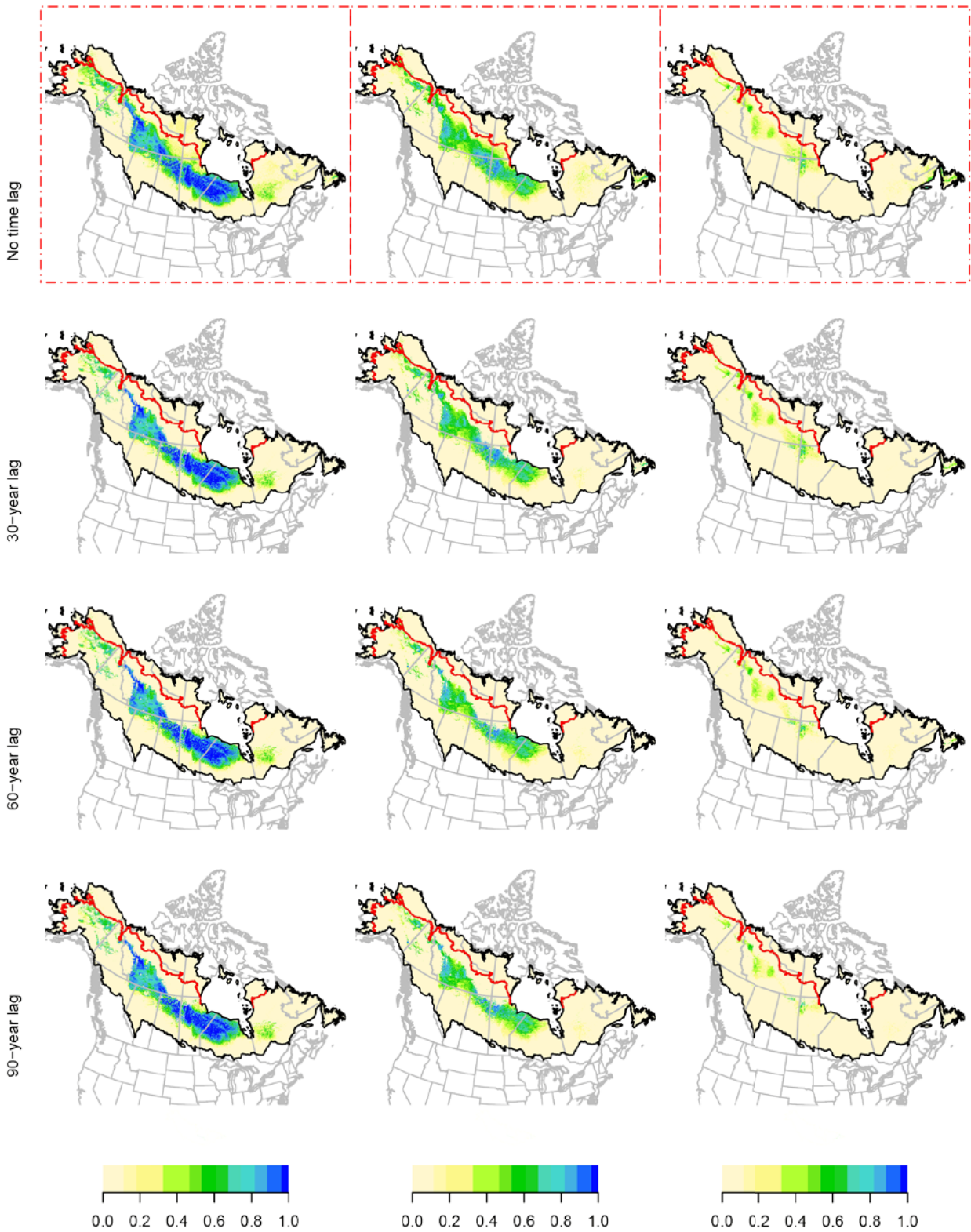


PAWA

a. 2011-2040

b. 2041-2070

c. 2071-2100

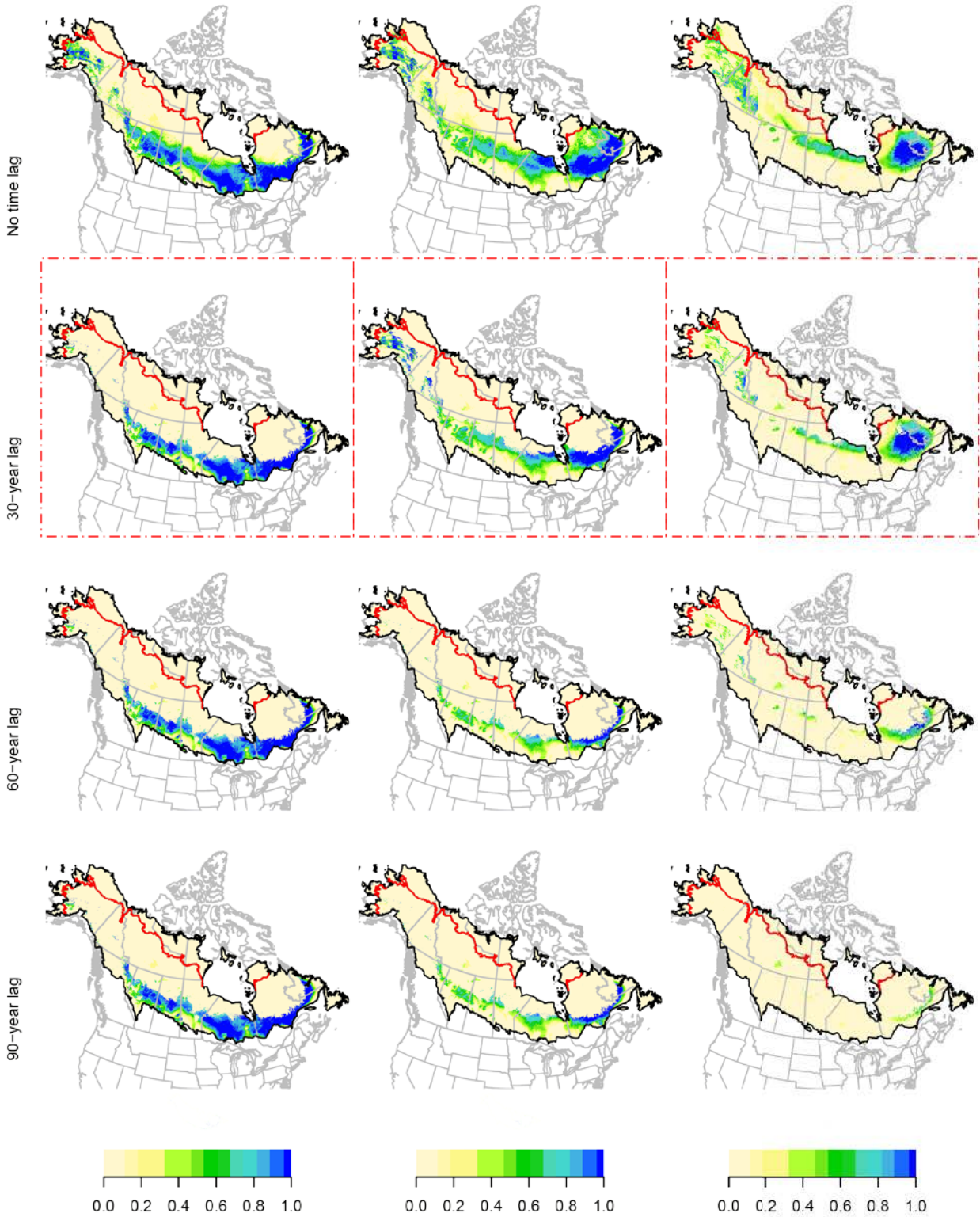


PHVI

a. 2011-2040

b. 2041-2070

c. 2071-2100

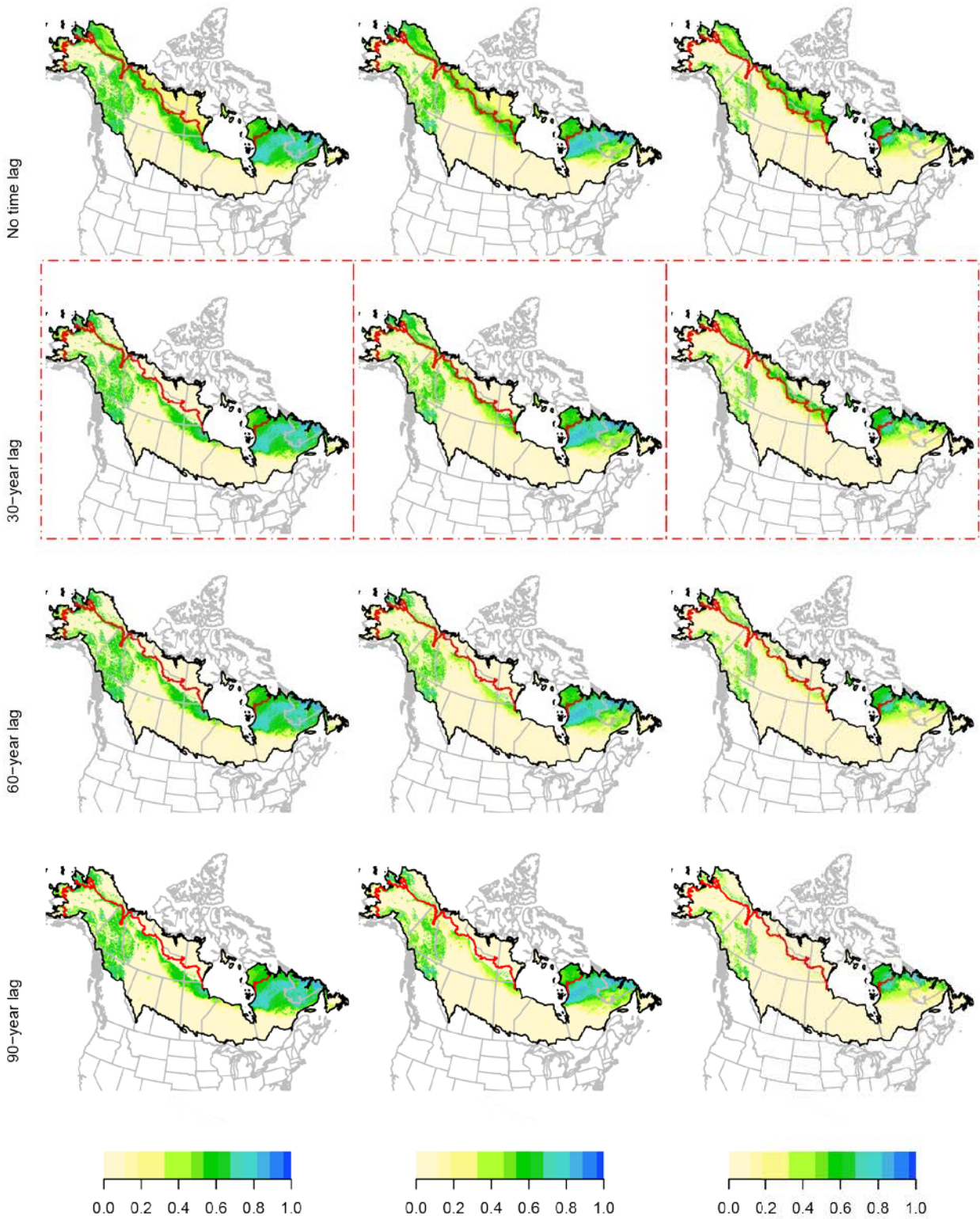


PIGR

a. 2011-2040

b. 2041-2070

c. 2071-2100

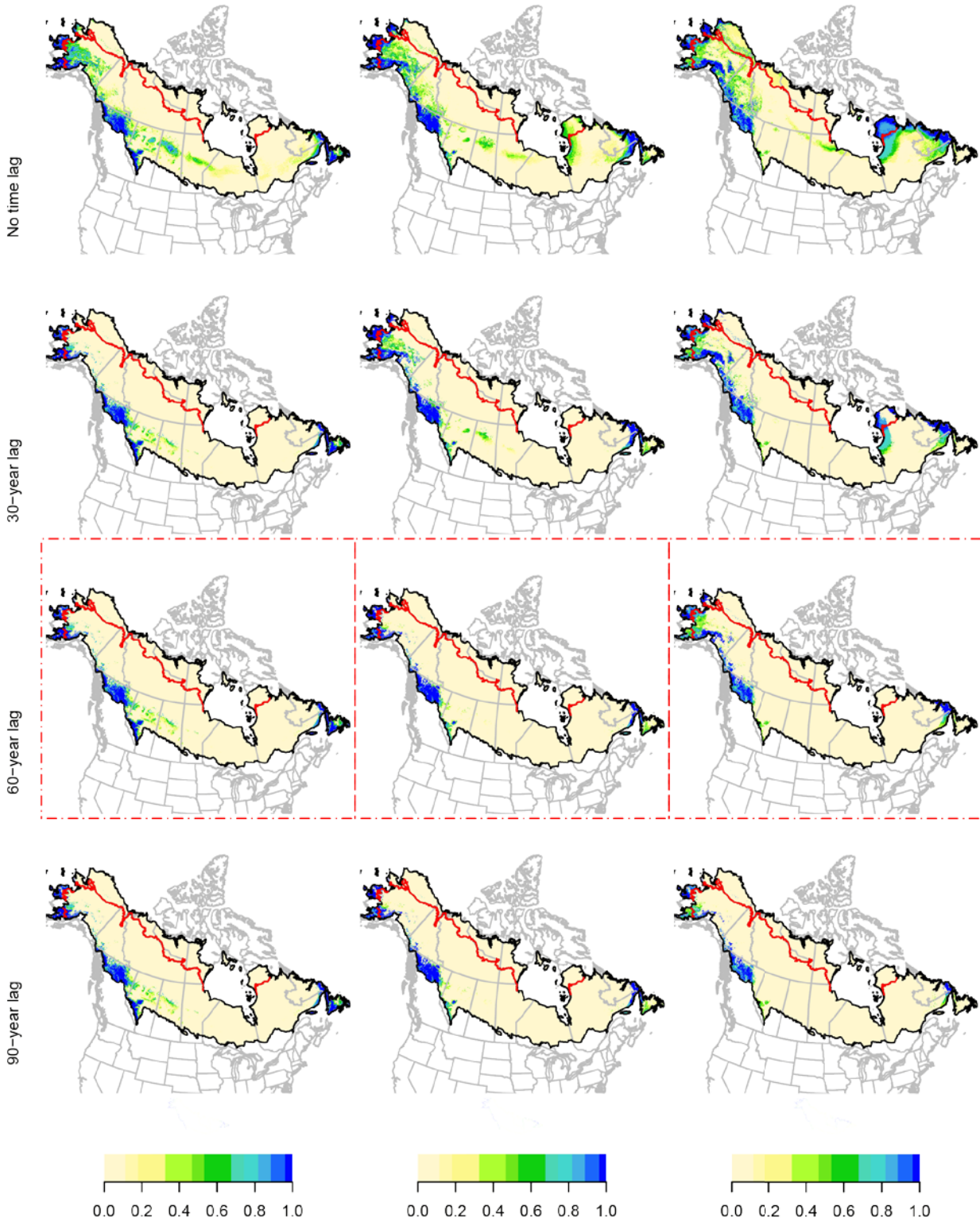


PISI

a. 2011-2040

b. 2041-2070

c. 2071-2100

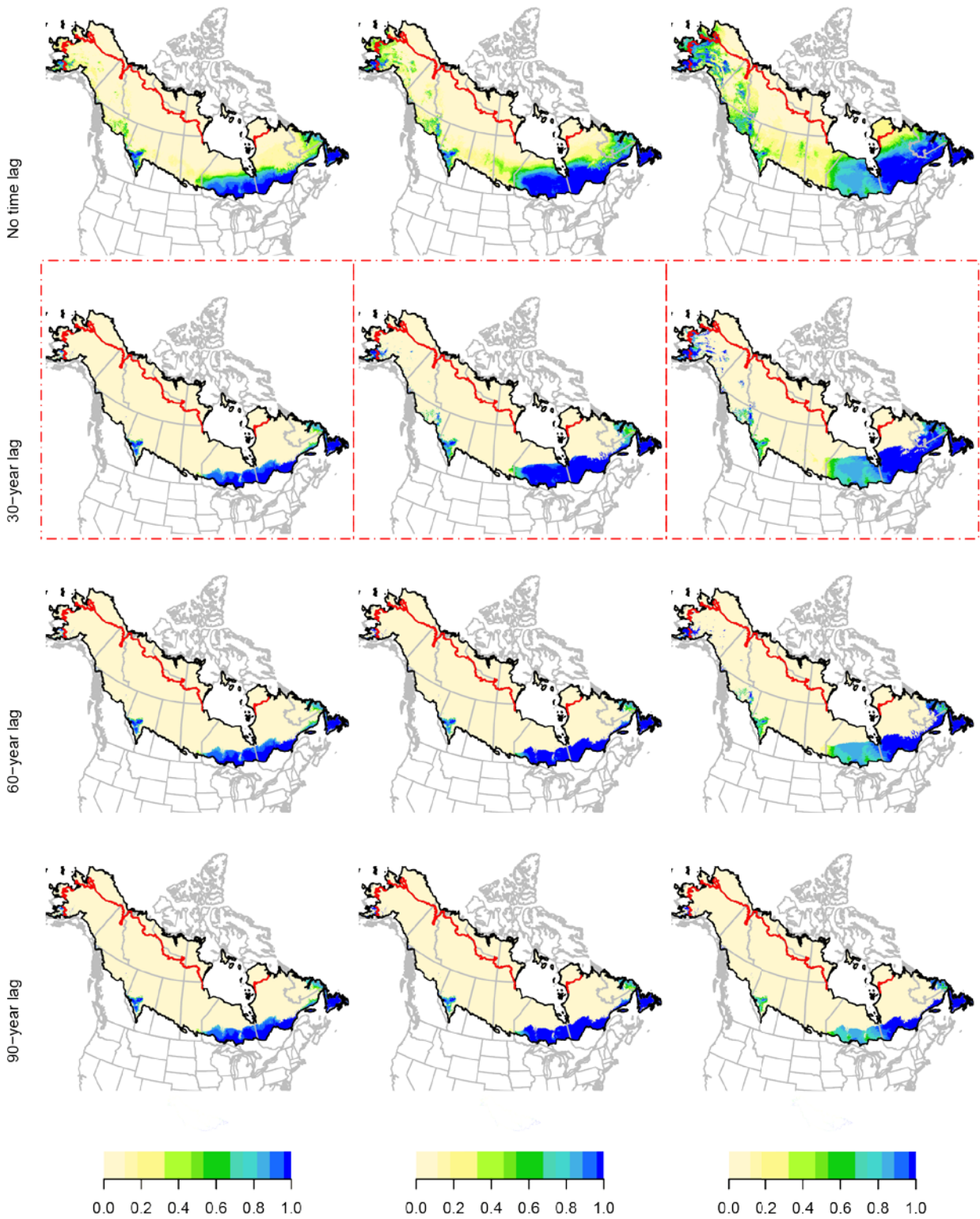


PUFI

a. 2011-2040

b. 2041-2070

c. 2071-2100

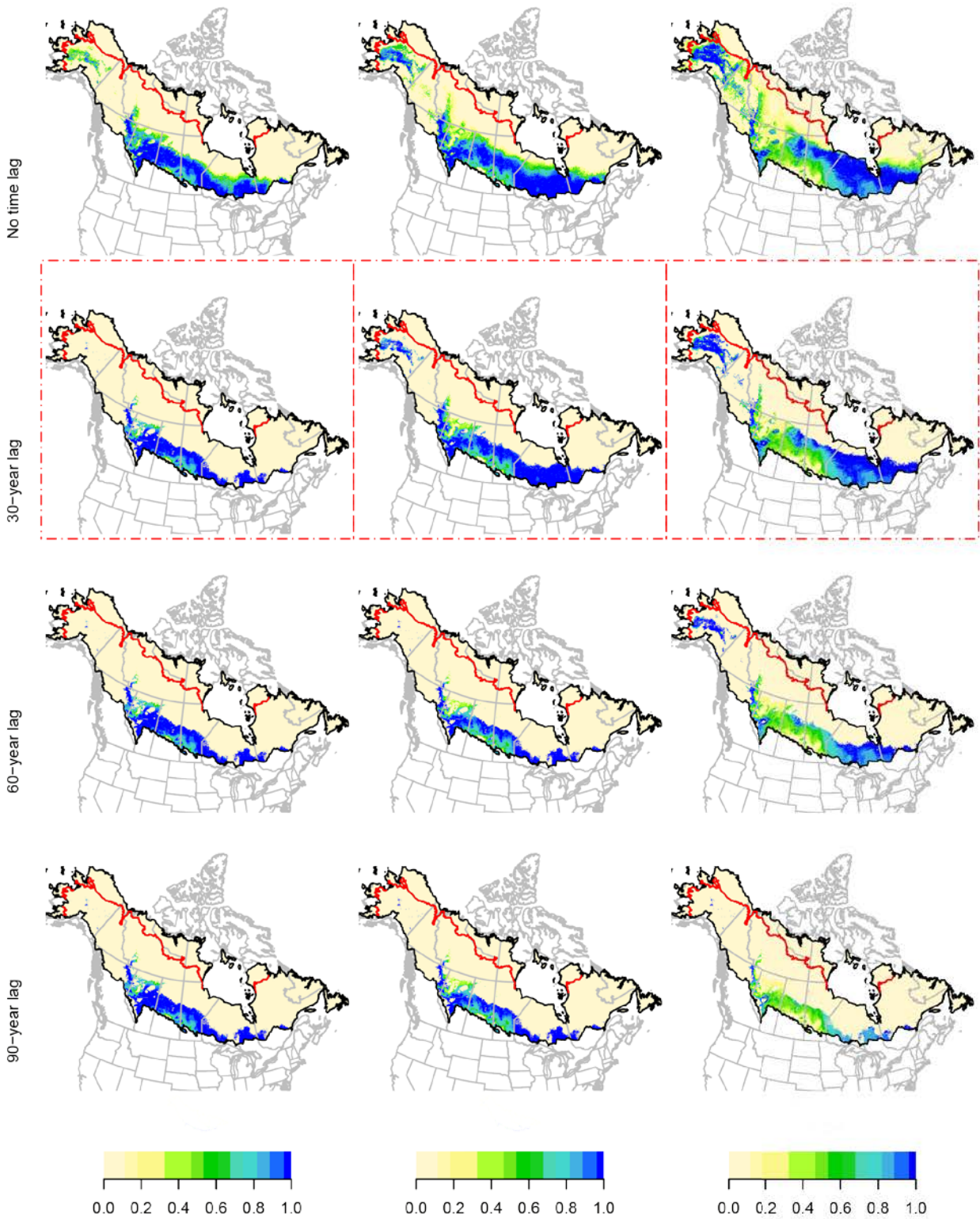


RBGR

a. 2011-2040

b. 2041-2070

c. 2071-2100

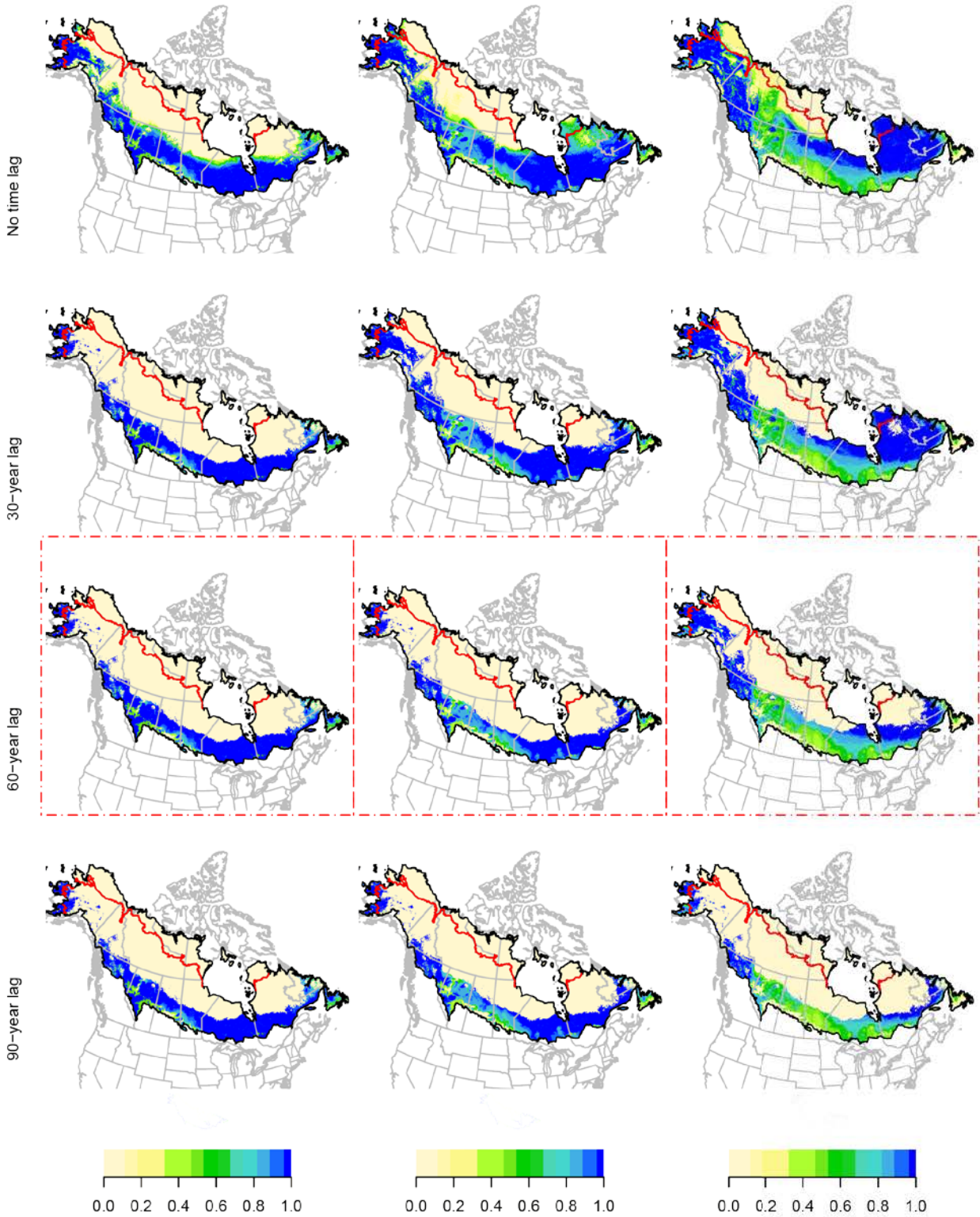


RBNU

a. 2011-2040

b. 2041-2070

c. 2071-2100

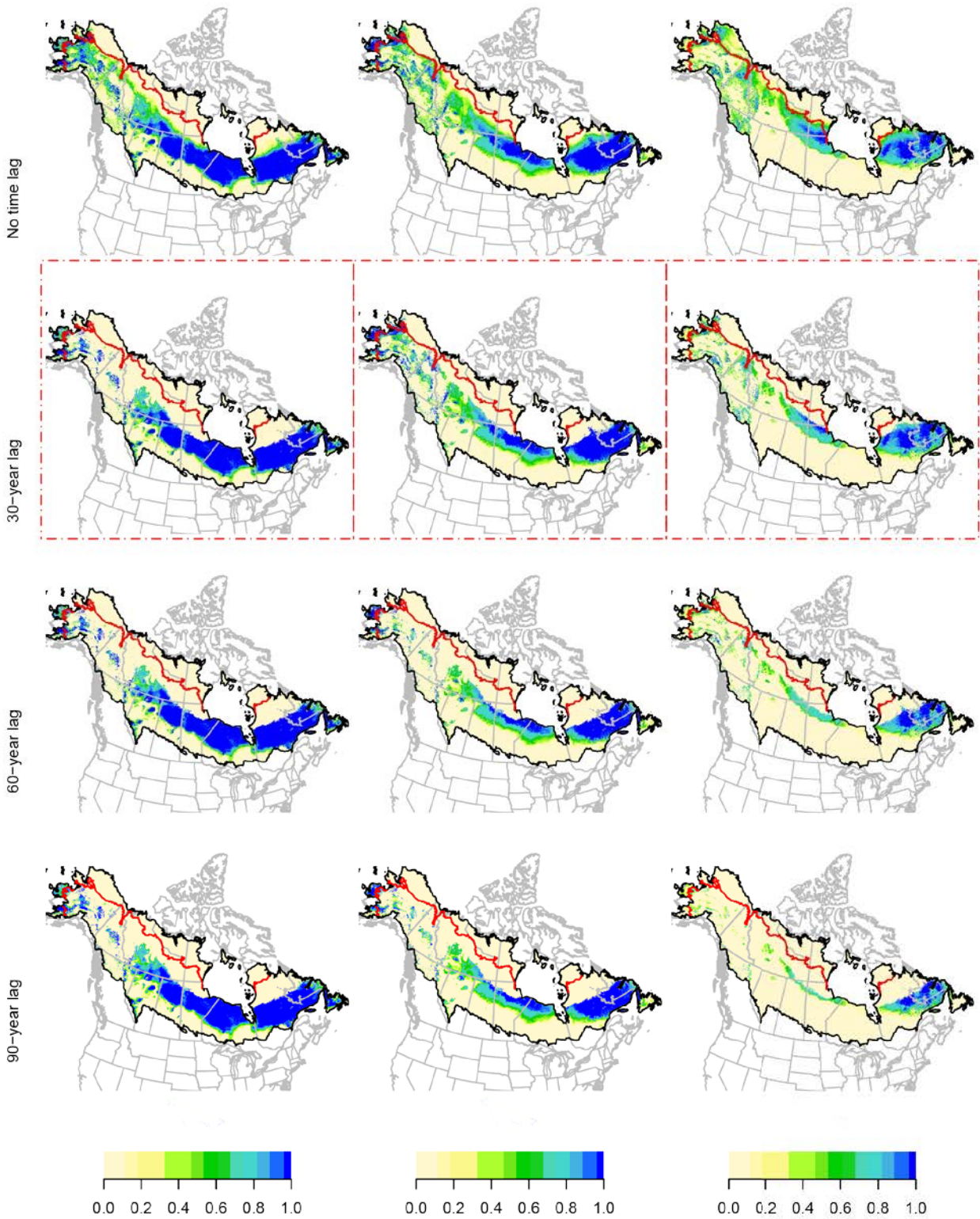


RCKI

a. 2011-2040

b. 2041-2070

c. 2071-2100

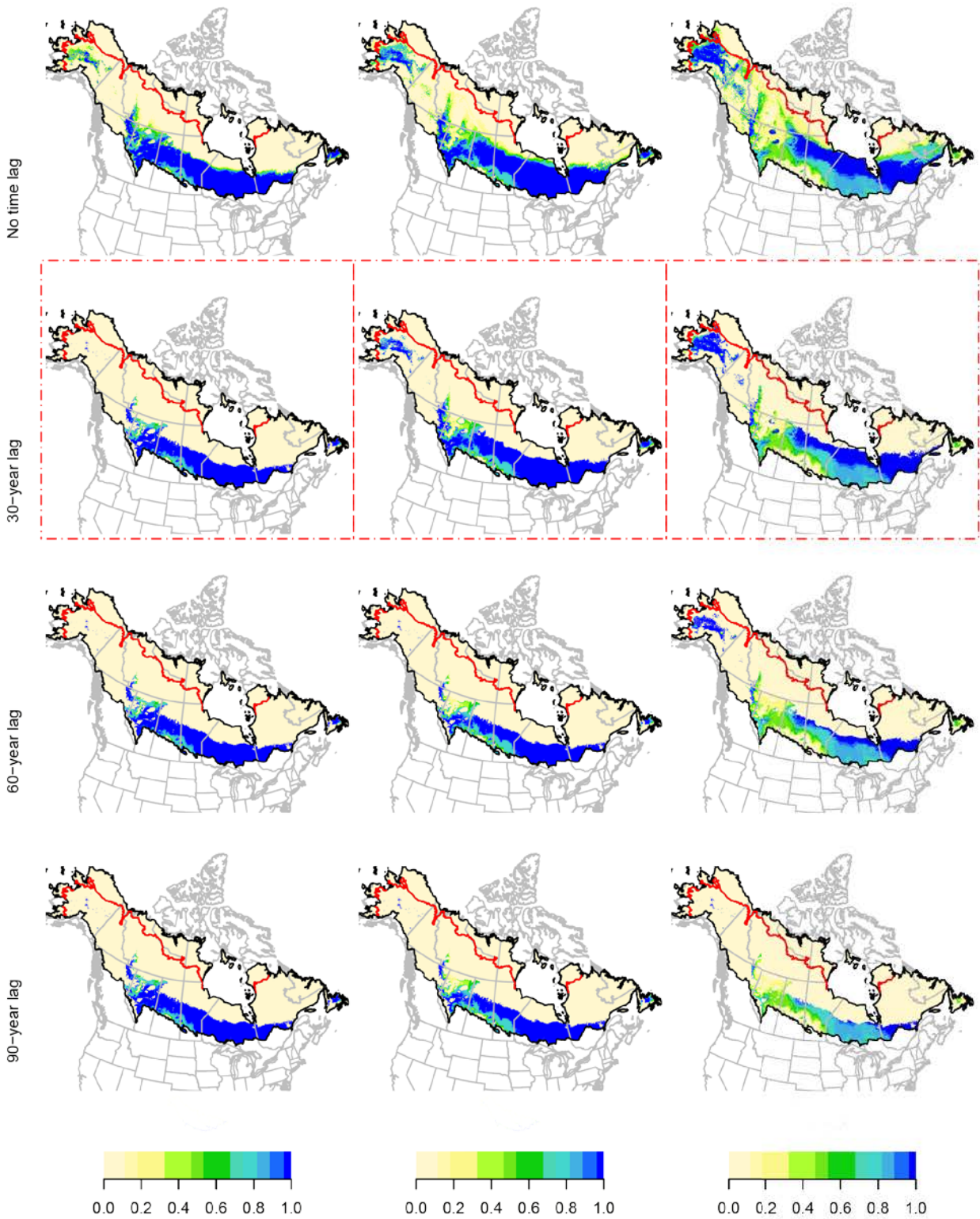


REVI

a. 2011-2040

b. 2041-2070

c. 2071-2100

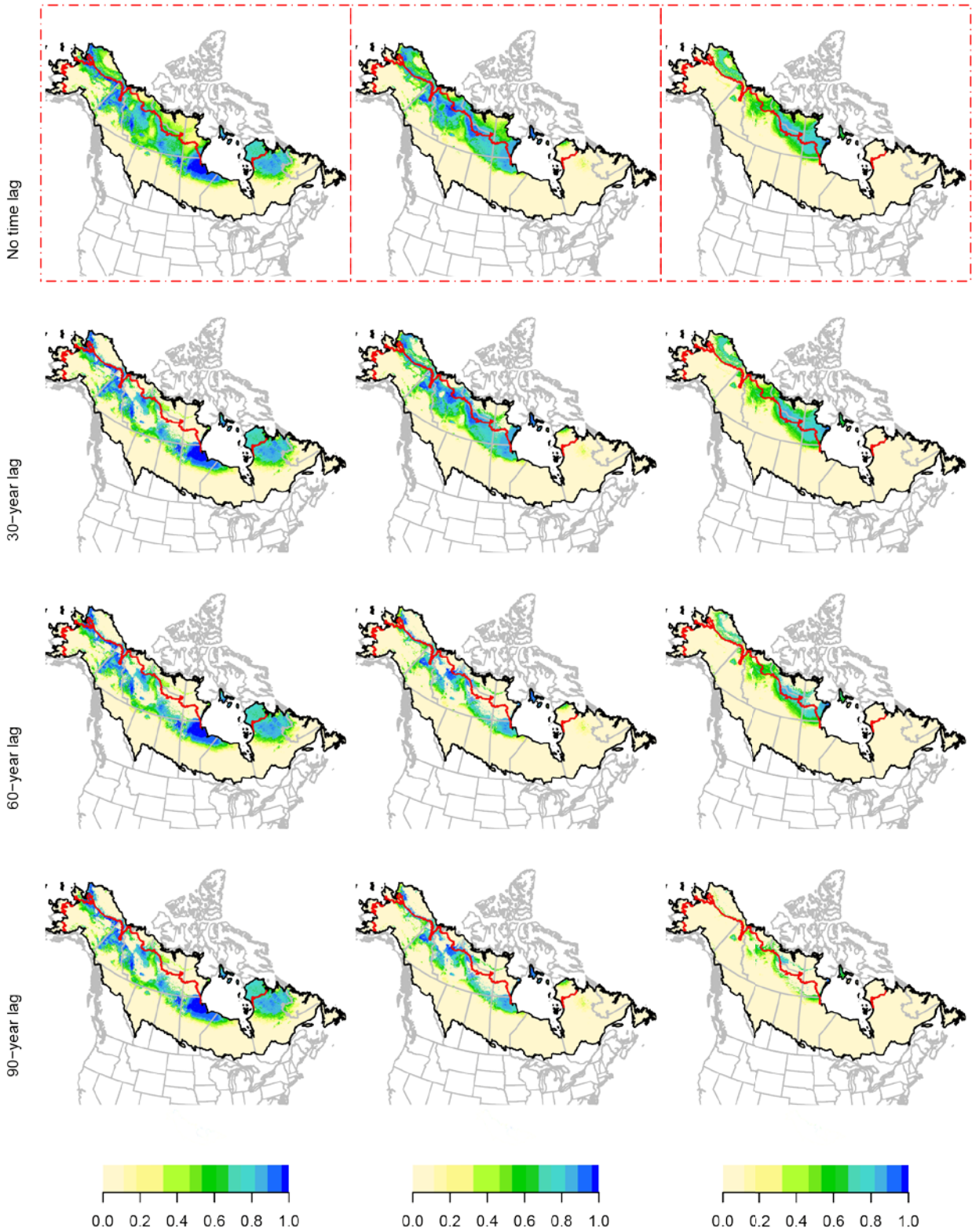


RUBL

a. 2011-2040

b. 2041-2070

c. 2071-2100

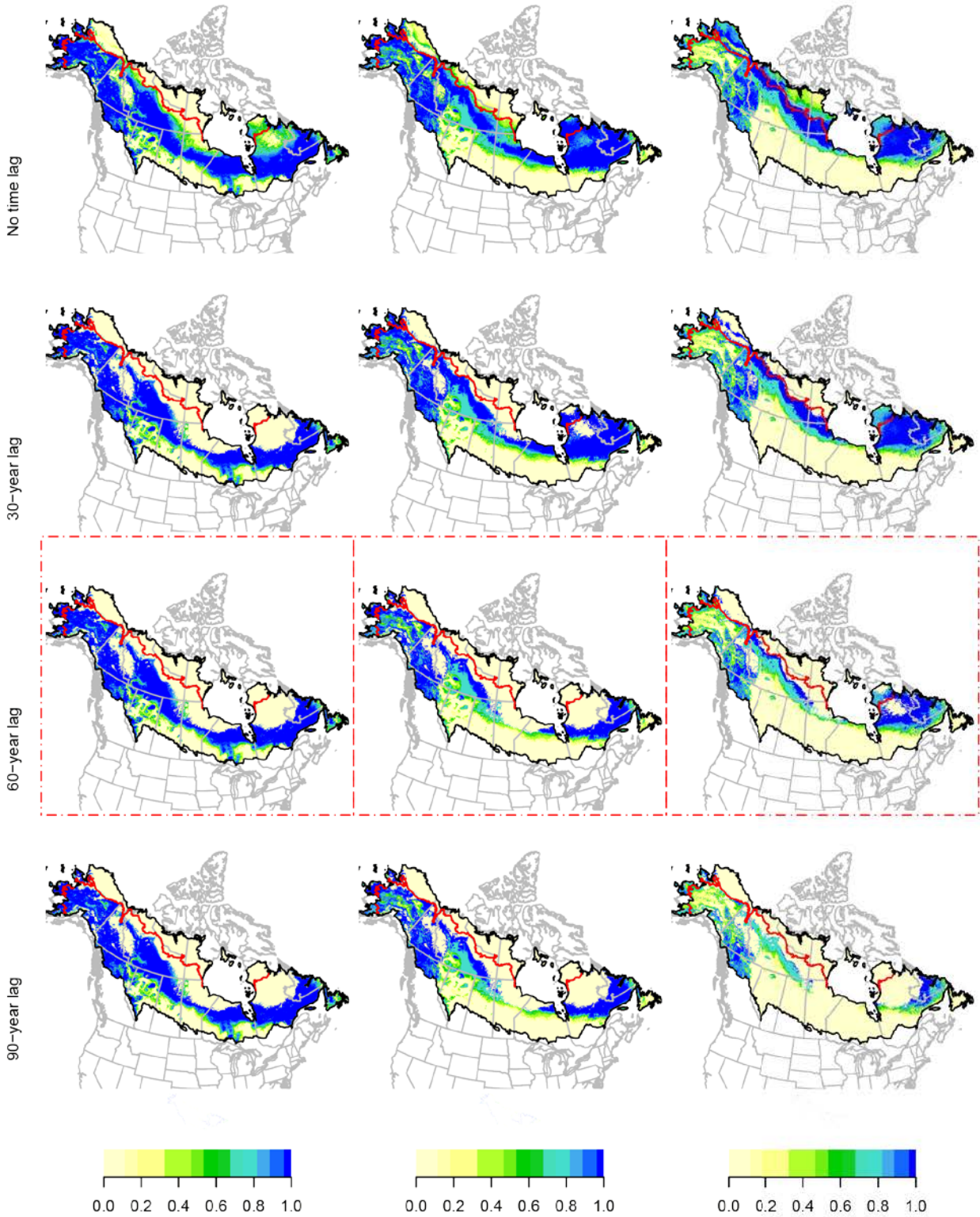


SWTH

a. 2011-2040

b. 2041-2070

c. 2071-2100

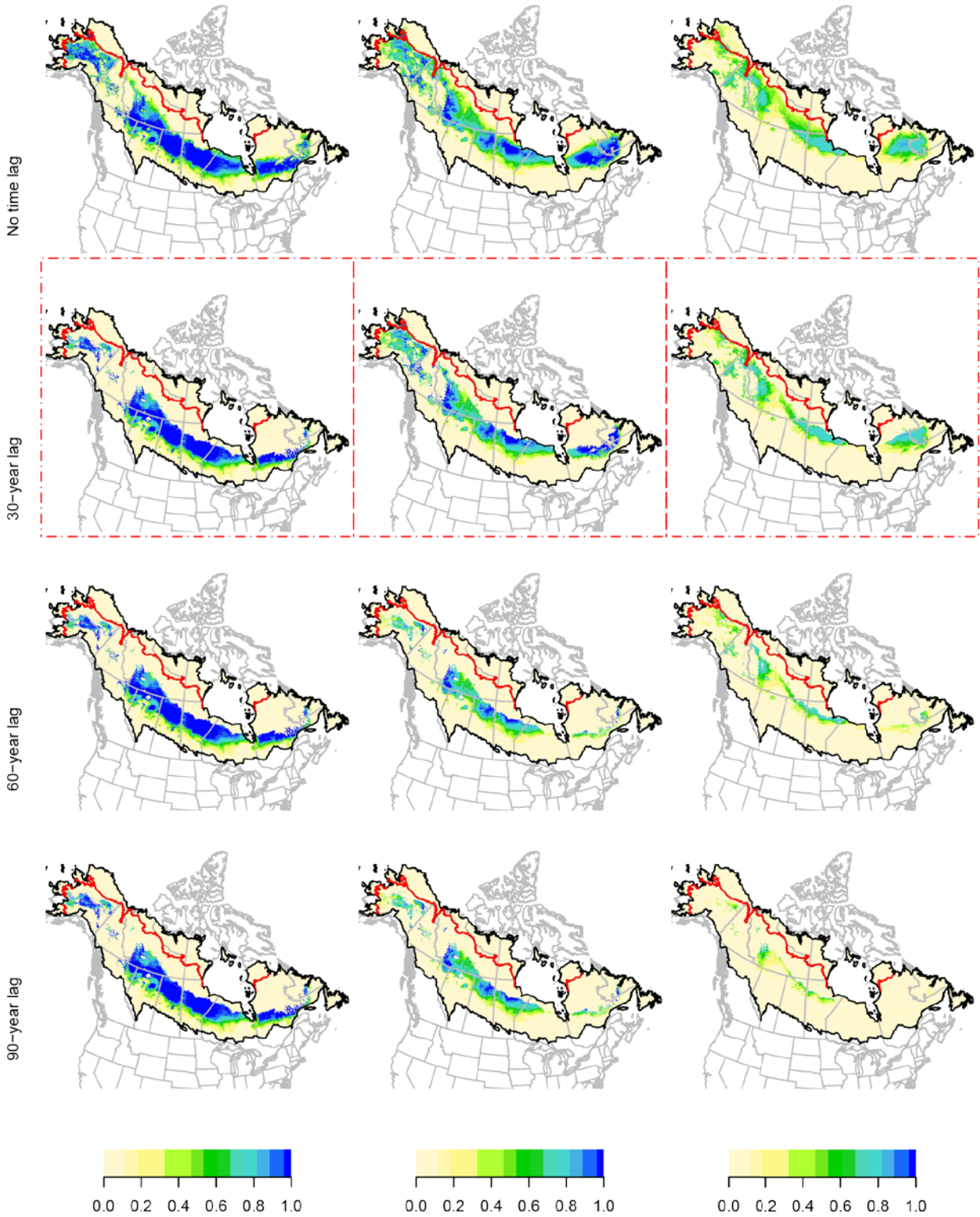


TEWA

a. 2011-2040

b. 2041-2070

c. 2071-2100

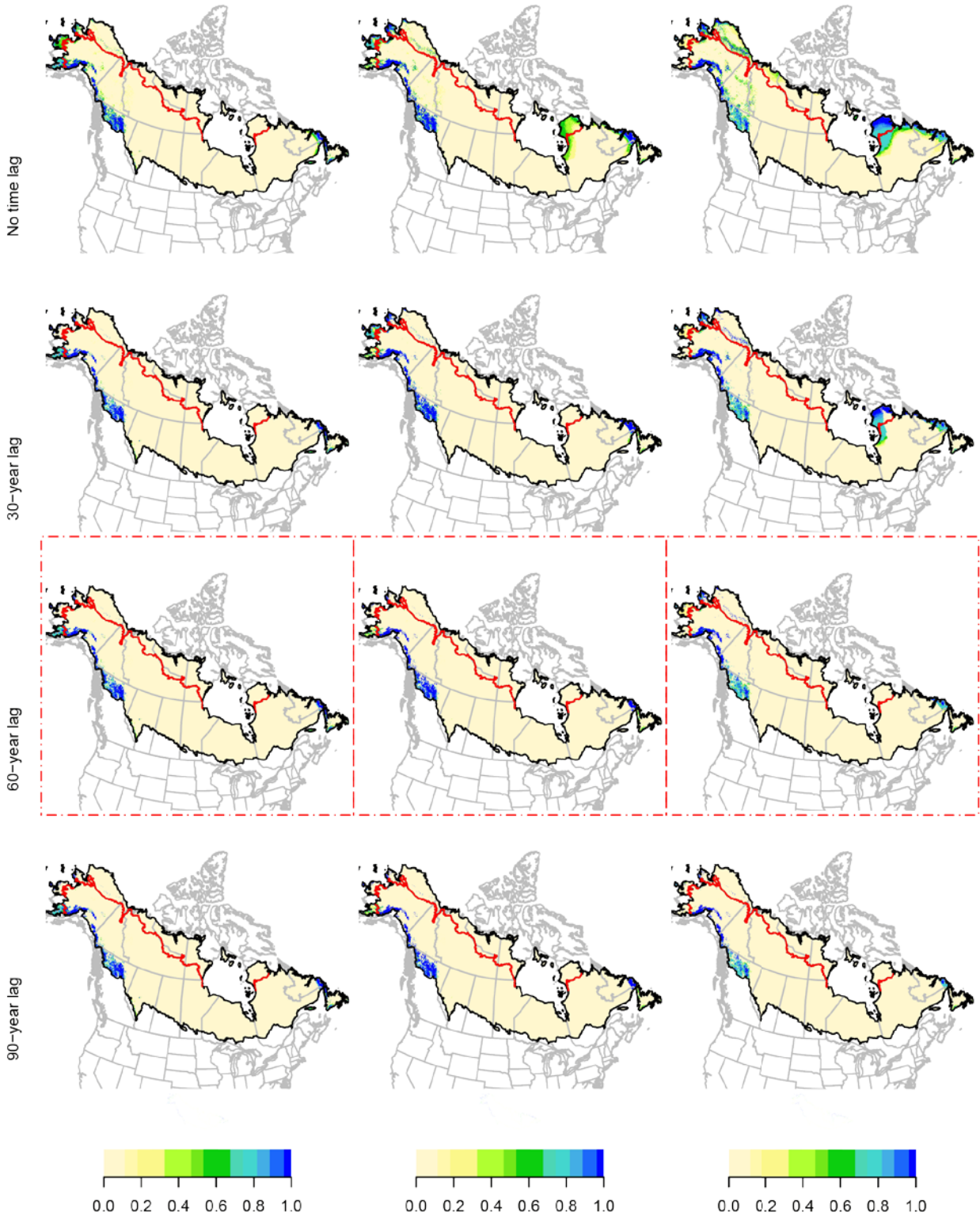


VATH

a. 2011–2040

b. 2041–2070

c. 2071–2100



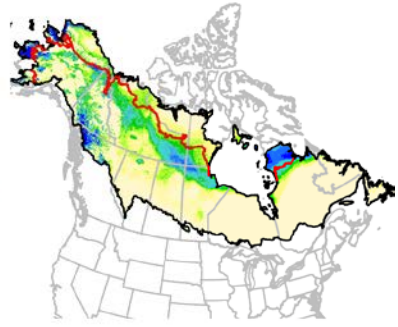
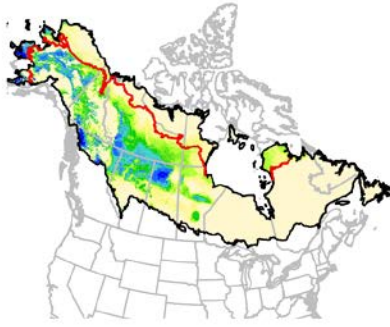
WETA

a. 2011-2040

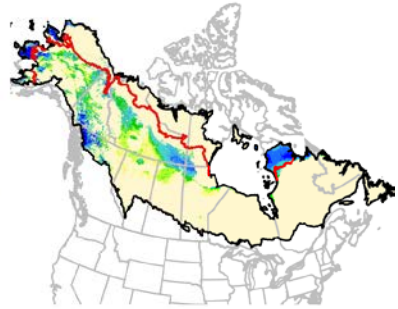
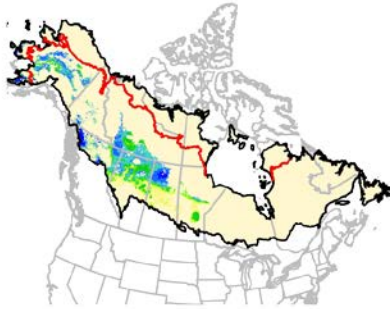
b. 2041-2070

c. 2071-2100

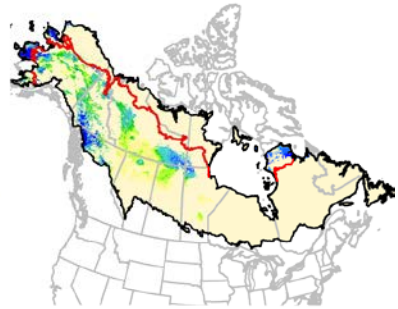
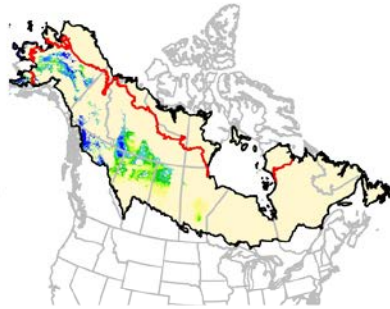
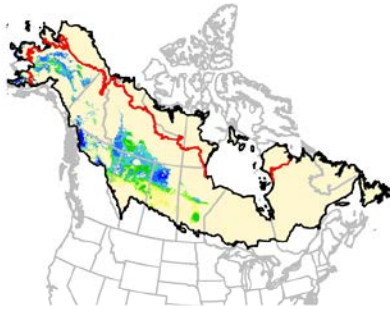
No time lag



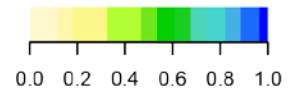
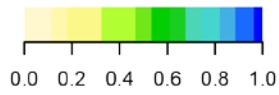
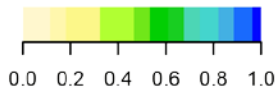
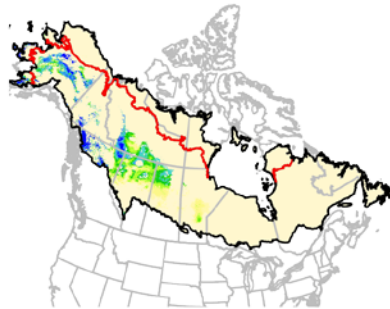
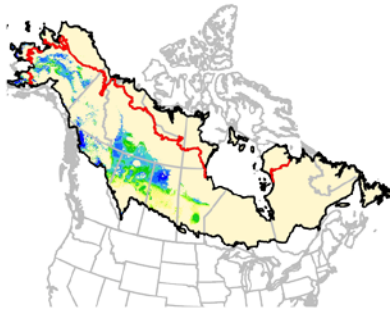
30-year lag



60-year lag



90-year lag

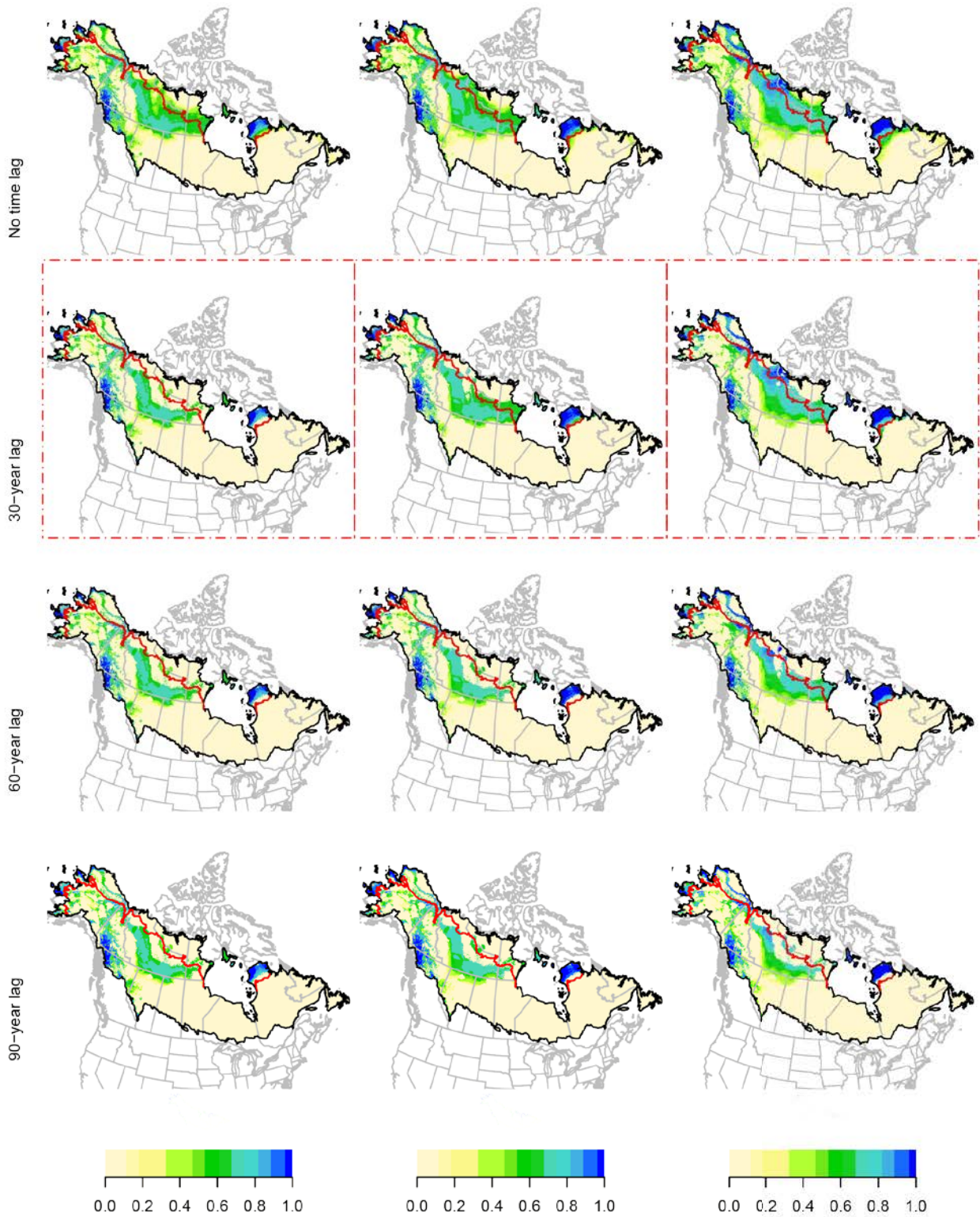


WEWP

a. 2011-2040

b. 2041-2070

c. 2071-2100

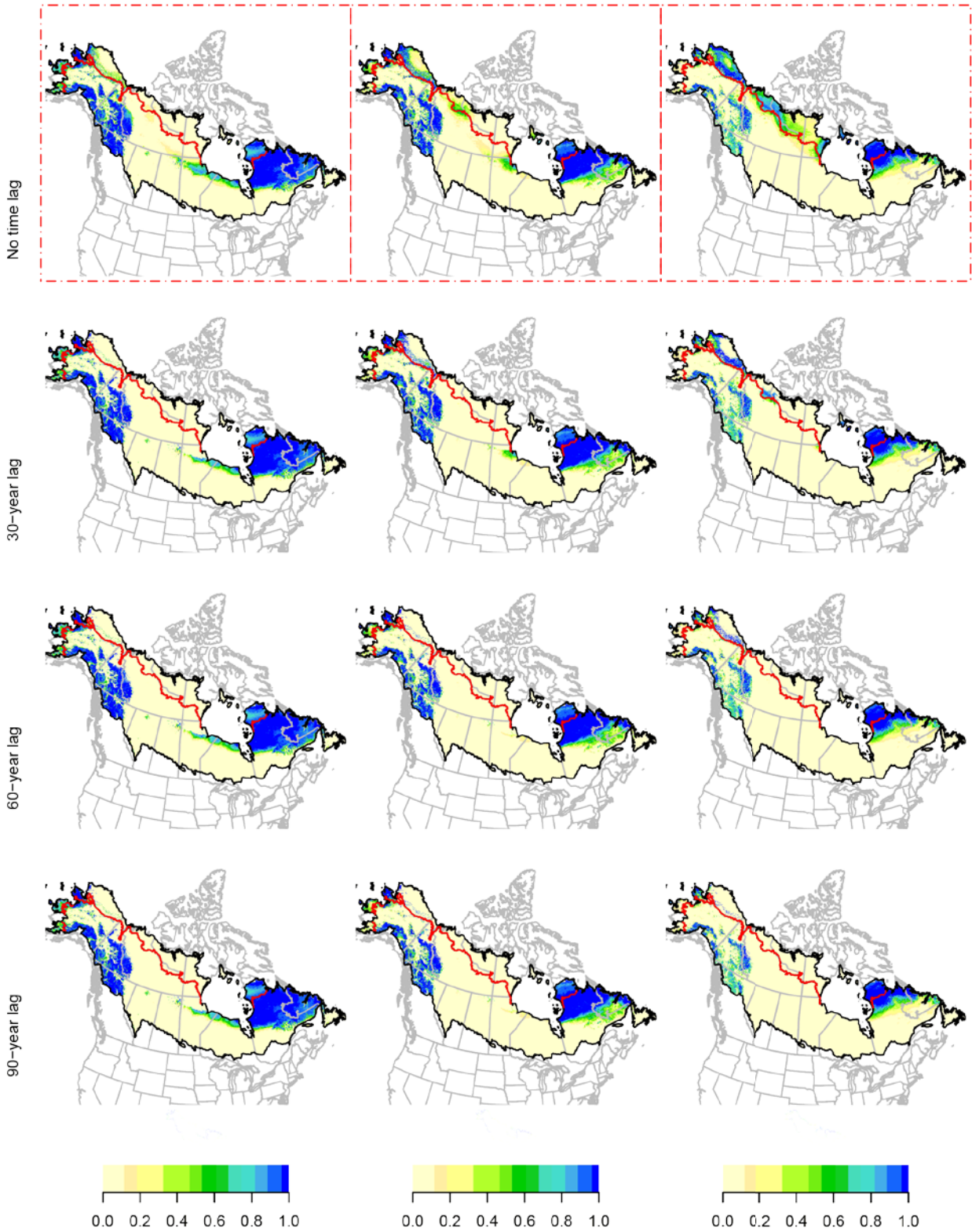


WIWA

a. 2011-2040

b. 2041-2070

c. 2071-2100

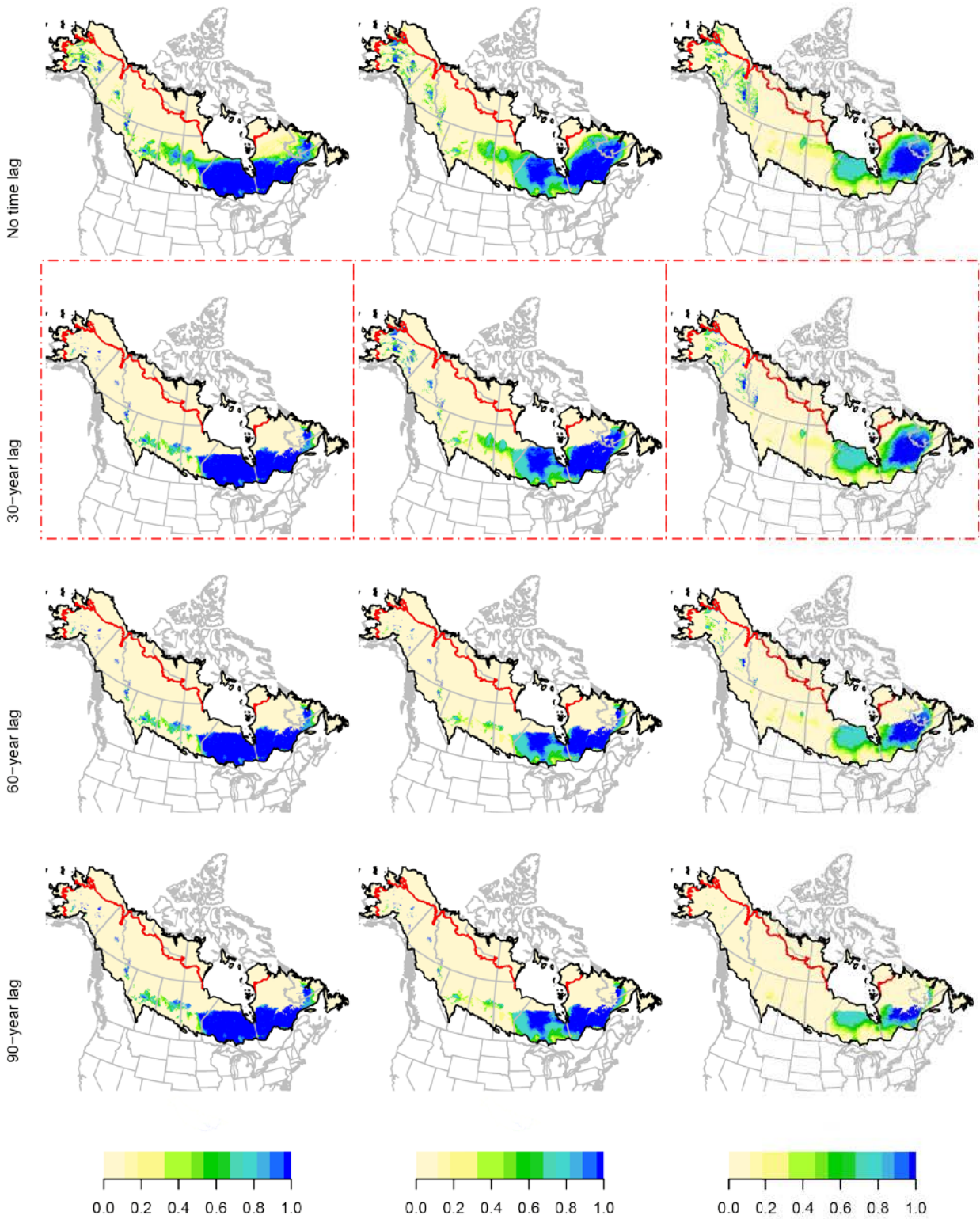


WIWR

a. 2011-2040

b. 2041-2070

c. 2071-2100

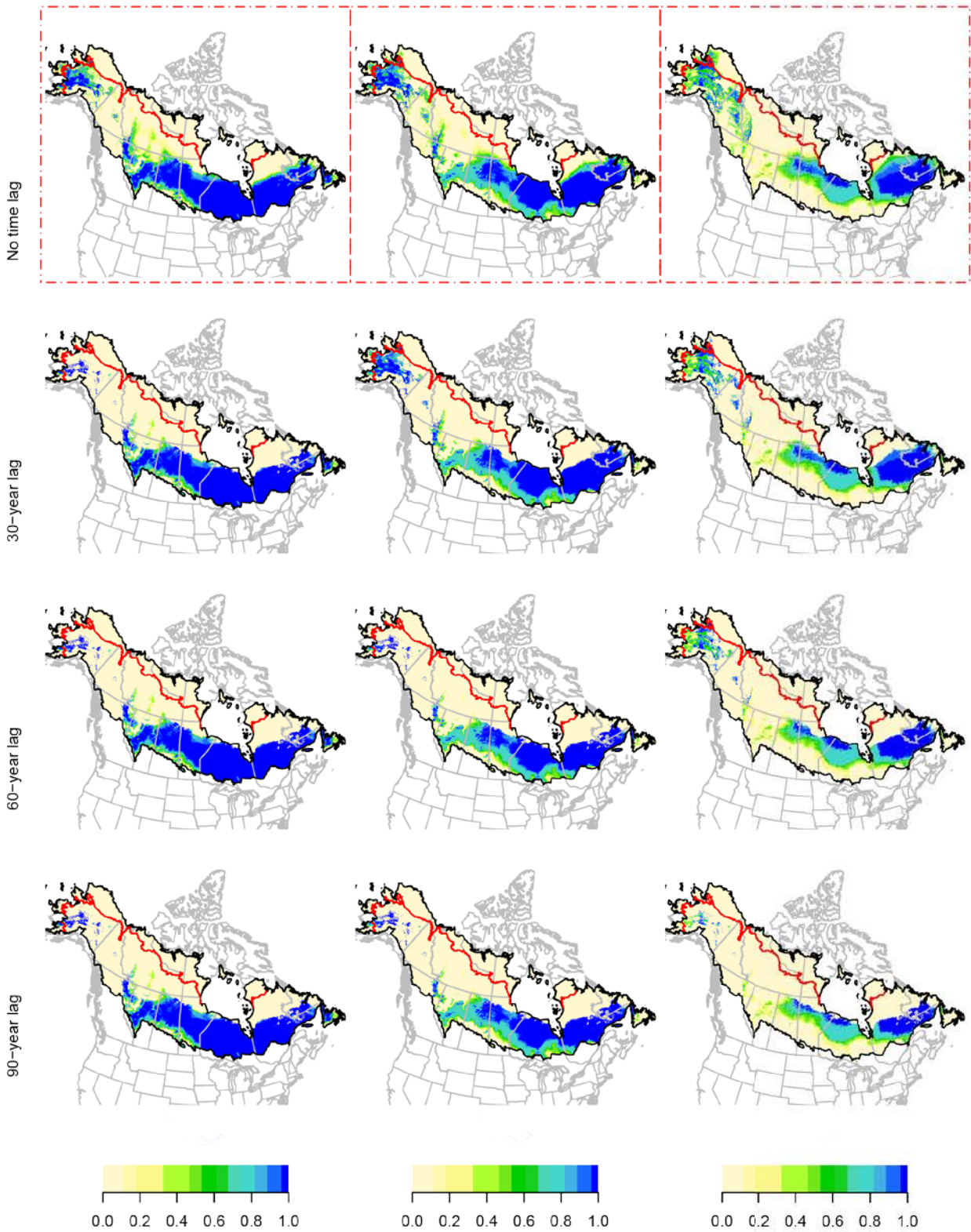


WTSP

a. 2011-2040

b. 2041-2070

c. 2071-2100

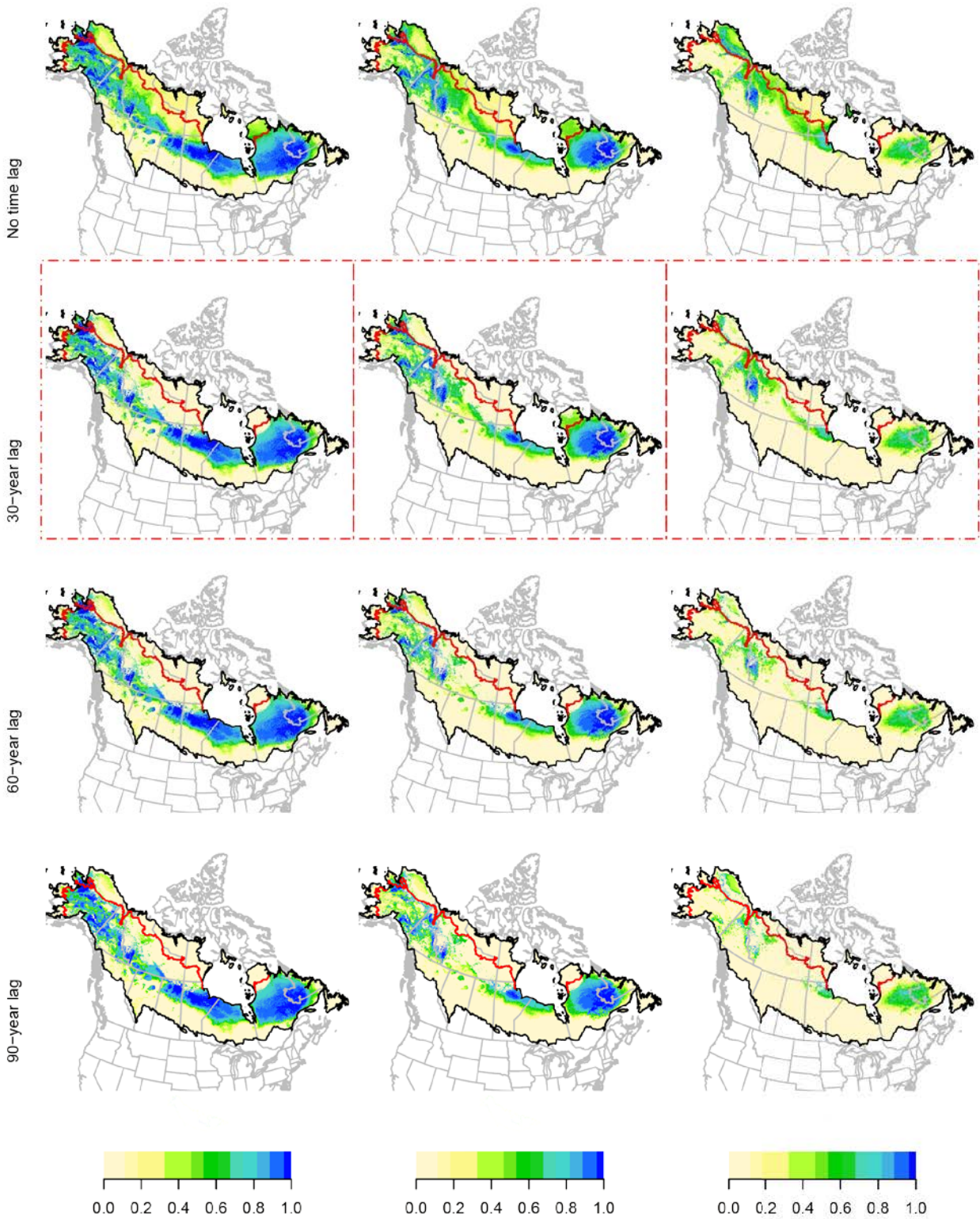


WWCR

a. 2011-2040

b. 2041-2070

c. 2071-2100

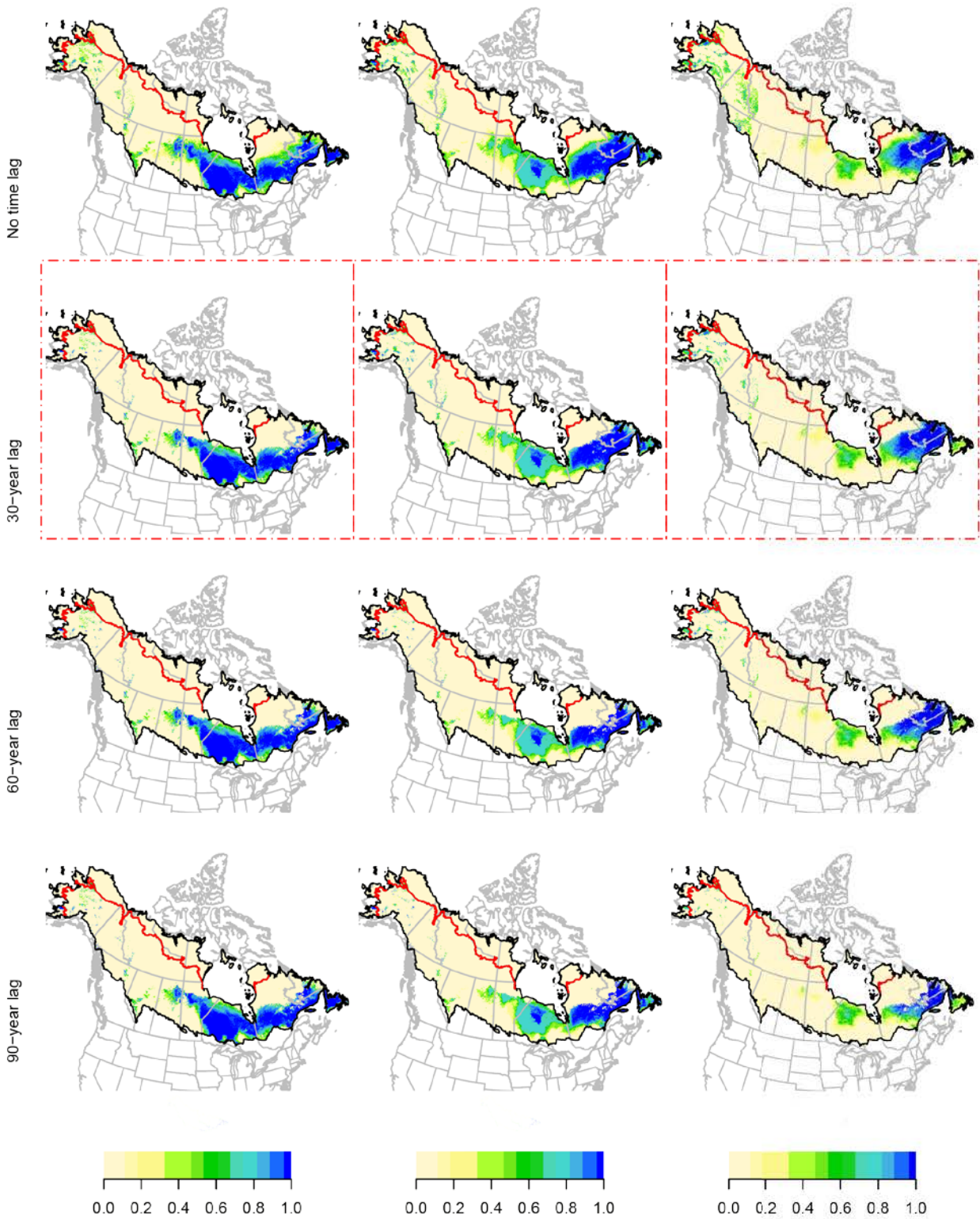


YBFL

a. 2011-2040

b. 2041-2070

c. 2071-2100

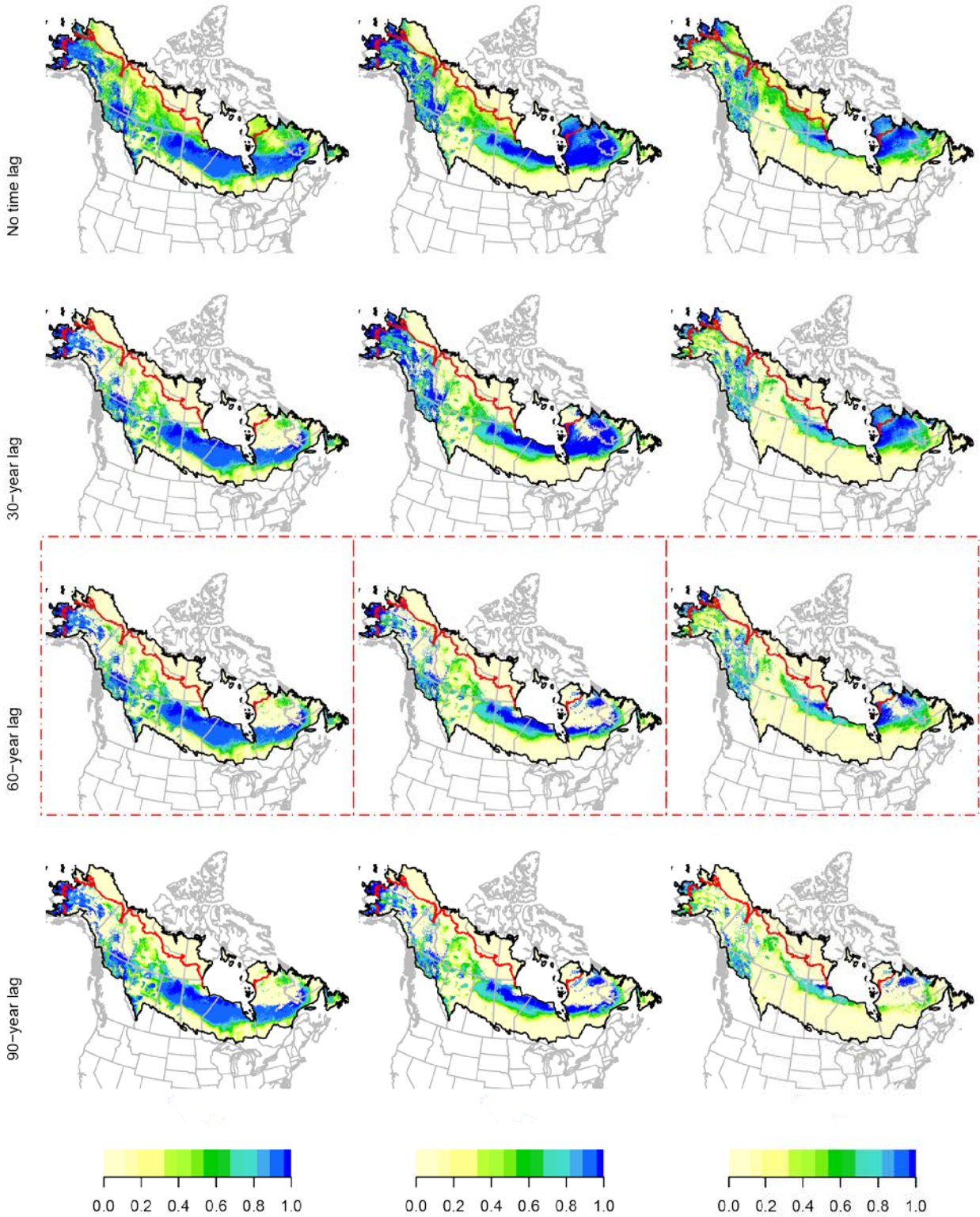


YRWA

a. 2011-2040

b. 2041-2070

c. 2071-2100



Appendix 2-D. R code to calculate core areas, strict refugia, and modified refugia

```
#####  
# R code to calculate core areas, strict refugia, and modified refugia  
library(raster) #Reading, writing, manipulating, analyzing and modeling of  
gridded spatial data  
  
# densdir <- density model means directory  
# refdir <- refugia output directory  
# w <- original model directory  
  
# speclistB: list of 53 boreal forest species  
# resultclip <- analysis area raster  
# study <- model-building area raster  
  
gcms <- c("cccma_cgcm3_1", "gfdl_cm2_1", "mpi_echam5", "ukmo_hadgem1") #  
four GCMs considered  
  
#####  
#Calculate core areas over time based purely on climatic suitability (mean  
density within model-building area)  
  
#Baseline  
for (j in 1:length(speclistB)) {  
  curr <- raster(paste(densdir,speclistB[j],"_currmean.asc",sep=""))  
  curr <- crop(curr, study)  
  curr <- mask(curr, study)  
  prev <- cellStats(curr, 'mean')  
  m <- c(0, prev, 0, prev+0.00001, 1000, 1)  
  rclmat <- matrix(m, ncol=3, byrow=TRUE)  
  core <- reclassify(curr, rclmat)  
  writeRaster(core,  
    file=paste(refdir,speclistB[j],"_corecurr.asc",sep=""),  
    format="ascii", overwrite=TRUE)  
  png(file=paste(refdir,speclistB[j],"_corecurr.png",sep=""))  
  plot(core)  
  dev.off()  
}  
  
#2011-2040  
for (j in 1:length(speclistB)) {  
  curr <- raster(paste(densdir,speclistB[j],"_currmean.asc",sep=""))  
  curr <- crop(curr, study)  
  curr <- mask(curr, study)  
  prev <- cellStats(curr, 'mean')  
  m <- c(0, prev, 0, prev+0.00001, 1000, 1)  
  rclmat <- matrix(m, ncol=3, byrow=TRUE)  
  mean2020 <- raster(paste(densdir,speclistB[j],"_2020mean.asc",sep=""))  
  core2020 <- reclassify(mean2020, rclmat)  
  core2020 <- crop(core2020, resultclip)  
  core2020 <- mask(core2020, resultclip)  
  writeRaster(core2020,  
    file=paste(refdir,speclistB[j],"_core2020.asc",sep=""),  
    format="ascii", overwrite=TRUE)  
  png(file=paste(refdir,speclistB[j],"_core2020.png",sep=""))  
  plot(core2020)  
  dev.off()  
}  
  
#2041-2070  
for (j in 1:length(speclistB)) {  
  curr <- raster(paste(densdir,speclistB[j],"_currmean.asc",sep=""))
```

```

curr <- crop(curr, study)
curr <- mask(curr, study)
prev <- cellStats(curr, 'mean')
m <- c(0, prev, 0, prev+0.00001, 1000, 1)
rclmat <- matrix(m, ncol=3, byrow=TRUE)
mean2050 <- raster(paste(densdir, speclistB[j], "_2050mean.asc", sep=""))
core2050 <- reclassify(mean2050, rclmat)
core2050 <- crop(core2050, resultclip)
core2050 <- mask(core2050, resultclip)
writeRaster(core2050,
  file=paste(refdir, speclistB[j], "_core2050.asc", sep=""),
  format="ascii", overwrite=TRUE)
png(file=paste(refdir, speclistB[j], "_core2050.png", sep=""))
plot(core2050)
dev.off()
}

#2070-2100
for (j in 1:length(speclistB)) {
  curr <- raster(paste(densdir, speclistB[j], "_currmean.asc", sep=""))
  curr <- crop(curr, study)
  curr <- mask(curr, study)
  prev <- cellStats(curr, 'mean')
  m <- c(0, prev, 0, prev+0.00001, 1000, 1)
  rclmat <- matrix(m, ncol=3, byrow=TRUE)
  mean2080 <- raster(paste(densdir, speclistB[j], "_2080mean.asc", sep=""))
  core2080 <- reclassify(mean2080, rclmat)
  core2080 <- crop(core2080, resultclip)
  core2080 <- mask(core2080, resultclip)
  writeRaster(core2080,
    file=paste(refdir, speclistB[j], "_core2080.asc", sep=""),
    format="ascii", overwrite=TRUE)
  png(file=paste(refdir, speclistB[j], "_core2080.png", sep=""))
  plot(core2080)
  dev.off()
}
#####

#####
#Calculate strict refugia for future time periods

#2020
for (j in 1:length(speclistB)) {
  curr <- raster(paste(densdir, speclistB[j], "_currmean.asc", sep=""))
  curr <- crop(curr, study)
  curr <- mask(curr, study)
  prev <- cellStats(curr, 'mean')
  m <- c(0, prev, 0, prev+0.00001, 1000, 1)
  m1 <- c(0, 1, 0, 1.000001, 1000, 1)
  rclmat <- matrix(m, ncol=3, byrow=TRUE)
  rclmat1 <- matrix(m1, ncol=3, byrow=TRUE)
  core <- reclassify(curr, rclmat)
  modelstack <- NULL
  for (i in 1:4) { #4 GCMS
    for (k in 1:11) { #11 bootstrap iterations
      r <-
        raster(paste(w, speclistB[j], "_brt_clim", k, "_", gcms[i], "_2020.asc",
          sep=""))
      r <- crop(r, resultclip)
      r <- mask(r, resultclip)
      ref <- reclassify(r, rclmat)
    }
  }
}

```

```

ref <- trim(ref + core)
ref1 <- reclassify(ref, rclmat1)
if(is.null(modelstack)) {modelstack <- stack(ref1)} else
  {modelstack <- addLayer(modelstack, ref1)}
rtop <-
raster(paste(w,speclistB[j],"_brt_climtop",k,"_",gcms[i],"_2020.as
c",sep=""))
  rtop <- crop(rtop, resultclip)
  rtop <- mask(rtop, resultclip)
  reftop <- reclassify(rtop, rclmat)
  reftop <- trim(reftop + core)
  reftop1 <- reclassify(reftop, rclmat1)
  modelstack <- addLayer(modelstack, reftop1)
}
}
modelmean <- mean(modelstack)
writeRaster(modelmean,
  file=paste(refdir,speclistB[j],"_ref2020combo.asc",sep=""),
  format="ascii", overwrite=TRUE)
png(file=paste(refdir,speclistB[j],"_ref2020combo.png",sep=""))
plot(modelmean)
dev.off()
}

#2050
for (j in 1:length(speclistB)) {
curr <- raster(paste(densdir,speclistB[j],"_currmean.asc",sep=""))
curr <- crop(curr, study)
curr <- mask(curr, study)
prev <- cellStats(curr, 'mean')
m <- c(0, prev, 0, prev+0.00001, 1000, 1)
m1 <- c(0, 1, 0, 1.00001, 1000, 1)
rclmat <- matrix(m, ncol=3, byrow=TRUE)
rclmat1 <- matrix(m1, ncol=3, byrow=TRUE)
core <- reclassify(curr, rclmat)
modelstack <- NULL
for (i in 1:4) { #4 GCMs
  for (k in 1:11) { #11 bootstrap iterations
    r <-
      raster(paste(w,speclistB[j],"_brt_clim",k,"_",gcms[i],"_2050.as
c",sep=""))
    r <- crop(r, resultclip)
    r <- mask(r, resultclip)
    ref <- reclassify(r, rclmat)
    ref <- trim(ref + core)
    ref1 <- reclassify(ref, rclmat1)
    if(is.null(modelstack)) {modelstack <- stack(ref1)} else
    {modelstack <- addLayer(modelstack, ref1)}
    rtop <-
      raster(paste(w,speclistB[j],"_brt_climtop",k,"_",gcms[i],"_2050
.asc",sep=""))
    rtop <- crop(rtop, resultclip)
    rtop <- mask(rtop, resultclip)
    reftop <- reclassify(rtop, rclmat)
    reftop <- trim(reftop + core)
    reftop1 <- reclassify(reftop, rclmat1)
    modelstack <- addLayer(modelstack, reftop1)
  }
}
}
modelmean <- mean(modelstack)

```

```

writeRaster(modelmean,
file=paste(refdir,speclistB[j],"_ref2050combo.asc",sep=""), format="ascii",
overwrite=TRUE)
png(file=paste(refdir,speclistB[j],"_ref2050combo.png",sep=""))
plot(modelmean)
dev.off()
}

#2080
for (j in 1:length(speclistB)) {
curr <- raster(paste(densdir,speclistB[j],"_currmean.asc",sep=""))
curr <- crop(curr, study)
curr <- mask(curr, study)
prev <- cellStats(curr, 'mean')
m <- c(0, prev, 0, prev+0.00001, 1000, 1)
m1 <- c(0, 1, 0, 1.00001, 1000, 1)
rclmat <- matrix(m, ncol=3, byrow=TRUE)
rclmat1 <- matrix(m1, ncol=3, byrow=TRUE)
core <- reclassify(curr, rclmat)
modelstack <- NULL
for (i in 1:4) { #4 GCMs
for (k in 1:11) { #11 bootstrap iterations
r <-
raster(paste(w,speclistB[j],"_brt_clim",k,"_",gcms[i],"_2080.as
c",sep=""))
r <- crop(r, resultclip)
r <- mask(r, resultclip)
ref <- reclassify(r, rclmat)
ref <- trim(ref + core)
ref1 <- reclassify(ref, rclmat1)
if(is.null(modelstack)) {modelstack <- stack(ref1)} else
{modelstack <- addLayer(modelstack, ref1)}
rtop <-
raster(paste(w,speclistB[j],"_brt_climtop",k,"_",gcms[i],"_2080
.asc",sep=""))
rtop <- crop(rtop, resultclip)
rtop <- mask(rtop, resultclip)
reftop <- reclassify(rtop, rclmat)
reftop <- trim(reftop + core)
reftop1 <- reclassify(reftop, rclmat1)
modelstack <- addLayer(modelstack, reftop1)
}
}
modelmean <- mean(modelstack)
writeRaster(modelmean,
file=paste(refdir,speclistB[j],"_ref2080combo.asc",sep=""), format="ascii",
overwrite=TRUE)
png(file=paste(refdir,speclistB[j],"_ref2080combo.png",sep=""))
plot(modelmean)
dev.off()
}
#####

#####
#Calculate modified refugia based on 30-year time lag for future periods

#2041-2070
for (j in 1:length(speclistB)) {
curr <- raster(paste(densdir,speclistB[j],"_currmean.asc",sep=""))
curr <- crop(curr, study)

```

```

curr <- mask(curr, study)
prev <- cellStats(curr, 'mean')
m <- c(0, prev, 0, prev+0.00001, 1000, 1)
m1 <- c(0, 1, 0, 1.00001, 1000, 1)
rclmat <- matrix(m, ncol=3, byrow=TRUE)
rclmat1 <- matrix(m1, ncol=3, byrow=TRUE)
core2020 <- raster(paste(densdir, speclistB[j], "_2020mean.asc", sep=""))
core <- reclassify(core2020, rclmat)
modelstack <- NULL
for (i in 1:4) { #4 GCMs
  for (k in 1:11) { #11 bootstrap iterations
    r <-
      raster(paste(w, speclistB[j], "_brt_clim", k, "_", gcms[i], "_2050.asc", sep=""))
    r <- crop(r, resultclip)
    r <- mask(r, resultclip)
    ref <- reclassify(r, rclmat)
    ref <- trim(ref + core)
    refl <- reclassify(ref, rclmat1)
    if(is.null(modelstack)) {modelstack <- stack(refl)} else {modelstack
      <- addLayer(modelstack, refl)}
    rtop <-
      raster(paste(w, speclistB[j], "_brt_climtop", k, "_", gcms[i], "_2050.as
c", sep=""))
    rtop <- crop(rtop, resultclip)
    rtop <- mask(rtop, resultclip)
    reftop <- reclassify(rtop, rclmat)
    reftop <- trim(reftop + core)
    reftop1 <- reclassify(reftop, rclmat1)
    modelstack <- addLayer(modelstack, reftop1)
  }
}
modelmean <- mean(modelstack)
writeRaster(modelmean,
  file=paste(refdir, speclistB[j], "_core2050combo_30yrlag.asc", sep=""),
  format="ascii", overwrite=TRUE)
png(file=paste(refdir, speclistB[j], "_core2050combo_30yrlag.png", sep=""))
plot(modelmean)
dev.off()
}

#2071-2100
for (j in 1:length(speclistB)) {
  curr <- raster(paste(densdir, speclistB[j], "_currmean.asc", sep=""))
  curr <- crop(curr, study)
  curr <- mask(curr, study)
  prev <- cellStats(curr, 'mean')
  m <- c(0, prev, 0, prev+0.00001, 1000, 1)
  m1 <- c(0, 1, 0, 1.00001, 1000, 1)
  rclmat <- matrix(m, ncol=3, byrow=TRUE)
  rclmat1 <- matrix(m1, ncol=3, byrow=TRUE)
  core2050 <- raster(paste(densdir, speclistB[j], "_2050mean.asc", sep=""))
  core <- reclassify(core2050, rclmat)
  core <- crop(core, resultclip)
  core <- mask(core, resultclip)
  modelstack <- NULL
  for (i in 1:4) { #4 GCMs
    for (k in 1:11) { #11 bootstrap iterations
      r <-
        raster(paste(w, speclistB[j], "_brt_clim", k, "_", gcms[i], "_2080.asc",
sep=""))

```

```

r <- crop(r, resultclip)
r <- mask(r, resultclip)
ref <- reclassify(r, rclmat)
ref <- trim(ref + core)
ref1 <- reclassify(ref, rclmat1)
if(is.null(modelstack)) {modelstack <- stack(ref1)} else {modelstack
  <- addLayer(modelstack, ref1)}
rtop <-
  raster(paste(w, speclistB[j], "_brt_climtop", k, "_", gcms[i], "_2080.as
c", sep=""))
rtop <- crop(rtop, resultclip)
rtop <- mask(rtop, resultclip)
reftop <- reclassify(rtop, rclmat)
reftop <- trim(reftop + core)
reftop1 <- reclassify(reftop, rclmat1)
modelstack <- addLayer(modelstack, reftop1)
  }
  }
modelmean <- mean(modelstack)
writeRaster(modelmean,
  file=paste(refdir, speclistB[j], "_core2080combo_30yrlag.asc", sep=""),
  format="ascii", overwrite=TRUE)
png(file=paste(refdir, speclistB[j], "_core2080combo_30yrlag.png", sep=""))
plot(modelmean)
dev.off()
}
#####

#####
#Calculate modified refugia based on 60-year time lag for future periods

#2071-2100
for (j in 1:length(speclistB)) {
  curr <- raster(paste(densdir, speclistB[j], "_currmean.asc", sep=""))
  curr <- crop(curr, study)
  curr <- mask(curr, study)
  prev <- cellStats(curr, 'mean')
  m <- c(0, prev, 0, prev+0.00001, 1000, 1)
  m1 <- c(0, 1, 0, 1.00001, 1000, 1)
  rclmat <- matrix(m, ncol=3, byrow=TRUE)
  rclmat1 <- matrix(m1, ncol=3, byrow=TRUE)
  core2020 <- raster(paste(densdir, speclistB[j], "_2020mean.asc", sep=""))
  core <- reclassify(core2020, rclmat)
  core <- crop(core, resultclip)
  core <- mask(core, resultclip)
  modelstack <- NULL
  for (i in 1:4) { #4 GCMs
    for (k in 1:11) { #11 bootstrap iterations
      r <-
        raster(paste(w, speclistB[j], "_brt_clim", k, "_", gcms[i], "_2080.asc",
          sep=""))
      r <- crop(r, resultclip)
      r <- mask(r, resultclip)
      ref <- reclassify(r, rclmat)
      ref <- trim(ref + core)
      ref1 <- reclassify(ref, rclmat1)
    }
    if(is.null(modelstack)) {modelstack <- stack(ref1)} else {modelstack
      <- addLayer(modelstack, ref1)}
    rtop <-
      raster(paste(w, speclistB[j], "_brt_climtop", k, "_", gcms[i], "_2080.as
c", sep=""))

```

```

    rtop <- crop(rtop, resultclip)
    rtop <- mask(rtop, resultclip)
    reftop <- reclassify(rtop, rclmat)
    reftop <- trim(reftop + core)
    reftop1 <- reclassify(reftop, rclmat1)
    modelstack <- addLayer(modelstack, reftop1)
  }
}
modelmean <- mean(modelstack)
writeRaster(modelmean,
  file=paste(refdir, speclistB[j], "_core2080combo_30yrlag.asc", sep=""),
  format="ascii", overwrite=TRUE)
png(file=paste(refdir, speclistB[j], "_core2080combo_30yrlag.png", sep=""))
  plot(modelmean)
  dev.off()
}
#####

```

Appendix 2-E. Zonation settings and inputs

#####

settings.dat file:

```
use groups = 0
use condition layer = 0
use retention layer = 0
removal rule = 1
BLP = 0.1
```

#####

sppequal20xx.bat file: (xx = time period, all species weighted equally)

```
call zig3 -r settings.dat sppequal20xx.spp out\sppequal20xx.txt 0.0 0 1.0 0
```

sppccweight20xx.bat file: (xx = time period, species climate-change weighted)

```
call zig3 -r settings.dat sppccweight20xx.spp out\sppccweight20xx.txt 0.0 0
1.0 0
```

#####

sppequal2020.spp file (2011-2040; all species weighted equally; modified refugia: core = no lag, ref = strict refugia)

1 1 1 1 1 AMRE_ref2020combo.asc	1 1 1 1 1 NAWA_core2020combo.asc
1 1 1 1 1 BAWW_ref2020combo.asc	1 1 1 1 1 NOWA_ref2020combo.asc
1 1 1 1 1 BBWA_ref2020combo.asc	1 1 1 1 1 OCWA_ref2020combo.asc
1 1 1 1 1 BCCH_ref2020combo.asc	1 1 1 1 1 OSFL_core2020combo.asc
1 1 1 1 1 BHVI_ref2020combo.asc	1 1 1 1 1 OVEN_ref2020combo.asc
1 1 1 1 1 BLBW_ref2020combo.asc	1 1 1 1 1 PAWA_core2020combo.asc
1 1 1 1 1 BLJA_core2020combo.asc	1 1 1 1 1 PHVI_ref2020combo.asc
1 1 1 1 1 BLPW_ref2020combo.asc	1 1 1 1 1 PIGR_ref2020combo.asc
1 1 1 1 1 BOCH_ref2020combo.asc	1 1 1 1 1 PISI_ref2020combo.asc
1 1 1 1 1 BRCR_ref2020combo.asc	1 1 1 1 1 PUFU_ref2020combo.asc
1 1 1 1 1 BTNW_ref2020combo.asc	1 1 1 1 1 RBGR_ref2020combo.asc
1 1 1 1 1 CAWA_ref2020combo.asc	1 1 1 1 1 RBNU_ref2020combo.asc
1 1 1 1 1 CEDW_core2020combo.asc	1 1 1 1 1 RCKI_ref2020combo.asc
1 1 1 1 1 CMWA_ref2020combo.asc	1 1 1 1 1 REVI_ref2020combo.asc
1 1 1 1 1 CONW_ref2020combo.asc	1 1 1 1 1 RUBL_core2020combo.asc
1 1 1 1 1 CORA_core2020combo.asc	1 1 1 1 1 SWTH_ref2020combo.asc
1 1 1 1 1 CORE_ref2020combo.asc	1 1 1 1 1 TEWA_ref2020combo.asc
1 1 1 1 1 DEJU_ref2020combo.asc	1 1 1 1 1 VATH_ref2020combo.asc
1 1 1 1 1 EVGR_ref2020combo.asc	1 1 1 1 1 WETA_ref2020combo.asc
1 1 1 1 1 FOSP_ref2020combo.asc	1 1 1 1 1 WEWP_ref2020combo.asc
1 1 1 1 1 GCKI_ref2020combo.asc	1 1 1 1 1 WIWA_core2020combo.asc
1 1 1 1 1 GCTH_ref2020combo.asc	1 1 1 1 1 WIWR_ref2020combo.asc
1 1 1 1 1 GRAJ_ref2020combo.asc	1 1 1 1 1 WTSP_core2020combo.asc
1 1 1 1 1 HETH_core2020combo.asc	1 1 1 1 1 WWCR_ref2020combo.asc
1 1 1 1 1 LEFL_ref2020combo.asc	1 1 1 1 1 YBFL_ref2020combo.asc
1 1 1 1 1 MAWA_ref2020combo.asc	1 1 1 1 1 YRWA_ref2020combo.asc
1 1 1 1 1 MOWA_core2020combo.asc	

sppccweight2020.spp file (2011-2040, species climate-change weighted; modified refugia: core = no lag, ref = strict refugia)

1.20 1 1 1 1 AMRE_ref2020combo.asc	1.15 1 1 1 1 BBWA_ref2020combo.asc
1.30 1 1 1 1 BAWW_ref2020combo.asc	1.25 1 1 1 1 BCCH_ref2020combo.asc

0.88	1	1	1	1	BHVI_ref2020combo.asc	1.27	1	1	1	1	OCWA_ref2020combo.asc
1.30	1	1	1	1	BLBW_ref2020combo.asc	0.5	1	1	1	1	OSFL_core2020combo.asc
0.96	1	1	1	1	BLJA_core2020combo.asc	1.13	1	1	1	1	OVEN_ref2020combo.asc
1.25	1	1	1	1	BLPW_ref2020combo.asc	1.28	1	1	1	1	PAWA_ref2020combo.asc
1.23	1	1	1	1	BOCH_ref2020combo.asc	1.17	1	1	1	1	PHVI_ref2020combo.asc
1.04	1	1	1	1	BRCR_ref2020combo.asc	1.37	1	1	1	1	PIGR_ref2020combo.asc
1.25	1	1	1	1	BTNW_ref2020combo.asc	1.60	1	1	1	1	PISI_ref2020combo.asc
1.08	1	1	1	1	CAWA_ref2020combo.asc	1.51	1	1	1	1	PUFI_ref2020combo.asc
1.22	1	1	1	1	CEDW_core2020combo.asc	1.21	1	1	1	1	RBGR_ref2020combo.asc
1.21	1	1	1	1	CMWA_ref2020combo.asc	1.15	1	1	1	1	RBNU_ref2020combo.asc
1.19	1	1	1	1	CONW_ref2020combo.asc	1.07	1	1	1	1	RCKI_ref2020combo.asc
0.87	1	1	1	1	CORA_ref2020combo.asc	1.17	1	1	1	1	REVI_ref2020combo.asc
1.43	1	1	1	1	CORE_ref2020combo.asc	1.08	1	1	1	1	RUBL_core2020combo.asc
1.09	1	1	1	1	DEJU_ref2020combo.asc	1.03	1	1	1	1	SWTH_ref2020combo.asc
1.34	1	1	1	1	EVGR_ref2020combo.asc	1.24	1	1	1	1	TEWA_ref2020combo.asc
1.24	1	1	1	1	FOSP_ref2020combo.asc	1.54	1	1	1	1	VATH_ref2020combo.asc
1.15	1	1	1	1	GCKI_ref2020combo.asc	1.53	1	1	1	1	WETA_ref2020combo.asc
1.56	1	1	1	1	GCTH_ref2020combo.asc	1.48	1	1	1	1	WEWP_ref2020combo.asc
1.13	1	1	1	1	GRAJ_ref2020combo.asc	1.07	1	1	1	1	WIWA_core2020combo.asc
1.10	1	1	1	1	HETH_ref2020combo.asc	1.07	1	1	1	1	WIWR_ref2020combo.asc
1.03	1	1	1	1	LEFL_ref2020combo.asc	1.09	1	1	1	1	WTSP_ref2020combo.asc
1.15	1	1	1	1	MAWA_ref2020combo.asc	1.12	1	1	1	1	WWCR_ref2020combo.asc
1.16	1	1	1	1	MOWA_ref2020combo.asc	1.01	1	1	1	1	YBFL_ref2020combo.asc
1.22	1	1	1	1	NAWA_ref2020combo.asc	1.14	1	1	1	1	YRWA_ref2020combo.asc
1.14	1	1	1	1	NOWA_ref2020combo.asc						

sppccweight2020.spp file (2011-2040, species climate-change weighted; strict refugia)

1.20	1	1	1	1	AMRE_ref2020combo.asc	1.22	1	1	1	1	NAWA_ref2020combo.asc
1.30	1	1	1	1	BAWW_ref2020combo.asc	1.14	1	1	1	1	NOWA_ref2020combo.asc
1.15	1	1	1	1	BBWA_ref2020combo.asc	1.27	1	1	1	1	OCWA_ref2020combo.asc
1.25	1	1	1	1	BCCH_ref2020combo.asc	0.86	1	1	1	1	OSFL_ref2020combo.asc
0.88	1	1	1	1	BHVI_ref2020combo.asc	1.13	1	1	1	1	OVEN_ref2020combo.asc
1.30	1	1	1	1	BLBW_ref2020combo.asc	1.28	1	1	1	1	PAWA_ref2020combo.asc
1.77	1	1	1	1	BLJA_ref2020combo.asc	1.17	1	1	1	1	PHVI_ref2020combo.asc
1.25	1	1	1	1	BLPW_ref2020combo.asc	1.37	1	1	1	1	PIGR_ref2020combo.asc
1.23	1	1	1	1	BOCH_ref2020combo.asc	1.60	1	1	1	1	PISI_ref2020combo.asc
1.04	1	1	1	1	BRCR_ref2020combo.asc	1.51	1	1	1	1	PUFI_ref2020combo.asc
1.25	1	1	1	1	BTNW_ref2020combo.asc	1.21	1	1	1	1	RBGR_ref2020combo.asc
1.08	1	1	1	1	CAWA_ref2020combo.asc	1.15	1	1	1	1	RBNU_ref2020combo.asc
1.61	1	1	1	1	CEDW_ref2020combo.asc	1.07	1	1	1	1	RCKI_ref2020combo.asc
1.21	1	1	1	1	CMWA_ref2020combo.asc	1.17	1	1	1	1	REVI_ref2020combo.asc
1.19	1	1	1	1	CONW_ref2020combo.asc	1.32	1	1	1	1	RUBL_ref2020combo.asc
0.87	1	1	1	1	CORA_ref2020combo.asc	1.03	1	1	1	1	SWTH_ref2020combo.asc
1.43	1	1	1	1	CORE_ref2020combo.asc	1.24	1	1	1	1	TEWA_ref2020combo.asc
1.09	1	1	1	1	DEJU_ref2020combo.asc	1.54	1	1	1	1	VATH_ref2020combo.asc
1.34	1	1	1	1	EVGR_ref2020combo.asc	1.53	1	1	1	1	WETA_ref2020combo.asc
1.24	1	1	1	1	FOSP_ref2020combo.asc	1.48	1	1	1	1	WEWP_ref2020combo.asc
1.15	1	1	1	1	GCKI_ref2020combo.asc	1.19	1	1	1	1	WIWA_ref2020combo.asc
1.56	1	1	1	1	GCTH_ref2020combo.asc	1.07	1	1	1	1	WIWR_ref2020combo.asc
1.13	1	1	1	1	GRAJ_ref2020combo.asc	1.09	1	1	1	1	WTSP_ref2020combo.asc
1.10	1	1	1	1	HETH_ref2020combo.asc	1.12	1	1	1	1	WWCR_ref2020combo.asc
1.03	1	1	1	1	LEFL_ref2020combo.asc	1.01	1	1	1	1	YBFL_ref2020combo.asc
1.15	1	1	1	1	MAWA_ref2020combo.asc	1.14	1	1	1	1	YRWA_ref2020combo.asc
1.16	1	1	1	1	MOWA_ref2020combo.asc						

sppccweight2020.spp file (2011-2040, species climate-change weighted; no lag)

0.63	1	1	1	1	AMRE_core2020combo.asc	0.58	1	1	1	1	BBWA_core2020combo.asc
0.90	1	1	1	1	BAWW_core2020combo.asc	1.25	1	1	1	1	BCCH_core2020combo.asc

0.88	1	1	1	1	BHVI_core2020combo.asc	1.11	1	1	1	1	OCWA_core2020combo.asc
0.63	1	1	1	1	BLBW_core2020combo.asc	0.50	1	1	1	1	OSFL_core2020combo.asc
0.96	1	1	1	1	BLJA_core2020combo.asc	0.74	1	1	1	1	OVEN_core2020combo.asc
1.04	1	1	1	1	BLPW_core2020combo.asc	1.04	1	1	1	1	PAWA_core2020combo.asc
0.92	1	1	1	1	BOCH_core2020combo.asc	0.58	1	1	1	1	PHVI_core2020combo.asc
0.38	1	1	1	1	BRCR_core2020combo.asc	1.20	1	1	1	1	PIGR_core2020combo.asc
0.68	1	1	1	1	BTNW_core2020combo.asc	1.27	1	1	1	1	PISI_core2020combo.asc
0.31	1	1	1	1	CAWA_core2020combo.asc	1.04	1	1	1	1	PUFI_core2020combo.asc
1.22	1	1	1	1	CEDW_core2020combo.asc	0.68	1	1	1	1	RBGR_core2020combo.asc
0.49	1	1	1	1	CMWA_core2020combo.asc	0.74	1	1	1	1	RBNU_core2020combo.asc
0.71	1	1	1	1	CONW_core2020combo.asc	0.77	1	1	1	1	RCKI_core2020combo.asc
0.43	1	1	1	1	CORA_core2020combo.asc	0.78	1	1	1	1	REVI_core2020combo.asc
1.20	1	1	1	1	CORE_core2020combo.asc	1.08	1	1	1	1	RUBL_core2020combo.asc
0.88	1	1	1	1	DEJU_core2020combo.asc	0.73	1	1	1	1	SWTH_core2020combo.asc
0.76	1	1	1	1	EVGR_core2020combo.asc	0.90	1	1	1	1	TEWA_core2020combo.asc
1.07	1	1	1	1	FOSP_core2020combo.asc	1.29	1	1	1	1	VATH_core2020combo.asc
0.71	1	1	1	1	GCKI_core2020combo.asc	0.97	1	1	1	1	WETA_core2020combo.asc
1.44	1	1	1	1	GCTH_core2020combo.asc	1.21	1	1	1	1	WEWP_core2020combo.asc
0.95	1	1	1	1	GRAJ_core2020combo.asc	1.07	1	1	1	1	WIWA_core2020combo.asc
0.88	1	1	1	1	HETH_core2020combo.asc	0.63	1	1	1	1	WIWR_core2020combo.asc
0.72	1	1	1	1	LEFL_core2020combo.asc	0.86	1	1	1	1	WTSP_core2020combo.asc
0.80	1	1	1	1	MAWA_core2020combo.asc	0.87	1	1	1	1	WWCR_core2020combo.asc
0.69	1	1	1	1	MOWA_core2020combo.asc	0.74	1	1	1	1	YBFL_core2020combo.asc
0.54	1	1	1	1	NAWA_core2020combo.asc	0.75	1	1	1	1	YRWA_core2020combo.asc
0.92	1	1	1	1	NOWA_core2020combo.asc						

sppccweight2050.spp file (2041-2070, species climate-change weighted; modified refugia:
core = no lag, ref = strict refugia, 30lag = 30-year lag time)

0.74	1	1	1	1	AMRE_30lag2050combo.asc	0.07	1	1	1	1	NAWA_core2050combo.asc
1.06	1	1	1	1	BAWW_30lag2050combo.asc	1.21	1	1	1	1	NOWA_30lag2050combo.asc
1.59	1	1	1	1	BBWA_ref2050combo.asc	1.36	1	1	1	1	OCWA_30lag2050combo.asc
1.23	1	1	1	1	BCCH_30lag2050combo.asc	0.68	1	1	1	1	OSFL_core2050combo.asc
1.16	1	1	1	1	BHVI_30lag2050combo.asc	1.24	1	1	1	1	OVEN_ref2050combo.asc
1.40	1	1	1	1	BLBW_ref2050combo.asc	1.35	1	1	1	1	PAWA_core2050combo.asc
0.27	1	1	1	1	BLJA_core2050combo.asc	1.2	1	1	1	1	PHVI_30lag2050combo.asc
1.61	1	1	1	1	BLPW_ref2050combo.asc	1.45	1	1	1	1	PIGR_30lag2050combo.asc
1.46	1	1	1	1	BOCH_ref2050combo.asc	1.69	1	1	1	1	PISI_ref2050combo.asc
1.22	1	1	1	1	BRCR_ref2050combo.asc	1.23	1	1	1	1	PUFI_30lag2050combo.asc
1.31	1	1	1	1	BTNW_ref2050combo.asc	0.75	1	1	1	1	RBGR_30lag2050combo.asc
1.17	1	1	1	1	CAWA_ref2050combo.asc	1.21	1	1	1	1	RBNU_ref2050combo.asc
0.8	1	1	1	1	CEDW_core2050combo.asc	1.17	1	1	1	1	RCKI_30lag2050combo.asc
1.52	1	1	1	1	CMWA_ref2050combo.asc	0.87	1	1	1	1	REVI_30lag2050combo.asc
1.59	1	1	1	1	CONW_ref2050combo.asc	1.35	1	1	1	1	RUBL_core2050combo.asc
0.4	1	1	1	1	CORA_core2050combo.asc	1.29	1	1	1	1	SWTH_ref2050combo.asc
1.71	1	1	1	1	CORE_ref2050combo.asc	1.32	1	1	1	1	TEWA_30lag2050combo.asc
1.21	1	1	1	1	DEJU_30lag2050combo.asc	1.59	1	1	1	1	VATH_ref2050combo.asc
0.91	1	1	1	1	EVGR_30lag2050combo.asc	1.63	1	1	1	1	WETA_ref2050combo.asc
1.59	1	1	1	1	FOSP_ref2050combo.asc	1.37	1	1	1	1	WEWP_30lag2050combo.asc
0.89	1	1	1	1	GCKI_30lag2050combo.asc	1.19	1	1	1	1	WIWA_core2050combo.asc
1.75	1	1	1	1	GCTH_ref2050combo.asc	0.9	1	1	1	1	WIWR_30lag2050combo.asc
1.27	1	1	1	1	GRAJ_30lag2050combo.asc	0.9	1	1	1	1	WTSP_core2050combo.asc
0.99	1	1	1	1	HETH_core2050combo.asc	1.32	1	1	1	1	WWCR_30lag2050combo.asc
0.78	1	1	1	1	LEFL_30lag2050combo.asc	1.07	1	1	1	1	YBFL_30lag2050combo.asc
1.09	1	1	1	1	MAWA_30lag2050combo.asc	1.36	1	1	1	1	YRWA_ref2050combo.asc
0.35	1	1	1	1	MOWA_core2050combo.asc						

sppccweight2080.spp file (2071-2100, species climate-change weighted; modified refugia:
core = no lag, ref = strict refugia, 30lag = 30-year lag time, 60lag = 60-year lag time)

0.56	1	1	1	1	AMRE_30lag2080combo.asc	1.44	1	1	1	1	NOWA_30lag2080combo.asc
0.99	1	1	1	1	BAWW_30lag2080combo.asc	1.42	1	1	1	1	OCWA_30lag2080combo.asc
1.77	1	1	1	1	BBWA_60lag2080combo.asc	0.94	1	1	1	1	OSFL_core2080combo.asc
0.82	1	1	1	1	BCCH_30lag2080combo.asc	1.18	1	1	1	1	OVEN_60lag2080combo.asc
1.27	1	1	1	1	BHVI_30lag2080combo.asc	1.77	1	1	1	1	PAWA_core2080combo.asc
1.13	1	1	1	1	BLBW_60lag2080combo.asc	1.39	1	1	1	1	PHVI_30lag2080combo.asc
0.00	1	1	1	1	BLJA_core2080combo.asc	1.60	1	1	1	1	PIGR_30lag2080combo.asc
1.78	1	1	1	1	BLPW_60lag2080combo.asc	1.64	1	1	1	1	PISI_60lag2080combo.asc
1.59	1	1	1	1	BOCH_60lag2080combo.asc	0.91	1	1	1	1	PUFI_30lag2080combo.asc
1.56	1	1	1	1	BRCR_60lag2080combo.asc	0.50	1	1	1	1	RBGR_30lag2080combo.asc
1.16	1	1	1	1	BTNW_60lag2080combo.asc	1.00	1	1	1	1	RBNU_60lag2080combo.asc
0.98	1	1	1	1	CAWA_60lag2080combo.asc	1.44	1	1	1	1	RCKI_30lag2080combo.asc
0.16	1	1	1	1	CEDW_core2080combo.asc	0.77	1	1	1	1	REVI_30lag2080combo.asc
1.71	1	1	1	1	CMWA_60lag2080combo.asc	1.64	1	1	1	1	RUBL_core2080combo.asc
1.68	1	1	1	1	CONW_60lag2080combo.asc	1.35	1	1	1	1	SWTH_60lag2080combo.asc
0.55	1	1	1	1	CORA_core2080combo.asc	1.60	1	1	1	1	TEWA_30lag2080combo.asc
1.72	1	1	1	1	CORE_60lag2080combo.asc	1.58	1	1	1	1	VATH_60lag2080combo.asc
1.46	1	1	1	1	DEJU_30lag2080combo.asc	1.78	1	1	1	1	WETA_ref2080combo.asc
0.55	1	1	1	1	EVGR_30lag2080combo.asc	1.30	1	1	1	1	WEWP_30lag2080combo.asc
1.79	1	1	1	1	FOSP_60lag2080combo.asc	1.33	1	1	1	1	WIWA_core2080combo.asc
0.81	1	1	1	1	GCKI_30lag2080combo.asc	1.12	1	1	1	1	WIWR_30lag2080combo.asc
1.92	1	1	1	1	GCTH_ref2080combo.asc	1.12	1	1	1	1	WTSP_core2080combo.asc
1.63	1	1	1	1	GRAJ_30lag2080combo.asc	1.68	1	1	1	1	WWCR_30lag2080combo.asc
1.31	1	1	1	1	HETH_core2080combo.asc	1.32	1	1	1	1	YBFL_30lag2080combo.asc
0.77	1	1	1	1	LEFL_30lag2080combo.asc	1.43	1	1	1	1	YRWA_60lag2080combo.asc
1.31	1	1	1	1	MAWA_30lag2080combo.asc						
0.13	1	1	1	1	MOWA_core2080combo.asc						
0.20	1	1	1	1	NAWA_core2080combo.asc						

Appendix 3-A. Confusion matrix for random forest vegetation predictions.

Code	Vegetation Classification	Ecosite	Class			
			Error	1	2	3
1	Poor-Xeric Grassland	PX	0.07	40	0	1
2	Poor-Xeric Jack Pine	PX	0.01	0	273	0
3	Poor-Mesic Grassland	PM	0.32	0	0	73
4	Poor-Mesic Pine	PM	0.25	0	0	1
5	Poor-Mesic Black Spruce	PM	0.07	0	0	3
6	Poor-Hygric Black Spruce	PG	0.00	0	0	0
7	Poor-Hydric Black Spruce / Larch	PD	0.00	0	0	0
8	Poor-Hydric Shrub	PD	0.33	0	0	0
9	Medium-Xeric Grassland	MX	0.06	0	0	1
10	Medium-Xeric Aspen Mix	MX	0.24	0	0	0
11	Medium-Xeric Pine	MX	0.30	0	1	0
12	Medium-Xeric Spruce	MX	0.23	0	1	0
13	Medium-Mesic Grassland	MM	0.00	0	0	0
14	Medium-Mesic Aspen	MM	0.15	0	0	0
50	Medium-Mesic Aspen Boreal Mixedwood	MM	0.12	0	0	0
15	Medium-Mesic Aspen Mix	MM	0.53	0	0	0
16	Medium-Mesic Pine	MM	0.22	0	0	0
17	Medium-Mesic Pine Mix	MM	0.42	0	0	0
18	Medium-Mesic White Spruce	MM	0.57	0	0	0
19	Medium-Hygric Grassland	MG	0.01	0	0	0
20	Medium-Hygric Poplar Mix	MG	0.11	0	0	0
21	Medium-Hygric Spruce Mix	MG	0.34	0	0	1
22	Medium-Hygric Black Spruce Mix	MG	0.37	0	0	0
25	Medium-Hydric Shrub (Poor Fen)	MD	0.71	0	0	0
26	Medium-Hydric Black Spruce Fen (Poor Fen)	MD	0.04	0	0	1
27	Rich-Mesic Grassland	RM	0.00	0	0	0
28	Rich-Hygric Shrubland	RG	0.30	1	0	0
29	Rich-Hygric Poplar	RG	0.03	0	0	0
30	Rich-Hygric Lodgepole Pine	RG	0.38	0	0	0
31	Rich-Hygric Spruce	RG	0.38	0	0	0
32	Rich-Hydric Grass Fen	RD	0.45	1	0	0
33	Rich-Hydric Shrub Fen	RD	0.26	0	0	0
34	Rich-Hydric Black Spruce	RD	0.19	0	0	0
37	Very Rich-Hydric Marsh	VD	0.20	0	0	0

Code	4	5	6	7	8	9	10	11	12	13	14	50	15	16
1	0	0	0	0	0	0	0	0	0	0	0	0	0	0
2	1	0	0	0	0	0	1	0	0	0	0	0	0	0
3	14	16	0	0	0	0	1	0	1	0	0	0	0	0
4	155	52	0	0	0	0	0	0	0	0	0	0	0	0
5	23	340	0	0	0	0	1	0	0	0	0	0	0	0
6	0	0	33	0	0	0	0	0	0	0	0	0	0	0
7	0	0	0	459	2	0	0	0	0	0	0	0	0	0
8	0	0	0	11	22	0	0	0	0	0	0	0	0	0
9	0	0	0	0	0	44	0	1	0	0	0	0	0	0
10	0	1	0	0	0	0	47	10	1	0	0	0	0	0
11	0	3	0	0	0	0	6	45	3	0	0	0	0	0
12	0	0	0	0	0	0	4	4	30	0	0	0	0	0
13	0	0	0	0	0	0	0	0	0	325	0	1	0	0
14	0	0	0	0	0	0	0	0	0	1	181	4	18	0
50	0	0	0	0	0	0	0	0	0	1	1	913	89	2
15	0	0	0	0	0	0	0	0	0	0	22	204	239	8
16	0	0	0	0	0	0	0	0	0	0	0	9	7	105
17	0	0	0	0	0	0	0	0	0	0	1	67	20	9
18	0	0	0	0	0	0	0	0	0	0	9	63	48	10
19	0	0	0	0	0	0	0	0	0	0	0	0	0	0
20	0	0	0	0	0	1	0	0	0	0	0	0	0	0
21	0	1	0	0	0	0	0	0	1	0	0	0	0	0
22	0	1	1	0	0	0	0	1	0	0	0	0	0	0
25	0	0	0	0	0	0	0	0	0	0	0	0	0	0
26	0	1	0	0	0	0	0	1	0	0	0	0	0	0
27	0	0	0	0	0	0	0	0	0	0	0	0	0	0
28	0	0	0	0	0	0	0	0	0	0	0	0	0	0
29	0	0	0	0	0	0	0	0	0	0	0	0	0	0
30	0	0	0	0	0	0	0	0	0	0	0	0	0	0
31	0	0	0	0	0	0	0	0	0	0	0	0	0	0
32	0	0	0	0	0	1	0	0	0	0	0	0	0	0
33	1	0	0	1	0	0	0	0	0	0	0	0	0	0
34	1	0	0	1	0	0	1	0	0	0	0	0	0	0
37	0	0	0	0	0	0	0	0	0	0	0	0	1	0

Code	17	18	19	20	21	22	25	26	27	28	29	30	31	32
1	0	0	0	0	0	0	0	0	0	1	0	0	0	0
2	0	0	0	0	0	0	0	0	0	0	0	0	0	0
3	0	0	0	0	1	0	0	0	1	0	0	0	0	0
4	0	0	0	0	0	0	0	0	0	0	0	0	0	0
5	0	0	0	0	0	0	0	0	0	0	0	0	0	0
6	0	0	0	0	0	0	0	0	0	0	0	0	0	0
7	0	0	0	0	0	0	0	0	0	0	0	0	0	0
8	0	0	0	0	0	0	0	0	0	0	0	0	0	0
9	0	0	1	0	0	0	0	0	0	0	0	0	0	0
10	0	0	0	2	0	0	0	1	0	0	0	0	0	0
11	0	0	0	4	0	0	1	1	0	0	0	0	0	0
12	0	0	0	0	0	0	0	0	0	0	0	0	0	0
13	0	0	0	0	0	0	0	0	0	0	0	0	0	0
14	0	8	0	0	0	0	0	0	0	0	0	0	0	0
50	16	20	0	0	0	0	0	0	0	0	0	0	0	0
15	12	28	0	0	0	0	0	0	0	0	0	0	0	0
16	8	6	0	0	0	0	0	0	0	0	0	0	0	0
17	143	8	0	0	0	0	0	0	0	0	0	0	0	0
18	7	104	0	0	0	0	0	0	0	0	0	0	0	0
19	0	0	122	0	0	0	0	0	1	0	0	0	0	0
20	0	0	0	232	18	9	0	0	0	0	0	0	0	0
21	0	1	1	31	85	4	0	0	0	0	0	0	0	0
22	0	0	0	18	9	58	0	3	0	0	0	0	0	0
25	0	0	0	0	0	0	12	29	0	0	0	0	0	0
26	0	0	0	0	0	1	4	235	0	0	0	0	0	0
27	0	0	0	0	0	0	0	0	36	0	0	0	0	0
28	0	0	2	0	0	0	0	0	0	7	0	0	0	0
29	0	0	0	0	0	0	0	0	0	0	475	2	14	0
30	0	0	0	0	0	0	0	0	0	0	3	13	5	0
31	0	0	0	0	0	0	0	0	0	0	32	5	61	0
32	0	0	1	0	0	0	0	0	2	1	0	0	0	24
33	0	0	0	2	0	0	0	0	0	0	0	0	0	5
34	0	0	0	0	0	2	0	4	0	0	0	0	0	1
37	0	0	0	0	0	0	0	0	0	0	0	0	0	0

Code	33	34	37
1	1	0	0
2	0	0	0
3	0	0	0
4	0	0	0
5	0	0	0
6	0	0	0
7	0	0	0
8	0	0	0
9	0	0	0
10	0	0	0
11	0	0	0
12	0	0	0
13	0	0	0
14	0	0	0
50	0	0	0
15	0	0	0
16	0	0	0
17	0	0	0
18	0	0	0
19	0	0	0
20	0	0	0
21	1	2	0
22	0	1	0
25	0	0	0
26	1	0	0
27	0	0	0
28	0	0	0
29	0	0	0
30	0	0	0
31	0	0	0
32	10	4	0
33	143	41	0
34	33	183	0
37	0	0	4

Appendix 3-B. Vegetation type projections (km²) by GCM for scenarios A, B1, and B2.

A = Climate-driven; B1 = fire-mediated; B2 = fire- and anthropogenic disturbance-mediated.

Upland Vegetation Type	Baseline	HadGEM 2030			HadGEM 2060			HadGEM 2090		
		A	B1	B2	A	B1	B2	A	B1	B2
Poor-Xeric Grassland	2	5	2	3	1,517	189	25	14,978	2,053	2,801
Poor-Xeric Jack Pine	15,021	14,839	15,002	14,997	13,661	14,830	14,651	244	13,000	11,965
Poor-Mesic Grassland	280	457	312	355	8,727	1,832	511	20,546	5,507	5,208
Poor-Mesic Pine	9,298	6,525	8,902	8,848	633	7,656	7,892	396	6,586	6,439
Poor-Mesic Black Spruce	15,978	18,335	16,286	16,293	13,806	15,551	16,709	2,361	12,622	12,984
Medium-Xeric Aspen Mix	488	537	489	489	83	434	497	72	375	462
Medium-Xeric Pine	123	23	112	111	29	102	93	14	92	81
Medium-Xeric Spruce	212	108	209	206	5	185	180	4	159	162
Medium-Mesic Grassland	57	57,138	7,054	8,833	171,156	29,080	24,491	202,411	56,420	53,489
Medium-Mesic Aspen	22,343	60,339	29,774	30,038	28,600	34,292	36,209	501	33,025	34,674
Medium-Mesic Aspen Boreal Mixedwood	122,428	27,430	107,783	106,967	6,252	91,345	91,354	3,184	75,103	74,568
Medium-Mesic Aspen Mix	36,889	23,008	34,872	34,073	508	29,574	30,443	422	24,070	24,870
Medium-Mesic Pine	6,493	510	5,555	5,266	54	4,573	3,526	54	3,629	2,615
Medium-Mesic Pine Mix	8,755	30,482	12,702	12,707	216	10,816	13,898	216	9,046	11,154
Medium-Mesic White Spruce	9,996	8,059	9,219	9,078	277	7,300	7,045	184	5,689	5,597
Non-Analog (Upland to Lowland)		569	87	98	2,838	602	836	2,776	986	1,290

Total 248,360 km²

Upland Vegetation Type	Baseline	HadCM3 2030			HadCM3 2060			HadCM3 2090		
		A	B1	B2	A	B1	B2	A	B1	B2
Poor-Xeric Grassland	2	4	2	2	7	3	4	160	35	31
Poor-Xeric Jack Pine	15,021	15,016	15,021	15,020	15,018	15,020	15,019	14,866	14,988	14,992
Poor-Mesic Grassland	280	400	306	337	889	429	536	5,009	1,478	1,490
Poor-Mesic Pine	9,298	9,392	9,445	9,408	5,678	8,853	8,833	2,350	7,491	7,581
Poor-Mesic Black Spruce	15,978	15,723	15,795	15,800	18,861	16,241	16,144	17,233	16,267	16,172
Medium-Xeric Aspen Mix	488	430	478	473	131	449	413	74	397	377
Medium-Xeric Pine	123	29	113	112	21	99	94	31	91	84
Medium-Xeric Spruce	212	87	207	202	59	192	166	4	146	143
Medium-Mesic Grassland	57	27,242	3,254	4,235	77,447	11,629	17,157	149,221	34,025	35,588
Medium-Mesic Aspen	22,343	32,159	24,563	24,574	43,760	30,591	31,287	43,353	39,827	38,974
Medium-Mesic Aspen Boreal Mixedwood	122,428	41,027	110,268	109,582	28,164	96,673	94,370	11,678	79,560	79,933
Medium-Mesic Aspen Mix	36,889	32,673	36,085	35,819	7,151	31,341	29,516	666	25,035	24,336
Medium-Mesic Pine	6,493	505	5,564	5,275	57	4,426	3,556	54	3,167	2,782
Medium-Mesic Pine Mix	8,755	40,336	13,397	13,466	35,254	18,313	17,919	412	14,586	14,715
Medium-Mesic White Spruce	9,996	33,020	13,829	14,009	15,129	13,987	13,155	1,579	10,761	10,633
Non-Analog (Upland to Lowland)		321	34	46	737	115	191	1,673	507	529
Total	248,360									

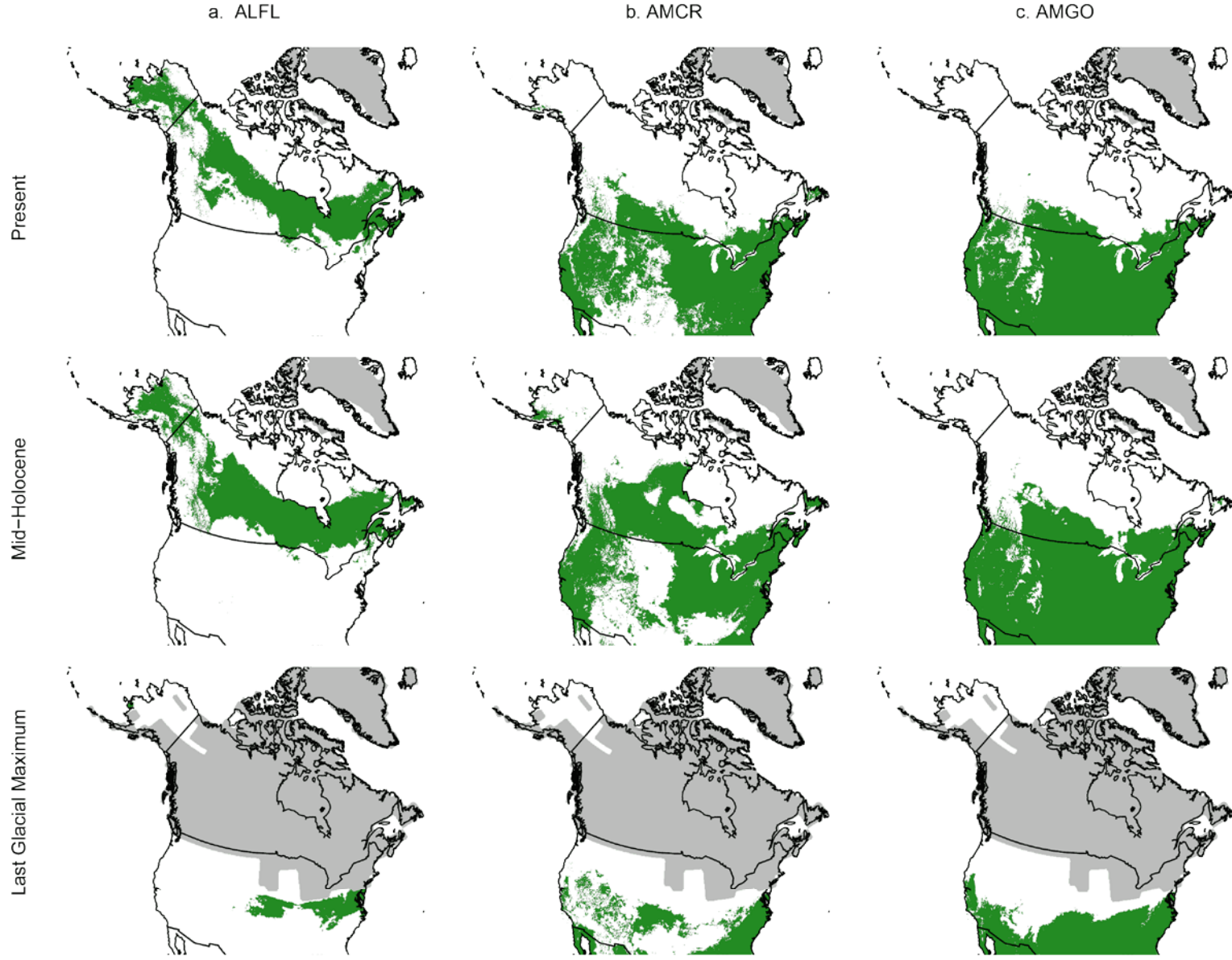
Upland Vegetation Type	Baseline	GFDL 2030			GFDL 2060			GFDL 2090		
		A	B1	B2	A	B1	B2	A	B1	B2
Poor-Xeric Grassland	2	57	2	13	13	9	13	5,638	732	587
Poor-Xeric Jack Pine	15,021	12,848	15,021	14,660	14,793	14,746	14,705	9,630	14,104	14,217
Poor-Mesic Grassland	280	1,312	306	590	708	522	678	8,120	2,182	2,377
Poor-Mesic Pine	9,298	7,664	9,445	8,936	3,440	8,134	8,012	506	6,610	6,544
Poor-Mesic Black Spruce	15,978	16,015	15,795	15,903	20,667	16,667	16,633	13,568	15,712	15,502
Medium-Xeric Aspen Mix	488	187	478	441	215	428	431	73	394	387
Medium-Xeric Pine	123	32	113	113	24	104	100	39	94	94
Medium-Xeric Spruce	212	32	207	190	57	169	168	4	129	144
Medium-Mesic Grassland	57	69,558	3,254	9,777	87,149	17,344	22,574	187,014	42,959	48,588
Medium-Mesic Aspen	22,343	85,005	24,563	35,716	72,832	46,259	45,774	13,993	47,757	46,291
Medium-Mesic Aspen Boreal Mixedwood	122,428	18,381	110,268	105,088	16,568	90,547	88,580	5,002	74,007	72,643
Medium-Mesic Aspen Mix	36,889	10,804	36,085	32,338	6,110	28,613	26,779	522	23,335	21,427
Medium-Mesic Pine	6,493	198	5,564	5,199	54	4,473	3,600	54	3,391	2,441
Medium-Mesic Pine Mix	8,755	12,131	13,397	9,442	17,733	11,063	11,220	216	8,843	9,133
Medium-Mesic White Spruce	9,996	10,886	13,829	9,401	6,528	8,665	8,436	280	6,709	6,465
Non-Analog (Upland to Lowland)		3,251	34	554	1,472	619	658	3,705	1,400	1,520

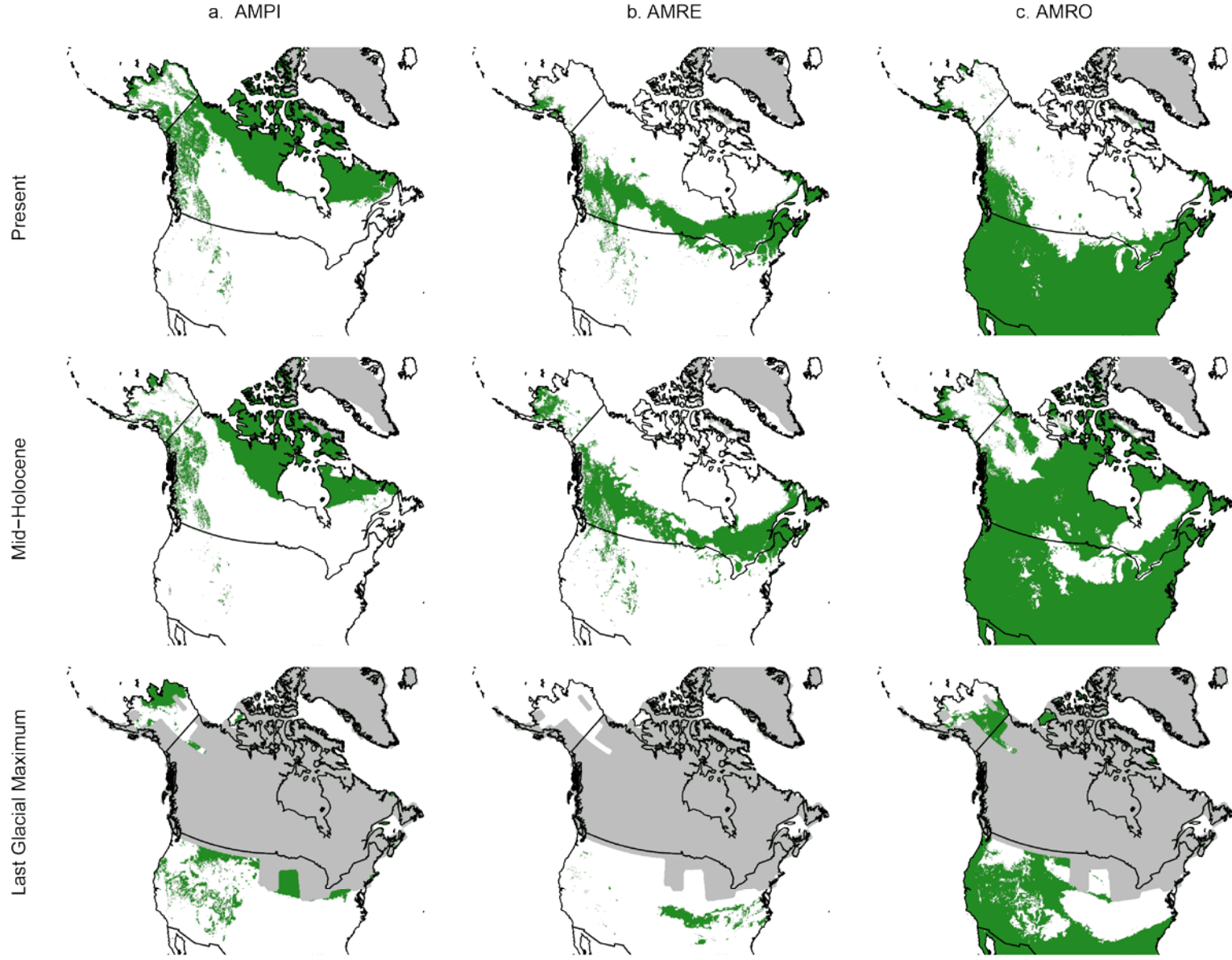
Total 248,360

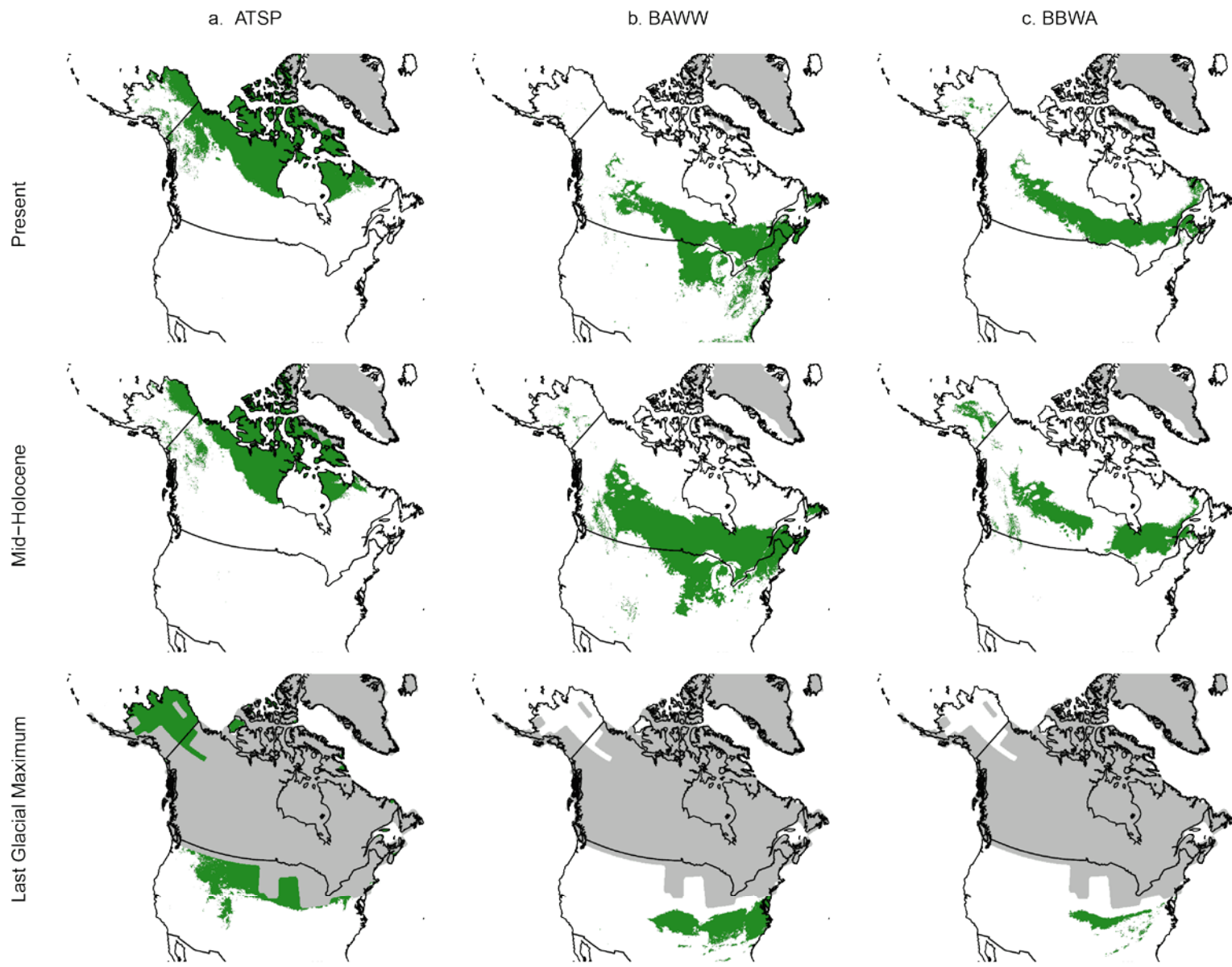
Upland Vegetation Type	Baseline	ECHAM 2030			ECHAM 2060			ECHAM 2090		
		A	B1	B2	A	B1	B2	A	B1	B2
Poor-Xeric Grassland	2	3	2	2	48	8	11	6,329	627	605
Poor-Xeric Jack Pine	15,021	14,978	15,016	15,015	14,520	14,939	14,941	7,761	14,256	14,324
Poor-Mesic Grassland	280	184	267	274	594	353	425	8,026	1,625	1,697
Poor-Mesic Pine	9,298	6,561	8,756	8,728	2,280	7,609	7,549	575	6,702	6,546
Poor-Mesic Black Spruce	15,978	18,732	16,517	16,537	21,729	17,365	17,313	12,731	16,376	16,377
Medium-Xeric Aspen Mix	488	540	490	491	190	453	448	73	410	391
Medium-Xeric Pine	123	51	115	114	19	103	98	22	97	91
Medium-Xeric Spruce	212	91	205	200	54	196	169	4	173	144
Medium-Mesic Grassland	57	13,516	1,777	2,461	85,093	12,579	16,869	187,747	31,683	36,338
Medium-Mesic Aspen	22,343	58,667	27,696	27,988	77,418	40,746	41,093	12,442	41,967	40,667
Medium-Mesic Aspen Boreal Mixedwood	122,428	81,465	117,002	116,448	23,826	99,875	98,807	5,782	87,056	86,616
Medium-Mesic Aspen Mix	36,889	35,318	36,551	36,283	6,831	31,726	29,651	488	27,415	25,894
Medium-Mesic Pine	6,493	2,396	5,847	5,726	58	4,713	3,734	54	4,016	2,931
Medium-Mesic Pine Mix	8,755	6,334	8,470	8,370	10,343	9,118	9,043	229	7,971	7,841
Medium-Mesic White Spruce	9,996	9,264	9,616	9,684	3,399	8,205	7,765	256	6,860	6,683
Non-Analog (Upland to Lowland)		260	33	39	1,959	372	444	5,843	1,126	1,216
Total	248,360									

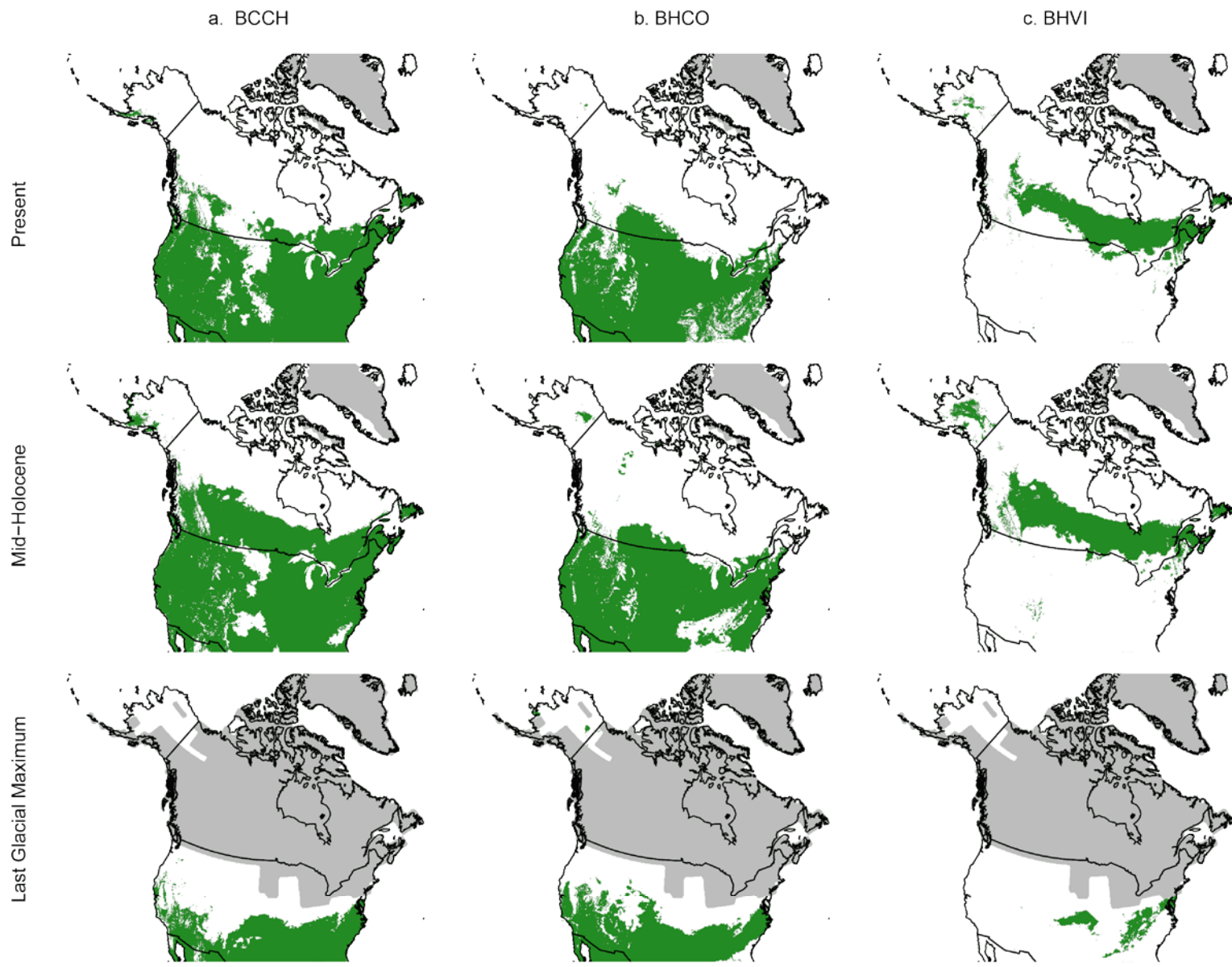
Appendix 4-A. Projected current and paleo-historical core area distributions based on the CCM1 global climate model.

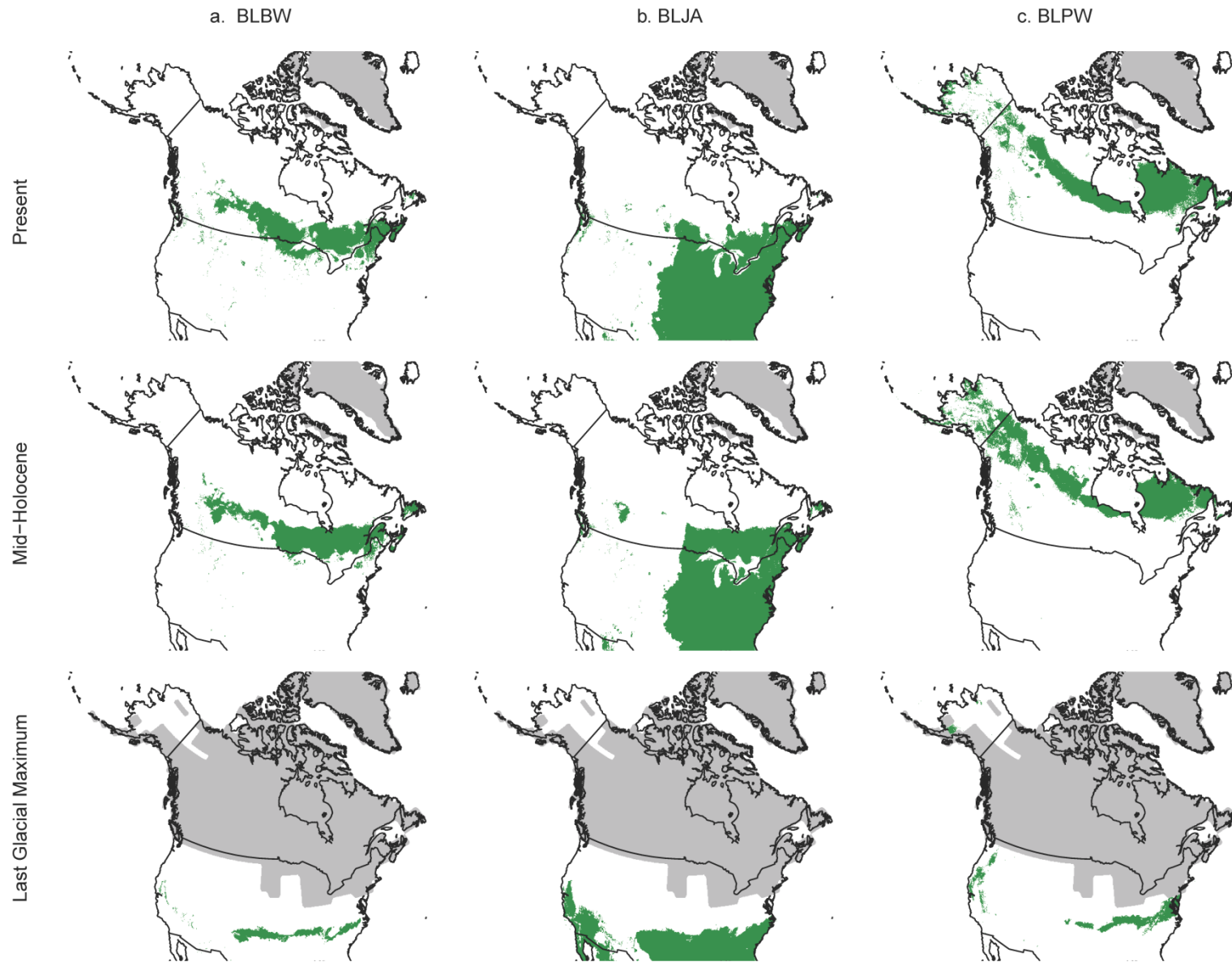
Present = 1961-1990; Mid-Holocene = 6,000 YBP; Last Glacial Maximum = 21,000 YBP. Core habitat was defined as areas where the species' predicted density exceeded its mean baseline predicted density within the boreal and sub-boreal model-building area. See Appendix 4-E for species code definitions.

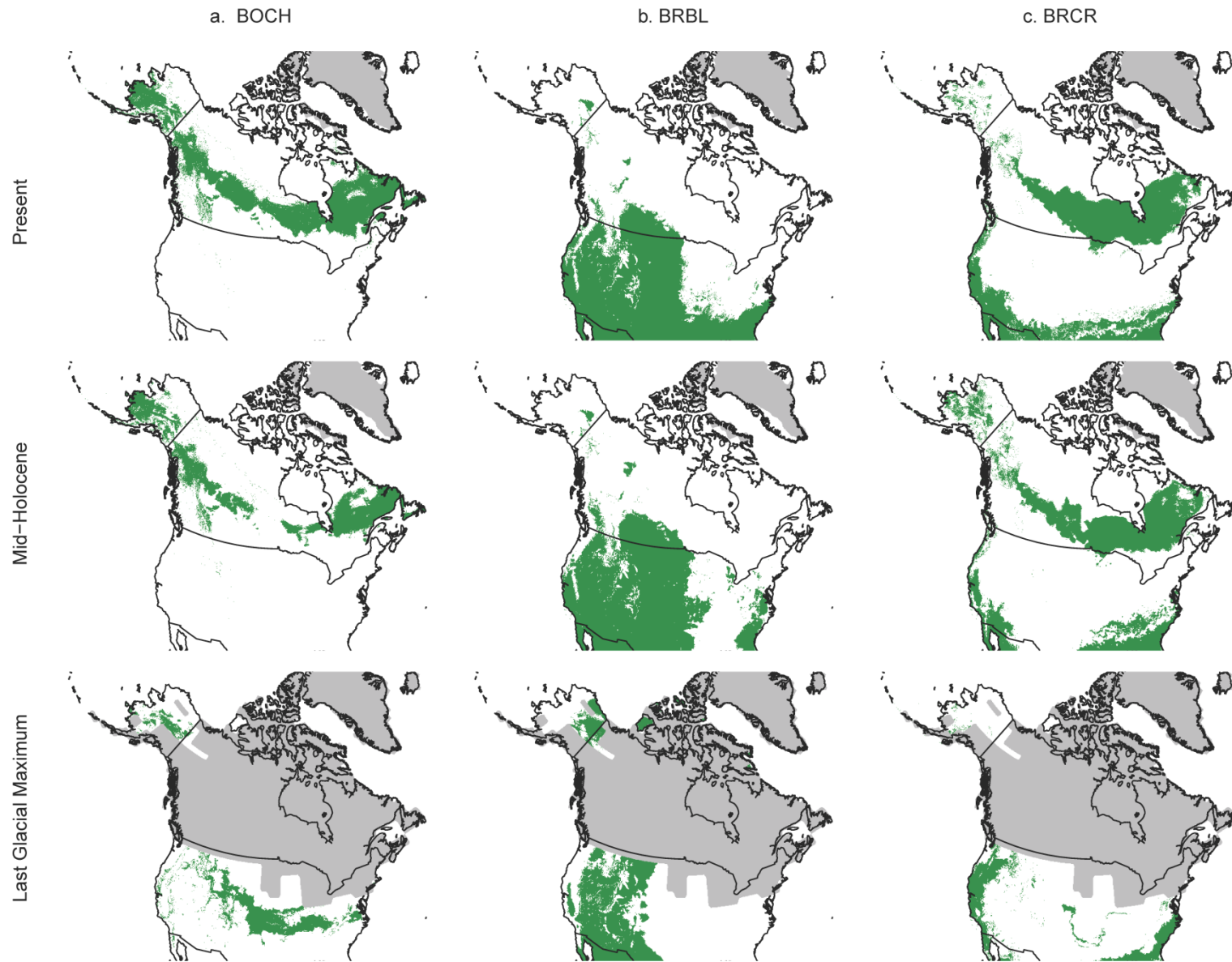


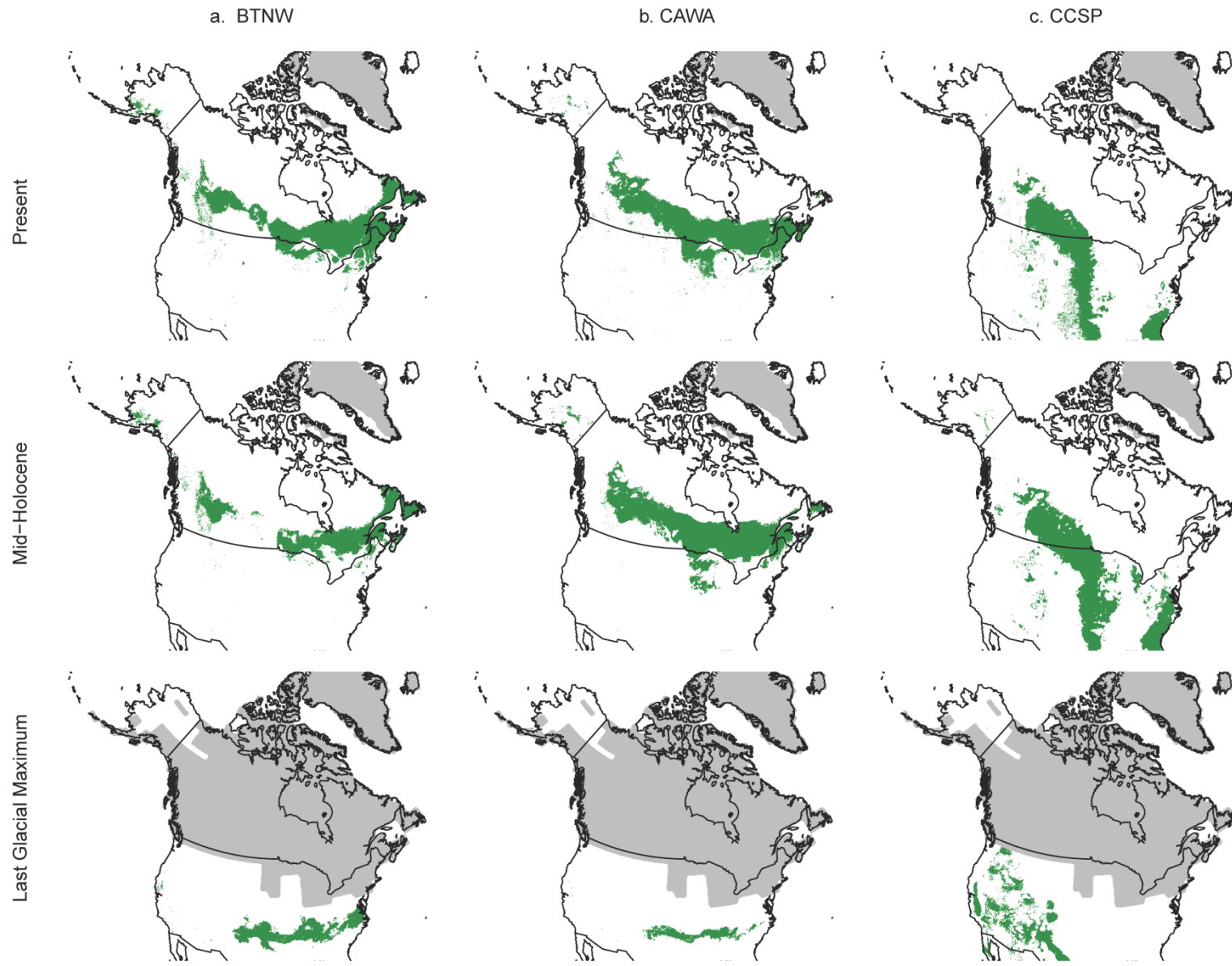


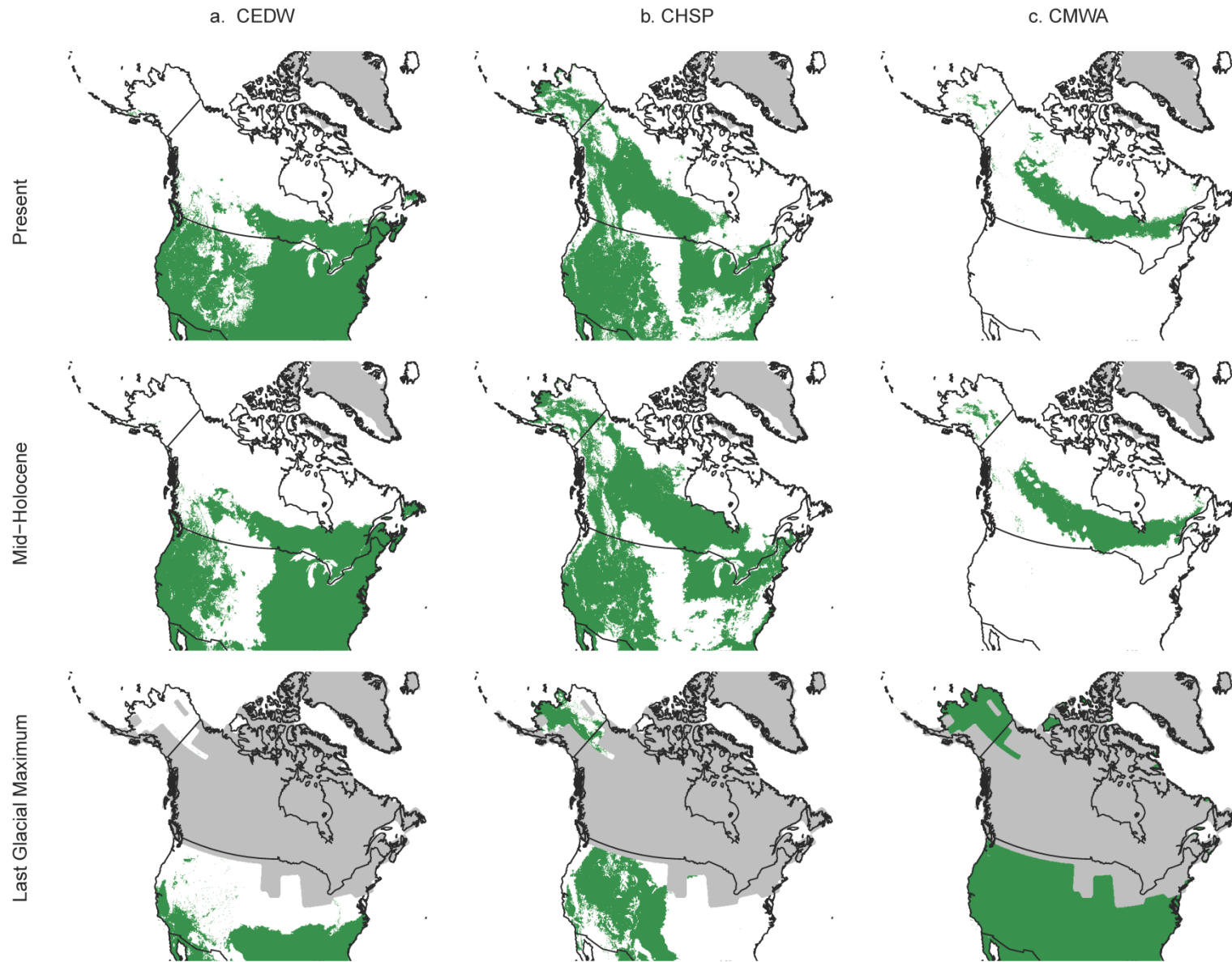


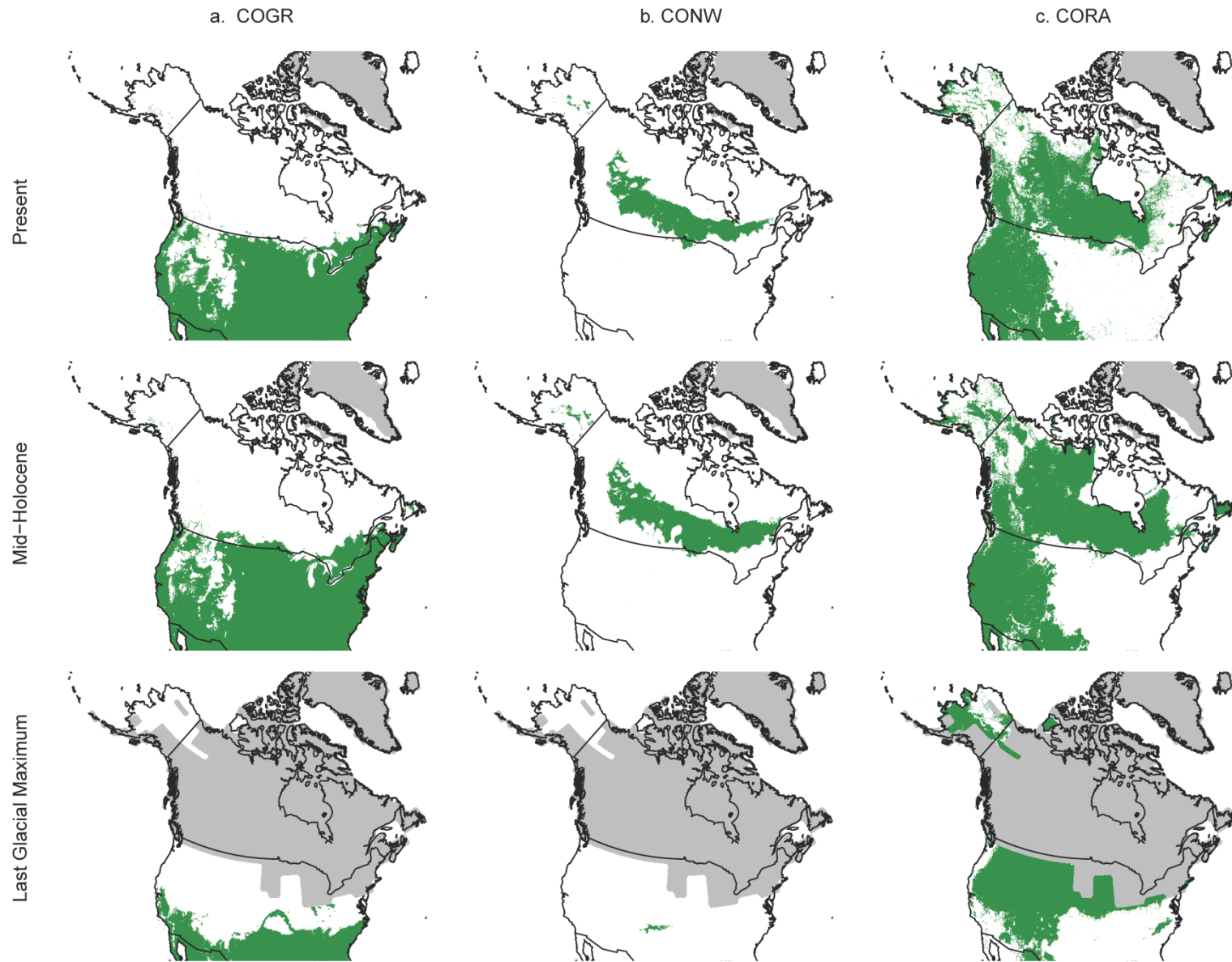


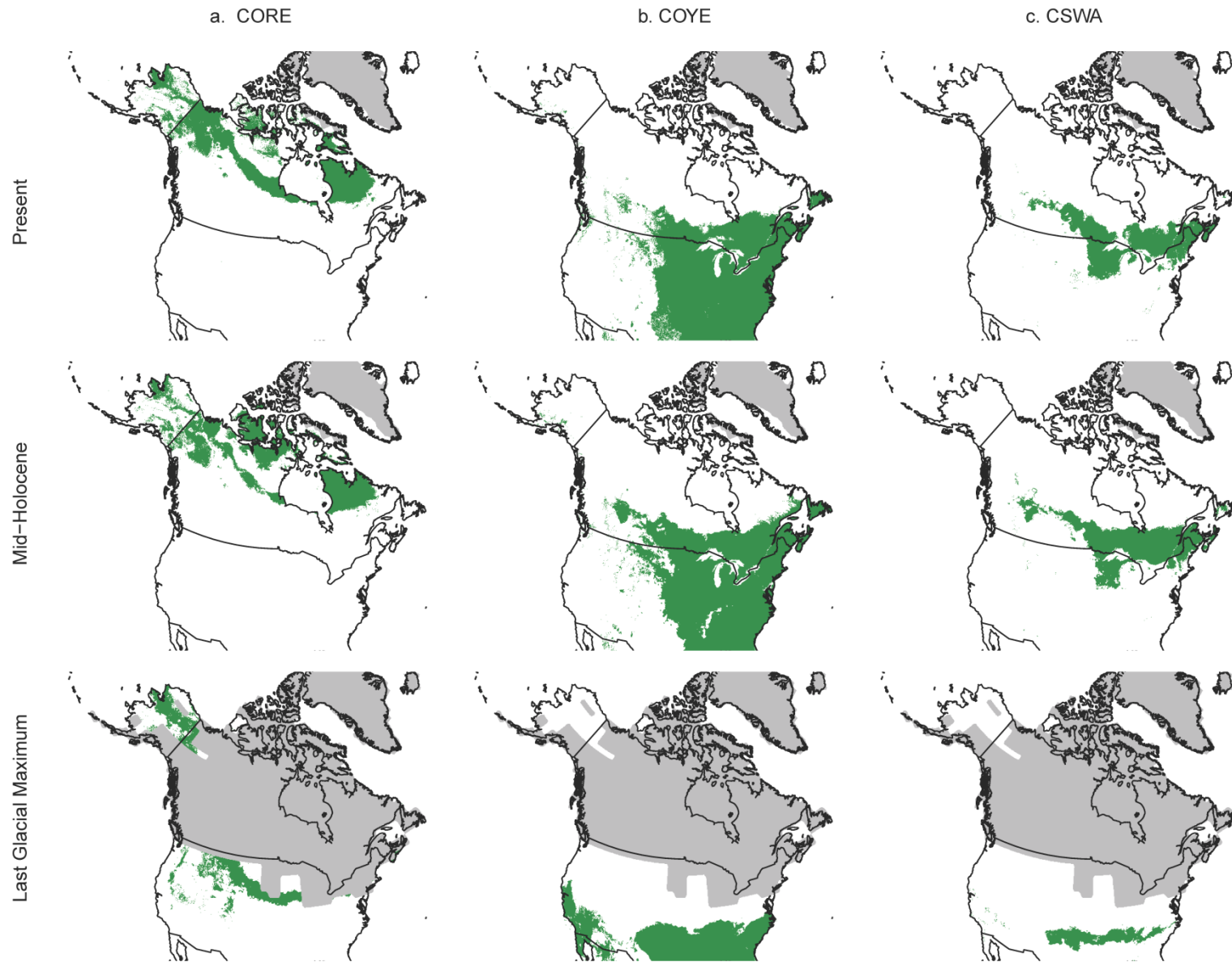


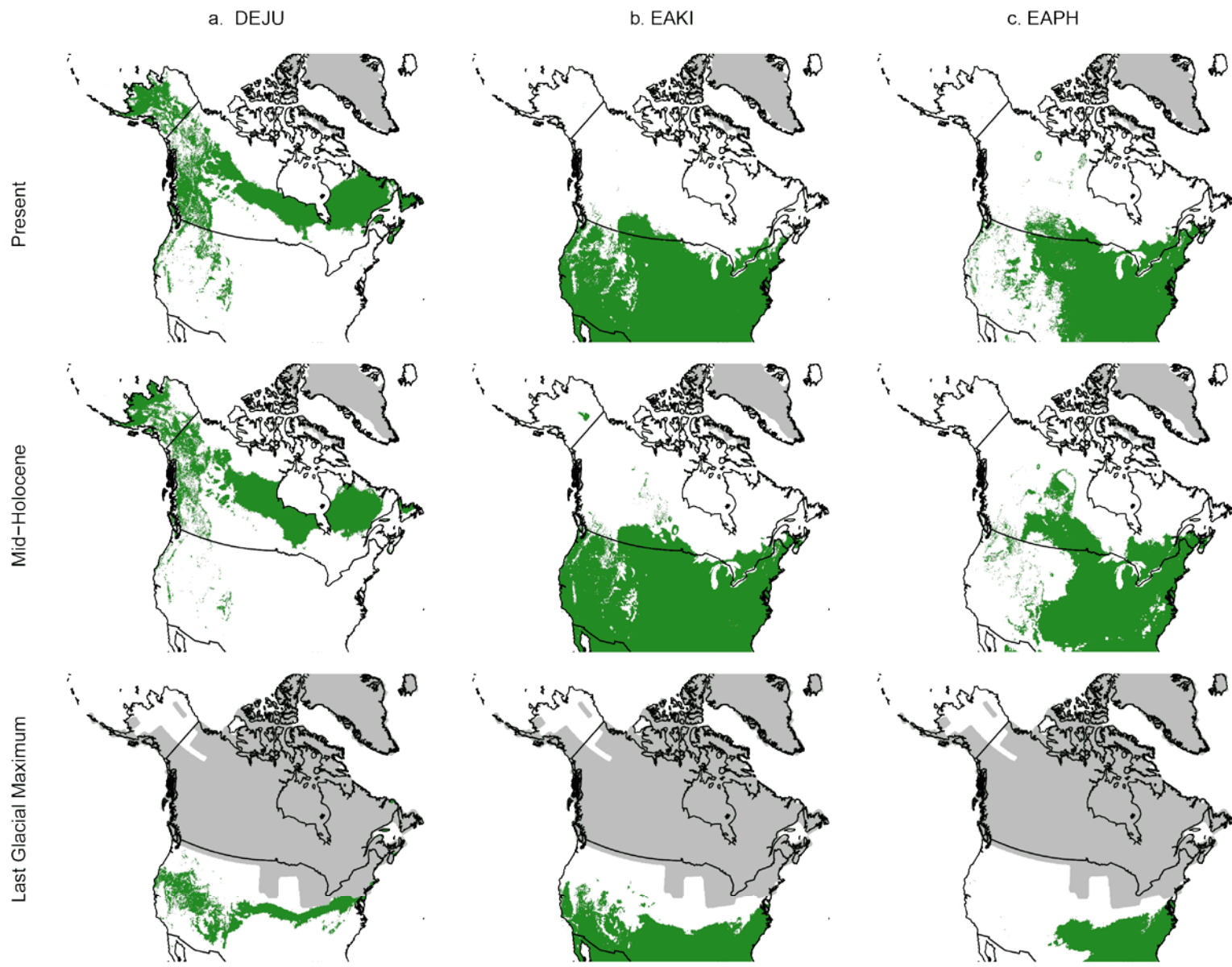


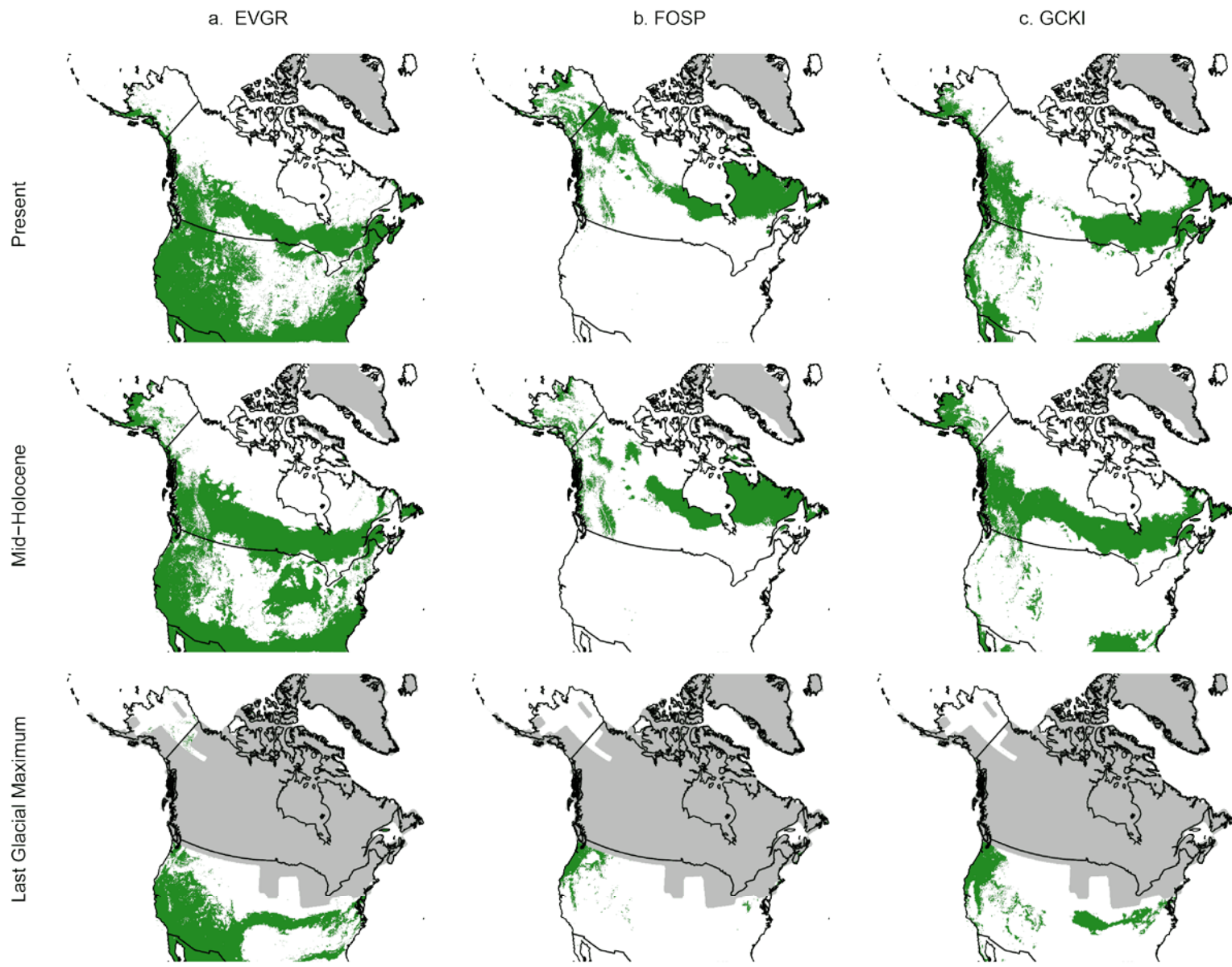


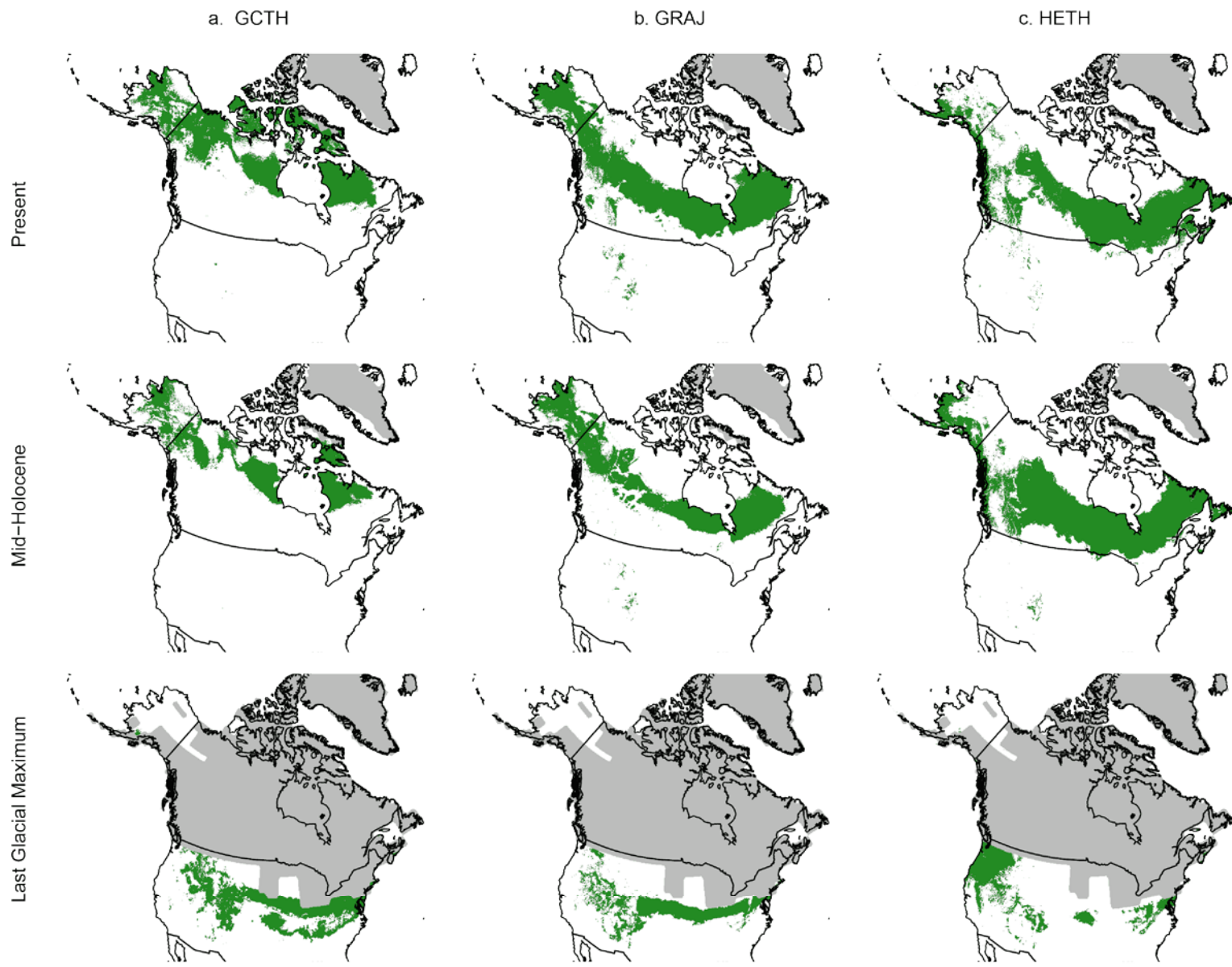


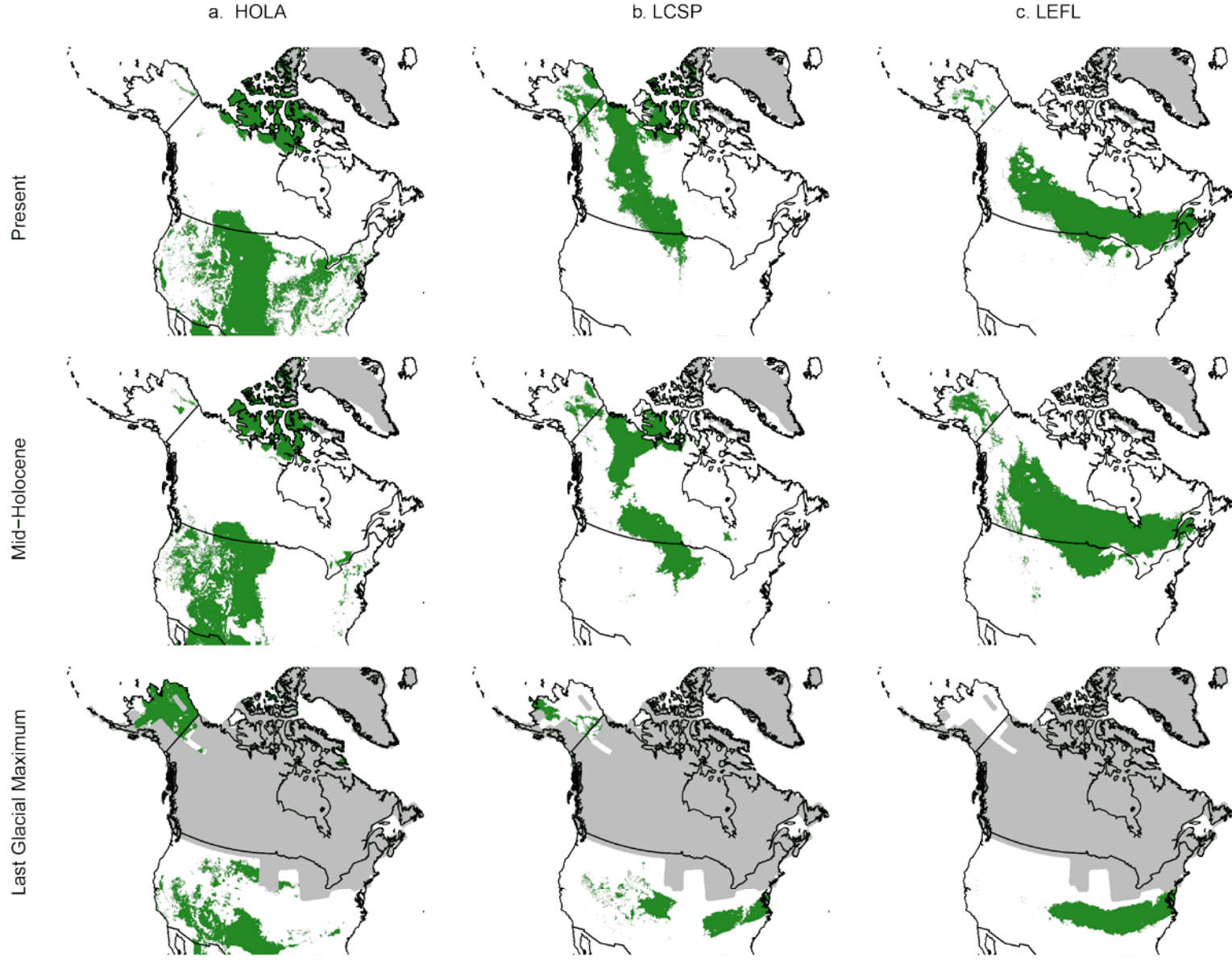


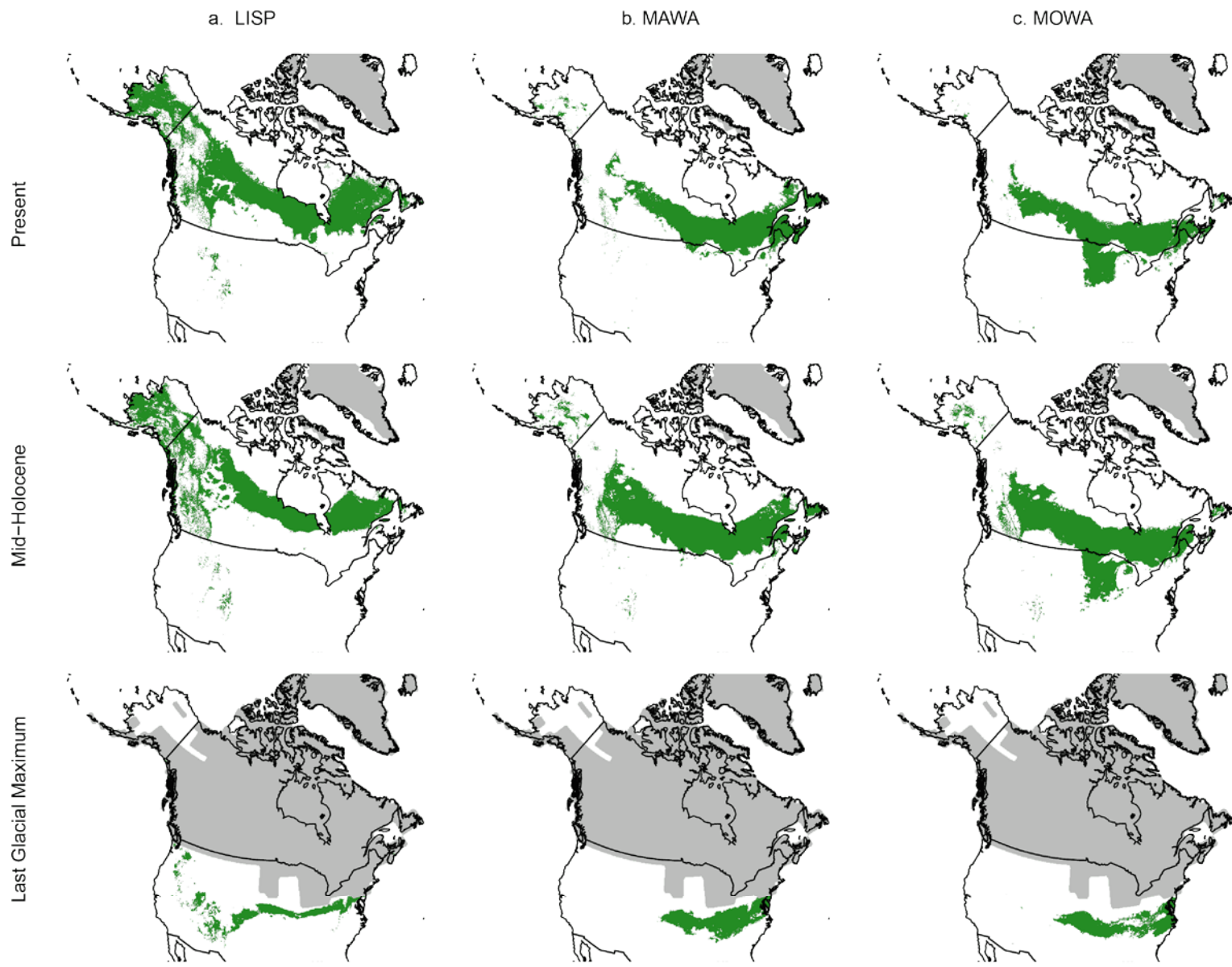


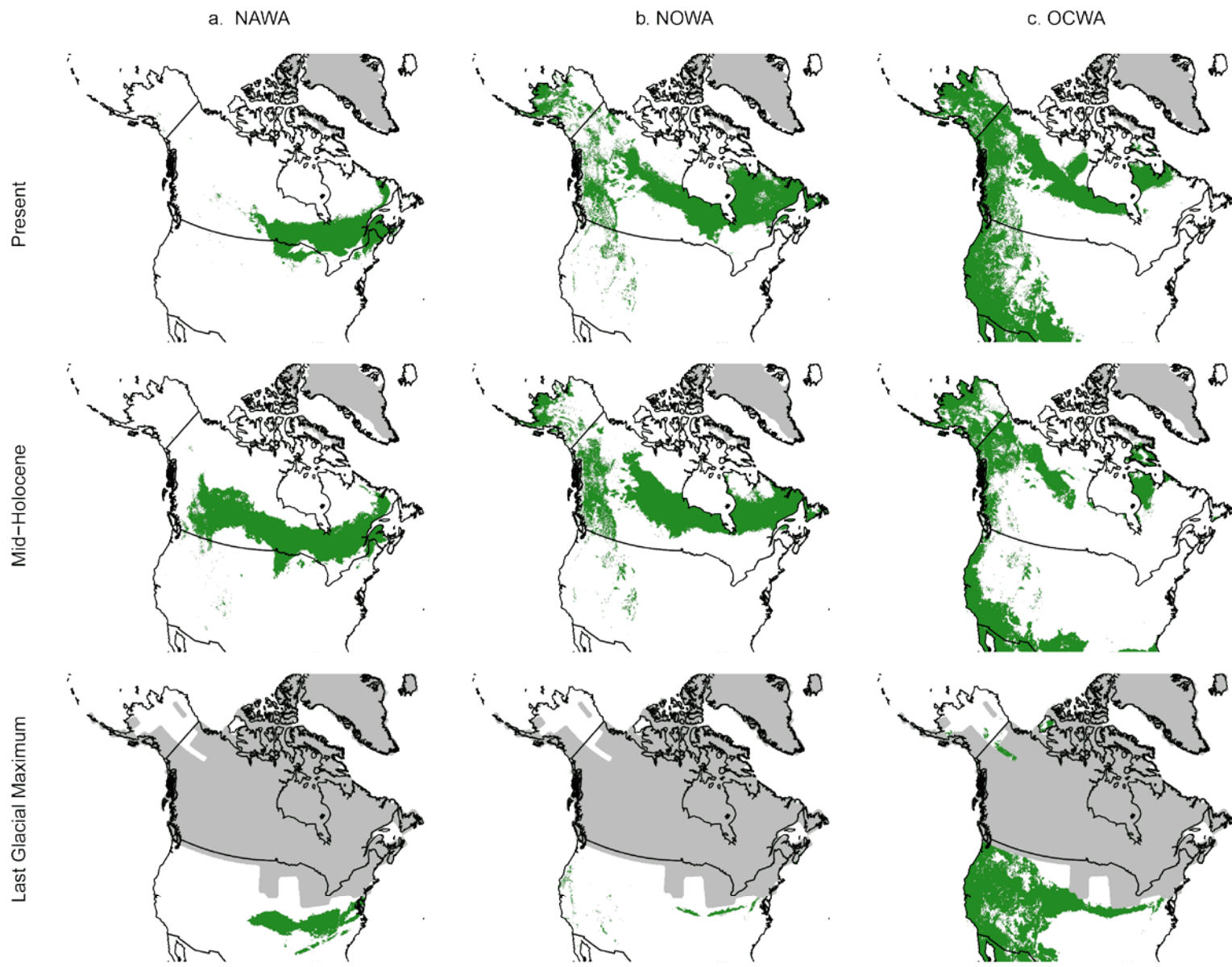


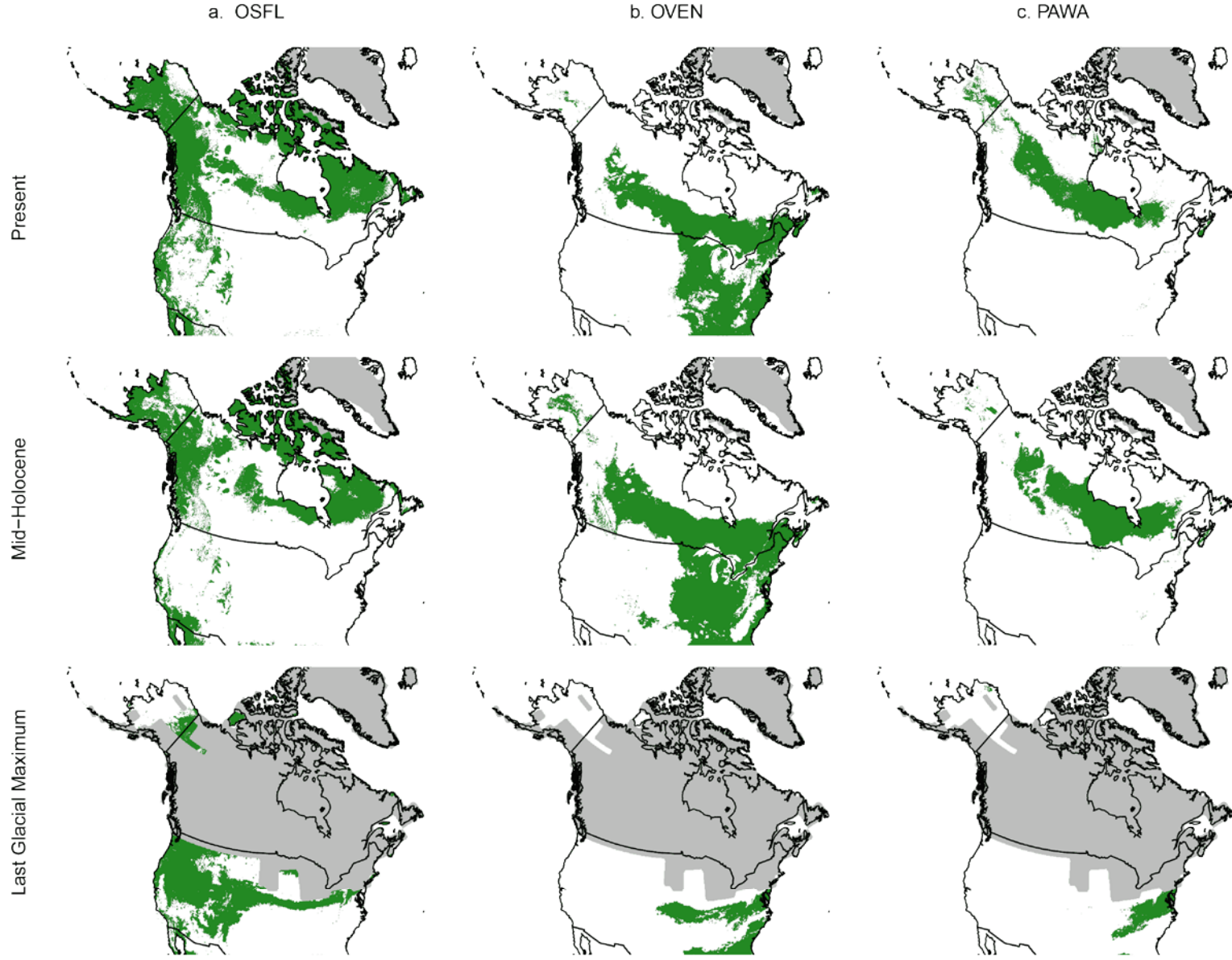


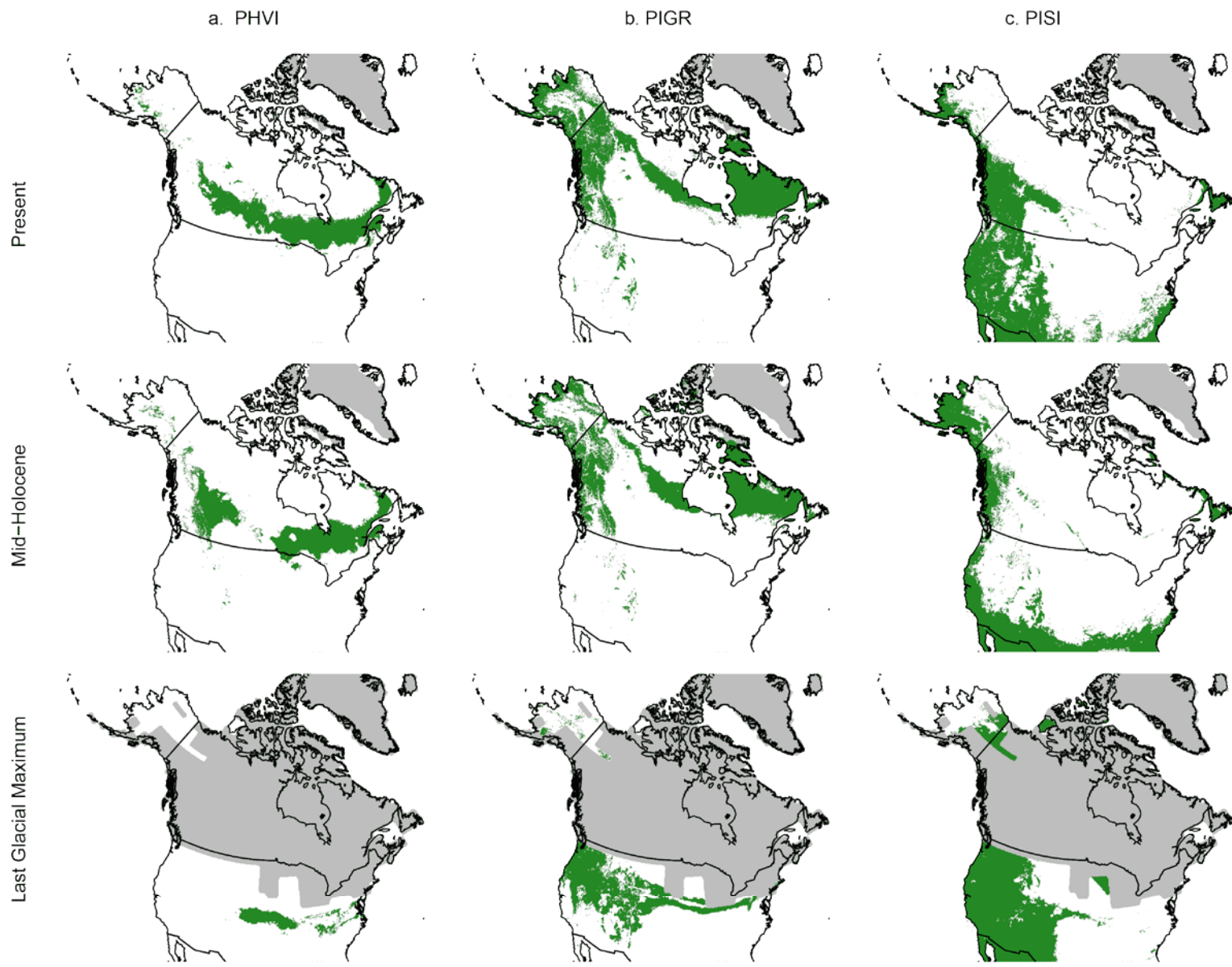


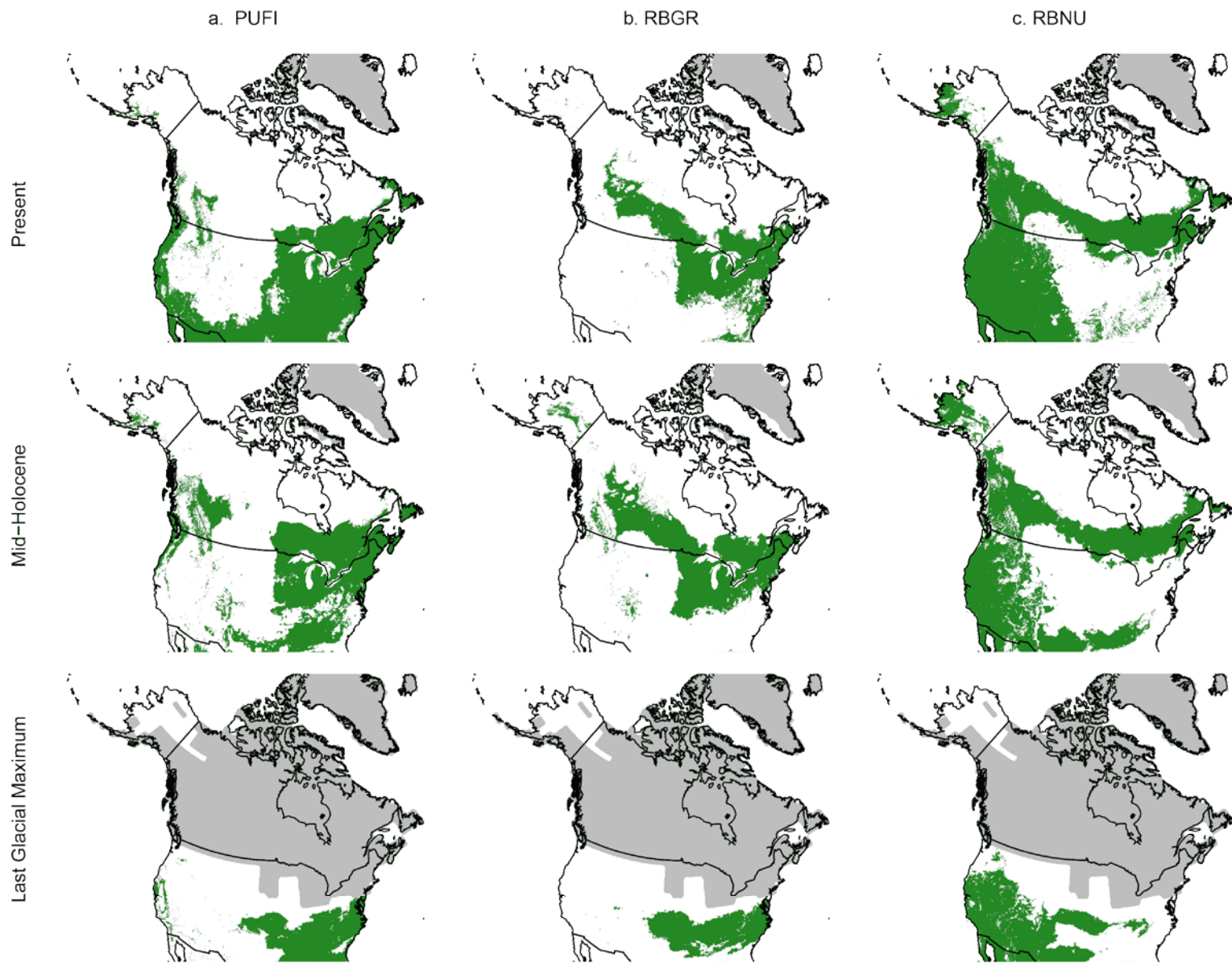


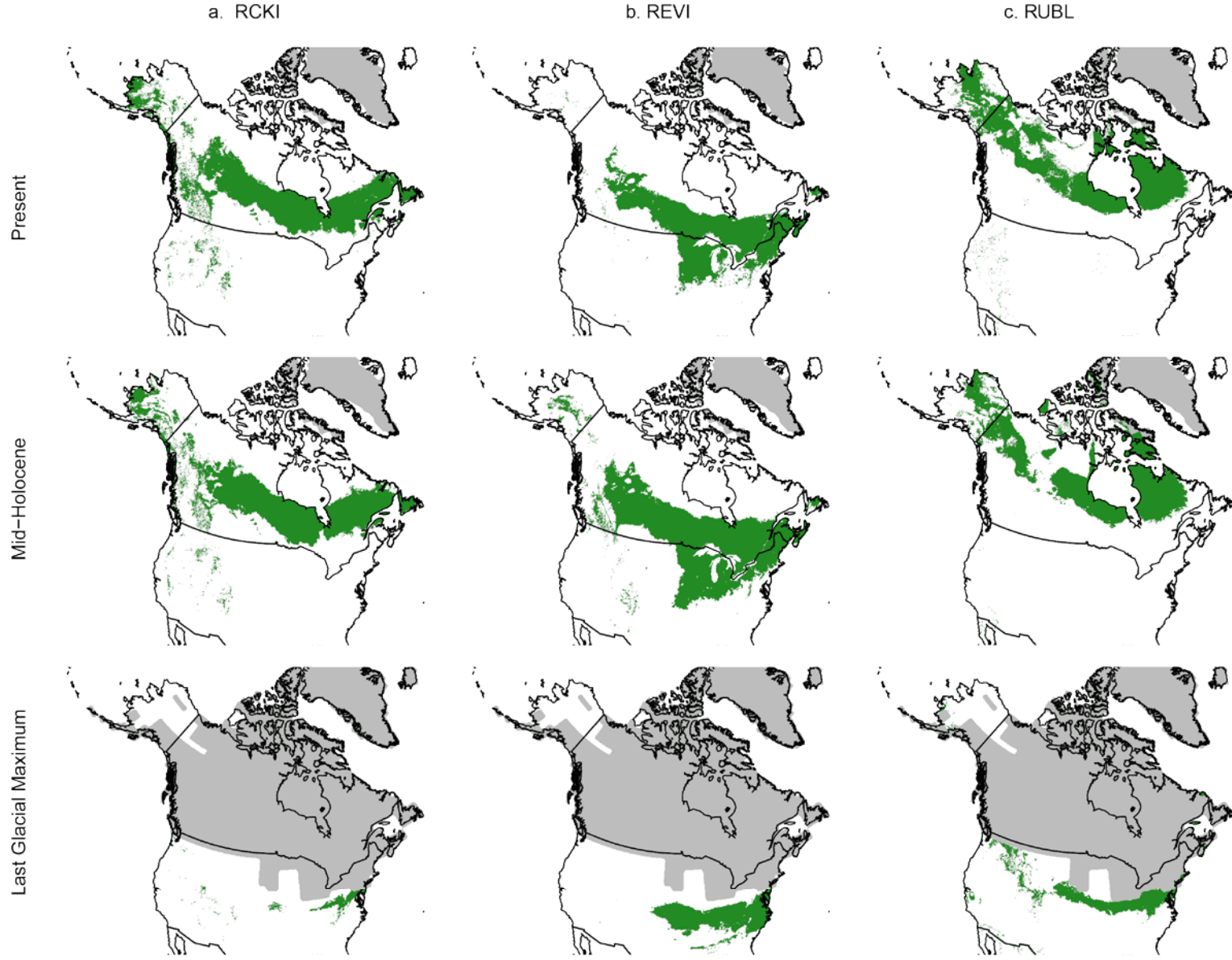


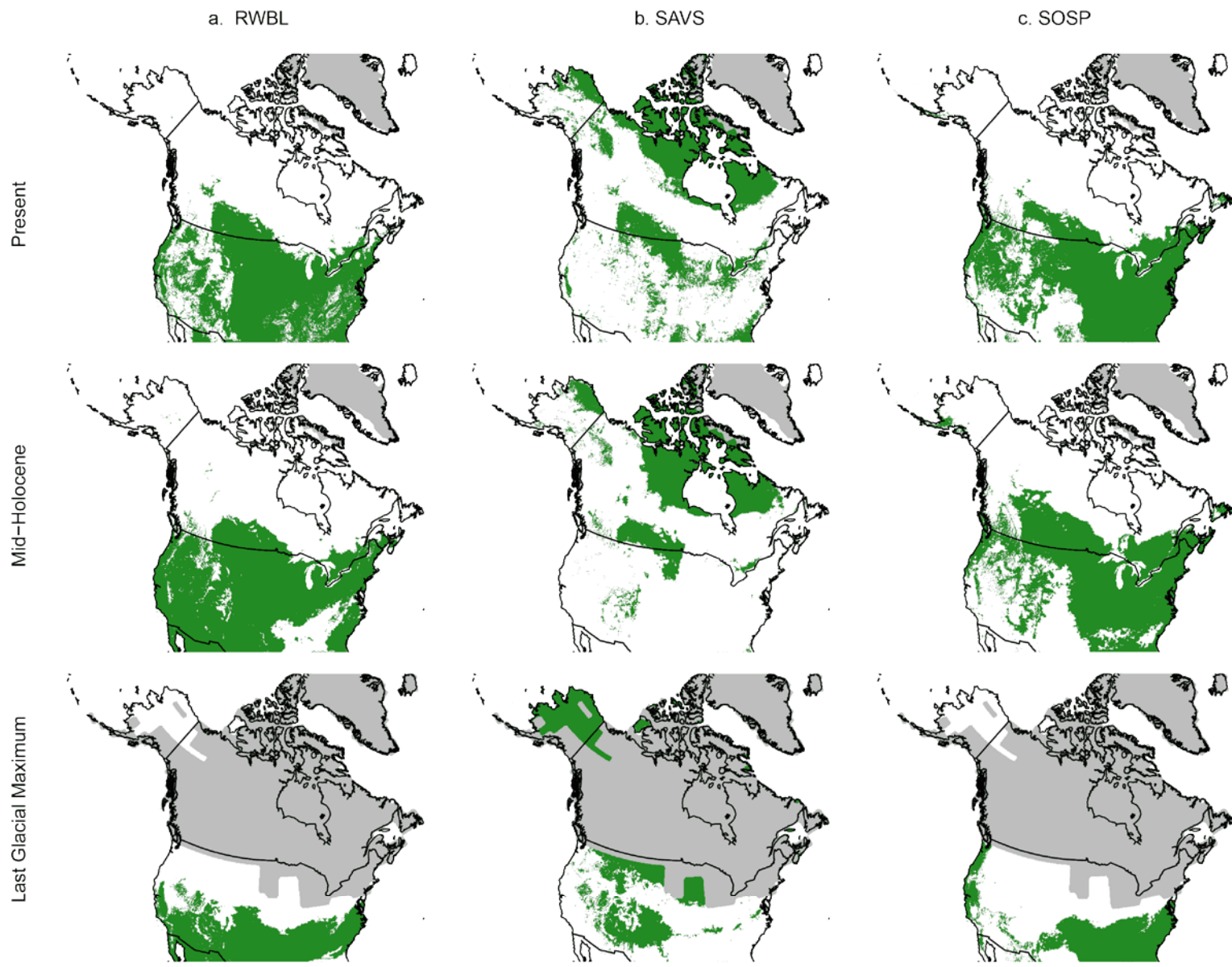


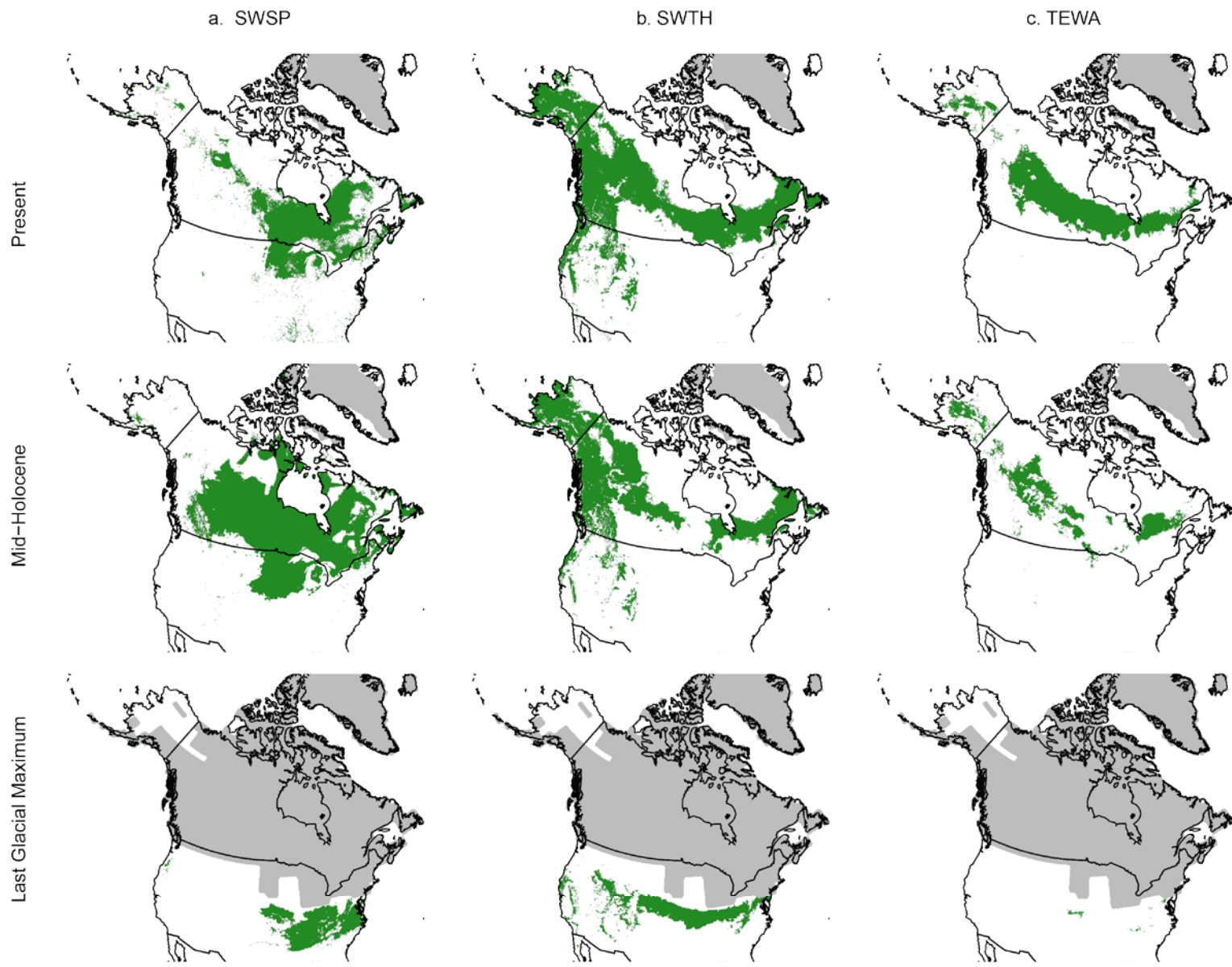


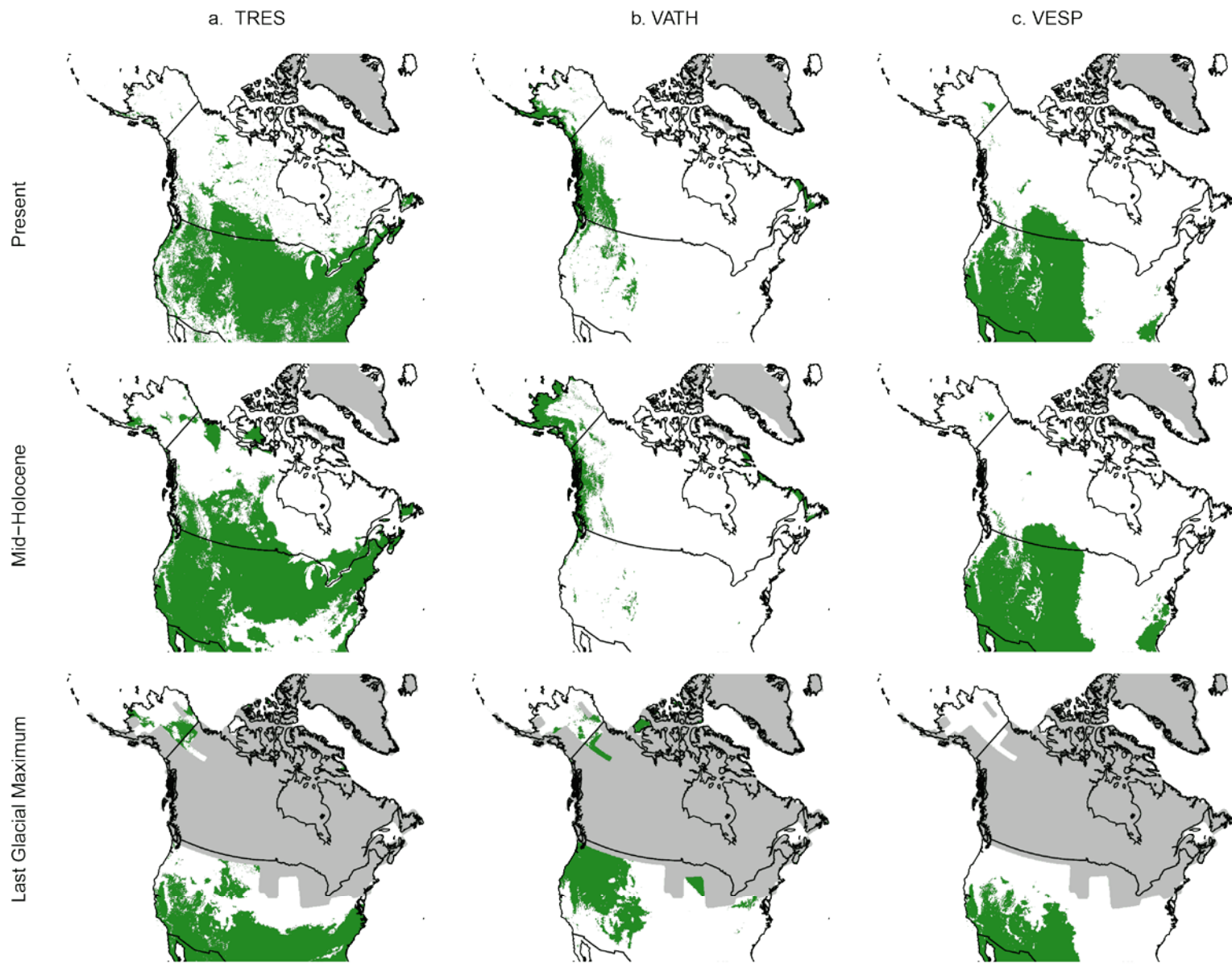


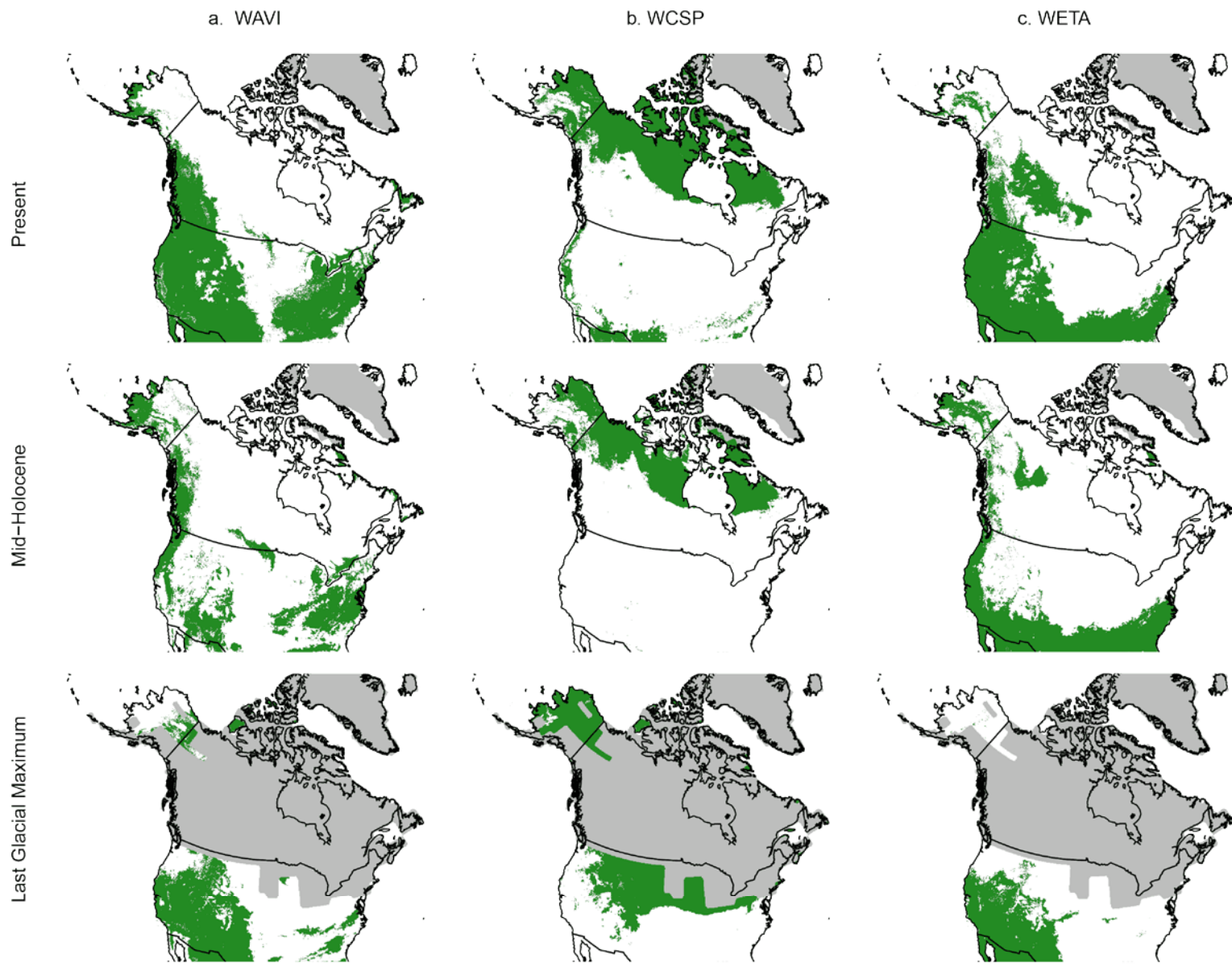


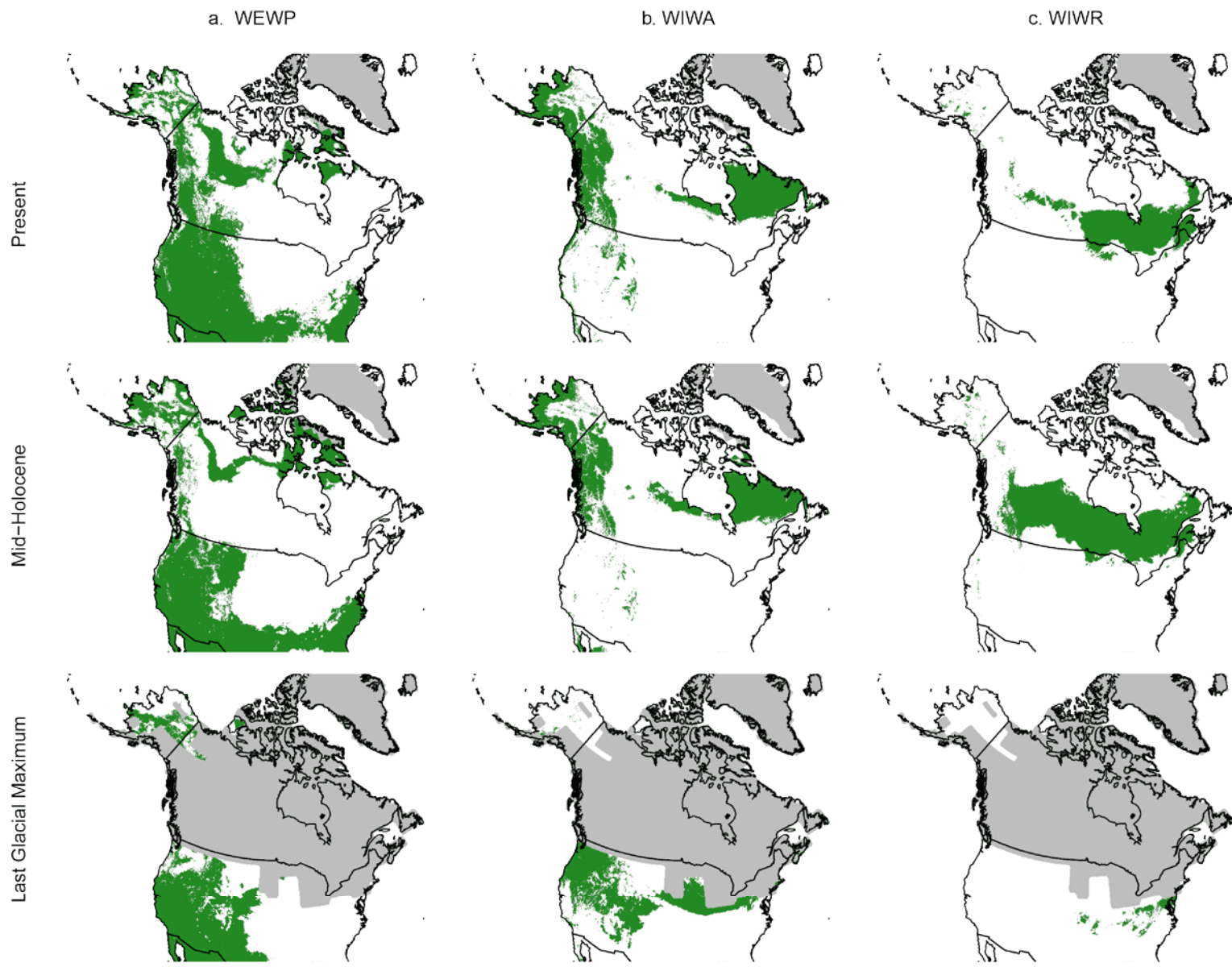


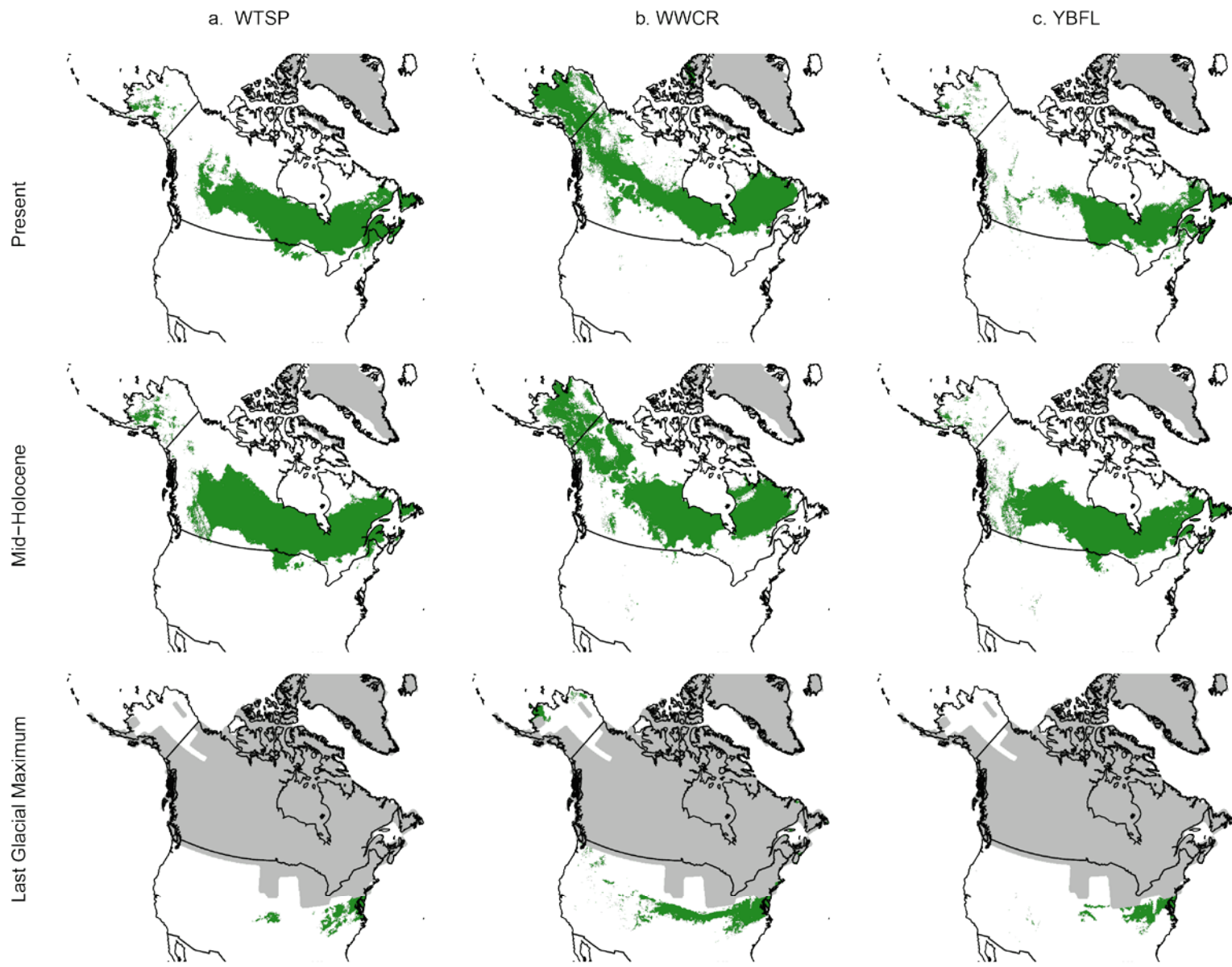


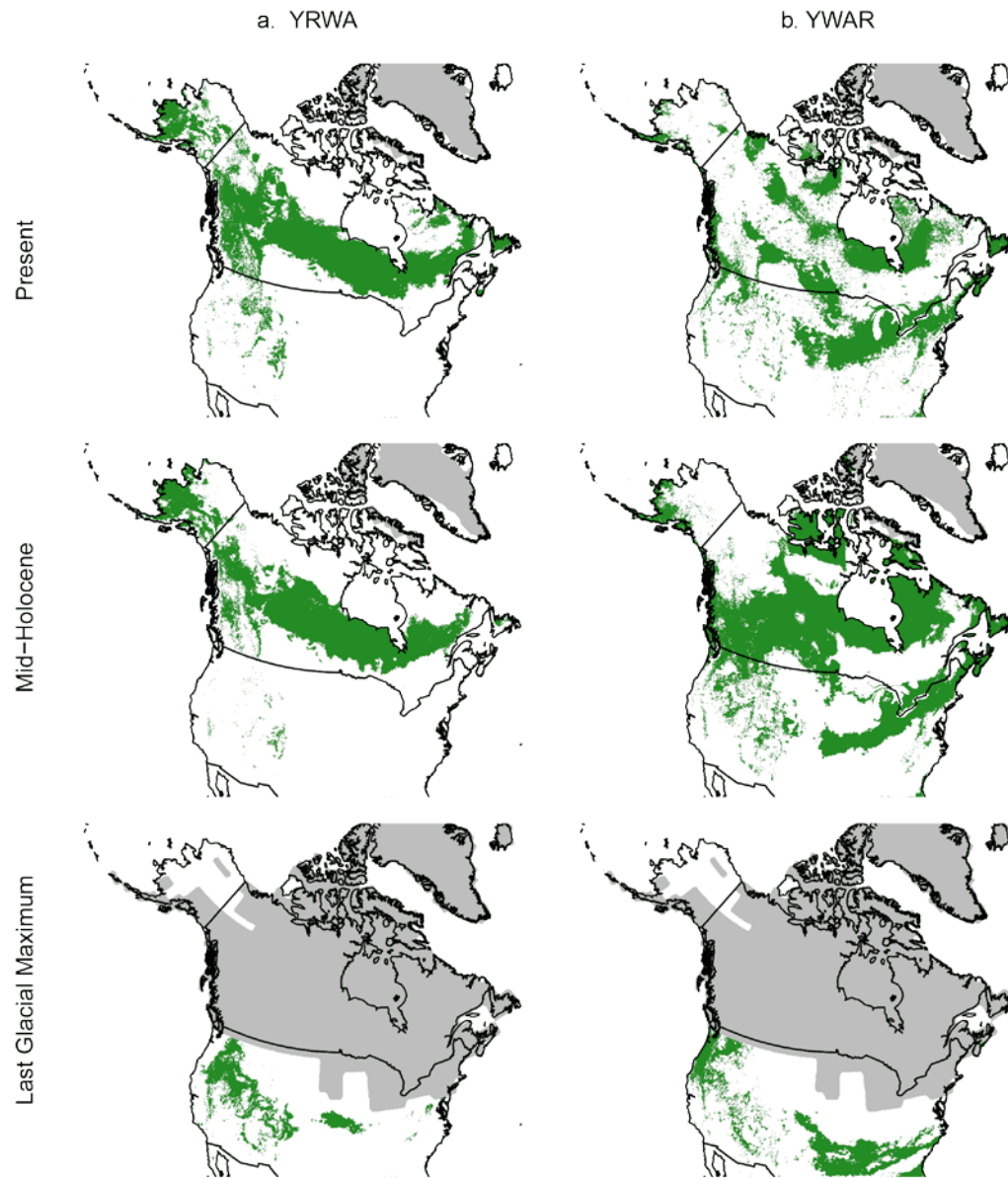






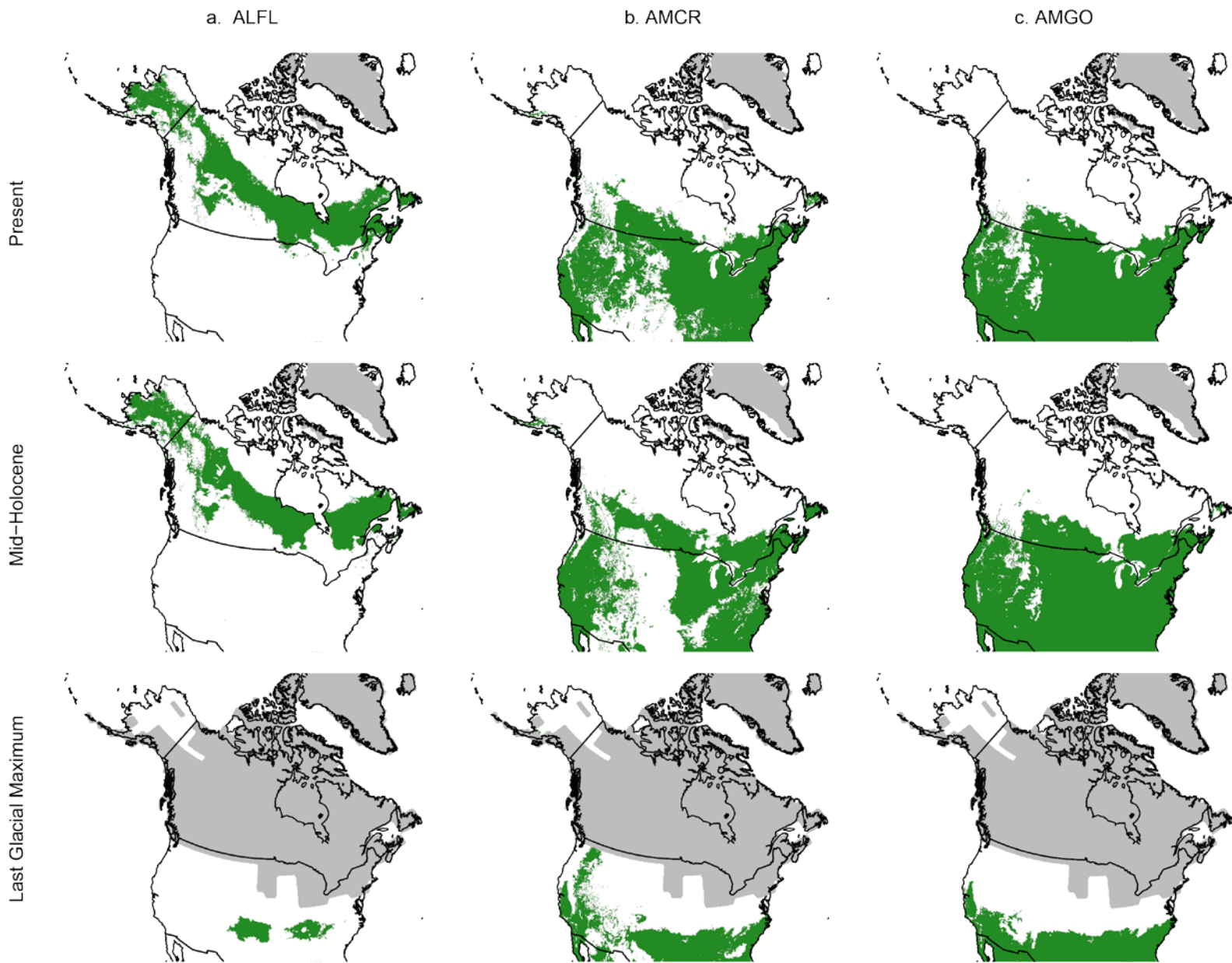


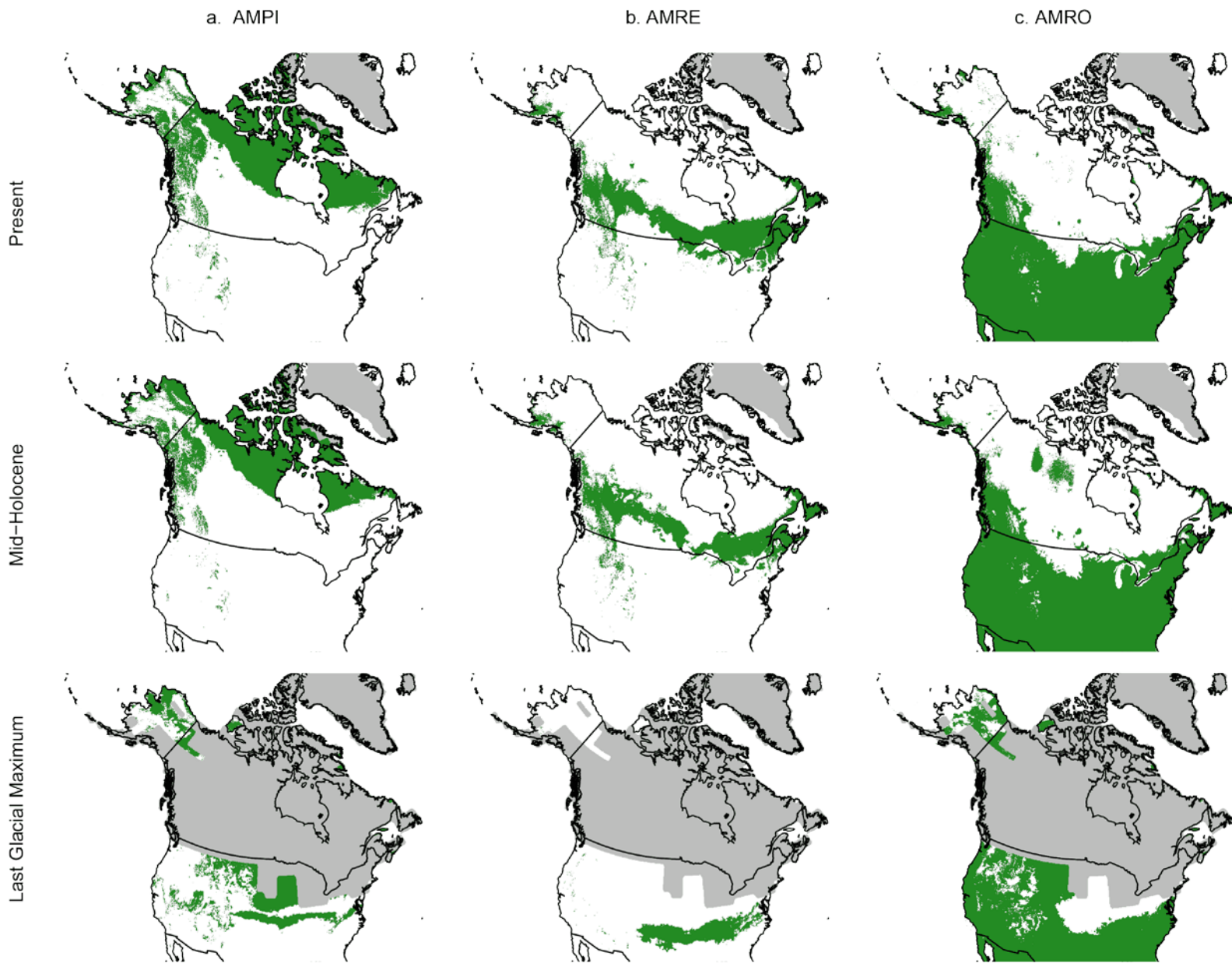


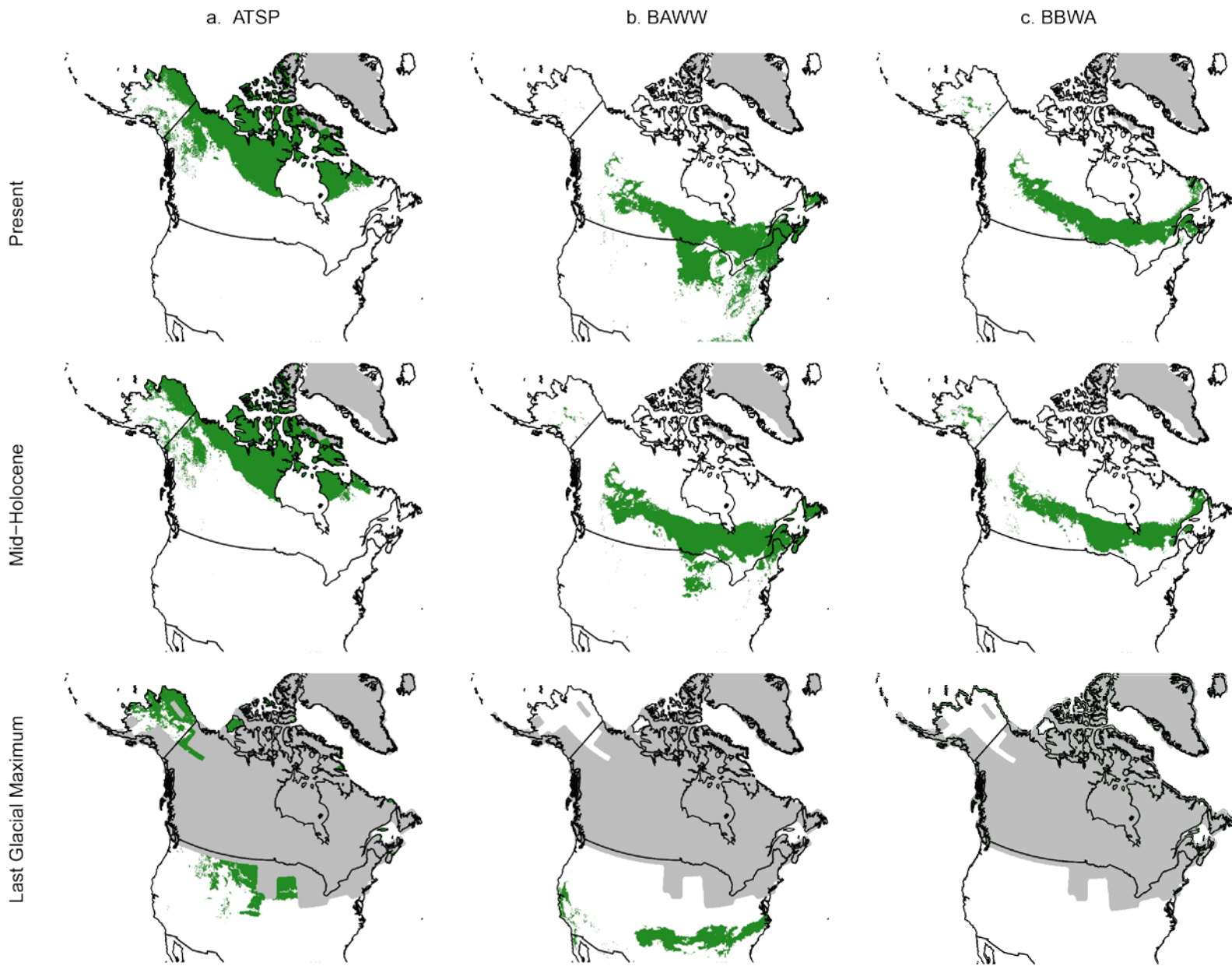


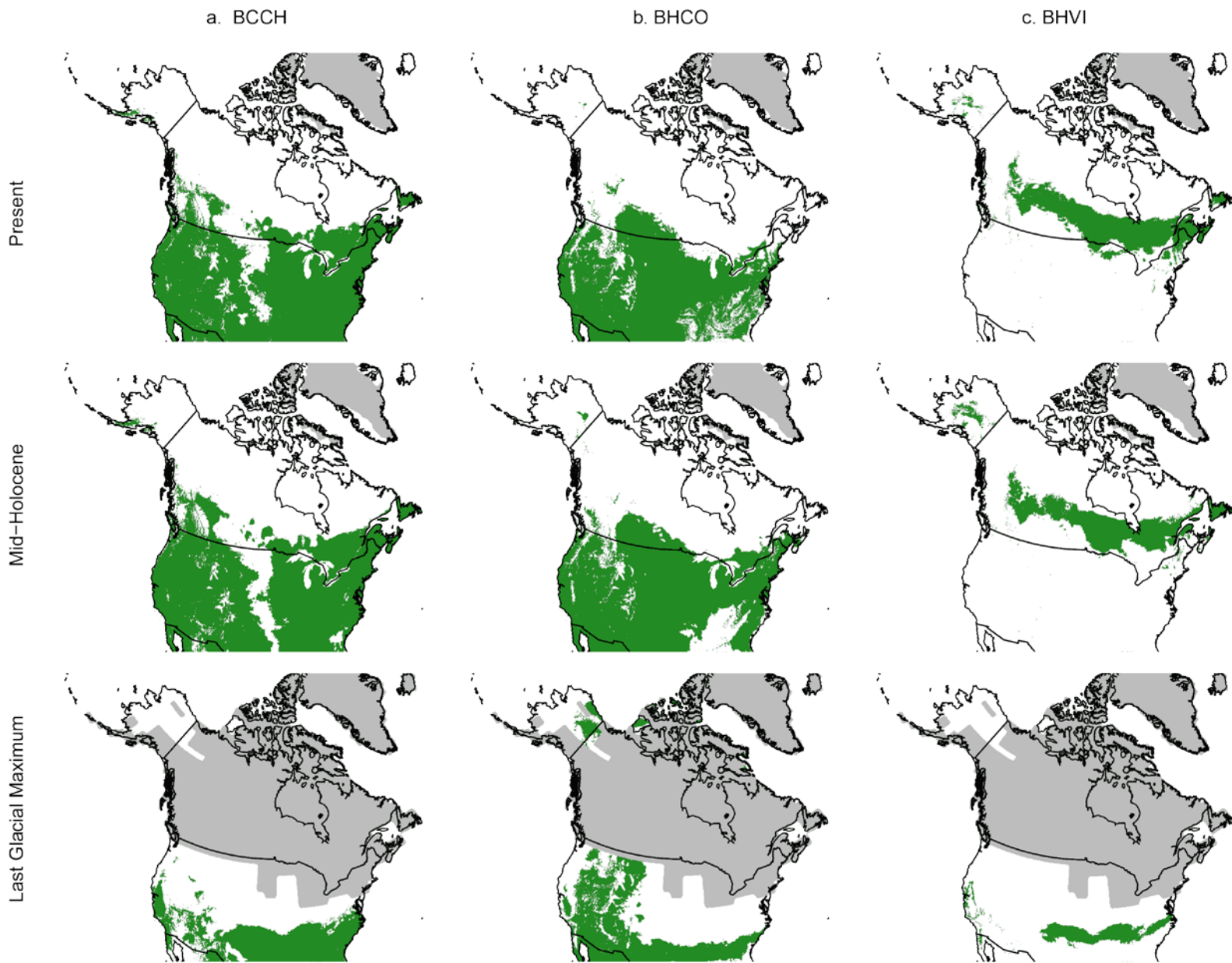
Appendix 4-B. Projected current and paleo-historical core area distributions based on the GFDL global climate model.

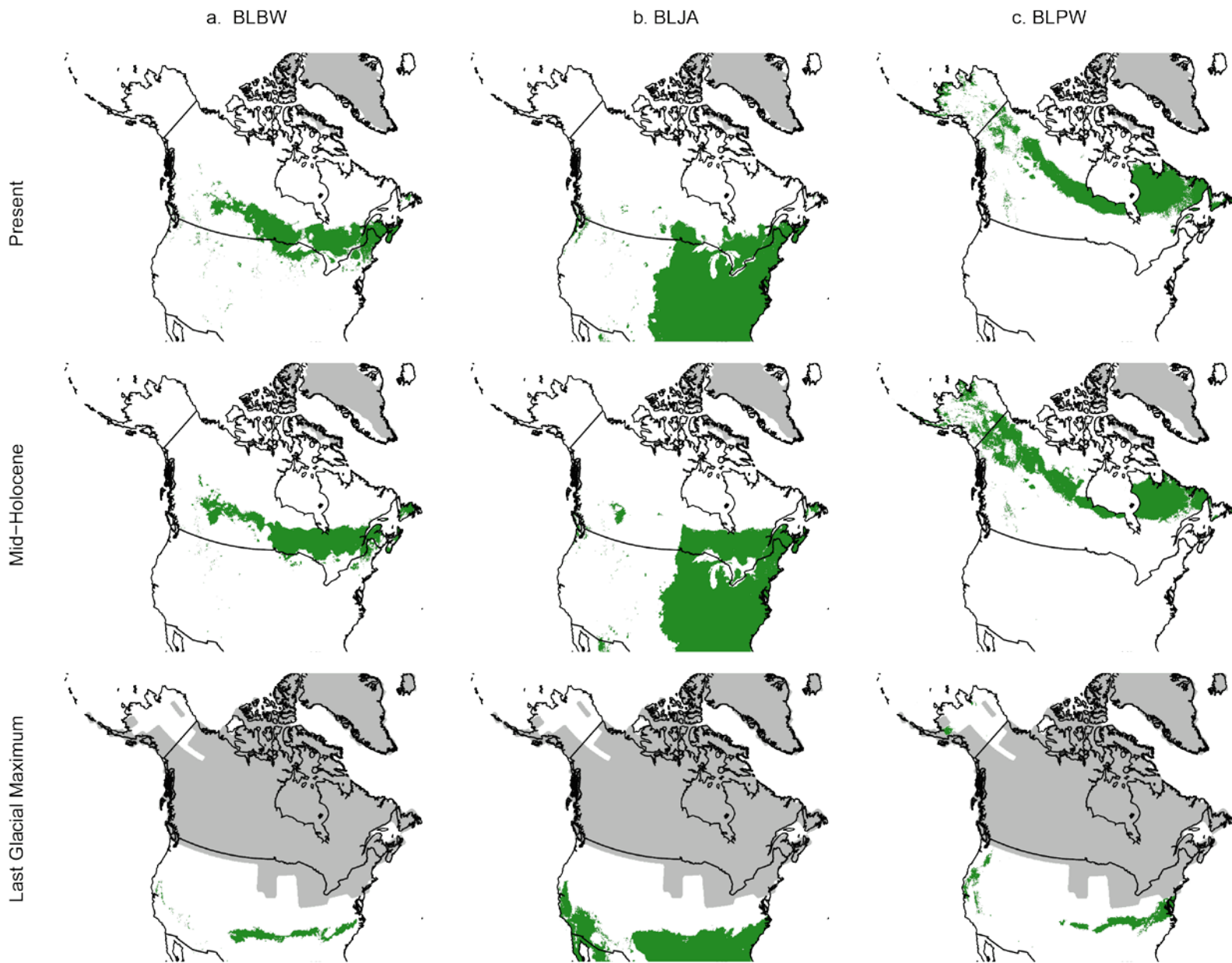
Present = 1961-1990; Mid-Holocene = 6,000 YBP; Last Glacial Maximum = 21,000 YBP. Core habitat was defined as areas where the species' predicted density exceeded its mean baseline predicted density within the boreal and sub-boreal model-building area. See Appendix 4-E for species code definitions.

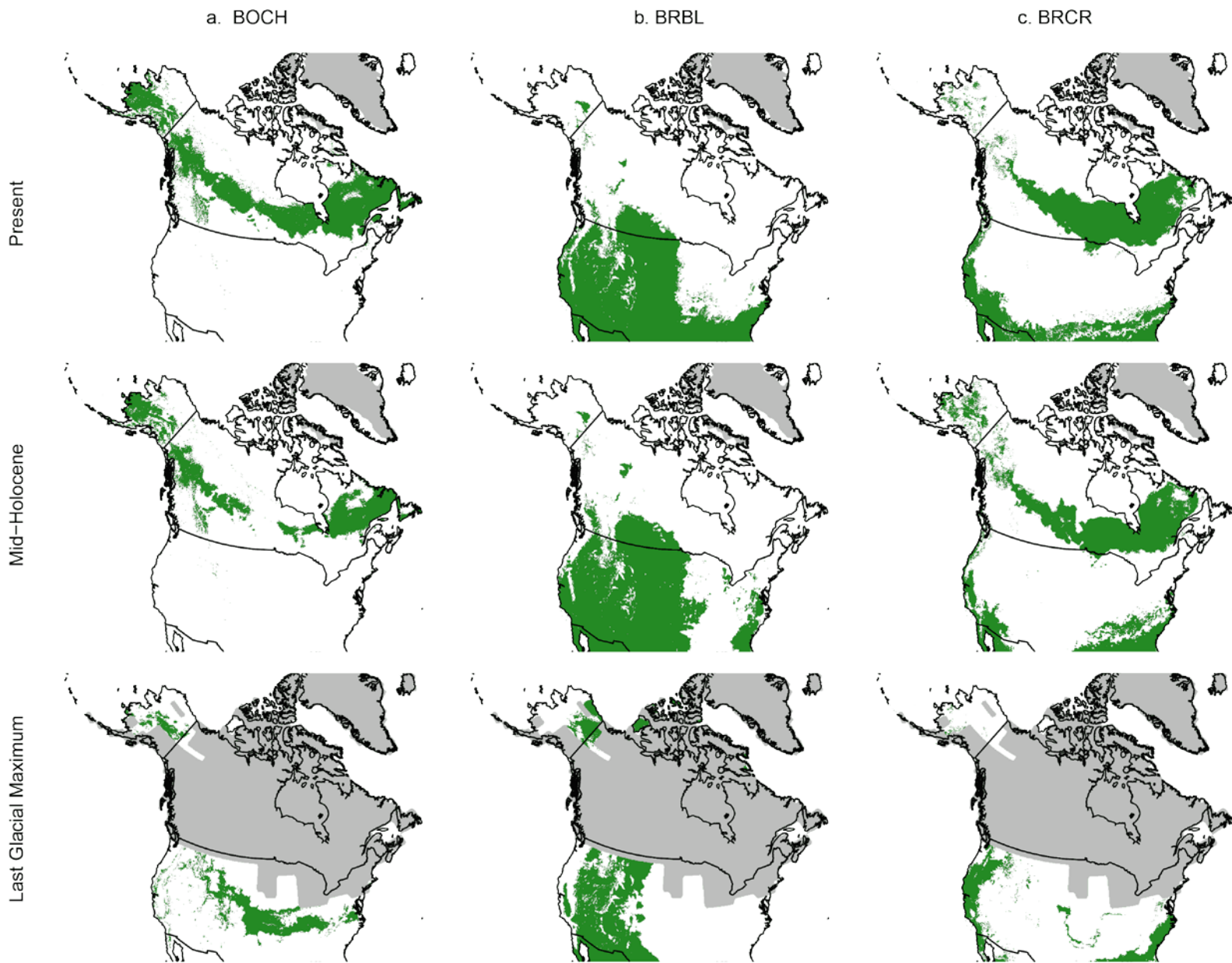


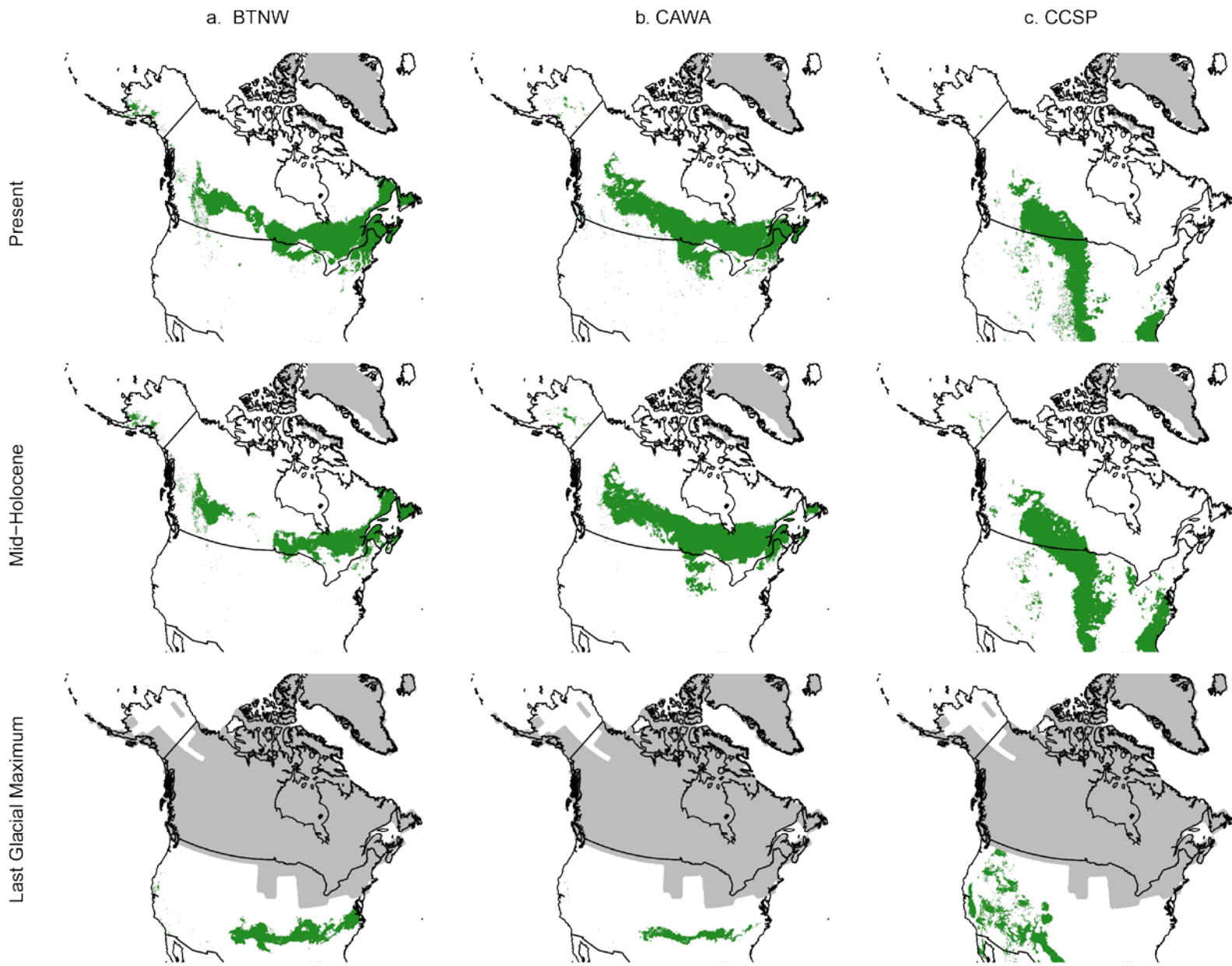


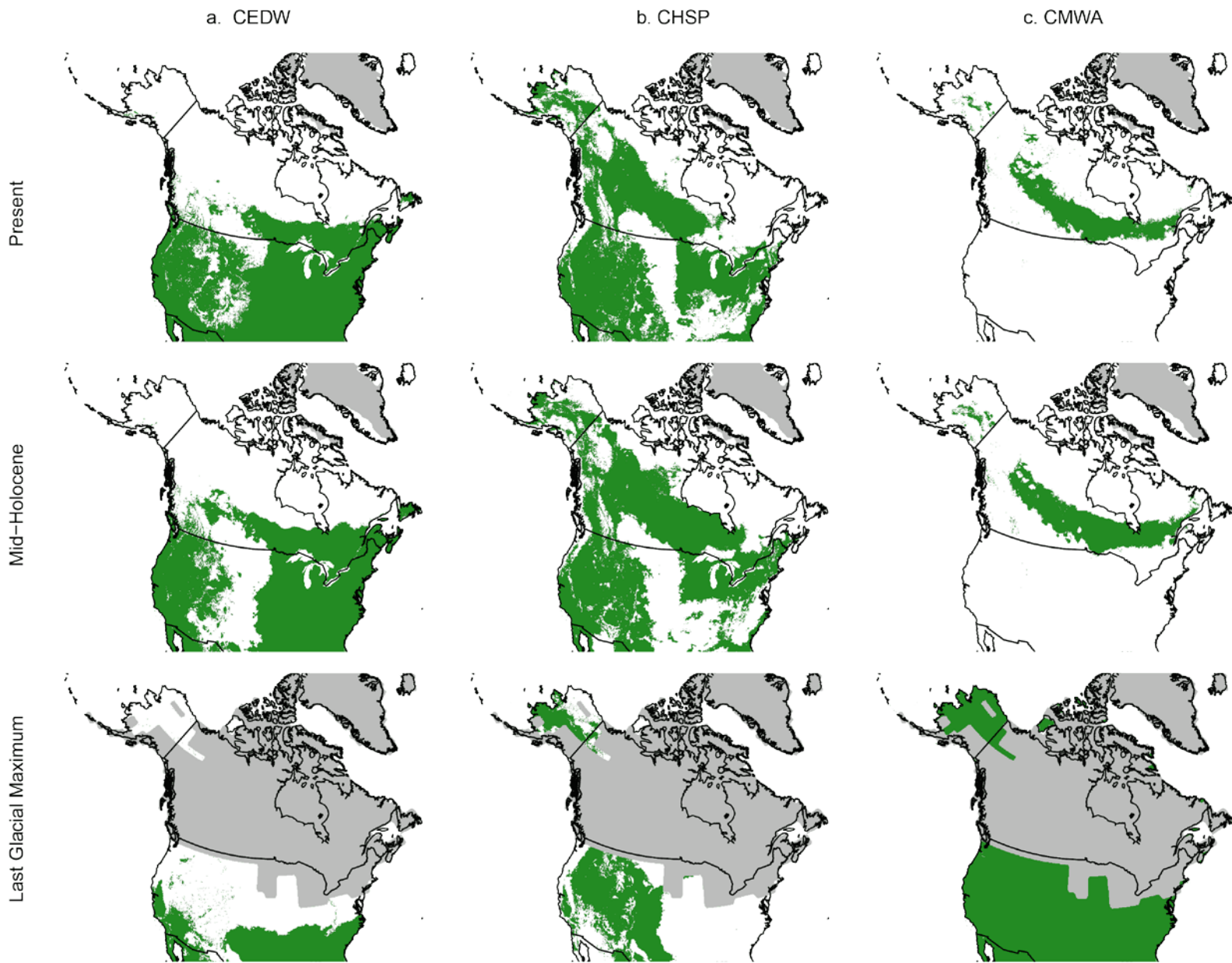


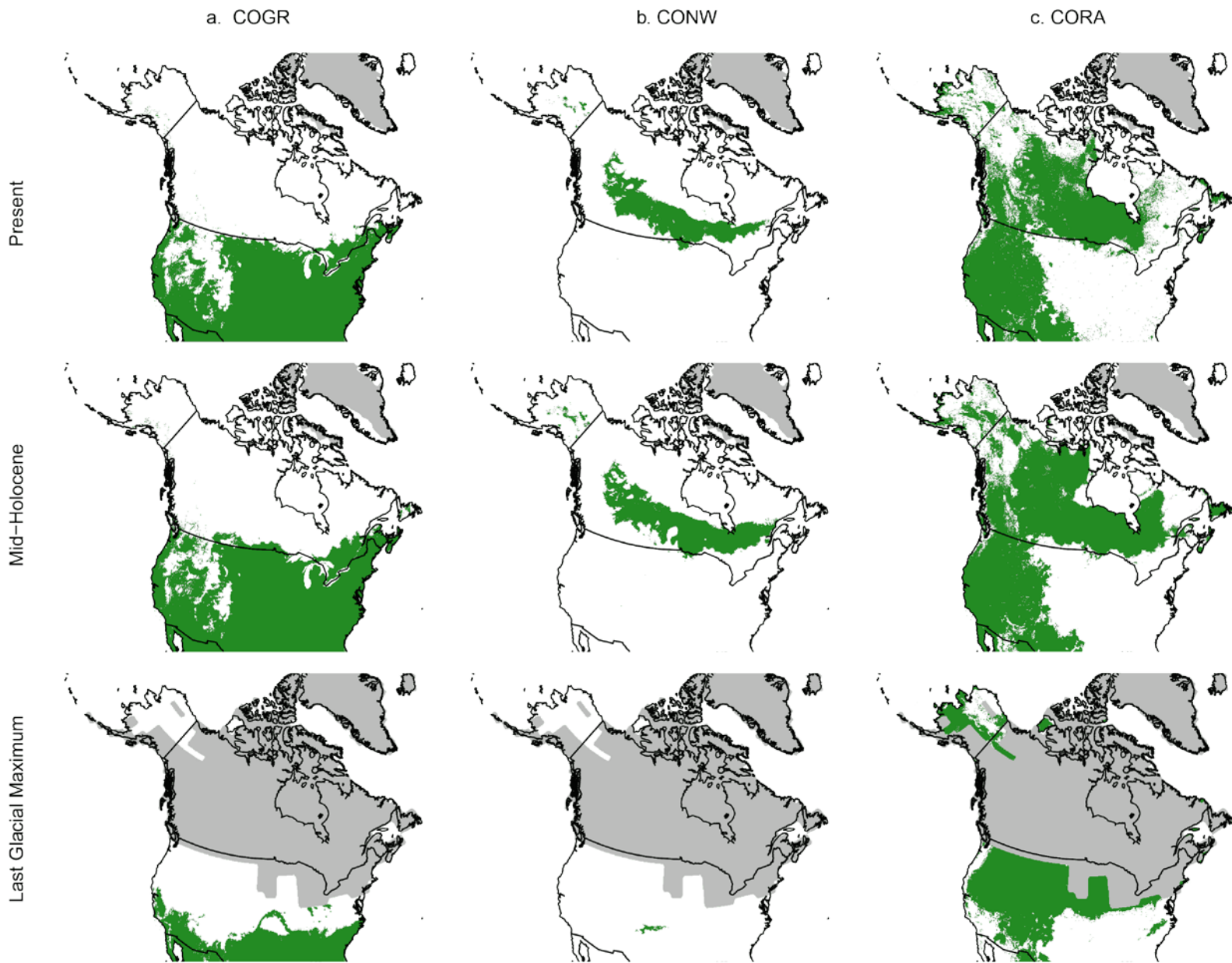


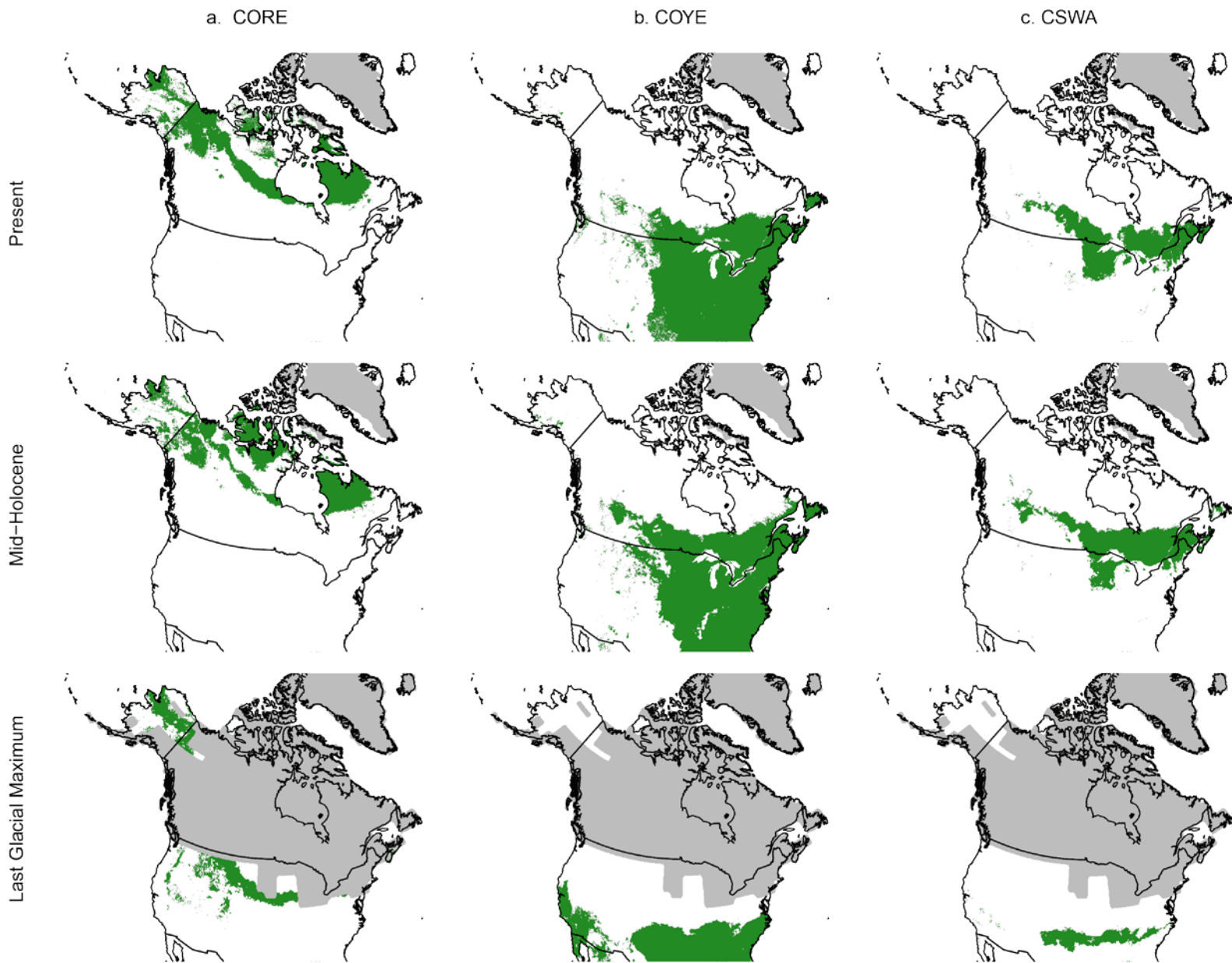


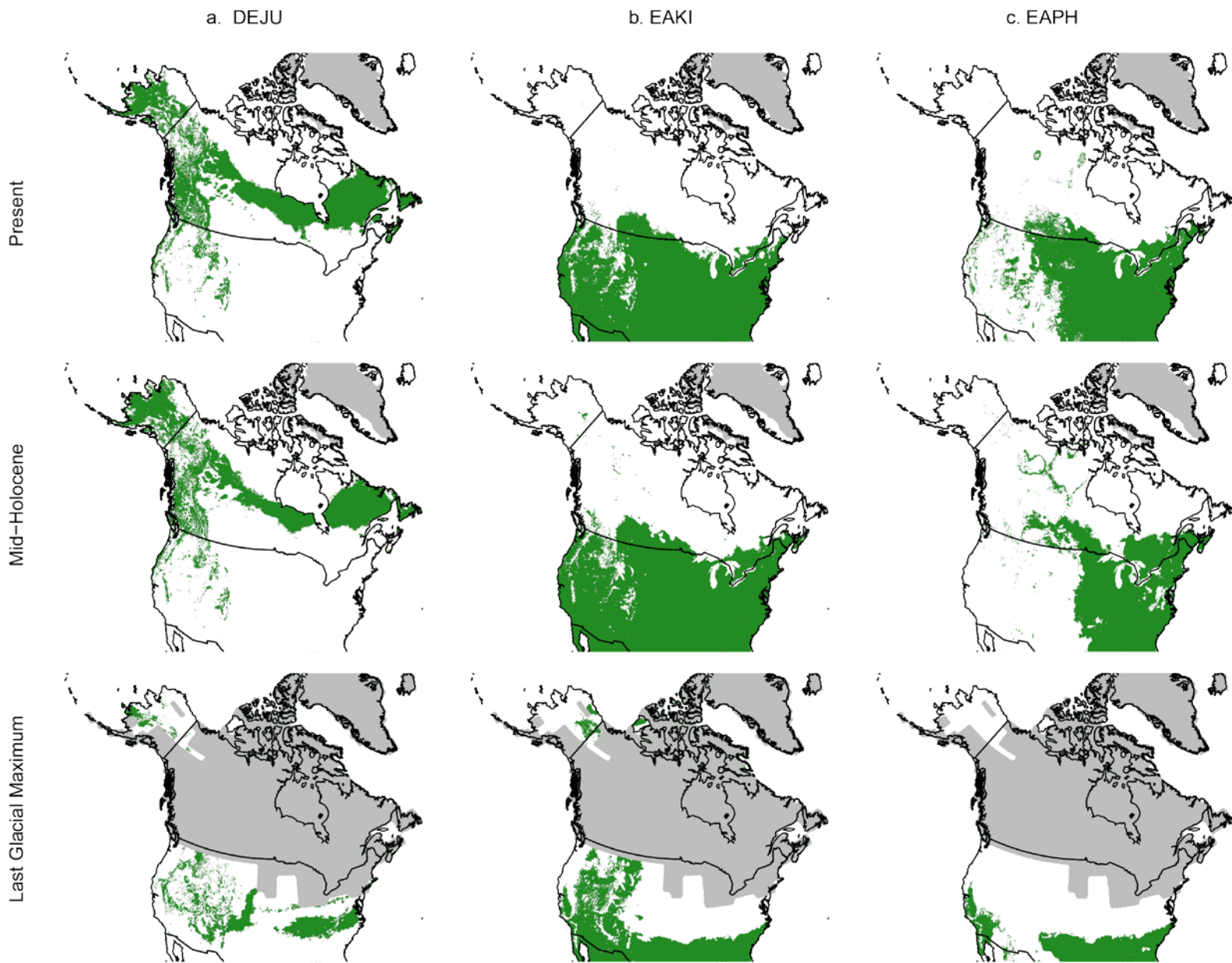


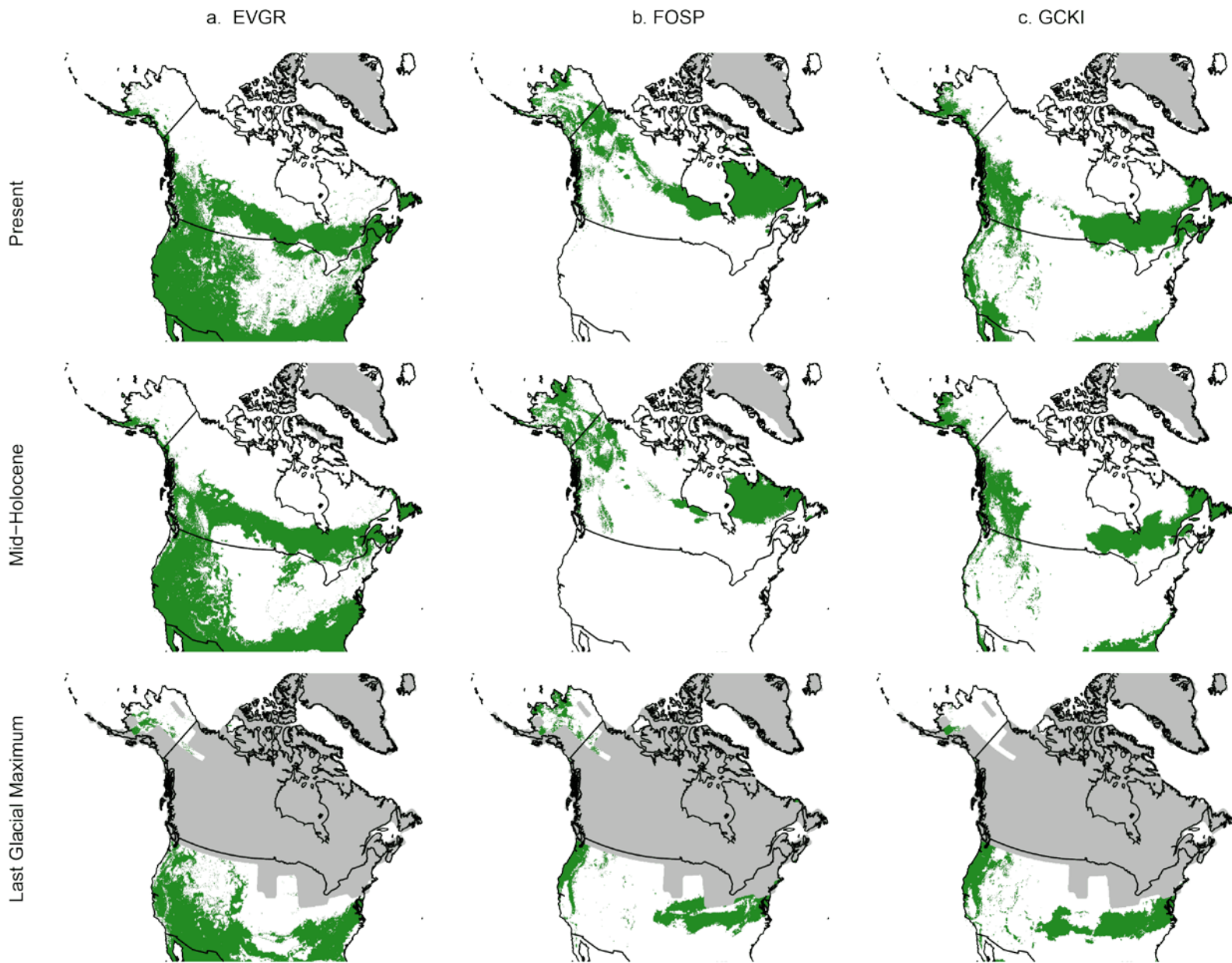


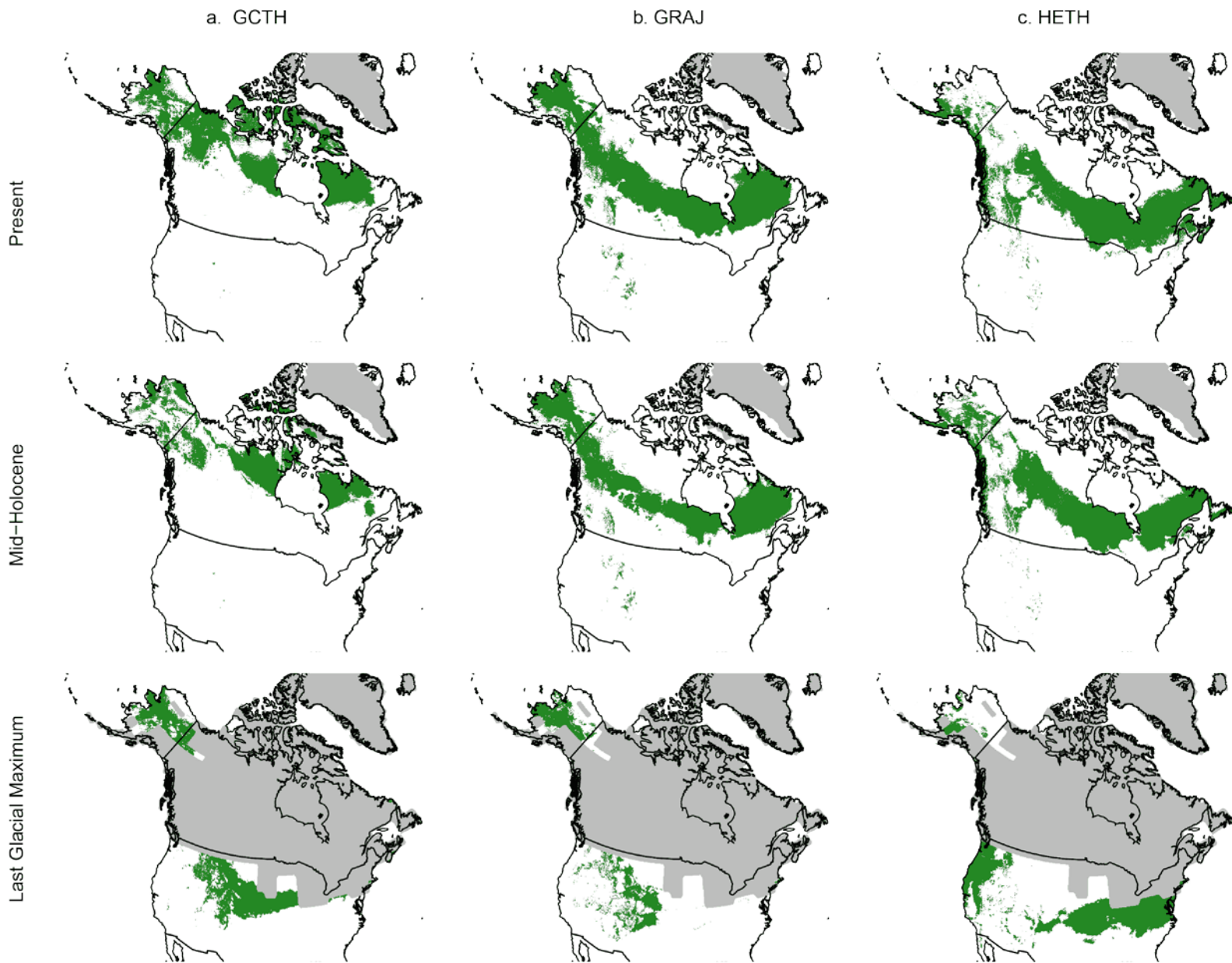


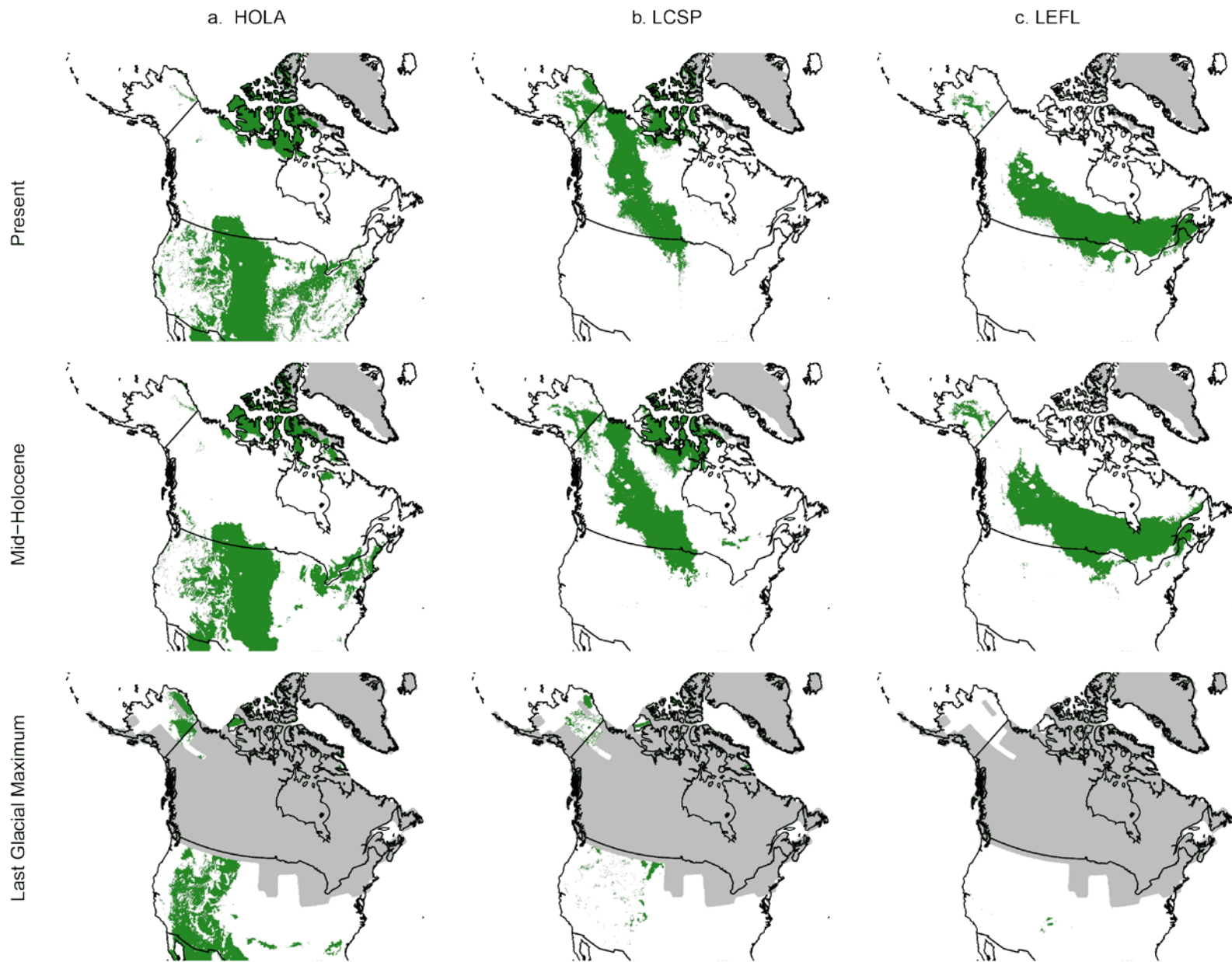


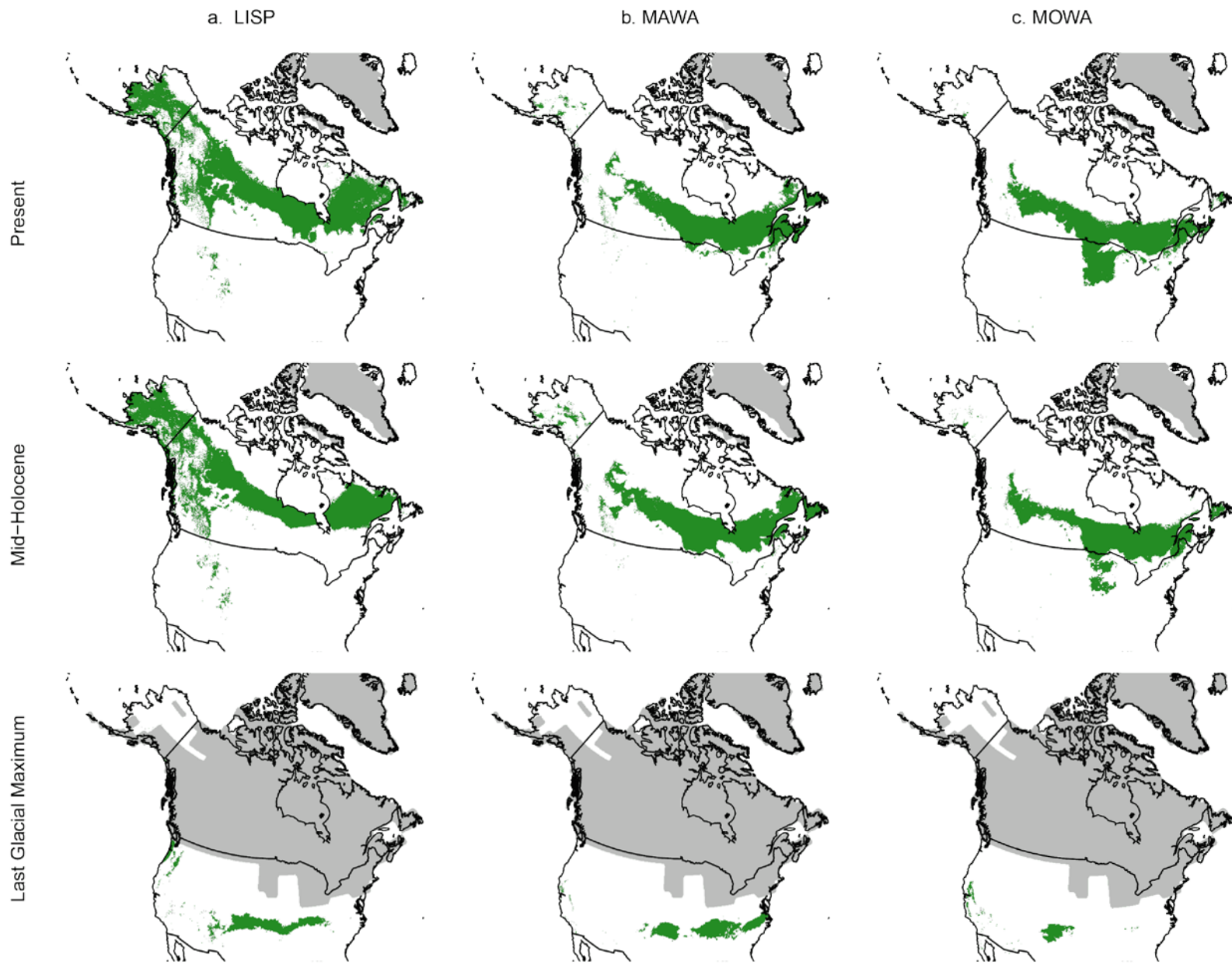


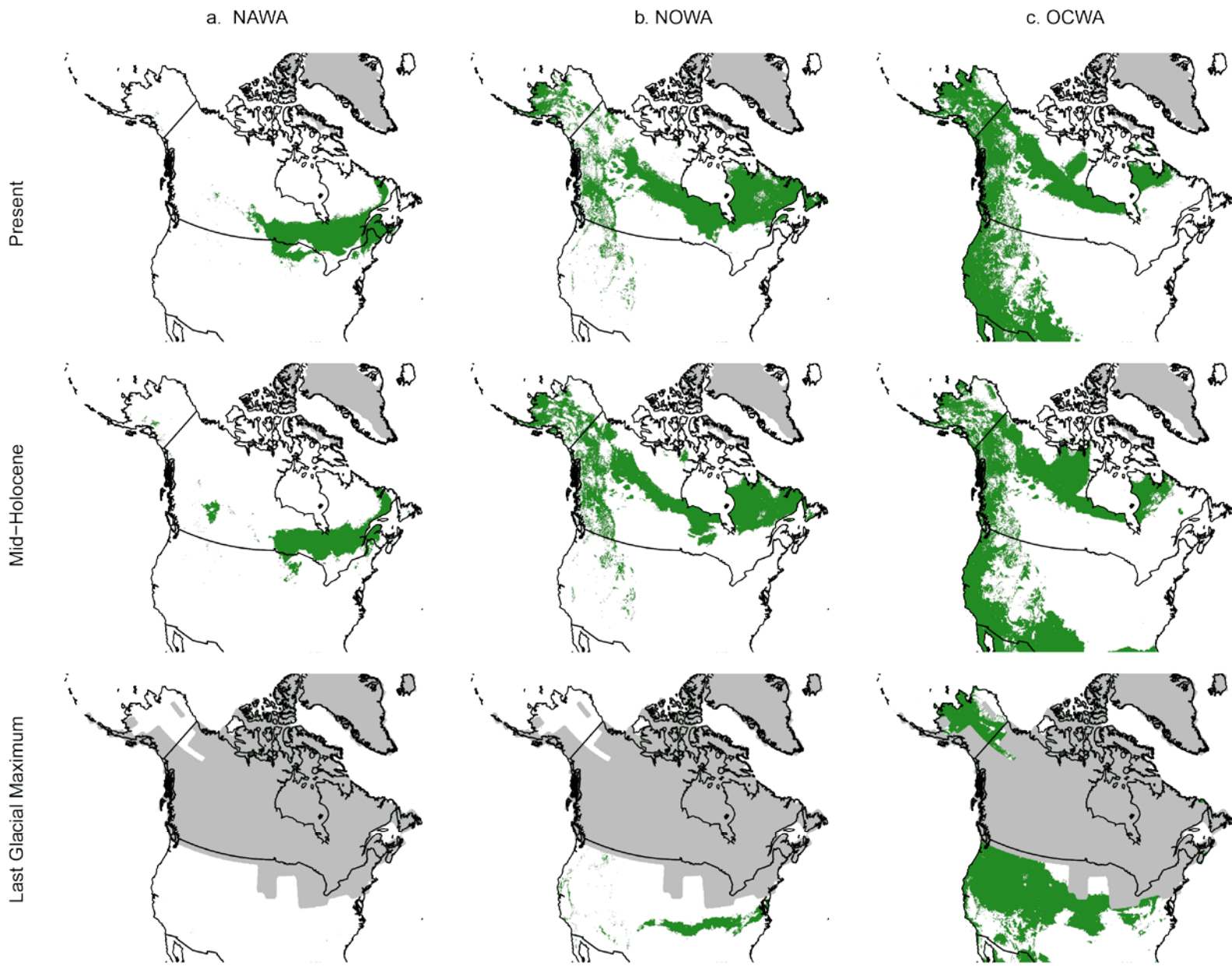


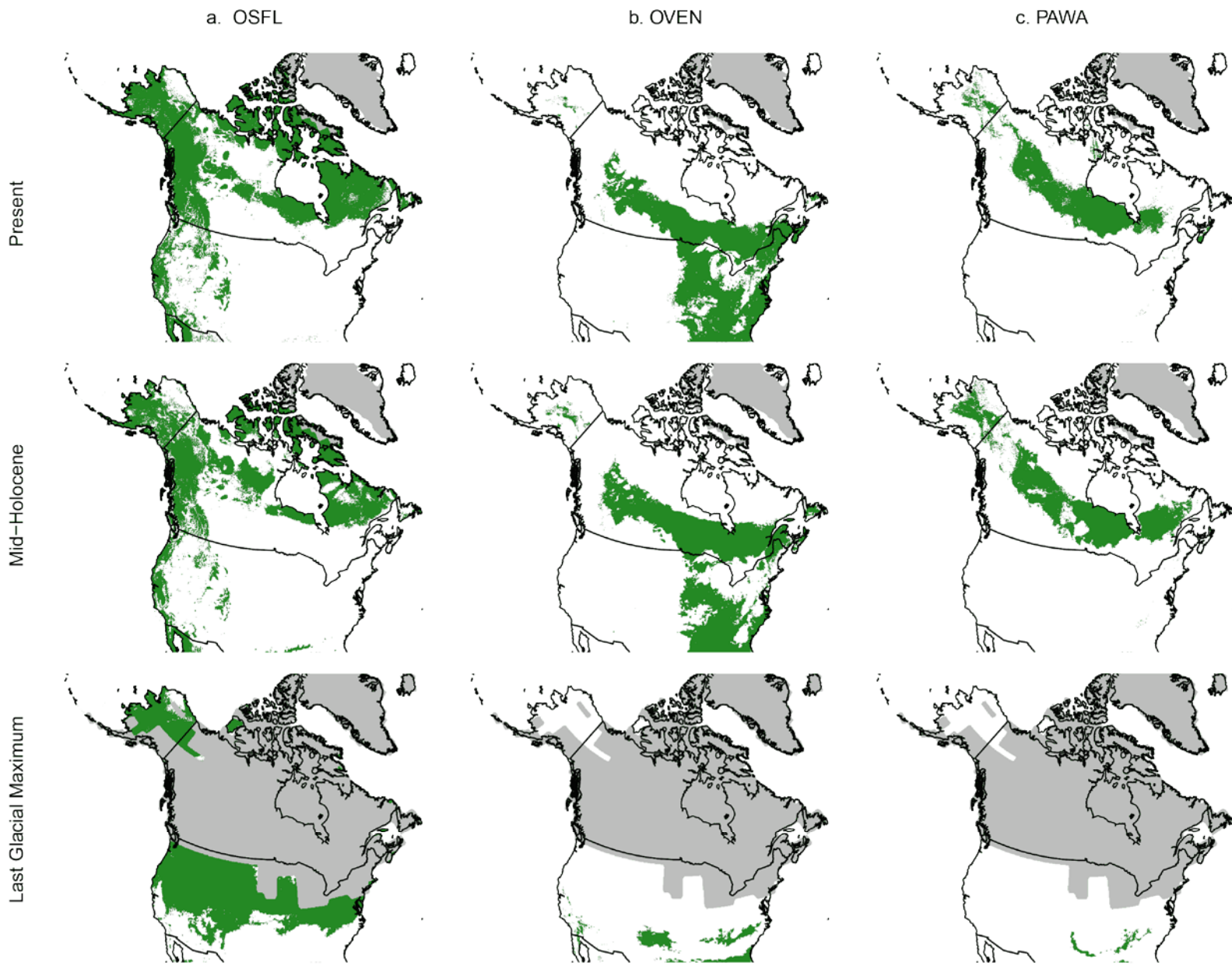


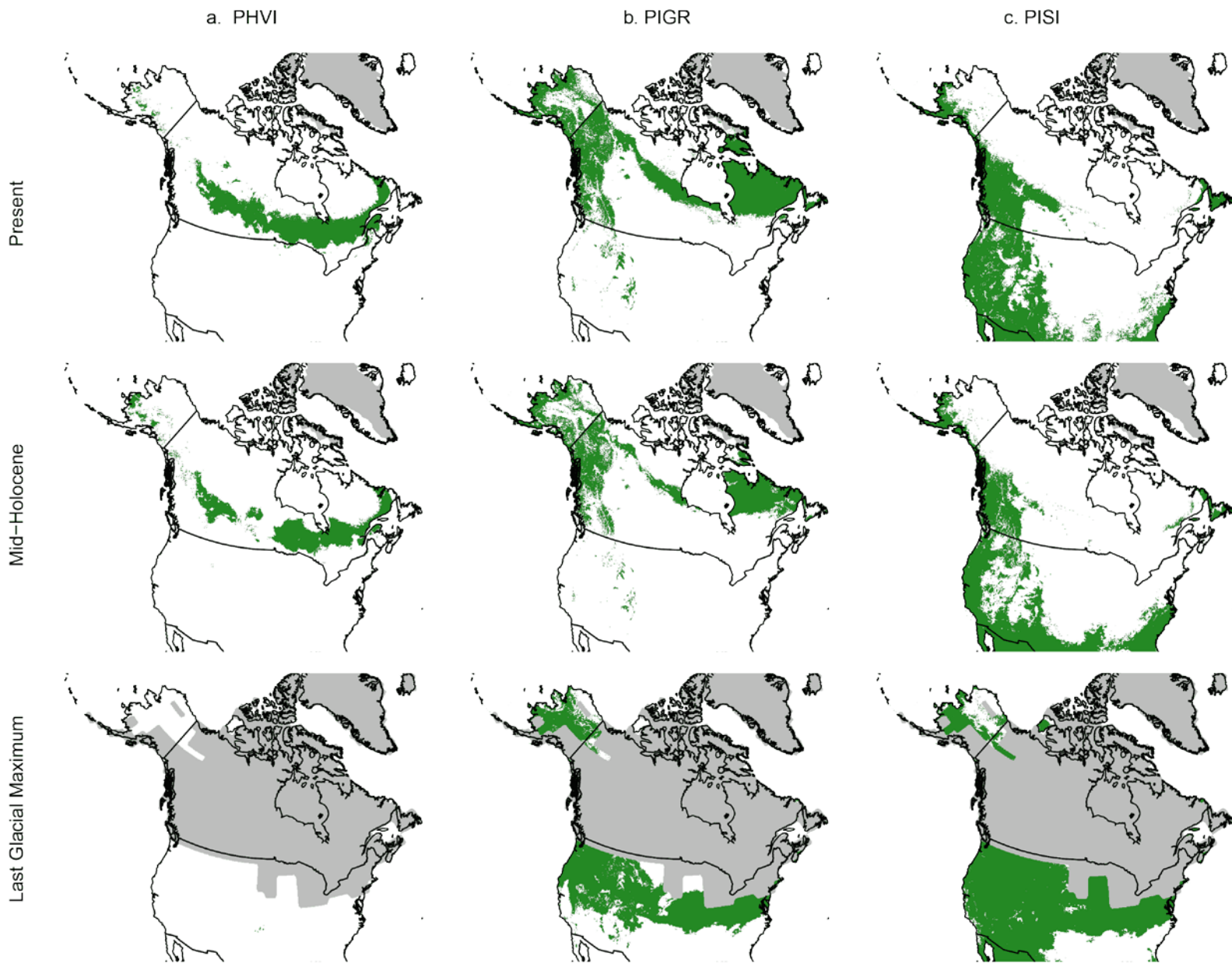


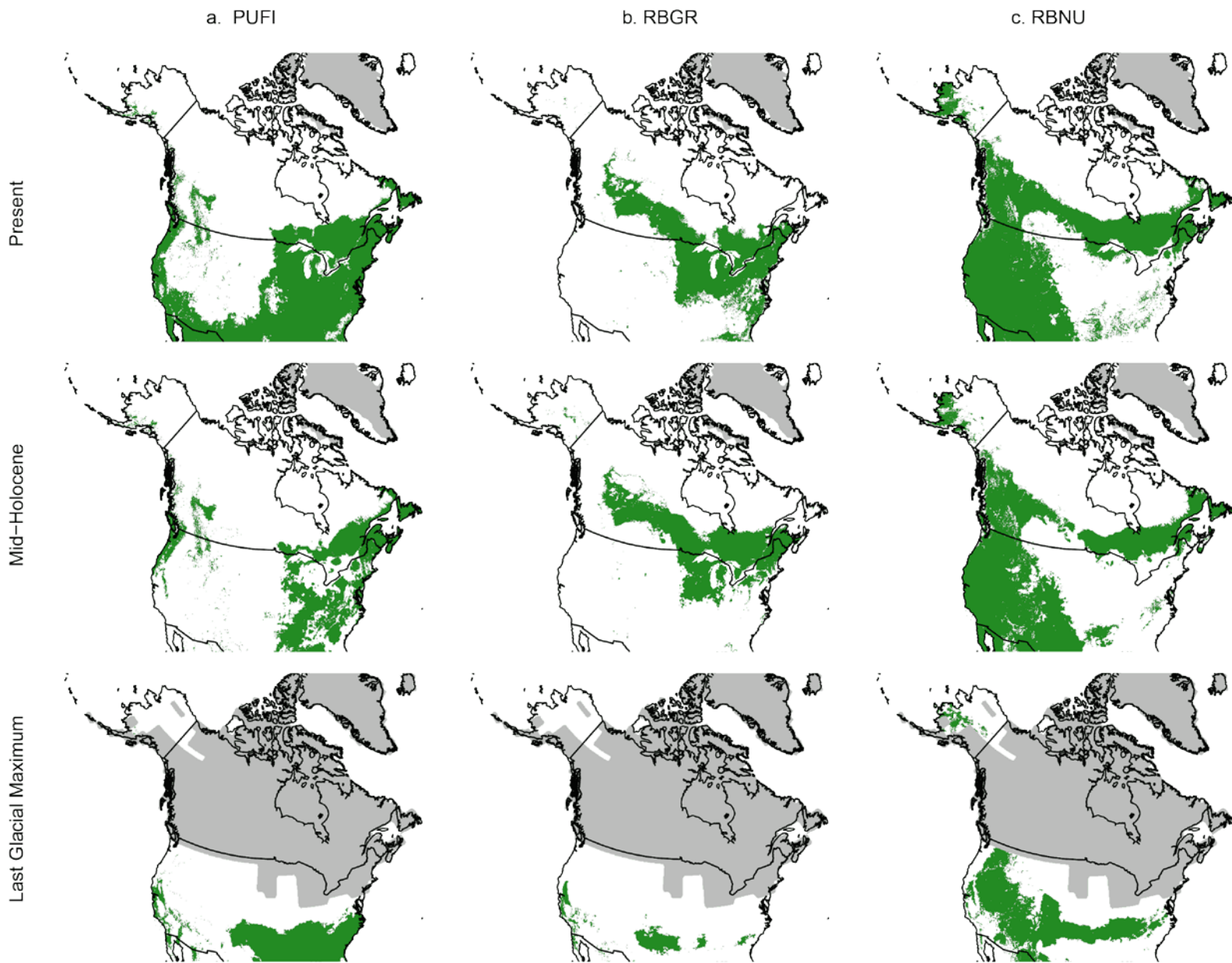


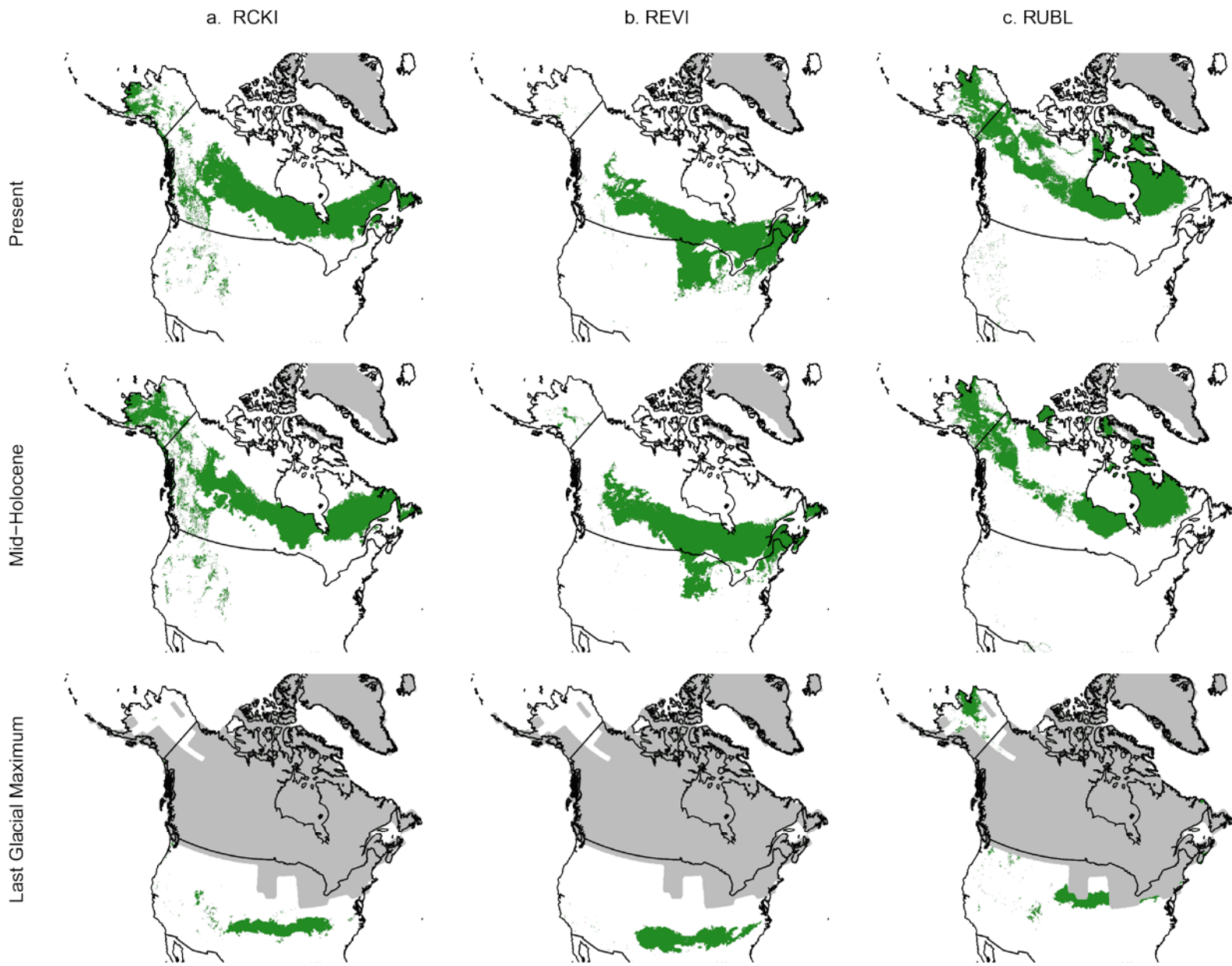


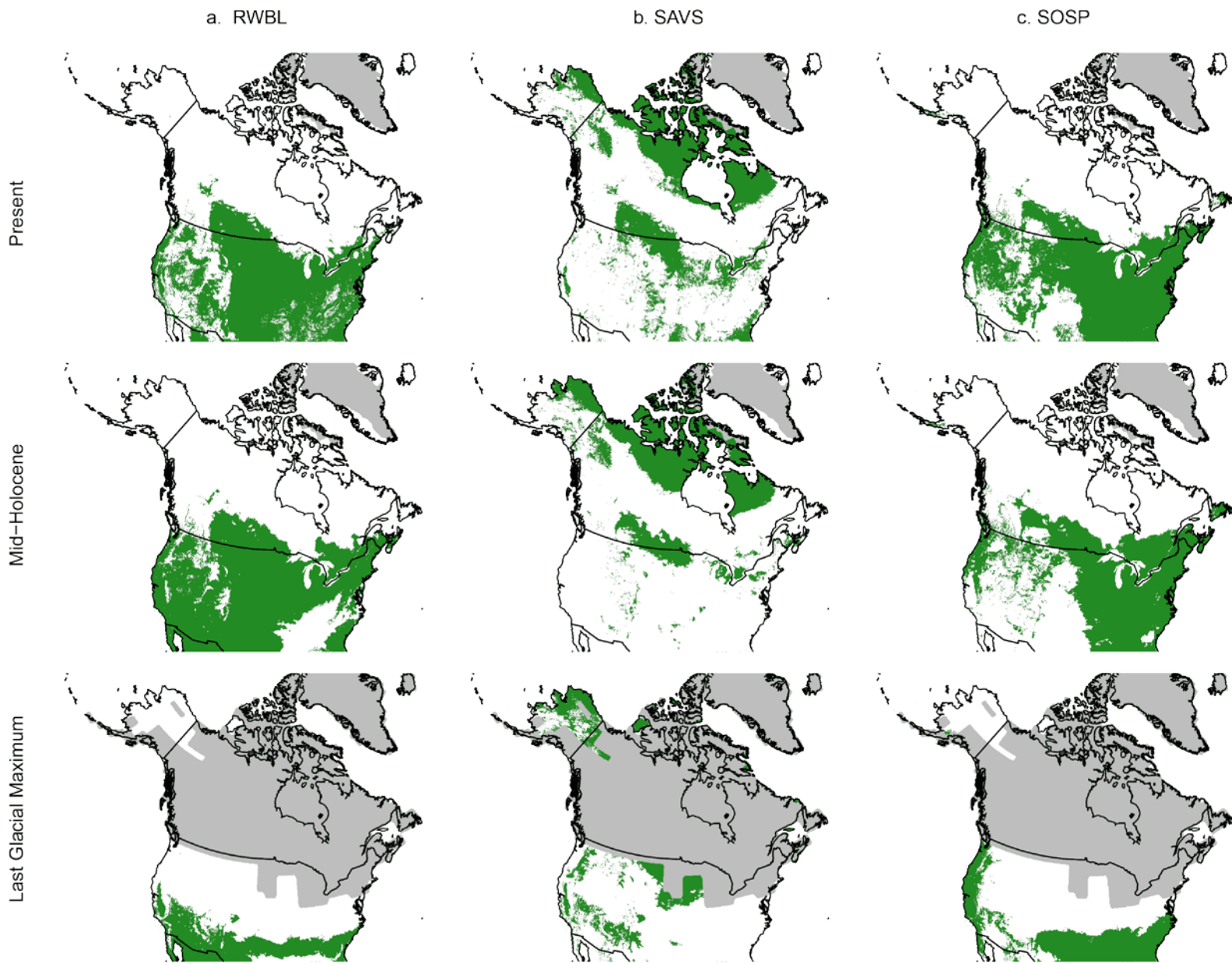


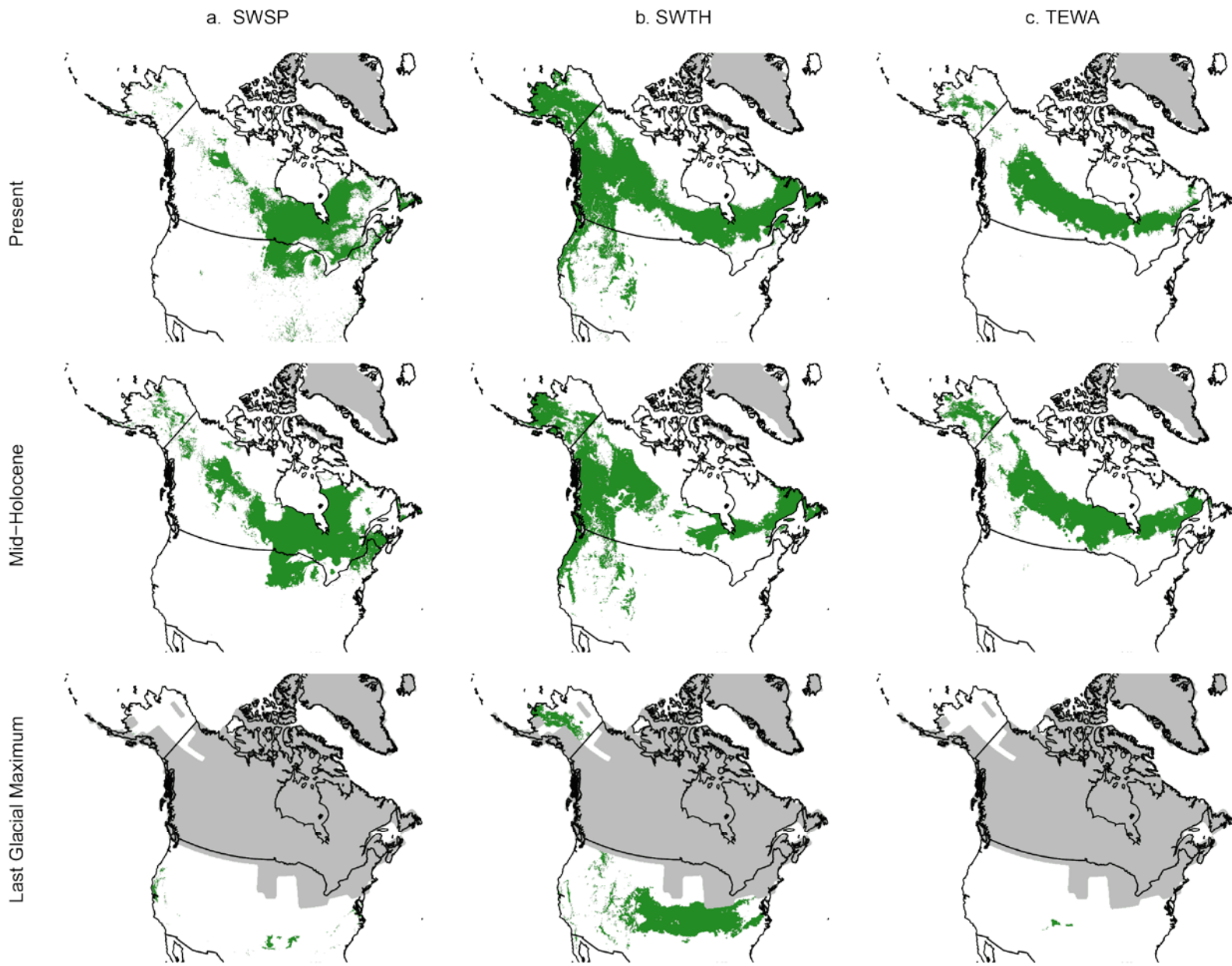


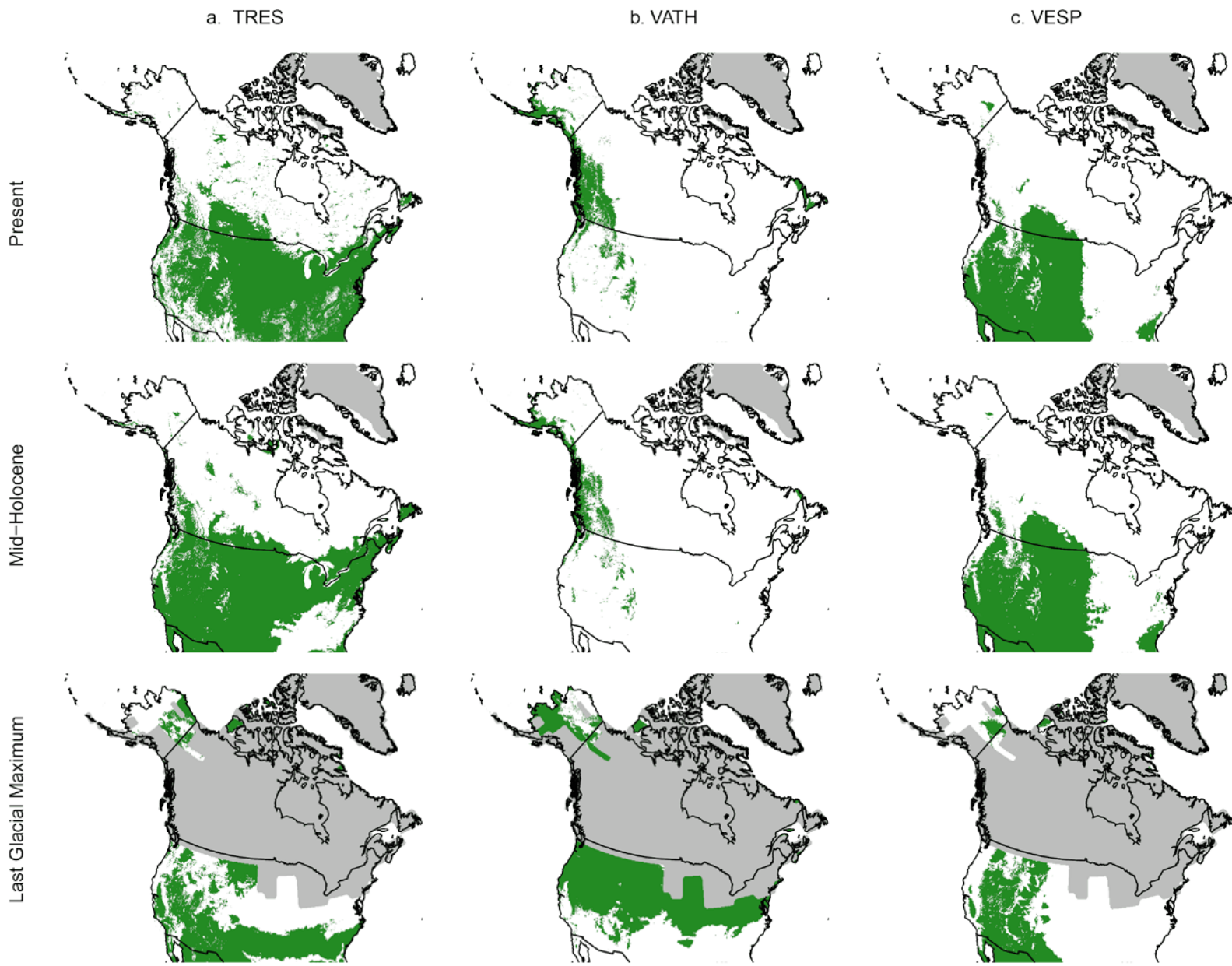


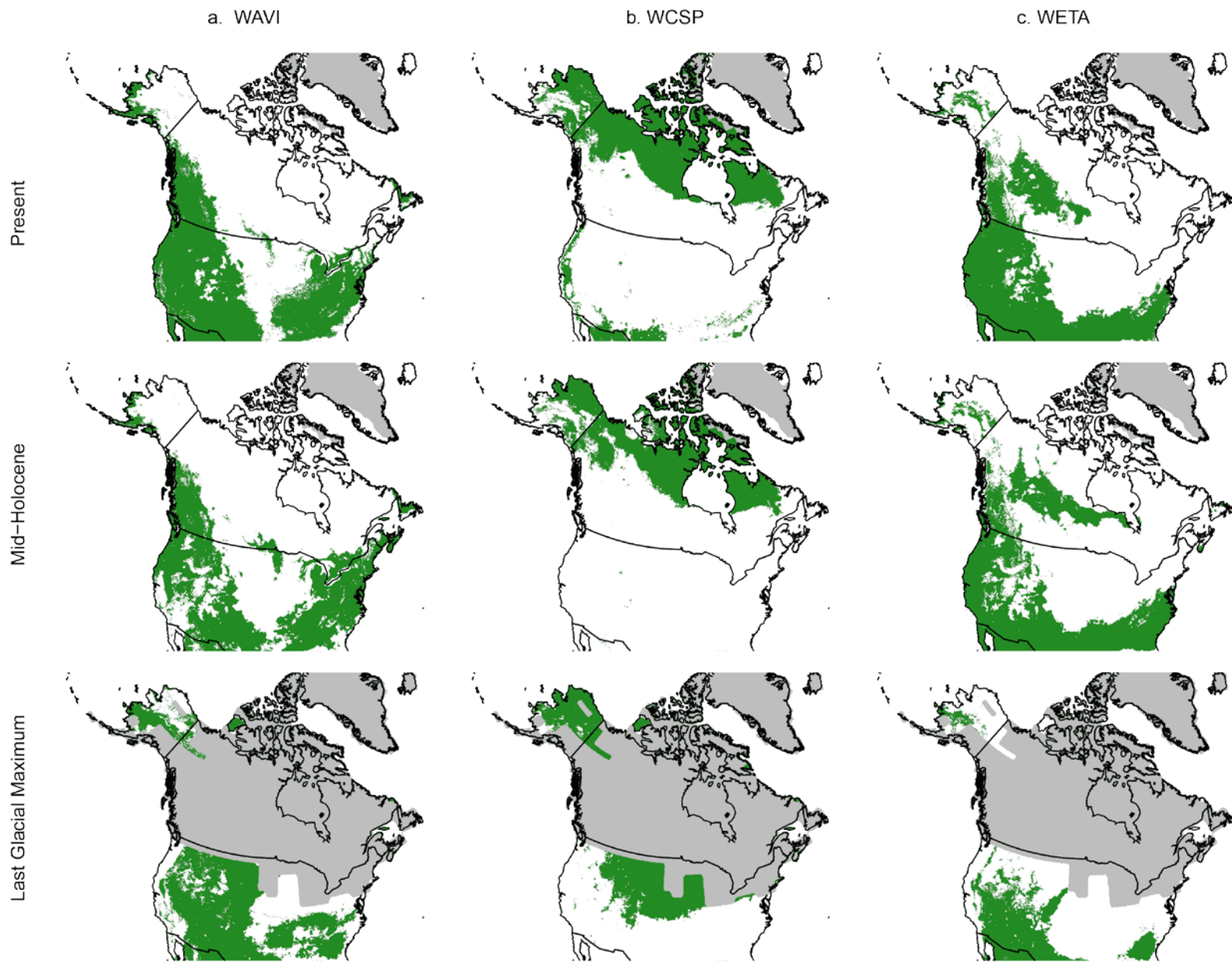


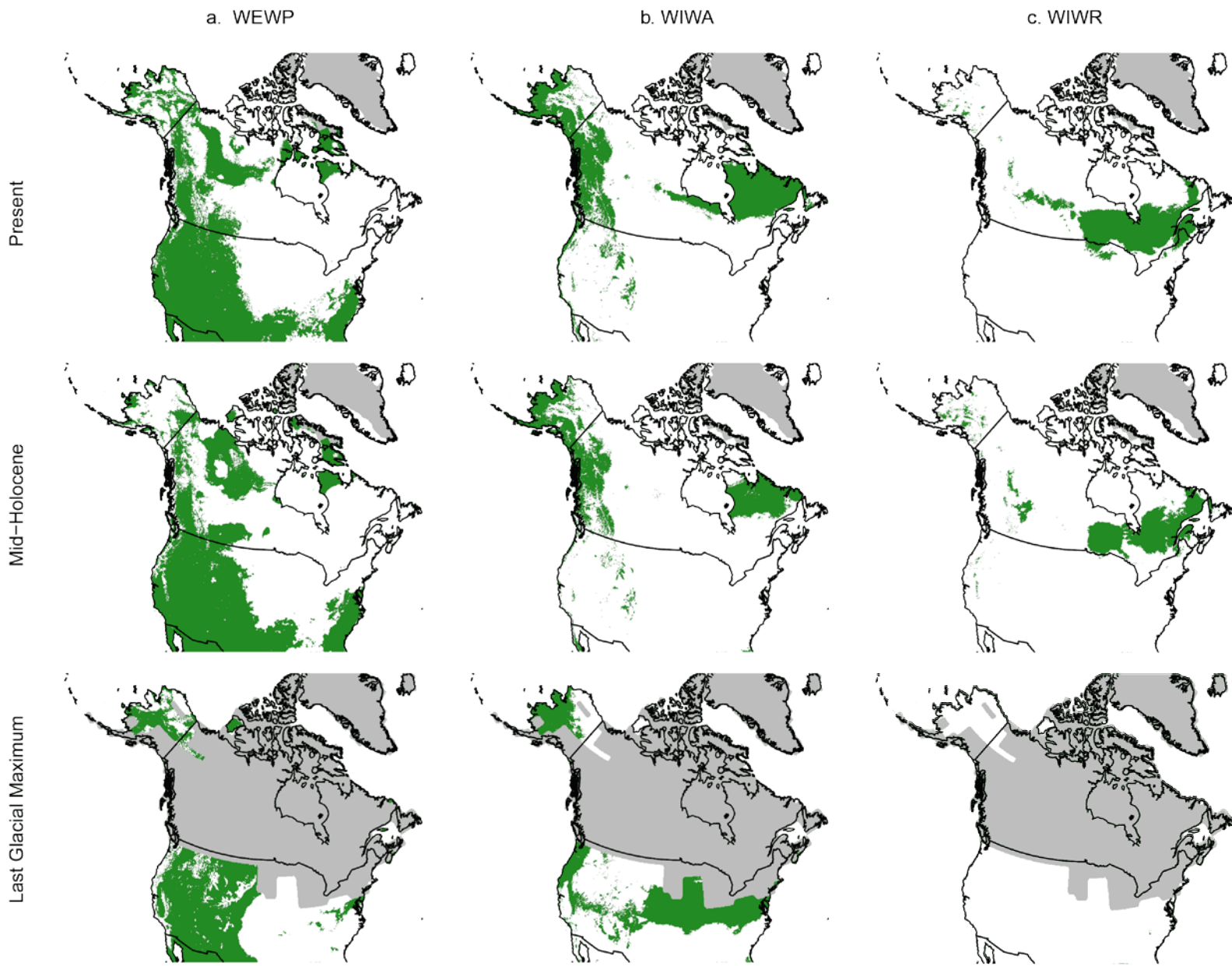


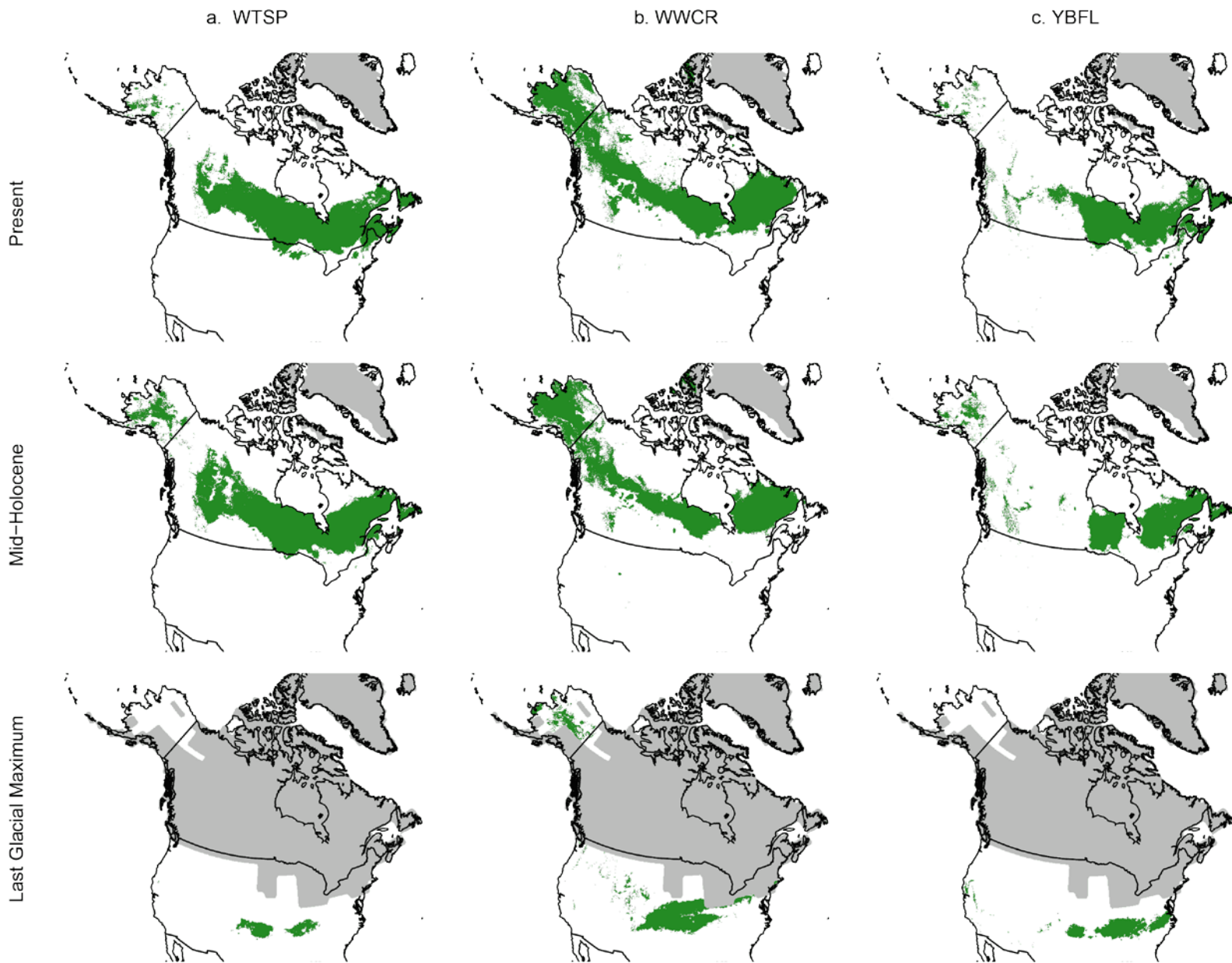


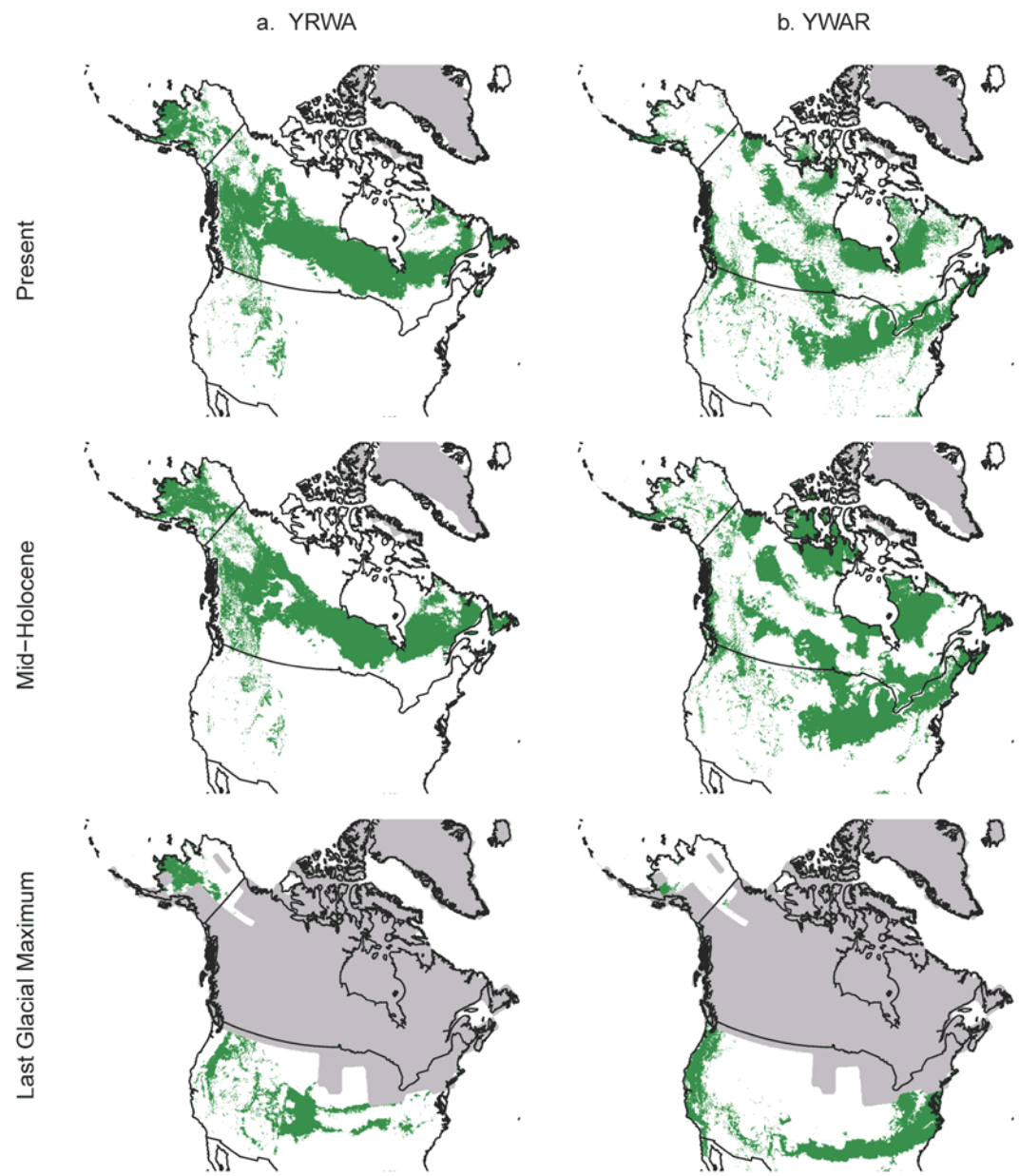












Appendix 4-C. Values of climate suitability variables for each species.

Units are the number of 16 km² (4-km x 4-km) grid cells in which the model-predicted density of a species exceeded the mean baseline predicted density for that species in the model-building area. Alaska Boreal = Alaska Boreal Interior ecoregion; NW Cord = Taiga + Boreal Cordillera ecoregions. CCM1 = Community Climate Model; GFDL = Geophysical Fluid Dynamics Laboratory model. Species currently occurring as regular breeders in the Alaska Boreal Interior (AK) according to Gibson and Withrow (2015) are indicated by ‘1.’

Common Name	AK	Current		Mid-Holocene		Last Glacial Maximum					
		Alaska Boreal	NW Cord	NW Cord CCM1	NW Cord GFDL	Alaska Boreal CCM1	Alaska Boreal GFDL	Western U.S. CCM1	Western U.S. GFDL	Eastern U.S. CCM1	Eastern U.S. GFDL
Alder Flycatcher (<i>Empidonax alnorum</i>)	1	21,489	14,840	24,794	20,962	0	0	0	7	48,435	30,523
American Crow (<i>Corvus brachyrhynchos</i>)	0	718	2,966	504	229	0	4	41,750	46,635	91,342	109,687
American Goldfinch (<i>Spinus tristis</i>)	0	272	1,308	16	4	0	0	47,429	47,669	158,546	118,396
American Pipit (<i>Anthus rubescens</i>)	1	1,004	14,427	28,644	39,289	6,134	9,941	14,730	11,157	119,994	150,324
American Redstart (<i>Setophaga ruticilla</i>)	0	1,784	5,859	13,825	5,984	0	29	426	124	24,625	52,426
American Robin (<i>Turdus migratorius</i>)	1	13,748	40,083	15,448	4,093	12,163	11,868	98,934	93,292	187,688	255,420
American Tree Sparrow (<i>Spizella arborea</i>)	1	2,121	18,299	11,749	22,607	25,312	12,185	6,068	508	147,294	116,301
Black-and-white Warbler (<i>Mniotilta varia</i>)	0	1,326	241	711	179	0	0	1	7,210	69,541	49,323
Bay-breasted Warbler (<i>Setophaga castanea</i>)	0	1,190	204	2,594	692	0	0	0	0	19,771	0
Black-capped Chickadee (<i>Poecile atricapillus</i>)	1	1,312	8,318	1,837	519	0	2	42,440	31,659	156,976	131,955
Brown-headed Cowbird (<i>Molothrus ater</i>)	0	9,483	16,491	48	268	838	5,808	73,504	90,175	132,270	89,941
Blue-headed Vireo (<i>Vireo solitarius</i>)	0	4,295	531	2,533	861	0	0	39	4,650	31,671	42,410
Blackburnian Warbler (<i>Setophaga fusca</i>)	0	2	5	269	15	0	0	9	1,021	58,748	22,275
Blue Jay (<i>Cyanocitta cristata</i>)	0	38	11	56	5	0	0	117	31,845	145,222	117,217
Blackpoll Warbler (<i>Setophaga striata</i>)	1	1,242	4,667	5,143	26,716	0	481	220	1,253	3,504	23,796
Boreal Chickadee (<i>Poecile hudsonicus</i>)	1	10,502	23,863	33,572	25,911	0	7,512	7,982	10,310	30,113	53,702
Brewer’s Blackbird (<i>Euphagus cyanocephalus</i>)	0	7,002	7,276	274	1,408	4,449	7,842	78,539	93,530	61,184	55,630
Brown Creeper (<i>Certhia americana</i>)	1	527	2,290	11,318	14,070	325	674	21,509	27,350	94,480	40,327

Common Name	AK	Current		Mid-Holocene		Last Glacial Maximum					
		Alaska Boreal	NW Cord	NW Cord	CCM1	GFDL	Alaska Boreal	Western U.S.		Eastern U.S.	
		CCM1	GFDL	CCM1	GFDL	CCM1	GFDL	CCM1	GFDL	CCM1	GFDL
Black-throated Green Warbler (<i>Setophaga virens</i>)	0	1,011	1,540	5,568	1,255	0	0	9	693	8,312	47,576
Canada Warbler (<i>Cardellina canadensis</i>)	0	802	148	2,138	344	0	0	1	55	73,482	19,869
Clay-colored Sparrow (<i>Spizella pallida</i>)	0	5,612	7,905	455	424	0	9	29,882	30,344	44,331	21,318
Cedar Waxwing (<i>Bombycilla cedrorum</i>)	0	589	1,989	334	94	8	27	37,586	45,009	147,412	128,834
Chipping Sparrow (<i>Spizella passerina</i>)	1	16,547	23,511	24,994	26,386	369	16,351	85,047	66,687	106,052	76,283
Cape May Warbler (<i>Setophaga tigrina</i>)	0	2,604	392	2,382	1,385	0	0	0	0	45,831	0
Common Grackle (<i>Quiscalus quiscula</i>)	0	1,056	15,390	535	572	0	0	40,675	41,258	134,912	123,037
Connecticut Warbler (<i>Oporornis agilis</i>)	0	501	118	2,564	496	0	0	466	0	55,158	2,252
Common Raven (<i>Corvus corax</i>)	1	2,609	7,926	17,104	17,555	5,049	14,590	95,614	73,229	97,670	178,911
Common Redpoll (<i>Acanthis flammea</i>)	1	5,327	24,595	17,233	27,671	285	12,228	7,621	3,435	61,381	52,797
Common Yellowthroat (<i>Geothlypis trichas</i>)	0	625	842	494	211	0	0	136	30,149	153,138	135,625
Chestnut-sided Warbler (<i>Setophaga pensylvanica</i>)	0	7	19	136	4	0	0	0	591	90,731	35,152
Dark-eyed Junco (<i>Junco hyemalis</i>)	1	14,119	17,896	38,319	31,964	0	4,097	33,565	17,178	59,913	55,293
Eastern Kingbird (<i>Tyrannus tyrannus</i>)	0	2,363	890	9,464	3,666	71	4,363	67,734	88,363	148,285	109,063
Eastern Phoebe (<i>Sayornis phoebe</i>)	0	379	6	0	0	0	0	80	21,280	125,894	95,626
Evening Grosbeak (<i>Coccothraustes vespertinus</i>)	0	1,719	9,818	19,936	33,840	284	4,334	91,631	79,891	71,286	115,391
Fox Sparrow (<i>Passerella iliaca</i>)	1	6,861	25,969	2	0	0	7,031	558	2,058	7,280	75,797
Golden-crowned Kinglet (<i>Regulus satrapa</i>)	1	3,818	13,924	23,202	13,332	0	1,216	19,461	17,862	31,783	78,617
Gray-cheeked Thrush (<i>Catharus minimus</i>)	1	12,134	33,746	28,821	25,083	108	20,439	17,121	8,564	102,412	83,824
Gray Jay (<i>Perisoreus canadensis</i>)	1	18,826	31,727	39,786	40,885	3	16,284	21,868	10,512	52,021	21,543
Hermit Thrush (<i>Catharus guttatus</i>)	1	2,145	11,755	19,004	19,511	0	4,505	14,094	10,485	19,961	101,801
Horned Lark (<i>Eremophila alpestris</i>)	1	471	4,050	32	184	23,120	5,673	32,121	75,850	72,394	31,900

Common Name	AK	Current		Mid-Holocene		Last Glacial Maximum					
		Alaska	NW	NW Cord		Alaska Boreal		Western U.S.		Eastern U.S.	
		Boreal	Cord	CCM1	GFDL	CCM1	GFDL	CCM1	GFDL	CCM1	GFDL
Le Conte's Sparrow (<i>Ammodramus leconteii</i>)	0	8,405	7,286	3,618	11,664	8,027	2,876	7,256	1,540	47,780	16,752
Least Flycatcher (<i>Empidonax minimus</i>)	0	5,578	1,056	6,612	1,786	0	0	50	31	74,517	865
Lincoln's Sparrow (<i>Melospiza lincolni</i>)	1	21,034	15,999	31,340	31,412	0	8	10,827	3,159	29,830	25,499
Magnolia Warbler (<i>Setophaga magnolia</i>)	0	1,925	484	1,892	965	0	0	0	533	52,210	31,439
Mourning Warbler (<i>Geothlypis philadelphia</i>)	0	78	57	1,399	140	0	0	16	2,822	48,404	8,329
Nashville Warbler (<i>Oreothlypis ruficapilla</i>)	0	6	148	299	416	0	0	0	7	50,475	18
Northern Waterthrush (<i>Parkesia noveboracensis</i>)	1	9,296	8,871	26,441	33,122	0	0	689	1,098	6,405	29,181
Orange-crowned Warbler (<i>Oreothlypis celata</i>)	1	21,864	46,555	46,134	43,517	175	23,377	95,865	73,552	69,016	126,589
Olive-sided Flycatcher (<i>Contopus cooperi</i>)	1	16,576	38,299	53,870	49,999	5,051	25,217	74,770	62,128	98,657	213,195
Ovenbird (<i>Seiurus aurocapilla</i>)	0	2,237	309	3,261	640	0	0	1	3,201	77,036	45,610
Palm Warbler (<i>Setophaga palmarum</i>)	0	5,546	1,960	1,028	9,148	4	0	0	0	33,433	9,357
Philadelphia Vireo (<i>Vireo philadelphicus</i>)	0	1,104	1,052	5,388	2,954	0	0	8	0	26,530	136
Pine Grosbeak (<i>Pinicola enucleator</i>)	1	7,085	37,650	40,285	45,649	1,709	22,086	39,554	45,200	49,698	134,601
Pine Siskin (<i>Spinus pinus</i>)	1	4,846	17,049	23,952	9,393	4,093	12,995	100,833	105,326	59,468	242,873
Purple Finch (<i>Haemorhous purpureus</i>)	0	951	5,260	2,575	403	0	25	4,778	12,697	125,494	120,291
Rose-breasted Grosbeak (<i>Pheucticus ludovicianus</i>)	0	207	113	1,395	196	0	0	320	8,767	97,542	23,185
Red-breasted Nuthatch (<i>Sitta canadensis</i>)	1	5,549	16,336	21,422	13,328	0	5,821	93,973	64,995	65,915	73,047
Ruby-crowned Kinglet (<i>Regulus calendula</i>)	1	4,005	4,884	13,851	19,782	0	72	951	2,826	12,351	34,456
Red-eyed Vireo (<i>Vireo olivaceus</i>)	0	1,458	229	1,989	312	0	0	5	125	71,675	47,435
Red-winged Blackbird (<i>Agelaius phoeniceus</i>)	1	11,851	27,751	26,516	37,060	87	5,909	3,478	243	59,221	40,449
Rusty Blackbird (<i>Euphagus carolinus</i>)	1	5,706	5,317	14	10	0	0	66,856	49,934	140,880	72,863
Savannah Sparrow (<i>Passerculus sandwichensis</i>)	1	2,703	14,536	8,621	17,558	25,309	12,563	26,563	21,960	153,967	115,252

Common Name	AK	Current		Mid-Holocene		Last Glacial Maximum					
		Alaska Boreal	NW Cord	NW Cord	CCM1	GFDL	Alaska Boreal	Western U.S.		Eastern U.S.	
		CCM1	GFDL	CCM1	GFDL	CCM1	GFDL	CCM1	GFDL	CCM1	GFDL
Song Sparrow (<i>Melospiza melodia</i>)	0	1,336	10,300	318	33	0	149	11,787	22,051	137,263	121,010
Swamp Sparrow (<i>Melospiza georgiana</i>)	0	1,319	1,894	759	8,388	0	4	0	1,114	65,106	4,810
Swainson's Thrush (<i>Catharus ustulatus</i>)	1	20,705	38,183	46,946	36,955	0	10,729	12,961	6,061	50,674	90,036
Tennessee Warbler (<i>Oreothlypis peregrina</i>)	0	5,761	2,443	8,395	8,746	0	0	0	0	1,970	1,473
Tree Swallow (<i>Tachycineta bicolor</i>)	1	5,034	12,049	660	562	9,587	5,534	84,125	74,230	167,505	154,703
Varied Thrush (<i>Ixoreus naevius</i>)	1	3,704	16,816	20,673	8,981	547	14,631	44,249	53,979	45,579	213,874
Vesper Sparrow (<i>Pooecetes gramineus</i>)	0	3,687	21,094	18,474	8,326	0	5,204	73,939	90,106	52,090	30,616
Warbling Vireo (<i>Vireo gilvus</i>)	0	3,171	17,551	45	1	5,573	14,162	87,246	68,899	79,214	186,446
White-crowned Sparrow (<i>Zonotrichia leucophrys</i>)	1	10,796	38,174	11,068	6,226	23,479	23,057	24,455	11,474	174,183	172,338
Western Tanager (<i>Piranga ludoviciana</i>)	0	10,822	9,825	17,566	19,532	148	6,503	93,296	74,125	30,880	50,816
Western Wood-Pewee (<i>Contopus sordidulus</i>)	1	15,266	28,503	48,294	40,068	13,446	15,769	102,047	100,488	62,205	132,474
Wilson's Warbler (<i>Cardellina pusilla</i>)	1	8,629	44,730	2,633	2,404	192	17,668	39,933	18,846	73,458	142,943
Winter Wren (<i>Troglodytes hiemalis</i>)	0	378	676	0	0	0	0	0	0	14,004	0
White-throated Sparrow (<i>Zonotrichia albicollis</i>)	0	2,375	1,226	4,915	4,983	0	0	0	43	20,528	16,776
White-winged Crossbill (<i>Loxia leucoptera</i>)	1	17,750	22,572	36,696	40,920	608	8,598	1,593	1,800	56,359	57,970
Yellow-bellied Flycatcher (<i>Empidonax flaviventris</i>)	0	475	743	4,103	3,105	0	0	42	756	23,627	31,170
Yellow-rumped Warbler (<i>Setophaga coronata</i>)	1	10,477	18,483	26,542	27,590	0	11,060	23,277	10,754	13,092	39,778
Yellow Warbler (<i>Setophaga petechia</i>)	1	3,003	3,345	4,442	10,104	0	977	10,983	16,806	63,724	76,175

Appendix 4-D. Values of calculated competition indices.

Maximum single-species phylogenetic correlation and sum of multi-species phylogenetic correlations with species currently occurring in the Alaska Boreal Interior. Higher values reflect higher phylogenetic relatedness. Species currently occurring as regular breeders in the Alaska Boreal Interior (AK) according to Gibson (2011) or Gibson and Withrow (2015) are indicated by ‘1.’

Scientific Name	Species	Alaska	Max	Sum
<i>Zonotrichia leucophrys</i>	White-crowned Sparrow	1	0.994	22.64
<i>Setophaga virens</i>	Black-throated Green Warbler	0	0.986	22.52
<i>Oreothlypis ruficapilla</i>	Nashville Warbler	0	0.977	22.32
<i>Melospiza georgiana</i>	Swamp Sparrow	0	0.976	22.40
<i>Setophaga castanea</i>	Bay-breasted Warbler	0	0.969	22.52
<i>Setophaga pensylvanica</i>	Chestnut-sided Warbler	0	0.967	22.52
<i>Zonotrichia albicollis</i>	White-throated Sparrow	0	0.966	22.58
<i>Melospiza melodia</i>	Song Sparrow	0	0.958	22.38
<i>Spizella pallida</i>	Clay-colored Sparrow	0	0.957	22.14
<i>Setophaga striata</i>	Blackpoll Warbler	1	0.948	22.55
<i>Setophaga petechia</i>	Yellow Warbler	1	0.948	22.55
<i>Euphagus cyanocephalus</i>	Brewer’s Blackbird	0	0.946	22.01
<i>Setophaga fusca</i>	Blackburnian Warbler	0	0.943	22.49
<i>Setophaga palmarum</i>	Palm Warbler	0	0.936	22.47
<i>Setophaga coronata</i>	Yellow-rumped Warbler	1	0.930	22.53
<i>Empidonax minimus</i>	Least Flycatcher	0	0.928	3.58
<i>Oreothlypis peregrina</i>	Tennessee Warbler	0	0.928	22.27
<i>Setophaga tigrina</i>	Cape May Warbler	0	0.926	22.45
<i>Setophaga ruticilla</i>	American Redstart	0	0.926	22.45
<i>Cardellina canadensis</i>	Canada Warbler	0	0.924	22.29
<i>Quiscalus quiscula</i>	Common Grackle	0	0.922	21.99
<i>Setophaga magnolia</i>	Magnolia Warbler	0	0.918	22.43
<i>Acanthis flammea</i>	Common Redpoll	1	0.915	20.34
<i>Loxia leucoptera</i>	White-winged Crossbill	1	0.915	20.34
<i>Carduelis tristis</i>	American Goldfinch	0	0.915	20.20
<i>Catharus guttatus</i>	Hermit Thrush	1	0.914	16.21
<i>Catharus minimus</i>	Gray-cheeked Thrush	1	0.914	16.21
<i>Contopus sordidulus</i>	Western Wood-Pewee	1	0.913	3.67
<i>Contopus cooperi</i>	Olive-sided Flycatcher	1	0.913	3.67
<i>Melospiza lincolni</i>	Lincoln’s Sparrow	1	0.900	22.42
<i>Passerculus sandwichensis</i>	Savannah Sparrow	1	0.900	22.42
<i>Junco hyemalis</i>	Dark-eyed Junco	1	0.900	22.55
<i>Empidonax alnorum</i>	Alder Flycatcher	1	0.897	3.65
<i>Corvus brachyrhynchos</i>	American Crow	0	0.896	11.38
<i>Molothrus ater</i>	Brown-headed Cowbird	0	0.893	21.96
<i>Mniotilta varia</i>	Black-and-white Warbler	0	0.890	22.23
<i>Agelaius phoeniceus</i>	Red-winged Blackbird	1	0.889	22.06
<i>Euphagus carolinus</i>	Rusty Blackbird	1	0.889	22.06

Scientific Name	Species	Alaska	Max	Sum
<i>Empidonax flaviventris</i>	Yellow-bellied Flycatcher	0	0.885	3.52
<i>Poecile atricapillus</i>	Black-capped Chickadee	1	0.884	14.27
<i>Poecile hudsonicus</i>	Boreal Chickadee	1	0.884	14.27
<i>Catharus ustulatus</i>	Swainson's Thrush	1	0.883	16.17
<i>Passerella iliaca</i>	Fox Sparrow	1	0.882	22.50
<i>Spizella arborea</i>	American Tree Sparrow	1	0.882	22.50
<i>Pooecetes gramineus</i>	Vesper Sparrow	0	0.873	22.27
<i>Ammodramus leconteii</i>	Le Conte's Sparrow	0	0.873	22.27
<i>Cardellina pusilla</i>	Wilson's Warbler	1	0.870	22.36
<i>Oporornis agilis</i>	Connecticut Warbler	0	0.866	22.21
<i>Geothlypis philadelphia</i>	Mourning Warbler	0	0.866	22.21
<i>Geothlypis trichas</i>	Common Yellowthroat	0	0.866	22.21
<i>Parkesia noveboracensis</i>	Northern Waterthrush	1	0.865	22.34
<i>Oreothlypis celata</i>	Orange-crowned Warbler	1	0.865	22.34
<i>Carduelis pinus</i>	Pine Siskin	1	0.863	20.28
<i>Sayornis phoebe</i>	Eastern Phoebe	0	0.863	3.45
<i>Seiurus aurocapilla</i>	Ovenbird	0	0.835	22.00
<i>Bombycilla cedrorum</i>	Cedar Waxwing	0	0.833	14.20
<i>Haemorhous purpureus</i>	Purple Finch	0	0.814	19.85
<i>Spizella passerine</i>	Chipping Sparrow	1	0.809	22.18
<i>Corvus corax</i>	Common Raven	1	0.771	11.48
<i>Zoothera naevia</i>	Varied Thrush	1	0.764	15.94
<i>Pinicola enucleator</i>	Pine Grosbeak	1	0.742	20.03
<i>Turdus migratorius</i>	American Robin	1	0.730	15.84
<i>Cyanocitta cristata</i>	Blue Jay	0	0.728	11.17
<i>Tyrannus tyrannus</i>	Eastern Kingbird	0	0.726	2.90
<i>Perisoreus canadensis</i>	Gray Jay	1	0.713	11.42
<i>Coccothraustes vespertinus</i>	Evening Grosbeak	0	0.695	19.56
<i>Pheucticus ludovicianus</i>	Red-breasted Grosbeak	0	0.673	20.43
<i>Piranga ludoviciana</i>	Western Tanager	0	0.673	20.43
<i>Troglodytes troglodytes</i>	Winter Wren	0	0.567	14.25
<i>Anthus rubescens</i>	American Pipit	1	0.542	18.43
<i>Vireo philadelphicus</i>	Philadelphia Vireo	0	0.520	10.56
<i>Vireo gilvus</i>	Warbling Vireo	0	0.520	10.56
<i>Vireo solitarius</i>	Blue-headed Vireo	0	0.520	10.56
<i>Vireo olivaceus</i>	Red-eyed Vireo	0	0.520	10.56
<i>Certhia americana</i>	Brown Creeper	1	0.512	14.68
<i>Sitta canadensis</i>	Red-breasted Nuthatch	1	0.512	14.68
<i>Regulus calendula</i>	Ruby-crowned Kinglet	1	0.491	14.30
<i>Regulus satrapa</i>	Golden-crowned Kinglet	1	0.491	14.30
<i>Tachycineta bicolor</i>	Tree Swallow	1	0.441	13.82
<i>Eremophila alpestris</i>	Horned Lark	1	0.441	13.82

Appendix 4-E. Predicted probability of occurrence within Alaska Boreal Interior ecoregion.

Predicted probability of occurrence within Alaska Boreal Interior ecoregion for 80 boreal-breeding species during the baseline period and three future time periods. Model numbers correspond with rankings in Table 4-3. Breeding status according to Gibson (2011) and Gibson and Withrow (2015) Breeding status codes: 2 = regular confirmed breeder; 1 = casual visitor with at least one recently confirmed breeding attempt or records of territorial singing males within region or in south-central Alaska; 0 = no record of regular breeding or territorial singing males in region. Most species listed have accidental records within interior or south-central Alaska and several are regular breeders in other parts of Alaska, especially the southeastern region.

Code	Common Name (Scientific Name)	Breeding Status	Baseline	2011-2040	2041-2070	2071-2100
ALFL	Alder Flycatcher (<i>Empidonax alnorum</i>)	2	0.923	0.986	0.989	0.987
AMCR	American Crow (<i>Corvus brachyrhynchos</i>)	0	0.040	0.653	0.881	0.978
AMGO	American Goldfinch (<i>Spinus tristis</i>)	0	0.067	0.655	0.939	0.994
AMPI	American Pipit (<i>Anthus rubescens</i>)	2	0.238	0.353	0.046	0.028
AMRE	American Redstart (<i>Setophaga ruticilla</i>)	0	0.519	0.970	0.990	0.997
AMRO	American Robin (<i>Turdus migratorius</i>)	2	0.975	0.992	0.991	0.993
ATSP	American Tree Sparrow (<i>Spizella arborea</i>)	2	0.868	0.912	0.616	0.061
BAWW	Black-and-white Warbler (<i>Mniotilta varia</i>)	0	0.007	0.553	0.950	0.995
BBWA	Bay-breasted Warbler (<i>Setophaga castanea</i>)	0	0.005	0.461	0.916	0.981
BCCH	Black-capped Chickadee (<i>Poecile atricapillus</i>)	2	0.878	0.992	0.997	0.999
BHCO	Brown-headed Cowbird (<i>Molothrus ater</i>)	1	0.774	0.955	0.961	0.971
BHVI	Blue-headed Vireo (<i>Vireo solitarius</i>)	0	0.013	0.528	0.902	0.990
BLBW	Blackburnian Warbler (<i>Setophaga fusca</i>)	0	0.000	0.286	0.971	0.998
BLJA	Blue Jay (<i>Cyanocitta cristata</i>)	0	0.000	0.330	0.965	0.998
BLPW	Blackpoll Warbler (<i>Setophaga striata</i>)	2	0.817	0.968	0.946	0.948
BOCH	Boreal Chickadee (<i>Poecile hudsonicus</i>)	2	0.985	0.997	0.998	0.997
BRBL	Brewer's Blackbird (<i>Euphagus cyanocephalus</i>)	0	0.176	0.570	0.612	0.699
BRCR	Brown Creeper (<i>Certhia americana</i>)	2	0.485	0.976	0.990	0.996
BTNW	Black-throated Green Warbler (<i>Setophaga virens</i>)	0	0.038	0.772	0.958	0.991
CAWA	Canada Warbler (<i>Cardellina canadensis</i>)	0	0.003	0.457	0.962	0.995
CCSP	Clay-colored Sparrow (<i>Spizella pallida</i>)	0	0.136	0.496	0.561	0.669
CEDW	Cedar Waxwing (<i>Bombycilla cedrorum</i>)	0	0.255	0.969	0.992	0.998

Code	Common Name (Scientific Name)	Breeding Status	Baseline	2011-2040	2041-2070	2071-2100
CHSP	Chipping Sparrow (<i>Spizella passerina</i>)	2	0.951	0.994	0.995	0.994
CMWA	Cape May Warbler (<i>Setophaga tigrina</i>)	1	0.014	0.634	0.927	0.976
COGR	Common Grackle (<i>Quiscalus quiscula</i>)	0	0.821	0.981	0.981	0.995
CONW	Connecticut Warbler (<i>Oporornis agilis</i>)	0	0.001	0.146	0.773	0.963
CORA	Common Raven (<i>Corvus corax</i>)	2	0.800	0.963	0.983	0.996
CORE	Common Redpoll (<i>Acanthis flammea</i>)	2	0.991	0.994	0.976	0.453
COYE	Common Yellowthroat (<i>Geothlypis trichas</i>)	0	0.045	0.874	0.982	0.998
CSWA	Chestnut-sided Warbler (<i>Setophaga pensylvanica</i>)	0	0.000	0.179	0.919	0.995
DEJU	Dark-eyed Junco (<i>Junco hyemalis</i>)	2	0.929	0.988	0.991	0.989
EAKI	Eastern Kingbird (<i>Tyrannus tyrannus</i>)	0	0.025	0.198	0.377	0.867
EAPH	Eastern Phoebe (<i>Sayornis phoebe</i>)	0	0.000	0.002	0.230	0.983
EVGR	Evening Grosbeak (<i>Coccothraustes vespertinus</i>)	0	0.723	0.974	0.991	0.997
FOSP	Fox Sparrow (<i>Passerella iliaca</i>)	2	0.927	0.980	0.961	0.898
GCKI	Golden-crowned Kinglet (<i>Regulus satrapa</i>)	2	0.840	0.984	0.992	0.996
GCTH	Gray-cheeked Thrush (<i>Catharus minimus</i>)	2	0.943	0.956	0.870	0.243
GRAJ	Gray Jay (<i>Perisoreus canadensis</i>)	2	0.993	0.999	0.999	0.995
HETH	Hermit Thrush (<i>Catharus guttatus</i>)	2	0.779	0.971	0.980	0.988
HOLA	Horned Lark (<i>Eremophila alpestris</i>)	2	0.158	0.222	0.049	0.044
LCSP	Le Conte's Sparrow (<i>Ammodramus leconteii</i>)	0	0.095	0.387	0.381	0.359
LEFL	Least Flycatcher (<i>Empidonax minimus</i>)	1	0.064	0.855	0.973	0.993
LISP	Lincoln's Sparrow (<i>Melospiza lincolni</i>)	2	0.861	0.986	0.991	0.987
MAWA	Magnolia Warbler (<i>Setophaga magnolia</i>)	0	0.029	0.588	0.918	0.986
MOWA	Mourning Warbler (<i>Geothlypis philadelphia</i>)	0	0.001	0.588	0.974	0.998
NAWA	Nashville Warbler (<i>Oreothlypis ruficapilla</i>)	0	0.003	0.286	0.812	0.977
NOWA	Northern Waterthrush (<i>Parkesia noveboracensis</i>)	2	0.665	0.975	0.989	0.991
OCWA	Orange-crowned Warbler (<i>Oreothlypis celata</i>)	2	0.975	0.993	0.990	0.959
OSFL	Olive-sided Flycatcher (<i>Contopus cooperi</i>)	2	0.849	0.958	0.956	0.877
OVEN	Ovenbird (<i>Seiurus aurocapilla</i>)	0	0.009	0.625	0.952	0.995

Code	Common Name (Scientific Name)	Breeding Status	Baseline	2011-2040	2041-2070	2071-2100
PAWA	Palm Warbler (<i>Setophaga palmarum</i>)	0	0.082	0.710	0.669	0.458
PHVI	Philadelphia Vireo (<i>Vireo philadelphicus</i>)	0	0.018	0.654	0.894	0.969
PIGR	Pine Grosbeak (<i>Pinicola enucleator</i>)	2	0.966	0.991	0.988	0.970
PISI	Pine Siskin (<i>Spinus pinus</i>)	2	0.878	0.986	0.993	0.994
PUFI	Purple Finch (<i>Haemorhous purpureus</i>)	1	0.201	0.878	0.957	0.988
RBGR	Rose-breasted Grosbeak (<i>Pheucticus ludovicianus</i>)	0	0.001	0.227	0.872	0.990
RBNU	Red-breasted Nuthatch (<i>Sitta canadensis</i>)	2	0.941	0.995	0.997	0.999
RCKI	Ruby-crowned Kinglet (<i>Regulus calendula</i>)	2	0.673	0.982	0.992	0.995
REVI	Red-eyed Vireo (<i>Vireo olivaceus</i>)	0	0.016	0.848	0.988	0.999
RUBL	Red-winged Blackbird (<i>Agelaius phoeniceus</i>)	2	0.782	0.914	0.846	0.385
RWBL	Rusty Blackbird (<i>Euphagus carolinus</i>)	2	0.286	0.748	0.823	0.927
SAVS	Savannah Sparrow (<i>Passerculus sandwichensis</i>)	2	0.877	0.925	0.686	0.140
SOSP	Song Sparrow (<i>Melospiza melodia</i>)	1	0.478	0.913	0.966	0.989
SWSP	Swamp Sparrow (<i>Melospiza georgiana</i>)	0	0.106	0.582	0.431	0.762
SWTH	Swainson's Thrush (<i>Catharus ustulatus</i>)	2	0.989	0.998	0.998	0.998
TEWA	Tennessee Warbler (<i>Oreothlypis peregrina</i>)	1	0.411	0.976	0.993	0.992
TRES	Tree Swallow (<i>Tachycineta bicolor</i>)	2	0.728	0.953	0.973	0.988
VATH	Varied Thrush (<i>Ixoreus naevius</i>)	2	0.844	0.953	0.957	0.947
VESP	Vesper Sparrow (<i>Pooecetes gramineus</i>)	0	0.142	0.639	0.801	0.897
WAVI	Warbling Vireo (<i>Vireo gilvus</i>)	0	0.720	0.944	0.970	0.985
WCSP	White-crowned Sparrow (<i>Zonotrichia leucophrys</i>)	2	0.973	0.986	0.950	0.484
WETA	Western Tanager (<i>Piranga ludoviciana</i>)	0	0.329	0.867	0.933	0.949
WEWP	Western Wood-Pewee (<i>Contopus sordidulus</i>)	2	0.818	0.956	0.957	0.944
WIWA	Wilson's Warbler (<i>Cardellina pusilla</i>)	2	0.966	0.991	0.989	0.976
WIWR	Winter Wren (<i>Troglodytes hiemalis</i>)	0	0.016	0.626	0.887	0.978
WTSP	White-throated Sparrow (<i>Zonotrichia albicollis</i>)	0	0.153	0.929	0.984	0.996
WWCR	White-winged Crossbill (<i>Loxia leucoptera</i>)	2	0.988	0.998	0.998	0.996
YBFL	Yellow-bellied Flycatcher (<i>Empidonax flaviventris</i>)	1	0.020	0.486	0.805	0.946

Code	Common Name (Scientific Name)	Breeding Status	Baseline	2011-2040	2041-2070	2071-2100
YRWA	Yellow-rumped Warbler (<i>Setophaga coronata</i>)	2	0.947	0.992	0.995	0.996
YWAR	Yellow Warbler (<i>Setophaga petechia</i>)	2	0.631	0.981	0.992	0.998

References

Gibson, D. D. 2011. Nesting shorebirds and landbirds of interior Alaska. Report to USGS. Ester, Alaska.

Gibson, D. D. and J. J. Withrow. 2015. Inventory of the species and subspecies of Alaska birds, second edition. *Western Birds* 46:94-185.